A THEORY OF PLASTICITY

FOR IDEAL FRICTIONLESS MATERIALS

DK 539. 214. 9 (043)
DK 624. 131. 53 (043)

A THEORY OF PLASTICITY

FOR IDEAL FRICTIONLESS MATERIALS

by

BENT HANSEN

Head of Research Department

Danish Geotechnical Institute

Application of a General Solution Method
to Plane Strain Problems in an
Ideally Plastic, Homogeneous and Isotropic Frictionless Material

With Summaries in English and Danish

TEKNISK FORLAG
COPENHAGEN 1965

PREFACE

This work is intended as a survey of the theory of plasticity applied to failure problems in plane strain, assuming the material to be an ideal homogeneous and isotropic clay in the undrained state. Since the basic assumptions for this material are identical to those for ideal plastic-rigid metals, the methods and some of the results from the classical theory of plasticity can be used directly.

However, the range of the classical methods is found to be too limited for the use on failure problems in soil mechanics. This is partly due to the fact that quite ordinary failure problems in soil mechanics may have rather complicated boundary conditions. Thus, a shallow foundation in the vicinity of a slope, and possibly on a stratified clay profile, cannot be termed an extraordinary problem in soil mechanics. However, the mathematically correct solution, even for the simple assumptions of ideal clay, is far more complicated than any one which has been published for metals.

Accordingly, one purpose of the present work is to indicate methods by which any given failure problem in ideal clay can be solved, at least in principle. It has been found that the types of rupture figures considered by the well known theory of plasticity are not sufficiently general to give a solution in all cases. With a few exceptions they are all statically determined rupture zones, or are simple combinations of such zones with line ruptures (in Brinch Hansen's theory). But a very important element, the so-called mixed boundary condition zones, separating rigid bodies of clay, have never been studied before, to the author's knowledge.

For the calculation of statically determined rupture zones in the general case, where the slip lines will be curved, a number of numerical methods are known, the most important ones using the radii of curvature for the slip lines, or the so-called equivalent coordinates. These methods can also be used for more general rupture zones, when the so-called rotation functions are introduced. It is found, however, that simpler numerical calculations are obtained by the introduction of a new method, the so-called method of chord lengths.

Although it may be important to know the mathematically correct solution to any failure problem, as for instance for research purposes, or when exact bearing capacity or earth pressure coefficients are to be calculated and published for reference, practical design work will in some cases require simpler approximate methods. This is because the calculation work involved in the finding of one correct solution in an ordinary engineering problem may be prohibitive for economical reasons.

A number of such approximate methods exist, ranging from very reliable quasi-correct solutions (Brinch Hansen's equilibrium method using his special boundary condition for line ruptures) to rather ill defined, purely empirical methods. By considering the work equation it is shown that a very general class of approximate solutions, the so-called 'kinematically admissible' ones, can be generalized to cover all practical needs. By a further specialization the so-called 'solutions with possible zones' are derived. This type of solutions, which forms the basis of the present work, has the advantage that within certain limits the complexity of the solutions can be chosen as required, ranging from simple line ruptures (the well known $\varphi = 0$ analysis) to the mathematically correct solution.

It must be admitted that the assumption of a homogeneous and isotropic clay is rather special in soil mechanics, although it may be a good approximation for metals. In undrained failure most clays are inhomogeneous, because the shear strength usually varies with depth. Besides, the most important problems in soil mechanics concern soils with internal friction. This limitation of the scope has been accepted in order to be able to study in details the general solution methods and the properties of the solutions. However, in many cases the solution methods can be extended quite easily to cover much more general problems. This aspect is discussed during the development of the methods.

The Danish Geotechnical Institute has worked on the theory of plasticity since 1951. Most of this work has been centered on theoretical and experimental studies of failure problems in sand, but ideal clay has also been studied all the time. As far as the theory of plasticity is concerned some results have been published, as for instance by Lundgren and Mortensen [1953], and Brinch Hansen [1957], whereas others as yet only exist as unpublished internal memoranda and masters theses (Damgaard [1951], Steen [1961]).

The author has been fortunate enough to participate in this work since 1954 when the Technical University of Denmark granted him a fellowship un-

der the direction of Professor H. Lundgren. Later, as head of the research department of the Institute under the directorship of Professor J. Brinch Hansen, the author has received every possible encouragement to continue the work. This work is a partial result of studies carried out during these years.

The author also wishes to express his gratitude to his friend and colleague Mr. N.H. Christensen who has patiently and competently checked the manuscript and has helped to clear up a number of doubtful points during subsequent discussions. Thanks are also due to Mr. K. Jensen-Jørgensen, Miss R. Steffensen, and Mrs. Hanne Nielsen who have prepared the drawings, and to Miss A. Weiss who prepared the preliminary typewritten edition. The author is also grateful for the very neat work done by Mrs. M. Jahn who has been a great help during the proof-reading, and by Mrs. B. Lauritzen who has prepared the final edition for printing. The actual reproduction and printing have been carried out by Messrs. S.L. Møllers Bogtrykkeri, Copenhagen, whom the author thanks for their excellent work.

CONTENTS

Preface 5

Contents 8

1 Introduction 11

11 The Theory of Plasticity 12
12 Short Historical Review 15
13 Proposed Revisions 19

2 Basic Principles 21

21 Preliminaries 22

211 General Assumptions 22
212 Types of Problems 23
213 Types of Solutions 28

22 Problem Parameters 33

221 Geometry of Failure Problems 33
222 Boundary Parts and Load Resultants 39
223 External Rigid Bodies 43

23 Fundamental Conditions 52

231 Equilibrium Conditions 52
232 The Failure Condition 54
233 The Stress Characteristics 56
234 Deformation Conditions 63
235 Velocity Fields 64

24 General Properties of Solutions 68

241 Deformation Work 68
242 Uniqueness of Solutions 72
243 Approximate Solutions 80
244 Admissible Solutions with Possible Zones 83
245 The Equilibrium Method 88
246 Possible and Quasi Possible Solutions 98

3 Rupture Figure Elements 108

31 Basic Equations 109

311 The Slip Line Field 109
312 Radii of Curvature 117

313 Equivalent Coordinates 121
314 Velocity Components 124

32 Calculation Methods 131

321 Fundamental Differential Equations 131
322 Riemann Integration 138
323 The Method of Finite Differences 145
324 Geometrical Methods 154
325 The Method of Chord Lengths 162
326 Stress Resultants Along Zone Boundaries 170

33 Boundary Conditions for Zones 175

331 Free Surfaces 175
332 Vertex Points 183
333 Discontinuity Lines 187
334 Transition and Discontinuity Points 193
335 Internal Boundaries 196
336 Boundaries to External Rigid Bodies 200
337 Boundaries to Rigid Bodies of Clay 214
338 Other Boundary Conditions 218

34 Stress Conditions for Line Ruptures 220

341 General Formulae 220
342 Free Surfaces 225
343 Internal Boundaries 227
344 Wall Points 229
345 Line Ruptures Meeting in Soil 232

4 Rupture Figures 242

41 General Introduction 243

411 Rupture Figure Types 243
412 Numerical Calculations 246

42 Simply Determined Rupture Figures 249

421 Statically Determined Rupture Zones 249
422 Simple Line Ruptures and Arc Zones 264
423 Rupture Figures with Simple Rigid Bodies 277
424 Straight Radial Zones and Band Zones 284
425 Systems of Line Ruptures 295
426 Kinematically Determined Rupture Zones 301

43 Rupture Zones with Mixed Boundary Conditions 305

431 Curved Radial and Rectangle Zones 305
432 Multiple Radial Zones 319
433 Combinations with Wall Zones and Simple Arc Zones 323
434 Open Rupture Zones 328
435 Rigid Bodies in Zones 334
436 Problems with Internal Boundaries 338

44 Special Problems 341

441 Stresses in Rigid Bodies 341
442 Statical Possibility 348
443 Rupture Figure Complexes 355
444 Approximate Movement Conditions 358

5 Construction of Solutions 361

51 Choice of Rupture Figure 362

511 General Problems 362
512 Rupture Figure Loci 366
513 Development of Rupture Figures 372
514 General Solution Method 377

52 Stability Investigations 379

521 Stability of Slopes 379
522 Stability of Structures 386

53 Earth Pressure Problems 391

531 Simple Earth Pressures 391
532 Special Surface Conditions 400
533 Yield Hinges and Partly Unsupported Earth Fronts 410
534 Interacting Walls 415

54 Bearing Capacity Problems 420

541 Simple Foundations 420
542 Complex Foundation Problems 430

6 Conclusions 435

61 Review of Methods 436

611 Solution Method 436
612 Calculation Methods 438

62 More General Applications 441

621 General Problems in Clay 441
622 Frictional Materials 448

Notations 451

References 455

Summary 461

Dansk Resumé 463

Index 465

1 INTRODUCTION

This chapter deals with the general problem of applying the theory of plasticity to failure problems in soil mechanics. It first reviews the basic approach of the theory, after which the present state of knowledge is summarized in a short historical review. Finally it is indicated where, in the author's opinion, revisions are necessary.

In the following chapters the proposed calculation methods are developed systematically. For the sake of continuity the parts of the theory which are already known are also included, at least to the extent that they are considered useful. After defining formally the basic assumptions and the failure problems to be considered, the fundamental conditions that the solutions must satisfy are formulated, and some general properties of the solutions are deduced. This development makes possible the precise definition of the class of approximate solutions used in the work.

For the approximate solutions considered - which solutions include the mathematically correct one as a special case - the most difficult computations are associated with the rupture zones. Such zones can be calculated by expressing the basic equilibrium and failure conditions in terms of a differential equation, which equation must be satisfied by certain auxiliary functions. The given boundary conditions can also be expressed in terms of these functions, and numerical methods can be introduced in order to solve the differential equation. A more direct approach to the computation of rupture zones is furnished by the so-called 'method of chord lengths' which leads to simpler numerical calculations. It should be mentioned, in passing, that the rupture figures corresponding to the approximate solutions are not restricted to rupture zones: indeed they may sometimes consist entirely of line ruptures. The method of chord lengths is directly applicable in either case, but a special set of stress conditions are necessary if an equilibrium method is to be used. The general principle for the development of such stress conditions is derived, and the necessary formulae are given.

On this basis, the general method for the calculation of any given rup-

ture figure with possible zones can be indicated. The most important rupture figure types are studied in detail together with some special problems, the most important of which concerns stresses in rigid bodies of clay. By a limiting condition, an alternative method to Brinch Hansen's approximate earth pressure distribution can be derived.

Finally the more practical problem of constructing solutions to a given failure problem is discussed in connection with some examples from soil mechanics. Here it is impossible to give a unique method, because the rupture figure to choose in any given case will also depend on practical engineering and economical questions. This can also be seen from the fact that it is necessary to have approximate solutions at all. However, a number of rupture figures are indicated which may be useful in future calculations.

11 THE THEORY OF PLASTICITY

Generally speaking the theory of plasticity is concerned with all deformations which are independent of time. A typical problem within this framework could therefore be formulated as follows.

Consider a (possibly three-dimensional) domain of a material with known, possibly inhomogeneous and anisotropic properties, acted upon by known boundary loadings and constraints, and sustaining a known stress distribution. The previous strain history from the unloaded state must also be known. For a known differential change of the boundary loadings and/or the geometry of the restraints it is required to find the corresponding stress and strain increments at any point in the material.

This can, at least in principle, be solved when the following conditions are formulated mathematically, by the solution of the resulting differential equations.

1. The equilibrium equations for the stresses.
2. The elastic deformation law, relating the elastic part of the strain increments to the stress increments.
3. The failure condition which the resulting state of stress must satis-

fy (or at least not exceed); it usually depends on the previous history of plastic strains.

4. The plastic deformation law, relating the plastic strain rates (zero if the stress function which represents the failure condition is below its critical value) to the resulting state of stress and the previous history of plastic strains.

5. The compatibility equations for the total (elastic and plastic) strain increments.

6. The boundary conditions for stresses, strains, and/or movements.

The mathematical formulation of these conditions amounts to the representation of the given physical problem by a mathematical model. How complicated the model has to be will of course depend on the actual properties of the materials, as measured by physical experiments, but it is also a question of economy (which deviations from a simple representation are considered so important that they must be included in the model, and which ones can be neglected). It will therefore also depend on the problem itself.

In this work the simplest possible model is considered. It can be obtained by the following specializations of the general conditions.

1. It is assumed that the clay experiences no work hardening or softening. This means that the failure condition is independent of the previous strains, so that when the state of failure has been obtained it can be maintained with constant stresses for arbitrarily large plastic strains.

2. In isotropic clay in the undrained state the failure condition will be independent of the mean normal stress increment (total stresses are used). Besides the plastic strain tensor can be assumed proportional to the tensor of deviator stresses, all deformations having zero volume change.

3. The above simplifications are reasonable assumptions for most clays in the undrained state. It is more doubtful in which problems it is permissible to assume the clay perfectly elastic, with a constant Young's modulus, when it is not in failure (the assumption of a perfectly elastic-plastic material). Some such assumption has to be made when for example the development of rupture figures under increased loadings, or shake-down problems are studied. In this work only final states of failure are considered. This means that movements are possible in the whole rupture figure under constant

external loadings. In this stage, which is asymptotic with respect to the intermediate elastic-plastic states, no further elastic deformations are obtained. Therefore, the deformation properties of the clay before failure are immaterial, and the clay can be considered as ideal plastic-rigid. Under this assumption possible elastic or even plastic prestressings in the clay are also immaterial (which they are not in more general elastic-plastic states).

4. Finally only plane strain problems are considered. This simplifies the theory considerably, especially as far as the calculation of the rupture zones is concerned. This follows from the fact that the stress and strain tensors have only three instead of six independent elements (two and five respectively, when the failure condition is taken into consideration). Besides, it is now possible in some cases to separate the calculations of stresses and strains. Thus, in plane problems statically determined rupture zones are possible (two equilibrium equations), which they are not in three dimensional problems (three equilibrium equations). In plane strain the failure condition is simply that the maximum shear stress must not exceed the shear strength.

As a minor point, the simplest possible calculations are obtained when the volume forces, which as a rule cannot be neglected in problems of soil mechanics, are assumed to be expressible as gradients of a scalar potential function. This is practically always the case, because in undrained clay the only active volume force will be the unit weight of the clay (possibly with a horizontal component resulting for example from an earthquake).

By the above simplifications simpler problems are obtained than those formulated in the beginning of this section. In both cases a loading programme may be assumed to be specified, but in the general case a solution must be found for each step, to be integrated into a load-deformation curve. In the simplified case with a plastic-rigid material only the final point of this curve is of any interest, so the problem can now be formulated as follows.

For a given domain of clay a programme for loading until failure is specified. The point in this programme at which the final state of failure is obtained, and the stress and strain rate distributions at this point are required.

Notice that because arbitrarily large plastic deformations can be obtained under constant loads, the absolute magnitudes of strains and deformations have no meaning. It is understood that the deformations can only be determined relative to each other. They are therefore termed deformation rates or velocities. Admittedly, the last mentioned term may be misleading, the parameter of differentiation being not the time, but another quantity, as for example a characteristic boundary movement, which governs the deformations in the clay. Nevertheless, it is widely employed elsewhere and is used for the sake of simplicity in the following.

12 SHORT HISTORICAL REVIEW

The method of considering final states of failure was the first method used in soil mechanics, probably because the stress distributions encountered are so complicated that an approach by the theory of elasticity is normally out of the question for practical design problems. Therefore, if possible, the design work is based on a specified safety against total failure. This is much more easy to calculate, at least when an approximate method is used. Such methods satisfy only some of the conditions, but they are usually defined so that a unique calculation result will still be obtained. As a rule they operate with a system of slip lines along which the failure condition is satisfied. At least one equilibrium condition is fulfilled for the soil domain bounded by the slip lines. The kinematic conditions are rarely satisfied, except when this can be done by simple geometrical considerations.

Coulomb [1773] in his earth pressure studies considered a family of straight slip lines, satisfying one equilibrium condition, and chose the slip line which gives an extreme value for the earth pressure. Rankine [1857], on the other hand, considered the equilibrium everywhere in a (correct) statically determined rupture zone under a horizontal surface. In both cases a pure friction material (sand) was considered, but the same methods can easily be transformed for application to undrained clay.

In later works, other methods of this kind have been elaborated, mostly in order to reproduce the effects of the radial zones which are known to

exist in the rupture figures for earth pressures on retaining walls, and which arise in the computation of bearing capacities under strip foundations. See for example discussions by Terzaghi [1943], Terzaghi and Peck [1948], Meyerhof [1951], and Caquot and Kerisel [1956]. Most of this work is concerned with sand, but methods of the same kind can also be used for clays.

These methods might be termed the classical methods of soil mechanics. They give approximate solutions to a number of problems resembling those where the classical theory of plasticity can also be applied (statically determined zone ruptures). Some modifications, as for example the intercession of shallow foundations, discontinuous surface loads, or irregular surface forms present no difficulties to the approximate methods. They may, however, be impossible to solve by the classical theory of plasticity.

A somewhat special case is presented by the pure extremum method which uses a single line rupture separating two rigid bodies of soil. A circular slip line is used in undrained clay, for kinematical reasons and in order to be able to use the moment equation around the centre of the circle, cf. Fellenius [1927]. In sand a logarithmic spiral allows the use of the moment equation around the pole (Rendulic [1940]). This method might be considered as an extension of Coulomb's method, but it is mostly used in failure problems, as for example stability investigations, where the classical theory of plasticity cannot be used at all.

The theory of plasticity proper has mainly been developed for metals, as described, among others, by Hill [1950]. Most of the later work in this field has been concerned with elastic-plastic problems, problems of strain hardening, three-dimensional problems, and problems with special failure conditions.

The application of the theory of plasticity to plane strain problems in plastic-rigid materials dates back to Tresca [1864-72], who proposed a failure condition with a maximum shear stress. A more general condition with a maximum distortion energy was originally formulated by Huber [1904], but was first made generally known by the works of Hencky [1923] and Mises [1913]. It gives the same result for plane strain, but it differs - and is in better accordance with experiments - for three-dimensional problems.

Considering only rupture zones Hencky proved that the stress distribution is most easily found by considering the so-called slip line net. He derived the equation which governs the stress variation along the slip lines; it is a special case of Kötter's equation [1903], which also takes a possible

internal friction into regard. From this the properties of constant angular differences in the net, and the differential equations for the radii of curvature (Hencky's theorems) can be derived. As shown by Hill this can be used for the numerical calculations of the geometry of the slip line field, starting from the known boundary conditions for stresses. As an alternative method the so-called equivalent coordinates (attributed to Mikhlin) can be used; they must satisfy much the same differential equations as the radii of curvature.

The properties of the basic differential equations for the auxiliary geometric functions have been studied from a rigorously mathematical point of view by Carathéodory and Schmidt [1923] and by Geiringer and Prager [1934]. Using the methods of applied mathematics, solutions can be obtained by series expansions or by Riemann integration. Simpler numerical calculations are obtained by some variant of the method of finite differences, see Prager and Hodge [1951], Hill [1950], and Sokolovski [1960], or by the geometrical method of pole trails indicated by Prager [1953].

The deformation conditions are based on the work of Saint Venant [1870-72]. For a more advanced theory the use of strain increments as proposed by Haar and v. Kármán [1909] are used. For numerical calculations in the plastic-rigid case the basic differential equations for the velocity components related to the slip line field were derived by Geiringer [1930].

The above development of the theory might be called the classical theory of plasticity. It has also been applied to problems in soil mechanics, as by Drucker and Prager [1952] and Kézdi [1962]. For undrained failure in clay the solutions for metals can in some cases be applied directly, cf. Prandtl [1920] for bearing capacity problems, but soils with internal friction are also considered, cf. Josselin de Jong [1959] and Sokolovski [1960]. By the introduction of the Mohr [1914] envelope almost completely general failure conditions can be considered, at least in plane strain.

In this way even very complex problems with statically determined rupture zones can be solved. But with rare exceptions (for example the kinematically determined rupture zones indicated by Sokolovski) this is also the only use which is made of the theory. In fact, in soil mechanics the theory of plasticity is usually taken to mean the calculation of statically determined rupture zones.

As a striking contrast, the potential possibilities of the more general theory have been demonstrated by the fact that the work equation can be used to show that solutions satisfying the general conditions of Sec. 11 are unique, cf. Hill [1950]. In this proof quite general stress and strain distributions

are considered. Nothing more is assumed about the rupture zones than that the basic conditions given above are satisfied. Similarly, the well known extremum principles of Drucker, Prager, and Greenberg [1951] are also deduced by means of the work equation only. They state that statically admissible stress distributions (satisfying the equilibrium conditions and boundary conditions for stresses, and not exceeding the failure condition) are on the safe side, and that kinematically admissible velocity fields (satisfying the condition of constant volume and the boundary conditions for movements) can be used to calculate solutions on the unsafe side. In the two cases, the upper and the lower limits respectively for a quantity defining the safety will be obtained, and will correspond to the mathematically correct solution.

These principles are frequently used in the theory of structures (limit design). They also assume nothing about the type or extension of the rupture zones. Some of the approximate methods in soil mechanics, especially the so-called $\varphi = 0$ analysis, may be considered as special applications of these principles. They do not lead to the correct solution, however, because it is not possible to change a sufficient number of parameters. Besides, the solution types for which a minimum safety is found may not admit of a kinematically admissible velocity field.

At an early stage in soil mechanics it was noticed by Terzaghi [1936] that some earth pressure problems, such as anchored sheet walls, cannot be solved by the usual approximate methods, as for example Coulomb's method, i.e. they cannot be solved by the theory of plasticity which they approximate, because the kinematic conditions would then be violated. The pure extemum method would in this case represent the true rupture figure quite well, but it could only be used to determine the necessary driving depth, not the earth pressure distribution along the wall. For such problems, more or less empirical methods, some of them based instead on the theory of elasticity, have been used until recently.

In order to be able to solve such problems Brinch Hansen [1953] introduced the so-called equilibrium method. It is based on the fact that for the $\varphi = 0$ analysis the extreme condition can be replaced by the three equilibrium equations for the moving rigid body of clay when a special boundary condition is used for the end point of the line rupture, and Kötter's equation (or Hencky's equation for undrained clay) is used to determine the stress distribution along the line rupture. He further introduced the idea of composite rupture figures, where a combination of line ruptures and statically determined rupture zones separate rigid bodies of clay. A preliminary classification of such rupture figures was given, and calculation methods were in-

dicated (except for a few special types, for example AfPfA where the zone is not statically determined).

For the practical calculation work Brinch Hansen indicated a special approximate method to calculate statically determined rupture zones (which can also be calculated exactly by the theory of plasticity), and proposed an assumption for the earth pressure distribution between a wall and a rigid body of clay (the resultant being known from the equilibrium method).

This gives a considerable increase in the range of failure problems which can be solved exactly, and it also introduces a type of very close approximations, namely the solutions that might be called quasi-correct, because all conditions are satisfied except for the end points of line ruptures, where a special stress condition is used.

However, the type of rupture figures considered by Brinch Hansen (which might be called simply or quasi-statically determined) do not represent the most general solution, as can be seen from the type AfPfA. This rupture figure contains a radial zone which must be determined partly from the stress conditions and partly from the movement conditions following from the fact that it is surrounded by rigid bodies of clay. Calculation methods for such zones have never been indicated, to the author's knowledge.

Besides, the special stress condition for line ruptures is not statically admissible, although it usually represents a good approximation. If mathematically correct solutions are required the line rupture must be replaced by a complex structure of rupture zones, one of which will also have mixed boundary conditions.

13 PROPOSED REVISIONS

From the summary of the existing theory which is given in the preceding section the following needs for revisions can be deduced.

1. In order to be able to calculate mathematically correct solutions methods must be developed for the calculation of zones with mixed boundary conditions. Some general rules must be formulated for

the combination of different types of rupture zones, including line ruptures, into rupture figures.

2. The existing numerical methods for rupture zones (using radii of curvature or equivalent coordinates) are rather laborious. The geometrical methods are much faster, but may be too inaccurate. A simple analytical method based on geometrical considerations would be useful, although not strictly necessary.

3. In order to be able to construct simple and well defined approximate solutions it will be necessary to utilize the extremum principles in a systematic way. This will also give a general proof of Brinch Hansen's equilibrium method, and will show exactly how this method is related to the $\varphi = 0$ analysis and to the mathematically correct solution.

4. By a simple application of the extremum principle it is possible to replace the earth pressure distribution proposed by Brinch Hansen with the investigation of a limiting state of stress in the rigid body of clay.

It is attempted to realize all the above points in the course of the following chapters.

2 BASIC PRINCIPLES

In this chapter the general assumptions and the considered types of failure problems are formally defined, and a preliminary classification of solution types is given.

The different parameters used to specify a failure problem are defined, and are represented analytically in a mathematical system of reference. In this way a generally applicable method is obtained to describe a given failure problem, and to analyze the mechanism of external rigid bodies in terms of loading and movement conditions for the boundaries of the clay. This formal description will not be needed in most cases where the calculations are performed by hand, but it may be useful in connection with calculations by an electronic computer.

The reference quantities of stress, strain, and velocity components are defined, and the basic conditions are interpreted in terms of these quantities.

Finally some general statements concerning the solutions and the solution methods are formulated. By means of the work equation the uniqueness of solutions is proved, and different types of approximate solutions, including the method with possible zones, are defined.

21 PRELIMINARIES

211 General Assumptions

In this work only plane strain conditions are considered. The material is assumed to be an ideal, homogeneous and isotropic clay in an undrained state with a constant shear strength, zero volume change at failure, and no internal friction. All considered stresses are total stresses. The principal stress and strain directions are always assumed to coincide.

The volume forces are assumed to be expressible as a gradient vector field to a continuous scalar function. There is no special problem involved in admitting piecewise continuous functions f. inst. by considering a stratified soil profile consisting of several clay layers, each with a different unit weight. It is also possible to assume different shear strengths for these layers. The methods to use under these assumptions are indicated, but most examples are concerned with one layer only.

Only such problems are considered where the material can be assumed plastic-rigid. Thus, it is assumed that a state of failure exists in which deformations are possible under constant stresses, so that during failure the material is not deformed elastically, but only pure plastic strains exist. This state of failure will be obtained asymptotically for clay with an arbitrary stress-strain relationship below failure, if

1. The material is acted upon by increasing loadings which produce increasing shear stresses until failure.
2. The work hardening or softening of the material, after the failure point (maximum shear stress) has been reached, is negligible.
3. Failure is obtained for deformations which are small in relation to the characteristic lengths (wall height, foundation width etc.) of the problem.
4. The stress increments due to the altered boundary conditions when boundaries are deformed, are small to at least the second order of deformations ($\Delta \sigma \sim \sigma \cdot \delta^2$) so that stability problems do not arise.

In the plastic-rigid state all movements and deformations may without any influence on the stress distribution be multiplied by a common arbitrary

factor of proportionality. For that reason they are termed movement rates or velocities, and it is understood that their magnitudes are only given relative to each other.

212 Types of Problems

By a failure problem is understood a given set of parameters specifying

1. A clay material which is bounded by a number of free surfaces and also by boundary curves to adjacent rigid bodies. There may also be internal boundaries separating different clay domains. For each domain a constant shear strength c is given, possibly divided by a partial safety coefficient. Correspondingly for each boundary to a rigid body an adhesive strength c_a is given.
2. A set of movement conditions for the rigid bodies, given as at most three conditions for each separate body, or as at most three conditions between the movement components of any two bodies (in case of interconnections).
3. A set of movement rates (the constant terms in the equations corresponding to the conditions under 2. above) which may be zero (for restraints) or may represent absolute movement vectors for one body or relative movements between any two bodies.
4. A set of loadings, possibly multiplied by individual partial coefficients, specified as:
   a. Volume forces for the clay.
   b. Surface loadings on the free surfaces.
   c. Line loadings and moments acting upon the rigid bodies (possibly coupled between any two bodies as actions and reactions).

According to the conditions under 2. some components of the forces under 4 c. may be taken directly by the restraints, whereas others are transmitted to the clay material.

To obtain a state of failure, where all equilibrium conditions must be satisfied, the problem may be formulated in one of the two following different ways:

1. Controlled strain: All specified forces are constant. A system of

movement rates, at least one of which is different from zero, is given (i.e. there must be at least one rigid body with at least one specified movement of restraints). The quantity defining failure is the total work W done by the specified movements (normalized in some way if several failure problems are to be compared) during failure in the material.

2. Controlled stress: No boundary movement different from zero is specified (possible rigid bodies must be free or be given a number of passive restraints). All forces are given in two parts, one of which is constant (possibly zero). The other part (with at least one force or loading different from zero) is for all forces multiplied by a common factor of proportionality f. The quantity defining failure is the value of f (which can be considered as an extra factor of safety above the demanded partial coefficients) corresponding to a state of failure in the material.

It is usually understood that the constant part of the loadings under 2. above shall not in itself produce failure. There will then be a positive and a negative value of f corresponding to failure, and it must be specified which one is desired (usually the positive one). The two states of failure may be termed complementary to the same problem. We have a similar case for positive and negative values of the movement components specified in controlled strain.

The above definition for failure problems is seen to be general enough to cover all practical problems in soil mechanics (earth pressures, bearing capacities, block foundations etc.), where it is investigated whether a given construction has a prescribed safety against failure.

In design problems it is required to find a set of geometrical quantities (constructional dimensions) so that a state of failure just exists in the clay, when the prescribed partial coefficients are applied to the forces and shear strengths. Such problems can also be described in terms of controlled stress or controlled strain.

1. If there are no external rigid bodies, or if all restraint movements are specified to be zero, the given loadings (which are constant) can be considered formally as a set of loading rates. One geometrical parameter can be found by the condition that f shall be exactly unity. In some cases a further number of parameters can be determined by the further conditions that f shall also be unity for a corresponding number of alternative rupture figures. This defi-

nition is not unique, however, because some parameters specifying the ratios between the movement rates in the different rupture figures can frequently be chosen arbitrarily, and the choice will influence the result. In such cases these ratios must be determined from considerations of optimum economy.

2. In controlled strain a number of restraint movements is specified, and one geometrical parameter can be determined by the condition that the work W done by these movements shall be exactly zero. In this case a further number of movement conditions can be imposed on the external rigid bodies, and possibly also on the rigid bodies of clay. The corresponding number of geometrical parameters can now be determined by the conditions that the imaginary restraint forces shall all be zero. By choosing appropriate modes of failure (f. inst. when possible, pure translations as preferable to rotations of the external rigid bodies in contact with the clay) an optimal set of dimensions can be obtained.

Notice that the ratios between movement rates, and also the imaginary restraint movements, can be chosen so that some parts of the rupture figure, although fully developed, will have zero plastic deformations in relation to the rest of the rupture figure (it is only on the verge of failure).

Example 21 a

The sheet wall construction shown in Fig. 21 A gives a good example of the great number of possible variations. Compare Brinch Hansen [1953].

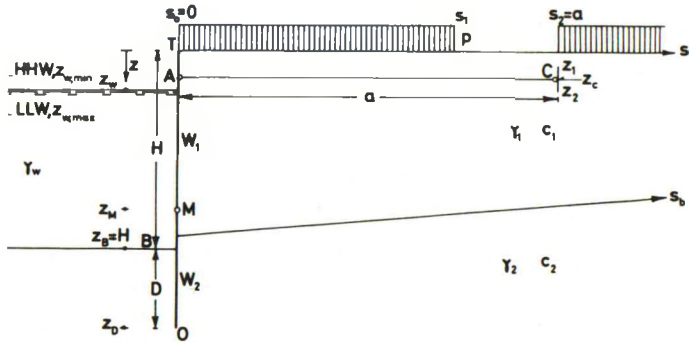

Fig. 21 A: An Anchored Sheet Wall Construction.

The wall OT is driven to the depth $z_D = H + D$ into a stratified soil profile with a sloping internal boundary s_b. Then the anchor wall C is constructed at the distance a from the sheet wall (between the depths z_1 and z_2 below the surface s), and is connected to the wall by the tie rods AC (supposed to be hinged at both ends). Finally the clay outside the wall is excavated to the depth $z_B = H$.

During the use of the wall the surface s is loaded by a variable normal load with the maximum intensity p. The water level outside the wall may vary between HHW (depth $z = z_{w,\,min}$ below the clay surface) and LLW ($z = z_{w,\,max}$). The wall is assumed plastic-rigid so that if the maximum moment M_m, acting at the point M where the transversal force Q in the wall is zero, is smaller than the yield moment M_y, the wall will act as one rigid plate. Otherwise, the wall will act as two rigid plates, W_1 and W_2, separated by the point M which acts as a hinge between the wall parts. M is still determined by the condition that $Q = 0$, but the moment at M between the wall parts will now act as a pair of constant external (moment) loads, equal to M_y.

It is seen that the external parameters may be subject to some variations, the most critical combination being unknown beforehand. The sheet wall construction may f. inst. give rise to the following problems.

1. For an existing wall construction (perhaps designed by means of an empirical method), where all geometrical parameters are known together with the yield moment M_y, the purpose of the calculations may f. inst. be to ascertain the safety of the wall after an increase of the surface load p, or of the excavation depth H. The problem may be considered as one of controlled stress, considering the known forces and unit weights, i. e. p, γ_1, γ_2, and γ_w, formally as loading rates. Thus, all these quantities are multiplied by a common factor of proportionality f (or, which amounts to the same thing, the resistancies c_1, c_2, and M_y are divided by f), the value of which corresponding to the final state of failure is determined. If the required partial coefficients (or total factors of safety) are applied to all forces and resistancies before this calculation, it can be stated, that $f \geq 1$ means that the construction is sufficiently safe, whereas $f < 1$ means that the safety is not satisfactory. f may also be put only on one quantity producing failure, f. inst. p. This may not give exactly the same solution, and the numerical value of f found in this way may be widely different. The above criterion for f will still be valid, however. During these calculations the position

of M must be ascertained by the condition Q = 0. It must further be ascertained whether this point is an ordinary point of maximum moment, or a yield hinge. In the first mentioned case we have two external rigid bodies, connected by the tie rods AC with constant lengths (their influence on the earth pressure on the wall is usually neglected), but otherwise free; in the last mentioned case there are three rigid bodies: two connected by the tie rods, and two others by a hinge. Similar complications may arise due to a possible longitudinal yield of the tie rods, or to the formation of a yield hinge in the anchor wall. Besides the external variable parameters, z_w and the quantities s_1, s_2 etc. defining the position of the surface load p, must be varied so that the combination is found for which f is a minimum.

2. In model tests the method of controlled stress may be difficult to realize in practice. Instead the problem may be considered as one of controlled strain, the specified movement being f. inst. a unit rotation of the wall (the upper wall part, if M is a yield hinge). The work W producing failure will in this case be equal to that of an unbalanced moment acting upon the wall, both equations of projection being satisfied. The criterion that the wall construction is sufficiently safe will be that $W \geq 0$, when the required partial coefficients are applied to the forces and resistancies.

3. In design one might use the method of controlled stress, determining f. inst. D and a, when all other design quantities are known, by the conditions that f = 1, and zero movement of the anchor wall in relation to the wall movement. A more general solution is obtained, however, when the 5 most important design quantities: D, a, z_1, z_c, and M_y are determined as follows. All movement components for the 3 external rigid bodies are chosen (9 quantities, subject to 1 condition from the tie rods and 2 conditions from the hinge M, i.e. 6 free parameters). During the calculation of the state of failure in the clay the position of M is found by the condition that Q = 0, the variable external parameters are determined by the condition that W shall be minimum, a value is assumed for the ratio z_1/z_2 (usually zero), and two of the free movement parameters are varied so that the walls are in equilibrium for the vertical forces. By successive calculations (if necessary) the 5 design quantities are varied until W and the remaining 4 imaginary restraint forces are zero. The anchor force in the tie rods, and the maximum moment

in the anchor wall are ordinary restraint forces (as M_m also is, when M is not a yield hinge). They are also determined during the calculations, possibly by a special procedure to be considered in a later section. By successive investigations as above the remaining 4 free movement components (and possibly the ratio z_1/z_2) may be varied until the total cost of the sheet wall construction is a minimum.

In practice the above mentioned investigations are performed in a somewhat simpler way. Thus, it is immediately clear that the most critical value for z_w is $z_{w,\,max}$. The optimal movement of the wall parts (and the optimal value of z_1/z_2) will frequently be known by experience, and (which is more dubious, however) the calculations of the state of failure are split up into a number of separate investigations (earth pressures and design of the wall, stability and design of the anchor construction) each with a separate critical distribution of the surface load.

Notice that the movement components frequently cannot be given in relation to one fixed scale. Thus, the movements of the anchor wall will usually be zero in relation to the movements of the sheet wall. But it is not the same thing to assume a zero translation and a zero rotation of the anchor wall. Therefore, the rotation of the anchor wall may well be zero in relation to its translational components, and thus be zero to the second order in relation to the sheet wall movements. Other constructions, f. inst. a possible shallow foundation at the clay surface, may in the same way have movement components which are zero in relation to the sheet wall movements, but are infinite, finite, or zero in relation to the anchor wall movements (when this relation has any practical importance).

213 Types of Solutions

By a solution to a given failure problem (with fixed external parameters, although these may later have to be varied in order to satisfy further conditions, f. inst. f = 1, W = 0, a restraint force = 0, f = min., W = min., or a cost function = min.) we understand:

1. A velocity field in the clay material. It will in the general case correspond to a number of rigid bodies of clay, rotating without any deformation, and separated by rupture zones which are deformed plastically. The transition of velocities from one rigid body to another is effected partly by deformations in the rupture zones,

partly by slidings (tangential velocity discontinuities), usually along the boundaries of the rigid bodies, but frequently also along curves through the rupture zones,

and/or

2. a stress distribution which is defined at least to the extent that the deformation work per unit volume can be determined at each point of the rupture zones, including the curves along which slidings take place.

The geometrical representation of the partitioning of the clay material into rigid bodies and rupture zones is called the rupture figure corresponding to the solution.

A solution is called mathematically correct if it satisfies the conditions for failure in an ideal plastic-rigid material, and further the special conditions pertaining to the given problem. More specifically it must satisfy the following conditions.

1. The velocity field satisfies the deformation condition (zero volume change) everywhere, and it agrees with the given boundary movements.

2. The stress distribution is completely determined in the rupture zones, except possibly for a constant hydrostatic pressure in each of a number of separated domains in failure. It satisfies the equilibrium conditions at each point in the rupture zones, and also the equilibrium conditions for all external rigid bodies, and all rigid bodies of clay (some of these conditions, possibly all of them, may not put any restraint on the stress distribution; they are used to find the restraining forces). For zones bounding to a free surface the stresses in the material along the boundary correspond to the given boundary loadings. In controlled stress all stress conditions are satisfied for a unique value of the factor f.

3. The principal stress and strain directions coincide everywhere in the rupture zones. At all points where the maximum shear strain is different from zero the failure condition (maximum shear stress equal to c) is also satisfied. Correspondingly, if there is a tangential movement between a rigid body and the clay, the shear stress acting upon the boundary curve will be equal to the adhesive strength c_a.

4. In each rigid body of clay a stress distribution satisfying the above condition No. 2 is possible with the maximum shear stress nowhere exceeding the shear strength, and shear stresses along boundary curves to external rigid bodies (if any) nowhere exceeding the adhesive strength.

5. At each point in the rupture zones the shear stresses and the shear strains have the same sign, i.e. the plastic deformation work per unit volume of the clay is non-negative at every point. Correspondingly, along boundary curves to external rigid bodies which are sliding upon the clay the shear stress (whose absolute value is equal to c_a) will point in the same direction as the sliding velocity.

Mathematically correct solutions must usually be found by numerical methods, so they can only be determined within a certain accuracy. They will still be termed correct (however inaccurate) if they contain the same number of elements, i.e. rigid bodies and rupture zone parts, as the exact ones. They are distinguished by the fact that no matter how far the numerical method is refined, they will still satisfy all the above conditions within the (increasing) accuracy of the method.

If the conditions are not all satisfied the solutions are termed approximate. Two types of approximate solutions may be distinguished:

1. Possible ones, which have much the same properties as the correct ones, but which may fail to satisfy the conditions No. 4 and/or 5. This class of solutions is introduced because in practice one can at most make sure beforehand that the conditions No. 1-3 will be satisfied. Solutions intended to be correct must therefore be calculated as possible ones, after which it is checked whether the conditions No. 4 and 5 are also satisfied.

2. Admissible ones which satisfy only a few of the above conditions, and, consequently, are simpler to calculate, but give less information than do the possible ones. However, they have the property that if the initial parameters are determined by an extremum condition the resulting solution is known to be closer to the correct one than for all other combinations.

An intermediate case is obtained by the so-called quasi-possible solutions which are known not to satisfy the condition No. 2 in the neighbourhoods of a finite number of points (usually end points for line ruptures). They are almost as accurate as the possible solutions, but may in some cases be much simpler to calculate.

In some cases a possible solution, or the extreme one of a family of admissible solutions, may be shown to be in fact the correct solution. If not, there is no one to one correspondence between the rupture figure elements of the exact and the approximate solution, and the last one can never become correct however much it is refined. The approximation can only be improved by choosing another type of rupture figure (usually a more complicated one with more initial parameters).

If the approximate solution is neither possible nor admissible, an extremum method may still be used, but nothing definite can be said about the position of the extreme solution in relation to the exact one. It may still be a good approximation, however. To this class of approximations belong the so-called quasi-admissible solutions, and solutions with approximate movement conditions. The important class of solutions with possible zones will be defined in a later section.

As to the practical calculations, the different rupture zone elements may be classified according to the type of boundary conditions from which they are calculated. The following types may be distinguished.

1. Statically determined zone elements, which may be calculated in closed form from boundary conditions relating to stresses only. These elements exist in direct contact with free surfaces with known surface loadings. They may be continued through radial zones to boundary zones in contact with rigid bodies (with known adhesion) or through transition points to other statically determined zone elements. A rupture figure consisting of such elements only is called statically determined.

2. Kinematically determined zone elements, the form of which is given uniquely by the boundary movements. The general case is rarely obtained, but a special case where the zone has degenerated to a single curve is very important. For kinematical reasons it must be a circle arc, the so-called line rupture. If a rupture figure consists only of statically determined zones together with line ruptures, the boundary movement conditions can easily be satisfied, after which purely statical conditions determine the rupture figure. It may in this case be called simply determined (or quasi statically determined). In special cases the line ruptures may be replaced by simple radial zones or band zones.

3. Mixed boundary zone elements separating clay bodies, but where the movement conditions are not sufficient to determine uniquely the

form of the zones. This type may be subdivided into a large number of classes, the most important division being between closed and open rupture zones. Especially in the latter class very complicated forms are possible. Rupture figures containing zones of this type are statically undetermined.

Example 21 b

The classical Prandtl rupture figure WPR, shown in Fig. 21 B (P in Brinch Hansen's notation) is a possible rupture figure. If the rotation point of the wall is in a certain domain below the foot point, it will also represent the mathematically correct solution. In all cases the rupture figure will be statically determined, no kinematical conditions at all being used for the calculation of the rupture zone (except for the determination of the sign of the shear stress along the wall, and to ascertain whether the zone is active or passive).

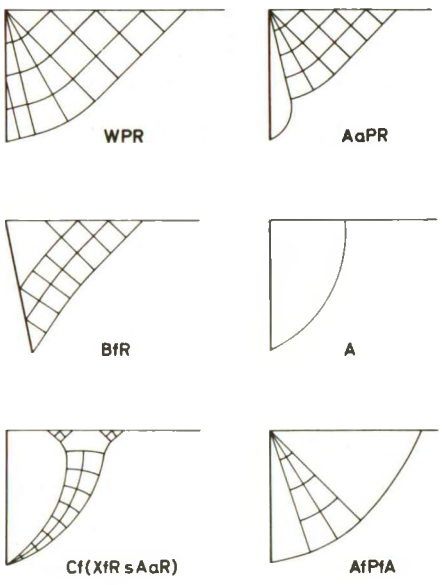

Fig. 21 B: Examples of Rupture Figure Types.

The rupture figure AaPR (AaP in Brinch Hansen's notation) is also possible. It is simply determined because the kinematical conditions for the rigid body of clay along the wall are easily expressed in terms of geometrical conditions for the line rupture.

The band zone rupture figure BfR is possible. If the surface conditions are simple enough, so that the boundaries of the Rankine zone are straight, it will also be simply determined, because the boundaries of the band zone will then be circle arcs, the form of which follows in a simple way from the kinematical conditions. Otherwise the band zone will be an open rupture zone with mixed boundary conditions.

The simple line rupture A represents a quasi-possible solution, the stress conditions being violated at the upper (and possibly also the lower) end point of the line rupture. This rupture figure is also simply determined,

when Brinch Hansen's approximate stress conditions are used.

The possible solution corresponding to the simple line rupture is rather complicated. It might be termed Cf (XfRsAaR), the letter C representing a closed rupture zone with mixed boundary conditions.

Finally, the rupture figure AfPfA represents an admissible solution, the number of free parameters being insufficient to satisfy all equilibrium conditions for the rigid bodies of clay. The form shown in Fig. 21 B is simply determined, because the radial zone has straight radial boundaries. If it is replaced by a closed zone C with curved boundaries one further parameter is obtained, but the rupture figure will now be statically undetermined. It will still only be admissible, however, the original AfPfA rupture figure having a deficiency of two parameters. Notice that the rupture figure WPR can frequently be used as a possible approximation in this case (a rotation point above the top point of the wall). It will not necessarily represent a better approximation, however.

22 PROBLEM PARAMETERS

221 Geometry of Failure Problems

Ordinary failure problems which are to be solved by means of numerical calculations by hand will not usually need a formal mathematical treatment of the problem parameters. As a rule even rather complex problems can be stated clearly by means of a sketch (cf. Fig. 21 A), if necessary by a drawing in scale (f.inst. by stability investigations), possibly with some explanation in form of a short text.

However, if the calculations are to be performed on an electronic computer all geometrical quantities will have to be represented by a set of numerical data. For that reason, and also in order to be able to refer to some well defined concepts, the following sections will give a concise representation of the different possible problem parameters in a numerical form.

All points referred to are described by their coordinates in a Cartesian

coordinate system x, y. There are no restrictions as to the position or orientation of the coordinate system, but once placed it defines the positive direction of rotations in the plane as the shortest one from the positive x-direction to the positive y-direction.

The geometry of a failure problem can be described by means of the following elements, cf. the sketch of principles shown in Fig. 22 A.

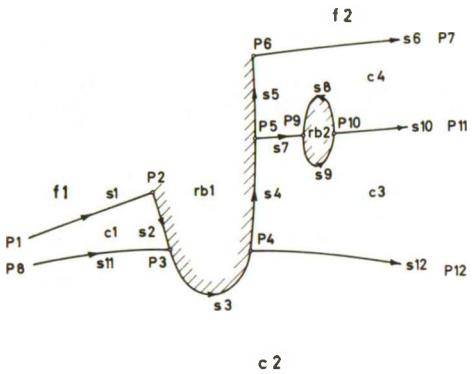

Fig. 22 A: General Topology of Failure Problems.

1. A number of characteristic points (P 1 - P 12) separating the different boundary parts.
2. A number of boundary parts (s 1 - s 12), each with a given positive orientation (the direction in which the arc length s is measured). Any boundary part may be characterized by the points it connects, and its orientation by the order in which the two points are mentioned, f. inst. s 4 connecting P 4 to P 5.
3. A number of domains which may be clay domains (c 1 - c 4, each with a constant value of c), external rigid bodies (rb 1 - rb 2), or free space (f 1 - f 2).

The points and boundary parts are chosen so that each boundary part separates two specific domains. The relative position of the domains can be indicated by the convention that the first mentioned one is located in the negative direction of rotations relative to the orientation of the boundary part. Thus, s 4 (between the points P 4 and P 5, in this order) separates the domains c 3 and rb 1, in this order.

At least one of the domains separated by any boundary part will be a clay domain. If only one of the domains is, the other being an external rigid body or free space, we have a part of the external boundary of the clay material. It can always be oriented so that the positive direction of s corresponds to the negative direction of rotations around the clay material, cf. s 1 - s 6 and s 8 - s 9 in Fig. 22 A. The same convention cannot be used in a unique way for internal boundaries, separating two clay domains.

It is frequently expedient to have a local system of coordinates for boundary points, cf. Fig. 22 B. It consists of a t-axis tangent to the boundary curve, positive in the positive s-direction, and an n-axis coinciding with the normal to the boundary, the rotation tn being in the positive direction of rotations. The angle between the x-axis and the t-axis is called β.

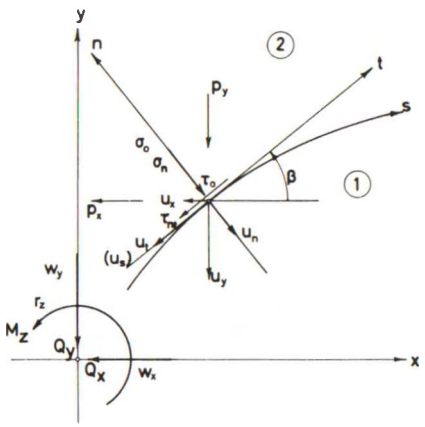

Fig. 22 B: Coordinate System. Surface Loading and Movement Components.

The problem parameters, mentioned in Sec. 212, can now be described as follows.

1. The topology of the failure problem: The numbers of characteristic points, boundary parts, and domains are given. For each boundary part one indicates the two end points and the two separated domains (type and No., in the correct order).

2. The geometry of the problem: For each boundary part its position in the xy-plane is indicated, f. inst. by giving x and y as functions of s. It is simpler, however, and usually accurate enough, to assume that each boundary part consists of a number of circle arcs, the parameters of which are given in the order of increasing values of s. The intermediate points between the circle arcs can then be treated as characteristic points.

3. For each clay domain: The shear strength c and the volume forces (usually only a unit weight).

4. Adhesion strengths: For each boundary part to an external rigid body a value for c_a is indicated. It must not exceed the value of c for the bounding clay domain (or, if it does it must be taken to

be equal to c). One might in the same way indicate adhesion strengths for the internal boundaries, representing the effect of an infinitely thin, weak layer, or a crack. In this case c_a must not exceed the value of c for the weaker of the two clay domains.

5. Boundary loads: All boundaries may be assumed to be loaded by external forces. Such loads may be given either by the normal component σ_o and the tangential component τ_o, both per unit length of the boundary, or by the components p_x and p_y parallel to the coordinate axes x and y, respectively, and given per unit length of the coordinate axes to which they are perpendicular.
   σ_o and τ_o are positive in the negative direction of n and t, respectively. p_x and p_y are positive if the loading for positive dy and dx, respectively (for a positive increase ds of the arc length), acts in the negative directions of the coordinate axes.

6. Total forces: All total force components (line loads on external rigid bodies, or force resultants of boundary loadings acting upon rigid bodies of clay) are given relative to the xy-coordinate system. The components Q_x and Q_y are positive when acting in the negative directions of the respective coordinate axes. M_z is a moment about the origin point, positive in the positive direction of rotations.

7. Movement conditions: The movement components w_x, w_y (translations), and r_z (a rotation) for rigid bodies are positive in the same directions as Q_x, Q_y, and M_z, respectively. They determine the velocity vector at each point of the rigid body. Its components u_x and u_y are parallel to the x- and y-direction, respectively, and are positive in the negative coordinate directions. For boundary points the components u_n and u_t can also be used; they are positive in the negative directions of the local coordinate axes n and t, respectively. A possible sliding is indicated by the fact that u_t is different for the two sides of the boundary. The sliding velocity $u_s = \Delta u_t$ is defined as the difference between the values of u_t for the material in the positive and in the negative direction of n (i.e. u_s is positive if the material in the positive direction of n slides in the negative direction of t upon the material in the negative direction of n).

All the above mentioned quantities are shown in Fig. 22 B. The elementary relations existing between them are indicated in the following, the symbol Δ meaning a function value for the domain No. 1 (in the negative direction of

n) minus the corresponding function value for the domain No. 2 (in the positive direction of n).

The components of boundary loading σ_o, τ_o, p_x, and p_y are related to each other, and to the stress components σ_n (in the n-direction, positive as compression) and τ_{nt} (in the t-direction, positive as a shear giving positive values of u_s) by the following equations, which also give the contribution to the total force components:

$$\sigma_o = p_y \cos^2\beta - p_x \sin^2\beta = \Delta\sigma_n$$
$$\tau_o = (p_y + p_x) \sin\beta \cos\beta = \Delta\tau_{nt} \qquad (2201)$$

$$p_x = -\sigma_o + \tau_o \cot\beta$$
$$p_y = \sigma_o + \tau_o \tan\beta \qquad (2202)$$

$$\begin{aligned} d(\Delta Q_x) &= p_x\, dy \\ &= (-\sigma_o \sin\beta + \tau_o \cos\beta)\, ds \\ &= -\sigma_o\, dy + \tau_o\, dx \end{aligned}$$

$$\begin{aligned} d(\Delta Q_y) &= p_y\, dx \\ &= (\sigma_o \cos\beta + \tau_o \sin\beta)\, ds \\ &= \sigma_o\, dx + \tau_o\, dy \end{aligned} \qquad (2203)$$

$$d(\Delta M_z) = y\, d(\Delta Q_x) - x\, d(\Delta Q_y)$$

Notice that for free surfaces (boundaries to free space) all functions with index 2 vanish, so that f.inst. $\Delta\sigma_n$ is identical to σ_n in the clay.

In practice (2201) is used for internal boundaries and free surfaces, where the stress distribution is important on both sides of (respectively along) the boundary. (2202) is used to calculate p_x and p_y from σ_o and τ_o if necessary, and (2203) is used in all cases where a rigid body exists on one or both sides of the boundary. Normally all boundary loadings are in this case taken in the first place as contributions to the total force components acting upon the rigid body. The equilibrium conditions for this body will then provide the necessary constraint upon the contact stresses σ_n and

τ_{nt} between the body and the clay.

The movement components satisfy the following equations:

$$u_x = u_t \cos\beta - u_n \sin\beta$$
$$u_y = u_t \sin\beta + u_n \cos\beta \tag{2204}$$

and

$$u_t = u_x \cos\beta + u_y \sin\beta$$
$$u_n = -u_x \sin\beta + u_y \cos\beta \tag{2205}$$

They are also valid for differences between the two sides of a boundary, but for kinematical reasons we must have:

$$-\Delta u_n = 0$$
$$-\Delta u_t = u_s \tag{2206}$$

so that

$$-\Delta u_x = u_s \cos\beta$$
$$-\Delta u_y = u_s \sin\beta \tag{2207}$$

For points of a rigid body we have:

$$u_x = w_x + y\, r_z$$
$$u_y = w_y - x\, r_z \tag{2208}$$

For clay material bounding to the rigid body this gives, when w_x, w_y, r_z, and u_s are assumed to be known:

$$u_x = w_x + y\, r_z - u_s \cos\beta$$
$$u_y = w_y - x\, r_z - u_s \sin\beta \tag{2209}$$

and

$$u_t = w_x \cos\beta + w_y \sin\beta + r_z\,(y \cos\beta - x \sin\beta) - u_s$$
$$u_n = -w_x \sin\beta + w_y \cos\beta - r_z\,(y \sin\beta + x \cos\beta) \tag{2210}$$

222 Boundary Parts and Load Resultants

The mathematical representation of the boundary parts can be obtained in different ways. For example, assuming each boundary part to consist of a number of circle arcs which are chosen sufficiently small, so that σ_o and τ_o can be taken to vary linearly with the arc length:

1. For any intermediate point No. i between the circle arcs, i.e. a discontinuity point for β, for the curvature $n_s = -\frac{d\beta}{ds}$ (or the radius of curvature $R_s = -\frac{ds}{d\beta}$), or for the surface load, beginning with the first end point of the boundary part ($s = 0$), one may indicate: the accumulated arc length s_i, the tangent angle β_i, and the curvature n_{si} (which may be zero) for the following circle arc (if any). Besides the values of σ_o and τ_o (and/or p_x and p_y) may be indicated just before and just after each point (i.e. the values for $s_i - 0$ and $s_i + 0$).
2. A more clear picture is obtained if the intermediate points are divided into geometrical discontinuities and load discontinuities. For the first mentioned ones the sets of s_i, β_i, n_{si} are given. The last mentioned ones are considered as a part of the information about the loads, so that a typical surface loading may be characterized by a set of the form s_1, σ_{o1}, τ_{o1}, s_2, σ_{o2}, τ_{o2}, or f.inst. x_1, p_{y1}, x_2, p_{y2} (cf. Ex. 21 a).
3. The above-mentioned scheme is reasonably simple and flexible, but it entails the measurement of arc lengths along sloped and possibly curved boundary parts. Alternatively the geometrical discontinuities may be indicated by the coordinates x_i, y_i to the intermediate points, together with n_{si}, R_{si}, or the half centre angle $\alpha_s = \frac{1}{2}(\beta_i - \beta_{i+1})$ for the circle arcs.

Which alternative to choose will depend on the particular properties of the given problem. Thus, the cases No. 1 and 2 are the simplest when there are only a few, mostly straight arcs in the boundary part. No. 1 is used when the load discontinuities are fixed and for the most part coincide with the geometrical discontinuities; No. 2 when the loads are moveable upon the surface. No. 3 is probably best for rather complex boundaries, f.inst. natural slopes in stability investigations.

In all cases it is easy to recalculate a boundary given in one repre-

sentation in terms of any other. Thus, for any given combination of values for the external parameters each boundary part can be assumed to consist of a number of circle arcs, each with a linear variation of σ_o and τ_o with the arc length.

Any such circle arc is defined completely by the chord length k_s, the angle ω_s between the positive x-direction and the chord (oriented in the positive direction of s), and the half centre angle α_s. One has, evidently, denominating the first end point of the arc by the subscript 1, and the second end point by 2 (taken in the positive direction of s):

$$\omega_s = \arctan \frac{y_2 - y_1}{x_2 - x_1} = \tfrac{1}{2}(\beta_2 + \beta_1) = \beta_1 - \alpha_s$$

$$\alpha_s = \tfrac{1}{2} s\, n_s = \tfrac{1}{2} \frac{s}{R_s} = \tfrac{1}{2}(\beta_1 - \beta_2)$$

$$k_s = s \frac{\sin \alpha_s}{\alpha_s} = \frac{2 \sin \alpha_s}{n_s} = 2 R_s \sin \alpha_s \qquad (2211)$$

$$= \sqrt{(x_2 - x_1)^2 + (y_2 - y_1)^2}$$

$$= (x_2 - x_1) \cos \omega_s + (y_2 - y_1) \sin \omega_s$$

s being the length of the circle arc.

The boundary loadings may be given by the components σ_{o1}, τ_{o1}, and σ_{o2}, τ_{o2} for the two end points. Defining:

$$\sigma_{om} = \tfrac{1}{2}(\sigma_{o2} + \sigma_{o1})$$

$$\Delta\sigma_o = \tfrac{1}{2}(\sigma_{o2} - \sigma_{o1}) \qquad (2212)$$

$$\tau_{om} = \tfrac{1}{2}(\tau_{o2} + \tau_{o1})$$

$$\Delta\tau_o = \tfrac{1}{2}(\tau_{o2} - \tau_{o1})$$

The loading components for a point t at the distance ts from the first end point ($0 \leq t \leq 1$) will be:

$$\sigma_{ot} = \sigma_{om} + (2t - 1)\,\Delta\sigma_o$$

$$\tau_{ot} = \tau_{om} + (2t - 1)\,\Delta\tau_o \qquad (2213)$$

The load resultants N_s, T_s, and M_s, referring to the middle point of the chord and positive as shown in Fig. 22C can easily be found by integration:

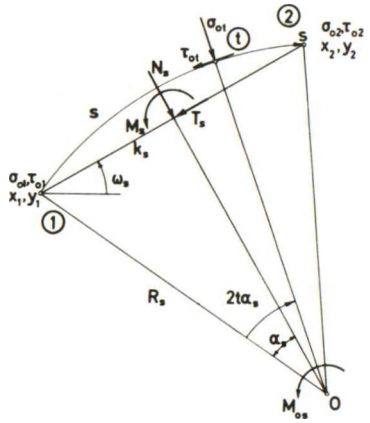

Fig. 22C: Circle Arc Element of Surface Curve. Components of Resultant Load.

$$N_s = k_s \frac{\alpha_s}{\sin \alpha_s} \int_0^1 [\sigma_{ot} \cos(2t - 1)\alpha_s - \tau_{ot} \sin(2t - 1)\alpha_s]\, dt$$

$$= k_s [\sigma_{om} - \frac{\Delta\tau_o}{\alpha_s}(1 - \alpha_s \cot \alpha_s)] \qquad (2214)$$

and

$$T_s = k_s \frac{\alpha_s}{\sin \alpha_s} \int_0^1 [\tau_{ot} \cos(2t - 1)\alpha_s + \sigma_{ot} \sin(2t - 1)\alpha_s]\, dt$$

$$= k_s [\tau_{om} + \frac{\Delta\sigma_o}{\alpha_s}(1 - \alpha_s \cot \alpha_s)] \qquad (2215)$$

M_s is found by means of the moment M_{os} about the centre of the circle arc:

$$M_{os} = k_s^2 \frac{\alpha_s}{2 \sin^2 \alpha_s} \int_0^1 \tau_{ot}\, dt = k_s^2 \frac{\tau_{om} \alpha_s}{2 \sin^2 \alpha_s}$$

so that:

$$M_s = \frac{k_s^2}{2 \sin^2 \alpha_s} [\tau_{om}(\alpha_s - \sin \alpha_s \cos \alpha_s) - \frac{\Delta\sigma_o}{\alpha_s} \sin \alpha_s \cos \alpha_s (1 - \alpha_s \cot \alpha_s)] \qquad (2216)$$

For a straight boundary element, i.e. in the limit for $\alpha_s \rightarrow 0$ (k_s being then equal to s), the equations (2214-6) reduce to:

$$N_s = k_s \sigma_{om}$$

$$T_s = k_s \tau_{om} \tag{2217}$$

$$M_s = -\frac{1}{6} k_s^2 \Delta \sigma_o$$

From the coordinates to the middle point of the chord:

$$x_m = \tfrac{1}{2}(x_2 + x_1) = x_1 + \tfrac{1}{2} k_s \cos\omega_s$$

$$y_m = \tfrac{1}{2}(y_2 + y_1) = y_1 + \tfrac{1}{2} k_s \sin\omega_s \tag{2218}$$

the contribution to the total load components Q_x, Q_y, and M_z are found to be:

$$\Delta Q_x = -N_s \sin\omega_s + T_s \cos\omega_s$$

$$\Delta Q_y = N_s \cos\omega_s + T_s \sin\omega_s \tag{2219}$$

$$\Delta M_z = M_s - x_m \Delta Q_y + y_m \Delta Q_x$$

In this way the resultant from a number of circle arcs, bounding f. inst. a rigid body of clay, can be summed. For a fraction of a circle arc, from point No. 1 to a point on the arc with a given value of t, the above equations (2214 - 9) can still be used, inserting:

$$\omega_t = \omega_s + (t - 1)\,\alpha_s$$

$$\alpha_t = t\,\alpha_s$$

$$k_t = k_s \frac{\sin\alpha_t}{\sin\alpha_s}$$

$$\Delta\sigma_{ot} = t\,\Delta\sigma_o$$

$$\sigma_{omt} = \sigma_{om} + (t - 1)\,\Delta\sigma_o \tag{2220}$$

$$\Delta\tau_{ot} = t\,\Delta\tau_o$$

$$\tau_{omt} = \tau_{om} + (t - 1)\,\Delta\tau_o$$

$$x_{mt} = x_1 + \tfrac{1}{2} k_t \cos \omega_t$$

$$y_{mt} = y_1 + \tfrac{1}{2} k_t \sin \omega_t$$

Thus, the total force components can be represented as continuous functions of the arc length s along the boundary part, calculating first the accumulated sums from s = 0 to all intermediate points (of any interest), and using afterwards (2220) and (2214-9) to interpolate between these values as necessary.

The total boundary load acting upon a rigid body of clay with a free boundary between $s = s_1$ and $s = s_2$ can then be determined by expressions of the form:

$$\begin{aligned} Q_x &= Q_x(s_2) - Q_x(s_1) \\ Q_y &= Q_y(s_2) - Q_y(s_1) \\ M_z &= M_z(s_2) - M_z(s_1) \end{aligned} \qquad (2221)$$

223 External Rigid Bodies

The movement conditions (physically given, or imaginary assumed for design purposes) for an external rigid body may be specified in several different ways, f.inst. as a fixed rotation point with or without a specified rotation, a hinge or one or more rod connections to other bodies etc. However, formally one can always construct all possible types by means of rod connections between one body and another. Each rod is assumed linear and hinged to both bodies, so that it can only take pure axial forces. It represents one movement condition, by specifying the rate of elongation (possibly zero) for the rod. In problems of controlled stress all rod elongations are zero.

Assume that there are $n_p + 1$ rigid bodies, one of which (No. 0, which may not be in contact with the clay) is the reference body with all movement components identically zero. The movement of each body is given by the three components w_x, w_y, and r_z in relation to the coordinate system, and all forces on the bodies are measured by the components Q_x, Q_y, and M_z.

When, for the sake of simplicity, the tensor notation is used the symbol w is used for all movement components, and Q for all force components. Thus, w_{pi} means movement component No. i ($1 \leq i \leq 3$) on rigid body No. p

($1 \leq p \leq n_p$). Product sums, such as $Q_{pi}\, w_{pi}$, are understood as sums of corresponding products for all components for all rigid bodies ($3n_p$ products).

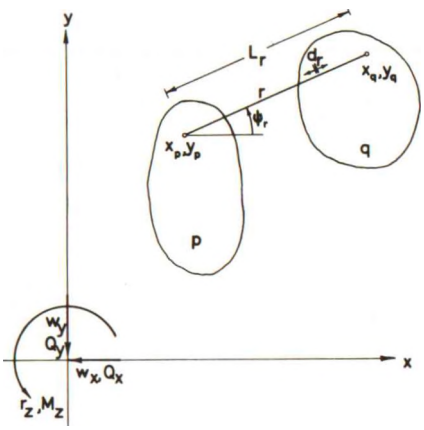

Fig. 22 D: Constraint by Rod Connection between External Rigid Bodies. Total Force and Movement Components.

Each *rod connection* (No. r) may be given by the coordinates (x_p, y_p) for the point of connection to the first rigid body, and (x_q, y_q) for the point of connection to the second rigid body in the pair. Alternatively the coordinates (x, y) to one point of the rod, and the angle ψ between the x-axis and the rod direction may be given (together with the numbers of the two bodies connected by the rod), cf. Fig. 22 D.

Using equation (2208) it is found that the projection of the velocity vector on the rod direction (positive in the negative rod direction) is:

$$u_r = u_x \cos\psi + u_y \sin\psi$$

$$= w_x \cos\psi + w_y \sin\psi + r_z (y \cos\psi - x \sin\psi); \qquad (2222)$$

it is seen to be immaterial which point on the rod is chosen.

When the elongation rate of the rod is specified to be d (possibly zero), we therefore have an equation of the form:

$$u_{rp} - u_{rq} = d_r \qquad (2223)$$

valid for rod No. r between body No. p and body No. q. In tensor notation:

$$w_{pi}\, a_{pir} = d_r \qquad (2224)$$

In this equation, which has the number r, a_{pir} is zero for all values of p corresponding to bodies not connected by the rod in question. For the two bodies p and q connected by the rod we have:

$$a_{p1r} = -a_{q1r} = \cos\psi_r$$

$$a_{p2r} = -a_{q2r} = \sin\psi_r \qquad (2225)$$

$$a_{p3r} = -a_{q3r} = y_p \cos \psi_r - x_p \sin \psi_r$$

where

$$\psi_r = \text{arc tan} \frac{y_q - y_p}{x_q - x_p} \tag{2226}$$

to be used when two points are given.

It is seen to be immaterial which points are chosen on the rod. If simpler calculations are obtained in this way, they may not be physical points on the bodies they are taken to connect.

To each rod, f.inst. No. r corresponds an initially unknown rod force P_r, positive as compression. One of the purposes of the calculation of the state of failure in the soil will usually be to determine the values of P_r, at least for the active constraints ($d_r \neq 0$).

The condition of a given (relative, and possibly zero) rotation of the rigid body can also be realized by means of rods, but it will usually be simpler to express this directly, i.e. by means of a row with

$$\begin{aligned} a_{p1r} &= a_{q1r} = a_{p2r} = a_{q2r} = 0 \\ a_{p3r} &= -a_{q3r} = -1 \end{aligned} \tag{2227}$$

In this case d_r and P_r will not have the same meaning as for the rods. d_r is now identical to the specified relative rotation:

$$d_r = r_{zq} - r_{zp} \tag{2228}$$

and P_r is identical to the (free) moment M_z acting between the two bodies in order to produce the specified rotation:

$$P_r = M_{zq} = -M_{zp} \tag{2229}$$

By means of the above elements all possible types of restraints can easily by obtained. For example:

1. If two bodies are bound to translate relative to each other (2227-9) are used with $d_r = 0$.
2. If the direction of relative translation is also known a rod (with $d_r = 0$) may further be introduced perpendicular to this direction. Alternatively the condition may be obtained by means of two parallel rods perpendicular to the direction. The position of the rod, or rods, is if possible chosen so that P_r has a direct physical signi-

ficance (reactions in the structural elements that impose the given constraint).

3. If further the rate of translation is known, a further rod (with $d_r \neq 0$) must be added. It cannot be perpendicular to the direction, but may if convenient form any other angle with it.

4. A hinge is represented by two rods ($d_r = 0$), intersecting each other in the hinge point, and with the directions corresponding to the required components of the reaction in the hinge. If the relative rotation in the hinge is known (2227-9) must again be used.

For connections to the completely fixed body (No. 0) the values a_{oir} are not taken into regard, because w_{oi} by definition is zero. Each equation (2224) or (2227) will therefore have $3n_p$ terms on the left hand side, only 3 or 6 of which are different from zero.

It is assumed that the movement conditions contain no superfluous or contradictory restraints. The resulting $3n_p$ by n_r coefficient matrix $[a_{pir}]$, where n_r is the total number of conditions ($0 \leq n_r \leq 3n_p$) is therefore assumed to have the rank n_r. There will then be $n_f = 3n_p - n_r$ equilibrium conditions for the system of rigid bodies to be satisfied by the stresses between the clay and the boundary surfaces, and n_r unknown rod forces (restraint components) to be found by the remaining n_r equilibrium conditions.

It is frequently convenient to solve partially the n_r equations (2224) to obtain the $3n_p$ movement components in the form:

$$w_{pi} = w^o_{pi} + v_f b_{pif} \tag{2230}$$

i.e. as a constant term plus a linear expression containing n_f free parameters v_f. The values of v_f are found during the solution of the failure problem so that the corresponding n_f equilibrium conditions are satisfied.

Using the restraint forces P_r the equilibrium equations can be written:

$$Q^p_{pi} = Q^e_{pi} - Q^{pc}_{pi} + P_r a_{pir} = 0 \tag{2231}$$

valid for all $3n_p$ combinations of the indices p and i. The superscripts e and pc indicate the resultant of the external forces acting upon the rigid body, and the resultant of the forces transmitted to the clay in contact with the body, respectively. Q^{pc}_{pi} is a force acting upon the clay; its reaction upon the rigid body is therefore taken with a negative sign. The summation in the last term is formally extended over all n_r restraints, but a_{pir} is zero for all bodies p which are not concerned by the restraint No. r.

From elementary matrix calculation it is known that when the n_r linearly independent rows a_{pir} are given we can find n_f linearly independent rows b_{pif}, each of which is orthogonal to all rows a_{pir}, i.e.

$$b_{pif}\, a_{pir} = 0 \tag{2232}$$

valid for all combinations of f and r. If each of the $3n_p$ equations (2231) is multiplied with the corresponding value b_{pif} for one value of f, and all equations are summed, we get for this value of f:

$$(Q^e_{pi} - Q^{pc}_{pi})\, b_{pif} + P_r\, a_{pir}\, b_{pif} = (Q^e_{pi} - Q^{pc}_{pi})\, b_{pif} = 0 \tag{2233}$$

by virtue of (2232). This can be done for all values of f. In this way the n_f remaining equilibrium equations are obtained.

It is further seen from (2232) that the movement components $w_{pi} = b_{pif}$ will be solutions to the homogeneous system of equations

$$w_{pi}\, a_{pir} = 0 \tag{2234}$$

They can therefore be used as elements of the general solution to (2224) in the way shown in (2230).

We can also define n_r rows c_{pin} with the property that for all combinations of r and n we have:

$$c_{pin}\, a_{pir} = \delta_{nr} \tag{2235}$$

δ_{nr} is here Kronecker's delta, which is equal to 1 when the two indices are equal, and zero otherwise. Multiplying each of the equations (2231) with the corresponding value c_{pin} for one value of n, and summing, we obtain:

$$(Q^e_{pi} - Q^{pc}_{pi})\, c_{pin} + P_r\, a_{pir}\, c_{pin} = (Q^e_{pi} - Q^{pc}_{pi})\, c_{pin} + P_n = 0 \tag{2236}$$

This can be done for all values of n, in which way the equations for the n_r restraint forces are obtained.

It is further seen that the row

$$w^o_{pi} = c_{pin}\, d_n \tag{2237}$$

is a solution to (2224), because:

$$c_{pin}\, d_n\, a_{pir} = d_n\, \delta_{nr} = d_r \tag{2238}$$

From (2237) we can therefore determine a constant term to be used as shown in (2230). Notice that to any row c_{pin} we may add any linear com-

bination of the rows b_{pif}. Correspondingly, to the solution w^o_{pi} found by (2237) may be added a term $v_f\, b_{pif}$ corresponding to any set of parameters v_f. This may be used in practice to choose the most likely basic movement w^o_{pi}.

Example 22a

In a great number of problems in practice there will be only one clay domain and one external rigid body. The boundary to this body is continued by one free surface in f.inst. earth pressure and one-sided bearing capacity problems. In two-sided problems, i.e. bearing capacities and/or both active and passive earth pressure on the same structure, the surface to the other side of the body will also have an influence. All boundary parts can usually be described by chains of linear parts.

The problems can frequently be considered as problems in controlled strain, and the movement restraints can in all cases be composed of at most 3 rods, or of at most 2 rods together with a known value of the rotation r_z.

A realistic diagram for the recording of the parameters of such problems is shown in Fig. 22 E. It may f.inst. be used as a standard input diagram for computer programs treating such problems. It contains the following items.

1. The job No. and the text called Problem Identification are supposed to be copied by the output procedures of the program for the identification of results.

2. The data of the problem are divided into 7 groups. For the specification of a problem at least one number in each group must be given. If the original data set is stored in the computer they can later be changed by a reading of only some of the groups.

   In this respect the groups are independent, except that:

   a. If Group 1 is appreciably changed one has in fact a completely new problem topology. In this case all other groups should be read in anew.

   b. If the number of restraints is changed in Group 6, the movements in Group 7 should be read in anew.

3. The reading of Group 1 starts a new parameter set. This set is characterized by a number, the remaining data in this group indicating the topology of the problem, and the necessary space for the

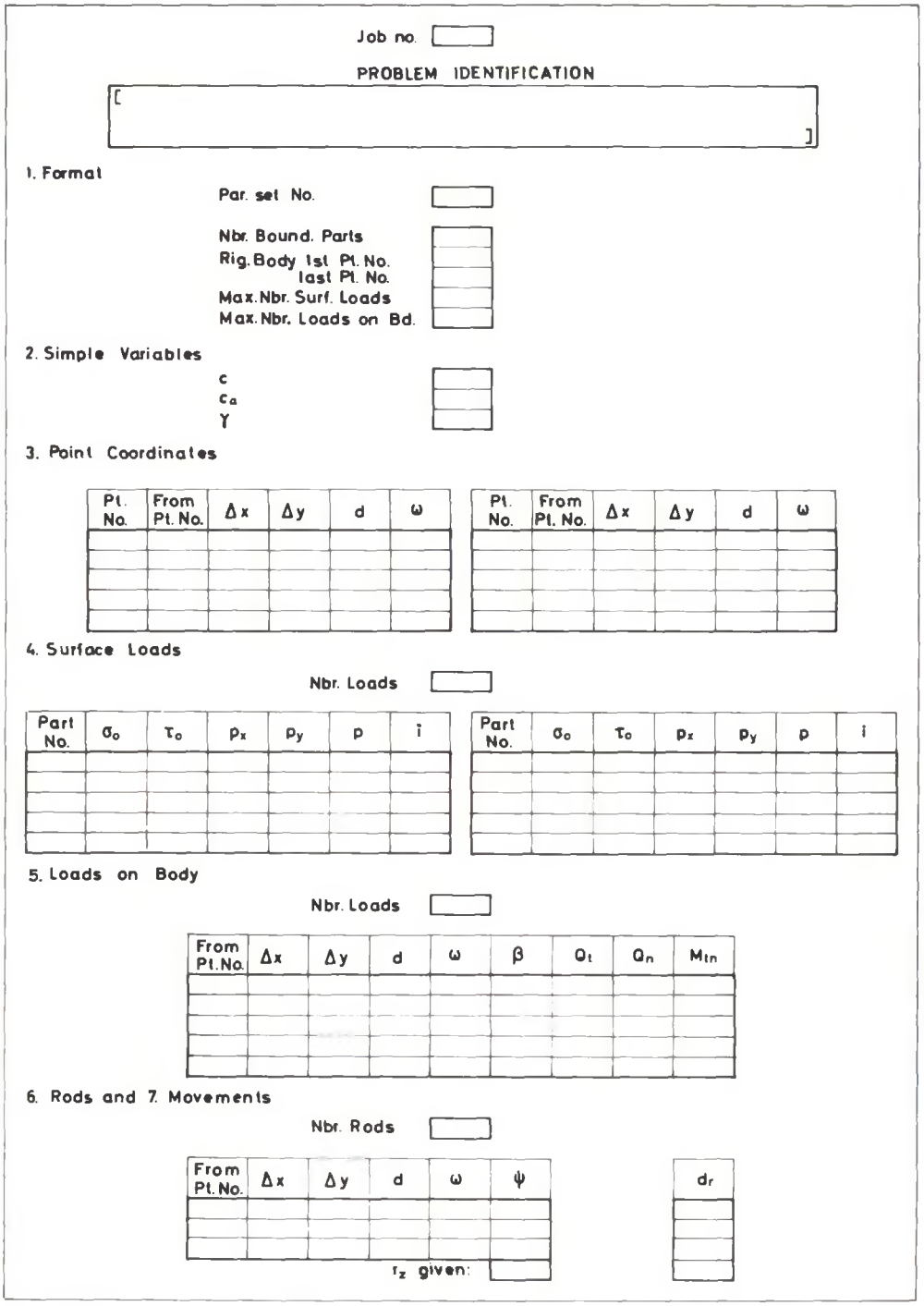

Fig. 22E: Input Diagram for Simple Problems in Controlled Strain.

storage of the parameters. All points are assumed to be given successive numbers in the positive direction of the boundary (starting with Point No. 0). The linear boundary parts have the same numbers as their end points in the positive direction (cf. Fig. 22 F).

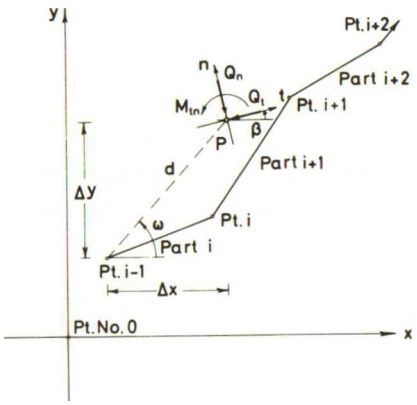

Fig. 22 F: Specification of Points and Line Loads.

4. The simple variables of Group 2 are self-explanatory. In Group 3 it is supposed that the points are indicated in a logical order so that the coordinates of each point can be calculated from information stored in the computer at the point of its reading. Point 0 has the coordinates 0, 0, and the coordinates to all other points can be indicated relative to this point or to any other point (already stored), the coordinate differences being given either directly or by their polar coordinates (direction and distance). Obviously, the input conventions must be made to show which alternative is used in each case (f. inst. by means of the terminator symbol used after the point No., or after the input numbers).

5. Correspondingly, the surface loads indicated in Group 4 may be given in 3 alternative ways (p and i are the load resultant and its inclination angle with the surface normal, respectively). They are supposed to be constant along the indicated surface parts, loads acting on parts covered by the rigid body being transmitted to this body, but it is also perfectly possible to devise an input convention that calls for 4 numbers for each part, giving a linearly distributed load. For subsequent corrections of the parameter set it is also necessary to indicate in some way whether the loads read in should be added to, or should replace the loads stored in the computer for the surface parts in question.

6. The loads on the rigid body in Group 5 (apart from the distributed loads indicated in Group 4) are given by their point of application (relative to any known point), the direction angle β to a local coordinate system, and the components relative to this system (cf. Fig. 22 F). In this way f. inst. normal and tangential forces acting at

certain heights on inclined walls may be given in a reasonably simple way. For corrections of existing parameter sets it is also here necessary to specify by a special convention exactly how the input data are to be understood.

7. The rods (if any) are specified by a point (indicated as above), and their direction angle ψ. In this Group No. 6 it is also indicated whether r_z is specified or not (1 or 0 in the corresponding place). The movements in Group 7 are given in the same order as the restraints, at least one movement being different from zero.

It is seen that the diagram of Fig. 22 E permits a rather flexible specification of a problem of the considered kind. In actual use it presupposes a program that is able to find solutions by means of one, or possibly several alternative rupture figures, or, possibly, is able to develop or choose itself a rupture figure that gives a solution within some specified standard of accuracy. What further input to give, specifying the rupture figure, the class of rupture figures, and/or the accuracy, will of course depend on the detailed needs and conventions of the program.

By the use of more advanced input conventions (f. inst. still based on the terminator symbols to the input numbers) the use of the diagram may be extended to cover also simple design problems, and, when two or more diagrams are used collectively, problems in controlled stress and/or problems with several rigid bodies and/or clay domains. In fact, a system may be devised so that all problems within the scope of the present work can be specified completely, using in all cases the diagram of Fig. 22 E as a standard input scheme.

23 FUNDAMENTAL CONDITIONS

231 Equilibrium Conditions

The state of stress may be represented by the stress components σ_x, σ_y, and τ_{xy} at any point in relation to the coordinate system, cf. Fig. 23 A.

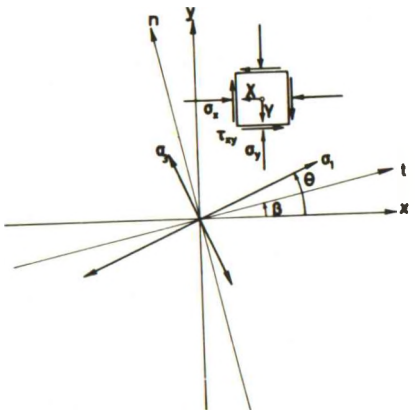

Fig. 23 A: Coordinate Systems. Stress Components and Volume Forces.

The *normal stresses*, σ_x and σ_y, acting on planes orthogonal to the coordinate axes indicated by the indices, are positive as compressions. The shear stress τ_{xy}, acting on the same planes, is positive when it tends to increase the right angle between the positive directions of the coordinate axes.

The stress components related to any other coordinate system f. inst. the local system of coordinates t, n for surface points, cf. Fig. 22 B, are evidently the stresses acting on another set of orthogonal planes through the same point. They may be found by means of Mohr's circle for stresses, cf. Fig. 23 B. From the given components the pole P can be constructed. The *normal stress* σ_n and the *shear stress* τ_{nt} corresponding to any section t may then be found as the coordinates (σ, τ) to the point of intersection between the circle and a line through P parallel to t.

If the angle between the positive directions of the x-axis and the t-axis is β we get:

$$\sigma_n = \sigma_x \sin^2 \beta + \sigma_y \cos^2 \beta - \tau_{xy} \sin 2\beta$$

$$\sigma_t = \sigma_x \cos^2 \beta + \sigma_y \sin^2 \beta + \tau_{xy} \sin 2\beta \qquad (2301)$$

$$\tau_{nt} = \tau_{xy} \cos 2\beta + \tfrac{1}{2} (\sigma_y - \sigma_x) \sin 2\beta$$

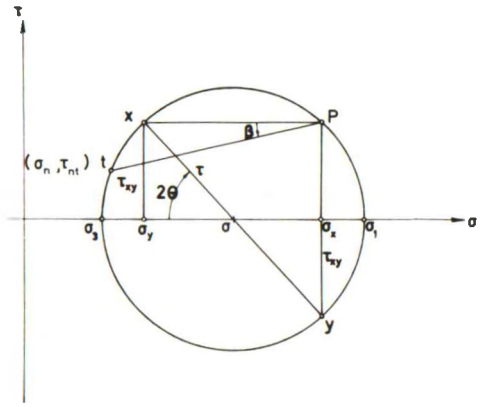

Fig. 23 B: Mohr Circle for Stresses.

Alternatively, if the mean normal stress σ, the maximum shear stress τ, and the angle θ between the x-axis and the major principal stress direction are known:

$$\sigma = \tfrac{1}{2}(\sigma_1 + \sigma_3) = \tfrac{1}{2}(\sigma_x + \sigma_y)$$

$$\tau = \tfrac{1}{2}(\sigma_1 - \sigma_3) = \sqrt{\tfrac{1}{4}(\sigma_x - \sigma_y)^2 + \tau_{xy}^2} \qquad (2302)$$

$$\tan 2\theta = \frac{2\tau_{xy}}{\sigma_x - \sigma_y}$$

all other stress components can be found by inserting the actual value of θ in the formulae:

$$\sigma_x = \sigma + \tau \cos 2\theta$$

$$\sigma_y = \sigma - \tau \cos 2\theta \qquad (2303)$$

$$\tau_{xy} = \tau \sin 2\theta$$

Notice that θ is in all cases measured from the (local) x-axis to the σ_1-direction, positive in the positive direction of rotations for the coordinate system in question.

If the volume force is expressed by the components X and Y, positive in the negative directions of the coordinate axes (cf. Fig. 23 A), the equilibrium equations are:

$$\frac{\partial \sigma_x}{\partial x} + \frac{\partial \tau_{xy}}{\partial y} + X = 0$$

$$\frac{\partial \sigma_y}{\partial y} + \frac{\partial \tau_{xy}}{\partial x} + Y = 0 \qquad (2304)$$

When the volume forces constitute a gradient vector field to a piecewise continuous function K, we may write:

$$X = \frac{\partial K}{\partial x}$$

$$Y = \frac{\partial K}{\partial y} \qquad (2305)$$

This is true if the following condition is satisfied:

$$\frac{\partial X}{\partial y} = \frac{\partial Y}{\partial x} \left(= \frac{\partial^2 K}{\partial x \partial y} \right) \tag{2306}$$

Then the equilibrium equations (2304) may be simplified by writing:

$$\begin{aligned} \frac{\partial (\sigma_x + K)}{\partial x} + \frac{\partial \tau_{xy}}{\partial y} &= 0 \\ \frac{\partial (\sigma_y + K)}{\partial y} + \frac{\partial \tau_{xy}}{\partial x} &= 0 \end{aligned} \tag{2307}$$

We see that if the local value of K is added to the normal stresses at any point, the resulting stress distribution must satisfy the equilibrium equations for zero volume forces. Therefore the following correction can be made to simplify the stress calculations.

From the known volume forces the function K can be calculated, except for an arbitrary additive constant, which can be chosen as will be most convenient. An additional normal loading $\sigma_o = K$ is then introduced on all free surfaces and boundaries to rigid bodies.

For internal boundaries separating different clay layers, K need not be the same on the two sides. A normal boundary loading σ_o must then be added, which is equal to the difference between the two K-values, and acts in the direction of the largest value of K.

As it is seen later, this correction does not affect the failure condition. Therefore the true rupture figure will be found, and also the true stress distribution, except that K must be subtracted from all normal stresses to obtain those corresponding to the original boundary loadings, and the original volume forces.

In the following the symbol K is suppressed in (2307). When no volume forces are indicated in the equilibrium equations, it is assumed either that they are zero (or can be neglected), or that the above mentioned correction has been performed.

232 The Failure Condition

An ideal plastic-rigid clay is in a state of failure when the maximum shear stress τ, equal to the radius in Mohr's circle for stresses, attains the value c, equal to the shear strength:

$$\tau = c \tag{2308}$$

This value can never be exceeded. If the equality (2308) is satisfied, plastic deformations of an arbitrary magnitude are possible, without affecting the value of c. For τ smaller than c the material is rigid, i.e. no deformations are possible.

If the material is known to be in failure, the stress distribution is therefore determined by σ and θ only. We get from (2303)

$$\begin{aligned} \sigma_x &= \sigma + c \cos 2\theta \\ \sigma_y &= \sigma - c \cos 2\theta \\ \tau_{xy} &= c \sin 2\theta \end{aligned} \tag{2309}$$

For rupture zones with sufficient boundary conditions for stresses, the two unknown quantities σ and θ can be determined uniquely by the two equilibrium equations (2307). This is the case of statically determined rupture figures.

Example 23 a

In some cases it is possible to obtain a solution directly from the basic equations (2302), (2304), and (2308), by a semiinverse method. Consider f.inst. the problem shown in Fig. 23 C, where a sloping clay layer on rock is acted upon by the normal surface loading σ_o, and the tangential stress τ_o (positive downslope).

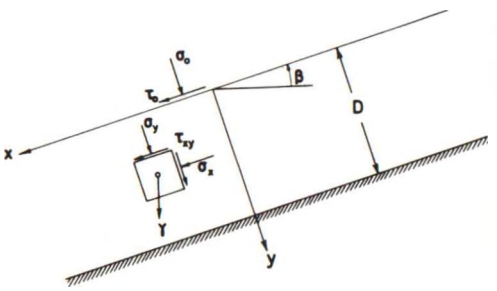

Fig. 23 C: Sloping Clay Layer on Rock.

If the slope is assumed infinitely long, we may assume that the same state of stress exists in all points along every line parallel to the clay surface. With the coordinate system shown in the figure we must therefore have zero derivatives with respect to x. We have also:

$$X = -\gamma \sin\beta, \quad Y = -\gamma \cos\beta \tag{2310}$$

so that we get from (2304) and the boundary conditions for the surface (at y = 0):

$$\tau_{xy} = \tau_o + \gamma\, y \sin\beta$$

$$\sigma_y = \sigma_o + \gamma\, y \cos\beta \qquad (2311)$$

σ_x can be found by means of (2302) and (2308):

$$\sigma_x = \sigma_y \pm 2\sqrt{c^2 - \tau_{xy}^2} \qquad (2312)$$

assuming that the whole clay layer is in a state of failure.

In the laboratory this state of stress can be realized if the rigid bottom is provided with a hinge in which a relative movement is produced, either decreasing or increasing the angle ($= \pi$) through the clay.

In the first mentioned case the upper sign in (2312) is valid, whereas the lower sign must be used for the second case. However, it is seen that the condition:

$$\tau_{xy}\ (y = D) = \tau_o + \gamma\, D \sin\beta \leq c \qquad (2313)$$

must be satisfied, in order that the slope shall not become unstable.

For a horizontal surface ($\beta = 0$) with no shear stress ($\tau_o = 0$) we have $\tau_{xy} = 0$ and $\sigma_y = \gamma y$. σ_x is $\gamma y \pm 2c$, and D may be infinite. This is the simple solution corresponding to Rankine's solution for sand.

233 The Stress Characteristics

Usually a numerical calculation method must be used. The necessary equations for this can be obtained by inserting (2309) in (2307). We get:

$$\frac{\partial \sigma}{\partial x} - 2c \sin 2\theta \frac{\partial \theta}{\partial x} + 2c \cos 2\theta \frac{\partial \theta}{\partial y} = 0 \qquad (2314a)$$

$$\frac{\partial \sigma}{\partial y} + 2c \cos 2\theta \frac{\partial \theta}{\partial x} + 2c \sin 2\theta \frac{\partial \theta}{\partial y} = 0 \qquad (2314b)$$

These equations might be used in the following way. Assume that a curve is given in the x, y plane (Fig. 23 D), and that σ and θ, regarded as scalar functions of x and y, are known along this curve.

The variation of σ and θ between two consecutive points A and B on the curve must satisfy the identities:

$$\cos\psi \frac{\partial \sigma}{\partial x} + \sin\psi \frac{\partial \sigma}{\partial y} = \frac{\delta \sigma}{\delta s} \qquad (2314c)$$

$$\cos\psi \frac{\partial \theta}{\partial x} + \sin\psi \frac{\partial \theta}{\partial y} = \frac{\delta \theta}{\delta s} \qquad (2314d)$$

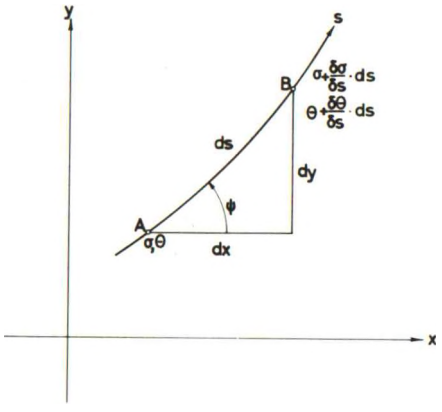

Fig. 23 D: Curve with a Known Variation of σ and θ in a Domain in Failure.

where $\cos\psi = \frac{\delta x}{\delta s}$ and $\sin\psi = \frac{\delta y}{\delta s}$. s is the arc length along the curve, and ψ is the tangent angle.

The four equations (2314a-d) determine the four unknown quantities $\frac{\partial\sigma}{\partial x}$, $\frac{\partial\sigma}{\partial y}$, $\frac{\partial\theta}{\partial x}$, and $\frac{\partial\theta}{\partial y}$, so that σ and θ can be found, possibly by numerical integration, in the vicinity of all ordinary curves of this kind. This process can be repeated for another curve, drawn inside the domain where σ and θ are known. In this way the two functions can be determined in a certain neighbourhood of the original curve.

However, this process breaks down if the curve is so chosen that by inserting ψ in the equations (2314) a vanishing determinant is obtained. If such curves are possible, the derivatives cannot be determined from known variations along the curves. These curves may therefore be discontinuity lines for the derivatives of σ and θ.

On the other hand, if the determinant of coefficients is zero, the rank of the augmented coefficient matrix, including the column on the right hand side of the equation signs, must be three, in order that the equations shall not be contradictory. Therefore, for such curves a relationship must exist between $\frac{\delta\sigma}{\delta s}$ and $\frac{\delta\theta}{\delta s}$.

Curves with these properties are called characteristics. In a certain sense they form the structure of the stress field, because it is along the characteristics that disturbancies are transmitted. Therefore, numerical calculations of the stress distributions are usually based on the system of stress characteristics.

The condition of a vanishing determinant of coefficients in (2314) can easily be reduced to:

$$\sin^2\psi\cos 2\theta - 2\sin\psi\cos\psi\sin 2\theta - \cos^2\psi\cos 2\theta = 0 \qquad (2315)$$

This is a second degree equation in $\tan\psi$ which has the real roots:

$$\tan\psi = \tan 2\theta \pm \sec 2\theta = \begin{cases} \tan\left(\theta + \frac{\pi}{4}\right) = \tan m \\ \tan\left(\theta + \frac{3\pi}{4}\right) = \tan\left(m + \frac{\pi}{2}\right) \end{cases} \qquad (2316)$$

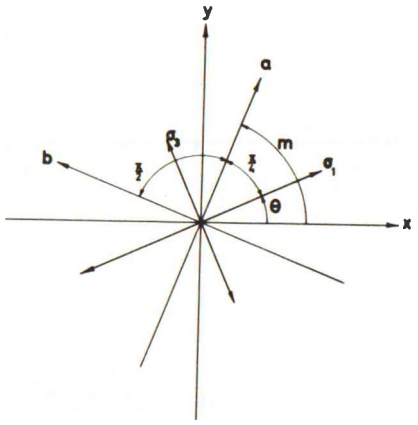

Fig. 23 E: Characteristic Directions Through a Point in a Failure Zone.

The angle $\theta + \frac{\pi}{4}$ is called m. It follows that there are two characteristic directions through each point where the clay is in failure, bisecting the right angles between the two principal stress directions. As shown in Fig. 23 E these directions are called a and b, respectively. They are defined so that the angular direction ab is positive (i.e. in the same direction as xy), and so that the minor principal stress direction bisects the first and third quadrant in the a,b coordinate system. The trajectory curves, whose tangents in each point are the a- and b-directions, respectively, are called the a- and b-lines.

The relation between σ and θ along the characteristic curves can be found f.inst. by replacing the fourth column of the coefficient matrix by the column of constant terms. Equating the resulting determinant to zero we get:

$$\cos\psi \frac{\delta\sigma}{\delta s} - 2c \sin(2\theta - \psi) \frac{\delta\theta}{\delta s} = 0 \qquad (2317)$$

The arc lengths along the a- and b-lines are called s_a and s_b, respectively. Inserting the values of ψ from (2316), and observing that $\frac{\delta\theta}{\delta s} = \frac{\delta m}{\delta s}$, we obtain:

$$\begin{aligned} \frac{\delta\sigma}{\delta s_a} + 2c \frac{\delta m}{\delta s_a} &= 0 \\ \frac{\delta\sigma}{\delta s_b} - 2c \frac{\delta m}{\delta s_b} &= 0 \end{aligned} \qquad (2318)$$

cf. Kötter [1903] and Hencky [1923].

When the characteristic lines are used, it may be preferable to take σ and m as the stress functions instead of σ and θ. (2309) must then be replaced by:

$$\begin{aligned} \sigma_x &= \sigma + c \sin 2m \\ \sigma_y &= \sigma - c \sin 2m \\ \tau_{xy} &= -c \cos 2m \end{aligned} \qquad (2319)$$

By inserting m = 0 in the above equations it is seen that $\sigma_a = \sigma_b = \sigma$, and $\tau_{ab} = -c$ (the right angle between the positive a- and b-directions is decreased by the plastic deformations).

It may be noticed that equations (2318) and (2319) are unchanged if both characteristic lines are oriented in the opposite directions. Furthermore, one may formally regard the difference between the two equations (2318) as a difference in the sign of c. This leads to the following observations.

1. If, from the same boundary conditions for stresses, two different stress distributions are calculated, one with positive and the other with negative signs for c throughout (it is seen later that the direction of boundary movements must then also be reversed), we obtain, using the same formulae and the same calculation procedure, the two complementary solutions to the same failure problem. This may be an advantage for some classes of problems (f. inst. earth pressures), in that only one calculation scheme has to be devised, although the two solutions are formally quite different. F. inst. the a- and b-directions in one solution may correspond to the b- and the negative a-direction, respectively, in the other.

2. If only one characteristic curve, or a series of such curves, is considered, f. inst. as the boundaries to a rigid body of clay, it may be an advantage to consider only the upper formula (2318), defining c to be positive when the curve is an a-line, and negative when it is a b-line. Here again the same formulae for stress resultants etc. can be used for both kinds of curves.

From equations (2319), and from Mohr's circle for stresses at failure (Fig. 23 F) it is seen that the directions a and b are those for which the failure condition in Coulomb's notation:

$$|\tau_{ab}| = \tau_{max} = c \qquad (2320)$$

is satisfied. They are therefore also called the slip line directions, from the point of view that they represent the most critically stressed sections, and that slips must therefore take place in these directions.

Strictly speaking this is not quite correct, because the most critically stressed sections should be those forming the angles $\pm (\frac{\pi}{4} - \varphi_r/2)$ with the major principal stress direction, where φ_r is Hvorslev's angle of internal friction (corresponding to constant volume). However, the a- and b-directions are stress characteristics, and, as shown later, they are also strain

characteristics, so slips do take place in these directions. For brevity they will therefore be called slip lines in the following.

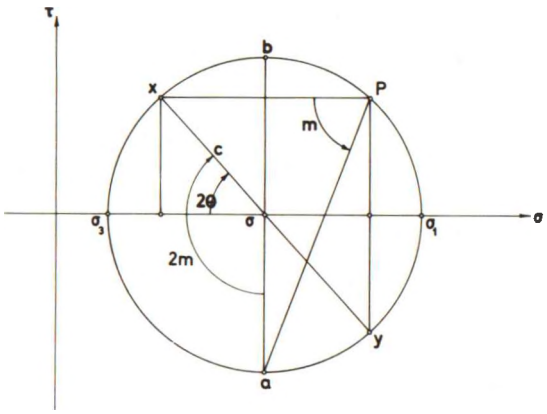

Fig. 23 F: Mohr Circle for Stresses for a Point in a Failure Zone.

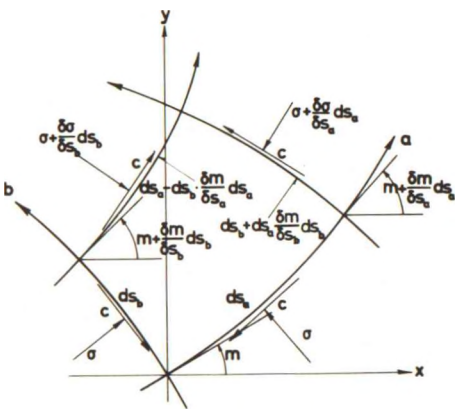

Fig. 23 G: Small Element in a Failure Zone Cut Out Between Consecutive Slip Lines.

Equations (2318) can also be deduced by a purely physical reasoning. If the equilibrium of a small soil element, cut out between consecutive slip lines (Fig. 23 G) is considered, it is used that the shear stresses are known along all four sides. Assuming that the increments Δm in m along the sides are small to the first order, we can put $\sin \Delta m \simeq \tan \Delta m \simeq \Delta m$, and $\cos \Delta m \simeq 1$. Retaining only quantities small to the second order in ds_a and ds_b, the equations (2318) are obtained by the projection of all forces to the a- and b-directions, respectively.

Example 23 b

The slip line field for the problem considered in example 23 a can be constructed when it is observed that according to (2311) and (2319) we must have:

$$\tau_o + \gamma y \sin\beta = -c \cos 2m \tag{2321}$$

or: $$dy = \frac{c}{\gamma \sin\beta} \; 2 \sin 2m \, dm \tag{2322}$$

For the a-lines we must have:

$$dx_a = dy \cot m = \frac{c}{\gamma \sin\beta} \; 4 \cos^2 m \, dm \tag{2323}$$

By integration we find:

$$\frac{\gamma \sin\beta}{c} x_a = A + 2m + \sin 2m \tag{2324}$$

where A is an arbitrary constant.

Correspondingly for the b-lines where $dx_b = -dy \tan m$ we have:

$$\frac{\gamma \sin\beta}{c} x_b = B - 2m + \sin 2m \tag{2325}$$

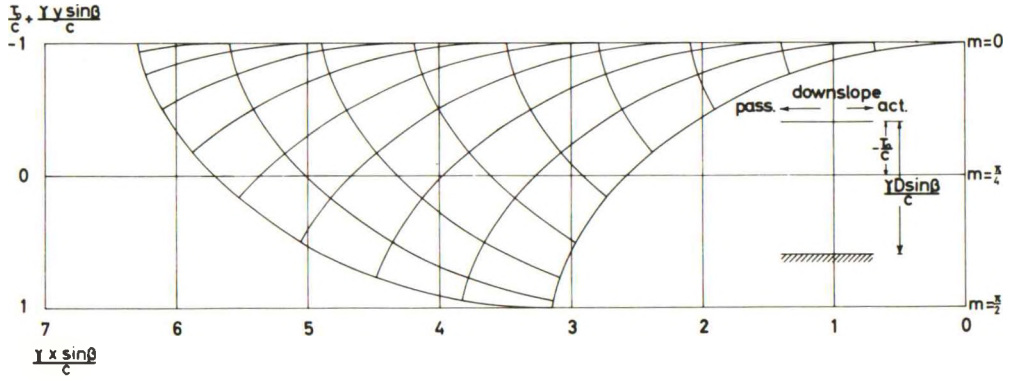

Fig. 23 H: Slip Line Field for a Sloping Clay Layer on Rock.

Using m as a parameter, the slip line field shown in Fig. 23 H can be drawn. It is seen from equations (2321), (2324), and (2325) that all slip lines are cycloidal arcs. The figure represents the solution for all combinations of the parameters τ_o, β, γ, c, and D. It can be used for any particular para-

meter set as sketched in the figure.

τ_o is positive when acting down the slope. To any given value of τ_o corresponds a position of the clay surface in Fig. 23 H (found by equating y to zero in (2321)). The rock surface will be at the distance $\frac{\gamma D \sin\beta}{c}$ below this level. As equation (2321) is unaltered when the signs are changed for τ_o, β, and c, simultaneously, it is seen that the figure can be used (formally with τ_o positive downslope, and c always positive) both for the passive and for the active case (major principal stress mostly parallel to or orthogonal to the horizon). In the first mentioned case (corresponding to the plus sign in (2312)) the surface slopes down for increasing values of x, in the other case for decreasing values of x.

If the clay surface is horizontal ($\beta = 0$) the part of the rupture figure to be used in Fig. 23 H degenerates to a point, i.e. the scale must be increased infinitely for any actual problem. This means that in the actual rupture figure the slip lines will be straight, with a constant value of m, given by (2321) throughout.

From (2311) and (2319) we have

$$\sigma = \sigma_o + c \sin 2m + \gamma y \cos\beta \tag{2326}$$

However, according to the correction introduced in (2307) the rupture figure may also be interpreted as resulting from no volume force in the clay, a constant shear stress τ_o on the clay surface, and a normal stress

$$\sigma'_o = \sigma_o + \gamma z = \sigma_o - \gamma x \sin\beta \tag{2327}$$

on the surface. In this equation z is the height above the origo of the coordinate system. Thus, in the general case, where the normal stress on the surface is given on the form:

$$\sigma'_o = a - bx \tag{2328}$$

we must insert in the above formulae:

$$\sigma_o = a$$

and (2329)

$$\frac{\gamma \sin\beta}{c} = \frac{b}{c}$$

This defines m by means of (2321):

$$-\cos 2m = \frac{\tau_o}{c} + \frac{by}{c} \tag{2330}$$

but in this case σ will be equal to the value from (2326) plus K, which is

equal to

$$K = \gamma z = -\gamma x \sin\beta - \gamma y \cos\beta \qquad (2331)$$

so that

$$\sigma = a - bx + c \sin 2m \qquad (2332)$$

according to (2329).

Notice that the same rupture figure can be obtained for several combinations of surface stresses and volume forces, the only condition being that the shear stress τ_o must be a constant, and the resulting normal stress $\sigma_o + K$ on the surface must be a linear function of x as in (2328).

234 Deformation Conditions

The magnitudes of the plastic deformations are not defined by the stresses alone. They must, however, satisfy the conditions of constant volume, and of coinciding principal stress and strain directions.

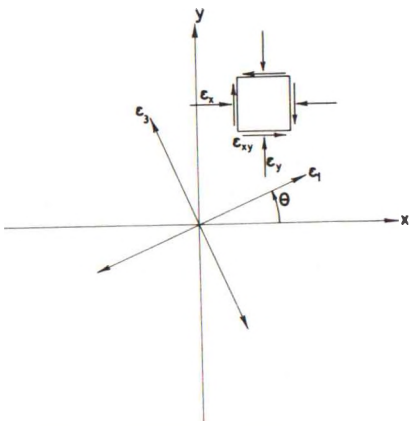

Fig. 23 I: Strain Components and Principal Strain Directions.

Defining the stress components as shown in Fig. 23 I, ϵ_x and ϵ_y are relative deformations of lines in the x- and y-directions, respectively, positive as shortenings. ϵ_{xy} is half the angular distortion of the right angle between the positive x- and y-directions, positive as an increase. The angle θ between the x-axis and the major principal strain directions ϵ_1, is equal to the corresponding angle θ in Fig. 23 A.

From Mohr's circle for deformations (Fig. 23 J) it is seen that the condition of zero volume change implies that the mean plastic strain is zero, i.e. the centre of the circle is known. This means that there are only two unknown quantities determining the state of strains: The radius ϵ of the circle, equal to the maximum shear strain and the angle θ. θ is known when the stress distribution is found, so only ϵ remains unknown.

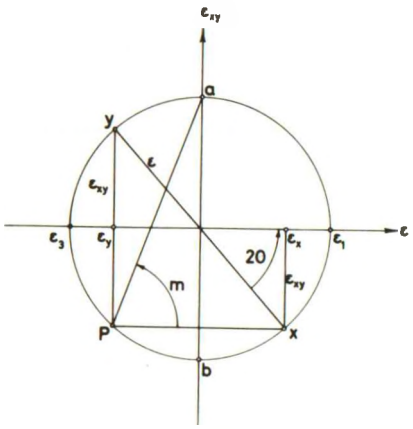

Fig. 23 J: Mohr Circle for Strains.

One has, evidently:

$$\epsilon_x = \epsilon \cos 2\theta$$
$$\epsilon_y = -\epsilon \cos 2\theta \qquad (2333)$$
$$\epsilon_{xy} = \epsilon \sin 2\theta$$

If these quantities are used to calculate the state of deformations, ϵ must be determined by the compatibility equation:

$$\tfrac{1}{2}\left(\frac{\partial^2 \epsilon_x}{\partial y^2} + \frac{\partial^2 \epsilon_y}{\partial x^2}\right) = \frac{\partial^2 \epsilon_{xy}}{\partial x\, \partial y} \qquad (2334)$$

which gives a second order differential equation in ϵ.

However, it is impractical to use this equation for calculation purposes. Instead the calculations are performed directly on the velocity field, in which case (2334) is satisfied identically.

Because the solution to (2334), or the corresponding equations in terms of the velocity components, may formally contain both positive and negative values of ϵ, it is necessary to impose the supplementary condition on the state of strains, that ϵ must always be positive or zero. This is because negative values of ϵ mean that ϵ_1 is negative and ϵ_3 is positive. If this were possible, ϵ_{xy} and τ_{xy} would have opposite signs, i.e. the deformation work done on a small soil element around the point in question would be negative. This is plainly impossible, because failure stresses in a medium cannot do active work (they are clearly resistive forces).

235 Velocity Fields

The velocity field is defined by the components u_x and u_y, positive in the negative directions of the coordinate axes (Fig. 23 K). These quantities define the state of strains by the equations

$$\epsilon_x = \frac{\partial u_x}{\partial x}$$
$$\epsilon_y = \frac{\partial u_y}{\partial y} \qquad (2335)$$
$$\epsilon_{xy} = \tfrac{1}{2}\left(\frac{\partial u_x}{\partial y} + \frac{\partial u_y}{\partial x}\right)$$

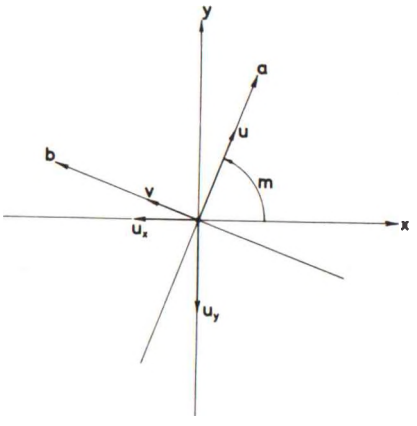

Fig. 23 K: Velocity Components.

The compatibility equation (2334) expresses the fact that the three strain quantities must correspond without contradictions to two velocity quantities, as indicated by (2335).

In analogy with the treatment of the stress functions in Sec. 233 we may assume that u_x and u_y are given along a curve in the x,y plane (see Fig. 23 D). The system of equations which may be used to determine the partial derivatives $\frac{\partial u_x}{\partial x}$, $\frac{\partial u_x}{\partial y}$, $\frac{\partial u_y}{\partial x}$, and $\frac{\partial u_y}{\partial y}$ in the neighbourhood of this curve are deduced from the condition of zero volume change:

$$\frac{\partial u_x}{\partial x} + \frac{\partial u_y}{\partial y} = 0 \qquad (2336\,a)$$

from the condition of coinciding principal axes:

$$\sin 2\theta \frac{\partial u_x}{\partial x} - \cos 2\theta \frac{\partial u_x}{\partial y} - \cos 2\theta \frac{\partial u_y}{\partial x} - \sin 2\theta \frac{\partial u_y}{\partial y} = 0 \qquad (2336\,b)$$

and from the two identities representing the variation of u_x and u_y along the curve:

$$\cos\psi \frac{\partial u_x}{\partial x} + \sin\psi \frac{\partial u_x}{\partial y} = \frac{\delta u_x}{\delta s} \qquad (2336\,c)$$

$$\cos\psi \frac{\partial u_y}{\partial x} + \sin\psi \frac{\partial u_y}{\partial y} = \frac{\delta u_y}{\delta s} \qquad (2336\,d)$$

As before the characteristic directions are determined by the vanishing of the determinant of coefficients. This gives the equation:

$$\sin^2\psi \cos 2\theta - 2 \sin\psi \cos\psi \sin 2\theta - \cos^2\psi \cos 2\theta = 0 \qquad (2337)$$

which is identical to (2315). It has, therefore, the same solutions:

$$\tan\psi = \begin{cases} \tan(\theta + \frac{\pi}{4}) = \tan m \\ \tan(\theta + \frac{3\pi}{4}) = \tan(m + \frac{\pi}{2}) \end{cases} \qquad (2338)$$

The a- and b-directions, defined as above, are therefore also deformation characteristics (see Fig. 23 E). As before, the relation between u_x and

u_y along the characteristic curves can be found by replacing the fourth column of the coefficient matrix by the column on the right hand side, and equating the resulting determinant to zero. One gets (after division with the common factor $\cos 2\theta$):

$$\cos\psi \frac{\delta u_x}{\delta s} + \sin\psi \frac{\delta u_y}{\delta s} = 0 \tag{2339}$$

This equation implies that the slip lines have zero elongation. The same result is also obtained from Mohr's circle of deformations (Fig. 23 J).

The velocity field may be calculated by means of (2339), inserting the values of ψ from (2338):

$$\begin{aligned} \cos m \frac{\delta u_x}{\delta s_a} + \sin m \frac{\delta u_y}{\delta s_a} &= 0 \\ -\sin m \frac{\delta u_x}{\delta s_b} + \cos m \frac{\delta u_y}{\delta s_b} &= 0 \end{aligned} \tag{2340}$$

However, it will usually be more convenient to use instead of u_x and u_y the components u and v in the slip line directions a and b, respectively (cf. Fig. 23 K). u and v are positive in the positive slip line directions. They are connected with u_x and u_y by the relations:

$$\begin{aligned} u &= -u_x \cos m - u_y \sin m \\ v &= u_x \sin m - u_y \cos m \end{aligned} \tag{2341}$$

or:

$$\begin{aligned} u_x &= -u \cos m + v \sin m \\ u_y &= -u \sin m - v \cos m \end{aligned} \tag{2342}$$

Inserting (2342) in (2340) we get:

$$\begin{aligned} \frac{\delta u}{\delta s_a} - v \frac{\delta m}{\delta s_a} &= 0 \\ \frac{\delta v}{\delta s_b} + u \frac{\delta m}{\delta s_b} &= 0 \end{aligned} \tag{2343}$$

cf. Geiringer [1930].

These equations can also be obtained by purely geometrical considerations. If consecutive points along an a-line and a b-line are considered, assuming Δm to be small to the first order (Fig. 23 L), we find (2343) when we express by projection on the a- and b-direction, respectively, that $\epsilon_a =$

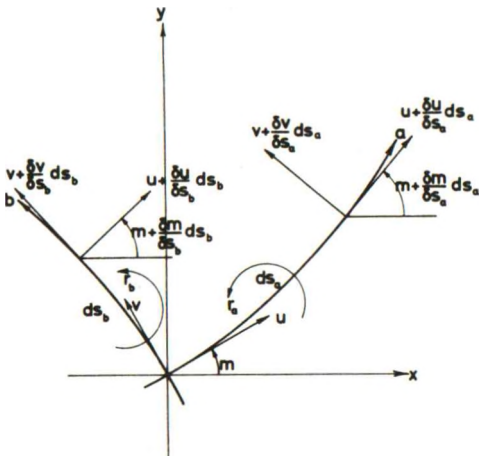

Fig. 23 L: Variation of Velocities Along Slip Lines. Rotations of Slip Line Directions.

$\epsilon_b = 0.$

The condition that $\epsilon_{ab} = -\epsilon$ must always be negative is, evidently, equivalent to the condition that the right angle between the positive a- and b-directions can only be decreased.

From Fig. 23 L it is seen that the rotation r_a of the a-direction (positive in the positive direction of rotation) is equal to:

$$r_a = \frac{\delta v}{\delta s_a} + u \frac{\delta m}{\delta s_a}$$

correspondingly (2344)

$$r_b = -\frac{\delta u}{\delta s_b} + v \frac{\delta m}{\delta s_b}$$

The above mentioned condition clearly demands that

$$2\epsilon = r_a - r_b = \frac{\delta v}{\delta s_a} + u \frac{\delta m}{\delta s_a} + \frac{\delta u}{\delta s_b} - v \frac{\delta m}{\delta s_b} \qquad (2345)$$

must always be positive.

From (2343) it is seen that not only the derivatives of the velocity components, but also u and v themselves may be discontinuous along the slip lines. Thus, different values of u may exist on the two sides of an a-line, and in the same way v may increase by a jump across a b-line. According to (2345) ϵ will in that case be infinite. It must still be positive, however, so the jumps Δu and Δv must always be positive in the positive directions of b and a, respectively.

24 GENERAL PROPERTIES OF SOLUTIONS

241 Deformation Work

For the investigation of some general properties of solutions, without any detailed study of stress or velocity distributions, different expressions for the deformation work are useful. The conclusions will also apply to much more general problems, viz. for clay materials with arbitrarily varying shear strengths and volume forces. They can easily be extended to three-dimensional problems, provided the failure condition and the deformation conditions are changed accordingly.

Assume that to a given failure problem a stress distribution, indicated by the symbol σ, and a velocity field, indicated by the symbol u, are considered. They satisfy the above mentioned conditions No. 1 and 2 (Sec. 213), i.e.:

1. The volume remains constant everywhere. For boundaries to rigid bodies the velocity components are compatible with the permissible movements (2230) for the system of bodies.
2. For the rupture zones ($\epsilon \neq 0$) the equilibrium equations (2304) are satisfied, the failure condition (2308) is not exceeded, and for free surfaces bounding such domains the boundary conditions f. inst. on the form (2301) are fulfilled. The total forces on boundaries to external rigid bodies satisfy the remaining equilibrium equations (2233). The rigid bodies of clay are also in equilibrium.

The deformation work for a small soil element dV will be:

$$dW_d = (\sigma_x \epsilon_x + \sigma_y \epsilon_y + 2 \tau_{xy} \epsilon_{xy})\, dV$$

$$= \left[\sigma_x \frac{\partial u_x}{\partial x} + \sigma_y \frac{\partial u_y}{\partial y} + \tau_{xy} \left(\frac{\partial u_x}{\partial y} + \frac{\partial u_y}{\partial x} \right) \right] dV \qquad (2401)$$

according to (2335). Integrating this quantity over the whole volume of clay we get, by integration by parts:

$$W_d = \int_v \left[\frac{\partial}{\partial x} (\sigma_x u_x + \tau_{xy} u_y) + \frac{\partial}{\partial y} (\sigma_y u_y + \tau_{xy} u_x) \right] dV$$
$$- \int_v \left[u_x \left(\frac{\partial \sigma_x}{\partial x} + \frac{\partial \tau_{xy}}{\partial y} \right) + u_y \left(\frac{\partial \sigma_y}{\partial y} + \frac{\partial \tau_{xy}}{\partial x} \right) \right] dV$$
$$= W_s + W_v \qquad (2402)$$

By Gauss' integral theorem the first integral may be transformed to:

$$W_s = \int_s \left[-(\sigma_x u_x + \tau_{xy} u_y)\, dy + (\sigma_y u_y + \tau_{xy} u_x)\, dx \right] \qquad (2403)$$

This integral is taken around the external boundary of the clay material in the positive direction of s (Fig. 22 B). It can easily be transformed to:

$$W_s = \int_s (\sigma_n u_n + \tau_{nt} u_t)\, ds \qquad (2404)$$

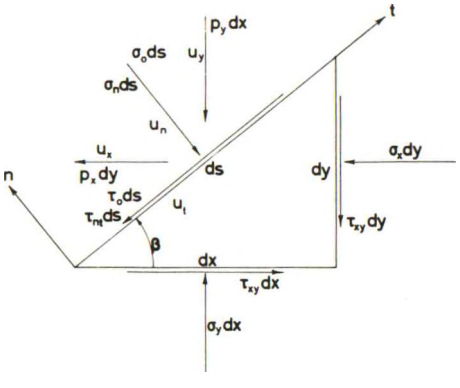

Fig. 24 A: Surface Element. Components of Surface Loading, Stresses, and Movements.

cf. Fig. 24 A. σ_n and τ_{nt} are the stresses in the clay acting upon the section t along the boundary.

For free surfaces this is equal to a corresponding expression including the surface loadings:

$$W_{fs} = \int_{fs} (\sigma_o u_n + \tau_o u_t)\, ds$$
$$= \int_{fs} (p_x u_x\, dy + p_y u_y\, dx) \qquad (2405)$$

cf. (2201) and (2205). If the surface bounds a rigid body of clay with movement components w_x^c, w_y^c, and r_z^c, the velocity components u_x and u_y can be expressed in terms of these quantities by (2208), and the integration can be performed according to (2203). We find:

$$W_{cs} = Q_x^c w_x^c + Q_y^c w_y^c + M_z^c r_z^c \qquad (2406)$$

using the total force components for this part of the surface (possibly calculated by means of (2212-21)). The superscript c indicates that the forces are external ones, acting upon a rigid body of clay.

For boundaries to external rigid bodies (2404) cannot directly be written in the form (2406), because u_n, u_t may not correspond to a rigid body movement of the clay. However, if σ_n and τ_{nt} are interpreted as surface

loadings (σ_o^{pc}, τ_o^{pc} with the corresponding components p_x^{pc}, p_y^{pc}) whose force resultants are the terms Q^{pc} in (2231), (2405) can be used together with (2203) and (2209), the movement components in the last mentioned equation No. being those of the external rigid body.

In this way we obtain:

$$W_{rs} = Q_x^{pc} w_x + Q_y^{pc} w_y + M_z^{pc} r_z - \int_{rs} \tau_{nt} u_s \, ds \tag{2407}$$

In this equation the last integral is the work done by a possible sliding between the rigid body and the clay. According to the above assumption No. 1 τ_{nt} cannot exceed the adhesion strength c_a.

Summing over all boundaries to external rigid bodies we find from (2231), (2230), (2237), (2235), and (2232):

$$\begin{aligned} Q_{pi}^{pc} w_{pi} &= Q_{pi}^{e} w_{pi} + P_r a_{pir} (c_{pin} d_n + v_f b_{pif}) \\ &= Q_{pi}^{e} w_{pi} + P_r d_r \end{aligned} \tag{2408}$$

that the total contribution from the bodies can be written:

$$W_{rs} = \sum_r P_r d_r + \sum_p \left[(Q_x^e w_x + Q_y^e w_y + M_z^e r_z) - \int_{rs} \tau_{nt} u_s \, ds \right] \tag{2409}$$

the sum r being a summation over all restraints, and sum p a summation over all external rigid bodies.

In (2409) the first expression contains the known restraint movements d_r, whereas the force components, P_r, are not given initially. The second and third expression contains known forces Q_{pi}^e and τ_{nt} but now the movements w_{pi} and u_s are not given initially.

The second integral in (2402) can by the equilibrium equations (2304) be transformed to:

$$W_v = \int_v (X u_x + Y u_y) \, dV \tag{2410}$$

It is therefore equal to the work done by the volume forces during the deformation. For the rigid bodies of clay (2304) need not be shown to be satisfied at all points. However, the equilibrium conditions must be satisfied for the body as a whole, so the expression (2410) must be true for the whole clay mass, when (2208) is used inside the rigid bodies of clay.

In the theory of structures equation (2402) is frequently used for struc-

tures loaded in controlled stress to determine total internal force components, such as normal and transversal forces, bending and torsional moments, by the principle of virtual displacements. This cannot be done for the type of problems considered here, because the stress distributions will usually be too complicated to be described by simple internal force components. Nevertheless, for an ideal plastic material the work equation may give important information because of a special property of the expression (2401).

If dW_d in this form is integrated by means of equation (2303) and (2333), assuming the angle θ_s between the x-axis and the major principal stress direction, and θ_d to the major principal strain direction, we obtain:

$$W_d = \int_v 2\tau \epsilon \cos 2(\theta_s - \theta_d)\, dV \tag{2411}$$

In this equation ϵ and θ_d are assumed to be determined directly from the velocity field by (2335) and (2333), so that ϵ is always positive. From (2411) it is seen that if a given velocity field satisfying the above condition No. 1 is used together with all possible stress distributions satisfying condition No. 2, a maximum for W_d is obtained for the stress distribution which satisfies the further conditions that $\theta_s = \theta_d$ and $\tau = c$ whenever ϵ is different from zero.

For in that case we have

$$W_d = \int_v 2c\epsilon\, dV \tag{2412}$$

which can evidently never be smaller than the right hand side of (2411) under the given assumptions.

Correspondingly, the sum of integrals constituting the last term of (2409) will attain its maximum value if τ_{nt} at every point has the same direction as u_s, and is equal to c_a (according to the assumption No. 2 above it does not exceed this value). To indicate that τ_{nt} satisfies this condition we may write:

$$\tau_{nt} = \tau_a = \pm c_a. \tag{2413}$$

where the positive or negative sign is used according to the sign of u_s.

Thus,

$$\sum_p \int_{rs} \tau_a u_s\, ds \geq \sum_p \int_{rs} \tau_{nt} u_s\, ds \tag{2414}$$

Furthermore, the expression (2412) and the integrals in (2409) are relatively easy to calculate for a given velocity field, which makes the work equation (2402) suitable for practical use.

242 Uniqueness of Solutions

A mathematically correct solution to a given failure problem is defined in Sec. 213. Thus, apart from the above mentioned conditions No. 1 and 2 the following supplementary conditions must be satisfied:

3. The principal stress and strain directions coincide everywhere in the rupture zones. Here also the failure condition (2308) is satisfied exactly, and $|\tau_{nt}| = c_a$ for all boundaries to external rigid bodies sliding upon the clay.

4. For all other points the maximum shear stress nowhere exceeds the shear strength of the material, and $|\tau_{nt}| \leq c_a$ along boundaries to rigid bodies which do not slide upon the clay.

5. The shear stress and the shear strain have the same sign everywhere in the rupture zones, and $\tau_{nt} = \tau_a$ points in the same direction as u_s.

From the comparison between (2411) and (2412) together with the relation (2414) it is seen that a mathematically correct solution satisfies an extremum condition. This is used in this section to investigate in what sense a solution of this type can be said to be unique.

More specifically, assume that two different solutions (σ, u) and (σ', u') exist to the same failure problem, giving the works $W = \sum_r P_r d_r$ and $W' = \sum_r P'_r d'_r$, respectively, done by the given movements (in controlled strain), or the two safety factors f and f', respectively (in controlled stress). The problem is to determine what relation if any exists between them.

This can be done by considering the deformation works ΔW_d and $\Delta W'_d$ done by the stress difference ($\sigma - \sigma'$) for the two velocity fields u and u', respectively. For each of these works the expression (2402) can be used, developing ΔW_s as shown in (2404-9), and ΔW_v as shown in (2410), when the force terms in these expressions are replaced by the corresponding differences. For the last term in (2409), (2413) is also used, and the equations (2411-2) are used to evaluate the deformation works themselves.

In controlled strain all force terms, except the restraint forces P_r, but including the adhesion shear stresses $\tau_{nt} = \tau_a$, are known. They are therefore the same for the two solutions, and the difference terms corresponding to (2405-6) and the two last terms in (2409) will be identically zero.

In the expressions for ΔW_d and $\Delta W'_d$ (2412) can be used for the combinations of σ with u, and σ' with u', whereas (2411) must be used when σ is combined with u', or σ' with u.

In this way we find for controlled strain:

$$\Delta W_d = \int_v 2\,[c - \tau' \cos 2(\theta' - \theta)]\epsilon\, dV + \sum_p \int_{rs} (\tau_a - \tau'_{nt})\, u_s\, ds$$

$$= \sum_r (P_r - P'_r)\, d_r \qquad (2415)$$

and

$$\Delta W'_d = \int_v 2\,[\tau \cos 2(\theta - \theta') - c\,]\epsilon'\, dV + \sum_p \int_{rs} (\tau_{nt} - \tau'_a)\, u'_s\, ds$$

$$= \sum_r (P_r - P'_r)\, d'_r \qquad (2416)$$

In these equations τ, θ, and ϵ are the maximum shear stress, the angle between the x-axis and the major principal stress direction, and the maximum shear strain, respectively, for the stress distribution σ. τ', θ', and ϵ' are the corresponding quantities for the stress distribution σ'. The first integrand in (2415) is only non-zero in the domains where $\epsilon \neq 0$, where it is also known that $\tau = c$. However, it cannot without proof be assumed that $\tau = \tau'$, or that $\theta = \theta'$. The corresponding relations are used for the integrand in (2416), which is only non-zero in the domains (not necessarily the same) where $\epsilon' \neq 0$. The second integrands in (2415-6) are non-zero along the boundary parts where $u_s \neq 0$ and $u'_s = 0$, or $u_s = 0$ and $u'_s \neq 0$, respectively.

In controlled stress all force terms R, including volume forces, surface loadings, and external loads on rigid bodies are assumed to be given on the form

$$R = R_1 + f\,R_2 \qquad (2417)$$

containing a constant term (index 1) and a loading rate (index 2), the latter one multiplied by the common factor of proportionality f (the factor of safety). It is assumed that all R_1 and R_2 are given so that there is no failure for values of f in a finite interval containing the point f = 0. The state of failure considered here corresponds to the positive end point of this interval.

Considering again the differences ΔW_d and $\Delta W'_d$ in deformation works, it is observed that all $d_r = 0$ and all force terms R_1 and R_2 are given. They are therefore the same for the two solutions σ and σ'. The terms corresponding to R_1 will therefore cancel out, whereas the terms corresponding

to R_2 will have the common factor $f - f'$. We find therefore:

$$\Delta W_d = \int_v 2\left[c - \tau' \cos 2(\theta' - \theta)\right]\epsilon \, dV + \sum_p \int_{rs} (\tau_a - \tau'_{nt})\, u_s \, ds$$

$$= (f - f')\left[\int_{fs} (p_{2x}\, u_x\, dy + p_{2y}\, u_y\, dx)\right.$$

$$\left. + \sum_p (Q^e_{2x}\, w_x + Q^e_{2y}\, w_y + M^e_{2z}\, r_z) + \int_v (X_2\, u_x + Y_2\, u_y)\, dV\right] \tag{2418}$$

and

$$\Delta W'_d = \int_v 2\left[\tau \cos 2(\theta - \theta') - c\right]\epsilon' \, dV + \sum_p \int_{rs} (\tau_{nt} - \tau'_a)\, u'_s \, ds$$

$$= (f - f')\left[\int_{fs} (p_{2x}\, u'_x\, dy + p_{2y}\, u'_y\, dx)\right.$$

$$\left. + \sum_p (Q^e_{2x}\, w'_x + Q^e_{2y}\, w'_y + M^e_{2z}\, r'_z) + \int_v (X_2\, u'_x + Y_2\, u'_y)\, dV\right] \tag{2419}$$

In these two equations the first integrals on the right hand side are performed over the free surfaces. The square brackets may for the sake of simplicity be called R_2u and R_2u', respectively. They are always positive, because $f\,R_2u$ and $f'\,R_2u'$ (with f and f' both positive) are the works done by the second part of the forces in (2417) under the velocity field u and u', respectively. This work must certainly be positive, because the works done by the complete forces R and R' according to Sec. 241 are equal to:

$$Ru = (R_1 + fR_2)\, u = \int_v 2c\epsilon \, dV + \sum_p \int_{rs} \tau_a\, u_s \, ds \tag{2420}$$

and

$$R'u' = (R_1 + f'R_2)\, u' = \int_v 2c\epsilon' \, dV + \sum_p \int_{rs} \tau_a\, u'_s \, ds \tag{2421}$$

respectively.

If the works R_1u and R_1u', respectively, could be equal to or greater than this, it would mean that a mathematically correct solution $\sigma_{(1)}$, u or $\sigma'_{(1)}$, u' could be found in equilibrium with the forces R_1, and with a failure condition $\tau_{(1)} = c_{(1)}$ where $c_{(1)} = c$ or $c_{(1)} > c$, contrary to the assumptions. Thus, the square brackets in (2418-9) are positive because of the assumption that the forces R_1 alone do not produce failure.

In (2415-6) we notice that $\Delta W_d \geq 0$ and $\Delta W'_d \leq 0$. However, $d_r = d'_r$ so that we must have $\Delta W_d = \Delta W'_d$. They must therefore both be zero together with the right hand term $W - W'$. Correspondingly, in (2418) we must have $\Delta W_d \geq 0$ and therefore $f - f' \geq 0$. However, in (2419) we must have $\Delta W'_d \leq 0$ and therefore $f - f' \leq 0$. The quantities ΔW_d, $\Delta W'_d$, and $f - f'$ must

therefore all be zero.

Considering the integral expressions for ΔW_d and $\Delta W'_d$ we find that the above results are only possible when:

1. $\tau' = c$ and $\theta' = \theta$ whenever $\epsilon \neq 0$,
   and $\tau'_{nt} = \tau_a$ whenever $u_s \neq 0$

and (2422)

2. $\tau = c$ and $\theta = \theta'$ whenever $\epsilon' \neq 0$,
   and $\tau_{nt} = \tau'_a$ whenever $u'_s \neq 0$.

Therefore, two solutions to the same failure problem, both satisfying the above conditions No. 1-5, and therefore both mathematically correct, must determine the same failure loads (in controlled stress) or the same work done by the prescribed movements (controlled strain). Moreover, all domains which are rupture zones in one solution ($\epsilon \neq 0$ and therefore $\tau = c$) will also be stressed to failure in the other one, and the slip line directions will be the same at every point ($\tau' = c$ and $\theta' = \theta$). Along boundaries to external rigid bodies where slidings take place in one solution the adhesion strength will also be mobilized in the other one. Because of (2236) all values of P_r will therefore also be the same.

Especially for design problems it has the consequence, as stated by Brinch Hansen, that when a mathematically correct solution has been found corresponding to a chosen mode of failure (a set of imaginary restraints with $d_r \neq 0$ but $P_r = 0$), no other more critical solution can be found corresponding to the given forces and movements, i.e. the construction as designed cannot fail in a more critical way than the one which is chosen.

Because of the assumption of a plastic-rigid material a certain ambiguity may still exist as to the velocity field or the mean normal stress σ.

Thus, apart from the trivial variation obtained by multiplying all velocities (in controlled stress) with a common factor of proportionality, two or more velocity fields u and u' may be possible for the same stress distribution σ at failure. Then, however, a family of linear combinations $\alpha u + \beta u'$ (also in agreement with the given boundary movements) will also be possible, subject only to the condition that $\alpha \epsilon + \beta \epsilon'$ shall be non-negative. For some problems in controlled stress a whole family of velocity fields may be possible, each member being characterized by an arbitrary function, with the only condition f. inst. that the function shall be non-negative and monotonously increasing in a certain direction.

For some of the different possible velocity fields the shear strains ϵ may become zero for a part of the rupture figure. A similar phenomenon is sometimes obtained when passing from one type of rupture figure to another, through a continuous variation of the boundary conditions. In such situations the domains in question are said to be on the verge of failure. They are usually included in the rupture zones, although they move as parts of rigid bodies of clay.

For some rupture zones where the stresses cannot be determined from known surface loadings or from equilibrium conditions for rigid bodies, an additive constant to the mean normal stress σ may be undetermined throughout the zones, subject only to certain limiting conditions to prevent secondary ruptures. However, as mentioned above this will have no influence on the failure load, or the work done by the prescribed movements, but some force components doing no work during the movement may be undetermined.

In the rigid bodies of clay the stress distribution is in principle undetermined, only the boundary stresses or (for boundaries to adjacent rigid bodies) the resultants of boundary stresses being known. Two otherwise identical solutions may therefore differ in this respect, f.inst. because of different prestressings before failure. However, if the structures adjacent to the clay material are also calculated by the theory of plasticity it is always possible to indicate limiting stress distributions on the verge of failure, from which the necessary bending moments etc. can be calculated.

Example 24a

The above mentioned uncertainties in velocity fields may be illustrated by the following few examples.

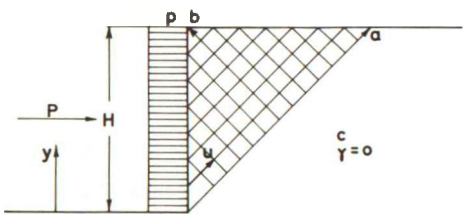

Fig. 24B: Failure Problem with Horizontal Surface, Vertical Earth Front, and Zero Unit Weight.

If a vertical, unsupported earth front (assuming zero unit weight for the clay) is loaded by a uniform loading p, failure will occur for the value $p = 2c$. The rupture figure is in this case the zone shown in Fig. 24B with straight a- and b-lines ($\theta = 0$, $m = \frac{\pi}{4}$ and $\sigma = c$ everywhere in the zone). The velocity field in the zone will be parallel to the a-lines, the velocity u being constant along each a-line.

In this case u is an arbitrary function of the height y, measured at the earth front, the only condition being that it must be non-negative and monotonously increasing with y. Evidently if $u > 0$ for $y = 0$ the whole rupture zone slides upon the clay material at rest. If u is discontinuous, slidings will also take place inside the rupture zone.

In practice there will of course always be inhomogeneities in the clay, so that in any given experiment failure will obtain along one (or possibly more) preferred slip lines. They cannot be determined beforehand, however, unless the assumption of a perfectly homogeneous clay is abandoned.

If the earth front is supported by a perfectly rigid, smooth wall which is loaded by a horizontal force resultant P at the height $y = H/2$ until failure (controlled stress), or if the horizontal movement component at the midpoint is made positive, f.inst. by a screw arrangement fixed to the wall through a hinge (controlled strain), the same rupture figure is obtained. But in this case the function u must be linear because of the wall:

$$u = a + b\,y \tag{2423}$$

where a and b are both positive. The expression (2423) may be taken to represent a linear combination of two different possible velocity fields, $u = a$ and $u = b\,y$. For the last mentioned one the wall rotates about its lower point. The first one corresponds to a translation. In this case we have effectively a line rupture following the lower boundary of the rupture figure, the rest of the rupture zone being only on the verge of failure. In both cases P (the failure load or the restraining force) is equal to $2\,c\,H$.

If the movement of the wall is further restricted, f.inst. by fixing the rotation point somewhere below the foot point, the velocity field will be completely determined both in controlled stress and in controlled strain (arranged as above).

The second example is a little more complicated (fig. 24 C). Assume that we have a construction, in this case a cofferdam, in the vicinity of a slope, and that its stability against horizontal forces P acting in the height y above the ground surface is investigated. This problem may be considered either as one of controlled stress ($P = f$ for a loading rate corresponding to a unit line load), or as one of controlled strain (P being the restraint force in a rod connection).

For y greater than a certain value h the local failure F_1 of the cofferdam will be the most critical one. Its rupture figure may, as shown by Brinch Hansen, be a single line rupture connecting the foot points of the

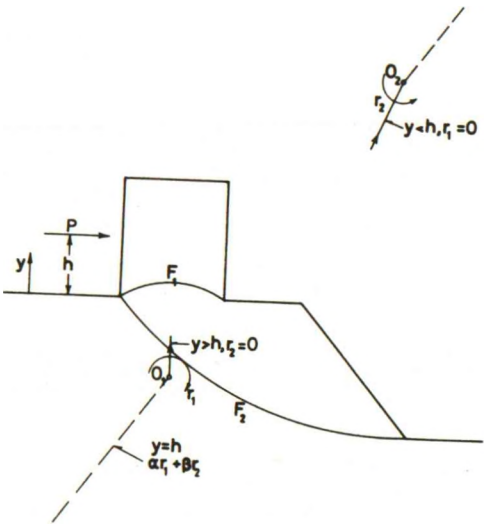

Fig. 24C: Movements in a Stability Problem for a Cofferdam.

sheet walls for the cofferdam. During this failure the cofferdam rotates about a centre O_1 located on the centre line of the construction.

When y is smaller than h the total slope failure F_2 is the most critical. Its rupture figure may also be a single line rupture corresponding to the rotation of the cofferdam about a point O_2 situated on the mean normal to the chord of F_2.

When y is exactly equal to h the two rupture figures are both mathematically correct. Any one of the above mentioned failure movements may therefore take place, and a linear combination $\alpha r_1 + \beta r_2$ will also be possible. Because we must have $\epsilon > 0$ everywhere, α and β must both be positive (with the directions of r_1 and r_2 as shown on Fig. 24C), and the resulting point of rotation cannot be located between the two points O_1 and O_2. Thus, if the height y of P above the clay surface is increased, passing through the value h shown in Fig. 24C, the resulting rotation point will, before this position is reached, approach O_2 along a straight line. While y is equal to h (so to speak) the rotation point will pass through the infinite point of the line O_1O_2, and will end up at O_1. Then for a further increase of the height y it will leave O_1 along a straight line.

Considered as a design problem, assume the magnitude of P to be given together with the height of application h. The two most important dimensions: the width of the cofferdam and its distance from the top of the slope

(assumed both to be desired as small as possible) may be chosen so that the rupture figures F_1 and F_2 are both just realized. The corresponding extra movement conditions are pure rotations r_1 and r_2, r_2 being imposed on the clay body above F_2, and r_1 on the cofferdam relative to this body. Notice that in this case the relative magnitudes of these rotations do not matter, so long as they have the correct signs. One of them may even be chosen to be zero relatively to the other (the corresponding line rupture being then only on the verge of failure).

Example 24 b

In Fig. 24 B the mean normal stress σ is given everywhere in the rupture zone by the boundary conditions $\sigma_o = \tau_o = 0$ for the free surface, and the stress equations (2318) for the variation along the slip lines.

In Fig. 24 C the boundary conditions for stresses do not determine σ for any one of the two line ruptures F_1 and F_2. However, (2318) still applies, and σ at one point (together with P and the centre angle for the circle arc) can in each case be found from the three equilibrium equations for the material and structure above the line rupture.

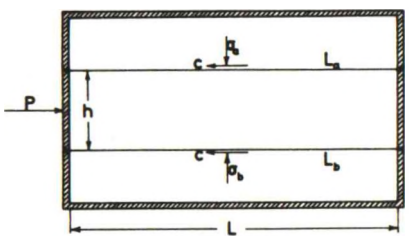

Fig. 24 D: A Special Shear Box Test with Fixed Upper and Lower Frames.

A (somewhat constructed) example where the value of σ is undetermined, is shown by the modified shear box test in Fig. 24 D. The upper and lower parts of the box are completely fixed, but the middle part can be moved horizontally (controlled stress or controlled strain).

In this case the rupture figure consists of two line ruptures L_a and L_b, and the failure load P is equal to 2 c L.

According to (2318) the normal stress σ is constant along each of the two line ruptures, but it is otherwise undetermined. In practice it will be given by the vertical prestressings of the clay material, but these cannot be found under the assumption of a plastic-rigid failure. It can only be deduced that in order to avoid secondary failures we must have $|\sigma_a - \sigma_b| \leq 2ch/L$.

Evidently the values of σ have no influence on the failure load (or on the work done by the prescribed movement).

Another example in which σ is undefined is given later in this work in Sec. 443 (Fig. 44 J).

243 Approximate Solutions

An approximate solution is defined by a velocity field and/or a stress distribution (i.e. by a rupture figure) as indicated in Sec. 213. By a solution method we understand a set of rules defining the permissible types of rupture figures, and indicating how any chosen rupture figure, permissible under the method, is calculated.

Thus, if a method of mathematically correct solutions could be found, it would only contain the solutions defined in Sec. 242 as permissible members. However, a unique calculation method cannot be indicated, so in practice methods containing a wider class of permissible solutions must be used, even if it is intended to find the mathematically correct solution.

As explained previously approximate solutions may also be used in their own right, f. inst. in order to obtain a calculation result within a reasonable expense of time and money.

In order to distinguish good approximate methods from less useful ones we shall in this work only consider such methods which satisfy the following conditions (apart from definiteness of permissible rupture figures and uniqueness of calculation method):

1. They should contain the mathematically correct solution as a permissible member.
2. It should be possible to determine whether a solution, permissible under the method, is the correct one.
3. If the solution is not correct it should be possible to indicate how it is related to the correct solution, i.e. whether it is on the safe or the unsafe side, how it should be corrected, or at least exactly what conditions are not satisfied.

One such method is the method of statically admissible solutions. A solution of this type satisfies the conditions No. 2 and 4 in Sec. 213 (or Sec. 241-2). It is therefore defined by a stress distribution σ which satisfies the equilibrium equations everywhere in the rupture zones and for all rigid bodies, and which further does not exceed the failure condition at any point. In practice it is rather difficult to construct a solution of this type in a simple way, so usually the method is only applied in the form that the correct

solution to another failure problem with the same geometry and the same forces, but with other prescribed movements, is used.

A statically admissible solution can be compared with the correct one by means of the appropriate one of the equations (2415) and (2418). It can therefore be concluded that $\Delta W_d \geq 0$, i.e. that $W_c \geq W$ (controlled strain) or $f_c \geq f$ (controlled stress), where W_c and f_c now represent the quantities corresponding to the correct solution. Thus, if the solution is not correct it will be on the safe side.

Notice that (2416) or (2419) cannot be used in this case, because a velocity field u corresponding to the stress distribution σ may not be defined (at least it is not calculated because one does not use it; f and the restraint forces P_r are found directly by the equilibrium conditions). Even if a velocity field u could be found one could not assume that $\Delta W'_d \geq 0$, because it is not certain that $\epsilon \geq 0$.

If one has a number of statically admissible solutions to the same problem, or if a stress distribution satisfying the above conditions can be made dependent of a number of parameters, the best approximation will therefore be given by the solution which has the maximum value of f or W. This may be used in some cases where stress distributions can be constructed in a sufficiently simple way, or where a family of correct solutions can be used. No simple general method can be indicated, however.

Notice that it is important that the failure condition $\tau \leq c$ is nowhere exceeded. If this is not ascertained ΔW_d may become negative according to (2415) or (2418). The solution might then be called quasi statically admissible. Solutions of this kind may evidently be on the unsafe, instead of on the safe side.

In practice the so-called method of kinematically admissible solutions, cf. Drucker, Greenberg, and Prager [1951], is more useful. Solutions of this type satisfy the conditions No. 1, 3, and 5 in Sec. 213 (or Sec. 241-2). They are therefore defined by a velocity field u for which the volume remains constant at every point, and which agrees with the boundary movement conditions. The stress distribution corresponding to this velocity field may formally be defined by the following conditions.

1. $\tau = c$ and $\theta_s = \theta_d$ whenever $\epsilon \neq 0$ (i.e. in the rupture zones).
2. σ in the rupture zones is determined so that the equality between the expressions in (2402) and the appropriate one of (2405-6), (2409), and (2410) is satisfied, i.e. by the equation of projection

upon the direction of the velocity vector at every point (for rigid bodies, also the bodies of clay: the moment equation about the rotation point or, for translated bodies, the projection upon the direction of translation).

If it is desired to satisfy both equilibrium equations (2304) it will therefore in the general case be necessary to introduce corrective volume forces and surface loadings perpendicular to the direction of the velocity vector at every point (for rigid bodies: total forces doing no work during the movement).

However, in practice the stress distribution is not needed, as the work equation (2402) can be used directly. We find, for controlled stress:

$$f\left[\int_{fs}(p_{2x}u_x\,dy + p_{2y}u_y\,dx) + \sum_p (Q^e_{2x}w_x + Q^e_{2y}w_y + M^e_{2z}r_z) + \int_v (X_2 u_x + Y_2 u_y)\,dV\right]$$
$$= \int_v 2c\epsilon\,dV + \sum_p \int_{rs} \tau_a u_s\,ds - \left[\int_{fs}(p_{1x}u_x\,dy + p_{1y}u_y\,ds) + \sum_p (Q^e_{1x}w_x + Q^e_{1y}w_y + M^e_{1z}r_z) + \int_v (X_1 u_x + Y_1 u_y)\,dV\right] \quad (2424)$$

from which the factor of safety f is determined, and for controlled strain:

$$W = \sum_r P_r d_r = \int_v 2c\epsilon\,dV + \sum_p \int_{rs} \tau_a u_s\,ds - \left[\int_{fs}(p_x u_x\,dy + p_y u_y\,dx) + \sum_p (Q^e_x w_x + Q^e_y w_y + M^e_z r_z) + \int_v (X u_x + Y u_y)\,dV\right] \quad (2425)$$

which determines the work W done by the prescribed movements d_r. In practice (2425) is also used for controlled stress: f is determined, or is if necessary assigned and subsequently changed by trial and error, until the minimum value of W is exactly zero.

The value of this method lies in the fact that any solution can be compared with the mathematically correct one by means of the equations (2416) and (2419), cf. the above definitions No. 1 and 2. $W - W_c$ and $f - f_c$ will therefore always be positive or zero, so that it can be stated that the solution if incorrect will be on the unsafe side.

Notice that (2415) or (2418) cannot be used in this case, because it is not certain that the equation of projection upon the direction of the correct velocity vector is satisfied. Even if it was it could not be deduced that ΔW_d was positive, because it is not certain that $\tau \leq c$ when $\epsilon = 0$ and $\epsilon_c \neq 0$.

The above mentioned extremum condition for this type of solutions makes it very simple to improve a given solution. The velocity field may be made dependent of as many parameters or even arbitrary functions as desired. The best solution will always be the one for which f or W as determined by (2424-5) is a minimum.

This makes the method extremely useful, especially for more general problems than those considered in the present work, f.inst. problems with arbitrarily varying volume forces and shear strengths, and even three-dimensional problems (if the failure condition of Huber, Hencky, and Mises is used). It certainly contains the mathematically correct solution as a permissible member; it is the solution which also satisfies the above conditions No. 2 and 4, i.e. for which all corrective volume forces, surface loadings, and line loads are zero, and for which $\tau \leq c$ also when $\epsilon = 0$.

However, although the deformation work in the rupture zones is not difficult to calculate by means of (2412), it is not easy only by varying the velocity field to obtain that the corrective volume forces and surface loadings on rupture zones become zero. Therefore, if closer approximations to the correct solution are required the method will have to be modified somewhat.

At least for the assumptions considered in the present work (Sec. 211) this is not difficult, because it is relatively easy to ensure by means of (2318) and (2343) that the equilibrium conditions and the movement conditions are satisfied at every point of the rupture zones. The boundary conditions for the stresses and movement along the zone boundaries can also be satisfied. Rupture zones defined in this way are called possible zones. Because of (2343) a velocity field will exist satisfying the above conditions No. 1 and 3, but not necessarily No. 5. Furthermore, the condition No. 2 need not be satisfied for the rigid bodies, and No. 4 also need not be satisfied.

244 Admissible Solutions with Possible Zones

From the considerations in Sec. 243 the so-called method of admissible solutions with possible zones can be defined. This method is new, mainly because the general case of possible zones is to a large extent unknown. However, a variant in which the zones are statically determined is used by Brinch Hansen [1953] for the solution of problems where the equilibrium method can be applied. In its most general formulation the method has much in common with the method of kinematically admissible solutions, but since

the velocity field in the rupture zones is calculated by means of (2343) ϵ may become negative. Unless the sign of ϵ is specially checked by means of (2345) it cannot therefore be concluded that $\Delta W'_d$ in (2416) or (2419) will always be negative or zero. The extreme member of a family of solutions may in this way be on the safe side instead of on the unsafe side.

A solution with negative values of ϵ is permissible under the method. If the solution is proved to have $\epsilon \geq 0$ everywhere it may be called admissible with kinematically possible zones. It is then known to be on the unsafe side, if it is not correct.

A rupture figure permissible under the method is defined not by a stress distribution or a velocity field, but in terms of a rupture figure type. By this we understand a specification, f. inst. in form of a graph, of the rigid bodies of clay, the line ruptures, and the different types of rupture zones which constitute the rupture figure. More specifically a rupture figure type can be defined as follows.

1. A collection of rupture zones and line ruptures specified by the number, type and relative position of zone boundaries, i.e. free surfaces, singular points (f. inst. vertex points of radial zones), internal boundaries, boundaries to external rigid bodies and to rigid bodies of clay, end points for line ruptures on free surfaces and rigid bodies, and intermediate points for line ruptures on internal boundaries and between line ruptures meeting in the clay.

2. A number of rigid bodies of clay located between and around the rupture zones and line ruptures.

3. To be permissible under the method the rupture figure type should be consistent and determinable, i.e. it should represent a reasonable transmission of velocity differences between the rigid bodies, and the different types of boundaries to the zones should be arranged so that no zone element is overdetermined according to the basic differential equations (2318) and (2343).

4. When applied to the given failure problem the rupture figure type should be relevant, i.e. it should be possible to identify the indicated zone boundaries with free surfaces, internal boundaries, and boundaries to external rigid bodies in the problem. It should further be possible to indicate which rigid bodies of clay are assumed to move together with specified external rigid bodies, which ones are assumed to slide upon external rigid bodies, and which ones are assumed to be moving freely. For sliding of rigid bodies of

clay the sign of u_s should also be indicated.

Each member of a type of rupture figures specified as above will represent a solution. It is determined by a number n_i of initial numerical parameters t_i which give the necessary information so that all rupture zones can be calculated from their boundary conditions, and all line ruptures are geometrically determined. The parameters for a given type of rupture figures can frequently be indicated in different ways; they will usually be: arc lengths along free surfaces to end points of slip lines, angle differences between tangents to slip lines in characteristic points of zone boundaries, ratios between sliding velocities along line ruptures, ratios between rotation velocities for rigid bodies of clay, and scale factors or angles of orientation for closed rupture zones.

In more complicated rupture figures, especially figures with open rupture zones and irregular surface conditions, it is not possible to carry through the calculations after estimating just the n_i parameters. A number n_e of extra parameters, representing further arc lengths and angle differences, may have to be estimated. They correspond to the same number of geometrical conditions and stress conditions which have to be satisfied during the calculation of the rupture figure in order that it shall correspond without contradiction to the geometrical boundary conditions and the boundary conditions for stresses.

On the other hand, in the actual calculations of a solution it may not be necessary to consider all the n_i parameters in an explicit way. For example, one may choose to keep some of them at fixed values, using f. inst. straight line ruptures, or straight zone boundaries as in the AfPfA rupture figure on Fig. 21 B, or the movement conditions for the external rigid bodies may make it possible to determine some of the parameters directly, cf. the rupture figures AaPR, BfR, and A on Fig. 21 B, where the movements of the wall and the geometry of the rigid body of clay are related in a simple way.

Therefore, when specifying the rupture figure type that should be used for the solution one should also indicate which parameters are to be considered as fixed, and which may be varied

1. to satisfy the movement conditions of the failure problem if any,

2. to obtain the extreme solution, i. e. the best approximation.

Let the number of parameters which can be varied be n_k.

The calculation of a solution must in principle proceed as follows for ordinary failure problems. Problems with variable external parameters and

design problems are treated separately in the following section.

1. A set of n_i initial parameters is chosen. For those which are fixed the known values are taken. The n_k others must be estimated, using the external movement conditions when possible. In controlled stress the value of f may also have to be estimated in order that the boundary conditions for stresses shall be defined.

2. The rupture zones can now be calculated, after which the geometry of the rupture figure is known. The velocity field in the clay material will then also be known, except for a common factor of proportionality for all velocities, and possibly also for certain constants characterizing the velocity field in statically determined rupture zones, cf. (2423).

3. It is ascertained that a set of movement components for the rigid bodies exist, which satisfy the conditions (2224) and are compatible with the velocity field in the clay. If not, some of the n_k parameters are changed, possibly by trial and error, until this is obtained. At most n_r parameters will be determined by these conditions. The actual number may be smaller, however, because of the existence of statically determined rupture zones, or when f.inst. two external rigid bodies are in contact with the same rigid body of clay (cf. the two sheet pile walls which will normally bound the cofferdam shown in Fig. 24C). For problems in controlled strain the factor of proportionality on the velocity field is also determined by this investigation.

4. The remaining parameters are changed, repeating the calculation under 2. and 3. above, until the minimum value for W as determined by (2425) is obtained. In controlled stress the estimated value of f is also changed until the minimum of W is exactly zero.

It should be noticed that when the rupture zones are calculated as possible zones, and the correction shown in (2307) is used to eliminate the volume forces, the work equation (2425) can be obtained in a somewhat simpler form.

Thus, when the surface loadings corresponding to the potential function K is introduced, cf. (2305), the last integral in (2425) will vanish.

The first integral on the right hand side of (2425) may be expressed as in (2402). W_v will be zero, and W_s may be expressed as in (2405-7) by means of the force resultants for the stresses along the zone boundaries.

The integral representing the free surfaces which bound zone ruptures is seen to cancel out, as will also the integral of $\tau_a u_s$ along the boundaries between external rigid bodies and rupture zones. The remaining terms represent works done by

1. External forces Q^e_{pi} and force resultants Q^{zp}_{pi} from rupture zones acting upon external rigid bodies (movement components w_{pi}).
2. External forces Q^c_{ci} and force resultants Q^{zc}_{ci} from rupture zones acting upon rigid bodies of clay (movement components w_{ci}).
3. Slidings along line ruptures (lengths L_{cc}, sliding velocities u_{cc}).
4. Slidings between external rigid bodies and rigid bodies of clay (lengths L_{cp}, sliding velocities u_{cp}).

In its simplest form Eq. (2425) can therefore be written:

$$W = \sum_r P_r d_r = \sum_{cc} c\, u_{cc} L_{cc} + \sum_{cp} \tau_a u_{cp} L_{cp} - \sum_{p,i} (Q^e_{pi} + Q^{zp}_{pi})\, w_{pi} - \sum_{c,i} (Q^c_{ci} + Q^{zc}_{ci})\, w_{ci} \qquad (2426)$$

This form is used for numerical calculations. The extremum condition that W shall be stationary for all admissible changes of the parameters t_k is normally used simply by calculating W or f for different sets of t_k. Each set is determined from the preceding ones by means of an iteration routine, ending with a solution which is estimated to be sufficiently close to the absolute minimum for W or f.

This procedure is well suited for computers, and if the rupture figure consists mostly of line ruptures, possibly with a few simple rupture zones, it will also be the simplest method. However, in the important special cases where the number of parameters is great enough, so that all equilibrium conditions for the rigid bodies can be satisfied, it may be an advantage to use the so-called equilibrium method instead of the extremum method.

This presupposes that the force resultants are also calculated along the line ruptures. But for the solutions of this type, the so-called quasi-possible and possible ones, they will frequently be needed for other purposes, f. inst. to calculate earth pressure components.

245 The Equilibrium Method

The equilibrium method, which has first been introduced by Brinch Hansen [1953], can if it is desired also be used as an alternative to the direct seeking of a minimum by means of (2426). It is observed that the two first sums in (2426) can be transformed into differences between the works done by the corresponding force resultants acting upon the external rigid bodies, and rigid bodies of clay in question.

Thus

$$\sum_{cp} \tau_a u_{cp} L_{cp} = -\left[\sum_{p,i} Q_{pi}^{cp} w_{pi} + \sum_{c,i} Q_{ci}^{pc} w_{ci} \right] \qquad (2427)$$

cf. (2406) and (2407). Q_{pi}^{cp} is a force component acting upon an external rigid body, whereas Q_{ci}^{pc} (= $-Q_{pi}^{cp}$ when external rigid body No. p is in contact with rigid body of clay No. c) is a force component acting upon a rigid body of clay. If no sliding obtains between the rigid bodies No. p and No. c, $w_{pi} = w_{ci}$ and the corresponding terms in (2427) cancel out.

Correspondingly

$$\sum_{cc} c\, u_{cc} L_{cc} = -\sum_{c,i} Q_{ci}^{cc} w_{ci} \qquad (2428)$$

where the sum includes all rigid bodies of clay.

Indicating now by Q_{pi} the sum of all force resultants No. i acting upon the external rigid body No. p, and in the same way by Q_{ci} the total force resultant No. i acting upon the rigid body of clay No. c, we find that (2426) can be written

$$W = -\left[\sum_{p,i} (Q_{pi}^{e} + Q_{pi}^{zp} + Q_{pi}^{cp})\, w_{pi} + \sum_{c,i} (Q_{ci}^{c} + Q_{ci}^{zc} + Q_{ci}^{pc} + Q_{ci}^{cc})\, w_{ci} \right]$$

$$= -\left[\sum_{p,i} Q_{pi} w_{pi} + \sum_{c,i} Q_{ci} w_{ci} \right] \qquad (2429)$$

The extremum condition applied to this equation gives that for all parameters t_k we must have in controlled strain:

$$\frac{\partial W}{\partial t_k} = -\left[\sum_{p,i} Q_{pi} \frac{\partial w_{pi}}{\partial t_k} + \sum_{c,i} Q_{ci} \frac{\partial w_{ci}}{\partial t_k} \right]$$

$$-\left[\sum_{p,i} \frac{\partial Q_{pi}}{\partial t_k} w_{pi} + \sum_{c,i} \frac{\partial Q_{ci}}{\partial t_k} w_{ci} \right]$$

$$= D_u + D_\sigma = 0 \qquad (2430)$$

In controlled stress the same equations are obtained, because when f takes a stationary value all terms derived from (2429), and containing the factor $\frac{\partial f}{\partial t_k}$, will vanish.

Each change of the parameters t_k will result in a changed rupture figure, and therefore in a changed velocity field and a changed stress distribution. The first term in (2430), called D_u, represents the change in the work done by the force resultants acting upon the original rigid bodies for the change in movement components for these bodies. The second term, called D_σ, represents the change of work done by the original movement components of the bodies for the change in force resultants arising from the changed stress distribution and the changed boundaries to the rigid bodies of clay. In this way known surface loadings Q^c_{ci} may give a contribution to D_σ although the loading components σ_o and τ_o are constant.

The principal point of the equilibrium method is that D_σ is identically zero. This is proved in the sequel for all normal boundaries to possible zones. On line ruptures singular points may exist (in quasi-possible solutions) where it is not possible to construct a unique Mohr circle to represent the state of stress. This introduces a set of extra parameters, usually tangent angles for the line rupture or line ruptures through the points. The corresponding conditions, which are stress conditions determining the value of σ on the line rupture, or the relation between values of σ on the line ruptures, through the point, can be found by the condition that $D_\sigma = 0$, identically. Thus, Brinch Hansen's boundary conditions for line ruptures, and also stress conditions for line ruptures meeting in the clay, can be derived from this theorem, cf. Sec. 341-5.

According to its definition D_σ is the limit value of the divided difference between the works done by two different stress distributions, σ corresponding to the parameter value t_k, and σ' corresponding to the parameter value $t_k + dt_k$. In both cases the velocity field u corresponds to the parameter value t_k.

By means of the work equation, cf. (2415-6) or (2418-9) we find:

$$D_\sigma = \lim_{dt_k \to 0} \frac{1}{dt_k} \left[\int_V 2[\tau' \cos 2(\theta' - \theta) - c]\,\epsilon dV + \sum_p \int_{rs} (\tau'_{nt} - \tau_a) u_s ds \right]$$

$$= \int_V \frac{\partial \tau}{\partial t_k} 2\,\epsilon dV + \sum_p \int_{rs} \frac{\partial \tau_{nt}}{\partial t_k} u_s ds \qquad (2431)$$

where τ', τ'_{nt}, and θ' are the stress parameters corresponding to the stress distribution σ'.

Consider first a zone boundary zb far from all walls and singularity points for the parameter value t_k. For the value $t_k + dt_k$ it is assumed to take the position zb', cf. Fig. 24E. The clay domain can be divided into four parts, distinguished by the values of ϵ and ϵ', the latter one of which corresponds to the velocity field u' for the parameter value $t_k + dt_k$.

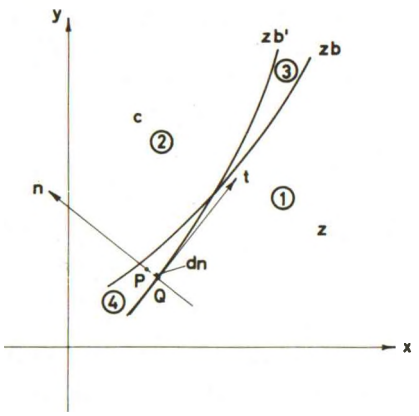

Fig. 24E: Change in the Position of a Boundary to a Possible Zone for an Infinitesimal Change of Parameters.

1. Domains where both ϵ and ϵ' are different from zero, i.e. domains which are rupture zones (z) in both solutions. Here $\tau = \tau' = c$, so that the contribution to D_σ is identically zero.
2. Domains where both ϵ and ϵ' are zero, i.e. domains which are rigid bodies in both solutions. By (2431) it is seen that the contribution to D_σ is zero.
3. Domains with $\epsilon = 0$ but $\epsilon' \neq 0$. The contribution to D_σ is zero according to (2431).

The fourth case where $\epsilon \neq 0$ but $\epsilon' = 0$ is more difficult, because here τ' is not defined. Since the solutions are kinematically admissible its magnitude relative to c is also unknown.

However, we may use the fact that every point P in the domain No. 4 is at an infinitesimal distance dn from a point Q on the zone boundary zb' which is a stress characteristic. Using a local system t,n of coordinates we find for the point P:

$$\tau'_P = \tau_P + \frac{\partial \tau}{\partial t_k} dt_k = \tau'_Q + \frac{\partial \tau'}{\partial n} dn \qquad (2432)$$

$\frac{\partial \tau'}{\partial n}$ is identically zero for negative values of dn, because inside the rupture

zone τ' is always equal to c. We shall now prove that although $\frac{\partial \sigma}{\partial n}$ may be discontinuous across a stress characteristic, $\frac{\partial \tau'}{\partial n}$ will be continuous, i.e. it will be zero also for positive values of dn.

In analogy with (2302) τ' at the point Q can be expressed as

$$\tau'_Q = \sqrt{\frac{1}{4}(\sigma_n - \sigma_t)^2 + \tau_{nt}^2} = c \tag{2433}$$

so that

$$\frac{\partial \tau'}{\partial n} = \frac{1}{\tau'}\left[\frac{1}{4}(\sigma_n - \sigma_t)\left(\frac{\partial \sigma_n}{\partial n} - \frac{\partial \sigma_t}{\partial n}\right) + \tau_{nt}\frac{\partial \tau_{nt}}{\partial n}\right] \tag{2434}$$

Along zb' we have, evidently, cf. (2307) and (2318-9):

$$\sigma_n = \sigma_t$$

$$\mp \tau_{nt} = \tau'_Q = c$$

$$\sigma_t = \sigma'_Q \mp 2c\, m_t \pm c \sin 2 m_t \tag{2435}$$

so that at the point Q:

$$\frac{\partial \tau'}{\partial n} = \frac{\partial \tau_{nt}}{\partial n} = -\frac{\partial \sigma_t}{\partial t} = \pm 2c \frac{\partial m_t}{\partial t}(1 - \cos 2 m_t) = 0$$

In (2435) the upper signs are valid when the zone boundary is an a-line, and the lower signs when it is a b-line. m_t is the angle between the t-axis and the tangent to the zone boundary. It is zero at the point Q.

Since σ_t is a one-valued function of t it follows that $\frac{\partial \tau'}{\partial n}$ must be continuous across the zone boundary, and moreover that it is equal to zero. According to (2432) the contribution to D_σ is therefore zero.

Notice that the proof is based on the fact that the equilibrium condition is satisfied for a small soil element in the vicinity of the zone boundary. In a corresponding way it can be shown that the contribution to D_σ will also be zero for possible triangular soil elements (with $\epsilon \neq 0$ but $\epsilon' = 0$) at the intersection points for zone boundaries with free surfaces, internal boundaries or boundaries to external rigid bodies. The conditions are found to be identical to the equilibrium conditions, i.e. the intersection angles and the values of σ shall be statically correct (Secs. 331 and 335-6, cf. also Secs. 342-4). Special singularities, such as vertex points, discontinuity lines, and discontinuity points (secs. 332-4) can also be shown to contribute nothing to D_σ (using the special conditions of geometry or relative movements valid for such points).

As shown in Sec. 341 the contribution to D_σ will also be zero for normal points on line ruptures. D_σ can therefore be shown to be identically zero in admissible solutions with possible zones, except possibly in the neighbourhood of stress singularities on line ruptures (where there are no geometrical or kinematical conditions as for singular points on zone boundaries). At such points the stress relations, which are also undetermined, can be chosen so that $D_\sigma = 0$, cf. Secs. 342-5.

This means that the last term in (2430) will always vanish, regardless of whether the solution is extreme or not. Denominating the coefficients:

$$m_{kpi} = \frac{\partial w_{pi}}{\partial t_k}$$
$$m_{kci} = \frac{\partial w_{ci}}{\partial t_k} \qquad (2436)$$

we find the complete set of equilibrium conditions:

$$\sum_{p,i} Q_{pi} m_{kpi} + \sum_{c,i} Q_{ci} m_{kci} + \frac{\partial W}{\partial t_k} = 0 \qquad (2437)$$

for controlled strain; and for controlled stress:

$$\sum_{p,i} Q_{pi} m_{kpi} + \sum_{c,i} Q_{ci} m_{kci} + \frac{\partial f}{\partial t_k}\left[\sum_{p,i} Q_{pi} w_{pi} + \sum_{c,i} Q_{ci} w_{ci}\right]_2 = 0 \qquad (2438)$$

where the index 2 indicates that only the work done by the second part of the force terms (2417) is to be considered (if necessary it must be calculated as in kinematically admissible solutions, cf. (2424)).

Eq. (2437-8) may be used instead of the extremum condition to find the best approximation ($\frac{\partial W_r}{\partial t_k} = \frac{\partial f}{\partial t_k} = 0$). The coefficients m_{kpi} and m_{kci} which can be considered as weighting factors to the force component No. i on the rigid body No. p and c, respectively, in equation No. k, can in simple rupture figures frequently be found quite easily as functions of the geometrical parameters for the line ruptures. In more complex rupture figures they may have to be found by numerical differentiation of the velocity fields, if desired. However, if the number of linearly independent equations (2437) or (2438) is equal to the number of remaining equilibrium conditions for the rigid bodies, i.e.

$$n_k = n_f + n_{cs} + 3\,n_{cf} \qquad (2439)$$

where n_{cs} is the number of rigid bodies of clay sliding upon external rigid bodies, and n_{cf} is the number of free rigid bodies of clay, it will not be

necessary to determine the coefficients at all, because it is known that (2437-8) will then be equivalent to the equilibrium conditions.

There are n_f equations on the form:

$$\sum_{p,i} Q_{pi}\, b_{pif} = \sum_{p,i} (Q^e_{pi} + Q^{zp}_{pi} + Q^{cp}_{pi})\, b_{pif} = 0 \qquad (2440)$$

cf. (2233) and (2429). Q^{cp}_{pi} are calculated by means of the equilibrium equations for the rigid bodies of clay in contact with the external rigid bodies:

$$\sum_{p,i} Q^{cp}_{pi}\, b_{pif} = \sum_{c,i} (Q^c_{ci} + Q^{zc}_{ci} + Q^{cc}_{ci})\, b_{cif} \qquad (2441)$$

where $b_{cif} = b_{pif}$ for clay bodies in contact with external rigid bodies, and otherwise zero.

The n_{cs} rigid bodies of clay sliding upon the external rigid bodies give rise to n_{cs} equations on the form:

$$\sum_{i} (Q^c_{ci} + Q^{zc}_{ci} + Q^{cc}_{ci})\, b_{cis} = \tau_a\, u_{cs}\, L_{cs} \qquad (2442)$$

where b_{cis} are the movement components of the rigid body of clay relative to the external rigid body, and corresponding to the sliding velocity u_{cs}.

Finally there are $3\,n_{cf}$ equilibrium equations for the free rigid bodies of clay:

$$Q_{cfi} = 0 \qquad (2443)$$

The replacement of (2437-8) by (2440-3) will usually mean an appreciable saving in calculation work, so if complicated rupture figures are used they might as well be made possible or at least quasi-possible ones.

(2437-8) may also be used to find the derivatives of W or f directly for a solution which is not the extreme one. This may be an advantage when a numerical iteration routine is used. It is a provision, however, that the coefficients m_{kpi} and m_{kci} can be found in a simple way. Under the same assumption, especially for systems of line ruptures, they can also be used to find some force resultants by means of observed changes in W or f for corresponding changes in the parameters t_k.

Thus, a restraint force in the extreme solution may be found by means of a further change of parameters, which violates the movement conditions for the external rigid bodies, so that this force makes a contribution to the work W. In this way an explicit calculation of force resultants along line ruptures may be saved. It is a provision, of course, that the rupture figure permits a movement of the restraint in question by a continuous (infinesimal) change of parameters. In some cases an additional (secondary) rupture figure

may have to be introduced in the rigid bodies of clay to obtain this, cf. Sec. 441. It should be noticed, however, that when the rupture figure does not represent a possible or a quasi-possible solution, forces doing no work during the movement may not be uniquely determined. This is because the equilibrium conditions (2440-3) are not all satisfied (only the weighted combinations (2437-8) are) so it may make a difference which force resultants are used to calculate the required restraint forces. Correspondingly, if the work equation is used, it may make a difference what parameters are used to make the restraint force contribute to the total work.

In order to find a unique calculation result, and at the same time the best possible approximation, one should as a rule, after a parameter has been changed, find the set of values for the other parameters that gives again an extreme solution. By this supplementary extremum condition, that amounts to the consideration of the failure problem as a special member of a more general class of problems, the above mentioned ambiguity is avoided. In certain cases, when secondary rupture figures have to be introduced, the condition may demand that the primary rupture figure is made more general by the introduction of supplementary free parameters.

Possible external parameters and geometrical design quantities will change the failure problem, and will also change the set of parameters t_k which corresponds to the extreme solution. In principle all such parameters should therefore be estimated beforehand, after which the rupture figure is calculated, and the extreme solution is found. This process is repeated with different sets of the external parameters, each set being determined from the preceding ones and from the corresponding extreme solutions, by means of an iteration routine, until all conditions have been satisfied.

In practice it is frequently possible to make some short cuts in this procedure. Thus, the extreme solution for the external and internal parameters may frequently be found in the same operation, where also the design conditions are satisfied simultaneously with the other equilibrium conditions. It may even be possible to revert the calculations, so to speak, in that only a group of the initial parameters is varied. For each solution, which is the extreme one relative to this group, it is determined what failure problem it solves, i.e. for which combination of the external and design parameters it is the extreme solution. By such short cuts a considerable amount of calculation work may be saved under favourable circumstances.

Example 24 c

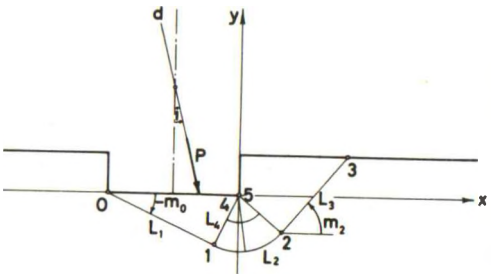

Fig. 24 F: Approximate Rupture Figure (SfPfS) with Two Straight Line Ruptures and a Simple Radial Zone.

Consider the problem of a strip foundation below the clay surface (Fig. 24 F). We assume the line of attack d for the foundation load to be given, f. inst. by a restraint bar between two hinges in controlled strain. It may be excentric and inclined in relation to the foundation. For the sake of simplicity we neglect the volume forces, and the vertical faces of the foundation are assumed to be unloaded free surfaces (i.e. the foundation is thin and rigid and is placed at the bottom of an excavation).

This problem can be investigated by means of a number of different rupture figures, all of them having possible rupture zones. In all cases the failure load P, equal to the restraint force, is also equal to the force between the foundation and the clay (i.e. the forces Q^e_{pi} are zero). The fixed velocity components w^o_{pi} corresponding to a unit elongation of the restraint bar, can be taken as a unit translation parallel to this bar. The two other movement rates b_{pif} can be taken as a translation perpendicular to the bar, and a rotation around any point, f. inst. the lower hinge, of the bar. The corresponding remaining equilibrium conditions are respectively a projection and a moment equation.

Assuming that no sliding takes place between the foundation and the clay one of the simplest rupture figures is shown in Fig. 24 F. It consists of a simple radial zone and two line ruptures separating three rigid bodies of clay. It has only two free parameters: $m_o = m_1$ and $m_2 = m_3$. There are 5 equilibrium conditions (corresponding to $n_f = 2$, $n_{cs} = 0$, and $n_{cf} = 1$). The movements of the clay bodies are pure translations with the velocities

$$u_c = \frac{1}{\sin(i - m_o)} \qquad (2444)$$

when $d_1 = 1$. The derivatives with respect to m_2 correspond to a translation for the free clay body perpendicular to its sliding direction (zero movement for the foundation). With respect to m_o we get a translation for the foundation perpendicular to the restraint bar (magnitude $1/\sin^2(i - m_o)$),

combined with a velocity increase $\Delta u_c = \cot(i - m_o)/\sin(i - m_o)$ for the free clay body. Thus, after using the work equation:

$$P = \frac{c}{\sin(i - m_o)} (L_1 + L_3 + 2 \Delta m L_4) \qquad (2445)$$

(because $\sigma_{(1)} = \sigma_{(2)} + 2c \Delta m$, where $\Delta m = m_2 - m_o$) we may find the optimal solution by varying m_o and m_2 either until a minimum of P has been found or until:

1. the total force component for the free clay body perpendicular to its sliding direction is zero,
2. the total forces for the foundation with adhering clay body, perpendicular to d (positive upwards), plus $\cos(i - m_o)$ times the total forces for the free clay body in the sliding direction are zero,

using Brinch Hansen's boundary condition for the end point (3) of the line rupture.

If it is required to find the positive bending moment in the foundation at the point of attack for P (which can be considered as a restraint force), a secondary zone rupture must be introduced in the adhering clay body in order to permit movements of the corresponding restraint (a hinge), cf. Ex. 44a. A movement in the hinge may now be realized by the introduction of a difference of curvature between the two parts of L_1, one of which becomes the boundary to the zone rupture. However, the difference being known from the imposed rotation of the hinge, the absolute values of the curvatures should be found by the extremum principle. This will for excentric loads give an overall curvature of L_1 (and thereby for L_3). Thus, in order to avoid inconsistencies the rupture figure shown in Fig. 24F cannot be used to solve the bearing capacity problem, if it is also required to find the bending moment in the foundation. At least one further parameter (a common radius of curvature for L_1 and L_3) must be introduced in this case.

Example 24d

As mentioned above Eq. (2437-8) represent, by the principle of virtual displacements, the most general form of all possible equilibrium equations for the rigid bodies. The two equations can be used to check the equilibrium conditions and also to find the forces which do no work during the movement. In the last mentioned case a variation must be used which violates the deformation condition, the restraint force of which is desired.

This use of the work equation has no special importance in quasi-pos-

sible or possible solutions for boundaries to rupture zones, where the stress resultants are calculated in order to find the deformation work. Evidently (2437-8) are then simply a combination of equilibrium equations for the same stress resultants, and these equations might as well be used directly. However, for rupture figures consisting mostly of line ruptures we may by this method avoid the calculation of the stress resultants. They are not used for the deformation work, cf. (2426), and by (2437-8) we consider changes in the deformation work.

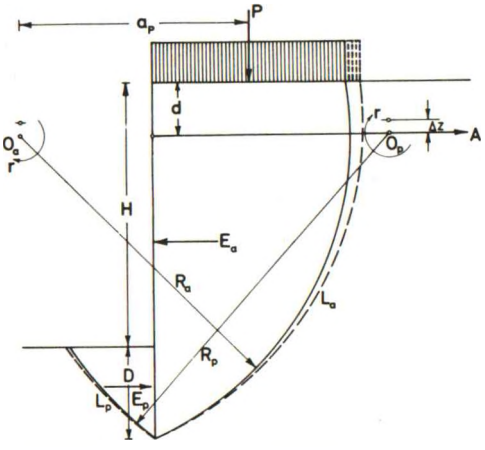

Fig. 24G: Smooth Anchored Sheet Wall Investigated by Simple Line Ruptures (A).

Thus, for the perfectly smooth sheet pile wall shown in Fig. 24G assume that the height H of the earth front, and the depth d of the anchor level are given. Using a rupture figure consisting of two line ruptures we find that for kinematical reasons the two centres O_a and O_p must be located in the anchor level in order that the movements of the two rigid bodies of clay and of the wall shall be compatible.

For any given position of O_a and O_p the total deformation work is evidently, the rotation r being the same for the two clay bodies:

$$W_d = r\,c\,(R_a L_a + R_p L_p) \quad (2446)$$

This must at failure be equal to the work done by the other forces acting upon the moving clay bodies, including f.inst. $W_P = r\,P\,a_P$ for the resultant of the surface loading. If the resulting work equation is divided through by the common factor r, we get a combined moment equation for the two clay bodies.

If D is given the stability of the construction is investigated by ascertaining that the minimum of W or f is positive. In design problems D is determined as the value for which the work equation is satisfied exactly, i.e. the value for which the minimum of $W = W_d - W_P$ etc. is exactly zero. By (2437) this is seen to be the value of D for which both equations of vertical projection for all forces acting upon each of the two clay bodies are satisfied (an infinitesimal horizontal movement of a rotation centre, keeping r constant, corresponds to a vertical translation of the rigid body).

If from the same extremum position the two centres are moved through the distance Δz in the vertical direction we may calculate the new rupture figure shown with dotted lines in Fig. 24G (including the increase in both P and a_P, but keeping r unchanged). Considering the differences $\Delta W_a = \Delta(r\,c\,R_a\,L_a) - \Delta(r\,Pa_P)$ etc., and $\Delta W_p = \Delta(r\,c\,R_p\,L_p)$ - etc., we can find the total earth pressures E_a and E_p, and the anchor force A, by the equations corresponding to (2437):

$$E_p = \frac{\Delta W_p}{r \Delta z}$$

$$E_a = \frac{\Delta W_a}{r \Delta z} \qquad (2447)$$

$$A = E_a - E_p$$

The positions of E_a and E_p can be obtained by using also the moment equations (the differential work equations for an increase in r for one of the rigid bodies and the wall). Notice that all calculations of σ or stress resultants can be completely avoided in this example. (A better accuracy is obtained in practice if E_p, E_a etc. are determined as the mean of values calculated from both a positive and a negative value of Δz with the same absolute magnitude, finding in each case the positions of O_a and O_p for which the vertical projections are satisfied exactly).

246 Possible and Quasi Possible Solutions

Solutions which are found by means of rupture figures with a sufficient number of initial parameters, so that (2440-3) can be used directly instead of the extremum condition, are called possible if they have no singular points on the line ruptures. If this condition is not maintained they might be called quasi-possible. These types of solutions form a subfamily of the admissible solutions with possible zones. The mathematically correct solution is evidently contained in this subfamily.

This does not mean, however, that solutions of this type will always be very complicated. On the contrary, most of the simple rupture figures treated by Brinch Hansen (except f. inst. AfPfA) do in fact correspond to possible or quasi-possible solutions, cf. Fig. 21 B. The same figure also shows an example of the great difference in calculation work one may have between a quasi-possible and a possible solution to the same failure problem (A and Cf (XfRsAaR)).

It also does not mean that a possible or quasi-possible solution will necessarily give a better approximation than an admissible solution with possible zones to the same failure problem. Thus, instead of the rupture figure AfPfA in Fig. 21 B the figure WPR may be used as a (statically but not kinematically) possible approximation. However, for rotation points of the wall not too far above the top point the admissible solution AfPfA will certainly represent the better approximation, cf. Ex. 42 a and 53 a.

After a possible or quasi-possible solution has been found it will satisfy the conditions No. 1-3 in Sec. 241-2 (except possibly for a finite number of singular points). As for admissible solutions with possible zones it can now be checked whether condition No. 5 is also satisfied. If this is the case, i.e. if $\epsilon \geq 0$ everywhere, the solution is kinematically possible or quasi possible. It is then known to be on the unsafe side, if it is not correct.

Since the equilibrium conditions for the rigid bodies of clay are all satisfied it is also possible to investigate whether the above condition No. 4 is fulfilled. This is done by considering secondary rupture figures on the verge of failure inside the rigid bodies of clay, cf. Sec. 442. If this is the case, i.e. if $\tau \leq c$ everywhere, the solution is statically possible. It is then known to be on the safe side, if it is not correct. The position of quasi statically possible solutions in relation to the mathematically correct one is not known, however.

Solutions which are both kinematically and statically possible are correct, or they will only differ from the correct solution in the way indicated in Sec. 242. Correspondingly quasi correct solutions may be defined as solutions which are both quasi kinematically and statically possible. They are known to be on the unsafe side, if they are not correct.

The method of possible solutions is the most selective solution method which can be chosen. For any given rupture figure permissible under the method it can only be ascertained after the calculations have been performed whether it is correct or not. If it is not correct another rupture figure must be chosen to the same failure problem. The results of the checks on kinematical and statical possibility will usually give some hints about how the first rupture figure must be changed in order that a closer approximation shall be obtained.

Thus, if $\epsilon < 0$ in a domain of a rupture zone, the correct solution will frequently have a rigid body of clay instead of a zone in this domain. Correspondingly, if $\tau > c$ in a rigid body of clay, this body will usually vanish, or will be divided into a number of rigid bodies, separated by line ruptures

and/or rupture zones. In the same way line ruptures with singularity points in quasi-possible solutions will frequently correspond to radial zones, arc zones or constructions as shown in Fig. 21 B in the correct solution. The problem of constructing rupture figures is considered in Chap. 5.

Example 24 e

The approximate solutions considered in the preceding sections can be summarized as follows.

I. Solutions defined by means of a rupture figure.
The geometrical parameters of the rupture zones and line ruptures form the basis of calculations.

A. Possible zones.
Equilibrium conditions, $\tau = c$, $\theta_s = \theta_d$, and constant volume.

1. Rigid bodies in equilibrium.
Sufficient number of variable parameters.

a. Possible solutions.
No singular point (with $\tau > c$) on line ruptures or rupture boundaries.

i Mathematically correct solutions.
$\epsilon \geq 0$ in zones, $\tau \leq c$ in rigid bodies.
correct

ii Kinematically possible solutions.
$\epsilon \geq 0$ in zones, $\tau > c$ or not proved.
unsafe

iii Statically possible solutions.
$\tau \leq c$ in rigid bodies, $\epsilon < 0$ or not proved.
safe

iv Unproved possible solutions.
Both τ and ϵ incorrect or not proved.
not known

b. Quasi-possible solutions.
Singular points with $\tau > c$ permitted.
i Quasi correct solutions.
$\epsilon \geq 0$ in zones, $\tau \leq c$ except at singular points.
unsafe

ii Quasi kinematically possible solutions.
$\epsilon \geq 0$, $\tau > c$ more extended or not proved.
unsafe

iii Quasi statically possible solutions.
$\epsilon < 0$ or not proved, $\tau \leq c$ except at singular points.
not known

iv Unproved quasi-possible solutions.
Both τ and ϵ incorrect or not proved.
not known

2. Corrective forces on rigid bodies (kinematically admissible movements). Deficiency of parameters (work equation must be used).

a. Kinematically possible zones.
$\epsilon \geq 0$ everywhere.
unsafe

b. Quasi kinematically possible zones.
$\epsilon < 0$ or not proved.
not known (mostly unsafe)

B. Statically possible zones with approximate movement conditions.
Equilibrium, $\tau = c$, and constant volume in the mean.

1. Rigid bodies in equilibrium.
Sufficient number of variable parameters.

a. Statically admissible solutions.
No singular point and $\tau \leq c$ everywhere.
safe

b. Quasi statically admissible solutions.
Singular points and/or $\tau > c$.
not known

2. Corrective forces on rigid bodies.
Deficiency of parameters (work equation must be used).
not known (mostly unsafe)

C. Statically possible zones with disregarded movement conditions. Only equilibrium and $\tau = c$ (arbitrary geometrical conditions).

1. Rigid bodies in equilibrium.
   Sufficient number of variable parameters.

   a. Statically admissible solutions.
      No singular point and $\tau \leq c$ everywhere.
      safe

   b. Quasi statically admissible solutions.
      Singular points and/or $\tau > c$.
      not known

2. Corrective forces on rigid bodies.
   Deficiency of parameters (arbitrary choice of equilibrium conditions).
   not known

D. Quasi admissible zones.
   Arbitrary zone boundaries, equilibrium only as a whole.

1. Clay domains in equilibrium.
   Sufficient number of (purely geometrical) parameters.
   not known (mostly safe)

2. Partial equilibrium of clay domains.
   Deficiency of parameters. Only some chosen conditions satisfied.
   not known

E. Kinematically possible zones.
   Constant volume and compatibility with rigid body movements.
   unsafe

II. Solutions defined by means of a velocity field.
   Kinematically admissible solutions.
   unsafe

III. Solutions defined by means of an (analytical) stress distribution.
All equilibrium conditions are satisfied.

A. Statically admissible solutions.
$\tau \leq c$ everywhere.
safe

B. Quasi statically admissible solutions.
$\tau > c$ somewhere (or not investigated).
not known

For the sake of completeness the list of solution methods has been extended to cover (almost) all cases that can reasonably be used in practice. For each method it is indicated whether solutions obtained by the method are safe or unsafe, when not correct, if this can be deduced. The following points should be noticed.

1. For the assumptions of this work the solutions with possible zones, items I A, can be applied to all problems in practice. In this case, therefore, it will hardly ever give any significant advantage to use less well defined solutions.

2. The method of statically admissible solutions may sometimes be utilized, however, when solutions to other, closely related problems are available (I B 1 a, I C 1 a and III). For a rough orientation some variants with statically possible zones (I B and I C) may also sometimes be useful (cf. Sec. 444). For other assumptions, f.inst. soils with internal friction, they may even represent the only available solution methods.

3. The method of kinematically admissible solutions is mostly used for inhomogeneous clays, and for problems in three dimensions. In the general case the defining velocity field may be given analytically (II), but in some types of plane problems it may be an advantage to consider kinematically possible zones (I E). They are based on the net of strain characteristics across the zone, which may facilitate the calculation of the deformation work in the zone, but the equilibrium conditions are not used.

4. The solutions with quasi admissible zones mentioned under I D are very close to some approximate solutions in soil mechanics. Notice, however, that even this method when used on rupture figures that

correspond closely to the correct ones may give very accurate results; cf. f.inst. Brinch Hansen's method for the calculation of zone ruptures [1953]. As a corollary, possible solutions may give rather poor approximations if $\epsilon < 0$ in major points of the zones, or if the supposed rigid bodies of clay are highly unstable (i.e. if the assumed rupture figure is very unlike the correct one).

As a conclusion it may be stated, that obviously the most important thing is to choose the approximate rupture figure (or velocity field, or stress distribution) in a reasonable way so that it corresponds as closely as possible to the correct solution. Under this condition the solution will of course be better the more closely all mathematical conditions are satisfied.

Consequently, in the following chapters of this work the so-called admissible solutions with possible zones, items I A above, are assumed to be used.

Example 24 f

The scope of the method of admissible solutions with possible zones is rather great, as can be seen from the number of different rupture figures that can all be used to give a solution to the bearing capacity problem considered in Ex. 24 c (Fig. 24 F). The most important examples are shown in Fig. 24 H (to be considered in more details in Chap. 4 and 5).

It is assumed that tractions cannot be taken between the foundation and the clay, so that either $\sigma_n \geq 0$, or the foundation will lift away from the clay surface.

The first example, letter a on Fig. 24 H, is a simple line rupture, L_1, as it is used in ordinary stability investigations. It can be used when, as in this example, there are two free movement parameters for the foundation. The rigid body of clay above L_1 is assumed to remain fixed upon the foundation, so the movement of the foundation is determined directly by the geometrical parameters of L_1. It will be a permissible movement when the centre O_1 is not located on the line of attack for the foundation load.

The two remaining equilibrium conditions for the foundation and the attached rigid body of clay correspond to the two parameters of L_1 (f.inst. the inclination of the chord and the centre angle, or the two coordinates to O_1). The solution is therefore quasi-possible (the end point A of the line rupture is a singular point), and the equilibrium method can be used as an alternative to the extremum method, as pointed out by Brinch Hansen. When the stresses in the rigid body of clay are investigated, they are found to ex-

ceed the failure condition, however, both in the vicinity of A and across a section from the corner of the foundation to L_1.

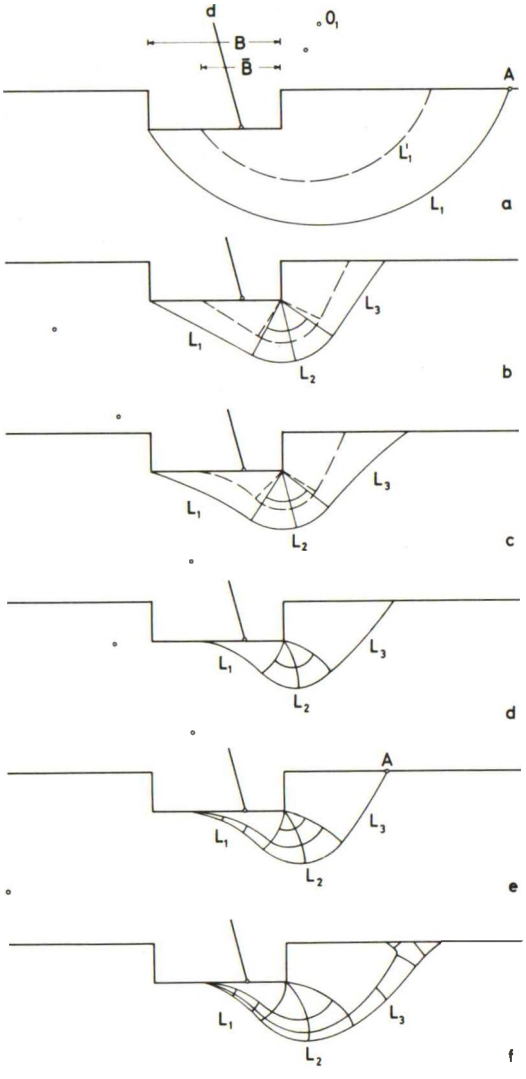

Fig. 24H: Admissible Solutions with Possible Zones to One-sided Bearing Capacity Problem.

This solution will be rather far off on the unsafe side. A better approximation, which is not kinematically admissible, however, can be obtained by a line rupture L_1' corresponding to an imaginary, centrically loaded foundation (with the width $\bar{B}$ symmetrically situated in relation to the intersection point between the line of attack and the foundation level). This modification will evidently be on the safe side.

The solution b on Fig. 24 H is the one considered in Ex. 24 c. It has also two parameters, but now there are two rigid bodies of clay, so there are 5 equilibrium conditions. The solution is admissible with a kinematically possible zone. Notice that the foundation load P must be found by the work equation (2426), cf. (2445). It will not give the same result to use an equation of projection for the rigid body of clay adhering to the foundation, or for the stress resultants along the lower boundary of the rupture figure (after the normal stresses have been found by means of Brinch Hansen's boundary condition).

The same rupture figure can be used if the foundation has a known direction of translation (but not if it has a known point of rotation). The restraint forces, a moment and a force perpendicular to the direction of translation, may in this case be determined by the equilibrium conditions, but again it makes a difference whether the stress resultants along the boundary to one rigid body of clay, or along the whole lower boundary of the rupture figure, are used. Correspondingly, if (2437) is used it makes a difference whether m_o is varied alone or together with m_2, cf. Fig. 24 F. Therefore, the best thing to do is to vary m_o and for each value of this quantity to find the value of m_2 that corresponds to a minimum of P. The approximation can also be improved in this case when an imaginary, centrically loaded foundation is assumed.

As shown under c in Fig. 24 H one further parameter can be introduced by assuming the line ruptures L_1 and L_3 to be circle arcs instead of straight lines. For kinematical reasons the radii of curvature R_1 and R_3 must be equal. In this way a rupture figure XfPfX (or AfPfA) is obtained instead of SfPfS. It has 3 initial parameters against 5 equilibrium conditions.

The approximation may be improved by assuming the foundation width $\bar{B}$ as under a. A more effective improvement is obtained by permitting the radii of curvature R_1 and R_3 to become different. We have now 4 parameters, but the movement conditions are only satisfied approximately in the rupture zone. Notice that for kinematical reasons the line rupture L_1 must either pass through the further corner of the foundation, or must have a

horizontal tangent at the foundation level.

A solution of this type may be made admissible with a possible zone by assuming curved radial zone boundaries. As shown in Chap. 4 this rupture figure has also 4 parameters against the 5 equilibrium conditions. In this case the coefficients m_{kpi} and m_{kci} in (2437) are rather difficult to calculate. The equilibrium method will therefore not be suitable, although it is perfectly possible to use it.

In e another parameter has been introduced by replacing the line rupture L_1 by a radial zone. This rupture figure has 5 parameters against the 5 equilibrium conditions, so it represents a quasi-possible solution (the end point A of the line rupture L_3 is still a singular point). Hence, the equilibrium method can be used directly, and the extremum principle will not usually be needed.

Finally, the singularity at the point A may be removed by a construction analogous to the one shown in Fig. 21 B, cf. the letter f on Fig. 24 H. This introduces 3 further parameters corresponding to the 3 equilibrium conditions for the small rigid body of clay. Thus, we have 8 parameters against 8 equilibrium conditions (plus one extra parameter to be found by a stress condition). This solution is possible, and is probably the mathematically correct one.

Notice that the rupture figures a-c are all geometrically determined from the parameters in very simple way. In the figures d-f it becomes an increasingly difficult task to compute the rupture zones. Since the number of parameters is also increased the computing time and expense will increase rapidly. Therefore, for the computation work in practice the choice between the 7 (or 9) rupture figures mentioned above must be based on an evaluation of the needed accuracy against the economy. For ordinary practical purposes the choice would probably be limited to the rupture figures b-d.

3 RUPTURE FIGURE ELEMENTS

This chapter deals with the formulation of all concepts, equations, and conditions necessary to calculate the rupture zones and line ruptures in admissible solutions with possible zones.

Thus, a frame of reference is defined for the rupture zones, viz. the so-called slip line field. A number of auxiliary functions related to the slip line field is also defined, and the conditions that they must satisfy in order that the rupture zone shall be possible are derived.

Next, numerical methods for calculating the functions are considered, and the alternative method of chord lengths in the slip line field is introduced. After this the different types of boundary conditions for the rupture zones are expressed in terms of the auxiliary functions, and of the method of chord lengths.

Finally, the special stress conditions for singular points on line ruptures are derived by means of the work equation.

The synthesis of the contents of this chapter into calculation procedures for rupture figures is given in Chap. 4, whereas Chap. 5 deals with the construction of rupture figures to obtain solutions to a given failure problem.

31 BASIC EQUATIONS

311 The Slip Line Field

Every rupture zone can be considered to be covered by the two families of slip lines, the a- and b-lines, which form the so-called slip line field, see f.inst. Hencky [1923], Hill [1950], or Sokolovski [1960]. By the geometric representation of rupture zones the slip lines forming the boundaries of the individual zone elements are usually drawn, and to indicate roughly the stress distribution inside the zones it is customary to draw some of the interior members of the slip line field, forming a net over the zone.

Being stress characteristics, the slip lines are very useful for calculating the stress distribution by means of (2318). These equations can be transformed in a simple way, so that for the clay properties here considered the stress distribution in a rupture zone can be regarded independently of the scale and position of the zone.

This is done by considering a system of curvilinear coordinates with the slip lines as coordinate curves. One possible set of coordinate values (a, b) are related in a very simple way to the stress functions σ and m.

As c is a constant, (2318) can be integrated directly. We get the following relations between the differences in σ and m for any two points on the same slip line:

$$\begin{aligned} &\Delta\sigma + 2c\Delta m = 0 \text{ (for a-lines)} \\ &\Delta\sigma - 2c\Delta m = 0 \text{ (for b-lines)} \end{aligned} \qquad (3101)$$

regardless of the actual arc length between the points, cf. Hencky [1923].

If a mesh OAPB in the slip line net is considered (Fig. 31 A), these relations applied to the corner points give:

$$\begin{aligned} \sigma_P - \sigma_O &= 2c(m_P - m_A) - 2c(m_A - m_O) \\ &= -2c(m_P - m_B) + 2c(m_B - m_O) \end{aligned} \qquad (3102)$$

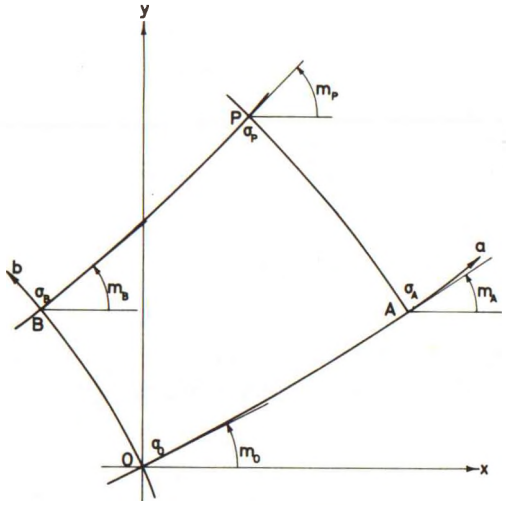

Fig. 31 A: Finite Cell in Slip Line Net.

Besides, evidently:

$$(m_P - m_A) + (m_A - m_O) = (m_P - m_B) + (m_B - m_O) \qquad (3103)$$

from which it can easily be deduced that:

$$\begin{aligned} m_P - m_B &= m_A - m_O = \Delta a \\ m_P - m_A &= m_B - m_O = \Delta b \end{aligned} \qquad (3104)$$

say.

The difference in m along all a-lines with end points on the same two b-lines will therefore be the same. According to (3101) this will also be true for the difference in σ. Correspondingly the differences in m and σ along all b-lines between the same two a-lines will be the same. A number, a, can thus be given to each b-line, and a number, b, to each a-line, so that the difference in m between points on the same a-line, or points on the same b-line, is equal to the corresponding difference Δa in a, or Δb in b.

The rupture zone may therefore be represented in a coordinate system a, b (Fig. 31 B). The reference point O may be chosen arbitrarily, but the values m_O and σ_O of the stress functions at this point determine uniquely the values m_P and σ_P at any other point P with the coordinates a_P, b_P:

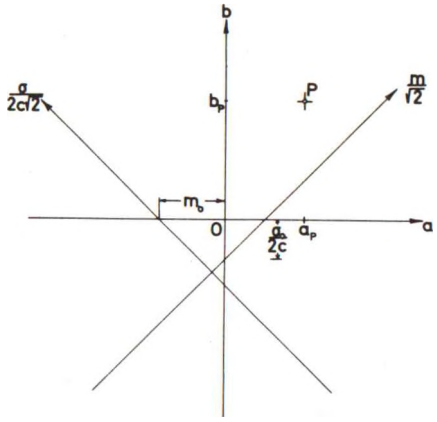

Fig. 31 B: a,b-Coordinate System, Showing Also σ, m-Coordinates.

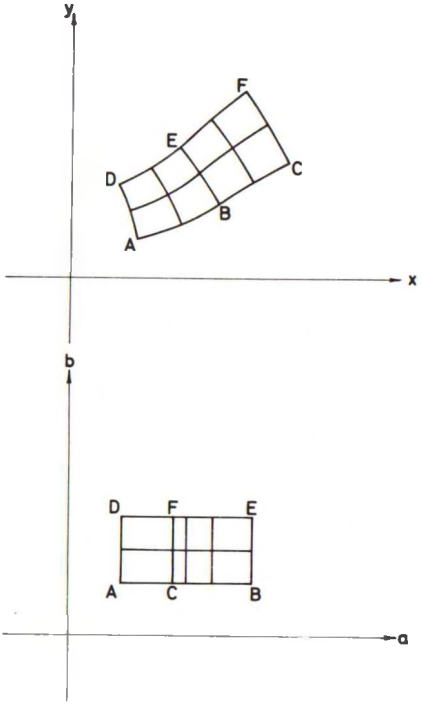

Fig. 31 C: Overlapping Rupture Zone Parts in the a,b-Plane. a-Lines with Points of Inflexion.

$$m_P = m_O + a_P + b_P$$
$$\sigma_P = \sigma_O + 2c\,(b_P - a_P) \qquad (3105)$$

Correspondingly, if m and σ are known for a point (f. inst. a boundary point with known surface loading), its coordinates a, b are given by the equations:

$$a = \frac{m - m_O}{2} - \frac{\sigma - \sigma_O}{4c}$$
$$b = \frac{m - m_O}{2} + \frac{\sigma - \sigma_O}{4c} \qquad (3106)$$

In the a,b-plane one might as well consider an m, σ coordinate system (shown in Fig. 31 B). However, for calculation purposes it is convenient that the characteristic directions are parallel to the coordinate axes. This system is also easier to generalize for more complicated materials. From (3106) it is seen that the stress condition at any point in a rupture zone with a known variation of a and b determines the whole stress distribution without any reference to the coordinate system x,y.

The a,b-plane is not directly suited for the representation of rupture zones, because a point will not in the general case be uniquely determined by its coordinates (a,b). For example, if m is decreasing in the positive direction of a slip line, the corresponding coordinate, a or b, will evidently also be decreasing. Therefore, if a slip line has a point of inflexion the corresponding coordinate will pass through an extremum point. In this way the representation of a normal rupture zone in

the a,b-plane may have overlapping parts (Fig. 31 C).

Furthermore, if f. inst. an a-line is rectilinear between any two b-lines, the same will be true for all a-lines between these two b-lines, and for this interval Δa will be zero. The same holds true for b-lines, so for rupture zones with elements where one or both of the slip line families are rectilinear the representation in the a,b plane will contain zone elements which have degenerated to line segments or points (Fig. 31 D).

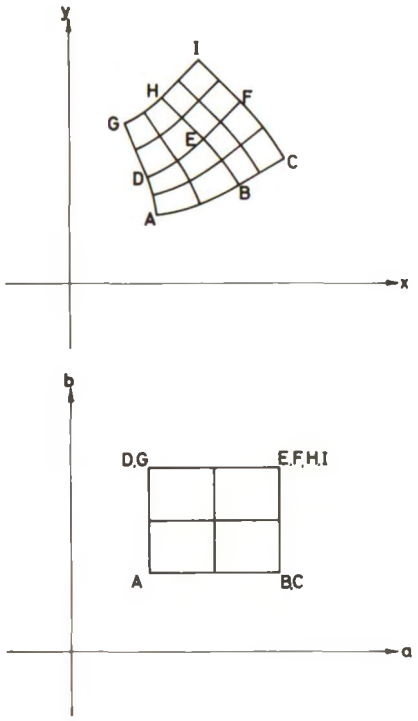

Fig. 31 D: Degenerate Rupture Zone Parts in the a,b-Plane. Straight Slip Line Parts.

Evidently this is inconvenient. Therefore a set of 'dummy' coordinates λ, μ may be used. They are both monotonically increasing in the positive direction of the corresponding slip lines, and they have different values for different b- and a-lines, respectively, so that the coordinate a is a unique function of λ, and b is a unique function of μ. But they have no computational significance, all calculations being still made in relation to a and b (f. inst. derivatives are taken in the form $\frac{\partial f}{\partial a}$ which is understood as

$$\lim_{\lambda \to \lambda_o} \frac{f(\lambda, \mu_o) - f(\lambda_o, \mu_o)}{a(\lambda, \mu_o) - a(\lambda_o, \mu_o)}$$

for the point with dummy coordinates λ_o, μ_o). For practical reasons λ and μ may be taken as real numbers, attaining integer values for the slip lines which are members of the final net to be calculated. The examples shown in Fig. 31 C-D will be simple rectangular zones in the λ, μ -plane.

In the x,y-plane rupture zones cannot overlap, because that would mean two different states of stress for the same point. Therefore slip lines of the same family cannot intersect at interior points of rupture zones. However, singular points may exist on the boundaries of rupture zones, as intersection points of all slip lines of one family. They can be regarded as a limiting case where a slip line of the other family has zero arc length but

a finite difference in m between the two end points. It has therefore degenerated to a single point. In this way a so-called radial zone is obtained (Fig. 31 E). It is represented in the λ, μ-plane (and also in the a, b-plane) by a simple rectangular zone.

Since line ruptures are also stress characteristics a rupture figure type can be indicated in a unique way by a drawing in the λ, μ-plane. The values of a and b corresponding to the characteristic points are different for different rupture figures of the same type, so the main purpose of the type sketch is to show the types and relative positions of the constituent rupture zones and line ruptures.

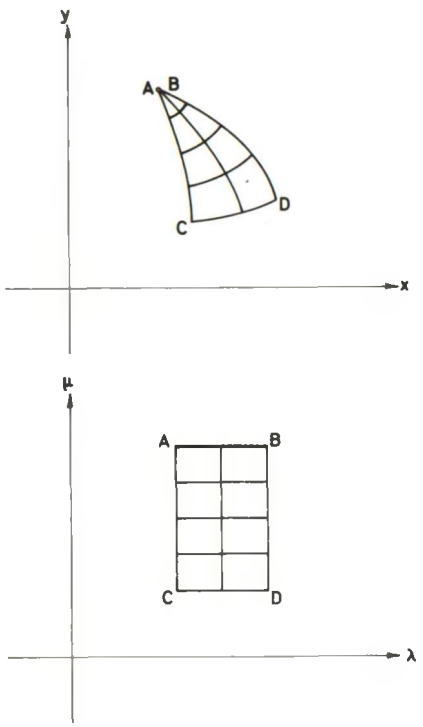

Fig. 31 E: Radial Zone with Singular (Vertex) Point A = B.

To define the rupture figure completely the different types of zone and boundary elements may be indicated by special signs. For example

1. Free surfaces by double lines.
2. Slip lines with a known geometrical position (singular points in radial zones) by heavy lines, cf. Fig. 31 E.
3. Boundaries to external rigid bodies (walls) by double dotted lines.
4. Slip line boundaries to rigid bodies of clay by heavy dotted lines, when slidings are assumed to take place, otherwise by thin full lines.
5. Points with a known position by large filled circles. Points which are known to be located on a given curve (f. inst. a free surface or a wall) by smaller filled circles. Other characteristic points by small open circles.

Signs for other types of zone elements will be indicated as necessary. Besides, the direction of a possible sliding of an external rigid body upon the clay may be indicated by a number e_t, which is zero if no sliding takes place, +1 if a sliding occurs with $\tau_{nt} = +c_a$, and -1 if $\tau_{nt} = -c_a$ (the two

last cases also for rupture zones; τ_{nt} is measured in a local system of coordinates, the direction of which follows from the fact that the orientation of the clay boundary encircles the clay domain in the negative direction of rotations).

In the λ, μ-plane a and b should be one valued functions of λ and μ, respectively. Therefore, it may not be possible to draw the whole rupture figure on one sheet, unless branch cuts are assumed in the plane.

Example 31 a

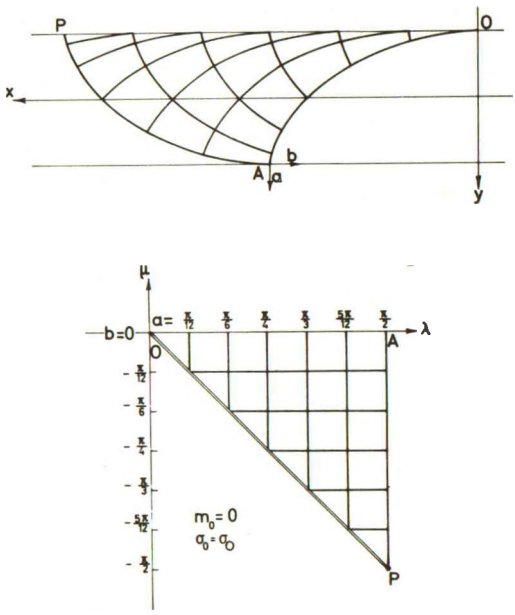

Fig. 31 F: Sloping Clay Layer. Representation of the Rupture Figure in the λ, μ-Plane.

For the zone rupture considered in examples 23 a and b (Fig. 23 H) we have in the passive case m-values between 0 and $\frac{\pi}{2}$. Taking the positive slip line directions as shown in Fig. 31 F we get the representation in the λ, μ-plane as shown in the second figure. Notice that in this case where the net spacing is equidistant in m we could as well use the original a,b-coordinate system.

Example 31 b

In the classical Prandtl-solution for the bearing capacity of a smooth strip foundation on a horizontal clay surface (Fig. 31 G) the representation in the a,b-plane would degenerate into two line segments. In the λ,μ -plane the structure of the zone-rupture can be described completely.

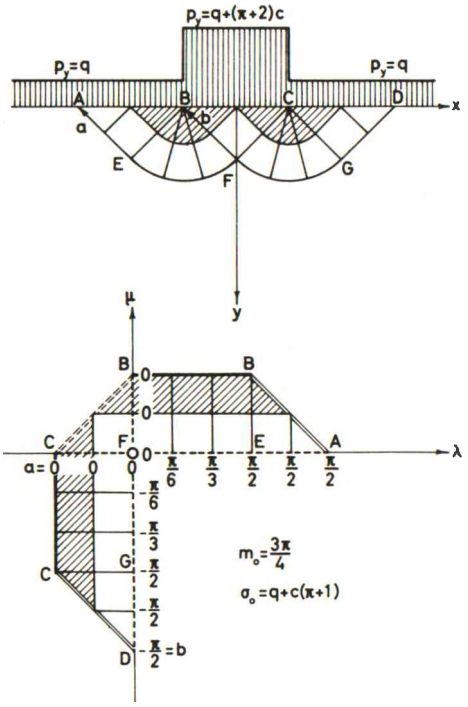

Fig. 31 G: Prandtl Solution for Bearing Capacities. Representation of the Rupture Figure in the λ,μ -Plane.

Notice that in the figure the positive direction of rotations is taken to be clockwise. m is accordingly measured clockwise from the positive direction of x to the positive direction of a. The symmetric position of the rupture figure in relation to the λ,μ coordinate system is obtained by choosing $m_O = \frac{3\pi}{4}$. The value of σ_O for this representation is found from (3105) by noticing that $\sigma_A = \sigma_D = q + c$, because at these points $p_y = \sigma_3 = \sigma - c$. Along BC we have $p_y = \sigma_1 = \sigma + c$.

According to Hill [1950] only the part of the rupture figure shown shaded in Fig. 31 G will actually be developed under a smooth foundation. Under a rough foundation the whole figure will be developed, but then the domains AEB, CGD, and BFC will remain rigid. The two first mentioned domains will be on the verge of failure, but this need not be the case for the last mentioned one. The stress distribution will here in principle be unknown (except for two limiting cases, one of which is shown on the figure, used for the calculation of bending moments in the strip foundation). However, the point F must still be a transition point (indicated by a large open circle), separating two rupture zones, and with the same values of m and σ determined from each of the two zones.

The velocity field in the rupture figure is to a certain degree undetermined. However, to obtain $\epsilon \geq 0$ everywhere in the rupture figure it must

correspond to a pure translation of the strip foundation (supposed rigid). The direction of movement for the foundation may deviate an arbitrary angle θ in the interval $-\frac{\pi}{4} \leq \theta \leq \frac{\pi}{4}$ from the y-axis.

Example 31 c

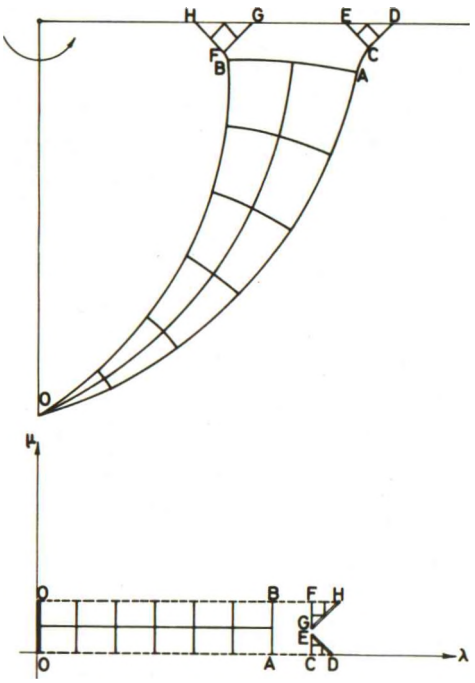

Fig. 31 H: Curved Radial Zone with a Surface Zone Complex. Representation in the λ, μ-Plane.

In Fig. 31 H is shown the rupture figure in the clay behind a vertical, perfectly smooth wall rotated about its upper point (calculated by Ole Steen [1961]). The representation in the λ, μ-plane shows that in order to avoid overlapping zone elements, and to emphasize that f. inst. the b-lines CE and FG may correspond to different values of a (in fact, the differences in a between A and C and between B and F will have different signs) a branch cut must be assumed to exist between the points E and G, extended in a Y-form ending at the points A and B. Alternatively, the constructions ACDE and BFGH may be drawn on two separate sheets of the λ, μ-plane. This will be necessary f. inst. when the figure is to be represented in a numerical form on an input data sheet for a computer.

Notice that to each rupture figure type corresponds a typical figure in the λ, μ-plane. Different rupture figures of the same type are distinguished by different values of a and b corresponding to the coordinates λ and μ, and different values of m_o and σ_o. For typographical reasons it may be practical to represent a type by a string of letters; in Brinch Hansen's terminology the type shown in Fig. 31 H might be termed: Cf (XfRsAaR), where C indicates a radial zone with curved radial slip lines. Alternatively a two-dimensional array of letters might be used as a sort of literal transcription of the figure in the λ, μ-plane, f. inst.:

$$\begin{array}{lll} LCa & & R \\ C \quad Ca = L & Cb = L & \\ LCb & R & \end{array} \qquad (3107)$$

where Ca and Cb (introduced in order to avoid an overlapping of letters in the array) are zone complexes of the type AaR and XfR, respectively. For a very useful class of relatively simple rupture figure types letter strings or letter arrays may characterize the different types in a simple way.

For more complicated rupture figures they become rather unwieldy, however, so they are not of much practical use for a general description of rupture figure types.

312 Radii of Curvature

In order to construct the rupture zone in the x,y-plane it is necessary to describe in some way the relations between this plane and the a,b-coordinates.

One possible way to do this is to use the local scale factors which for each point give the relation between arc length elements and differences in a and b, cf. Hencky [1923].

Thus, the two functions R and S may be defined by the equations:

$$\begin{aligned} R &= \frac{ds_a}{da} \\ S &= \frac{ds_b}{db} \end{aligned} \qquad (3108)$$

considering f. inst. s_a as a function of a with b as a parameter.

Because the differences in a and b are by definition differences in m, i.e. in direction angles to tangents, R and S are seen to be the radii of curvature for the two slip lines through the point in question (Fig. 31 I). They are positive when a and b increase in the positive slip line directions.

When R and S are known as functions of λ and μ, and therefore of a and b, the coordinates to any mesh point in the net can be found by direct integration, using the equations:

$$\begin{aligned} dx &= ds_a \cos m = R \cos m \, da \\ dy &= ds_a \sin m = R \sin m \, da \end{aligned} \qquad (3109a)$$

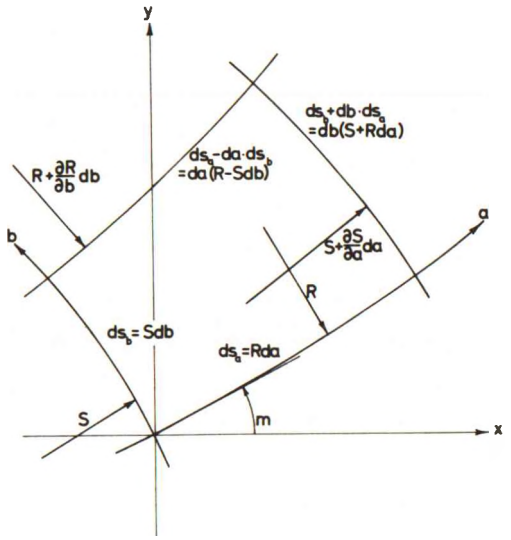

Fig. 31 I: Radii of Curvature and Arc Length Increments for a Cell Element in the Slip Line Net.

for a-lines, and

$$dx = -ds_b \sin m = -S \sin m \, db$$

$$dy = ds_b \cos m = S \cos m \, db \qquad (3109\,b)$$

for b-lines.

From (3109) we may find:

$$\frac{\partial^2 x}{\partial a \partial b} = \frac{\partial (R \cos m)}{\partial b} = \frac{\partial R}{\partial b} \cos m - R \sin m$$

$$= -\frac{\partial (S \sin m)}{\partial a} = -\frac{\partial S}{\partial a} \sin m - S \cos m \qquad (3110)$$

and also

$$\frac{\partial^2 y}{\partial a \partial b} = \frac{\partial (R \sin m)}{\partial b} = \frac{\partial R}{\partial b} \sin m + R \cos m$$

$$= \frac{\partial (S \cos m)}{\partial a} = \frac{\partial S}{\partial a} \cos m - S \sin m \qquad (3111)$$

because $\frac{\partial m}{\partial a} = \frac{\partial m}{\partial b} = 1$. As the two expressions in each equation must be identical for all values of m, we must have

$$\frac{\partial S}{\partial a} - R = 0$$

$$\frac{\partial R}{\partial b} + S = 0 \qquad (3112)$$

The same result can also be obtained by simple geometry, cf. Fig. 31 I. For example, the first equation (3112) is obtained by expressing that $(S + dS)\, db = ds_b + \Delta ds_b$, retaining only first order increments.

Equations (3112) may be integrated numerically as a preliminary to the calculation of coordinates by (3109). By direct integration one obtains from (3108):

$$\Delta S = \Delta s_a$$

$$\Delta R = -\Delta s_b \qquad (3113)$$

along any a-line, and b-line, respectively.

It is evident that along any a-line S must have the same sign throughout the rupture zone, in order that neighbouring slip lines shall not intersect. For different a-lines, S may have different signs, however. It follows from (3113) that S at any point of a rupture zone must not be numerically smaller than the arc length along the a-line from the point to the boundary of the zone, measured in the positive or negative direction of s_a according to whether S is negative or positive. The corresponding statement is true for the variation of R along b-lines.

For a linear segment of an a-line R is infinite, and correspondingly S is infinite for linear segments of b-lines. (3112) cannot be used in these cases, but (3113) is still valid. According to (3104) if an a-line is linear between any two b-lines, all other a-lines will also be linear between the same two b-lines. From Fig. 31 I it is seen that all these line segments will have the same length Δs_a, and from (3113) it follows that the increase ΔS_a in S along all a-line segments will be the same, and will be equal to Δs_a. It will always be positive in the positive a-direction.

This corresponds to a discontinuity for S along a b-line in the a,b-plane (not in the λ, μ-plane, however), and the derivative $\frac{\partial S}{\partial a}$ will be infinite. From (3113) it is seen that discontinuities in S along a-lines are also possible ($\frac{\partial S}{\partial b}$ infinite). Thus, S may be different on the two sides of an a-line (f. inst. the line BF in Fig. 31 G). It is seen, however, that the jump ΔS_b must be the same along the whole a-line; it may have either sign. Correspondingly, for linear b-line segments we have S infinite, and $\Delta R_b = -\Delta s_b$,

always negative in the positive b-direction. Besides R may be discontinuous in the a-direction along any b-line. There are no restrictions on the sign or magnitude of ΔR_a.

It is a disadvantage by the use of R and S that they may become arbitrarily large, even infinite, and also that they have to be calculated with a rather high accuracy if equations (3109) are to give consistent results. Therefore these functions are not well suited for preliminary, rather rough calculations. On the other hand, the functions R and S are invariant to arbitrary translations and rotations of the coordinate system, so zone elements may be calculated and tabulated without any regard to their position in the x,y-plane.

Example 31 d

Considering again the zone rupture shown in Fig. 23 H, we get from (2324) and (2325):

$$\frac{\gamma \sin\beta}{c} \frac{dx_a}{dm} = 4 \cos^2 m = \frac{\gamma \sin\beta}{c} R \cos m$$
$$\frac{\gamma \sin\beta}{c} \frac{dx_b}{dm} = -4 \sin^2 m = -\frac{\gamma \sin\beta}{c} S \sin m \qquad (3114)$$

so that for this zone rupture we have:

$$\frac{\gamma \sin\beta}{c} R = 4 \cos m = 4 \cos(a + b)$$
$$\frac{\gamma \sin\beta}{c} S = 4 \sin m = 4 \sin(a + b) \qquad (3115)$$

It is seen that these two functions satisfy (3112). Both functions are continuous throughout the zone, but at the two boundaries corresponding to the surface for $\tau_o = -c$, and the rock surface when the sliding condition (2313) is satisfied exactly, we have a special case with S, respectively R equal to zero, and the other radius of curvature finite.

This case, where the boundary is an envelope to the slip line field, is normal for boundaries to rigid bodies with $c_a = c$ (provided a full zone rupture and not only a single line rupture is developed along the boundary).

Mathematically such envelope curves are characterized by the fact that in the general case the determinant of coefficients in (2314) is zero (i.e. $\psi = m$ or $\frac{\pi}{2} + m$ plus an integer multiple of π), but the rank of the augmented matrix of coefficients is four (i.e. (2317) is not satisfied, cf. (2332)). They will therefore represent singular cases with infinite derivatives of σ

and θ (except in the direction of the curve).

Reverting to the original equilibrium equations (2307) we find, however, that the stress derivatives used here are perfectly normal. In the local t,n coordinate system (cf. Fig. 22 B) τ_{nt} will be $\pm c$, and $\frac{\partial \tau_{nt}}{\partial n} \neq 0$. The rupture zone cannot therefore be continued through such a curve. It will normally be a boundary curve to an external rigid body (where τ may be greater than c). In certain special cases, however, it may conceivably be a boundary to a rigid body of clay. Such cases are very rare, and will not be considered further in the following.

313 Equivalent Coordinates

Alternatively the coordinates may be calculated by means of another set of sectionally smooth functions of a and b, the so-called equivalent coordinates $\bar{x}$ and $\bar{y}$ that are attributed to Mikhlin, cf. Hill [1950].

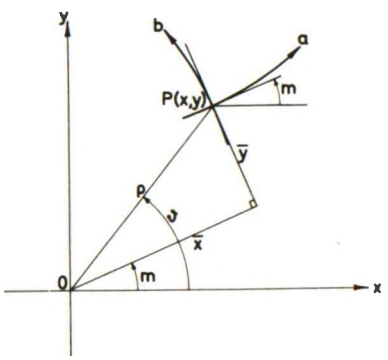

Fig. 31 J: Equivalent Coordinates to a Point in a Rupture Zone.

As shown in Fig. 31 J they are defined for any point P in the rupture zone from the coordinates x,y of P, and the value of m at P, by the equations:

$$\begin{aligned} \bar{x} &= x \cos m + y \sin m \\ &= \rho \cos (\vartheta - m) \\ \bar{y} &= -x \sin m + y \cos m \\ &= \rho \sin (\vartheta - m) \end{aligned} \qquad (3116)$$

where ρ, ϑ are polar coordinates in the x,y-plane.

Correspondingly, if the equivalent coordinates $\bar{x}, \bar{y}$ are known for a point, where also m is known, the coordinates are given by:

$$\begin{aligned} x &= \bar{x} \cos m - \bar{y} \sin m \\ y &= \bar{x} \sin m + \bar{y} \cos m \end{aligned} \qquad (3117)$$

If the increase in $\bar{x}$ and $\bar{y}$ is considered, when the point P is moved along the a- and b-line, respectively, we obtain from (3116), using also (3108) and (3109):

$$\frac{\partial \bar{x}}{\partial a} = \frac{\partial x}{\partial a} \cos m + \frac{\partial y}{\partial a} \sin m - x \sin m + y \cos m = R + \bar{y} \quad (3118a)$$

$$\frac{\partial \bar{x}}{\partial b} = \frac{\partial x}{\partial b} \cos m + \frac{\partial y}{\partial b} \sin m - x \sin m + y \cos m = \bar{y} \quad (3118b)$$

and in the same way

$$\frac{\partial \bar{y}}{\partial a} = -\bar{x} \quad (3118c)$$

$$\frac{\partial \bar{y}}{\partial b} = S - \bar{x} \quad (3118d)$$

It is seen, therefore, that the equivalent coordinates must satisfy the conditions:

$$\frac{\partial \bar{y}}{\partial a} + \bar{x} = 0$$
$$\frac{\partial \bar{x}}{\partial b} - \bar{y} = 0 \quad (3119)$$

i.e. a set of differential equations of the same type as (3112). They are related to R and S by the equations:

$$R = \frac{\partial \bar{x}}{\partial a} - \bar{y} = -\left(\bar{y} + \frac{\partial^2 \bar{y}}{\partial a^2}\right)$$
$$S = \frac{\partial \bar{y}}{\partial b} + \bar{x} = \bar{x} + \frac{\partial^2 \bar{x}}{\partial b^2} \quad (3120)$$

from which one set of functions can be found when the other set is known.

From (3119) it is seen that $\bar{x}$ may be a discontinuous function of a. There will then be a point of discontinuity at all a-lines where they are intersected by the same b-line, and the jump $\Delta \bar{x}$ will be the same for all a-lines. $\bar{y}$ has the same property in relation to b-lines. The jumps $\Delta \bar{x}_a$ and $\Delta \bar{y}_b$ correspond to linear slip line segments. They are always positive in the positive slip line directions, and are equal to the arc lengths Δs_a and Δs_b of the line segments.

Compared with the functions R and S, the equivalent coordinates have the advantage that they can never become infinite in a finite domain. Furthermore, by a rough calculation of $\bar{x}$ and $\bar{y}$ for a rupture zone rough but consistent values of the coordinates x,y for the mesh points are obtained. On the other hand all values of $\bar{x}$ and $\bar{y}$ will be changed if the coordinate system is translated or rotated (the corrections are quite simple, however).

For a radial zone we have the special consideration that the singular point is determined simply by R = 0 or S = 0, whereas $\bar{x}$ and $\bar{y}$ are some-

what more complicated functions. Except for the special case where the singular point is at the origin of the coordinate system ($x = y = \bar{x} = \bar{y} = 0$) they will be trigonometric functions with the same amplitude (same value of ρ in (3116)) and period (2π), but with the phase difference $\frac{\pi}{2}$ between $\bar{x}$ and $\bar{y}$.

For this case, and also f. inst. in the case of a circle arc boundary curve with a constant value of τ_{nt} (or c_a), it is a standard procedure to translate the coordinate system so that for each rupture zone element the most convenient origin point for $\bar{x}$ and $\bar{y}$ is used. By this method most of the above mentioned disadvantages are avoided. For some solutions, especially those obtainable in a closed form, the functions R and S give the simplest formulae. This does not matter when the calculations are performed numerically, so in the general case the method of equivalent coordinates is probably the most widely applicable.

It should be noticed that for more general assumptions than those considered in this work (f. inst. inhomogeneous clay with arbitrary volume forces) the method of radii of curvature becomes too complicated for practical use. (3119) is valid for any orthogonal curve net, however, when the derivatives are taken in relation to m, so for an extended theory of plasticity the method of equivalent coordinates becomes in fact the only (or at least the simplest) method for numerical calculations.

The method of chord lengths mentioned in a later section is a numerical method which combines some of the advantages of both methods.

Example 31 e

For the rupture zone shown in Fig. 23 H we have (for the full zone with $y = 0$ for $m = \frac{\pi}{4}$) from (2321):

$$\frac{\gamma \sin\beta}{c}\, y = -\cos 2m = -\cos 2(a + b) \tag{3121}$$

From (2324-5) we have correspondingly:

$$\frac{\gamma \sin\beta}{c}\, x = 2a + \sin 2a + [-2(a + b) + \sin 2(a + b) + 2a - \sin 2a]$$

$$= 2(a - b) + \sin 2(a + b) \tag{3122}$$

x being measured first along the a-line through $(0, -\frac{c}{\gamma \sin\beta})$, i.e. $(a, b) = (0, 0)$, until the intersection point with the b-line through the point in question, and then along the b-line until the point. Notice that all b-values are negative.

From (3116) we now obtain:

$$\frac{\gamma \sin\beta}{c}\,\bar{x} = 2\,(a - b)\cos(a + b) + \sin(a + b)$$

$$\frac{\gamma \sin\beta}{c}\,\bar{y} = -2\,(a - b)\sin(a + b) - \cos(a + b) \qquad (3123)$$

These two functions are seen to satisfy equations (3119). By comparison with (3115) it is seen that (3120) is also satisfied.

In this case the equivalent coordinates are evidently not especially suited as the formulae (3123) are actually more complicated than those for the coordinates. However, this would be immaterial if the zone was to be computed numerically. Then the most important thing would be the boundary conditions f. inst. along the upper boundary ($\frac{\gamma \sin\beta}{c}\,y = -1$, i.e. $a + b = 0$), and they are relatively simple:

$$\frac{\gamma \sin\beta}{c}\,\bar{x} = 2\,(a - b) = 4a$$

$$\frac{\gamma \sin\beta}{c}\,\bar{y} = -1 \qquad (3124)$$

They are as easily calculated as are those for R and S ($\frac{\gamma \sin\beta}{c}R = 4$, and $\frac{\gamma \sin\beta}{c}\,S = 0$). For this special rupture zone the latter functions will of course also be the simplest to calculate numerically, because they are functions of a + b only.

314 Velocity Components

The movements in a rupture figure form a two-dimensional velocity field. According to definitions (Fig. 23 K) the velocity vector $\bar{w}$ has at each point O the components u_x and u_y, positive in the negative coordinate directions.

Considering the velocity differences between neighbouring points in a rupture zone (Fig. 31 K) it is seen, that because of the deformation condition $\epsilon_a = \epsilon_b = 0$ the velocity increments $\overline{dw_a}$ and $\overline{dw_b}$ for consecutive points on the a- and b-line through O must be orthogonal to the corresponding slip lines.

Therefore, if the velocities of points in the rupture zone are represented in the hodograph plane u_x, u_y, the a- and b-directions through any point are represented by orthogonal directions through the image point, form-

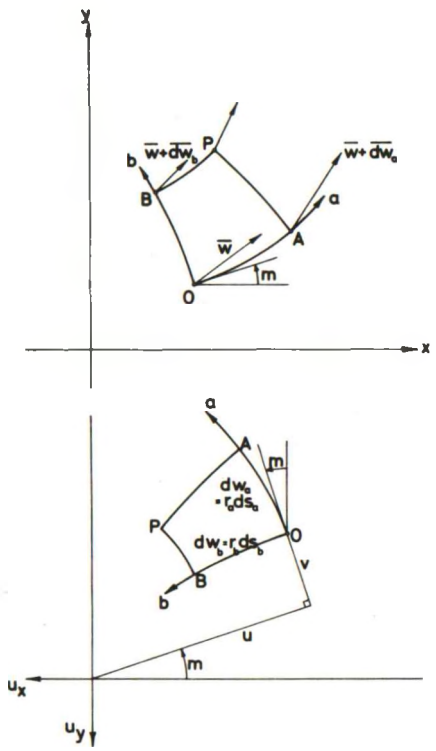

Fig. 31 K: Velocity Increments in the Slip Line Field. Cell Element in the Hodograph Plane.

ing the angles m and $90^o + m$ with the negative u_y-direction. A mesh OABP in the slip line field is in this way represented by a mesh OABP in the hodograph plane, corresponding directions forming the same angles with the x-direction and the negative u_y-direction.

If the angular velocities r_a and r_b are both positive, the image slip lines in the hodograph plane will be oriented in the same directions as the original slip lines in the x,y-plane. This is the case of Fig. 31 K. If one, or both, of the rotations are negative, the corresponding image slip line will go in the opposite direction. The tangent angles m are still measured as indicated above, but the arc lengths dw_a and dw_b are then taken as negative.

According to their definition the velocity components u and v are measured as indicated in Fig. 31 K, cf. Fig. 23 K and (2341-2). They are evidently equivalent coordinates in the hodograph plane, so they must satisfy the equations obtained from (3119) when $\bar{x}$ is replaced by v and $\bar{y}$ by $-u$ (compare Fig. 31 J). However, the same equations can be obtained in a simpler way directly from (2343). By multiplying these two equations with $\frac{ds_a}{da}$ and $\frac{ds_b}{db}$, respectively, we obtain:

$$\frac{\partial u}{\partial a} - v = 0$$

$$\frac{\partial v}{\partial b} + u = 0 \qquad (3125)$$

i.e. differential equations of the same type as (3112) and (3119), cf. Geiringer [1930].

Considering now the arc lengths dw_a and dw_b for a small element in the hodograph plane we get:

$$dw_a = r_a\, ds_a = r_a\, R\, da = F da$$
$$dw_b = r_b\, ds_b = r_b\, S\, db = G db \qquad (3126)$$

In this way the rotation functions F and G are defined. They are evidently radii of curvature for the image slip lines in the hodograph plane, so they must satisfy the equations obtained from (3112) when R is replaced by F and S by G:

$$\frac{\partial G}{\partial a} - F = 0$$
$$\frac{\partial F}{\partial b} + G = 0 \qquad (3127)$$

The relations between F, G and u, v can be found by substituting in (3120) as indicated above. However, they can also be found directly from (2344):

$$r_a = \frac{\delta v}{\delta s_a} + u \frac{\delta m}{\delta s_a} = \frac{1}{R}\left(\frac{\partial v}{\partial a} + u\right) = \frac{F}{R}$$
$$r_b = \frac{\delta u}{\delta s_b} + v \frac{\delta m}{\delta s_b} = \frac{1}{S}\left(-\frac{\partial u}{\partial b} + v\right) = \frac{G}{S} \qquad (3128)$$

so that:

$$F = u + \frac{\partial v}{\partial a} = u + \frac{\partial^2 u}{\partial a^2}$$
$$G = v - \frac{\partial u}{\partial b} = v + \frac{\partial^2 v}{\partial b^2} \qquad (3129)$$

By this notation the condition (2345) may be written:

$$2\epsilon = r_a - r_b = \frac{F}{R} - \frac{G}{S} \geq 0 \qquad (3130)$$

From (3129), (3127) can be found by direct differentiation, using also (3125).

When F and G are known as functions of λ and μ, and therefore also of a and b, the velocity field can be determined by integration of (3129), or by the equations:

$$du_x = dw_a \sin m = F \sin m\, da$$
$$du_y = -dw_a \cos m = -F \cos m\, da \qquad (3131\,a)$$

for integration along a-lines, and

$$du_x = dw_b \cos m = G \cos m \, db$$

$$du_y = dw_b \sin m = G \sin m \, db \qquad (3131\,b)$$

for integration along b-lines.

The functions F, G and u, v being respectively radii of curvature and equivalent coordinates in the hodograph plane, they have much the same properties as R, S and $\bar{x}, \bar{y}$. Thus, linear image slip line segments, f. inst. Δw_a, may occur. Then all other image a-lines will be linear between the same two image b-lines, and the length Δw_a of all line segments will be the same. For such segments F is infinite, and between the two image b-lines bounding the strip of a-line segments we have a constant increase in G equal to Δw_a. Notice that these two b-lines have the same a-coordinate, and that they may also coincide in the λ, μ-plane. If they do, there is a finite velocity difference (sliding) between the two sides of the b-line.

This corresponds with the fact that according to (3125) v may be discontinuous, regarded as a function of a. We will then have the same discontinuity Δv_a on all a-lines at the points where they are intersected by the same b-line. The jump Δv_a is equal to the length Δw_a in the hodograph plane.

The corresponding properties exist for linear image b-line segments. As mentioned previously the condition that $\epsilon \geq 0$ everywhere means that velocity jumps Δu and Δv must always be positive in the positive slip line directions. Therefore, in the following relations between the velocity functions for line segments, all quantities must be positive:

$$\text{a-line segments (u const., F infinite): } \Delta G_a = \Delta w_a = \Delta v_a$$

$$\text{b-line segments (v const., G infinite): } \Delta F_b = -\Delta w_b = \Delta u_b \qquad (3132)$$

Besides we may have discontinuities ΔF_a and ΔG_b in the a- and b-direction, respectively, constant but of an arbitrary sign and magnitude, along any b- respectively a-line.

For computational reasons it may be practical to reserve two coordinate values in the λ, μ-plane for each slip line along which slidings take place. Corresponding mesh points in the two rows will then have the same physical and equivalent coordinates, but the velocity components will be different according to (3132). Thus, line segments in the x, y-plane and in the hodograph plane are treated in the same way in order that all functions have unique values at all mesh points.

In the hodograph plane rupture figures may overlap, and neighbouring image slip lines of the same family may intersect. Thus, in the positive slip line directions the arc lengths w_a or w_b may not increase (as the corresponding functions s_a and s_b will always do), but may decrease or may remain constants. This may give rather complicated pictures of the rupture zones, which will frequently not be very illustrating, and where geometrical constructions may be almost impossible. Therefore, this representation is often used only formally, arc lengths etc. being treated as purely numerical quantities, and all calculations are performed in the λ, μ -plane.

For rupture zones where the geometry is influenced by the velocity conditions, and where the slip line field and the velocity field are therefore calculated simultaneously, the computations are always based either on the radii of curvature or on the equivalent coordinates throughout. Thus, one uses either the function set R, S, F, G or the set $\bar{x}, \bar{y}, u, v$. The factors influencing the choice between these two methods have previously been discussed for the geometrical functions. The same points of view apply for the corresponding velocity functions. Thus, the first mentioned set may give the simplest formulae for mathematical solutions, based f. inst. on function series, but for numerical solution methods, especially by means of finite differences, the second set is the most widely applicable. It is also the one to be used in a more general theory of plasticity.

In this connection it may be mentioned, that exactly as for the functions $\bar{x}, \bar{y}$ it is an easy standard procedure to translate the u_x, u_y-coordinate system to obtain convenient boundary conditions for the functions u, v. Evidently this corresponds to the addition of a constant vector to all velocities. A constant rotation r_o may also be added to all values of r. This gives a rather complicated transformation of the hodograph plane, $r_o \bar{x}$ being added to all v-values, and $- r_o \bar{y}$ to all u-values in all rupture zones. In this way one can obtain that at least one of the rigid bodies bounding the zone element in question is at rest. If so desired, f. inst. in order to make a geometrical construction possible, one can also in this way make all arc lengths dw_a and dw_b positive, except for Δw_b-segments by slidings along a-lines, which are always negative, and possibly also for other domains with arbitrarily high, possibly infinite rotations in the negative direction.

Example 31 f

Consider the Prandtl rupture figure (cf. Fig. 31 G) for a rough strip foundation which is moved during failure in a translation w_o inside the permissible limits of deviation from the vertical y-axis.

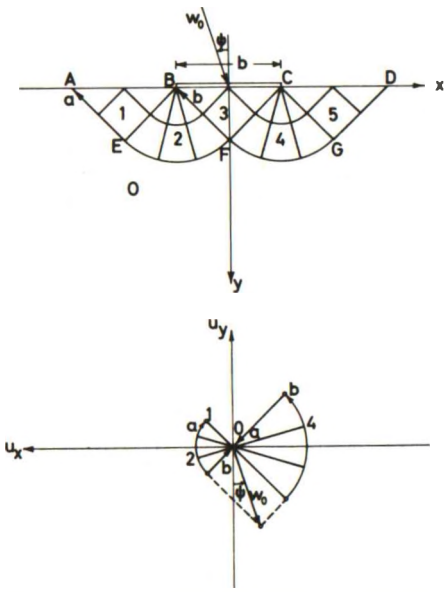

Fig. 31 L: Prandtl Rupture Figure. Representation in the Hodograph Plane of the Velocity Field.

As shown in Fig. 31 L, where the different domains in the x,y-plane are designated by the numbers 0-5, there are 4 rigid bodies of clay. Body No. 0 remains at rest, whereas No. 3 has the same velocity as the strip foundation. It slides upon the two radial zones, Nos. 2 and 4, which are represented in the hodograph plane by two circle arcs. The clay material in the radial zones, and the two rigid bodies Nos. 1 and 5, slide upon the body at rest, but there are no slidings between the domains No. 1 and 2, or between No. 4 and 5.

From this representation it can be deduced, that for deviation angles ψ between the positive y-axis and the w_0-direction in the interval $-\frac{\pi}{4} \leq \psi \leq \frac{\pi}{4}$, all r_a-values will be positive or zero, and all r_b-values will be negative or zero, so the condition (3130) is always satisfied.

The construction in Fig. 31 L is quite simple. However, for a small variation of the boundary conditions, so that the radial slip lines in the zones No. 2 and 4 become slightly curved, possibly with inflexion points, it is easy to see that the figure may become rather intricate with sets of points, and families of image slip lines almost, but not quite, coinciding.

If we add a constant rotation (equal to $\frac{16\, w_{oy}}{3\, b}$, where b is the foundation width) we obtain Fig. 31 M, where all characteristic points in the rupture figure are clearly separated. To get a clear picture of the slidings all points are designated both by a letter and by a number corresponding to the domains in Fig. 31 K. Thus, there are four points F corresponding to the fact that the velocity vector is different in all four quadrants formed by the slip lines through this point.

By the construction of the figure the following rule, which is self-evident, is frequently used:

The boundaries to a rigid body of clay will in the hodograph plane be represented by a figure which is similar to the corresponding figure in the

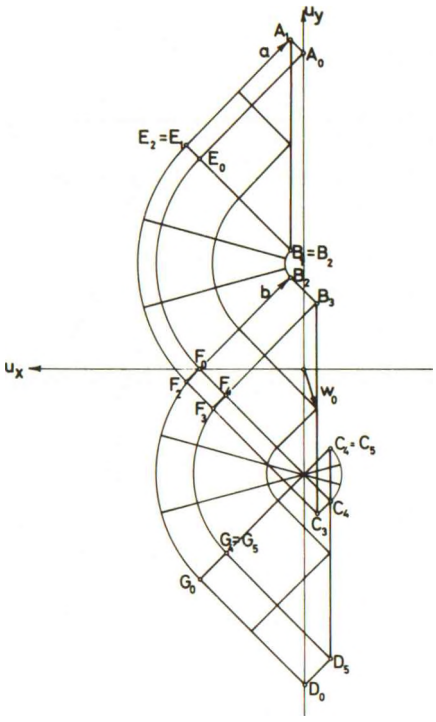

Fig. 31 M: Hodograph Plane for Prandtl Rupture Figure. Modified by Adding a Uniform Rigid Body Rotation.

x, y-plane, but is turned $\frac{\pi}{2}$ in the positive direction u_x, u_y. Its centre of rotation will coincide with the origin point, and its scale factor $(\frac{u_x}{y} = -\frac{u_y}{x})$ will be the value of its angular velocity r (taken with sign).

It is seen that in Fig. 31 M most of the arc lengths w_a and w_b are positive. However, the image b-lines along the a-line AEFC, such as $A_o - A_1$ or $C_4 - C_3$, and in the neighbourhood of the point C, have negative arc lengths. Here the rotation r_b is negative and arbitrarily large.

For numerical reasons it is not an ideal procedure to add a great positive number to a set of small positive and negative quantities. Therefore, if the calculations are performed analytically this method presents no special advantage. In this case it is safer, and not more difficult, to use the original arc lengths w_a and w_b.

32 CALCULATION METHODS

321 Fundamental Differential Equations

In the preceding section we have shown that the stress conditions are all fulfilled in a rupture zone when the slip line field of orthogonal curve families satisfies a special condition for the tangent angles (the Hencky condition (3104)). Correspondingly, the deformation condition is fulfilled when the image slip lines in the hodograph plane satisfy the same condition.

In order to facilitate the construction of such nets two function sets, $\bar{x}$, $\bar{y}$, u, v and R, S, F, G, representing equivalent coordinates and radii of curvature for the original and image slip line fields, have been defined, and Hencky's condition has been utilized to define a special coordinate system (a, b, or the corresponding domain space λ, μ, introduced to obtain a unique functional dependence), in which a set of differential equations are valid for each pair of functions.

In this section the problem of calculating these functions is discussed. The computation methods are based partly on the differential equations, from which some important properties of the solutions can be deduced, partly on direct geometrical reasoning, based again on the Hencky properties.

For the purely analytical methods it is first observed that all differential equations considered, i.e. (3112), (3119), (3125), and (3127), are of the same type, which can be written:

$$\frac{\partial f}{\partial a} - g = 0$$

$$\frac{\partial g}{\partial b} + f = 0 \qquad (3201)$$

The function set f, g may be identified with each of the pairs S, R; $-\bar{y}$, $\bar{x}$; u, v; and G, F. The calculation method is therefore the same for all the above functions, and only the typical form (3201) need to be treated in detail.

From this equation it is seen that each of the functions f and g, i.e. each of the functions R, S, $\bar{x}$, $\bar{y}$, u, v, F, and G, must satisfy the equation:

$$\frac{\partial^2 h}{\partial a \, \partial b} + h = 0 \qquad (3202)$$

cf. Carathéodory and Schmidt [1923].

This is a well known type of hyperbolic differential equations, a special case of the so-called Telegraphist's equation. Its characteristic directions (in the a,b-plane) are parallel to the coordinate directions.

From the theory of linear differential equations we can immediately deduce the following properties of solutions.

1. If two functions h_1 and h_2 are solutions to (3202), any linear combination $\alpha h_1 + \beta h_2$ will also be a solution. The derivatives $\frac{\partial h_1}{\partial a}$ and $\frac{\partial h_1}{\partial b}$ etc., and integrals $\int_{a_o}^{a} h_1(\alpha, b)\, d\alpha$ and $\int_{b_o}^{b} h_1(a, \beta)\, d\beta$ to an arbitrary order will also be solutions. From this it is seen that an arbitrary linear differential and integral functional containing any number of solution functions will itself be a solution (cf. equations (3120) and (3129)).

2. From a given solution, f or g, a conjugate solution, g or f, can be defined by means of (3201). In principle any solution may be considered as an f- or g-function, subject to certain limitations as to whether steps and infinity points are permissible, and if so what signs they should have. If in a given functional all solution functions are replaced by their conjugate solutions, a new functional is obtained which is the conjugate solution to the original one.

3. It is seen that the solutions are not as a rule continuous and differentiable, as they are for elliptic differential equations. For any given problem the solution is determined by the specified boundary conditions. It is here not permissible to assume the function h or its derivative $\frac{\partial h}{\partial n}$ to be known along the periphery of a closed boundary curve. As a rule, in order to avoid contradiction both h and $\frac{\partial h}{\partial n}$ must be known, but only along part of the boundary. On the other hand, the value of h at an interior point of the domain is not influenced by all arbitrary changes of the boundary conditions. Only changes inside a region of influence, bounded by the characteristics through the point, will have any influence on the value of h at the point.

From this it follows that numerical calculations, f.inst. by the method of finite differences, do not as a rule correspond to the simultaneous solution of a large number (equal to the number of mesh points) of equations with the same large number of unknown quantities. It is a step by step procedure

in which the values of h at the mesh points are found successively, using in each step the values at the neighbouring mesh points. Thus, the problems considered here are typical initial value problems, as contrary to boundary value problems. Correspondingly, the direction through the rupture zone in which the calculations are performed, beginning at the initial values, has a real significance, as it can be seen from the fact that regions of influence can be defined.

In a number of problems we have an exception to this rule, arising from the fact that we do not know the necessary initial values for the solution functions. Instead we have certain conditions which the solution must satisfy at the other end of the domain. Even in this case the problem is essentially an initial value problem. The values at the interior points do not enter the equations to satisfy, which are only equations for the boundary points. In order to formulate these equations it may be necessary to calculate some values at the interior points, but this can in most cases be done without any regard to the desired solution function, by means of influence factors on the unknown initial values to the final conditions to satisfy.

We may distinguish between the following three types of pure initial value problems, leading to unique solutions:

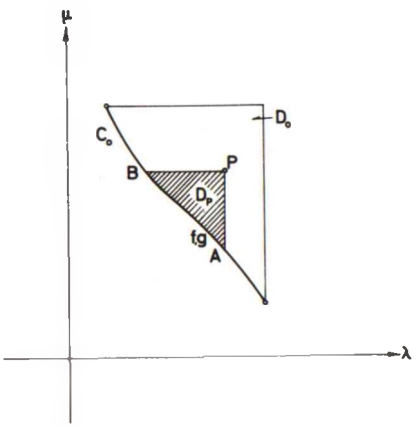

Fig. 32 A: First (Cauchy) Initial Value Problem Type: f and g Known on a Given Curve.

1. The first type, the Cauchy initial value problem (Fig. 32 A) specifies one function h and both its derivatives $\frac{\partial h}{\partial a}$ and $\frac{\partial h}{\partial b}$ (or, alternatively, h and $\frac{\partial h}{\partial n}$, or two conjugate functions f and g) on an arc C_o of a regular curve which is neither a characteristic nor touches any characteristic. The curve will therefore intersect each characteristic at most once. The given initial conditions determine h (or f and g) in a region D_o bounded by C_o and a characteristic of each family. Each point P of this region determines a sub-region D_P, so that h (or f and g) at P are determined by the initial values on the portion of C_o which is bounded by the characteristics through P.

The region D_o defined in this way is called a triangle zone, or a Rankine zone. The above holds true for any of the four possible positions of C_o in relation to the bounding characteristics (in any of the four quadrants), corresponding to the four possible directions of calculation in the λ, μ-plane.

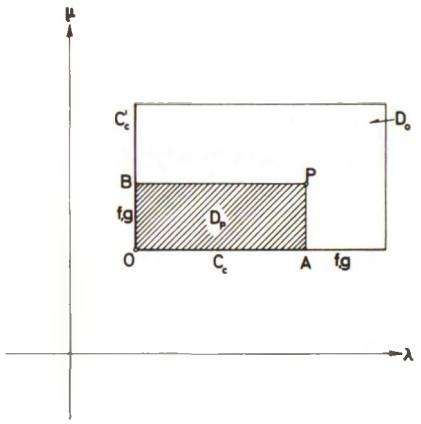

Fig. 32B: Second Initial Value Problem Type: f (and g) Known Along Two Characteristics.

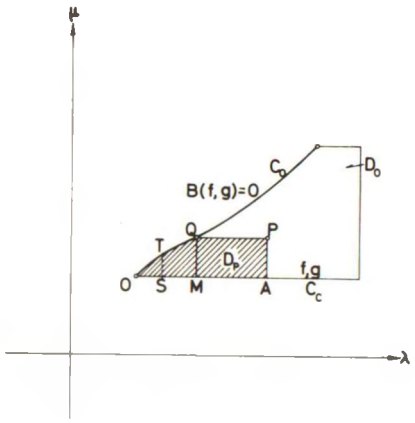

Fig. 32C: Third Initial Value Problem Type: f (and g) Known Along One Characteristic. Known Relation Along a Given Curve.

2. The second type prescribes both conjugate functions f and g (or any one of them; the other is then given by (3201)) on two intersecting characteristics C_c and C'_c (Fig. 32B). The region D_o is in this case bounded by two given characteristics, and the characteristics through their end points. The values of f and g at a point P in this region are determined by the initial values on the portions OA and OB of C_c and C'_c between their intersection point O and the characteristics through P. D_o is in this case called a rectangle zone (possibly a radial zone if one of the bounding characteristics degenerates to a point in the x,y-plane). This zone too has four possible positions in relation to the bounding characteristics.

3. The third type (Fig. 32C) prescribes a relationship $B(f,g) = 0$, or $g = g(f)$, $f = f(g)$ on an arc C_o specified as above. In addition f and g are given (cf. (3201)) on a characteristic C_c through one end point O of C_o. The region D_o is bounded by C_o, C_c, and the characteristics through the other end points of C_o and C_c (only the last mentioned one, if it has the smallest abscissa of the two). D_P is bounded by the cha-

racteristics through P. The region D_o is here called a wall zone, because physically it always occurs in contact with an external rigid body.

The last type is known in a variant where the position of C_o in the a,b-plane is not given (except for the point O), but where we know both f and g along C_o together with a relationship between a and b (possibly dependent on f).

Other types which are not strictly initial value problems may in practice present some difficulties, because they cannot without supplementary conditions be proved to yield unique solutions. Thus, a rectangle zone (cf. Fig. 32B) where f and g are given along two opposite characteristics of the same family is not defined by this information only. If nothing further is given one may f.inst. include an arbitrary number of strips of linear slip line segments (or sliding discontinuities) parallel to the known characteristics, or one may insert an arbitrary number of branch sheets in the a,b-plane, letting the coordinate orthogonal to the known characteristics pass through a number of maximum and minimum points, instead of increasing monotonously from one characteristic to the other.

For zones with mixed boundary conditions we have no complete set of initial values for any of the two sets of conjugate functions f_1, g_1 and f_2, g_2, which refer to the geometry and the velocity field, respectively. Instead we have along some of the zone boundaries relationships between corresponding functions of the two sets, of the type $\alpha f_1 + \beta f_2 = 0$. Such problems too cannot be solved by simple initial value operations. However, we will usually not have the difficulties indicated above. For, because of the relationships between geometric and velocity functions, the zone will in all practical cases turn out to have a sufficient number of conditions.

The general solution to (3202) may be built up of function series. Thus, any function of the type

$$A_p(a,b) = \left(\frac{a}{b}\right)^{\frac{p}{2}} J_p\left(2\sqrt{ab}\right)$$

$$= \frac{a^p}{p!} - \frac{a^{p+1}b}{(p+1)!\,1!} + \frac{a^{p+2}b^2}{(p+2)!\,2!} - \ldots \qquad (3203\,a)$$

$$B_q(a,b) = \left(\frac{b}{a}\right)^{\frac{q}{2}} J_q\left(2\sqrt{ab}\right)$$

$$= \frac{b^q}{q!} - \frac{a\,b^{q+1}}{1!\,(q+1)!} + \frac{a^2 b^{q+2}}{2!\,(q+2)!} - \ldots \qquad (3203\,b)$$

with

$$A_o(a,b) = B_o(a,b) = J_o(2\sqrt{ab})$$
$$= 1 - \frac{ab}{1!\,1!} + \frac{a^2b^2}{2!\,2!} - \ldots \qquad (3203\,c)$$

is a solution to (3202). J_p is here the Bessel function of the order p. From the elementary differential formulae for Bessel functions we have:

$$\begin{aligned} \frac{\partial}{\partial a} A_p &= A_{p-1} \qquad (p > 0) \\ \frac{\partial}{\partial b} A_p &= -A_{p+1} \\ \frac{\partial}{\partial a} B_q &= -B_{q+1} \\ \frac{\partial}{\partial b} B_q &= B_{q-1} \qquad (q > 0) \end{aligned} \qquad (3204)$$

which can also be deduced from the power series in (3203). From (3204), and also directly from the power series we see that (3202) is satisfied.

This can be used f. inst. to solve the second initial value problem (Fig. 32B). We define m_o and σ_o so that C_c and C'_c coincide with the coordinate axes a = 0 and b = 0. For b = 0 all functions B_q are identically zero, and A_p are simply the power terms $\frac{a^p}{p!}$. Correspondingly, B_q are the power terms $\frac{b^q}{q!}$ for the b-axis. Thus, if the MacLaurin series are known for the two given initial functions:

$$\begin{aligned} h_a(a) &= h(0) + h'_a(0)\frac{a}{1!} + h''_a(0)\frac{a^2}{2!} + \ldots \\ h_b(b) &= h(0) + h'_b(0)\frac{b}{1!} + h''_b(0)\frac{b^2}{2!} + \ldots \end{aligned} \qquad (3205)$$

we get immediately the solution:

$$h(a,b) = hA_o + h'_a A_1 + h'_b B_1 + h''_a A_2 + h''_b B_2 + \ldots \qquad (3206)$$

h, h'_a, h'_b etc. being the values of the initial functions and their derivatives at the origin point.

However, this method is only useful for certain simple types of functions. A small number of step functions can be treated by subdividing the rectangle zone into a number of rectangles, each with a continuous initial value function, and calculating the rectangles in a systematic order, starting with the lower left hand corner. But the series (3206) are not generally easy to calculate.

For the two other initial value problems the solution is not obtained in a closed form. One must build up a series of Bessel functions so that the known conditions on the curves C_o are satisfied. This is feasible, f.inst. after an orthogonalization process, but it is not as simple as the methods considered in the following.

Example 32a

For the rupture zone shown in Fig. 23 H (and Fig. 31 F) we have found the radii of curvature (3115) and the equivalent coordinates (3123). Transforming the a,b-coordinate system so that the origin coincides with the point A in Fig. 31 F ($a' = a - \frac{\pi}{2}$) we can consider the problem as a second initial value problem type.

In the new coordinate system ($-\frac{\pi}{2} \leq a' \leq 0$, $-\frac{\pi}{2} \leq b \leq 0$) we have the following functions (common scale factor: $\frac{\gamma \sin\beta}{c}$):

$$R = -4 \sin(a' + b)$$
$$S = 4 \cos(a' + b) \tag{3207}$$

$$\bar{x} = \cos(a' + b) - \pi \sin(a' + b) - 2(a' - b) \sin(a' + b)$$
$$\bar{y} = \sin(a' + b) - \pi \cos(a' + b) - 2(a' - b) \cos(a' + b) \tag{3208}$$

The last expressions can be somewhat simplified, if the x,y-coordinate system is also moved, so that its origin point is A. By this transformation we subtract π from x and 1 from y, i.e. according to (3116):

$$\Delta\bar{x} = -\pi \cos(a+b) - \sin(a+b) = \pi \sin(a'+b) - \cos(a'+b)$$
$$\Delta\bar{y} = \pi \sin(a+b) - \cos(a+b) = \pi \cos(a'+b) + \sin(a'+b) \tag{3209}$$

so that we get:

$$\bar{x}' = -2(a' - b) \sin(a'+b)$$
$$\bar{y}' = 2[\sin(a'+b) - (a' - b) \cos(a'+b)] \tag{3210}$$

All four functions (3207) and (3210) can easily be expressed by their MacLaurin series for $b = 0$ and $a' = 0$. However, it is rather inconvenient to obtain the solutions as series of Bessel functions. For example

$$R = 4 \left[-\left(\frac{a'}{b}\right)^{\frac{1}{2}} J_1 (2\sqrt{a' b}) + \left(\frac{a'}{b}\right)^{\frac{3}{2}} J_3 (2\sqrt{a' b}) - \ldots \right.$$
$$\left. -\left(\frac{b}{a'}\right)^{\frac{1}{2}} J_1 (2\sqrt{a' b}) + \left(\frac{b}{a'}\right)^{\frac{3}{2}} J_3 (2\sqrt{a' b}) - \ldots \right] \qquad (3211)$$

The series are difficult to calculate, except when a' and b are both small numbers. It takes a special knowledge of Bessel functions to know that they are identical to the much simpler expressions (3207) and (3210).

It should be noticed that in special cases, f.inst. for polynomial expressions for h(a) and h(b) with only a small number of terms, (3206) may be useful. The functions A_p and B_q are defined according to their power series also when a and b have different signs. Corresponding terms with Bessel functions N_p of the second kind (to be used with Laurent's series) are also solutions.

322 Riemann Integration

The Riemann-Volterra integral method is based on the fact that for a self-adjoint differential operator L, as f.inst. the one considered in (3202):

$$L[h] = \frac{\partial^2 h}{\partial a \, \partial b} + h \qquad (3212)$$

a certain functional containing L will when applied to any two functions, φ and ψ, be the divergence of a vector function, P, Q:

$$\psi \, L[\varphi] - \varphi \, L[\psi] = \frac{\partial P}{\partial a} + \frac{\partial Q}{\partial b} \qquad (3213)$$

The functions P and Q will of course depend on the operator L and on the choice of φ and ψ.

By integrating both sides of (3213) over any domain in the a,b-plane we obtain, using Gauss' integral theorem:

$$\int_V (\psi \, L[\varphi] - \varphi \, L[\psi]) \, da \, db = \int_S (-P db + Q da) \qquad (3214)$$

the surface integration being performed in the negative direction of rotations in the a,b-plane. The differential increments da and db are taken with signs.

This may be applied to find the value of the solution function h to (3202) at a point P in the a,b-plane (Fig. 32 D) by choosing the functions φ and ψ in the following way:

ψ is identified with the function h, and φ is the Riemann function $G_R(a, b; a_P, b_P)$ of a and b, and also of the coordinates a_P, b_P to the point P.

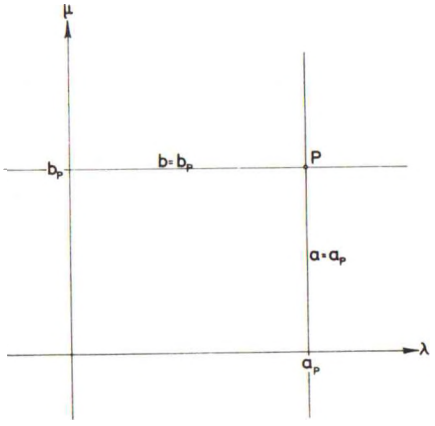

Fig. 32 D: Characteristics Through the Point P Where the Function Values are Sought.

A Riemann function to a given differential operator L is defined by the following properties:

1. Regarded as a function of a and b it satisfies the differential equation:

$$L\,[\,G_R\,] = 0 \qquad (3215)$$

2. Along the characteristics through P the derivatives of G_R in the characteristic directions are zero. Thus:

$$\text{for } b = b_P\text{: } \frac{\partial G_R}{\partial a} = 0 \qquad \text{for } a = a_P\text{: } \frac{\partial G_R}{\partial b} = 0 \qquad (3216)$$

3. At the point P, and therefore also along the characteristics through P we have:

$$G_R\,(a_P, b_P; a_P, b_P) = 1 \qquad (3217)$$

From (3202) and (3215) we see that the left hand side of (3214) is identically zero. The right hand side is evaluated by means of (3202):

$$h\,L\,[\,G_R\,] - G_R\,L\,[\,h\,] = h\,\frac{\partial^2 G_R}{\partial a\,\partial b} - G_R\,\frac{\partial^2 h}{\partial a\,\partial b}$$

$$= \frac{1}{2}\left[\frac{\partial}{\partial a}\left(h\,\frac{\partial G_R}{\partial b} - G_R\,\frac{\partial h}{\partial b}\right) + \frac{\partial}{\partial b}\left(h\,\frac{\partial G_R}{\partial a} - G_R\,\frac{\partial h}{\partial a}\right)\right] \qquad (3218)$$

Therefore, from (3214):

$$\int_S \left[\left(h\,\frac{\partial G_R}{\partial a} - G_R\,\frac{\partial h}{\partial a}\right)da - \left(h\,\frac{\partial G_R}{\partial b} - G_R\,\frac{\partial h}{\partial b}\right)db\right] = 0 \qquad (3219)$$

The different boundary value problems are solved by means of this equation, using suitable paths of integration.

The function G_R is uniquely determined by the above conditions. Assuming it to be a function of the single variable $t = (a_P - a)\,(b_P - b)$, which will assure that (3216) is always satisfied, we obtain from (3215), cf. (3202):

$$\frac{\partial^2 G_R}{dt^2}\,\frac{\partial t}{\partial a}\,\frac{\partial t}{\partial b} + \frac{dG_R}{dt}\,\frac{\partial^2 t}{\partial a\,\partial b} + G_R = 0 \qquad (3220)$$

Inserting the expression for t we see that since $\frac{\partial t}{\partial a}\,\frac{\partial t}{\partial b} = t$ and $\frac{\partial^2 t}{\partial a\,\partial b} = 1$, we have:

$$t \frac{d^2 G_R}{dt^2} + \frac{d G_R}{dt} + G_R = 0 \tag{3221}$$

the general solution of which is

$$G_R = A J_o (2\sqrt{t}) + B N_o (2\sqrt{t}) \tag{3222}$$

J_o and N_o are the Bessel functions of zero order, and of the first and second kind. A and B are arbitrary constants to be determined by the normalizing condition (3217). It is only satisfied when A = 1 and B = 0, so we have:

$$G_R = J_o \left(2 \sqrt{(a_P - a)(b_P - b)} \right) = J_o (2\sqrt{t})$$

from which

$$\begin{aligned} G_{R,a} &= \frac{d G_R}{da} = \sqrt{\frac{b_P - b}{a_P - a}} \; J_1 \left(2 \sqrt{(a_P - a)(b_P - b)} \right) \\ &= (b_P - b) \frac{J_1 (2\sqrt{t})}{\sqrt{t}} \\ G_{R,b} &= \frac{d G_R}{db} = \sqrt{\frac{a_P - a}{b_P - b}} \; J_1 \left(2 \sqrt{(a_P - a)(b_P - b)} \right) \\ &= (a_P - a) \frac{J_1 (2\sqrt{t})}{\sqrt{t}} \end{aligned} \tag{3223}$$

The functions $J_o (2\sqrt{t})$ and $t^{-\frac{1}{2}} J_1 (2\sqrt{t})$ are the so-called Bessel-Clifford functions of zero and first order. They are defined for both positive and negative values of t. For brevity the symbols G_R, $G_{R,a}$, and $G_{R,b}$ will be used in the following instead of the full expressions (3223).

By the practical application of (3219) we choose an integration path following the two characteristics through the point P where h is desired, and the known boundary curves (i.e. the boundary of the influence domain). By integration along curves such as C_o in Fig. 32 A it is used that for any function h:

$$\frac{\delta h}{\delta s} = \frac{\partial h}{\partial a} \frac{\delta a}{\delta s} + \frac{\partial h}{\partial b} \frac{\delta b}{\delta s} \tag{3224}$$

s need not here be the arc length, but may be any continuous function of this variable. It may f. inst. be put equal to a or b.

Using (3224) to evaluate the left hand side of (3219), this equation can be transformed to:

$$\int_s \frac{\delta}{\delta s} (h G_R) \, ds - 2 \int_s (G_R \frac{\partial h}{\partial a} \, da + h G_{R,b} \, db) = 0 \tag{3225}$$

or:

$$-\int_S \frac{\delta}{\delta s}(h G_R)\,ds + 2\int_S (h G_{R,a}\,da + G_R \frac{\partial h}{\partial b}\,db) = 0 \qquad (3226)$$

Any one of these two expressions may be used, inserting one of the functions f or g instead of h. Because of (3201) derivatives can be eliminated when (3225) is used for h = f, and (3226) for h = g.

By the first type of initial value problems (Fig. 32 A) the integration is performed along the path ABPA. We get:

1. Along AB: The integral (3219) may be used for both f and g, finding one of the derivatives from (3201) and the other from (3224), putting s equal to a or b. The two forms (3225) for f and (3226) for g are simpler, however.
2. Along BP: (3226) is used, observing that $G_R = 1$ and db = 0. This integral is therefore equal to $-h(P) + h(B)$.
3. Along PA: (3225) is used, observing that $G_R = 1$ and da = 0. This integral is therefore equal to $h(A) - h(P)$.

As a result we obtain by inserting and contracting:

$$f(P) = f(B) - \int_{AB} (g G_R\,da + f G_{R,b}\,db) \qquad (3227)$$

and

$$g(P) = g(A) + \int_{AB} (g G_{R,a}\,da - f G_R\,db) \qquad (3228)$$

In the limit, when the curve AB is an a-line or a b-line, these two formulae follow directly from (3201). They are simpler to use than the formula given by Hill [1950].

By the second type of initial value problems (Fig. 32 B) the integration is performed along the path OBPAO. For BP and PA we use (3226) and (3225), respectively, but for OB and AO we may use either. In this way we get the following two expressions for h(P), representing any of the two functions f and g:

$$h(P) = h(A) + h(B) - h(O)\,G_R(O) - \int_{OA} h G_{R,a}\,da - \int_{OB} h G_{R,b}\,db \qquad (3229)$$

$$= h(O)\,G_R(O) + \int_{OA} G_R \frac{\partial h}{\partial a}\,da + \int_{OB} G_R \frac{\partial h}{\partial b}\,db \qquad (3230)$$

cf. Hill [1950].

If only one of the functions is desired, one of these expressions must be used. (3230) is the simplest in that it only needs a table of $J_0(2\sqrt{t})$ for

numerical calculations. By interpreting the integrals as Stieltjes-integrals, i.e. as limiting sums of the type:

$$\int_{OA} G_R \frac{\partial h}{\partial a}\, da = \int_{OA} G_R\, dh = \lim_{\Delta a \to 0} \sum_{OA} G_R\, \Delta h \tag{3231}$$

they are also defined for step functions. (3229) is even defined when h includes delta functions.

By a combination of the two methods, and by the use of (3201) the results can also be expressed directly in f and g as follows:

$$f(P) = f(B) + \int_{OA} g G_R\, da - \int_{OB} f G_{R,b}\, db \tag{3232}$$

$$g(P) = g(A) - \int_{OA} g G_{R,a}\, da - \int_{OA} f G_R\, db \tag{3233}$$

They are probably the simplest to use when both f and g are given, and are desired at P.

For the third type of initial value problems (Fig. 32C) it is not possible to obtain a solution in closed form. However, an expression can be found for the variation of f and g along C_o. When this is solved for the portion OQ inside the region of influence for P we can find the value at P by integration along the path OQPAO. The last procedure is also the one to use for combined boundary conditions, f. inst. as here a rectangle zone continuing a triangle zone.

For the first part of the problem, to find the variation along C_o, we obtain an integro-differential equation which for any point T on the curve OQ expresses the derivative of a functional of f and g (and therefore by the known relationship B (f, g) = 0 of one of the functions) in terms of an integral of the already found values along OT, and the known values along OS. This procedure is not suited for numerical calculations, so for this type of initial value problems (and especially for the variants where the position of C_o in the a,b-plane is not known beforehand) a direct numerical integration can only be performed by means of the method of finite differences.

When the values in the triangle zone OQM have been found, the value at P can be calculated by Riemann integration, if so desired.

In some cases, when the known initial values are given as simple functions of a and b, the integrals can be evaluated directly. The method may then give the solution in a closed form. Most often, however, the integrations must be performed numerically, f. inst. by means of Simpson's formula.

Then the method gives rather laborious calculations, if the solution has to be found in the mesh points of a reasonably closely spaced net.

In such cases the method of finite differences will frequently be more economical. Riemann integration will then only be used when only a few points are needed, f. inst. for preliminary calculations, giving only the corner points of major zone elements, or important transition points. Such points may also be determined as a check on numerical calculations by another method.

Example 32 b

For the rupture zone shown in Fig. 31 F we found in Example 31 e the equivalent coordinates (3123) with the boundary conditions (3124) along the upper boundary OP.

Neglecting the common scale factor $\frac{\gamma \sin\beta}{c}$, assume that we want $\bar{x}$, $\bar{y}$ at the lowest point A $(a, b = \frac{\pi}{2}, 0)$ by means of Riemann integration. From (3227-8) we find, equating f to $-\bar{y}$ and g to $\bar{x}$ and changing the signs of (3227):

$$\bar{x}(A) = \bar{x}(P) + \int_{PO} (\bar{x}\, G_{R,a}\, da + \bar{y}\, G_R\, db)$$
$$\bar{y}(A) = \bar{y}(O) + \int_{PO} (\bar{x}\, G_R\, da - \bar{y}\, G_{R,b}\, db) \qquad (3234)$$

Expressing all integrals in terms of a, using that along OP we have $b = -a$, and inserting (3223) we obtain:

$$\bar{x}(A) = 2\pi - \int_0^{\frac{\pi}{2}} 4a \sqrt{\frac{a}{\frac{\pi}{2} - a}}\; J_1\left(2\sqrt{(\tfrac{\pi}{2} - a)\,a}\right) da$$
$$- \int_0^{\frac{\pi}{2}} J_o\left(2\sqrt{(\tfrac{\pi}{2} - a)\,a}\right) da \qquad (3235)$$
$$\bar{y}(A) = -1 - \int_0^{\frac{\pi}{2}} 4a\, J_o\left(2\sqrt{(\tfrac{\pi}{2} - a)\,a}\right) da$$
$$+ \int_0^{\frac{\pi}{2}} \sqrt{\frac{\frac{\pi}{2} - a}{a}}\; J_1\left(2\sqrt{(\tfrac{\pi}{2} - a)\,a}\right) da$$

According to (3123) the result is $\bar{x} = 1$, $\bar{y} = -\pi$.

Table 32 A: Rupture Zone. Equivalent Coordinates. Riemann Integration Along Diagonal.

Point no.	$A = a_P - a$	$B = b_P - b$	t	$C_o = J_o(2\sqrt{t})$	$C_1 = \frac{J_1(2\sqrt{t})}{\sqrt{t}}$	$\bar{x}$	$\bar{y}$	D
0	0	1.5708	0	1.0000	1.0000	6.2832	-1	1
1	0.0873	1.4835	0.1295	0.8749	0.9366	5.9341	-1	4
2	0.1745	1.3963	0.2437	0.7708	0.8830	5.5851	-1	2
3	0.2618	1.3090	0.3427	0.6856	0.8382	5.2360	-1	4
4	0.3491	1.2217	0.4265	0.6169	0.8014	4.8869	-1	2
5	0.4363	1.1345	0.4950	0.5630	0.7721	4.5379	-1	4
6	0.5236	1.0472	0.5483	0.5224	0.7498	4.1888	-1	2
7	0.6109	0.9599	0.5864	0.4942	0.7341	3.8397	-1	4
8	0.6981	0.8727	0.6092	0.4775	0.7248	3.4907	-1	2
9	0.7854	0.7854	0.6169	0.4720	0.7217	3.1416	-1	4
10	0.8727	0.6981	0.6092	0.4775	0.7248	2.7925	-1	2
11	0.9599	0.6109	0.5864	0.4942	0.7341	2.4435	-1	4
12	1.0472	0.5236	0.5483	0.5224	0.7498	2.0944	-1	2
13	1.1345	0.4363	0.4950	0.5630	0.7721	1.7453	-1	4
14	1.2217	0.3491	0.4265	0.6169	0.8014	1.3963	-1	2
15	1.3090	0.2618	0.3427	0.6856	0.8382	1.0472	-1	4
16	1.3963	0.1745	0.2437	0.7708	0.8830	0.6981	-1	2
17	1.4835	0.0873	0.1295	0.8749	0.9366	0.3491	-1	4
18	1.5708	0	0	1.0000	1.0000	0	-1	1

By numerical integration, using 5°-intervals ($-\Delta a = \Delta b = \frac{\pi}{36} = 0.0873$) and inserting directly into (3234), we may use a table like the one shown in Table 32 A.

D is the multiplier in Simpson's formula. We obtain, cf. (3223):

$$
\begin{aligned}
F_1 &= \sum B\, C_1\, \bar{x}\, D = 147.25 \\
F_2 &= \sum C_o\, \bar{y}\, D = -34.38 \\
F_3 &= \sum C_o\, \bar{x}\, D = 108.16 \\
F_4 &= \sum A\, C_1\, \bar{y}\, D = -34.38
\end{aligned}
\qquad (3236)
$$

$$
\begin{aligned}
\bar{x}\,(A) &= 2\pi + \frac{\Delta a}{3} F_1 + \frac{\Delta b}{3} F_2 \\
&= 6.2832 - 4.2835 - 1.0001 \\
&= 0.9996
\end{aligned}
$$

$$
\begin{aligned}
\bar{y}\,(A) &= -1 + \frac{\Delta a}{3} F_3 - \frac{\Delta b}{3} F_4 \\
&= -1.0000 - 3.1464 + 1.0001 \\
&= -3.1463
\end{aligned}
$$

$-\Delta a = \Delta b$ is here inserted as 0.08727.

The result is reasonably accurate, and is also relatively easy to calculate. Evidently, a table like the above has to be constructed for (almost) every point to calculate, so this method is only economical for one or a few points.

323 The Method of Finite Differences

The most direct way to solve the equations (3201) and (3202) numerically is by means of a finite difference approximation. For a theory of plasticity with more general assumptions, where the stress distribution cannot be found simply by introducing the a, b coordinate system, it may even be the only possible method. For the ideal clay considered here alternative methods exist, but this method may still be preferred in some cases.

The rupture zone is covered by a slip line net which is represented

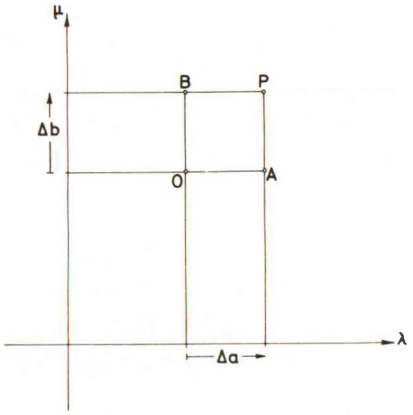

Fig. 32E: Unit Cell in the Slip Line Net. Method of Finite Differences.

in the λ,μ-plane by a rectangular net. Except for certain regions in the vicinity of special boundaries, the rupture zone is usually divided into subnets, each with equal net spacings Δa and Δb in the coordinate directions. If possible it is convenient to have $\Delta a = \Delta b$ (numerically), but it may be necessary to have different values for the two quantities in order to have an integer number of equal spacings across the rupture zone.

The unit step in calculations by this method is shown in Fig. 32E. The two functions, f and g, or any one of them, h, is known at the three mesh points O, A, and B, and it is desired to find the values at the fourth corner, P, to the same cell.

The following notation may now be used:

1. Δa is positive when m (and therefore a) is increasing in the positive direction of the a-lines, i.e. for increasing values of λ. Correspondingly Δb is positive when m, and therefore b, increases for increasing values of μ. It is seen that Δa and Δb have the same signs as R and S, respectively.
2. For simplicity the half centre angles $\alpha_a = \frac{1}{2}\Delta a$ and $\alpha_b = \frac{1}{2}\Delta b$ may be used.
3. The directions of calculation may be indicated by the two numbers e_a and e_b. e_a is equal to +1 or -1 according to whether the directions OA and BP is the positive or the negative direction of the a-lines. Correspondingly, e_b is equal to +1 or -1 according to whether OB and AP correspond to increasing or decreasing values of μ. The ratio e_a/e_b (equal to the product $e_a e_b$) is called e_f.

The difference equation corresponding to (3201) will then be:

$$f(P) - f(B) = e_a \alpha_a [g(B) + g(P)]$$
$$g(P) - g(A) = -e_b \alpha_b [f(A) + f(P)] \qquad (3237)$$

cf. Hill [1950].

These formulae are also valid when α_a and/or α_b are equal to zero. For the radii of curvature R, S, F, G the right hand sides of (3237) will usually have limit values which are finite, when $\alpha_a = 0$ and R or F infinite, or $\alpha_b = 0$ and S or G infinite. As explained previously the four limit values will be $\Delta s_a = \Delta S = \Delta \bar{x}$, $\Delta G = \Delta v$, $\Delta s_b = -\Delta R = \Delta \bar{y}$, and $\Delta F = \Delta u$, respectively, constant along the whole strip of unit cells.

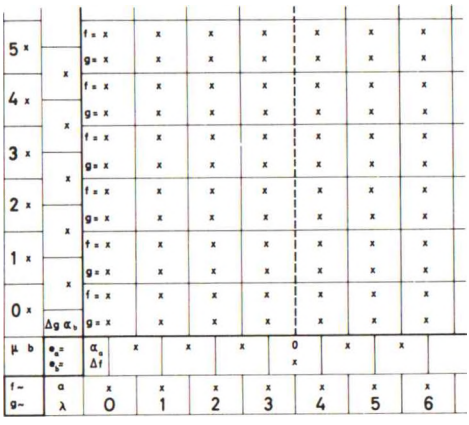

Fig. 32F: Layout for a Calculation Table by the Method of Finite Differences.

For that reason the steps across such strips need not be calculated or recorded explicitly. The numerical calculations may be performed (by hand) in a table with a lay-out in principle like the one shown in Fig. 32F. Notice that both functions f and g are recorded in the same table, together with the necessary information about a, b, α_a, α_b, e_a, and e_b. The functions R, S, $\bar{x}$, $\bar{y}$ etc. may also be recorded directly, however. In this case Eq. (3237) must be transformed as indicated in Sec. 321 (variables may have to be interchanged, and when $\bar{y}$ is used instead of f signs must also be changed).

In Fig. 32F a cross indicates that information is written into the table on the place in question. Discontinuities and strips of straight slip line sections may be indicated as shown in the table ($\lambda = 3$ and 4) by a dotted line separating the two slip lines which are placed on the two sides of the discontinuity. The values recorded for these slip lines are those for the preceding, respectively the following step, so all values recorded will usually be finite. Across the discontinuity α_a (or α_b) will be zero. As a supplementary information Δf (or Δg) may be recorded. It is zero for an ordinary discontinuity, but it will have a finite value for a strip of straight slip line sections, or for a slip line with slidings when the velocity functions are recorded.

For suitable values of α_a and α_b the function values may be inserted directly, the difference equations being solved by inspection. If f.inst. $\alpha_a = \alpha_b = .01$ (which is simpler than f.inst. $1^o = .01745$) the function values can be calculated directly with four significant figures, all differences having then two figures, which can easily be estimated beforehand.

For larger, and possibly unequal differences, (3237) may be solved explicitly:

$$f(P) = \frac{f(B) + e_a \alpha_a [g(A) + g(B)] - e_f \alpha_a \alpha_b f(A)}{1 + e_f \alpha_a \alpha_b}$$
$$g(P) = \frac{g(A) - e_b \alpha_b [f(A) + f(B)] - e_f \alpha_a \alpha_b g(B)}{1 + e_f \alpha_a \alpha_b} \qquad (3238)$$

Somewhat simpler formulae, which have also a more unfavourable propagation of errors, however, are obtained if the function values for the point O are taken into regard. If the formulae for $f(O)$ and $g(O)$ are found by the same procedure - they are identical to (3238), only with changed signs for e_a and e_b - and are subtracted from the expressions in (3238), we find:

$$f(P) = f(O) - f(A) + f(B) + \frac{2 \alpha_a}{1 + e_f \alpha_a \alpha_b} [g(A) + g(B)]$$
$$g(P) = g(O) + g(A) - g(B) - \frac{2 \alpha_b}{1 + e_f \alpha_a \alpha_b} [f(A) + f(B)] \qquad (3239)$$

If only one function is known, or is desired, (3202) may be used. The corresponding difference formula is:

$$h(P) - h(B) - h(A) + h(O) + e_f \alpha_a \alpha_b [h(O) + h(A) + h(B) + h(P)] = 0 \qquad (3240)$$

which gives:

$$h(P) = \frac{1 - e_f \alpha_a \alpha_b}{1 + e_f \alpha_a \alpha_b} [h(A) + h(B)] - h(O) \qquad (3241)$$

When $e_f \alpha_a \alpha_b$ is negative the above formulae will, strictly speaking, be divergent. The multiplication factor is so near unity, however, that usually it is of no practical importance.

The formulae (3237-41) and the lay-out shown in Fig. 32 F can be used directly for the types of initial value problems considered in the preceding section, with only the lay-out of the calculations varying a little between the types.

1. For the first type (Fig. 32 A) the curve C_o will in Fig. 32 F be represented by a diagonal string of cells, each mesh point on C_o being an end point (in the positive or negative slip line direction) of one a-line and one b-line. Between two neighbouring points on C_o we have $\Delta\lambda = \pm 1$ and $\Delta\mu = \pm 1$ dependent on the orientation of the curve and of the two families of slip lines in relation to the curve.

Thus, in passive zones we have always $\Delta\lambda = -\Delta\mu$, and in active zones $\Delta\lambda = \Delta\mu$. If possible the points on C_o are chosen so that the net spacings Δa and/or Δb are at least sectionally equal. For irregular, or irregularly loaded surfaces this may be difficult to obtain without a rather large work of interpolations. The fact that one set of net spacings is equal will also not give much simpler calculations, unless the other set of net spacings is also equal. Alternatively, for very large nets it may be an advantage to choose the net spacings Δa and Δb beforehand. All points on C_o which are end points either for a-lines or for b-lines (not in general coincident) with the chosen net spacings are then found by interpolation. After the calculation of a band of irregular cells along C_o (with fractional net spacings), the major part of the slip line net can then be calculated with sectionally equal values of Δa and Δb.

2. For the second type (Fig. 32 B) the two boundary slip lines, C_c and C_c', represented in Fig. 32 F by a row and a column of cells, can frequently be divided into sections where a or b are monotonic. In each of these sections we can use equal net spacings Δa or Δb, so all cells will be regular. The same may not be true if one of the slip line families is continued from another zone element, f. inst. a triangular zone as under 1. above.

3. For wall zones (Fig. 32 C) the curve C_o will be represented in Fig. 32 F by a diagonal string of cells, but the a-values or the b-values in the net may not be known, except for the point O. For the slip line through O the boundary condition for the curve C_o is known to be satisfied. For the next one, f. inst. ST on Fig. 32 C, the appropriate one of the equations (3237) may be used to find f (T) and g (T) if Δb (or Δa) and the relationship B (f, g) = 0 are known. Alternatively it may be used to find Δb (or Δa) if both f (T) and g (T) are known, also if they are known as functions of b (or a, or f. inst. a + b).

   The first slip line parallel to C_c can now be placed through the point T, and the first row of cells between this line and C_c can be calculated, all cells being regular. From the first point on the line the next slip line parallel to ST can now be calculated, intersecting C_o. In this way we can continue until the whole zone has been calculated.

In all three cases the calculation process ends with the bounding slip

lines, the exact position of which, i.e. the fractional spacings Δa or Δb, may not be known beforehand. Instead we have a supplementary condition f. inst. that the bounding slip lines for the zone must pass through a given point (a foot point for a wall) or must together with the bounding slip lines for another zone form a transition point (they intersect at the same point in the x,y-plane, and for this point they determine the same values of σ and m).

In such cases the simplest procedure is to continue the zone with equal net spacings outside the final boundaries, and to find the position of the boundaries by interpolation in the table. As a final step one may check the boundary strips with the spacings found in this way, possibly by trial and error, to ascertain that the supplementary conditions are satisfied with the desired accuracy.

Example 32 c

For the rupture zone considered in Example 32 b the results of a calculation of $\bar{x}$ and $\bar{y}$ by the method of finite differences are shown in Table 32 B. The same spacings ($\Delta a = \Delta b = 5^o = 0.0873$) are used as in the preceding example, and we start from the same boundary conditions. e_a and e_b are both equal to +1. Since the final results will normally only be needed in the mesh points of a net with f. inst. 30^o-intervals, the table shows only the 5^o-net in one cell of the large net, together with the final results.

For the first strip along the diagonal a + b = 0 we must use the formulae (3238). If f is replaced by $-\bar{y}$ and g by $\bar{x}$ they become:

$$\bar{x}(P) = \frac{\bar{x}(A) + 0.0436\,[\bar{y}(A) + \bar{y}(B)] - 0.0019\,\bar{x}(B)}{1.0019}$$

$$\bar{y}(P) = \frac{\bar{y}(B) - 0.0436\,[\bar{x}(A) + \bar{x}(B)] - 0.0019\,\bar{y}(A)}{1.0019} \qquad (3242)$$

All other cells may be calculated by means of (3239) which are transformed to:

$$\bar{x}(P) = \bar{x}(O) + \bar{x}(A) - \bar{x}(B) + 0.0871\,\left[\bar{y}(A) + \bar{y}(B)\right]$$

$$\bar{y}(P) = \bar{y}(O) - \bar{y}(A) + \bar{y}(B) - 0.0871\,\left[\bar{x}(A) + \bar{x}(B)\right] \qquad (3243)$$

The last mentioned formulae are easier to handle, but (3242) have a more favourable propagation of errors. In these formulae we have only one leading term, $\bar{x}(A)$ respectively $\bar{y}(B)$, and possible errors are transmitted

along the characteristics (b-lines, respectively a-lines), being slightly decreased or increased, according to whether Δa and Δb have the same, or opposite signs.

In (3243) we form still higher differences between the initial values in the diagonal direction (the terms $\bar{x}(A) - \bar{x}(B)$ and $\bar{y}(B) - \bar{y}(A)$). This means that an isolated error, which is not balanced by corresponding errors in the opposite direction, may be propagated with multiplication factors increasing as the binomial coefficients. This may not be dangerous for round-off errors in functions which are calculated from closed formulae, because such errors tend to balance out. However, it will always be necessary when possible to check the variation of differences along the diagonal.

In this example the control is simple because the differences along the diagonals parallel to the initial one ($a + b = 0$) are constant. The result is seen to be reasonably accurate, compare Table 32C where the exact values according to (3123) are given.

However, it is seen that the spacing $\Delta a = \Delta b = 5^{\circ}$ is not well suited. It could not be chosen much higher if the simple approximation (3237) should not be too inaccurate. On the other hand the full formulae (3242) have to be used for a rather high number of cells. It would probably be more economical to use either more accurate formulae (f. inst. the method of chord lengths) on a smaller number of cells (f. inst. $\Delta a = \Delta b = 15^{\circ}$), or the much simpler formulae (3237) directly on smaller cells ($\Delta a = \Delta b = 0.02$). As an example Table 32D shows the first part ($0 \leq a \leq 0.16$) of the calculations corresponding to Table 32B with small cells. In these cells the table values can be written down directly by inspection, possibly with an occasional correction of the last digit.

In this connection it should be noticed that if (3237) is used iteratively, inserting estimated values for f (P) and g (P) on the right hand side to obtain corrected values on the left hand side, the convergence will be very fast for Δa and Δb values of this order of magnitude.

Table 32 B: Rupture Zone. Equivalent Coordinates.
Finite Difference Integration Starting at Diagonal.

1. Cell with 5°-intervals ($\Delta a = \Delta b = 0.0873$)

a =	0	5°	10°	15°	20°	25°	30°	b =
$\bar{x}$ =	0	0.2613	0.5180	0.7565	0.9995	1.2154	1.4092	0
$\bar{y}$ =	-1.0000	-1.0114	-1.0454	-1.1014	-1.1784	-1.2749	-1.3891	
		0.3491	0.6090	0.8618	1.1028	1.3276	1.5318	5°
		-1.0000	-1.0418	-1.1059	-1.1916	-1.2976	-1.4222	
			0.6981	0.9568	1.2056	1.4400	1.6556	10°
			-1.0000	-1.0722	-1.1665	-1.2818	-1.4168	
				1.0472	1.3045	1.5493	1.7772	15°
				-1.0000	-1.1025	-1.2270	-1.3721	
					1.3963	1.6523	1.8931	20°
					-1.0000	-1.1329	-1.2875	
						1.7453	2.0000	25°
						-1.0000	-1.1633	
							2.0944	30°
							-1.0000	

2. Net with 30°-intervals ($\Delta a = \Delta b = 0.5236$)

a =	0	30°	60°	90°	b =
$\bar{x}$ =	0	1.4092	1.9200	1.0124	0
$\bar{y}$ =	-1.0000	-1.3891	-2.3128	-3.1432	
		2.0944	3.2230	2.9695	30°
		-1.0000	-2.4351	-4.1255	
			4.1888	5.0383	60°
			-1.0000	-3.4811	
				6.2832	90°
				-1.0000	

Table 32C: Rupture Zone. Equivalent Coordinates. Theoretical Values.

1. Cell with 5°-intervals ($\Delta a = \Delta b = 0.0873$)

a =	0	5°	10°	15°	20°	25°	30°	b =
$\bar{x}$ =	0	0.2610	0.5174	0.7646	0.9980	1.2135	1.4069	0
$\bar{y}$ =	-1.0000	-1.0114	-1.0454	-1.1014	-1.1785	-1.2751	-1.3896	
		0.3491	0.6088	0.8612	1.1018	1.3261	1.5299	5°
		-1.0000	-1.0418	-1.1060	-1.1918	-1.2979	-1.4226	
			0.6981	0.9565	1.2049	1.4389	1.6541	10°
			-1.0000	-1.0723	-1.1667	-1.2821	-1.4172	
				1.0472	1.3042	1.5487	1.7761	15°
				-1.0000	-1.1027	-1.2273	-1.3725	
					1.3963	1.6520	1.8925	20°
					-1.0000	-1.1331	-1.2879	
						1.7453	1.9997	25°
						-1.0000	-1.1635	
							2.0944	30°
							-1.0000	

2. Net with 30°-intervals ($\Delta a = \Delta b = 0.5236$)

a =	0	30°	60°	90°	b =
$\bar{x}$ =	0	1.4069	1.9132	1.0000	0
$\bar{y}$ =	-1.0000	-1.3896	-2.3138	-3.1416	
		2.0944	3.2207	2.9604	30°
		-1.0000	-2.4368	-4.1276	
			4.1888	5.0345	60°
			-1.0000	-3.4840	
				6.2832	90°
				-1.0000	

Table 32 D: Rupture Zone. Equivalent Coordinates.
Finite Difference Integration with Small Steps.

Cell with intervals $\Delta a = \Delta b = 0.02$

a =	0	0.02	0.04	0.06	0.08	0.10	0.12	0.14	0.16	b =
$\bar{x}$ =	0	0.0600	0.1200	0.1798	0.2394	0.2988	0.3581	0.4169	0.4754	0
$\bar{y}$ =	-1.0000	-1.0006	-1.0024	-1.0054	-1.0096	-1.0150	-1.0216	-1.0294	-1.0383	
		0.0800	0.1400	0.1999	0.2596	0.3191	0.3785	0.4375	0.4962	0.02
		-1.0000	-1.0022	-1.0056	-1.0100	-1.0158	-1.0228	-1.0310	-1.0403	
			0.1600	0.2200	0.2798	0.3394	0.3990	0.4581	0.5170	0.04
			-1.0000	-1.0038	-1.0088	-1.0150	-1.0224	-1.0310	-1.0408	
				0.2400	0.2999	0.3597	0.4194	0.4787	0.5378	0.06
				-1.0000	-1.0054	-1.0120	-1.0198	-1.0288	-1.0390	
					0.3200	0.3799	0.4397	0.4992	0.5585	0.08
					-1.0000	-1.0070	-1.0152	-1.0246	-1.0352	
						0.4000	0.4599	0.5196	0.5791	0.10
						-1.0000	-1.0086	-1.0184	-1.0294	
							0.4800	0.5399	0.5996	0.12
							-1.0000	-1.0102	-1.0216	
								0.5600	0.6199	0.14
								-1.0000	-1.0118	
									0.6400	0.16
									-1.0000	

324 Geometrical Methods

By the geometrical methods we consider the construction of finite cells in the slip-line field. The quantities that are used (such as chord lengths and centre angles) will therefore describe the entire cells. Considered as functions, their domains are therefore not the continuous x,y- or a,b-planes, but are the discrete (usually finite) set of cells.

The solution by geometrical methods may be obtained graphically; in fact some of the methods were made for that purpose. This may be an advantage in some cases, mainly for statically determined zones where only a

rough approximation is needed, but frequently a geometrical construction will be too inaccurate, and also too slow, f. inst. for a zone with mixed boundary conditions that have to be satisfied iteratively by several constructions back and forth over the zone. However, it is always possible to make the same calculations analytically. Then they can be as accurate as we desire, and we still have the advantage of using only a finite number of quantities. For the final nets, where all conditions are satisfied, we can then calculate the necessary coordinates to mesh points etc., so that they can be drawn if so desired.

One of the best known geometrical methods is the method of pole trails, introduced by Prager [1953]. It is based on the fact that for points on the same slip line the poles in Mohr's diagram will lie on a fixed curve. This can be seen from Fig. 32G. When σ and m are known for a point O, we can construct Mohr's circle for the point; it will have its centre at the point $\sigma = \sigma_O$. The pole P_O can also be constructed as the intersection point between the circle and a line through the lower tangent point a_O, forming the angle m_O with the σ-axis (positive in the positive direction of rotations).

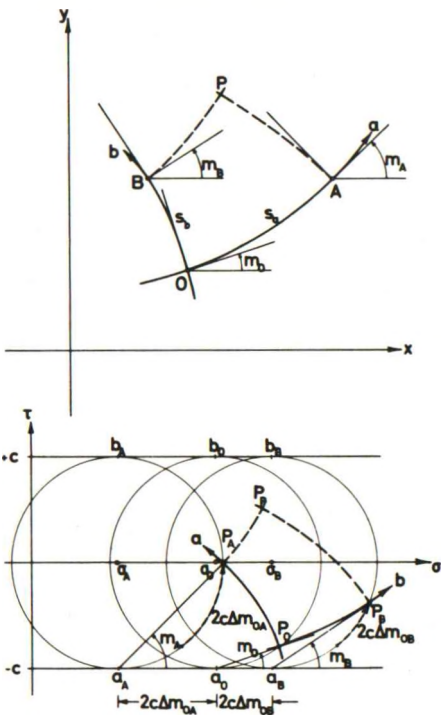

Fig. 32G: Pole Trails in Mohr Diagram Corresponding to Slip Lines in a Rupture Zone.

For a point A on the a-line through O we can construct Mohr's circle when the tangent angle m_A is known. The position of the centre point $\sigma = \sigma_A$ is found from (3101), and the pole can be constructed from the new tangent angle m_A. In the same way Mohr's circle and the pole can be found for a point B on the b-line through O, when the tangent angle m_B is known.

It is seen that this construction is independent of the arc lengths s_a and s_b. The pole trails $P_O P_A$ and $P_O P_B$ will only depend on the tangent angles m. It is further seen that the arc length measured on Mohr's circles between the positions of P_O and P_A is equal to the radius, c, times twice the differ-

ence in centre angle, $2\,\Delta m_{OA}$, i.e. equal to the distance between the two centres. The corresponding property is found for the movement of the pole from P_O to P_B. This means that the pole trails are cycloidal arcs through the point P_O. For the a-line we may obtain the pole trail by rolling the circle without sliding on the lower envelope $\tau = -c$ (in the negative direction of the σ-axis for increasing values of m). Correspondingly, for the b-line the circle is rolled without sliding on the upper envelope $\tau = c$, in the positive σ-direction for increasing values of m.

Therefore, the pole P_P for the intersection point P of the b-line through A and the a-line through B, i.e. the fourth corner point of the cell OAPB, can easily be constructed as the intersection point of the a-cycloid through P_B and the b-cycloid through P_A. Indeed, if σ and m are known for one point of a rupture zone, where also the net spacings Δa and Δb, and the number of cells in each direction are known (or its image in the λ, μ-plane with corresponding values of a and b for all system lines) the poles for all net points can be found as the mesh points in the corresponding net of cycloidal arcs in Mohr's plane. As all the cycloids are similar, only one curve need be calculated for a given scale in the σ, τ-plane. All other curves can then be found by translations parallel to the σ-axis, and by symmetry about the σ-axis. In practice only the chords $P_O P_A$ etc. need be drawn. Their directions and lengths can be measured on one (or two symmetrical) cycloids which are placed in a fixed position in relation to the σ, τ coordinate system, and are provided with divisions corresponding to the necessary values of m.

The net of pole trails obtained in this way can be used in two ways. For any point where it is desired Mohr's circle can be drawn, and the state of stress is obtained graphically in a direct way. One can also start with known boundary stresses (σ_n, τ_{nt}), construct the Mohr circles and the poles, and from these initial data draw the pole trail net for the whole zone. The corresponding cells in the xy-plane can be constructed, at least approximately, by observing that the chords AP and BP (Fig. 32G) for sufficiently small values of Δm_{OB} and Δm_{OA} will be nearly orthogonal to the chords $P_A P_P$ and $P_B P_P$ in the σ, τ-plane. From the position of P_P the tangent angle m_P for the a-line through P can be constructed, so the slip line sections AP and BP can be drawn as smooth arcs between their known endpoints, where also their tangent directions are known.

This method is fairly simple to use. It permits the construction of a whole rupture figure (at least if it is statically determined) on a drawing-board without any numerical calculations. The image slip lines in the hodo-

graph plane (Fig. 31 K) can also be constructed from the net of pole trails when sufficient boundary conditions for the velocities are known. Here the chords AP and BP can be assumed approximately parallel to the chords $P_A P_P$ and $P_B P_P$, respectively.

However, if the initial boundary stresses are not given graphically, which will hardly ever be the case, we cannot avoid some analytical calculations to find the initial pole positions. The method will therefore in practice never be purely graphical. Even if we want to find the slip line field graphically, we might then as well avoid the use of Mohr's circles altogether, by using Hencky's conditions (3104), and the properties (3105) of the a,b coordinate system. We only need a table of a- and b-coordinates for the (b- and a-) slip lines in the net. For any two points, such as A and P in Fig. 32G we can then find m_A and m_P from (3105). The chord direction can be defined by the mean value:

$$m_k = \frac{m_A + m_P}{2} \tag{3244}$$

The chord can now be drawn parallel, or, for b-lines, orthogonal to this direction. For graphical constructions one may easily find the directions corresponding to the different m-values by means of a scaled circle arc.

Notice that (3244) does not give exactly the same result as the method of pole trails, which defines the chord directions in another way. Both methods are approximations, however, and of the same order of accuracy, so from this point of view there is no reason to prefer one method to the other.

However, the last mentioned method has the advantage that, except possibly for initially given slip lines where x,y, and m are given for all points, and where (3244) therefore may not apply, all slip line sections can be drawn as circle arcs; and the angles between chord directions (such as between OB and AP, or between OA and BP) are equal to the corresponding differences in m (Δa and Δb, respectively). This follows directly from (3104), f. inst.:

$$\begin{aligned} m_{BP} - m_{OA} &= \frac{m_P + m_B}{2} - \frac{m_A + m_O}{2} \\ &= \frac{m_P - m_A}{2} + \frac{m_B - m_O}{2} = \Delta a \end{aligned} \tag{3245}$$

The geometry of a cell by this method is shown in Fig. 32H. Assume that the chords OA and OB are known together with the angle differences $2\alpha_a = \Delta a$ and $2\alpha_b = \Delta b$. We must then in the normal case, where the

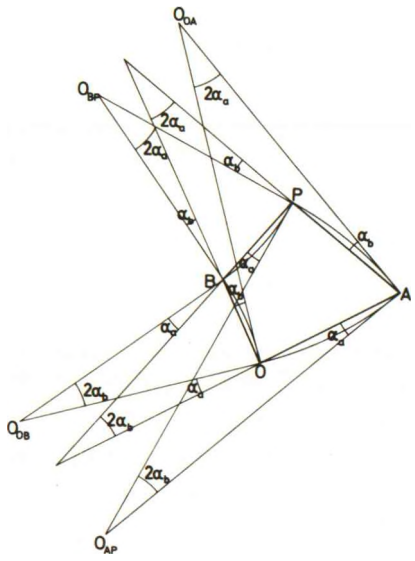

Fig. 32H: Cell in a Slip Line Net. Line Elements Approximated by Circle Arcs.

slip line sections OA and OB are circle arcs, have that the angle AOB satisfies the condition:

$$\angle AOB = \frac{\pi}{2} - \alpha_a + \alpha_b \qquad (3246\,a)$$

The chord directions AP and BP are then found simply by the fact that they form the angles $2\,\alpha_a$ and $2\,\alpha_b$ with OB and OA, respectively. Evidently we have:

$$\angle OAP = \frac{\pi}{2} - \alpha_a - \alpha_b$$

$$\angle OBP = \frac{\pi}{2} + \alpha_a + \alpha_b \qquad (3246\,b\text{-}d)$$

$$\angle APB = \frac{\pi}{2} + \alpha_a - \alpha_b$$

It is seen that opposite angles in the quadrangle OAPB are supplementary, so the figure can be inscribed in a circle (this is the geometrical consequence of Hencky's condition). The centres for the circle arcs can if desired be constructed as shown on the figure.

In special cases, where OA and/or OB are not circle arcs, f.inst. because they are boundary slip lines to rupture zones where the theoretically correct solutions are found in closed form, the correct slip line directions must be given at A and B, i.e. the directions AO_{AP}, AO_{OA}, BO_{OB}, and BO_{BP} are known. The directions AP and BP are then found from the fact that they form the angles α_b and α_a with AO_{OA} and BO_{OB}, respectively. The slip line sections AP and BP can then again be drawn as circle arcs.

The same constructions can be performed in the hodograph plane, so it is also possible to find the velocity fields by this method. All possible boundary conditions can be stated in terms of the cell elements shown on Fig. 32H, so in principle any failure problem can by this method be solved graphically.

However, this method can in a relatively simple way be expressed analytically. The calculations can then be made more accurate, and also faster. In this formulation the method is called the method of chord lengths. As ex-

plained above it is an alternative to the methods which use geometrical and velocity functions defined at any point in the rupture zones.

Example 32 d

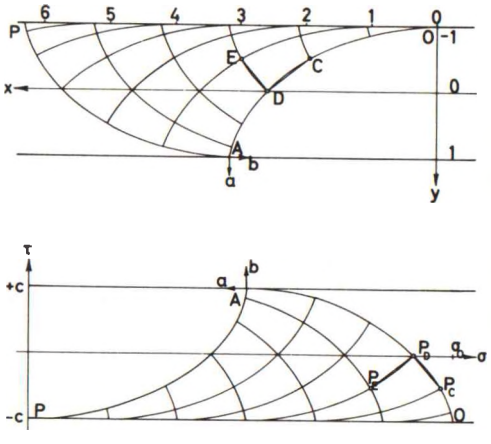

Fig. 32 I: Net of Pole Trails for the Rupture Zone in a Sloping Clay Layer.

For the rupture zone considered in the previous examples the net of pole trails is shown in Fig. 32 I. In this case it is similar to the slip line net, but the method of pole trails will not give the exact result. This is because for finite angle differences a chord such as CD, which is parallel to the pole trail chord $P_E P_D$, will not be orthogonal to the corresponding pole trail chord $P_C P_D$ (i.e. in finite cells of the cycloidal net the chords do not form orthogonal quadrangles even if $\alpha_a = \alpha_b$).

By the method of chord lengths we can construct a net of cells with constant angular differences $\Delta a = \Delta b = 2\alpha$, assuming the points along the upper boundary to be known:

$$m = 0, \quad x = 4a, \quad y = -1 \tag{3247}$$

We have here omitted the scale factor $\frac{\gamma \sin\beta}{c}$ on all coordinates and chord lengths.

It is easily seen that all mesh points with the same value of $m = a + b$ will be on the same line $y = \text{const.}$, and will be equidistant with the spacing:

$$A = \Delta x = 8\alpha \tag{3248}$$

all cell constructions based on two such points being similar.

For the construction No. q of this kind, between the line corresponding to $m = 2(q - 1)\alpha$ and the line for $m = 2q\alpha$, we have the triangle shown in Fig. 32 J. Notice that by the definition of the method the chords will here be orthogonal when $\Delta a = \Delta b$. For the a-line we find:

$$\Delta x_a = A \cos^2 (2q - 1)\alpha = 4\alpha[1 + \cos 2(2q - 1)\alpha]$$

$$\Delta y_a = A \cos (2q - 1)\alpha \sin (2q - 1)\alpha = 4\alpha \sin 2(2q - 1)\alpha \tag{3249}$$

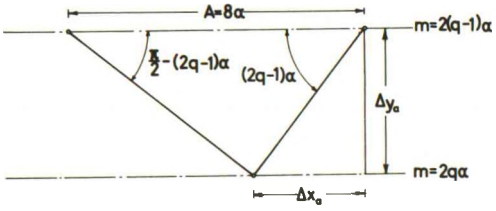

Fig. 32 J: Unit Cell Construction by the Method of Chord Lengths for a Sloping Clay Layer.

Summing the increments (3249) from q = 1 to q = n (x_o = 0 and y_o = -1) we obtain, f. inst. by using the construction in Fig. 32 K, and observing that 2 n α = m:

$$x_a^{(\alpha)} = 4n\alpha + \frac{2\alpha}{\sin 2\alpha} \sin 4n\alpha = 2m + K \sin 2m \qquad (3250)$$

$$y_a^{(\alpha)} = -1 + \frac{2\alpha}{\sin 2\alpha} (1 - \cos 4n\alpha) = -1 + K(1 - \cos 2m) \qquad (3251)$$

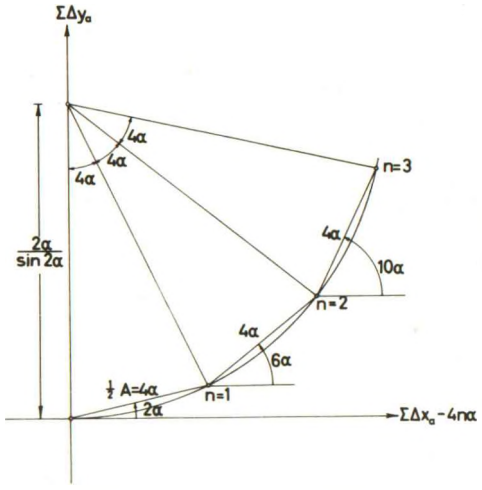

Fig. 32 K: Coordinate Increments by the Method of Chord Lengths for Zone in Fig. 32 I.

where

$$K = \frac{2\alpha}{\sin 2\alpha} \qquad (3252)$$

In the coordinate system x, y shown in Fig. 32 I we have the theoretically correct values for the a-line OA, cf. (2321) and (2323):

$$x_a = 2m + \sin 2m$$
$$y_a = -\cos 2m \qquad (3253)$$

The mesh points found by the method of chord lengths will therefore have the following errors in the coordinates:

$$e_x^{(\alpha)} = x_a^{(\alpha)} - x_a = (K - 1) \sin 2m$$
$$e_y^{(\alpha)} = y_a^{(\alpha)} - y_a = (K - 1)(1 - \cos 2m) \qquad (3254)$$

The distance between the approximate and the correct points will therefore be

$$d_\alpha = \sqrt{(e_x^{(\alpha)})^2 + (e_y^{(\alpha)})^2} = 2(K - 1) \sin m \qquad (3255)$$

provided the numerical calculations (or the graphical constructions) are performed with perfect accuracy.

According to (3255) the error in the position of the mesh points will increase along the a-line, its maximum value being obtained for the point A ($m = \frac{\pi}{2}$) where it is

$$d_{max} = 2\,(K - 1) = 2\,(\frac{2\,\alpha}{\sin 2\,\alpha} - 1) \qquad (3256)$$

which should be compared with the total arc length (= 4) or the total coordinate differences ($\Delta x = \pi$, $\Delta y = 2$).

The value d_{max} is shown as a function of the angle difference $2\,\alpha$ in Fig. 32 L. For the whole range we may with a good approximation take $d_{max} \simeq \frac{(2\,\alpha)^2}{3}$.

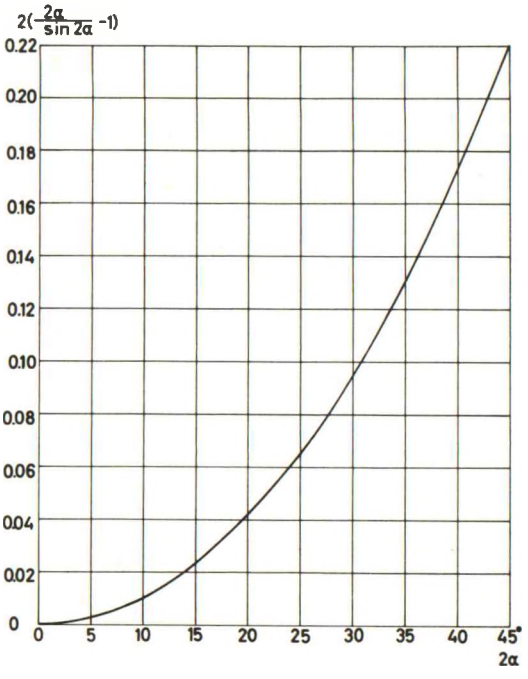

Fig. 32 L: Maximum Relative Point Error ($\Delta x = \pi$, $\Delta y = 2$, Total Arc Length = 4) by the Method of Chord Lengths for Zone in Fig. 32 I.

To the result of the above calculations the following remarks may be made.

1. Because of the rapidly changing curvature of the slip lines this is a rather severe test of the method of chord lengths. In most other rupture zones the slip lines will be more nearly circle arcs, so the maximum error (over a total tangent rotation of $\frac{\pi}{2}$) shown in Fig. 32 L will usually be an overestimation.

2. By the finite difference method (Table 32 B compared with Table 32 C) we found a maximum error of 0.0124 ($\bar{x}$ for the point A) with a net spacing $\Delta a = \Delta b = 5^{\circ}$. This value also includes a round-off error, which by comparison of the values of $\bar{y}$ at the same point (-3.1432 against the theoretical value $-\pi$) can be estimated to be of an order of magnitude not exceeding 0.0025. The maximum error e_y resulting from the method of finite differences can therefore be estimated to about 0.01. From Fig. 32 L it is seen that by the method of chord lengths we would for the same net spacing find $e_y = 0.0025$. If we allowed an error of about 0.01, the spacing $\Delta a = 2\alpha = 10^{\circ}$ would be sufficient. Thus, by using the method of chord lengths the number of cells to compute could be reduced to about one quarter and give the same accuracy as before.

3. In practice a value of d_{max} of 0.02 - 0.05 (for rough calculations possibly 0.10) would be acceptable. Therefore angle differences 2α of about 15°-30° should give results which are accurate enough for all practical purposes.

4. For rupture figures where it is important that the accuracy is known (and is better than a given standard) the calculations can be performed simultaneously with two different net spacings. Assuming all e_x and e_y (or errors Δk on the chord lengths) to be proportional to the second power of the net spacing, the accuracy can be estimated, and corrected values can be deduced from the differences between the two results. If so desired the same method can be used by the method of finite differences. The accumulation of too great round-off errors is prevented by the use of one or two more figures in the calculations than are needed in the result.

325 The Method of Chord Lengths

This method is concerned with geometrical quantities, viz. chord lengths and centre angles for the cells in the slip line net, which are taken to be independent of the directions of calculations. These directions are, as

in Sec. 323, characterized by the numbers e_a and e_b, which are equal to +1 when the calculations are performed in the positive directions of the slip lines, and to -1 when in the negative slip line directions.

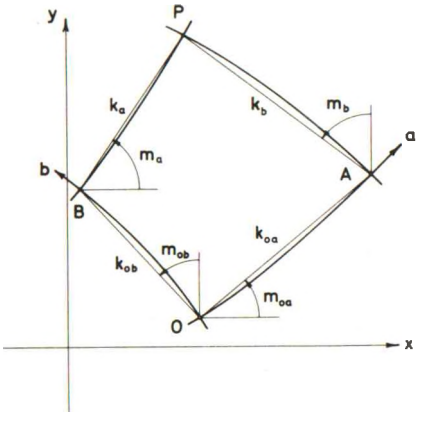

Fig. 32 M: Unit Cell in the Slip Line Field by the Method of Chord Lengths.

The notations are shown in Fig. 32 M (for e_a and e_b both equal to +1). The known points are A and B, and usually also O, so that the directions of calculations are always BP (along an a-line) and AP (along a b-line). The unknown chords are correspondingly k_a and k_b, whereas k_{oa} and k_{ob} are known if they exist. Chord lengths are always positive (if the slip line net is geometrically possible). The inclinations of the chords are defined by means of the stress function m. The quantities m_{oa}, m_{ob}, m_a, and m_b are defined by the following equations, which also indicate their relations to the net spacings $\Delta a = 2\,\alpha_a$ and $\Delta b = 2\,\alpha_b$.

$$
\begin{aligned}
m_{oa} &= \tfrac{1}{2}(m_O + m_A) = m_O + e_a\,\alpha_a \\
m_{ob} &= \tfrac{1}{2}(m_O + m_B) = m_O + e_b\,\alpha_b \\
m_a &= \tfrac{1}{2}(m_B + m_P) = m_O + e_a\,\alpha_a + 2\,e_b\,\alpha_b \\
m_b &= \tfrac{1}{2}(m_A + m_P) = m_O + 2\,e_a\,\alpha_a + e_b\,\alpha_b
\end{aligned}
\qquad (3257)
$$

α_a and α_b being positive when a increases for increasing values of λ, and b increases for increasing values of μ, respectively, so that:

$$
\begin{aligned}
m_A &= m_O + 2\,e_a\,\alpha_a \\
m_B &= m_O + 2\,e_b\,\alpha_b \\
m_P &= m_O + 2\,e_a\,\alpha_a + 2\,e_b\,\alpha_b
\end{aligned}
\qquad (3258)
$$

The geometrical formulae for the cell are derived from the relations:

$$x_P = x_B + e_a k_a \cos m_a = x_O - e_b k_{ob} \sin m_{ob} + e_a k_a \cos m_a$$

$$= x_A - e_b k_b \sin m_b = x_O + e_a k_{oa} \cos m_{oa} - e_b k_b \sin m_b \tag{3259}$$

$$y_P = y_B + e_a k_a \sin m_a = y_O + e_b k_{ob} \cos m_{ob} + e_a k_a \sin m_a$$

$$= y_A + e_b k_b \cos m_b = y_O + e_a k_{oa} \sin m_{oa} + e_b k_b \cos m_b$$

For normal cells in the interior of rupture zones k_{oa} and k_{ob} are both known. From (3259) we may find

$$k_a = \frac{k_{oa} \cos(\alpha_a + e_f \alpha_b) - e_b k_{ob} \sin 2\alpha_a}{\cos(\alpha_a - e_f \alpha_b)}$$

$$k_b = \frac{e_a k_{oa} \sin 2\alpha_b + k_{ob} \cos(\alpha_a + e_f \alpha_b)}{\cos(\alpha_a - e_f \alpha_b)} \tag{3260}$$

using also (3257) and the abbreviation $e_f = e_a e_b = e_b/e_a$. $e_f e_a = e_b$ and $e_f e_b = e_a$, because $e_a^2 = e_b^2 = 1$. From (3260) the coordinates (x_P, y_P) can be found (and checked) by means of (3259).

In the first initial value problem (Fig. 32 A) k_{oa} and k_{ob} are not defined for the first string of cells along the curve C_o. In this case one may assume the coordinates (x_A, y_A) and (x_B, y_B) to be known. From (3259) we can then find:

$$k_a = e_a \frac{(x_A - x_B) \cos m_b + (y_A - y_B) \sin m_b}{\cos(\alpha_a - e_f \alpha_b)}$$

$$k_b = e_b \frac{(x_A - x_B) \sin m_a - (y_A - y_B) \cos m_a}{\cos(\alpha_a - e_f \alpha_b)} \tag{3261}$$

If the curve C_o can be approximated with a circle arc between the points B and A, cf. Sec. 222, Eq. (3261) can be obtained in a simpler way. Let the curve be oriented by defining the positive direction of s, and let β be the angle between the x-axis and the tangent direction t. A circle arc between the points A and B may be defined by the chord length k_s (always positive), the angle ω_s between the x-axis and the chord (positive as β), the half centre angle $\alpha_s = -\frac{1}{2}\Delta\beta$, positive when β is decreasing in the positive direction of s, and a number e_s which is equal to +1 when the direction

from B to A is in the positive direction of s, and is equal to -1 when this direction is in the negative direction of s.

It is seen that k_s, ω_s, and α_s are purely geometrical quantities which define the circle arc, whereas the relative positions of A and B, which also depend on which slip line family should be used through each point, are given by the number e_s. As it is shown in Sec. 331, a unique relation exists between e_a, e_b, and e_s. For simple geometrical reasons e_s must be equal to $-e_f = -e_a e_b$.

From the above definitions we obtain:

$$x_A - x_B = e_s k_s \cos\omega_s = -e_f k_s \cos\omega_s$$
$$y_A - y_B = e_s k_s \sin\omega_s = -e_f k_s \sin\omega_s \tag{3262}$$

Inserting these expressions in (3261) we find:

$$k_a = e_a e_s k_s \frac{\cos(m_b - \omega_s)}{\cos(\alpha_a - e_f \alpha_b)} = -e_b k_s \frac{\cos(m_b - \omega_s)}{\cos(\alpha_a - e_f \alpha_b)}$$
$$k_b = e_b e_s k_s \frac{\sin(m_a - \omega_s)}{\cos(\alpha_a - e_f \alpha_b)} = -e_a k_s \frac{\sin(m_a - \omega_s)}{\cos(\alpha_a - e_f \alpha_b)} \tag{3263}$$

It should be noticed that the directions of calculation are related to the values of m in relation to ω. In geometrically possible zones k_a and k_b must both be positive, so the values of e_a and e_b are evidently determined by the quadrant in which the angles $(m_b - \omega_s)$ and $(m_a - \omega_s)$ are located.

Normally, the quantity which is given directly at the points A and B will be $m_t = m - \beta$. It can be introduced by observing that

$$m_b - \omega_s = m_{tA} + e_b \alpha_b - e_s \alpha_s$$
and
$$m_a - \omega_s = m_{tB} + e_a \alpha_a + e_s \alpha_s \tag{3264}$$

By means of the above formulae the two first initial value problem types can be solved directly. For boundary points in a wall zone, where x,y, and m are known as functions of the arc length s, we may have to solve (3259) directly, using also (3257), so that the given boundary conditions are satisfied. This problem is considered separately in the following section on boundary conditions.

The construction of finite cells may be used in the hodograph plane to find the velocity field in a rupture zone. We have seen that Hencky's condi

tion is also valid in this plane. Therefore, if we approximate the slip line sections by circle arcs, and take the deformation condition to mean that the chord length between any two consecutive net points must remain unaltered, the above construction and analytical formulae can be applied directly, cf. Fig. 32 N.

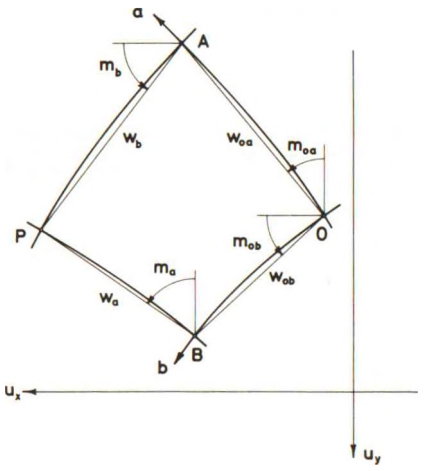

Fig. 32 N: Unit Cell in the Hodograph Plane.

The velocity difference $\Delta \bar{w}_{BP}$ between the end points of a chord BP along an a-line will therefore be orthogonal to the corresponding chord in the x, y-plane, i.e. it will form the angle m_a with the negative direction of the u_y-axis, and it will be equal to

$$w_a = r_a k_a \tag{3265}$$

where r_a is the angular velocity of the chord, positive in the positive direction of rotations.

For a unit cell OAPB in the hodograph plane we use the same convention of directions of calculation, and the same indices for the chord lengths w as in the physical plane. Notice that w has the same sign as r.

The unknown chord lengths w_a and w_b may be found by any one of two formulae corresponding to (3260) and (3261). Usually a formula corresponding to (3263) will have no practical use. We have, evidently:

$$\begin{aligned} u_{xP} &= u_{xB} + e_a w_a \sin m_a = u_{xA} + e_b w_b \cos m_b \\ u_{yP} &= u_{yB} - e_a w_a \cos m_a = u_{yA} + e_b w_b \sin m_b \end{aligned} \tag{3266}$$

from which we find:

$$\begin{aligned} w_a &= e_a \frac{(u_{xA} - u_{xB}) \sin m_b - (u_{yA} - u_{yB}) \cos m_b}{\cos (\alpha_a - e_f \alpha_b)} \\ w_b &= e_b \frac{-(u_{xA} - u_{xB}) \cos m_a - (u_{yA} - u_{yB}) \sin m_a}{\cos (\alpha_a - e_f \alpha_b)} \end{aligned} \tag{3267}$$

These equations are seen to be completely equivalent to (3261) when, as mentioned previously, x is replaced by $-u_y$, and y by u_x. If the chord lengths w_{oa} and w_{ob} are known, (3267) may be transformed to:

$$w_a = \frac{w_{oa} \cos(\alpha_a + e_f \alpha_b) - e_b w_{ob} \sin 2\alpha_a}{\cos(\alpha_a - e_f \alpha_b)}$$

$$w_b = \frac{e_a w_{oa} \sin 2\alpha_b + w_{ob} \cos(\alpha_a + e_f \alpha_b)}{\cos(\alpha_a - e_f \alpha_b)} \qquad (3268)$$

which are evidently equivalent to (3260).

As explained previously a sliding Δu or Δv along an a-line or a b-line, respectively, will give rise to a row of cells with α_b or α_a equal to zero, and with all $w_b = -\Delta u$ or $w_a = \Delta v$. Such cells, which have k_b or k_a equal to zero, can be treated as perfectly normal cases by the formulae (3260-1) and (3267-8).

The condition of positive maximum shear strain ϵ can be tested approximately by observing that for any chord k_a in the a-direction we have:

$$r_a = \frac{w_a}{k_a}$$

Correspondingly (3269)

$$r_b = \frac{w_b}{k_b}$$

For the four chords meeting at any mesh point (for boundary points possibly only two chords) we may therefore take the condition to mean that the smallest one of the two quantities r_a must be greater than or equal to the largest one of the quantities r_b.

Notice that since the chord lengths k_a and k_b are found by purely geometrical considerations it is not certain that the equilibrium conditions are satisfied for any cell regarded as a whole. The calculation of the deformation work for a rupture zone by means of the stress resultants along the zone boundaries will not, therefore, be strictly consistent. The error will decrease with decreasing values of α_a and α_b, however.

For statically determined rupture zones we might refine the method so that the stress resultants become much more correct. We could divide each circle arc, such as BP, into two arcs, each with the centre angle α_a, but with different chord lengths k_{a1} and k_{a2}. We could then satisfy four con-

ditions, viz. the two geometric ones and the two equations of projection, by the four unknown quantities k_{a1}, k_{a2}, k_{b1}, and k_{b2} in each cell.

In this way we should have a method very similar to Brinch Hansen's equilibrium method for rupture zones, but more general because both families of slip lines in the net could be considered (and not just the bounding slip line of one family, although this would be sufficient for most practical purposes). The method would satisfy the equilibrium conditions very accurately, so quite large centre angles could be used. However, the corresponding cells in the hodograph plane would then also become large, and here we have no supplementary conditions corresponding to the equilibrium equations. The accuracy in the velocity field would therefore decrease, so the method could only be used when the details in the velocity field had no special importance, i.e. only in statically determined zones and not in mixed boundary condition zones.

For the first mentioned purpose the method might give the final solution in one operation. However, it is a question whether the calculation work is much reduced. By the normal method of chord lengths each step consists in the insertion into simple, linear formulae, and even if this must be done several times it may actually be easier than the solution of four equations, two of the first and two of the second degree, in four unknown quantities. Therefore, in the following the normal method of chord lengths, which is also more generally applicable, is assumed to be used.

Example 32 e

The recording of calculation results obtained by the method of chord lengths cannot be done in a simple way by using the table shown in Fig. 32 F. Instead a lay-out like the one shown in Fig. 32 O may be used.

At the places marked P functions characterizing the mesh points are recorded. For the geometrical construction of the slip line net the coordinates (x, y) and possibly also values of σ and m are indicated as required. For velocity fields the components u_x, u_y and possibly also u, v are indicated.

The places marked A and B are intended for the chords in the a- and b-direction, respectively. Thus, at A the chord lengths k_a and w_a are indicated together with m_a and possibly other quantities characterizing the circle arcs (f. inst. radius or coordinates to centre).

Finally, at the places marked C the coefficients in the formulae may be indicated as necessary. For example:

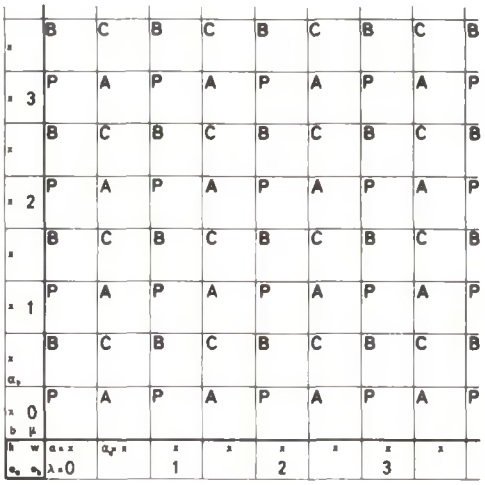

Fig. 32O: Layout for a Calculation Table by the Method of Chord Lengths.

$$K_{aa} = K_{bb} = \frac{\cos(\alpha_a + e_f\,\alpha_b)}{\cos(\alpha_a - e_f\,\alpha_b)}$$

$$K_{ab} = -e_b\,\frac{\sin 2\,\alpha_a}{\cos(\alpha_a - e_f\,\alpha_b)} \qquad (3270)$$

$$K_{ba} = e_a\,\frac{\sin 2\,\alpha_b}{\cos(\alpha_a - e_f\,\alpha_b)}$$

cf. (3260) and (3268).

If the chords in a rectangle zone with n_a net spacings in the a-direction and n_b spacings in the b-direction are represented in an Algol program by the arrays $k_a\,[\,1{:}n_a,\ 0{:}n_b\,]$ and $k_b\,[\,0{:}n_a,\ 1{:}n_b\,]$, Eq. (3260) and the sign rules can be summarized by the formulae

$$\begin{aligned} k_a\,[\,i_a,\ i_b\,] &= K_{aa}\,k_a\,[\,i_a,\ i_b - e_b\,] + K_{ab}\,k_b\,[\,i_a - e_a,\ i_b\,] \\ k_b\,[\,i_a,\ i_b\,] &= K_{ba}\,k_a\,[\,i_a,\ i_b - e_b\,] + K_{bb}\,k_b\,[\,i_a - e_a,\ i_b\,] \end{aligned} \qquad (3271)$$

the subscript limits for k_a and k_b, and the subscript expressions being indicated in square brackets for the sake of clarity (in accordance with the Algol conventions).

In practical calculations by hand a table like the one shown in Fig. 32 O will frequently take up too much space. It may then be subdivided into a number of smaller tables, each containing the places marked P, A, or B in the larger table.

326 Stress Resultants Along Zone Boundaries

As explained in Chap. 2 the stress resultants along the zone boundaries are used in the calculation of the rupture figure, either directly or for the calculation of the deformation work. They may be expressed as curve integrals in the following way.

For boundaries to external rigid bodies the local surface coordinate system t, n is used as in Sec. 222. It corresponds to an orientation s of the boundary curve encircling the clay material in the negative direction of rotations, cf. Fig. 32 P.

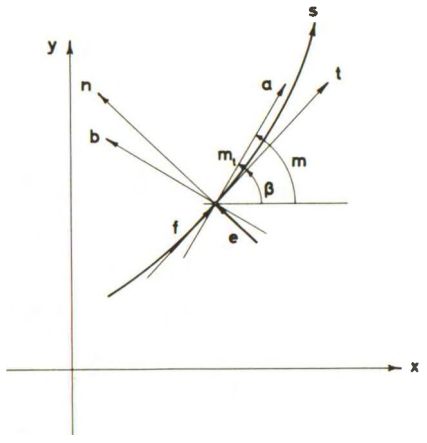

Fig. 32 P: Earth Pressure Components Along a Boundary to an External Rigid Body.

At each boundary point the tangent angle β is known together with the stress functions σ and m, and therefore also the angle $m_t = m - \beta$. The earth pressure components $e = \sigma_n$ and $f = \tau_{nt}$ acting upon the rigid body can be found by means of Mohr's circle. Since there will always be slidings between an external rigid body and the clay in a rupture zone, one must have

$$f = \tau_a = e_t c_a = -c \cos 2 m_t \quad (3272)$$

As explained in Sec. 311 the number e_t (equal to +1 or -1) indicates the sign of u_s, and therefore of τ_{nt}. The last expression in (3272) is used to determine m_t when the rupture zone is calculated, cf. Sec. 331 and 336.

One must also have

$$e = \sigma - c \sin 2 m_t \quad (3273)$$

cf. (2319).

The contribution from an arc element ds to the force components Q_i^{zp} and to the work expression $W = Q_i^{zp} w_i$ will then be:

$$\begin{aligned} d Q_x^{zp} &= (e \sin\beta - f \cos\beta)\, ds \\ d Q_y^{zp} &= -(e \cos\beta + f \sin\beta)\, ds \\ d M_z^{zp} &= y\, d Q_x^{zp} - x\, d Q_y^{zp} \end{aligned} \tag{3274}$$

and

$$\begin{aligned} d W &= w_x\, d Q_x^{zp} + w_y\, d Q_y^{zp} + r_z\, d M_z^{zp} \\ &= -(e\, u_n + f\, u_t)\, ds \end{aligned} \tag{3275}$$

cf. (2210). The movement and velocity components are those for the rigid body.

For boundaries to rigid bodies of clay expressions of the same kind may be obtained. If the direction of integration is chosen so that the rigid body is encircled in the positive direction of rotation (i.e. the rupture zones in the negative direction), and it is used that the boundary curves are slip lines, the stress parameters σ and m can be introduced. One finds:
for a-lines:

$$\begin{aligned} d Q_x^{zc} &= (\sigma \sin m + c \cos m)\, ds_a \\ d Q_y^{zc} &= (-\sigma \cos m + c \sin m)\, ds_a \\ d M_z^{zc} &= (\bar{x}\sigma + \bar{y}c)\, ds_a \end{aligned} \tag{3276}$$

and

$$d W = (\sigma v - c u)\, ds_a$$

for b-lines:

$$\begin{aligned} d Q_x^{zc} &= (\sigma \cos m + c \sin m)\, ds_b \\ d Q_y^{zc} &= (\sigma \sin m - c \cos m)\, ds_b \\ d M_z^{zc} &= (\bar{x}c + \bar{y}\sigma)\, ds_b \end{aligned} \tag{3277}$$

and

$$d W = (-\sigma u + c v)\, ds_b$$

In these formulae the arc elements

$$ds_a = Rda = d\bar{x} - \bar{y}da$$

and (3278)

$$ds_b = Sdb = d\bar{y} + \bar{x}db$$

cf. (3108) and (3120), must be taken with signs.

The expressions (3276-8) are used when the rupture zone has been calculated by means of f. inst. the method of finite differences. When the method of chord lengths is used the integrations can be performed for each circle arc, R or S being constant between the end points, when also (3105) is used. In this case the total force resultants can therefore be obtained as sums of finite expressions for the individual circle arcs.

However, for that purpose it may be simpler to use one set of expressions, independent of the type of slip line and the direction of integration. If Brinch Hansen's notation is used we find the following conventions and sign rules, cf. Fig. 32Q.

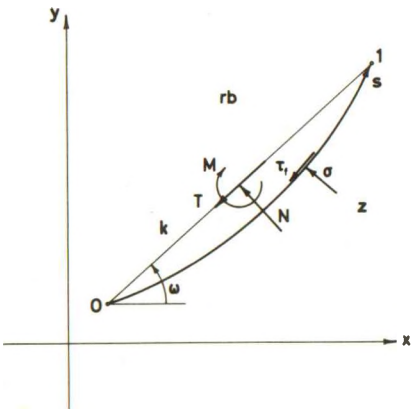

Fig. 32Q: Stress Resultants Along a Circle Arc Slip Line.

Consider a slip line arc between the points No. 0 and 1, separating a rigid body of clay, marked rb, from a rupture zone, marked z. Since the rigid body is encircled in the positive direction of rotations it must necessarily be located in the positive direction from the direction 0-1. Let the direction of integration, as in the preceding sections, be indicated by the two numbers e_a and e_b (e_a = +1 when the direction 0-1 is in the positive a-direction, and -1 when it is in the negative a-direction; correspondingly e_b = +1 or -1 according to whether the direction 0-1 is in the positive or negative b-direction).

The circle arc has the chord length k, the inclination ω, and the half centre angle α, which are found by the following formulae.

$$k = k_a \quad \text{for a-lines}$$

$$= k_b \quad \text{for b-lines} \qquad (3279)$$

$$\alpha = e_a \alpha_a \quad \text{for a-lines}$$
$$= -e_b \alpha_b \quad \text{for b-lines} \tag{3280}$$

$$\omega = m_a + (e_a - 1)\frac{\pi}{2} + 2p\pi \quad \text{for a-lines}$$
$$= m_b + e_b \frac{\pi}{2} + 2p\pi \quad \text{for b-lines} \tag{3281}$$

where p is an arbitrary integer number (positive or negative, or zero).

The rigid body is acted upon by a shear stress τ_f, positive in the direction from 1 to 0, which is equal to

$$\tau_f = c \quad \text{for a-lines}$$
$$= -c \quad \text{for b-lines} \tag{3282}$$

and by a normal stress σ, equal to the mean normal stress, which varies linearly between the end points of the circle arc. Let σ_m be the value of σ at the mid point of the arc.

$$\sigma_m = \sigma_{(0)} - 2\tau_f \alpha = \sigma_{(1)} + 2\tau_f \alpha$$
$$= \sigma_{(0)} - \tau_f N^Z = \sigma_{(1)} + \tau_f N^Z \tag{3283}$$

with Brinch Hansen's notation.

The resultant force components N, T, and M, acting in the mid point of the chord, and positive as shown in Fig. 32Q are found by the following expressions, cf. Brinch Hansen [1957]; they can also be derived from (2214-16).

$$N = k\sigma_m = k(\sigma_{(0)} - \tau_f N^Z)$$
$$= k(\sigma_{(1)} + \tau_f N^Z)$$
$$T = \tau_f k T^Z \tag{3284}$$
$$M = \tau_f k^2 M^Z$$

where

$$N^Z = 2\alpha$$
$$T^Z = 2\alpha \cot\alpha - 1 \tag{3285}$$
$$M^Z = \frac{1}{2}(\alpha - \alpha \cot^2\alpha + \cot\alpha)$$

These quantities are tabulated as functions of α by Brinch Hansen [1957].

It should be noticed that, strictly speaking, the direction of integration in Fig. 32Q is defined in the opposite direction of the one used by Brinch Hansen. This difference is of no practical importance, however.

If the coordinates to the mid point of the chord are called (x_m, y_m), the contribution from the circle arc to the total force resultants for the rigid body of clay, and to the work expression for this body, will be:

$$\Delta Q_x^{zc} = N \sin\omega + T \cos\omega$$

$$\Delta Q_y^{zc} = -N \cos\omega + T \sin\omega \tag{3286}$$

$$\Delta M_z^{zc} = y_m \Delta Q_x^{zc} - x_m \Delta Q_y^{zc} - M$$

and

$$\Delta W = w_x^c \Delta Q_x^{zc} + w_y^c \Delta Q_y^{zc} + r_z^c \Delta M_z^{zc} \tag{3287}$$

The formulae are not especially simple, but it is easy to devise a table of calculations, or an Algol routine for the use with computers, which makes it possible to record the constituent terms with a reasonable safety against mistakes. The above formulae and sign rules may also be used for line ruptures. For free surfaces to rigid bodies of clay the necessary formulae have been indicated in Sec. 222.

33 BOUNDARY CONDITIONS FOR ZONES

331 Free Surfaces

In section 33 the different possible boundary conditions are formulated in terms of the functions defined in section 31, and are evaluated in the light of the calculation methods considered in section 32. Thus, for each type of boundary the conditions prescribed for each of the function sets $\bar{x}$, $\bar{y}$, u, v (equivalent coordinates) and R, S, F, G (radii of curvature) are indicated, together with the corresponding conditions for calculations by the method of chord lengths.

For free surfaces the notation shown in Fig. 33 A is used (cf. Fig. 22 B). The local surface coordinate system t,n is at any point defined by the coordinates x,y to the point, and the tangent angle β, assuming n to point outwards from the clay.

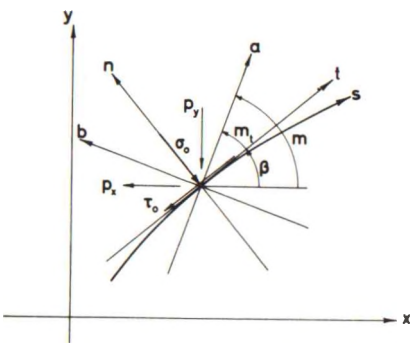

Fig. 33 A: Local Surface Coordinate System and Loading Components for a Free Surface.

The loading on the surface is given by the components p_x, p_y in the negative coordinate directions -x and -y, respectively, or, alternatively, by the normal and shear stress components σ_o and τ_o.

The state of stress for any point in the rupture zone is characterized by the mean normal stress σ and the tangent angle m to the positive a-direction, or, alternatively by the coordinates a,b to the surface point in the a,b-plane, assuming a reference set σ_O, m_O for the origin point in this plane to be chosen. For simplicity we use also the angle m_t between the positive t-direction and the positive a-direction.

From (2203) and (2319) we find:

$$\sigma_n = \sigma_o = p_y \cos^2\beta - p_x \sin^2\beta = \sigma - c \sin 2m_t$$
$$\tau_{nt} = \tau_o = (p_x + p_y) \sin\beta \cos\beta = -c \cos 2m_t \tag{3301}$$

These equations determine m_t and σ. However, a certain ambiguity exists, partly because it does not follow from the surface loadings whether the normal stress component σ_t parallel to the surface is greater than or smaller than σ_n. The absolute value of the difference between σ_n and σ_t is given, however, by the fact that the clay is in failure. According to (2319) we have:

$$\sigma_t - \sigma_n = 2c \sin 2m_t = \pm 2c \sqrt{1 - (\tau_o/c)^2} \tag{3302}$$

Besides we can define the positive direction of a in two possible ways when the position of the a-line through the point is given. Both of these ambiguities follow from the periodicity of the trigonometric functions in (3301).

In the equation:

$$\cos 2m_t = -\frac{\tau_o}{c} \tag{3303}$$

we call the principal solution i ($0 \leq i \leq \frac{\pi}{2}$ for $-1 \leq \frac{\tau_o}{c} \leq 1$). We then have the following two solutions:

$$m_{to} = \pm i \tag{3304}$$

In the first case we have $\sigma_t \geq \sigma_n$, cf. (3302). It is called the passive state of failure corresponding to the given boundary stresses. Correspondingly in the active state of failure we have $\sigma_t \leq \sigma_n$. The two cases coincide for $\tau_o = \pm c$. The surface will then be a tangent to a slip line at the point.

Which of the two possible states of failure to assume for a given boundary zone must be determined from other boundary conditions. In this respect the stress distribution in the zone can be said to depend on the movements of surrounding rigid bodies.

m_t is defined as the pertinent angle given by (3304) plus a multiple of π, to orient the slip lines in the desired directions, and to bring the zone into its correct position in the a,b-plane in relation to possible other zones in the rupture figure. By definition m is equal to m_t found in this way plus the tangent angle β:

$$m_t = m_{to} + p\pi$$
$$m = m_t + \beta \tag{3305}$$

For a small soil element in contact with the surface the slip line directions are shown for the two states of stress in Fig. 33 B, assuming $p \neq 0$ in (3305). In the same figure Mohr's circles are shown. The passive case is indicated by an index 1, and the active case by 2.

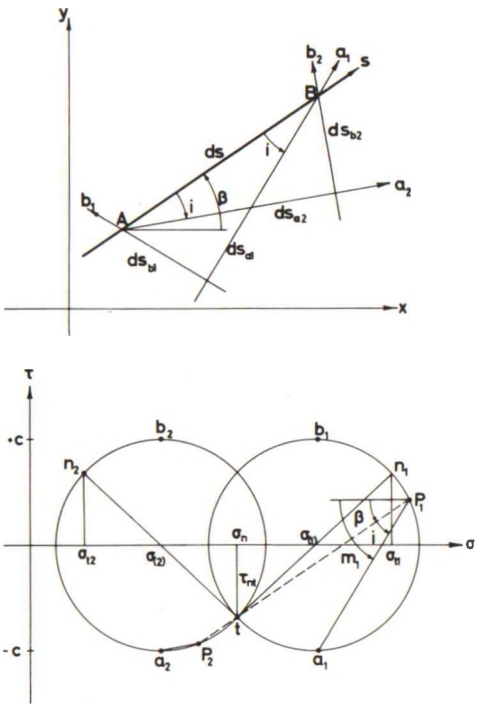

Fig. 33 B: Zone Element and Mohr Circle for Stresses at Surface. Passive and Active Case.

From this figure, or directly from (3301), the values of the mean normal stress σ in the two cases are found to be:

$$\sigma = \sigma_o + c \sin 2 m_t = \sigma_o \pm c \sin 2 i$$

$$= \sigma_o \pm c \sqrt{1 - (\tau_o / c)^2} \qquad (3306)$$

the positive sign being valid for the passive, and the negative sign for the active case.

By the formulae (3304-6) m and σ can be found for all surface points. For the representation in the a,b-plane, or to determine the a- and b-values for chosen system lines in the λ,μ-plane, we need a reference set σ_O, m_O, valid for a = b = 0. When it is chosen, or is known from other parts of the rupture figure, we find:

$$a = \frac{\beta - m_O}{2} - \frac{\sigma_o - \sigma_O}{4c} \pm \frac{1}{2}\left(i - \frac{1}{2}\sin 2i\right) \qquad (+ p\tfrac{\pi}{2})$$

$$b = \frac{\beta - m_O}{2} + \frac{\sigma_o - \sigma_O}{4c} \pm \frac{1}{2}\left(i + \frac{1}{2}\sin 2i\right) \qquad (+ p\tfrac{\pi}{2}) \qquad (3307)$$

cf. (3106). The positive and negative signs are valid for the passive and the active case, respectively.

The state of failure, and the value of p will normally be the same when applying (3305-7) to all boundary points for the same zone. When these points have been decided, an arbitrary number of image points in the a,b-plane to surface points with known coordinates x,y can therefore be constructed.

If a and b vary monotonically along the surface one may choose a constant spacing Δa or Δb for one of these functions. By interpolation the other function and the corresponding coordinates x,y can then be found. Alternatively one may choose a number of surface points, f. inst. at equal intervals along the arc length, and let two system slip lines start from each point (λ and μ both changing by one unit).

In the last mentioned case it is seen that in the positive direction of s we have always:

1. In the passive case: $(\Delta\lambda, \Delta\mu) = (1, -1)$ and $(e_a, e_b) = (-1, -1)$ for even, and $(\Delta\lambda, \Delta\mu) = (-1, 1)$, $(e_a, e_b) = (1, 1)$ for uneven values of p in (3305). By the method of chord lengths $e_s = -1$.
2. In the active case: $(\Delta\lambda, \Delta\mu) = (1, 1)$ and $(e_a, e_b) = (1, -1)$ for even, and $(\Delta\lambda, \Delta\mu) = (-1, -1)$ and $(e_a, e_b) = (-1, 1)$ for uneven values of p. $e_s = 1$.

Thus, the active and passive case may be distinguished by the sign of e_s, and the two different orientations of the slip lines by the sign of $e_m = e_s \Delta\mu$. Hence, $\Delta\lambda = -e_b = e_m$ and $\Delta\mu = e_a = e_s e_m$. In the λ, μ-plane free surfaces are represented by two parallel straight lines in a diagonal direction.

The quantities which are given for a free surface will normally be e_s and e_m. However, one can also formally assume e_a and e_b to be given. The two other quantities can then be derived by the conditions that $e_m = -e_b$ and $e_s = -e_a e_b = -e_f$.

The values of the geometric functions $\bar{x}$, $\bar{y}$ and R, S are known for any point along a free surface. This is evident for the equivalent coordinates which are directly given by (3116) when x,y, and m are known. For the radii of curvature we see from Fig. 33 B that the slip line arc lengths between two consecutive points A and B in the positive s-direction are:

$$\begin{aligned} ds_a &= R\,da = ds \cos m_t \\ ds_b &= S\,db = -ds \sin m_t \end{aligned} \tag{3308}$$

so that we have:

$$\begin{aligned} R \frac{\delta a}{\delta s} &= \cos m_t \\ S \frac{\delta b}{\delta s} &= -\sin m_t \end{aligned} \tag{3309}$$

$$\text{i.e. } \frac{\cos m_t}{R} - \frac{\sin m_t}{S} = \frac{\delta a}{\delta s} + \frac{\delta b}{\delta s} = \frac{\delta m}{\delta s} = \frac{\delta \beta}{\delta s} + \frac{\delta m_t}{\delta s}$$

valid for both the passive and the active case, and also for any value of p in (3305) and (3307).

The initial conditions by the method of chord lengths are exactly those assumed in (3262-3) when the surface curve can be assumed to consist of circle arcs. If not the formulae (3261) must be used.

From the above it follows that for the calculation of the geometric functions free surfaces are curves of the type C_o in Fig. 32A. They will therefore directly determine triangle zones by the first initial value problem type. Such zones, which are geometrically completely determined when the bounding portion of the surface has been specified, are called Rankine zones. On the other hand, no conditions exist for the velocity functions along free surfaces, so in this respect they are just boundary curves to the domains where the velocity field is of any interest.

Notice that we might formally consider only one state of stress in contact with free surfaces, using only one sign in the formulae (3302), (3304), and (3306-7). For corresponding zone elements the two possible states of stress are realised in the two conjugate solutions to the same problem (reversed movements, or opposite signs of the safety factor f), which can be distinguished by changing the sign of c. This would lead to simpler formulae, and would also be quite simple for statically determined rupture figures. However, for more complicated rupture figures the notation would not be simplified. Here we may have both passive and active Rankine zones in the same rupture figure, so nothing would be gained, as one would then have to calculate with different signs for c in different zone elements. For that reason the above notation is retained in the following.

Example 33a

As an example consider the Rankine zone generated under a reentrant corner, rounded off by a circle arc with the radius r_o, cf. Fig. 33C. The angle between the surface tangents at the two end points of the circle arc is 2θ. The surface is assumed to be loaded by the constant normal load σ_o, and the passive case is considered.

From the influence domains for the different surface curves, cf. Fig. 32A, it is seen that there will be two domains, I and III, under the straight surface portions which only depend on these portions. We have here

$$\sigma_n = \sigma_o$$
$$\tau_{nt} = 0 \qquad (3310)$$

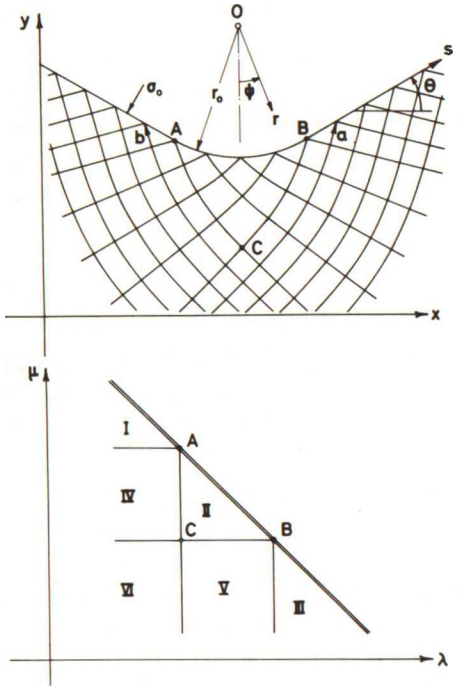

Fig. 33 C: Surface Zone Under a Rounded Reentrant Corner on a Free Surface.

and therefore

$$m_t = i = \frac{\pi}{4}$$

$$\sigma = \sigma_o + c \qquad (3311)$$

and $m = \frac{\pi}{4} \pm \theta$

where the positive sign is valid for the domain III, and the negative sign for I.

This means that they are classical Rankine zones with straight slip lines (constant values of a and b). From Hencky's conditions it is seen that the a-lines will also be straight in the domains IV and VI, and the b-lines will also be straight in V and VI. The last mentioned domain will therefore also be an ordinary Rankine zone with constant values of a and b.

If we choose σ_O and m_O corresponding to this domain, i.e.

$$\sigma_O = \sigma_o + c\,(1 + 2\,\theta)$$

$$m_O = \frac{\pi}{4} \qquad (3312)$$

we find a = 0 for the domains I, IV, and VI, and a = θ for III. Correspondingly, b = 0 for III, V, and VI, and b = $-\theta$ for I.

The domain II is generated by the circle arc. Using the tangent angle ψ as a parameter we find along this curve:

$$m = \frac{\pi}{4} + \psi$$

$$\sigma = \sigma_o + c$$

so that (3313)

$$a = \frac{\psi + \theta}{2}$$

$$b = \frac{\psi - \theta}{2}$$

If the coordinates (x,y) are calculated with the origo at the centre O for the circle arc, i.e.

$$x = r_o \sin\psi$$
$$y = -r_o \cos\psi \qquad (3314)$$

the initial values for the equivalent coordinates will be:

$$\bar{x} = -r_o \sin(m - \psi) = -\frac{\sqrt{2}}{2} r_o$$
$$\bar{y} = -r_o \cos(m - \psi) = -\frac{\sqrt{2}}{2} r_o \qquad (3315)$$

cf. (3116). They are therefore constants. From (3309) we find, observing that $\frac{\delta s}{\delta \theta} = r_o$ so that $\frac{\delta s}{\delta a} = \frac{\delta s}{\delta b} = 2 r_o$:

$$R = -S = r_o \sqrt{2} \qquad (3316)$$

i.e. the radii of curvature are also constants.

In this case the solution can be obtained by direct integration, cf. (3234). However, it is possible to use a semi-inverse method, utilizing that the stresses must be radially distributed about O.

In polar coordinates the equilibrium conditions are:

$$\frac{\partial \sigma_r}{\partial r} + \frac{1}{r}\frac{\partial \tau_{r\psi}}{\partial \psi} + \frac{\sigma_r - \sigma_\psi}{r} = 0$$
$$\text{and} \quad \frac{1}{r}\frac{\partial \sigma_\psi}{\partial \psi} + \frac{\partial \tau_{r\psi}}{\partial r} + 2\frac{\tau_{r\psi}}{r} = 0 \qquad (3317)$$

the stress components being defined in Fig. 33 D.

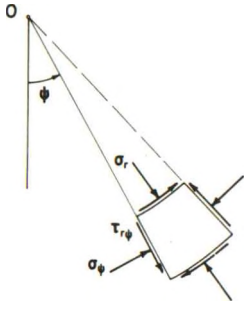

Fig. 33 D: Stress Components in Polar Coordinates.

Assume that the minor principal stress direction for any point in the domain II will pass through the point O, and that the stress components will be the same for all points with the same value of r, independent of ψ. Then

$$\tau_{r\psi} = 0$$
$$\sigma_\psi - \sigma_r = 2c \qquad (3318)$$

and all derivatives

$$\frac{\partial}{\partial \psi} = 0$$

When these assumptions are inserted in (3317) it is seen that the second equation is satisfied identically. From the first equation we find, using the boundary condition $\sigma_r = \sigma_o$ (and $\tau_{r\psi} = 0$) for $r = r_o$:

$$\sigma_r = \sigma_o + 2c \ln \frac{r}{r_o}$$

and from (3318): (3319)

$$\sigma_\psi = \sigma_o + 2c \left(1 + \ln \frac{r}{r_o}\right)$$

Since the a-lines always form the angle $\frac{\pi}{4}$ with the radius vector, they are seen to be logarithmic spirals with the tangent angle $\frac{\pi}{4}$. A point with the coordinates (a, b) will therefore have the polar coordinates.

$$\psi = a + b$$

$$r = r_o e^{\theta - a + b} \tag{3320}$$

and the Cartesian coordinates:

$$x = r_o e^{\theta - a + b} \sin(a + b)$$

$$y = -r_o e^{\theta - a + b} \cos(a + b) \tag{3321}$$

The equivalent coordinates will therefore be

$$\bar{x} = \bar{y} = -\frac{\sqrt{2}}{2} r_o e^{\theta - a + b} \tag{3322}$$

and the radii of curvature:

$$R = -S = \sqrt{2} r_o e^{\theta - a + b} \tag{3323}$$

cf. (3120). These functions are seen to satisfy (3112), (3119), and the boundary conditions.

The points in the domains IV and V are easily found from (3322). Thus, for a point (a, b) in the domain IV, where a is always equal to zero, $\bar{x}$ and $\bar{y}$ may be found from (3322). $\bar{y}$ will remain constant along an a-line in IV, but $\bar{x}$ may be decreased by an arbitrary amount (equal to Δs_a measured along the a-line from the curve AC).

By the method of chord lengths we may define an angle difference $\Delta\psi$. For the initial circle arc between ψ and $\psi + \Delta\psi$ we have:

$$e_s = -1$$

$$e_m = 1$$

$$\alpha_s = -\frac{1}{2}\Delta\psi \qquad (3324)$$

$$\omega_s = \psi + \frac{1}{2}\Delta\psi$$

$$k_s = 2\,r_o \sin\frac{\Delta\psi}{2}$$

Along the straight surface parts one may take the same chord lengths (and the same values of e_s and e_m), but here $\alpha_s = 0$ and $\omega_s = -\theta$ for the domain I and $+\theta$ for III.

332 Vertex Points

The image curve C_o of a free surface in the a,b-plane (and in the λ,μ-plane) will only be continuous if a and b are continuous functions of s. From (3307) it is seen that this will normally not be the case unless β, σ_o, and τ_o are all continuous. This means that the surface must be a smooth curve with no corner points, and that the surface loading must vary continuously.

In this case $\overline{x}$ and $\overline{y}$ will also be continuous functions of s, and therefore also of a and b along the curve. However, R and S may be discontinuous. From (3307) it is seen that $\frac{\delta a}{\delta s}$ and $\frac{\delta b}{\delta s}$ are discontinuous functions of s if $\frac{\delta \beta}{\delta s}$ is, i.e. if the radius of curvature for the surface suddenly changes.

If there is a discontinuity, f.inst. a corner point at the surface as shown in Fig. 33 E, a rupture zone in contact with the surface on both sides of the point may not be geometrically possible. In the cases where it is, the discontinuity point will be singular, being an ordinary corner point for two triangle zones and one rectangle zone, and a vertex point for two intermediate radial zones.

Vertex points can be regarded as degenerated slip lines corresponding to a finite interval in a or b, but with zero arc length, cf. Fig. 31 E. They have therefore radii of curvature equal to zero, and are in the x,y-plane intersection points for all slip lines of the other family inside the given interval of a or b (the so-called radial slip lines). However, for computational purposes they are ordinary slip lines, all normally used formulae being valid. Thus, from (3112) it is seen that all radial slip lines have the same radius of curvature at the vertex of the radial zone. If equivalent coordinates

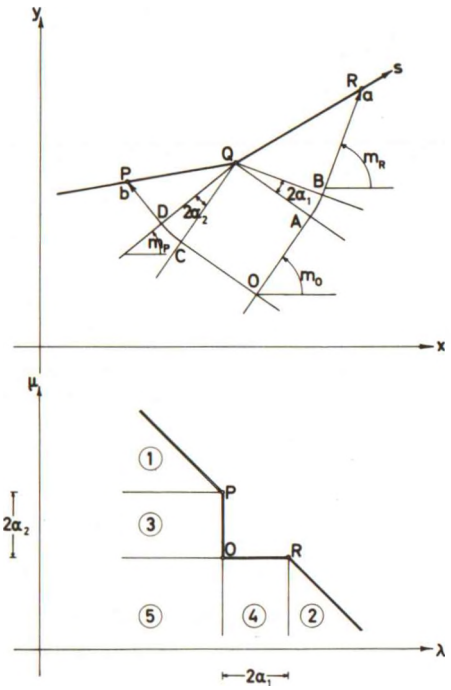

Fig. 33 E: Zone Elements with Radial Zones Under a Sharp Reentrant Corner on a Free Surface.

are used, the origin point for the x,y coordinate system is usually placed at the vertex point. We then have the boundary condition $\bar{x} = \bar{y} = 0$. It is also possible to define one or more cells bounded along one side by the vertex slip line. If calculated by the method of chord lengths all such cells will of course have one chord equal to zero (and will in reality be triangles instead of quadrangles), but this has no influence on the validity of the general formulae. The degenerated slip lines (with a known position in the physical plane) are indicated in the λ,μ-plane by heavy lines.

In the physical plane a vertex is a stress singularity, because at the point we have, according to (3101), different values for σ and m at different directions through the point. It will usually also be a singular point of the velocity field, different velocity vectors obtaining at different directions through the point. As an example vertices obtain in the classical Prandtl rupture figure for strip foundations, cf. the points B and C of Fig. 31 G (Example 31 b). For the velocity field around such points, compare Fig. 31 L-M of Example 31 f.

In Fig. 33 E is shown a small soil element OPR bounded by slip lines and in contact with the surface PQR (taken in this order in the positive direction of s) where we have a corner point Q. The passive state of stress is assumed in the figure.

The sub-elements PQD and QRB are ordinary surface zone elements as in Fig. 33 B (and Fig. 33 C). The stress functions m_P, σ_P, a_P, b_P, and m_R, σ_R, a_R, b_R are calculated in the usual way from (3303-7). The sub-elements QBA and QCD are transitional radial zones with an a-line and a b-line vertex in Q, respectively. Finally QAOC is an ordinary rectangle zone element with the stress functions m_O, σ_O, a_O, and b_O. Notice that even for arbitrarily small soil elements the stress distribution cannot be assumed constant

in the radial zones as it can be in the other zone elements. This is due to the singularity at the point Q.

In the active state of failure we have much the same figure, but now OP will be an a-line and RO a b-line. The radial zone QBA will therefore now be a b-line vertex, and QCD an a-line vertex.

The centre angles $2\alpha_1$ and $2\alpha_2$ of the a- and b-line vertex, respectively (independent of the orientations of the slip lines), are found by the following equations, obtained by using (3101) on the degenerate slip lines:

$$\begin{aligned} 2(\alpha_1 + \alpha_2) &= m_R - m_P \\ 4c(-\alpha_1 + \alpha_2) &= \sigma_R - \sigma_P \end{aligned} \tag{3325}$$

from which

$$\begin{aligned} 2\alpha_1 &= \frac{m_R - m_P}{2} - \frac{\sigma_R - \sigma_P}{4c} = a_R - a_P \\ 2\alpha_2 &= \frac{m_R - m_P}{2} + \frac{\sigma_R - \sigma_P}{4c} = b_R - b_P \end{aligned} \tag{3326}$$

valid for both states of stress.

In the passive case we have:

$$\begin{aligned} a_O &= a_P, \quad b_O = b_R \\ m_O &= m_P + 2\alpha_2 = m_R - 2\alpha_1 = a_P + b_R \\ \sigma_O &= \sigma_P + 4c\alpha_2 = \sigma_R + 4c\alpha_1 = 2c(-a_P + b_R) \end{aligned} \tag{3327}$$

and for the active case:

$$\begin{aligned} a_O &= a_R, \quad b_O = b_P \\ m_O &= m_P + 2\alpha_1 = m_R - 2\alpha_2 = a_R + b_P \\ \sigma_O &= \sigma_P - 4c\alpha_1 = \sigma_R - 4c\alpha_2 = 2c(-a_R + b_P) \end{aligned} \tag{3328}$$

assuming $\sigma = 0$, $m = 0$ for $a = b = 0$. Notice that $\alpha_a = e_m \alpha_1$ and $\alpha_b = e_m e_s \alpha_2$.

In the λ,μ-plane the singular point Q is represented by the two line segments PO and OR. The figure will be slightly different for different orientations of the a- and b-lines, and for the two possible states of stress. Thus, for the passive case, and when both positive slip line directions point

towards the clay surface Fig. 33 E will apply. All other possible cases are obtained by rotating the figure through an arbitrary number of quarter rotations in the λ,μ-plane (the wedge POR pointing always towards the clay from the surface).

Along PO and OR we know x,y and the variation of m, so $\bar{x}$ and $\bar{y}$ can be calculated directly. We also know that R or S is equal to zero, and that correspondingly S or R, respectively, will be constant, equal to the values found at P and R from (3309). Thus, all four geometric functions are known along the slip line segments PO and OR. We therefore have sufficient initial values to be able to calculate the zones 1 and 2 (first problem) and then 3, 4, and 5 (second problem).

Notice that (3237-8) are also valid when the curve AB (Fig. 32 A) has sections parallel to the coordinate axes (and also whether a and b vary monotonically along AB or not). The integral method can therefore be used directly. The method of finite differences, or the method of chord lengths can also be used directly, without any special problems.

However, in order that the rupture figure shall be geometrically possible we must have α_1 and α_2 both positive, i.e. we must have $a_R \geq a_P$ and $b_R \geq b_P$, or, according to (3326):

$$\begin{aligned} 0 &\leq m_R - m_P \\ -2c(m_R - m_P) &\leq \sigma_R - \sigma_P \leq 2c(m_R - m_P) \end{aligned} \tag{3329}$$

Thus, the rupture figure is possible for a reentrant corner of an unloaded surface, and also for a surface where τ_o is suddenly increased in the positive s-direction (passive case) or decreased (active case). It is not possible by extruding corners on unloaded or normally loaded surfaces or by any jump in a pure normal loading on a smooth surface.

If one of the equalities in the lower formula (3329) is satisfied, one of the radial zones in Fig. 33 E will disappear. The rectangle zone QAOC will then be separated from the corresponding surface zone by a normal slip line only. If the above conditions are not satisfied, the correct solution will contain a rigid body of clay at least to one side of the discontinuity point Q. However, it is still possible to construct statically possible solutions with rupture zones on both sides of Q, if discontinuity lines are used.

Vertices will rarely occur at interior points in homogenous clay domains. If they do it is a condition that $u = v = 0$. They usually obtain at boundaries where the boundary conditions specify two different values of m, and possibly also two values of σ with a difference which is inconsistent

with the corresponding difference in m, or two different velocity vectors, at two sides of the same point. Apart from the case considered above (normally two radial zones) they are mostly attached to external rigid bodies, f. inst. at intersection points with free surfaces, and at corner points. It is seen that at the end point in the positive direction of s for a continuous surface curve one will always have a b-line vertex in the passive case, and an a-line vertex in the active case. For end points in the negative direction of s the opposite rule is valid.

333 Discontinuity Lines

A discontinuity line is a curve separating two rupture zones with different values of the stress component σ_t on the two sides of the curve.

To maintain equilibrium in the rupture zones the normal stress σ_n and the shear stress τ_{nt} acting on the curve must be the same on the two sides. Therefore, since the clay is in failure on both sides of the curve, the two states of stress separated by the curve must be the passive (marked by index 1) and active (2) case corresponding to the same values of the curve stresses σ_n and τ_{nt}, cf. Fig. 33 F. The corresponding Mohr circles are shown in Fig. 33 B. By the transition of a discontinuity line the sign of either e_a or e_b will be changed.

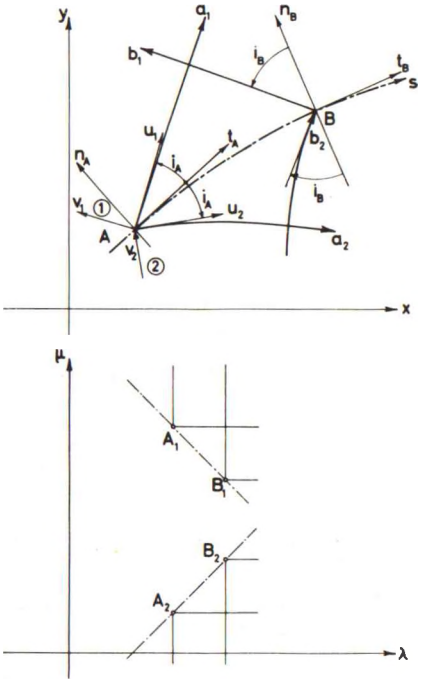

Fig. 33 F: Zone Elements Separated by a Discontinuity Line.

We may therefore define the angle i by Eq. (3303-4). The following transition formulae are then obtained from (3302) and (3305-7).

For the tangential stresses:

$$\sigma_{t1} - \sigma_{t2} = 4c \sin 2i$$

$$= 4c \sqrt{1 - (\tau_{nt}/c)^2} \qquad (3330)$$

For m and σ:

$$m_1 - m_2 = 2i \qquad (\pm p\,\pi)$$
$$\sigma_{(1)} - \sigma_{(2)} = 2c \sin 2i = 2c \sqrt{1 - (\tau_{nt}/c)^2} \tag{3331}$$

and for a and b:

$$a_1 - a_2 = i - \frac{1}{2}\sin 2i \qquad (\pm p\,\frac{\pi}{2})$$
$$b_1 - b_2 = i + \frac{1}{2}\sin 2i \qquad (\pm p\,\frac{\pi}{2}) \tag{3332}$$

Thus, to a discontinuity line corresponds two image lines in the λ,μ-plane (indicated by thin dash-dotted lines).

From (3331) it is seen that at any point the discontinuity line and its normal are the bisectrices of the angles between the positive directions of the two pairs of slip lines through the point, each pair consisting of the two slip lines of the same family, one from either side of the curve. However, except for the special case where both families of slip lines, and the curve itself are rectilinear, this is only a necessary, not a sufficient condition. In the general case both conditions (3331), or (3332), must therefore be used to construct a discontinuity line.

Discontinuity lines are used to obtain statically determined rupture figures in cases where continuous solutions would not be geometrically possible, or for other reasons do not exist. As a rule their position in the x,y-plane will not be known beforehand, except that usually they must start at a given point, where the tangent direction can easily be calculated. In the general case the calculations become rather complicated, entailing the solution of some new types of boundary value problems. Examples of this are, cf. Fig. 33 G (for the sake of simplicity drawn with rectilinear slip lines):

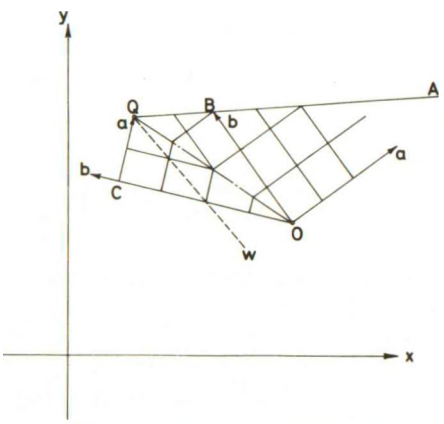

Fig. 33 G: Examples of Problems with Discontinuity Lines.

1. Statically determined zone - characteristic (type ZL): A zone is determined f. inst. by a free surface QA, and a characteristic, f. inst. OC or QC is known. It may be given as a boundary characteristic for another statically determined rupture zone. The disconti-

nuity line OQ is given by the conditions that it must pass through a given point (O or Q, determined so that (3332) is satisfied), and must have the form so that when (3332) is used to find the boundary conditions for the zone OCQ from the known stress distribution in the zone OQA, the characteristic found through O or Q shall be identical with the given one.

2. Statically determined zone - wall (type ZW). A zone is given e.g. by the surface QA, and a wall QW is known (i.e. the position of the curve QW, and the variation of m, but not σ, is known along this curve). The discontinuity line OQ is given by the fact that it must pass through the point Q with an inclination found by (3331), and must have the form so that the zone OQW (determined by (3332)) has the correct values of m along QW.

These two types are the most frequent. However, more complicated types exist, f. inst. ZZ, where we have given two statically determined rupture zones, and must find two discontinuity lines through a given point so that the zone between these two curves is consistent with the boundary conditions on both curves, each being derived from one of the given rupture zones. There even exist problems where three discontinuity lines must intersect in a given point.

Such problems are quite easy to solve when all curves considered are rectilinear, because then m and σ (or a and b) are constants for each rupture zone. In the general case the position of the discontinuity line must be found iteratively by choosing a curve and changing its position until the given conditions are satisfied.

By the method of finite differences this can be done by subsequent interpolations in the full zone Z, defining the curve in the same way as a free surface, f. inst. by a function of the type $y = y(x)$, $\beta = \beta(x)$, or $\beta = \beta(\lambda)$. By the method of chord lengths it may be simpler to define the curve by the assumption that it passes through a specified number of mesh points. In each point β, and therefore $m - \beta$, i, etc., are found by numerical differentiation. The position of the curve is changed by changing the initial points which define the slip line net. In some cases a further iteration is necessary f. inst. to ensure that the final mesh points will coincide with the mesh points on the known characteristic. However, nothing is gained by using statically determined zones when the discontinuity lines become too complicated to calculate. They are therefore mostly used in the rectilinear case. In the general case one might as well use the correct rupture figure, or an admis-

sible solution with a simpler type of possible zones.

Along discontinuity lines the velocity field will frequently not be assumed to be continuous. However, in order to avoid discrepancies we must impose the restriction that the normal component u_n of the velocity vector must be the same on the two sides of the curve (cf. Fig. 33 F):

$$u_1 \sin(m_1 - \beta) + v_1 \cos(m_1 - \beta)$$

$$= u_2 \sin(m_2 - \beta) + v_2 \cos(m_2 - \beta) \qquad (3333)$$

or, according to (3304-5):

$$u_1 \sin i + v_1 \cos i = \pm(-u_2 \sin i + v_2 \cos i) \qquad (3334)$$

The negative sign may be necessary if a multiple of π has been added to one or both of the m-values (3305), and the difference in p for the two sides of the curve is an uneven number.

In the general case the tangential velocity component u_t will be different on the two sides of the curve. The velocity jump $u_s = \Delta u_t$ (positive when u_t increases in the positive direction of n) may be positive or negative. If its sign is opposite that of τ_{nt}, the deformation work done by τ_{nt} is evidently negative, and the solution is not kinematically possible.

Notice that a physical sliding need not take place, even if u_s is different from zero. We may assume the discontinuity line to be a mathematical curve which has a fixed position in the x,y-plane, so that the clay particles during the movement pass across the curve. Neighbouring particles will then still be neighbours after the passage, but all particle paths have a sudden change of directions when passing the curve.

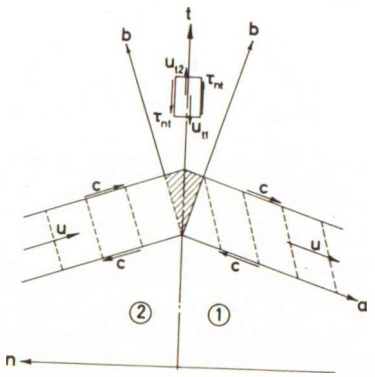

Fig. 33 H: Straining of Clay Elements Transgressing a Discontinuity Line.

However, even in this case all clay elements will be strained in the opposite direction of the shear stresses, if the signs of τ_{nt} and u_s are different; compare the angles between the shown dotted lines and the a-lines in Fig. 33 H before and after the element has crossed the discontinuity line (v is assumed zero, and u is the same between two consecutive a-lines; the negative sign is used in (3334)).

When τ_{nt} and u_s have opposite signs the boundary conditions for the zones may in some cases permit one to assume $u_s = 0$ as an alternative. In Fig. 33 H this would be equivalent to the assumption of the shaded domain being a rigid body of clay, translated in a direction between the directions u on the two sides of the discontinuity lines. However, this would correspond to negative values of Δv_a for one or both of the two b-lines bounding the rigid body.

The deformation condition will also be violated when u_s and τ_{nt} have the same sign. The unit deformation work along a curve element ds:

$$dW'_{ds} = \tau_{nt} u_s ds \tag{3335}$$

is then positive. However, it should correspond to an infinite strain parallel to the t-axis, i.e. with principal strain directions forming the angles $\pm \frac{\pi}{4}$ with this direction. Thus, calculated from the velocity field the kinematically correct deformation work rate would be:

$$dW_{ds} = c u_s ds \tag{3336}$$

The discrepancy between (3335) and (3336) is due to the fact that for the infinite strain the principal stress and strain directions do not coincide. In this case the alternative velocity field in the zone with $u_s = 0$ will not as a rule be in agreement with the boundary conditions for the zone.

Thus, rupture zones containing discontinuity lines will not be kinematically possible, unless either $u_s = 0$ along the curves, or $\tau_{nt} = c$, numerically, and u_s has the same sign as τ_{nt} (but in this case the curves are normal slip lines). Discontinuity lines with $u_s = 0$ may obtain in mathematically correct rupture figures, however (f. inst. the neutral surface in a bar which is bent plastically). For the use in soil mechanics they are exceedingly rare, except in the limiting case as discontinuity points (zero arc length).

Ordinary discontinuity lines (rectilinear, with rectilinear slip lines) are frequently used to construct statically possible rupture figures consisting of zone ruptures only.

Example 33 b

Consider the soil element in the neighbourhood of a corner point (Fig. 33 E) when α_1 and α_2 are not both positive. For the sake of simplicity we need only consider the passive case with pure normal stresses σ_o on the surface ($\tau_o = 0$, i.e. $m_t = \frac{\pi}{4}$).

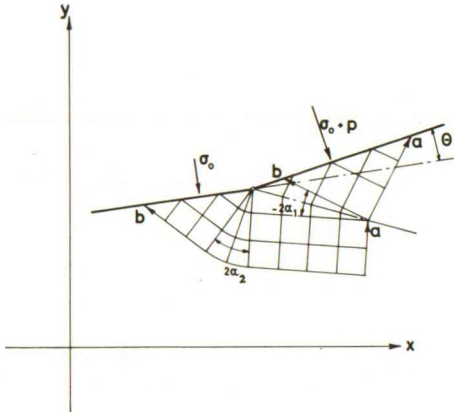

Fig. 33 I: Zone Element with a Discontinuity Line Under a Corner on a Free Surface.

We define the quantities θ and p by the equations (cf. Fig. 33 I):

$$m_R - m_P = \beta_R - \beta_P = \theta$$
$$\sigma_R - \sigma_P = \sigma_{o(R)} - \sigma_{o(P)} = p \qquad (3337)$$

so that in the normal case (two radial zones) we have from (3325):

$$\alpha_1 + \alpha_2 = \frac{\theta}{2} \qquad (3338)$$

$$-\alpha_1 + \alpha_2 = \frac{p}{4c} \qquad (3339\,a)$$

If we use discontinuity lines when one or both of the two angles become negative, (3338) is still valid. From (3331) we see, however, that (3339 a) must be replaced by one of the following:

$$\alpha_1 \leq 0, \quad \alpha_2 \geq 0: \; -\frac{1}{2}\sin 2\alpha_1 + \alpha_2 = \frac{p}{4c} \qquad (3339\,b)$$

$$\alpha_1 \geq 0, \quad \alpha_2 \leq 0: \; -\alpha_1 + \frac{1}{2}\sin 2\alpha_2 = \frac{p}{4c} \qquad (3339\,c)$$

$$\alpha_1 \leq 0, \quad \alpha_2 \leq 0: \; -\frac{1}{2}\sin 2\alpha_1 + \frac{1}{2}\sin 2\alpha_2 = \frac{p}{4c} \qquad (3339\,d)$$

Evidently, the last mentioned case is only possible when θ is negative.

We have $\alpha_1 \leq 0$ for:

$$\frac{p}{2c} \geq \theta \text{ when } \theta \geq 0$$
$$\text{and } \frac{p}{2c} \geq \sin\theta \text{ when } \theta \leq 0 \qquad (3340)$$

Correspondingly $\alpha_2 \leq 0$ for:

$$\frac{p}{2c} \leq -\theta \text{ when } \theta \geq 0$$
$$\text{and} \qquad (3341)$$
$$\frac{p}{2c} \leq -\sin\theta \text{ when } \theta \leq 0$$

It presents no special difficulty to find the two angles from (3338-9). In the three cases we have:

$$\alpha_1 + \frac{1}{2}\sin 2\alpha_1 = \frac{\theta}{2} - \frac{p}{4c} \qquad (3342\,b)$$

$$\alpha_2 + \frac{1}{2}\sin 2\alpha_2 = \frac{\theta}{2} + \frac{p}{4c} \qquad (3342\,c)$$

$$\sin(\alpha_2 - \alpha_1) = \frac{p}{4c\cos\frac{\theta}{2}} \qquad (3342\,d)$$

to be used in each case together with (3338).

For geometrical reasons we must have α_1 and $\alpha_2 \geq -\frac{\pi}{4}$. Therefore, from (3342 b-c):

$$-(\pi + 2 + 2\theta) \leq \frac{p}{c} \leq \pi + 2 + 2\theta \qquad (3343)$$

valid for the domains where one radial zone and one discontinuity line exist, cf. Fig. 33 I.

A soil element found by the above equations can be extended arbitrarily if we are in the rectilinear case (straight boundaries with piecewise constant surface loadings). In the general case we only find the tangent directions for the slip lines and possible discontinuity lines, i.e. the initial conditions at the point in question.

334 Transition and Discontinuity Points

The points considered in this section have the property in common that they are vertices for two rigid wedges of soil, separating two rupture zones, cf. Fig. 33 J. Being one-point connections between the two zones they do not relate the radii of curvature at the point for one zone to the corresponding values for the other zone. The two zones may therefore be calculated from two sets of boundary conditions, quite independent of each other. However, the fact that the zones are connected at the point permit relative movements to take place between the wedges.

Transition points (O in Fig. 33 J) are distinguished by the fact that the two zones are of the same kind (the positive a- and b-directions both go through the point). This implies that the shear stresses acting upon the faces of the two rigid wedges all point away from (the passive case) or towards (the active case) the point. The assumption that the two wedges remain rigid will in this case only be possible when the vertex angles are both $\frac{\pi}{2}$, and when σ is the same for both zones at the point. If these conditions are not satisfied, the failure condition can be shown to be exceeded in at least one wedge.

Therefore transition points are ordinary points, the same values of m and σ being obtained from the two rupture zones. The possible relative move-

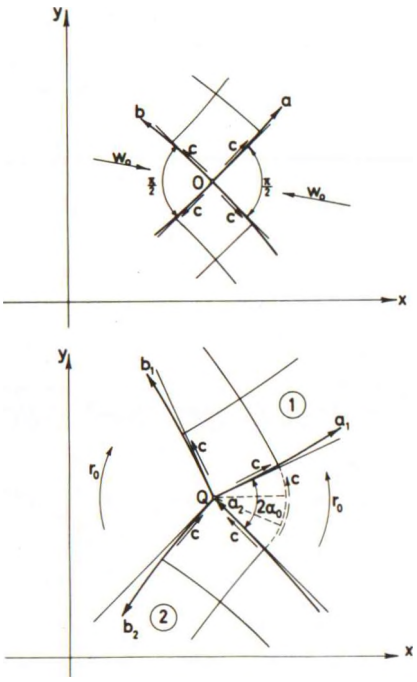

Fig. 33 J: Transition Point O and Discontinuity Point Q.

ment between the two wedges depends on the curvatures for the boundary slip lines, cf. (3130). For straight slip lines through the point the wedges can only be translated by a relative movement w_o the direction of which lies wholly inside the rigid wedges. Any rotation would give negative values of ϵ in one of the rupture zones. When the slip lines are curved so that $\frac{\Delta u}{R} - \frac{\Delta v}{S} > 0$, Δu and Δv being measured from the rigid bodies to the zones, for at least one of the zones a relative rotation r_o between the wedges may also obtain. Considered as a positive quantity it must be smaller than the value of the expression indicated above (the maximum permissible value will be proportional to w_o, since Δu and Δv are). The principal relative movement of the two wedges will be that for passive zones they approach each other, and for active ones they retract.

For geometrical reasons the zone boundaries must evidently be considered as mathematical curves which are passed across by the clay particles during the movement.

For discontinuity points (Q in Fig. 33 J) one of the zones meeting at the point is passive (marked 1), and the other (marked 2) is active. The stress functions m and σ cannot in this case be determined for one zone when they are known for the other, because the two rigid wedges can now support a certain stress difference even if the smallest vertex angle $2\alpha_o$ is smaller than $\frac{\pi}{2}$. However, in order that the radial zone shown with dotted lines in Fig. 33 J shall not become possible we must have:

$$\sigma_{(1)} - \sigma_{(2)} \leq 4c\,\alpha_o \qquad (3344)$$

All geometric functions, including a and b, may be discontinuous in the point.

No sliding between the two wedges is possible at the point Q, because a relative movement of this kind would always induce slidings along the boundary slip lines for the zones, at least one of which would go in the opposite direction of the shear stress. The only possible relative movement

is therefore a pure rotation r_o around Q. It must correspond to the types of the zones, compressing the passive and extending the active one. Thus, a discontinuity point acts as a hinge between the two wedges.

Notice that the above mentioned static conditions for the wedges at transition and discontinuity points are only necessary but not sufficient conditions. In a given rupture figure a wedge satisfying these conditions may well be statically impossible farther away from its vertex point, f. inst. if the boundary slip lines converge.

Transition and discontinuity points are indicated in the λ, μ-plane by large open circles. The two image points corresponding to one discontinuity point (if represented on the same sheet) are connected by a thin dash-dotted line.

Example 33 c

A transition point has previously been considered, cf. the point F in the Prandtl rupture figure for strip foundations, Fig. 31 L-M of Ex. 31 f.

Discontinuity points may f. inst. obtain in rupture figures of the type shown in Fig. 31 H (Ex. 31 c) when the radial zone is sufficiently inclined. An example of this is shown in Fig. 33 K where the rough wall OW is translated with a constant velocity vector w forming the angle θ with the negative x-axis (the horizon).

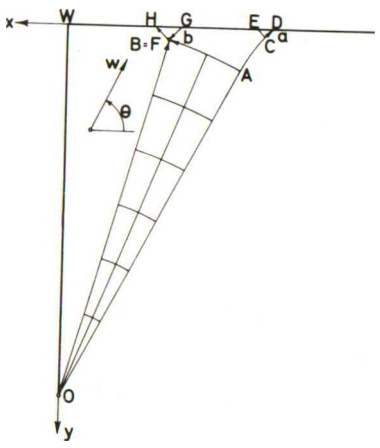

Fig. 33 K: Rupture Figure (Radial Zone with Surface Zone Complex) with a Discontinuity Point B = F.

For sufficiently large values of θ we obtain a rupture figure much like the one shown in Fig. 31 H, only the radial slip lines, f. inst. OA and OB, being rectilinear. When θ is decreased the chord length for the line rupture BF will also decrease, until it (for θ about 78°) becomes zero. At this point the equation sign in (3344) will still be valid, as it is for a finite line rupture when $2\alpha_o$ is taken to mean the centre angle for the circle arc.

For smaller values of θ, however, calculations assuming a line rupture would give a negative chord length, so this type of rupture figure is geometrically

impossible. Instead we have the discontinuity point B = F. Now the equality (3344) is no longer valid, and b for the line OB will no longer be equal to the value for FH (the centre angle AOB will then decrease for decreasing values of θ).

On the other hand, if the rupture figure shown in Fig. 31 H is calculated under the assumption that B = F is a discontinuity point (the free parameter k_{BF} being replaced by the centre angle AOB), the solution would show that (3344) was not satisfied. This assumption would therefore not be statically possible. The corresponding result would obtain if A = C was assumed to be a discontinuity point, or if this assumption was made for both points ($\angle$ AOB and σ_A will then both be free parameters instead of k_{BF} and k_{AC}).

It is seen that line ruptures and discontinuity points perform much the same functions in the rupture figure. They may connect rupture zones derived from quite independent boundary conditions, and they separate rigid bodies rotating in relation to each other. The example shows how it is determined which one to apply in a given case. Notice that the general proof of the uniqueness of solutions ensures that the two alternatives cannot both be possible in the same rupture figure.

335 Internal Boundaries

Internal boundaries are curves with a fixed position which separate clay domains with different shear strengths. The volume forces acting upon the domains may also be different, so because of the correction (2307) a continuously varying normal loading may act upon the boundary.

In the rupture figure internal boundaries may act in several different ways:

1. In the interior of rigid bodies of clay they will of course have no special importance, except that the normal loading contributes to the total forces acting upon the body.
2. If a zone rupture only develops in the weaker clay domain, whereas the stronger domain remains rigid, the boundary will in effect be a boundary to an external rigid body. The adhesion strength c_a will be equal to the shear strength of the weaker clay, and the boundary will be a slip line or an envelope of slip lines.
3. In this section are considered the cases where a rupture zone develops in both clay domains. Except for very special cases the two

zones will be of the same type, but because of the difference in c and the surface loading the boundary will have some features in common with discontinuity lines.

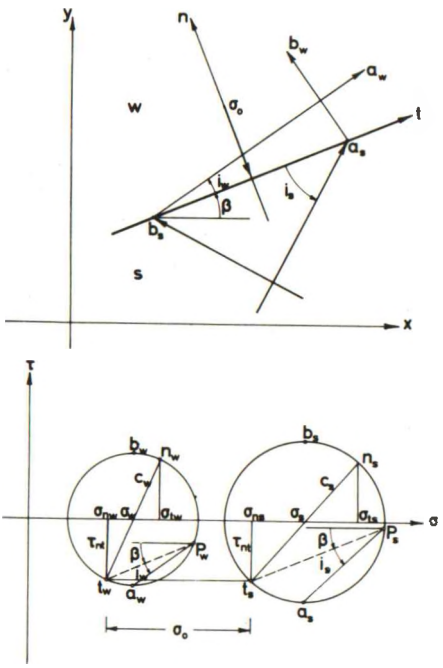

Fig. 33 L: Zone Elements Separated by an Internal Boundary. Mohr Circles for Stresses.

A small element of an internal boundary is shown on Fig. 33 L. The weaker domain is marked by index w, and the stronger one by index s. The normal loading σ_o is positive when it acts in the direction towards the stronger material.

Evidently we must have:

$$\tau_{nt(s)} = \tau_{nt(w)}$$
$$\sigma_{n(s)} = \sigma_{n(w)} + \sigma_o \qquad (3345)$$

From the equations corresponding to (3301), and from Mohr's circles, cf. Fig. 33 L, we find:

$$c_s \cos 2i_s = c_w \cos 2i_w$$

and (3346)

$$\sigma_s \mp c_s \sin 2i_s = \sigma_w \mp c_w \sin 2i_w + \sigma_o$$

the upper sign being valid for the passive, and the lower sign for the active case. Besides:

$$m_s = m_w \pm (i_s - i_w) \qquad (3347)$$

the positive sign being valid when both zones are passive. For boundaries of this kind the same multiple of π will usually be added to m on the two sides. e_a and e_b will therefore also be the same on the two sides.

From the first equation (3346) it is seen that we get a sort of refraction of the slip line field over an internal boundary. i_s will have a smaller range than i_w. Its extremum values are obtained when $i_w = 0$ or $\frac{\pi}{2}$, i.e.

$$\cos 2i_s = \pm \frac{c_w}{c_s} \qquad (3348)$$

In this case we have $\tau_{nt} = \pm c_w$. It is a special case, because the internal boundary will then act as a loaded surface with $|\tau_{nt}| < c_s$ for the stronger clay, but as a boundary to an external body for the weaker clay. Thus, the boundary may be deformed by deformations in the zone rupture in

the stronger clay, but in the zone rupture in the weaker clay it may be an envelope to slip lines.

In relation to statically determined rupture zones we may have two different cases.

1. The boundary crosses over the Rankine zone, i.e. the region of influence for the free surface curve. σ and m will then both be statically determined for the upper clay layer, and by (3346-7) they can also be found for the lower clay layer. As a rule the velocity field must be calculated under the assumption that $\Delta u_n = \Delta u_t = 0$ across the boundary; it may not be kinematically possible, however, cf. Sec. 436.

2. The boundary is outside the direct region of influence. The surface zone must then be continued, usually through a radial zone and a wall zone, to the boundary. The special case mentioned above will frequently obtain, i.e. the wall zone is calculated under the assumption that $\tau_{nt} = \pm c_w$. By the subsequent calculation of the velocity field Δu_t may be different from zero (but it must have the same sign as τ_{nt}).

For more general rupture figures extremely complex constructions may obtain, the clay around the boundary breaking up into rigid bodies separated by local rupture zones. In practice approximate solutions using systems of line ruptures are very useful. If it cannot be avoided that the internal boundaries pass through rupture zones (especially with mixed boundary conditions) one might use kinematically admissible solutions with velocity fields corresponding to solutions with possible zones in homogeneous clay.

The condition that $\Delta u_n = 0$ is evidently equivalent to, cf. (3334):

$$u_s \sin i_s + v_s \cos i_s = u_w \sin i_w + v_w \cos i_w \tag{3349}$$

This condition must always be satisfied. If also $\Delta u_t = 0$, i.e.

$$u_s \cos i_s - v_s \sin i_s = u_w \cos i_w - v_w \sin i_w \tag{3350}$$

the following relations obtain:

$$\begin{aligned} u_s &= u_w \cos(i_s - i_w) + v_w \sin(i_s - i_w) \\ v_s &= -u_w \sin(i_s - i_w) + v_w \cos(i_s - i_w) \end{aligned} \tag{3351}$$

or the corresponding equations where the suffixes w and s have been interchanged.

Internal boundaries may be represented in the λ,μ-plane by wavy lines (in the diagonal directions).

Example 33 d

On Fig. 33 M is shown the (somewhat constructed) example of a smooth foundation AO placed with one edge over an interface OG forming the angle θ with the vertical y-axis, between two clay domains with different shear strengths c_s and c_w ($c_s \geq c_w$). The unit weight γ is assumed to be the same everywhere in the clay.

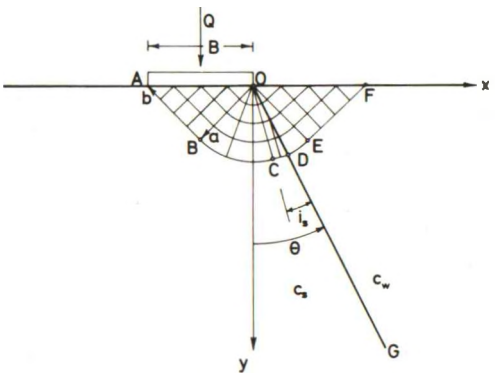

Fig. 33 M: A Bearing Capacity Problem Modified by an Internal Boundary.

The rupture figure is a modified Prandtl rupture, with a triangle zone OCD along the interface in order that the boundary condition (3347) shall be satisfied.

Along the interface we have $i_w = 0$, and therefore according to (3348):

$$\cos 2 i_s = \frac{c_w}{c_s} \tag{3352}$$

At the same place we have

$$\sigma_w = c_w \left(1 + \frac{\pi}{2} - 2\theta\right) \tag{3353}$$

From (3346) we find, σ_o being zero (passive case):

$$\sigma_s = \sigma_w + c_s \sin 2 i_s = c_w \left(1 + \frac{\pi}{2} - 2\theta\right) + \sqrt{c_s^2 - c_w^2} \tag{3354}$$

The unit bearing capacity of the foundation is found as σ_1 along OA, which is equal to σ along OB plus c_s:

$$\frac{Q}{B} = \sigma_s + c_s \left(1 + \frac{\pi}{2} + 2\theta - 2i_s\right) \tag{3355}$$

$$= c_s \left[(\pi + 2) \cos^2 i_s + 4\theta \sin^2 i_s - (2i_s - \sin 2i_s) \right] \tag{3356}$$

when i_s, defined by (3352), is used as the parameter characterizing the relative strengths of the clay domains. The solution is valid for the interval:

$$-\left(\frac{\pi}{4} - i_s\right) \leq \theta \leq \frac{\pi}{4} \tag{3357}$$

We must have, evidently

$$0 \leq i_s \leq \frac{\pi}{4} \tag{3358}$$

The lower limit corresponds to the normal Prandtl case ($c_s = c_w$), whereas the upper limit corresponds to $c_w = 0$, i.e. a strip foundation on the edge of a slope OG.

(3352-8) give no solution when $c_w > c_s$. If the two symbols are interchanged in Fig. 33 M the triangle zone OCD will develop on the other side of the interface OG. We may then again use (3352), and find in the same way as above (active case):

$$\frac{Q}{B} = c_s \left[(\pi + 2) \cos^2 i_s - 4\theta \sin^2 i_s - (2 i_s - \sin 2 i_s) \right] \tag{3359}$$

valid for:

$$-\frac{\pi}{4} \leq \theta \leq \frac{\pi}{4} - i_s \tag{3360}$$

Notice, however, that in this case it is necessary to investigate whether a rupture figure to the other side of the foundation will not be more critical. This will always be the case unless some sort of confinement exists, f. inst. as a rigid wall at a small distance from A.

336 Boundaries to External Rigid Bodies

Along a boundary between a rupture zone and an external rigid body there will always be slidings, the sign of which is indicated by the number e_t (cf. Sec. 311). Therefore $\tau_{nt} = e_t c_a$ is known, and m_t, and also m, can be found from (3303-5).

Defining the angle i_w from the equation

$$\cos 2\, i_w = \frac{c_a}{c} \tag{3361}$$

$(0 \leq i_w \leq \frac{\pi}{4})$ one must have:

$$m_t = -e_s \left[\frac{\pi}{4} + e_t \left(\frac{\pi}{4} - i_w \right) \right] \tag{3362}$$

the sign of $e_s = -e_a\, e_b$ indicating whether the rupture zone is in the active ($e_s = +1$) or the passive ($e_s = -1$) case. By this notation it is assumed that the direction of calculations in the rupture zone is roughly parallel to the normal to (i.e. away from) the boundary.

In some cases this formula may be used directly. Since σ_n is not given initially - as explained in Sec. 231 a possible surface loading σ_o is transmitted directly to the external rigid body - (3306) cannot be used. However, σ_n might be assumed as a function of s after which the boundary may be treated as if it were a free surface. In this way the problem has been transformed to one of the first initial condition type, cf. Sec. 321, but with a supplementary condition (a specified functional dependence) on one or both of the derived zone boundaries, from which the assumed function σ_n can be checked and readjusted.

However, in most cases a wall zone will be calculated as a third initial value problem, i.e. from a previously calculated zone boundary (slip line), so that e_a and e_b are both specified and correspond to a direction of calculations which is roughly parallel to the surface. The position of the wall in the λ, μ-plane (indicated by a double dotted line in a diagonal direction) may be specified by the number e_w (+1 if the direction of calculations is in the positive direction of s, and -1 if it is in the negative direction of s). Finally e_t specifies the sign of τ_{nt} as indicated above. This quantity will also depend on the tangential movement of the external rigid body in relation to the wall.

The eight possible combinations of e_a, e_b, e_w are shown in a schematical way on Fig. 33 N where it is also used that the positive direction of s corresponds to a rotation in the negative direction about the clay material.

With this notation (3362) must be replaced by:

$$m_t = -e_f \left[\frac{\pi}{4} + e_t \left(\frac{\pi}{4} - i_w \right) \right] + p\, \pi \tag{3363}$$

so that

$$m = m_t + \beta$$

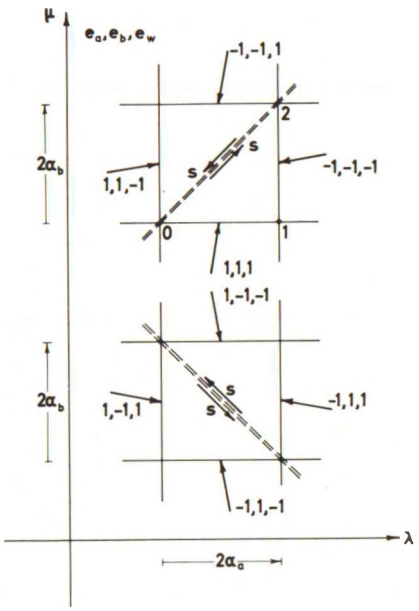

Fig. 33 N: Signs of Indicators e_a, e_b, and e_w for Different Types of Wall Zones and Directions of Calculations.

where p is an even number when $e_a e_w$ is positive, and uneven when this quantity is negative. The value of p will be given by the geometry of the failure problem, cf. Sec. 421.

As explained in Sec. 322 the method of Riemann integration cannot be used in this case, but the method of finite differences or the method of chord lengths must be applied. The calculations are performed in principle as indicated in Sec. 321. Thus, in a unit step two points are assumed to be known, one (No. 0) located on the boundary and the other (No. 1) on a slip line through this point. A third point (No. 2), which is the intersection point between the boundary and the other slip line through the second point, is sought. From Fig. 33 N, where the point numbers are indicated for the case $e_a = e_b = e_w = 1$, it is seen that the known slip line between the two first mentioned points is an a-line (i.e. α_a is known for the step) when $e_a e_b e_w = e_f e_w = +1$, and a b-line ($\alpha_b$ is known) when $e_f e_w = -1$.

By the method of finite differences the calculations must be based upon the equivalent coordinates or the radii of curvature. In the general case, where β and c_a are arbitrary functions of s the calculations may be rather cumbersome, an interpolation procedure being necessary in each step.

Thus, if the equivalent coordinates are used $\bar{x}$ and $\bar{y}$ are assumed to be known at the point No. 1. Along the boundary β, m_t, x, and y are known as functions of s. The equivalent coordinates $\bar{x}$ and $\bar{y}$ will therefore also be known as functions of s, cf. (3116). The point No. 2 may now be determined by the following procedure.

Assume the value of s for the point No. 2. This determines m_2, $\bar{x}_2$, and $\bar{y}_2$. We can now find:

$$\alpha_b = \frac{1}{2} e_b (m_2 - m_1) \text{ for } e_f e_w = 1$$
$$\alpha_a = \frac{1}{2} e_a (m_2 - m_1) \text{ for } e_f e_w = -1 \qquad (3364)$$

and from (3119), cf. (3237):

$$\bar{x}_2 = \bar{x}_1 + e_b \alpha_b (\bar{y}_1 + \bar{y}_2) \text{ for } e_f e_w = 1$$
$$\bar{y}_2 = \bar{y}_1 - e_a \alpha_a (\bar{x}_1 + \bar{x}_2) \text{ for } e_f e_w = -1 \qquad (3365)$$

If necessary the value of s_2 is changed by trial and error until the value found by (3365) is equal to the known value corresponding to the assumed value of s_2.

If c_a is constant along the boundary, which will normally be the case, m_t will also be constant according to (3361) and (3363). It can further be used that the boundary curve will normally, at least in sections, be formed as a circle arc, or be a straight line; cf. Fig. 33 O. In the former case the origin point for the coordinate system can be placed at the centre for the circle arc (this may necessitate a re-calculation of $\bar{x}$ and $\bar{y}$ along the given initial slip line C_c of Fig. 32 C). If the radius of the boundary curve is

$$r_o = -\frac{ds}{d\beta} \qquad (3366)$$

we find that $\bar{x}$ and $\bar{y}$ are constants along the boundary:

$$\bar{x} = r_o \sin m_t$$
$$\bar{y} = r_o \cos m_t \qquad (3367)$$

They are therefore known beforehand. The only unknown quantities are α_b or α_a which can be found directly from (3365):

$$\alpha_b = e_b \frac{\bar{x}_2 - \bar{x}_1}{\bar{y}_2 + \bar{y}_1} \text{ for } e_f e_w = 1$$
$$\alpha_a = -e_a \frac{\bar{y}_2 - \bar{y}_1}{\bar{x}_2 + \bar{x}_1} \text{ for } e_f e_w = -1 \qquad (3368)$$

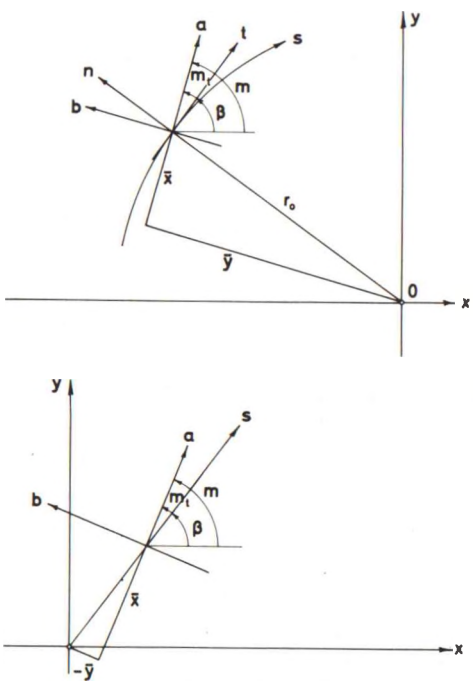

Fig. 33 O: Circular and Straight Boundaries to External Rigid Bodies (Constant Value of c_a). Optimal Position of Origin Point for Equivalent Coordinates.

Besides

$$s_2 = s_o - r_o (m_2 - m_o) = s_o - 2 r_o (e_a \alpha_a + e_b \alpha_b) \qquad (3369)$$

If the boundary is a straight line m will be constant along the boundary, because β and m_t are. This means that a + b = const., or

$$e_a \alpha_a + e_b \alpha_b = 0 \qquad (3370)$$

valid for both signs of $e_f e_w$. The known variation of $\bar{x}$ and $\bar{y}$ with s:

$$\begin{aligned} \bar{x} &= s \cos m_t \\ \bar{y} &= -s \sin m_t \end{aligned} \qquad (3371)$$

can be used together with (3365) to find s_2:

$$\begin{aligned} s_2 &= \frac{\bar{x}_1 + e_b \alpha_b \bar{y}_1}{\cos m_t + e_b \alpha_b \sin m_t} \quad \text{for } e_f e_w = 1 \\ s_2 &= \frac{e_a \alpha_a \bar{x}_1 - \bar{y}_1}{\sin m_t - e_a \alpha_a \cos m_t} \quad \text{for } e_f e_w = -1 \end{aligned} \qquad (3372)$$

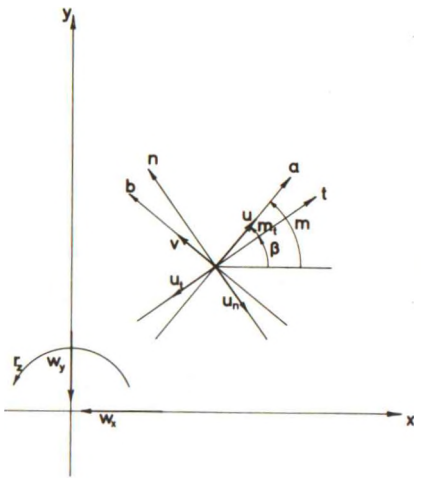

Fig. 33 P: Velocity Components at a Point on a Boundary to an External Rigid Body. Movement Components for the Rigid Body.

By the calculation of the velocity field, characterized in the rupture zone by means of the components u and v, the geometrical functions and all angle differences must be assumed to be known, f. inst. from a preliminary calculation as indicated above with estimated values for all unknown parameters. The coordinates x, y will therefore be known as functions of λ (or μ) along the boundary curve. Since the velocity of a clay particle on the boundary can only differ from the velocity of the corresponding particle on the external rigid body by an amount corresponding to the sliding velocity $u_s = \Delta u_t$ (positive in the positive direction of n), one must have, cf. Fig. 33 P:

$$u = -w_x \cos m - w_y \sin m - r_z \bar{y} + u_s \cos m_t = u_r + u_s \cos m_t$$
$$v = w_x \sin m - w_y \cos m + r_z \bar{x} - u_s \sin m_t = v_r - u_s \sin m_t \tag{3373}$$

u_r and v_r being the velocity components for the external rigid body. The same formulae are used when the external body is not rigid but is deformed elastically or plastically, the boundary being f. inst. an internal boundary satisfying (3348).

Inserting u and v (with index 2) in the equations corresponding to (3125), cf. (3365):

$$v_2 = v_1 - e_b \alpha_b (u_1 + u_2) \quad \text{for } e_f e_w = 1$$
$$u_2 = u_1 + e_a \alpha_a (v_1 + v_2) \quad \text{for } e_f e_w = -1 \tag{3374}$$

we may find u_s:

$$u_{s(2)} = \frac{v_{r(2)} - v_1 + e_b \alpha_b (u_1 + u_{r(2)})}{\sin m_t - e_b \alpha_b \cos m_t} \quad \text{for } e_f e_w = 1$$
$$u_{s(2)} = \frac{-u_{r(2)} + u_1 + e_a \alpha_a (v_1 + v_{r(2)})}{\cos m_t + e_a \alpha_a \sin m_t} \quad \text{for } e_f e_w = -1 \tag{3375}$$

from which u_2 and v_2 are given by means of (3373).

If the radii of curvature are used the boundary condition is given by (3309). By the method of finite differences this equation can be interpreted on the form:

$$e_a \alpha_a (R_2 + R_o) = (s_2 - s_o) \cos m_t$$
and
$$e_b \alpha_b (S_2 + S_o) = -(s_2 - s_o) \sin m_t \tag{3376}$$

This may be used together with (3112), cf. (3365):

$$R_2 = R_1 - e_b \alpha_b (S_1 + S_2) \quad \text{for } e_f e_w = 1$$
$$S_2 = S_1 + e_a \alpha_a (R_1 + R_2) \quad \text{for } e_f e_w = -1 \tag{3377}$$

Thus, when s_2 has been estimated α_b or α_a can be found from (3364). S_2 and R_2 are then given by (3376), and the estimate for s_2 can be checked by means of (3377).

If the boundary curve is circular (Fig. 33 O) $s_2 - s_o$ may be replaced by $-r_o \Delta\beta = -2 r_o (e_a \alpha_a + e_b \alpha_b)$ so that (3376) and the appropriate equation (3377) form 3 equations with the 3 unknown quantities α_b or α_a, R_2, and S_2.

For straight boundary curves (3370) may be used so that we have 3 linear equations in the 3 unknowns Δs, R_2, and S_2. From (3309) we find in this case that $S_2 \cos m_t = R_2 \sin m_t$.

The boundary condition for the rotation functions may be found by means of Fig. 33 Q. The figure is drawn for $e_a = e_w = 1$, $e_b = -1$, and the quantities da and db relate, as does ds, to the change from the point No. 0 to No. 2. Notice that the two points No. 0 and 2 are represented in the hodograph plane by two sets of points, 0_b and 2_b corresponding to the surface of the rigid body, and 0_c, 2_c corresponding to the clay sliding upon this surface. The distance between 0_b and 2_b is $r_z\, ds$, where r_z is the rotation of the rigid body. The distance $0_b - 0_c$ is the tangential sliding u_s which is assumed to be large in relation to the rest of the figure.

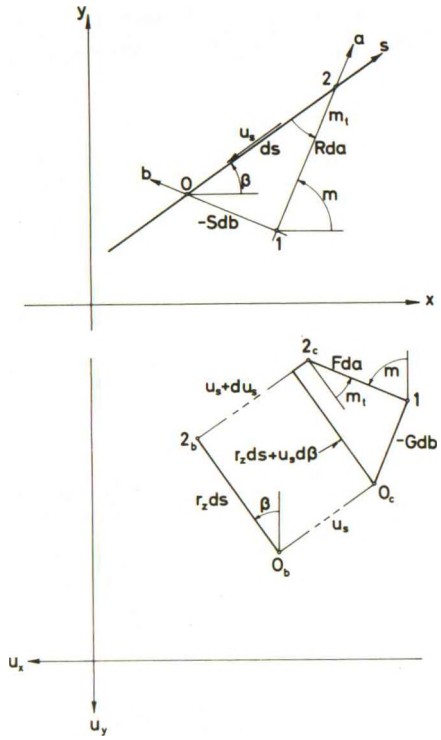

Fig. 33 Q: Zone Element Along a Boundary to an External Rigid Body. Image Element in the Hodograph Plane.

From the figure we find, valid for all combinations of e_a, e_b, and e_w:

$$\begin{aligned} Fda &= (r_z\, ds + u_s\, d\beta) \cos m_t \\ &\quad - du_s \sin m_t \\ Gdb &= -(r_z\, ds + u_s\, d\beta) \sin m_t \\ &\quad - du_s \cos m_t \end{aligned} \qquad (3378)$$

Inserting (3309) we find, assuming m_t different from 0 and from $\frac{\pi}{2}$ (+ p π):

$$\begin{aligned} F &= R \left[r_z + u_s \frac{\delta \beta}{\delta s} - \frac{\delta u_s}{\delta s} \tan m_t \right] \\ G &= S \left[r_z + u_s \frac{\delta \beta}{\delta s} + \frac{\delta u_s}{\delta s} \cot m_t \right] \end{aligned} \qquad (3379)$$

If $m_t = 0$ we have either $S = 0$ or $db = 0$, cf. (3309). In the first case the boundary is an envelope of a-lines. G cannot then be found from (3379), but (3378) must be used. In the last case the boundary is itself an a-line. G is then undetermined, but from (3378-9) we find:

$$\frac{\delta u_s}{\delta s} = 0$$

$$F = R\, r_z + e_a\, e_w\, u_s \qquad (3380\,a)$$

the factor to u_s depending on whether n is in the positive or the negative direction of b ($\frac{\delta \beta}{\delta s} = \pm \frac{1}{R}$).

Correspondingly, for $m_t = \frac{\pi}{2}$ the boundary is either an envelope of b-lines, in which case F must be found from (3378), or a b-line itself. For a b-line we find:

$$\frac{\delta u_s}{\delta s} = 0$$

$$G = S\, r_z + e_b\, e_w\, u_s \qquad (3380\,b)$$

the factor to u_s depending on whether n is in the positive or the negative direction of a ($\frac{\delta \beta}{\delta s} = \mp \frac{1}{S}$).

In the normal case where the boundary is not a slip line it is seen that F and G can only be determined simultaneously with the variation of u_s along the boundary. Even when R, S, α_a, and α_b are all known the calculations will be rather cumbersome. In each step we must evidently estimate $u_{s(2)}$, and find F_2 and G_2 by a numerical differentiation by means of (3379). For example, $\frac{\delta \beta}{\delta s}$ will usually be a known constant, $\frac{1}{r_o}$, which is equal to zero when the boundary is straight, and m_t will normally also be constant. R and S are assumed to be known, and r_z for the rigid body is also known (or estimated). $\frac{\delta u_s}{\delta s}$ can be estimated by means of a numerical differentiation formula.

The estimate of $u_{s(2)}$ can be checked by means of the equations corresponding to (3127), cf. (3365):

$$F_2 = F_1 - e_b\, \alpha_b\, (G_1 + G_2) \quad \text{for } e_f\, e_w = 1$$

$$G_2 = G_1 + e_a\, \alpha_a\, (F_2 + F_1) \quad \text{for } e_f\, e_w = -1 \qquad (3381)$$

By the method of chord lengths we must in the general case assume s_2 from which x_2, y_2, and m_2 are given. α_b or α_a are then found from (3364), and m_b or m_a from:

$$m_b = \tfrac{1}{2}(m_1 + m_2) = m_1 + e_b\, \alpha_b = m_2 - e_b\, \alpha_b \quad \text{for } e_f\, e_w = 1$$

$$m_a = \tfrac{1}{2}(m_1 + m_2) = m_1 + e_a\, \alpha_a = m_2 - e_a\, \alpha_a \quad \text{for } e_f\, e_w = -1 \qquad (3382)$$

This value is checked by the geometrical condition corresponding to (3259):

$$m_b = \arctan\frac{y_2 - y_1}{x_2 - x_1} - e_b \frac{\pi}{2} \quad (+ p\,\pi) \qquad \text{for } e_f e_w = 1$$

$$m_a = \arctan\frac{y_2 - y_1}{x_2 - x_1} + (1 - e_a)\frac{\pi}{2} \quad (+ p\,\pi) \quad \text{for } e_f e_w = -1 \tag{3383}$$

the value of p being chosen so that $\cos m_b$ and $\sin m_b$ (or $\cos m_a$ and $\sin m_a$) both have the correct signs.

When agreement has been obtained k_b or k_a can be found from the equation:

$$\left.\begin{matrix} k_b \\ k_a \end{matrix}\right\} = \sqrt{(x_2 - x_1)^2 + (y_2 - y_1)^2} \tag{3384}$$

for $e_f e_w = 1$ or -1, respectively.

If the boundary is a circle arc or a straight line the estimate may instead be based on the half centre angle α_w, or on the chord length k_w:

$$\alpha_w = \frac{1}{2} e_w (\beta_o - \beta_2)$$

$$k_w = 2\, r_o \sin\alpha_w \tag{3385}$$

These quantities are independent of e_w. k_w is always positive, and α_w is positive when β is decreasing in the positive direction of s. For a straight boundary line $\alpha_w = 0$.

One may define the quantities (cf. Fig. 33 R):

$$m_a = m_1 - (e_f e_w)\, e_a\, \alpha_a = m_1 - e_w e_b \alpha_a$$

$$m_b = m_1 + (e_f e_w)\, e_b\, \alpha_b = m_1 + e_w e_a \alpha_b$$

$$\begin{aligned} \omega_w &= m_1 + e_f e_w (2\, e_b\, \alpha_b + e_w\, \alpha_w) - m_t \\ &= m_1 - e_f e_w (2\, e_a\, \alpha_a + e_w\, \alpha_w) - m_t \\ &= m_1 - m_t + e_w (e_a\, \alpha_b - e_b\, \alpha_a) \end{aligned} \tag{3386}$$

which represent the mean values of m between the end points of the chords k_a and k_b, and the mean value of β between the end points of k_w, respectively. In the last equation the identity

$$e_a\, \alpha_a + e_b\, \alpha_b + e_w\, \alpha_w = 0 \tag{3387}$$

is used. It is valid when m_t is a constant along the boundary.

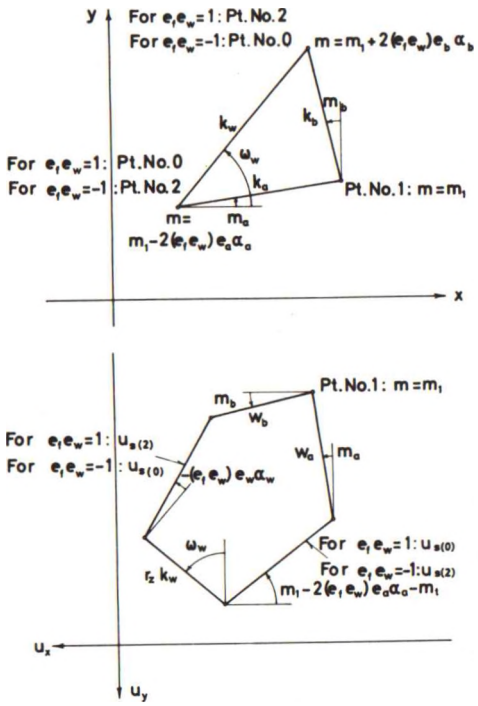

Fig. 33 R: Cell Element Adjacent to a Boundary to an External Rigid Body. Image Cell in the Hodograph Plane.

The two geometrical identies:

$$\begin{aligned} e_a k_a \cos m_a - e_b k_b \sin m_b &= e_w k_w \cos \omega_w \\ e_a k_a \sin m_a + e_b k_b \cos m_b &= e_w k_w \sin \omega_w \end{aligned} \tag{3388}$$

can now be used to find the solution:

$$\begin{aligned} k_a &= e_a e_w k_w \frac{\cos (m_b - \omega_w)}{\cos (m_a - m_b)} \\ &= e_a e_w k_w \frac{\cos (m_t + e_w e_b \alpha_a)}{\cos (\alpha_a + e_f \alpha_b)} \end{aligned} \tag{3389}$$

$$\begin{aligned} k_b &= -e_b e_w k_w \frac{\sin (m_a - \omega_w)}{\cos (m_a - m_b)} \\ &= -e_b e_w k_w \frac{\sin (m_t - e_w e_a \alpha_b)}{\cos (\alpha_a + e_f \alpha_b)} \end{aligned}$$

cf. (3263). It is seen that k_a and k_b must satisfy the condition:

$$e_a k_a \sin (m_t - e_w e_a \alpha_b) + e_b k_b \cos (m_t + e_w e_b \alpha_a) = 0 \tag{3390}$$

These equations are used as follows. If the boundary is a circle arc, α_w is assumed after which the unknown quantity α_b or α_a is found from (3387). k_w is determined in two ways: from (3385) and from the appropriate equation (3389), containing the known chord length k_a or k_b. If necessary the value of α_w is changed by trial and error until the two values of k_w are identical. Finally the unknown chord length k_b or k_a is found from (3390) (or (3389) which gives the same result).

If the boundary is a straight line $\alpha_w = 0$, and α_b or α_a can be found directly from (3387), cf. (3370). k_b or k_a can then be found from (3390) and k_w from (3389).

The formulae for the velocities are rather complicated. We find, cf. Fig. 33 R:

$$\Delta u_x(0\to 2) = e_a w_a \sin m_a + e_b w_b \cos m_b = e_w r_z k_w \sin \omega_w$$
$$- [\, u_{s(2)} \cos(\omega_w - e_w \alpha_w) - u_{s(0)} \cos(\omega_w + e_w \alpha_w)\,] \qquad (3391)$$
$$-\Delta u_y(0\to 2) = e_a w_a \cos m_a - e_b w_b \sin m_b = e_w r_z k_w \cos \omega_w$$
$$+ [\, u_{s(2)} \sin(\omega_w - e_w \alpha_w) - u_{s(0)} \sin(\omega_w + e_w \alpha_w)]$$

The solution is:

$$w_a \cos(m_a - m_b) = e_a \,[\, e_w r_z k_w \cos(\omega_w - m_b)$$
$$+ u_{s(2)} \sin(\omega_w - m_b - e_w \alpha_w)$$
$$- u_{s(0)} \sin(\omega_w - m_b + e_w \alpha_w)\,] \qquad (3392)$$
$$w_b \cos(m_a - m_b) = e_b \,[\, e_w r_z k_w \sin(\omega_w - m_a)$$
$$- u_{s(2)} \cos(\omega_w - m_a - e_w \alpha_w)$$
$$+ u_{s(0)} \cos(\omega_w - m_a + e_w \alpha_w)\,]$$

The unknown quantities are $u_{s(2)}$ and either w_b or w_a. The first mentioned quantity is found from the equation which contains the known chord length, and when its value has been inserted in the other equation the unknown chord length is given.

Example 33 e

The complete formulae to be used by the method of chord lengths, f. inst. (3260-3), (3279-85), and (3389), are necessary for a smooth administration of calculations by a computer. They are also useful to avoid mistakes in large calculation tables when the computations are performed by hand. However, for simpler calculations it will normally be easier to adopt a modified scheme based on direct geometrical reasoning. To avoid confusions the chord lengths and centre angles (always positive) may in this case be distinguished by means of integer suffixes (not letters).

As an example consider the rupture figure shown in Fig. 33 S, corresponding to the active earth pressure on a retaining wall when the clay surface is loaded on the part OA, and is unloaded outside this part.

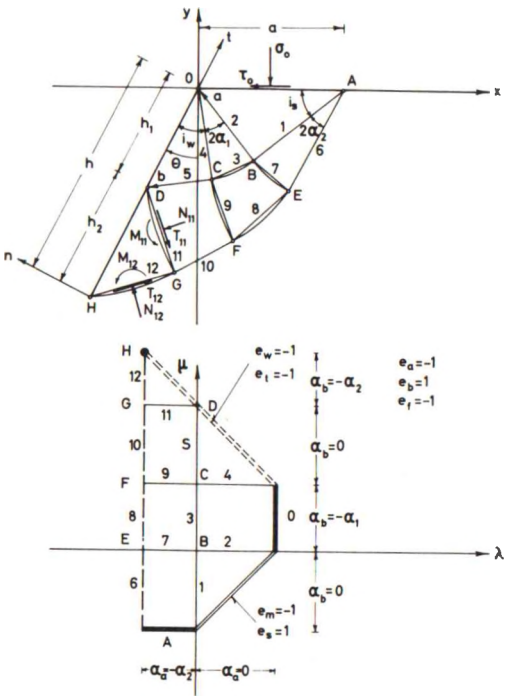

Fig. 33 S: Zone Rupture Behind a Retaining Wall with a Discontinued Surface Loading. Solved by the Method of Chord Lengths.

The rupture figure depends on the 4 dimensionless parameters θ, $\frac{c_a}{c}$, $\frac{a}{h}$, and $\frac{\tau_o}{c}$, and on the sign of $\tau_{nt} = f$ along the wall. This quantity is determined by the movement of the wall. It is assumed to be given so that the zone rupture shown in Fig. 33 S represents a kinematically possible solution with $\tau_{nt} = f = -c_a$. It is also assumed that the other parameters (and $\frac{\sigma_o}{c}$) have such values that the rupture figure is geometrically and statically possible.

Notice that Fig. 33 S has been drawn with the maximal chord lengths under the condition that zone elements shall be distinguished. As an alternative one might f. inst. approximate the arc AEF by one circle arc (and possibly FGH by another). This would be perfectly possible, using the known points A and C, and the known value of i_w at H, but a poorer approximation would be obtained. If possible, zone element boundaries, i. e. slip lines which are discontinuity lines for the radius of curvature, should always be represented by circle arcs. Interior slip lines in zone elements may be dis-

regarded, however, if this will not give too great angles along the element boundaries.

With the notations shown in the figure the centre angles α_a and α_b, and the indicators e_a, e_b etc. are found as indicated. From the formulae in the preceding sections, or from direct geometrical considerations the following calculation procedure can now be derived.

1. Calculate:

$$i_s = \text{arc tan} \sqrt{\frac{\tau_f + \tau_o}{\tau_f - \tau_o}}$$

$$i_w = \text{arc tan} \sqrt{\frac{\tau_f + \tau_a}{\tau_f - \tau_a}} \qquad (3393)$$

with $\tau_f = -c$, $\tau_a = -c_a$;

and $\alpha_1 = \frac{1}{2}(\theta + i_s - i_w)$

2. If $\alpha_1 < 0$ the zone is not geometrically possible. The problem cannot therefore be solved by means of the assumed rupture figure.

3. If $\frac{h_1}{h} = \frac{a}{h}\frac{\sin i_s}{\cos i_w} \geq 1$ the strip AEFGH will not develop, but the rupture figure will be an ordinary Prandtl zone. In this case the actual surface part covered by the rupture figure will not be a, but $OA_1 = a_1$ where:

$$\frac{a_1}{h} = \frac{\cos i_w}{\sin i_s}$$

Else, if $\frac{h_1}{h} < 1$ take: (3394)

$$\frac{a_1}{h} = \frac{a}{h}$$

4. Calculate:

$$\frac{k_1}{h} = \frac{a_1}{h} \cos i_s$$

$$\frac{k_2}{h} = \frac{k_4}{h} = \frac{a_1}{h} \sin i_s$$

$$\frac{k_3}{h} = 2 \frac{k_2}{h} \sin \alpha_1$$

$$\frac{k_5}{h} = \frac{k_4}{h} \tan i_w \qquad (3395)$$

$$\frac{e_O}{c} = \frac{e_D}{c} = \frac{\sigma_o}{c} - \sin 2 i_s - \sin 2 i_w - 4 \alpha_1$$

$$\frac{f_O}{c} = \frac{f_D}{c} = -\frac{c_a}{c}$$

5. If $\frac{h_1}{h} < 1$ take $\frac{k_6}{h} = \frac{k_1}{h}$ and estimate the value of α_2.

6. Calculate:

$$\frac{k_7}{h} = 2 \frac{k_1}{h} \sin \alpha_2$$

$$\frac{k_8}{h} = \frac{k_3}{h} \frac{\cos (\alpha_1 - \alpha_2)}{\cos (\alpha_1 + \alpha_2)} + \frac{k_7}{h} \frac{\sin 2 \alpha_1}{\cos (\alpha_1 + \alpha_2)}$$

$$\frac{k_9}{h} = \frac{k_3}{h} \frac{\sin 2 \alpha_2}{\cos (\alpha_1 + \alpha_2)} + \frac{k_7}{h} \frac{\cos (\alpha_1 - \alpha_2)}{\cos (\alpha_1 + \alpha_2)}$$

$$\frac{k_{10}}{h} = \frac{k_5}{h} \qquad (3396)$$

$$\frac{k_{11}}{h} = 2 \frac{k_5}{h} \sin \alpha_2 + \frac{k_9}{h}$$

$$\frac{k_{12}}{h} = \frac{k_{11}}{h} \tan (i_w + \alpha_2)$$

$$\frac{h_2}{h} = \frac{k_{11}}{h} \sec (i_w + \alpha_2)$$

7. If $\frac{h_1}{h} + \frac{h_2}{h} \neq 1$ then choose another value for α_2 (by means of an iteration routine) and go to No. 6 above. Else, if the condition is satisfied within the required accuracy calculate:

$$\frac{e_H}{c} = \frac{e_D}{c} - 8\,\alpha_2 \qquad (3397)$$

$$\frac{f_H}{c} = -\frac{c_a}{c}$$

8. The calculations may be continued by the finding of the coordinates (x_B, y_B), (x_C, y_C) etc., and of the total earth pressure components $E = -Q_n$, $F = -Q_t$, and $M = M_{tn}$ acting upon the wall (related to the t,n-coordinate system with origo at the foot point H of the wall). The latter quantities are easily found by means of the stress resultants:

$$\frac{N_{11}}{ch} = \frac{k_{11}}{h}\left[\frac{\sigma_D}{c} - N^z(\alpha_2)\right]$$

$$\frac{T_{11}}{ch} = \frac{k_{11}}{h}\,T^z(\alpha_2) \qquad (3398)$$

and

$$\frac{M_{11}}{ch^2} = \left(\frac{k_{11}}{h}\right)^2 M^z(\alpha_2)$$

etc., the resultants being positive in the directions shown on Fig. 33 S when α_2 is inserted as a positive quantity ($\tau_f = +c$).

337 Boundaries to Rigid Bodies of Clay

The boundaries between rupture zones and rigid bodies of clay may either be internal boundaries or slip lines. In the first mentioned case the position is known initially, so the boundary will in fact have the same properties as a boundary to an external rigid body.

For slip lines in homogeneous clay the position will not be known initially. In some cases it may be constructed directly (statically determined zones) or after a number of initial parameters have been estimated (open rupture zones with mixed boundary conditions). The boundary conditions along some of the zone boundaries will then be used to calculate the velocity field in the rupture zone. If there are estimated initial parameters in the rupture figure the boundary conditions along some other zone boundaries can

afterwards be used to check the values of these parameters. In an important special case (closed rupture zones with mixed boundary conditions) the above mentioned calculations can be performed in one closed operation independent of the position and scale of the rupture zone. In the λ,μ-plane slip lines without sliding are represented by thin full lines, and slip lines with sliding by heavy dotted lines.

In homogeneous clay the boundary slip lines are perfectly normal. Thus, the shear stress is known (equal to c), and the normal stress (equal to σ) can be calculated by means of (3101). We need only know one of a set of two conjugate auxiliary functions, since the other can always be calculated by means of (3201). Therefore, from a boundary condition in terms of f.inst. R and F the corresponding one in terms of S and G can always be deduced by differentiation (along b-lines) or integration (along a-line).

Sliding may obtain along such boundaries. It follows from (3132) that the velocity difference $u_s = \Delta u_t$ will be constant along the boundary, equal to $-\Delta u_b$ or Δv_a, dependent on whether the boundary is an a-line or a b-line. As mentioned previously Δu_b and Δv_a must always be positive. For brevity these two quantities are called u_d and v_d, respectively, in the following.

In this case the boundary conditions can be expressed independent of the directions of calculations. However, since the value of m_t depends on whether the rigid body is to the positive or the negative side of the orthogonal slip lines it will be necessary to distinguish between these two cases. Let e_r be equal to +1 in the former, and to -1 in the latter case. From (3373) we shall then find (r_z being the rotation of the rigid body of clay):

For a-lines ($m_t = \frac{\pi}{2}(1 - e_r)$, $u_s = -u_d$):

$$u = -w_x \cos m - w_y \sin m - r_z \bar{y} - e_r u_d = u_r - e_r u_d$$
$$v = w_x \sin m - w_y \cos m + r_z \bar{x} = v_r \qquad (3399)$$

For b-lines ($m_t = \frac{\pi}{2} e_r$, $u_s = v_d$):

$$u = -w_x \cos m - w_y \sin m - r_z \bar{y} = u_r$$
$$v = w_x \sin m - w_y \cos m + r_z \bar{x} - e_r v_d = v_r - e_r v_d \qquad (33100)$$

It is seen that in the first case v, and in the second case u, is independent of u_d and v_d, respectively.

From (3380) we have directly for a-lines:

$$F = Rr_z - e_r u_d$$

and by integration: (33101)

$$G - G_o = (S - S_o)\, r_z - e_r u_d\, (a - a_o)$$

where a_o, S_o, and G_o are known function values at the same point of the boundary.

Correspondingly, for b-lines:

$$G = Sr_z - e_r v_d$$

and by integration: (33102)

$$F - F_o = (R - R_o)\, r_z - e_r v_d\, (b - b_o)$$

These formulae are simpler than the corresponding (3399-100). Besides they are independent of the position of the boundary. Therefore, at least in homogeneous clay they are the most useful for the calculation of closed rupture zones.

By the method of chord lengths we may in the same way insert into (3392), using that $u_{s(2)} = u_{s(0)}$ in all cases. For example, for a-lines $e_w = e_r e_a$, $\omega_w = m_a + (1 - e_r)\frac{\pi}{2}$, $e_w \alpha_w = -e_a \alpha_a$, and $u_s = -u_d$. The second Eq. (3392) then becomes an identity, but the first equation gives:

$$w_a = r_z k_a - 2 e_r u_d \sin \alpha_a \qquad (33103)$$

In the same way we find for b-lines:

$$w_b = r_z k_b - 2 e_r v_d \sin \alpha_b \qquad (33104)$$

These simple formulae can also be obtained by direct geometrical considerations. Since they give a linear relationship between chord lengths in the physical plane and in the hodograph plane they are extremely well suited for the calculation of rupture zones with mixed boundary conditions.

Example 33 f

The velocity field in the rupture figure considered in Ex. 33 e (Fig. 33 S) can be found in a simple way by means of the method of chord lengths. Assume that the movement components of the wall are w_n, w_t, r_z relative to the t,n-coordinate system shown in the figure. Since the clay outside the rupture figure is unmoved we must have at the point H, v_d being the sliding velocity along AEFGH ($e_r = -1$):

$$-w_n = v_d \cos i_w \tag{33105}$$

i.e.

$$v_d = -w_n \sec i_w$$

and

$$u_s = w_t - v_d \sin i_w = w_t + w_n \tan i_w \tag{33106}$$

u_s must be negative, so we must have $w_t \leq -w_n \tan i_w$. From (33104) we find ($r_z = 0$ for the rigid body of clay):

$$\begin{aligned} w_{12} &= -2 v_d \sin \alpha_2 \\ w_{10} &= w_6 = 0 \\ w_8 &= -2 v_d \sin \alpha_1 \end{aligned} \tag{33107}$$

cf. Fig. 33 S.

During the calculation of the velocity field we have evidently $e_a = 1$, $e_b = -1$, $e_f = -1$, and $e_w = 1$. Along the wall $\alpha_w = 0$, and for the cells HGD and DCO we have, respectively:

$$\begin{aligned} &\text{For HGD:} \quad m_a = m_b = \omega_w + i_w + \alpha_2 \\ &\text{For DCO:} \quad m_a = m_b = \omega_w + i_w \end{aligned} \tag{33108}$$

Therefore, from (3268) and (3392) we find:

$$\begin{aligned} u_{s(D)} &= u_{s(H)} - r_z h_2 \tan (i_w + \alpha_2) + w_{12} \sec (i_w + \alpha_2) \\ w_{11} &= r_z h_2 \sec (i_w + \alpha_2) - w_{12} \tan (i_w + \alpha_2) \\ w_9 &= w_{11} \\ w_5 &= 0 \\ w_7 &= w_9 \frac{\cos (\alpha_1 - \alpha_2)}{\cos (\alpha_1 + \alpha_2)} - w_8 \frac{\sin 2\alpha_2}{\cos (\alpha_1 + \alpha_2)} \\ w_3 &= -w_9 \frac{\sin 2\alpha_1}{\cos (\alpha_1 + \alpha_2)} + w_8 \frac{\cos (\alpha_1 - \alpha_2)}{\cos (\alpha_1 + \alpha_2)} \\ w_1 &= 0 \\ u_{s(O)} &= u_{s(D)} - r_z h_1 \tan i_w + w_5 \sec i_w \\ w_4 &= r_z h_1 \sec i_w - w_5 \tan i_w \\ w_2 &= w_4 \end{aligned} \tag{33109}$$

The velocity vectors can now be constructed from the known vector at H, and from (3269) it can be investigated whether the rupture zone is kinematically possible or not.

338 Other Boundary Conditions

The boundary conditions considered in the preceding sections are the most generally encountered in soil mechanics. Other types may occasionally be met with, some of them giving extremely complicated calculations. For example:

1. External bodies may be deformable instead of rigid. Thus, they may themselves be deformed plastically (cf. the line DG in Fig. 33 M), or a rupture figure may develop in the clay because of an elastic deformation of f. inst. a sheet wall. Especially in the last mentioned case the boundary loadings and movements may be connected by a differential equation which must be solved simultaneously with the calculation of the rupture figure.
2. Similar problems are obtained if the surface loading is not acting directly upon the clay surface but f. inst. through an elastic (or unstretchable) membrane with a known adhesion strength c_a to the clay surface.
3. The forces acting upon the system of external rigid bodies may not be constants, but may depend on the movements (elastic links). Different kinds of variable systems may also obtain. Thus, the contact between the clay and an external rigid body may be assumed to break if negative values of σ_n are obtained, the contact area may not be known initially (a circle arc in point contact with a straight clay surface) etc.
4. As mentioned previously internal boundaries may represent cracks or thin soft clay layers, so an adhesion strength $c_a < c_w \leq c_s$ may be defined. Cracks may also develop into external free surfaces if it is assumed that negative normal stresses cannot be taken.

Although they may be very complicated all the above types can be solved within the framework of the present theory. Special problems are encountered for boundary conditions where adhesion strengths are replaced by frictional forces, i. e. stress conditions of the type $\tau_{nt} = e_t \mu \sigma_n$ instead of $\tau_{nt} = e_t c_a$.

In such cases the arguments of Secs. 24 cannot strictly speaking be applied, and it is not possible to prove the uniqueness of solutions or to define the different classes of approximate solutions in the same way as it is done in these sections. This is because the contributions to the deformation work can no longer be separated into terms where the stress quantity (f. inst. c or τ_f) is known, and terms where the deformation quantity (f. inst. u_n or d_r) is known.

Such problems, which are outside the scope of the present work, are mostly encountered by soils with internal friction. They cannot be solved simply by considering the work equation, using also Gauss' s integral theorem, but the stress distribution must be considered more closely.

For the sake of simplicity the boundary conditions mentioned in this section will not be considered further in the present work.

34 STRESS CONDITIONS FOR LINE RUPTURES

341 General Formulae

As explained in Sec. 245 line ruptures in contrast to rupture zones have the special property that the values of σ at the singular points, usually the end points, cannot be found directly from the equilibrium and stress conditions. This is not important when the energy method is used, because the unknown values of σ do not influence the terms in (2426). If the equilibrium method is used σ must be determined by the condition that the two methods shall give the same result, i.e. that $D_\sigma = 0$, cf. (2430).

Considering also (2427) and (2429), and observing that $\frac{\partial Q^e_{pi}}{\partial t_k} = 0$ identically and that we have shown $\sum_{c,i} \frac{\partial Q^{zc}_{ci}}{\partial t_k} w_{ci}$ to vanish when possible zones are considered, this condition can be written:

$$-D_\sigma = \sum_{c,i} \frac{\partial Q^{cc}_{ci}}{\partial t_k} w_{ci} + \sum_{c,i} \frac{\partial Q^{c}_{ci}}{\partial t_k} w_{ci}$$

$$-\sum_{cp} \tau_a u_{cp} \frac{\partial L_{cp}}{\partial t_k} + \sum_{p,i} \frac{\partial Q^{zp}}{\partial t_k} w_{pi} = 0 \qquad (3401)$$

For any variation of parameters the calculation of the three last terms in (3401) is straightforward. Notice that the first term cannot be transformed by means of (2428) on a form like $\sum_{cc} c\, u_{cc} \frac{\partial L_{cc}}{\partial t_k}$, because the position of the line ruptures and therefore the values of u_{cc} may change even if all components w_{ci} are constants. However, the transformation of the third term by means of (2427) is permissible since boundaries between the clay and external rigid bodies are fixed in space. u_{cp} will therefore be constants when the components w_{pi} and w_{ci} are unchanged.

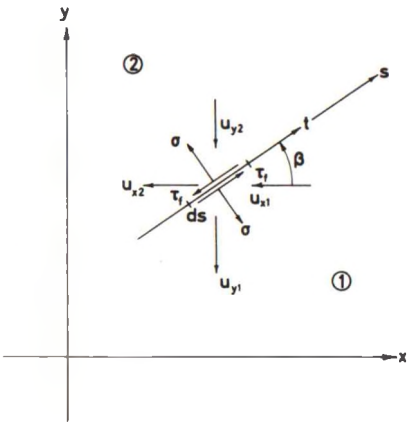

Fig. 34 A: Line Rupture Element Separating Two Rigid Bodies (No. 1 and 2).

The quantity

$$W^{cc} = -\sum_{c,i} Q_{ci}^{cc} w_{ci} \qquad (3402)$$

can be obtained by integrating the contribution $-w_{ci}\, dQ_{ci}^{cc}$ along all line ruptures, cf. Fig. 34 A. Let each line rupture be oriented by introducing a positive direction for the arc length s, and let the rigid bodies of clay separated by the line rupture be termed No. 1 (in the negative direction from the s-direction) and No. 2, respectively. β is the angle between the x-axis and the tangent direction to the line rupture. σ is the normal stress and τ_f is the shear stress, equal to +c or -c according to whether the sliding velocity $u_f = u_{t(1)} - u_{t(2)} = \pm u_{cc}$ is positive or negative. Notice that u_f has the opposite sign of u_s as defined in Sec. 221. This sign rule has been introduced so that u_f and τ_f are positive along a-lines (the signs of u_s and u_f are in accordance with Brinch Hansen's notation). From Fig. 34 A it is seen that:

$$W^{cc} = -\sum_{cc} \int_L \Big[(\sigma \sin\beta + \tau_f \cos\beta)\, \Delta u_x + (-\sigma \cos\beta + \tau_f \sin\beta)\, \Delta u_y \Big] ds \qquad (3403)$$

where Δ indicates the difference between the corresponding quantities for body No. 2 and body No. 1.

Inserting that for the sake of continuity we must have

$$-\Delta u_x \sin\beta + \Delta u_y \cos\beta = 0$$
$$-\Delta u_x \cos\beta - \Delta u_y \sin\beta = u_f \qquad (3404)$$

so that

$$\Delta u_x = -u_f \cos\beta$$
$$\Delta u_y = -u_f \sin\beta \qquad (3405)$$

we find

$$W^{cc} = \sum_{cc} \int_L \tau_f u_f \, ds = \sum_{cc} \tau_f u_f L = \sum_{cc} c \, u_{cc} L_{cc} \tag{3406}$$

as stated in (2428).

When the variation δW^{cc} in W^{cc} is sought, corresponding to a variation in the stress function σ, and possibly also in the position of the line rupture, but keeping the movement components $w_{x(1)}$, $w_{y(1)}$ ... etc. constant, (3403) must be transformed, using f.inst. x as the independent variable. Since W^{cc} and δW^{cc} are both invariant to transformations of the coordinate system, it is seen that the assumption used in the following that the line rupture should correspond to a one valued function y of x with finite derivatives is not essential. If necessary the coordinate system may be given any affine transformation so that this condition is satisfied.

Using that

$$\begin{aligned} \tan \beta &= \frac{dy}{dx} = y' \\ \sin \beta &= \frac{y'}{\sqrt{1 + (y')^2}} \\ \cos \beta &= \frac{1}{\sqrt{1 + (y')^2}} \\ ds &= dx \sqrt{1 + (y')^2} \end{aligned} \tag{3407}$$

and that

$$\begin{aligned} \Delta u_x &= \Delta w_x + y \Delta r_z \\ \Delta u_y &= \Delta w_y - x \Delta r_z \end{aligned} \tag{3408}$$

we find:

$$\begin{aligned} W^{cc} = -\sum_{cc} \int_{x_1}^{x_2} & [(\sigma y' + \tau_f) (\Delta w_x + y \Delta r_z) \\ & + (-\sigma + \tau_f y') (\Delta w_y - x \Delta r_z)] \, dx \end{aligned} \tag{3409}$$

The variation of this expression may be divided into the contribution from a variation $\delta \sigma$ in σ, and the contribution from the changed position of the line rupture. The first contribution is identically zero, cf. (3403-6). The second one can be found from a well known result in the calculus of variations. We may use that the variation of the integral of a general function F of the three variables x, y, and y' can be written:

$$\delta \int_{x_1}^{x_2} F(x,y,y')\,dx = F(x_2, y_2, y_2')\,\delta x_2$$

$$- F(x_1, y_1, y_1')\,\delta x_1 + \frac{\partial F}{\partial y'}\,\delta y \Big]_{x_1}^{x_2} \qquad (3410)$$

$$- \int_{x_1}^{x_2} \left[\frac{d}{dx}\left(\frac{\partial F}{\partial y'}\right) - \frac{\partial F}{\partial y}\right] \delta y\,dx$$

If this result is applied to the variation of (3409) for a line rupture which is moved from the position I to II (Fig. 34 B), we find, considering σ as a function (along the line rupture) of x alone:

$$\frac{d}{dx}\left(\frac{\partial F}{\partial y'}\right) - \frac{\partial F}{\partial y}$$

$$= \frac{d\sigma}{dx}\left(\Delta w_x + y \Delta r_z\right) - 2\tau_f \Delta r_z$$

$$= \frac{d\sigma}{dx}\,\Delta u_x - 2\tau_f \Delta r_z$$

$$= -u_f \left(\frac{d\sigma}{ds} + 2\tau_f \frac{d\beta}{ds}\right) \qquad (3411)$$

using also (3408), (3405), (3407), and the fact that

$$u_f = R\,\Delta r_z = \Delta r_z \frac{ds}{d\beta} \qquad (3412)$$

R being the radius of curvature for the line rupture.

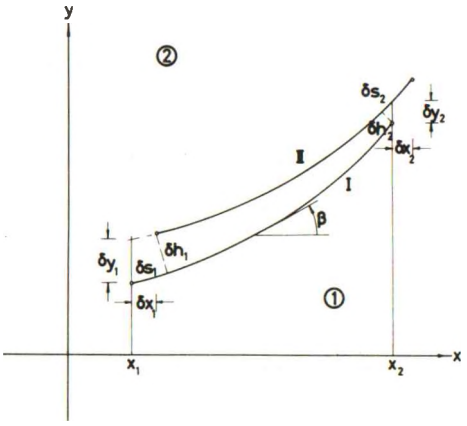

Fig. 34 B: Variation of a Line Rupture Arc from Position I to II.

We also have:

$$F\,\delta x + \frac{\partial F}{\partial y'}\,\delta y$$

$$= \left[\left(\sigma y' + \tau_f\right)\delta x + \sigma\,\delta y\right]\Delta u_x$$

$$+ \left[\left(-\sigma + \tau_f y'\right)\delta x + \tau_f\,\delta y\right]\Delta u_y \qquad (3413)$$

Inserting (3405) and (3407) we find, introducing the quantities δh and δs which are invariant to changes in the coordinate system:

$$\delta h = \delta y \cos \beta$$

$$\delta s = \frac{\delta x}{\cos \beta} + \delta y \sin \beta \tag{3414}$$

or:

$$\delta x = -\delta h \sin \beta + \delta s \cos \beta$$

$$\delta y = \frac{\delta h}{\cos \beta} \tag{3415}$$

that (3413) can be written:

$$F \delta x + \frac{\partial F}{\partial y'} \delta y = -u_f (\sigma \delta h + \tau_f \delta s) \tag{3416}$$

Inserting (3411) and (3416) in (3410) we find that (3401) is equivalent to:

$$\begin{aligned} -D_\sigma = & \sum_{cc} u_f \int_L \left(\frac{d\sigma}{ds} + 2 \tau_f \frac{d\beta}{ds}\right) \frac{\partial h}{\partial t_k} ds \\ & - \sum_{el} u_f \left(\sigma \frac{\partial h}{\partial t_k} + \tau_f \frac{\partial s}{\partial t_k}\right) + \sum_{c,i} \frac{\partial Q^c_{ci}}{\partial t_k} w_{ci} \\ & - \sum_{cp} \tau_a u_{cp} \frac{\partial L_{cp}}{\partial t_k} + \sum_{p,i} \frac{\partial Q^{zp}}{\partial t_k} w_{pi} = 0 \end{aligned} \tag{3417}$$

The first summation is extended over all line rupture arcs, and the second one over all end points of line ruptures. In the first summation δh is positive in the positive n-direction (defined in relation to s as in Fig. 33 A). In the second summation δs is always positive as increases of arc lengths, and for end points δh is positive when corresponding to a positive rotation of the line rupture position (in this way the sums are seen to be independent of the direction of integration).

The condition that (3417) shall be satisfied for all possible variations of the rupture figure will not, strictly speaking, give a unique distribution of σ along the line ruptures. Since only a finite number of parameters t_k can be changed, it is evident that (3417) cannot be used to find an unknown function σ of the variable s. However, although it might be possible to find special distributions (dependent on the geometry of the rupture figure and the number and kind of parameters which can be varied) that would satisfy (3417) a more general solution will certainly be obtained, when the distribution of σ in all cases is determined so that (3417) is satisfied by any variation of the

rupture figure. It is found that a unique solution is obtained if $\frac{\partial h}{\partial t_k}$ is regarded as a completely arbitrary function of s, although in reality its variation is restricted by the fact that the line ruptures must remain circle arcs.

Under this assumption the condition that the first summation in (3417) shall be identically zero will be:

$$\frac{d\sigma}{ds} + 2\tau_f \frac{d\beta}{ds} = 0 \qquad (3418)$$

which is always satisfied, considering that the line ruptures are stress characteristics, cf. (2318). Notice that τ_f is always positive for a-lines, and negative for b-lines, independent of the direction of s.

The condition that the second summation together with the following terms shall be zero will when applied to any possible point of singularity give the necessary conditions for the values of σ.

342 Free Surfaces

Considering a surface point S, cf. Fig. 34C, we find, assuming first that S is a point on a smooth surface curve with a continuous surface loading:

$$-u_f \left(\sigma \frac{\partial h}{\partial t_k} + \tau_f \frac{\partial s}{\partial t_k}\right) = -u_f \frac{\partial s_b}{\partial t_k} \left[-\sigma \sin(\beta - \beta_s) + \tau_f \cos(\beta - \beta_s)\right]$$

and

$$\frac{\partial Q^c_{ci}}{\partial t_k} w_{ci} \qquad (3419)$$

$$= \frac{\partial s_b}{\partial t_k} \left[(-\sigma_o \sin\beta_s + \tau_o \cos\beta_s)\Delta u_x + (\sigma_o \cos\beta_s + \tau_o \sin\beta_s)\Delta u_y\right]$$

$$= -u_f \frac{\partial s_b}{\partial t_k} \left[\sigma_o \sin(\beta - \beta_s) + \tau_o \cos(\beta - \beta_s)\right]$$

The remaining terms in (3417) are identically zero for the vicinity of the point S.

The contribution from this point to D_σ will therefore be zero if

$$\sigma = \sigma_o + (\tau_f + \tau_o) \cot(\beta - \beta_s) \qquad (3420)$$

This is Brinch Hansen's boundary condition. If $\beta = \beta_c$, the statically correct angle corresponding to the given values of β_s and τ_o:

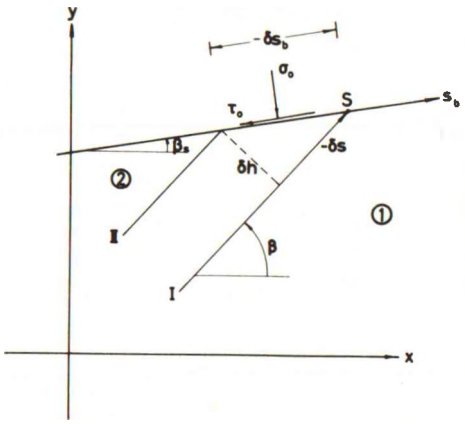

Fig. 34C: Variation of a Line Rupture in the Vicinity of a Surface Point S.

$$\cos 2(\beta_c - \beta_s) = -\frac{\tau_o}{\tau_f}$$

or

$$\cot(\beta_c - \beta_s) = \pm\sqrt{\frac{\tau_f - \tau_o}{\tau_f + \tau_o}} \qquad (3421)$$

cf. (3303), τ_o and τ_f being taken with the correct sign, σ will be equal to the statically correct value σ_c as determined from (3306):

$$\sigma_c = \sigma_o + \tau_f \sin 2(\beta_c - \beta_s)$$

In the above formulae we may without loss of generality assume that

$$0 \leq \beta - \beta_s \leq \pi. \qquad (3422)$$

(3420) is valid for all values of β (except β_s or $\beta_s + \pi$ when $\tau_o \neq -\tau_f$), but in practice a surface zone will be used in connection with the line rupture whenever this is possible. This is frequently the case when β is outside the limits indicated by (3421), i.e.

$$\pi - i \leq \beta - \beta_s \leq \pi$$

or

$$0 \leq \beta - \beta_s \leq i \qquad (3423)$$

cf. (3303-4), and the convex side of the line rupture points towards the surface.

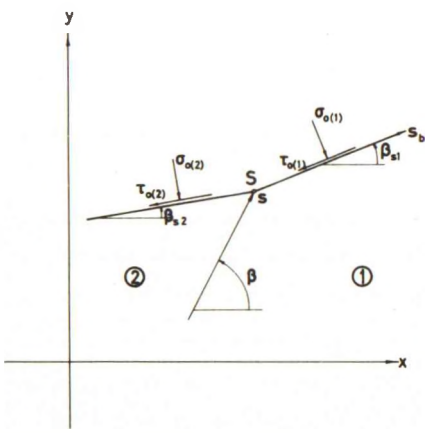

Fig. 34D: Corner Point S (and/or Point of Loading Discontinuity) on a Free Surface.

If the point S is a corner point of the surface, or a discontinuity point for the surface loading, (3420) will give different values of σ for the two sides of the point, cf. Fig. 34D. This means that σ is undetermined in such cases. On the other hand one free parameter is lost when the rupture figure is calculated under the assumption that the line rupture through S must pass through a known surface point. In the case of quasi possible solutions σ can therefore be found by the equilibrium method.

This means that σ for this line rupture arc will be determined by the condition that the term D_u shall be zero for the pertinent rigid bodies, cf. (2430). Therefore, assuming that (3417) is satisfied for all other singular points, we have directly from (2430) and (3419):

$$\frac{\partial W}{\partial t_k} = D_\sigma = u_f \frac{\partial s_b}{\partial t_k}\left[(\sigma_o - \sigma)\sin(\beta - \beta_s) + (\tau_f + \tau_o)\cos(\beta - \beta_s)\right] \tag{3424}$$

for any variation which moves the intersection point S away from the corner point.

Since the condition that we have at least a local extremum when the line rupture passes through the corner point is that $\frac{\partial W}{\partial t_k} \geq 0$ for any variation, we must therefore have:

$$\frac{\sigma_{o(2)}}{c} + \left(1 + \frac{\tau_{o(2)}}{c}\right)\cot(\beta - \beta_{s2}) \leq \frac{\sigma}{\tau_f}$$

and (3425)

$$\frac{\sigma}{\tau_f} \leq \frac{\sigma_{o(1)}}{c} + \left(1 + \frac{\tau_{o(1)}}{c}\right)\cot(\beta - \beta_{s1})$$

valid for both signs of τ_f (notice that u_f has the same sign as τ_f, and that $\frac{\partial s_b}{\partial t_k}$ is positive when the point is moved in the positive direction of s_b, and negative otherwise).

The condition (3425) can only be satisfied when the right hand expression is greater than or equal to the left hand one. Thus, if $\sigma_{o(1)} = \sigma_{o(2)}$ and $\tau_{o(1)} = \tau_{o(2)}$ it is a provision that $\beta_{s1} \geq \beta_{s2}$ (a reentrant corner), and if $\tau_{o(1)} = \tau_{o(2)}$ and $\beta_{s1} = \beta_{s2}$ we must have $\sigma_{o(1)} \geq \sigma_{o(2)}$ when $\tau_f > 0$ (a-lines), and $\sigma_{o(1)} \leq \sigma_{0(2)}$ when $\tau_f < 0$ (b-lines).

If (3425) is not satisfied it can be stated that the solution cannot be the extreme one, provided the free parameters permit the variation corresponding to (3424). In some cases it can then be concluded directly from (3425) which way to move the line rupture.

343 Internal Boundaries

For an intersection point B on an internal boundary (Fig. 34E) we find:

$$-\sum u_f \left(\sigma \frac{\partial h}{\partial t_k} + \tau_f \frac{\partial s}{\partial t_k}\right)$$

$$= -u_f \frac{\partial s_b}{\partial t_k} \left[(-\sigma_s + \sigma_w) \sin(\beta - \beta_b) + (\tau_{fs} - \tau_{fw}) \cos(\beta - \beta_b)\right]$$

and (3426)

$$\frac{\partial Q^c_{ci}}{\partial t_k} w_{ci} = \frac{\partial s_b}{\partial t_k} \left[-\sigma_o \Delta u_x \sin \beta_b + \sigma_o \Delta u_y \cos \beta_b\right]$$

$$= -u_f \frac{\partial s_b}{\partial t_k} \sigma_o \sin(\beta - \beta_b)$$

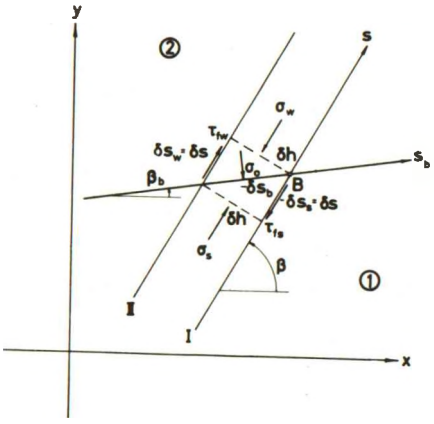

Fig. 34 E: Variation of a Line Rupture Near an Intersection Point B With an Internal Boundary.

the corrective normal force σ_o, equal to $K_s - K_w$, cf. (2305-7), being positive when it acts in the direction from w to s, see also Fig. 33 L. τ_{fs} and τ_{fw} are taken with signs. For kinematical reasons they will always have the same sign.

The contribution from the point B to D_σ will therefore be zero if

$$\sigma_s = \sigma_w + \sigma_o + (\tau_{fs} - \tau_{fw}) \cot(\beta - \beta_b) \quad (3427)$$

Notice that the normal stress σ_n and the shear stress τ_{nt} on the boundary do not enter the expression (3427), because they do no work during the movement.

The statically correct case obtains when $\beta - \beta_b = \frac{\pi}{4}$ or $\frac{3\pi}{4}$. Corner points may be treated as above, cf. Fig. 34 D; we find that a local minimum will only be possible (provided the contributions from all other singular points to D_σ are zero) if $\beta_{b1} - \beta_{b2}$ has the same sign as $\tau_{fs} - \tau_{fw}$. The difference $\sigma_s - \sigma_w$ must, if it is desired, be found from the equilibrium conditions. It must be in the interval:

$$\frac{\sigma_o}{\tau_{fs}} + \left(1 - \frac{\tau_{fw}}{\tau_{fs}}\right) \cot(\beta - \beta_{b2}) \leq \frac{\sigma_s - \sigma_w}{\tau_{fs}}$$

and $\frac{\sigma_s - \sigma_w}{\tau_{fs}} \leq \frac{\sigma_o}{\tau_{fs}} + \left(1 - \frac{\tau_{fw}}{\tau_{fs}}\right) \cot(\beta - \beta_{b1})$ (3428)

344 Wall Points

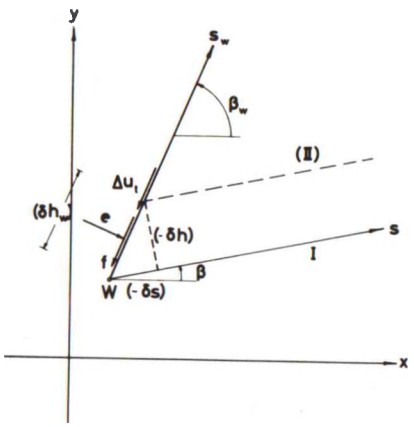

Fig. 34F: The Neighbourhood of an End Point W of a Wall (Variation From I to II not Kinematically Possible).

For an end point W of an external rigid body the contribution to D_σ will be identically zero, cf. Fig. 34F, because a variation of the line rupture from the position I to a position II with another intersection point with the wall is not kinematically possible. Therefore no condition for σ exists at this point; it must be found by means of (3418) used along the line rupture. Correspondingly, the extreme solution can be found without any knowledge of the earth pressure components e (= σ_n) and f (= τ_{nt}) at the point W.

This does not mean that they are completely undetermined. If the rigid body is sliding upon the clay, i.e. if $u_w = \Delta u_t \neq 0$, we know that f is numerically equal to c_a and has the same sign as u_w. In this case we might assume with Brinch Hansen that e has the same value as if it was a normal stress on a free surface assigned corresponding to the known values of σ and f, cf. (3420):

$$e = \sigma + (\tau_f + f) \cot (\beta_w - \beta) \qquad (3429)$$

This is not a necessary condition, however. When possible it may in some cases be more natural to find e from a radial zone and a wall zone starting from the known line rupture at W.

The same holds true when $u_w = 0$, in which case f is unknown. (3429) cannot then be used, but e and f may then also be found simply by constructing the Mohr circle for the clay element at W.

In practice e is only needed when it is required to find an estimate for the earth pressure distribution between the external rigid body and the rigid body of clay. However, this is usually done simpler, and also more accurately, by considering limiting states of stress inside the clay body, cf. Sec. 441.

Line ruptures meeting at a wall are obtained f. inst. in the rupture figure shown in Fig. 34G (AwX in Brinch Hansen's notation). For kinemat-

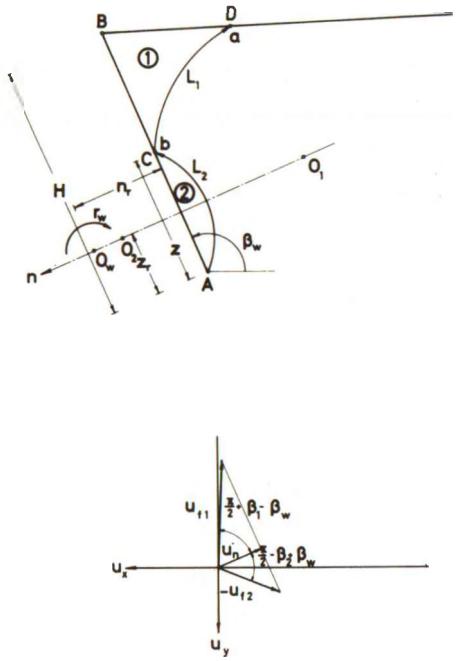

Fig. 34G: Line Ruptures Meeting at a Wall (Rupture Figure AwX). Velocity Conditions.

ical reasons the two centres O_1 and O_2 for the line ruptures No. 1 and 2, respectively, must lie on the same normal to the wall as the rotation point O_w for the wall. The wall rotation r_w may be positive or negative; it is seen that L_1 and L_2 always belong to different families of line ruptures so that $\tau_{f(2)} = -\tau_{f(1)}$. If we take $\tau_{f(1)} = \tau_f$ we must evidently assume τ_f to be of the same sign as r_w.

The sliding velocities u_{f1}, u_{f2} (along the line ruptures), u_{w1}, and u_{w2} (along the wall parts) may be found when r_w, z_r, z (= 2 z_r in Fig. 34G), and the distance n_r from the wall to the rotation point O_w are known. We have evidently at the point C:

$$\begin{aligned} u_n &= u_{f1} \sin(\beta_w - \beta_1) \\ &= -u_{f2} \sin(\beta_2 - \beta_w) \\ &= r_w (z - z_r) \end{aligned} \qquad (3430)$$

to be used in (3417), and:

$$u_{w1} = r_w \left[n_r + (z - z_r) \cot(\beta_w - \beta_1) \right] = r_w n_r + u_n \cot(\beta_w - \beta_1)$$

$$u_{w2} = r_w \left[n_r - (z - z_r) \cot(\beta_2 - \beta_w) \right] = r_w n_r - u_n \cot(\beta_2 - \beta_w) \qquad (3431)$$

Notice that τ_{nt} will always have the same sign as u_w. Therefore, indicating these signs by the two integers e_{t1} and e_{t2} (+1 when the wall slides downwards, and -1 when it slides upwards relative to the clay; and 0 when no sliding occurs), we find that the change indicated by the second last term in (3417) for a change in the position of C (positive upwards) will be:

$$\begin{aligned} -\sum_{cp} \tau_a u_{cp} \frac{\partial L_{cp}}{\partial t_k} &= -c_a \frac{\partial z}{\partial t_k} (-e_{t1} u_{w1} + e_{t2} u_{w2}) \\ &= c_a \frac{\partial z}{\partial t_k} u_n \left[(e_{t1} - e_{t2}) \frac{r_w n_r}{u_n} + e_{t1} \cot(\beta_w - \beta_1) \right. \\ &\quad \left. + e_{t2} \cot(\beta_2 - \beta_w) \right] \end{aligned} \qquad (3432)$$

Evidently $e_{t1} = e_{t2}$ when O_w is outside the interval O_1O_2. If O_w coincides with one of these points e_{t1} or e_{t2} will be zero, but $\frac{r_w n_r}{u_n}$ will be equal to either $-\cot(\beta_w - \beta_1)$ or $\cot(\beta_2 - \beta_w)$. A formula containing only the two last terms could therefore be used generally, except when O_w is between O_1 and O_2 (and $n_r \neq 0$).

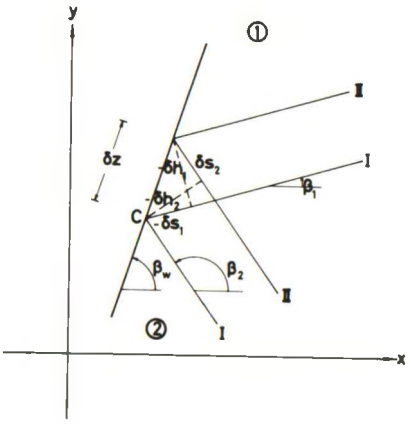

Fig. 34H: Variations of Two Line Ruptures Meeting at a Wall Point C.

Notice that the earth pressure components e and f are internal forces in this respect, doing no work during the movement, cf. (2427), except for the work done by the sliding between the wall and the clay. The only remaining term in (3417) is therefore the second one which can be found from Fig. 34H.

$$\frac{\partial h_1}{\partial t_k} = -\frac{\partial z}{\partial t_k}\sin(\beta_w - \beta_1)$$

$$\frac{\partial s_1}{\partial t_k} = -\frac{\partial z}{\partial t_k}\cos(\beta_w - \beta_1) \qquad (3433)$$

$$\frac{\partial h_2}{\partial t_k} = -\frac{\partial z}{\partial t_k}\sin(\beta_2 - \beta_w)$$

$$\frac{\partial s_2}{\partial t_k} = \frac{\partial z}{\partial t_k}\cos(\beta_2 - \beta_w)$$

Inserting also (3430) we obtain:

$$-\sum_{el} u_f\left(\sigma\frac{\partial h}{\partial t_k} + \tau_f\frac{\partial s}{\partial t_k}\right)$$

$$= u_n\frac{\partial z}{\partial t_k}\left[\sigma_1 - \sigma_2 + \tau_f(\cot(\beta_w - \beta_1) - \cot(\beta_2 - \beta_w))\right] \qquad (3434)$$

$\tau_{f(2)}$ being equal to $-\tau_f$.

Inserting (3432) and (3434) in (3417) we find, finally:

$$\sigma_2 = \sigma_1 + \tau_f\left[\cot(\beta_w - \beta_1) - \cot(\beta_2 - \beta_w)\right]$$

$$+ c_a\left[(e_{t1} - e_{t2})\frac{r_w n_r}{u_n} + e_{t1}\cot(\beta_w - \beta_1) + e_{t2}\cot(\beta_2 - \beta_w)\right] \qquad (3435)$$

If so desired estimates for e_1, f_1, e_2, and f_2 might be obtained by means of (3429) when u_{w1} and u_{w2} are both different from zero. Even if $f_1 \neq f_2$ and/or $e_1 \neq e_2$ the properties pertaining to loading discontinuities on a free surface (Fig. 34 D) do not apply in this case, because the discontinuity is not fixed in space; it moves together with the point C.

If the rotation point O_w for the wall is fixed in the given failure problem the position of the point C will not in fact be moved to find the extreme solution. In such cases (3435) will not be a necessary condition for the use of the equilibrium method, as can be seen from the fact that σ_2 does not enter the projection parallel to the wall of the forces acting upon the rigid body No. 2 in Fig. 34 G. However, if the restraint forces at O_w are required they must be determined by the value of σ_2 given by (3435). By the extremum method they are given by differences in deformation works corresponding to movements of O_w which also will move the point C away from its fixed position.

If there is a rupture zone above the point C (rupture figure AwP in Brinch Hansen's notation) the contributions from the line rupture L_1, and from the sliding between the wall and the rigid body No. 1, will vanish in (3417). On the other hand the last term $\sum_{p,i} \frac{\partial Q^{zp}_{pi}}{\partial t_k}$ will now give a contribution. In this way a formula corresponding to (3420) is obtained, with $\sigma_o = e_1$ and $\tau_o = f_1 = e_{t1}\, c_a$ at the lower point of the rupture zone, but with a corrective term if e_{t2} is different from e_{t1}.

Alternatively (3435) may still be used as it can be seen by comparison with (3420). $\sigma_1 + (\tau_f + c_a\, e_{t1}) \cot (\beta_w - \beta_1)$ is evidently equal to e_1; $\frac{\partial z}{\partial t_k} (e_1\, u_n + c_a\, e_{t1}\, r_w\, n_r)$ is equal to $\sum_{p,i} \frac{\partial Q^{zp}}{\partial t_k}\, w_{pi}$ so this term corresponds exactly to the terms with index 1 in (3435). This is of course a consequence of the fact that all equilibrium conditions are satisfied in the rupture zone.

345 Line Ruptures Meeting in Soil

As shown in Fig. 34 I three line ruptures may meet at an interior point of the clay. In the general case the line ruptures may be denominated and directed as shown in the figure, cf. Fig. 34 J. The clay domain bounded by the numerically greatest angle ($= \pi + \beta_2 - \beta_1$) has the line ruptures L_1 and

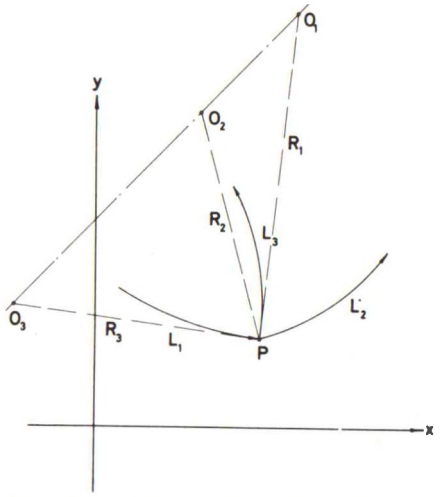

Fig. 34 I: Three Line Ruptures Meeting in the Soil. Circle Arc Centres.

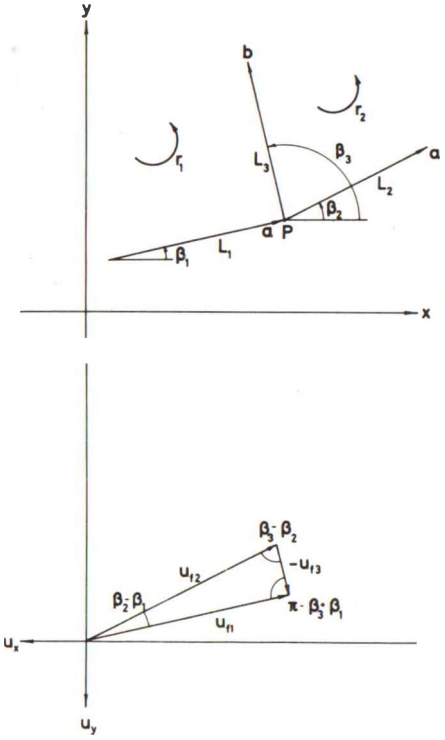

Fig. 34 J: Three Line Ruptures Meeting in the Soil. Velocity Conditions.

L_2 as boundary curve, taken in this order and directed in the negative direction of rotations around the domain. Without loss of generality this rigid body of clay can always be assumed to be at rest. The line rupture L_3 points away from this domain.

In certain cases with two equal angles between $\frac{\pi}{2}$ and π this definition is not unique. It does not matter which one of the two (in a special case even three) possible clay domains is chosen. Even if it is unique the above definition is not the only possible one. The same result is obtained for any choice where

$$\beta_1 - \frac{\pi}{2} \leq \beta_2 \leq \beta_1 + \frac{\pi}{2}$$

$$\beta_2 \leq \beta_3 \leq \beta_2 + \pi \qquad (3436)$$

and

$$\beta_1 \leq \beta_3 \leq \beta_1 + \pi$$

From the figure in the hodograph plane (Fig. 34 J) it is seen that the sliding velocities can be expressed as:

$$u_{f1} = u \sin(\beta_3 - \beta_2)$$

$$u_{f2} = u \sin(\beta_3 - \beta_1) \qquad (3437)$$

$$u_{f3} = -u \sin(\beta_2 - \beta_1)$$

where u is a constant factor of proportionality. We can always take $\tau_{f(1)} = \tau_{f(2)} = \tau_f$; $\tau_{f(3)}$ will then be $+\tau_f$ or $-\tau_f$ according to the sign of u_{f3} relative to the signs of u_{f1} and u_{f2}.

Besides, assuming the rotations r_1 and r_2 for the two rigid bodies above the line L_1L_2 (relative to the third body) we must have at the point P:

$$u_{f1} = r_1 R_1$$

$$u_{f2} = r_2 R_2 \tag{3438}$$

$$u_{f3} = -(r_2 - r_1) R_3$$

the radii of curvature R being defined as $\frac{ds}{d\beta}$ for the orientations shown in Fig. 34J. Inserting (3437) and eliminating the quantities u, r_1, and r_2 we find:

$$\frac{\sin(\beta_3 - \beta_1)}{R_2} = \frac{\sin(\beta_3 - \beta_2)}{R_1} + \frac{\sin(\beta_2 - \beta_1)}{R_3} \tag{3439}$$

This can easily be transformed to an equation of the form:

$$\frac{R_2 \cos\beta_2 - R_3 \cos\beta_3}{R_1 \cos\beta_1 - R_3 \cos\beta_3} = \frac{-(R_2 \sin\beta_2 - R_3 \sin\beta_3)}{-(R_1 \sin\beta_1 - R_3 \sin\beta_3)} \tag{3440}$$

which is evidently the condition that the three centres O_1, O_2, and O_3 shall lie on the same straight line (provided R_1, R_2, and R_3 are all finite), cf. Fig. 34I. As a general rule the coordinates to the centre No. i (i = 1, 2, 3) are:

$$x_i = x_P - R_i \sin\beta_i$$

$$y_i = y_P + R_i \cos\beta_i \tag{3441}$$

The ratio in (3440) is equal to the ratio $\frac{O_2O_3}{O_1O_3}$ which is equal to $\frac{r_1}{r_2}$. If one of the radii is infinite the line will be normal to the corresponding (straight) line rupture.

The stress conditions for the singular point are derived from (3417) in which only the second term is not identically zero, cf. Fig. 34K. Notice that in this case we must find two unknown stress differences, f. inst. $\sigma_1 - \sigma_3$ and $\sigma_3 - \sigma_2$ as against only one in the preceding cases. On the other hand we have two free parameters for the movement of P, f. inst. the distance δa and the angle ψ shown in Fig. 34K corresponding to a change δt_k of parameters, and it is required that (3417) is satisfied for any set of values for these two quantities.

From the sign rules for δs and δh we find by simple geometry:

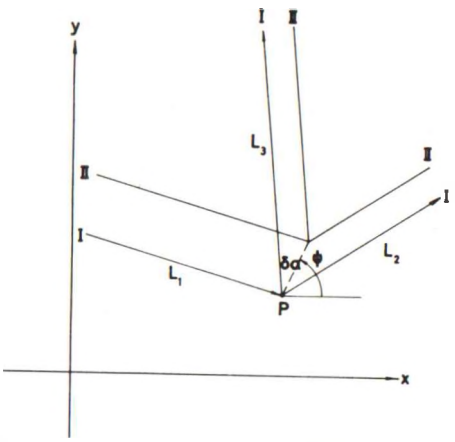

Fig. 34 K: Variations of Three Line Ruptures Meeting in the Soil.

$$\frac{\partial h_1}{\partial t_k} = \frac{\partial a}{\partial t_k} \sin(\psi - \beta_1)$$

$$\frac{\partial s_1}{\partial t_k} = \frac{\partial a}{\partial t_k} \cos(\psi - \beta_1)$$

$$\frac{\partial h_2}{\partial t_k} = -\frac{\partial a}{\partial t_k} \sin(\psi - \beta_2)$$

$$\frac{\partial s_2}{\partial t_k} = -\frac{\partial a}{\partial t_k} \cos(\psi - \beta_2) \qquad (3442)$$

$$\frac{\partial h_3}{\partial t_k} = -\frac{\partial a}{\partial t_k} \sin(\psi - \beta_3)$$

and

$$\frac{\partial s_3}{\partial t_k} = -\frac{\partial a}{\partial t_k} \cos(\psi - \beta_3)$$

Inserting in (3417) we find:

$$-\sum_{el} u_f \left(\sigma \frac{\partial h}{\partial t_k} + \tau_f \frac{\partial s}{\partial t_k}\right) = -u \frac{\partial a}{\partial t_k} \Big[\sigma_1 \sin(\beta_3 - \beta_2) \sin(\psi - \beta_1)$$

$$-\sigma_2 \sin(\beta_3 - \beta_1) \sin(\psi - \beta_2)$$

$$+ \sigma_3 \sin(\beta_2 - \beta_1) \sin(\psi - \beta_3)$$

$$+ \tau_{f(1)} \sin(\beta_3 - \beta_2) \cos(\psi - \beta_1)$$

$$- \tau_{f(2)} \sin(\beta_3 - \beta_1) \cos(\psi - \beta_2)$$

$$+ \tau_{f(3)} \sin(\beta_2 - \beta_1) \cos(\psi - \beta_3) \Big]$$

$$= 0 \qquad (3443)$$

Isolating factors to $\sin\psi$ and $\cos\psi$ respectively and equating to zero we obtain after division with the common factor $-u \frac{\partial a}{\partial t_k}$

$$\sigma_1 \cos\beta_1 \sin(\beta_3 - \beta_2) - \sigma_2 \cos\beta_2 \sin(\beta_3 - \beta_1)$$
$$+ \sigma_3 \cos\beta_3 \sin(\beta_2 - \beta_1)$$
$$+ \tau_{f(1)} \sin\beta_1 \sin(\beta_3 - \beta_2) - \tau_{f(2)} \sin\beta_2 \sin(\beta_3 - \beta_1)$$
$$+ \tau_{f(3)} \sin\beta_3 \sin(\beta_2 - \beta_1) = 0$$

and (3444)

$$\sigma_1 \sin\beta_1 \sin(\beta_3 - \beta_2) - \sigma_2 \sin\beta_2 \sin(\beta_3 - \beta_1)$$
$$+ \sigma_3 \sin\beta_3 \sin(\beta_2 - \beta_1)$$
$$= \tau_{f(1)} \cos\beta_1 \sin(\beta_3 - \beta_2) - \tau_{f(2)} \cos\beta_2 \sin(\beta_3 - \beta_1)$$
$$+ \tau_{f(3)} \cos\beta_3 \sin(\beta_2 - \beta_1)$$

We now use that $\tau_{f(1)} = \tau_{f(2)} = \tau_f$; $\tau_{f(3)}$ is expressed as $e_3 \tau_f$, where e_3 is +1 or -1 according to whether L_3 is of the same family as L_1 and L_2 or not. (3444) can then be contracted to:

$$(\sigma_1 - \sigma_3) \cos\beta_1 \sin(\beta_3 - \beta_2) + (\sigma_3 - \sigma_2) \cos\beta_2 \sin(\beta_3 - \beta_1)$$
$$= \tau_f (1 - e_3) \sin\beta_3 \sin(\beta_2 - \beta_1)$$

and (3445)

$$(\sigma_1 - \sigma_3) \sin\beta_1 \sin(\beta_3 - \beta_2) + (\sigma_3 - \sigma_2) \sin\beta_2 \sin(\beta_3 - \beta_1)$$
$$= -\tau_f (1 - e_3) \cos\beta_3 \sin(\beta_2 - \beta_1)$$

It is seen immediately that if $e_3 = 1$ both right hand sides become identically zero. This means that we must in this case have $\sigma_1 = \sigma_2 = \sigma_3$ unless the determinant

$$D = \sin(\beta_2 - \beta_1) \sin(\beta_3 - \beta_2) \sin(\beta_3 - \beta_1) \quad (3446)$$

is also zero. This may obtain in some special cases (f. inst. $\beta_1 = \beta_2 = \beta_3$ in which case (3437) must be replaced by the condition $u_{f1} = u_{f2} + u_{f3}$) which may be treated separately. As a general rule the assumption that $\sigma_1 = \sigma_2 = \sigma_3$ will evidently always give a solution, however. For the case $\beta_1 = \beta_2$ compare (3420) with $\tau_o = -\tau_f$.

The remaining case, $e_3 = -1$, has the solution:

$$\sigma_1 - \sigma_3 = 2 \tau_f \cot(\beta_3 - \beta_2)$$
$$\sigma_3 - \sigma_2 = -2 \tau_f \cot(\beta_3 - \beta_1) \quad (3447)$$

At the first sight it seems curious that when f. inst. $\beta_3 - \beta_1 = \frac{\pi}{2}$ and $\beta_3 - \beta_2 \neq \frac{\pi}{2}$ we should have $\sigma_2 = \sigma_3$ but $\sigma_1 \neq \sigma_3$, because in this case a rupture zone may be constructed in the wedge between L_1 and L_3, and this would certainly seem to imply that $\sigma_1 = \sigma_3$ (whereas σ_2 might be different).

This argument is a fallacy, however, because a rupture zone is not in fact statically possible in the vicinity of a singularity point as P in Fig. 34 J unless $\beta_3 - \beta_1$ and $\beta_3 - \beta_2$ are both equal to $\frac{\pi}{2}$. Besides, in considering the extreme solution the rupture figure must be considered as a whole, and the introduction of a rupture zone between L_1 and L_3 would give a new rupture figure with another set of parameters and conditions.

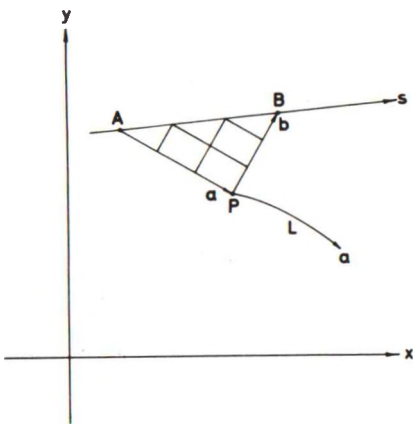

Fig. 34 L: Rupture Zone Continued by a Line Rupture.

Another problem is that a rupture zone, f. inst. a surface zone, may be continued by a line rupture, cf. Fig. 34 L. In the general case this construction is undetermined, however, because for a given position of the line rupture L the singularity point P on L can be moved arbitrarily by a change of the points A and B which define the surface zone. Therefore we must either have the condition that P shall lie on a given curve, fixed arbitrarily or given f. inst. as an internal boundary, or the positions of A and B must also be determined by the extremum condition.

In the first mentioned case σ for the line rupture is found by (3420), regarding the curve as a free surface with surface loadings determined by the known stresses in the zone. In the second case we find that the zone will either contract to a point (i. e. the line rupture intersects the surface), or it will take a position so that P becomes a normal point on the line rupture ($\beta_1 = \beta_2$). Therefore the construction shown in Fig. 34 L need not be considered separately. Except for special cases transition points between line ruptures and rupture zones must be ordinary point.

Example 34 a

The simple bearing capacity problem for a strip foundation on a horizontal clay surface can be solved approximately by simple line ruptures or systems of line ruptures. This has no value in itself since the mathematically correct solution is known (Prandtl's rupture figure Fig. 31 G, Ex. 31 b), but it shows how far a radial zone can be approximated with three line ruptures meeting in the soil.

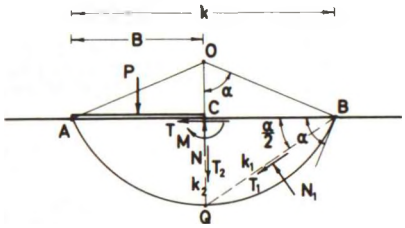

Fig. 34 M: Bearing Capacity Problem Solved by One Circular Line Rupture. Secondary Line Rupture CQ.

The solution with one single line rupture (Fig. 34 M) is very easy to find. It is also rather far off. Since the solution is quasi possible the equilibrium method can be used. Assume the chord AB to be given. The centre angle is then found from the condition that

$$T = ck\, T^Z(\alpha) = ck\,[2\,\alpha \cot \alpha - 1] = 0 \qquad (3448)$$

cf. (3285), Fig. 32 Q. The solution to this equation, that can also be written:

$$\tan \alpha = 2\,\alpha \qquad (3449)$$

is $\alpha = 1.1656 = 66.78^\circ$.

From (3420) we find $\sigma_B = \cot \alpha$ and therefore:

$$N = ck\,[\cot \alpha + 2\,\alpha] = 2.7601\, ck$$
$$M = \frac{1}{2} ck^2 [\alpha - \alpha \cot^2 \alpha + \cot \alpha] = \frac{1}{4} kN \qquad (3450)$$

cf. (3285). The last equation follows from the condition (3448). It is seen that the centre O must be located above the foundation edge C, if the load P is acting centrically ($B = \frac{1}{2} k$).

The unit bearing capacity is thus:

$$\frac{P}{cB} = 2\,\frac{N}{ck} = 5.52 \qquad (3451)$$

which is about 7.5 % on the unsafe side, the mathematically correct value being $\pi + 2 = 5.14$.

It is seen that the stress condition is satisfied at the point A if the foundation is assumed to be uniformly loaded:

$$\frac{P}{cB} = \sigma_A + \cot \alpha = \sigma_B + 4\,\alpha + \cot \alpha = 4\,\alpha + 2 \cot \alpha = 2\,\frac{N}{ck} \qquad (3452)$$

according to (3450). Therefore, the foundation may be replaced by a uniform load on the surface to the left of the point C. Failure may then take place along any number of circular line ruptures, similar about the point C. A continuous, kinematically admissible velocity field may be built up in this way, but it will not form a possible rupture zone, even if ϵ is finite in a certain domain around C. It is seen to be impossible to draw the family of secondary slip lines in such a way that they satisfy the Hencky conditions in the zone. This solution with a continuous velocity field is an example of the solutions with kinematically (but not statically) possible zones mentioned under item IC in Ex. 24e.

The poorness of the estimate (3451) stems from the fact that the rupture figure is not quasi statically possible. The rigid body above the line rupture is found to be unstable when a secondary slip line CQ through the foundation edge is investigated.

By a projection of the forces acting upon the body CQB on the vertical we find:

$$N_1 \cos\frac{\alpha}{2} - T_1 \sin\frac{\alpha}{2}$$

$$= ck_1 \left[(\cot\alpha + \alpha)\cos\frac{\alpha}{2} - (\alpha\cot\frac{\alpha}{2} - 1)\sin\frac{\alpha}{2} \right]$$

$$= ck_1 (\cot\alpha \cos\frac{\alpha}{2} + \sin\frac{\alpha}{2}) \qquad (3453)$$

which is evidently greater than

$$T_2 = ck_1 \sin\frac{\alpha}{2} \qquad (3454)$$

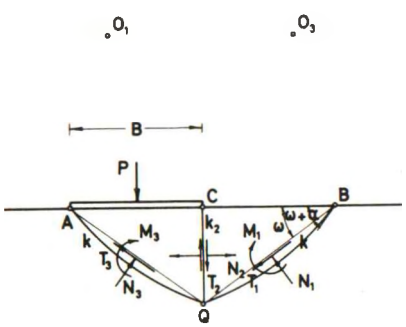

Fig. 34N: Improved Solution With Three Line Ruptures Meeting in the Soil.

A better approximation can therefore be expected if the rupture figure is replaced by one in which three line ruptures meet at the point Q. In principle such a figure has 5 free parameters, but in this case it is easy to show that it must be symmetrical about the vertical through C. It has then only two parameters, ω and α, cf. Fig. 34N.

From (3420) and (3447) we find:

$$\sigma_B = c \cot(\omega + \alpha)$$

and at the point Q:

$$\sigma_{Q(1)} = \sigma_B + 4\,c\,\alpha$$

$$\sigma_{Q(2)} = \sigma_{Q(1)} + 2\,c\tan(\omega - \alpha) \tag{3455}$$

$$\sigma_{Q(3)} = \sigma_{Q(1)} + 4\,c\tan(\omega - \alpha)$$

The parameters ω and α, and the unit bearing capacity $\frac{P}{cB}$ should be found by the conditions that all three equilibrium equations must be satisfied for both rigid bodies of clay.

The moment equation about the middle point of the chord $k_1 = k$ gives:

$$M_1 = ck^2 M^z(\alpha) = \tfrac{1}{2}\,k\cos\omega\,T_2 = \tfrac{1}{2}\,ck^2\sin\omega\cos\omega \tag{3456}$$

that is:

$$M^z(\alpha) = \tfrac{1}{2}\sin\omega\cos\omega \tag{3457}$$

This also satisfies the moment equation for the second rigid body (below the foundation), if P is assumed to act centrically.

The horizontal projection for the first rigid body gives:

$$N_1\sin\omega + T_1\cos\omega = N_2$$

or

$$ck\left[(\cot(\omega + \alpha) + 2\,\alpha)\sin\omega + T^z(\alpha)\cos\omega\right] \tag{3458}$$

$$= ck\sin\omega\left[\cot(\omega + \alpha) + 4\,\alpha + 2\tan(\omega - \alpha)\right]$$

which can be written:

$$T^z(\alpha)\cos\omega = 2\sin\omega\left[\alpha + \tan(\omega - \alpha)\right] \tag{3459}$$

The horizontal projection for the second rigid body turns out to give the same equation.

Finally, the vertical projection for the first rigid body gives:

$$N_1\cos\omega - T_1\sin\omega = T_2 \tag{3460}$$

which can be reduced to:

$$\left[1 + T^z(\alpha)\right]\sin\omega = \cos\omega\left[\cot(\omega + \alpha) + 2\,\alpha\right] \tag{3461}$$

By trial and error ω can be estimated after which α is found from (3457). The correct value of ω satisfies both of the equations (3459) and (3461). This can be shown by rather laborious transformations, but since the calculations must be performed numerically it is simpler in practice to check this point directly.

The unit bearing capacity is found in the simplest way by the vertical equilibrium condition for the entire domain above the boundary slip line AQB:

$$\frac{P}{cB} = \frac{k}{B}\left[(N_1 + N_3)\cos\omega\right]$$

$$= \left[\cot(\omega + \alpha) + 2\alpha\right] + \left[\cot(\omega + \alpha) + 4\alpha + 4\tan(\omega - \alpha) + 2\alpha\right]$$

$$= 2\cot(\omega + \alpha) + 8\alpha + 4\tan(\omega - \alpha) \qquad (3462)$$

This is seen to satisfy also the stress condition at the point A when (3429) is used. The foundation may therefore again be replaced by a constant load to the left of C, and a kinematically admissible velocity field with finite values of ϵ (except along the line CQ and possibly also along the boundary slip line AQB) may be defined. It corresponds to a kinematically, but not statically possible zone.

The result of the calculations according to the equations (3457), (3459), (3461), and (3462) is:

$$\omega = 35.85^\circ$$

$$\alpha = 20.58^\circ \qquad (3463)$$

$$\frac{P}{cB} = 5.29$$

which is about 3 % on the unsafe side.

The approximation could be further improved by the introduction of more branch points (symmetrically situated about the vertical through C). However, the result (3463) seems to be accurate enough for all practical purposes; except, possibly, when a horizontal internal boundary is situated somewhat below the clay surface. In this case it might be necessary to use a rupture figure with two branch points instead of one.

4 RUPTURE FIGURES

This chapter deals with the problem of calculating a solution, specified by a given rupture figure type applied to a given failure problem, assuming the solution to be admissible with possible zones.

As explained in the preceding chapters the main problem consists in the calculation of the rupture zones. By changing the parameters of the zones the solution is made to agree with the conditions of the failure problem by means of the energy method. If the solution is quasi possible the equilibrium method can be used as an alternative. In possible solutions all boundary conditions can be satisfied exactly, so the special stress conditions for line ruptures are not necessary.

Since the rupture zones are the most important elements of the rupture figure, the different rupture figure types can be classified according to the complexity of the principal rupture zone. The sections in this chapter deals with rupture figures of increasing difficulty, starting with the simple types built up of line ruptures and statically determined rupture zones, and ending with rather complex open zones with mixed boundary conditions.

In the final sections some special problems are considered, the most important being the determination of limiting states of stress in the rigid bodies of clay, and the investigation of whether a given rupture figure is statically possible or not. These two problems are closely connected to the more general problem of rupture figure complexes. Finally rupture zones with approximate movement conditions are discussed.

41 GENERAL INTRODUCTION

411 Rupture Figure Types

A rupture figure type is a partitioning of a clay domain into rigid bodies of clay separated by rupture zones and line ruptures. It may be represented by means of a sketch in the x,y-plane, or, more concisely, by a figure in the λ,μ-plane. In practice other conventions may also be used, f. inst. a string of letter symbols as in Brinch Hansen's notation, or a purely numerical representation which can be read by a computer.

A calculation procedure can in principle be defined on this basis since the following purely mathematical operations can be performed.

1. The number and kinds of numerical parameters which define the rupture figure are ascertained.
2. It is checked that all rupture zones are determinable, i.e. that a complete (necessary and sufficient) set of boundary conditions exists, that the whole rupture figure is geometrically determined, and that all movements and forces can be calculated from the assumed boundary conditions.
3. The extra (geometrical and stress) conditions implied by the rupture figure in order to avoid inconsistencies are also ascertained.

These points are independent of the failure problem to which the rupture figure shall be applied. However, in practice, the formulation of the actual procedure to follow in each case must be made dependent on the parameters of the problem. This will frequently also determine the choice of initial parameters and the order in which they are used, at least when the economy in calculations is important in relation to simplicity in the formulation of procedures. In computer programs it may be an advantage to have a simple and straightforward procedure without too many special cases, even if this in some cases means a little more computer time than is strictly necessary, but the calculation economy will nevertheless usually be important as it certainly is in calculations by hand.

Therefore, in the following it is assumed that a failure problem is known, and a rupture figure type has been chosen as a solution to this pro-

blem. It is then possible to treat as special cases rupture figure types which can be calculated in a simple way because they are used in simple failure problems. A rough classification in the order of increasing complexity may be given as follows.

A. Simply determined rupture figures, whose rupture zones can be calculated in one closed operation.

1. Statically determined rupture zones (no internal parameters).

a. Surface zones, possibly continued through radial zones and wall zones until contact with one or two external rigid bodies (simple earth pressures and squeezing between two walls).

b. Surface zones continued from two different surfaces to contact at a transition point under an external rigid body, possibly with squeezing because of other (unmoving) rigid bodies (punching, bearing capacity).

c. The general case with several surfaces and external rigid bodies (interacting foundations).

2. Combinations with line ruptures (introducing movement parameters in a simple way).

a. Pure line ruptures and systems of line ruptures (no rupture zones).

b. Line ruptures connecting one external rigid body to a, possibly continued, surface zone (the types LaZ and LfZ in Brinch Hansen's notation).

c. The general case with systems of line ruptures connected to general statically determined zones.

3. Special cases with more complicated rupture figures applied to simple failure problems.

a. Connections between statically determined rupture zones, line ruptures, and simple (circular) arc zones.

b. Connections with simple radial zones (straight radial slip lines). Slidings along circular or radial slip lines.

c. Kinematically determined rupture zones.

B. Rupture figures containing zones with mixed boundary conditions.

1. Closed rupture zones (only connected by line ruptures to surface zones).
   a. Single radial zones with curved radial slip lines, and closed rectangle zones.
   b. Multiple radial zones and rectangle zones.
   c. Closed radial zones continued by wall zones.
   d. (A transitional case): Closed rupture zones connected by circular arc zones to simple surface zones.
2. Open rupture zones, directly connected to surface zones.
   a. General arc zones.
   b. More complex combinations, including free rigid bodies of clay.

Special problems may be encountered when two or more rupture figures are developed simultaneously. In order to satisfy all movement and equilibrium conditions of the failure problem it may in such cases be necessary to calculate the rupture figure complex as a whole, although the individual rupture figures may be separated.

Since a general program, which is able to calculate any given rupture figure applied to any given failure problem, can hardly be conceived, a general convention for reading rupture figures into a computer (by means of a sort of input data sheet) will not have any great use. In practice the following two types of more general computer programs might be useful.

1. Programs which are able to calculate one given class of rupture figure types applied to different types of failure problems. The calculation procedures may be more or less specialized, so the limitations of the permissible failure problems may be more or less severe. The input data for such programs are problem parameters, and possibly also some data limiting or regulating the choice between the rupture figures covered by the program (f. inst. a first estimate on the rupture figure and the values of its initial parameters).

   As examples the following rupture figures and failure problems might be considered.

   a. Statically determined rupture zones, and combinations of such zones to be used on zone ruptures in earth pressure and bearing

capacity theory, including problems with interacting walls and foundations, and squeezing.

b. Single line ruptures or systems of line ruptures to be used on stability investigations, earth pressure problems (with rigid walls) and combined problems of earth pressures and stability.

c. Combinations of line ruptures, and simple arc zones, surface zones, radial zones, and wall zones to be used on a class of earth pressure and bearing capacity problems with one wall and one (f. inst. straight and uniformly loaded) surface.

2. Programs which are able to solve a given class of failure problems, choosing between (possibly constructing itself) different types of rupture figures. For example:

a. Sheet pile walls, possibly with yield hinges, and possibly including design of the wall.

b. Foundations, possibly in shallow depths and with inclined and excentric loads.

Compared with the programs under 1 above these programs have a shorter range of problems (identified in the input data by a set of simple variables), but a wider range of rupture figure types.

The difference between the two types of programs is mostly one of points of view. The contents of Chap. 4 corresponds to the type No. 1 above (the solutions that can be obtained by a given rupture figure type), whereas the problem of constructing solutions to a given failure problem is considered in Chap. 5.

412 Numerical Calculations

The numerical calculation of a given rupture figure applied as a solution to a given failure problem is assumed to be performed by the method of admissible solutions with possible zones, using either the energy method or the equilibrium method as explained in Sec. 244-6.

By the calculation of the rupture zones one of the methods indicated in Sec. 32 is used. Thus, one may use continuous functions, either the equivalent coordinates $\overline{x}$, $\overline{y}$, u, and v or the radii of curvature R, S, F, and G calculated by means of Riemann integration or by the method of finite differences, or he may use the method of chord lengths (the complete formulae of

Sec. 325 and 331-8 for large calculations, and simpler formulae based on direct geometrical reasoning in simpler problems).

As a general rule, when exact solutions cannot be obtained, the method of chord lengths will always give the simplest calculations. Consequently most weight has been placed on this method in the following sections. If for some reason it is desired to use continuous functions the equivalent coordinates will be the most generally useful, and will also give the simplest calculations except for closed rupture zones. In this case the radii of curvature are specially suited. They may also be used in other cases, but they are not so simple, especially when wall zones are present, or when other types of geometrical conditions must be satisfied.

The method of finite differences is the most widely useful method, but it is not as a rule suited to the calculation of zones with mixed boundary conditions. Closed rupture zones can be calculated by means of Riemann integration, which can also be used as a check in other cases, but open rupture zones with mixed boundary conditions are difficult to calculate by means of continuous functions whatever method is used.

Apart from the idealization of the original (physical) failure problem, the estimate of the loadings that will become actual, and the determination of the shear strengths, all of which are outside the scope of the present work, all calculations contain the following sources of error:

1. Choice of rupture figure.
2. Maximum step lengths (or centre angles) used in the calculations.
3. Accuracy of iterations to find the extreme solution or to satisfy the movement and/or equilibrium conditions.
4. Round off errors during the calculations.

The factor No. 1 is a consequence of the fact that the method of admissible solutions permits the same failure problem to be solved by a number of different, more or less correct approximations. No. 2, 3, and 4 must be decided upon before the calculations are started. Notice that the characteristic point in using the method of chord lengths is that because of the greater accuracy of the method good numerical results can be obtained by larger step lengths than with the other methods.

It is clear that the calculations in any given case should be planned so that the four sources of error mentioned above are balanced in a reasonable way, and give a reasonable overall economy of the calculations. In order that it shall be possible to check the results numerically the round off er-

rors should always be small. This is easily obtained by taking one or two more figures in the calculations than are needed in the result (by calculations by hand). It is usually also relatively easy to bring down the errors of iteration to a sufficiently small amount. In order to obtain a unique calculation result which can easily be checked this should also be done whenever possible, at least when the equilibrium method is used.

It is more difficult to adjust the influence of the two first mentioned sources of error. The influence of the maximum step length on the calculation work is relatively unimportant for statically determined zones. For closed rupture zones with mixed boundary conditions the influence is greater, but still the number of circle arcs along the zone boundaries is not as important as the number of initial parameters in the rupture figure. In open rupture zones each circle arc will in principle contribute one initial parameter. Of course, all initial parameters do not contribute by the same amount to the calculation work, and the value of the maximum centre angle is more critical in some rupture zones than in other, so a general rule which is strictly valid in all cases cannot be obtained.

However, as a rough approximation we find that in statically determined rupture zones the maximum centre angle should be taken small enough so that all important zone elements are distinguished, and the calculation error is relatively small. Zone elements, i.e. rectangular or triangular zone parts with continuous radii of curvature, should also be distinguished in closed and in open rupture zones with mixed boundary conditions, but in this case it is rarely justified to take more divisions along the zone boundaries than are absolutely necessary for this purpose. Thus, boundaries to zone elements should be single circle arcs unless one of the following cases apply.

1. The rupture zone is statically determined.
2. The variation in R (or S) along the zone boundary is very steep.
3. The rupture figure is possible, or at least quasi possible, and a very high accuracy is needed.

This result is used in the following sections. The problem of choosing rupture figures is discussed in Chap. 5.

Calculation formulae for a given rupture figure are frequently expressed in the form where the shear strength c is replaced by a failure stress τ_f. Conjugate solutions corresponding to failure problems with the same geometry and movement conditions, but with the signs reversed on all known

loadings and all prescribed movement rates d_r, may then be obtained simply by inserting $\tau_f = c$ or $\tau_f = -c$.

42 SIMPLY DETERMINED RUPTURE FIGURES

421 Statically Determined Rupture Zones

Surface (or Rankine) zones are generated from free surfaces as explained in Sec. 331. In Sec. 332 it is shown how surface zones are continued by means of radial zones. A further continuation by wall zones is shown in Sec. 336.

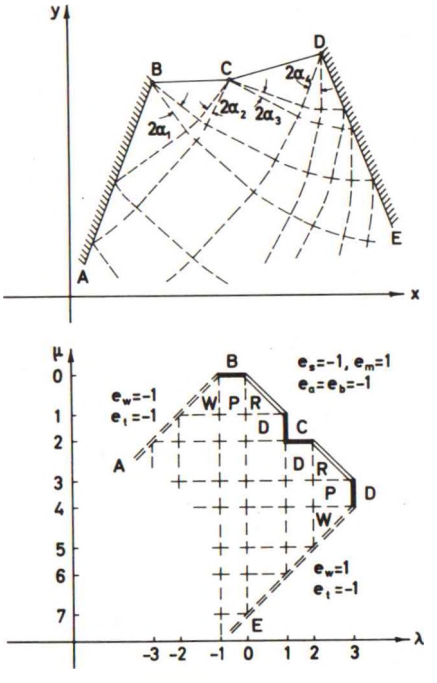

Fig. 42 A: Surface Zones Continued by Radial Zones and Wall Zones.

A surface zone, possibly containing radial zones at corner points of the surface, and possibly continued at one or both of the end points of the free surface by a radial zone and possibly also a wall zone, is a statically determined rupture zone. It is completely determined by two parameters, cf. Fig. 42 A which shows a fairly general example.

When the indicators e_s, e_m (or e_a, e_b), and e_t for any wall which is in contact with the rupture zone, have been determined, the centre angles $\alpha_1, \ldots, \alpha_4$ for all radial zones are given uniquely. The full rupture zone can then be constructed as far as the walls permit. It is seen to consist of a pattern of rectangular and triangular zone elements, obtained by continuing the primary Rankine (R), Prandtl (P), and

wall (W) zones which are determined directly by the conditions at the surface and the walls. The pattern may be described as a network of radial zones which are reflected from the walls, with meshes consisting of triangular surface zones and wall zones, and of rectangle zones.

If one of the centre angles shown in Fig. 42 A becomes negative, the rupture zone can only be continued through the corresponding point as a statically determined zone if a discontinuity line is used. It will be reflected from the wall in much the same way as are the radial zones, but the rupture figure will certainly not be kinematically possible.

In some cases a wall zone need not start as in the points B and D of Fig. 42 A. Provided that the external rigid body is perfectly rough ($c_a = c$), or that we have an internal boundary to a clay domain with a sufficiently high shear strength, it may be contacted by a boundary slip line of the rupture zone in a point which is not a surface point, cf. Fig. 42 B. In this figure the extension of the rupture zone to the right is limited by the contact point T. Beyond this point, along the part TD the clay remains rigid however far down the wall BA is continued. Like all other perfectly rough boundaries the part TE may be an envelope of slip lines (being convex to the boundary) or may coincide with a slip line (with the same radius of curvature as the boundary). If the slip line is concave to the boundary a rigid body of clay will remain between TE and the rupture zone.

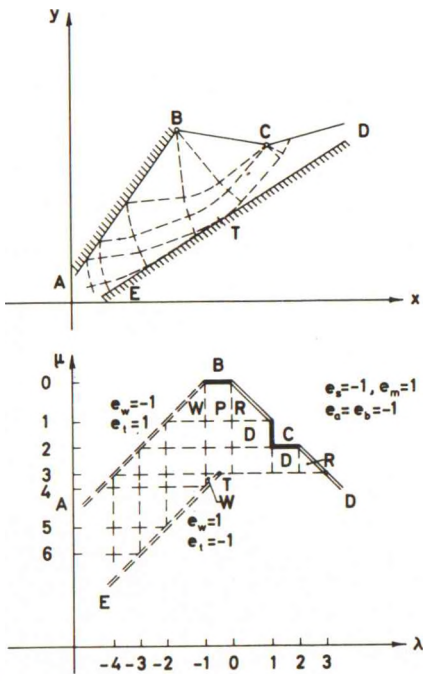

Fig. 42 B: Squeezing Zones Below the Contact Point T.

In practice the full zone will frequently not be needed. If the slip lines forming the zone element boundaries are characterized by integer values of λ and μ as shown in Fig. 42 A and B, beginning at the first point (in the positive direction of s) of the free surface, the following convention may be used:

1. Along parts of the free surface λ and μ are interpolated linearly in relation to s.

2. Along degenerate slip lines (in vertex points) λ or μ is interpolated linearly in relation to m.

3. Along parts of boundaries to rigid bodies $|\Delta\lambda| = |\Delta\mu|$ in each unit triangle cell.

This defines a set (λ, μ) for all points in the rupture zone. Any (possibly continued) surface zone may be characterized by the set (λ_P, μ_P) corresponding to its end point P (i.e. the zone is limited by the a- and b-line through the point P).

As a more qualitative indication one may give a letter string enumerating the types of zone elements bounding the rupture zone (taken in the order of increasing values of s). Thus

1. R indicates a pure surface zone. End point in Fig. 42 A f. inst. (0.2, 0.8), (2.2, 2.8), or (0.2, 2.8) when one does not wish to emphasize that there are radial zones inside the Rankine zone. (If this is required the last mentioned rupture zone might be termed RDR, the letter D being used instead of P to distinguish a radial zone under a surface discontinuity from a radial zone between a surface zone and a wall zone).

2. PR, DR, RP, or RD is a Rankine zone continued by a radial zone. F. inst. (-0.5, 0.5), (0.4, 1.5) or (1.5, 2.5). Correspondingly PRD or PRP (-0.4, 1.6) or (-0.4, 3.5).

3. WPR, WPRD, WPRP, and WPRPW are surface zones continued by both radial zones and wall zones. F. inst. (-1.5, 0.5), (-1.5, 1.5 or 3.5), and (-2.5, 5.5).

4. Squeezing may be indicated by the letter s; thus WPRsW (-2.6, 4.2) in Fig. 42 B. Types on the form PRsW etc. are also possible.

When a set (λ_P, μ_P) is given the rupture zone ending in this point can easily be calculated by means of the methods indicated in Chap. 3. If continuous functions are used, f. inst. the equivalent coordinates $\bar{x}, \bar{y}$, the initial points on the surface may be placed so that the boundary slip lines for the rupture zone intersect the surface, possibly after one or more reflections from walls, in two known points. Alternatively a fixed spacing may be used on the surface, independent of λ_P and μ_P. The rupture zone is then calculated until and including the cell in which P is located, after which the boundary slip lines may be found by interpolation.

By the method of chord lengths neither procedure is quite satisfactory. In the first case, where the boundary slip lines are calculated in their full

lengths through all reflections up to the surface, a relatively large number of cells with irregular centre angles may have to be calculated. On the other hand, direct interpolation in the boundary cells is difficult, linear interpolation being normally too inaccurate.

As a compromise one may calculate the rupture zone up to, but not including the cell containing the end point P with a fixed spacing determined by the zone element boundaries, possibly with subdivisions of the zone elements dependent on the maximum permissible centre angle. The boundary slip lines are then calculated by two special strips of cells ending at P and starting at the nearest reflection points on walls, or at surface points if no reflections are present. In the latter case the initial cells are perfectly normal, but in the former case they must be determined by a linear interpolation along the first circle arc of the neighbouring slip lines; cf. Fig. 42 C where the boundary cells with fractional centre angles are indicated by dotted lines. The point Q is obtained by a linear interpolation in μ along the circle arc AB. AQR is calculated as a normal wall cell from the known arc AQ. The surface cell CDE is perfectly normal, since the point E can be found when μ_P is known.

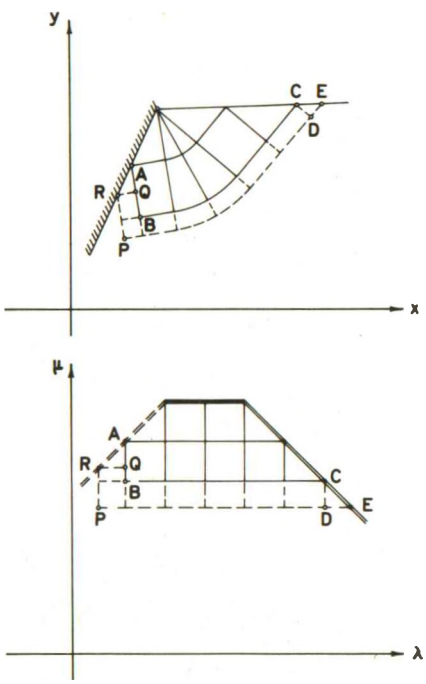

Fig. 42C: Extrapolation to the Point P by Fractional Net Spacings.

Surface zones obtain in a great number of rupture figures. For each zone the two parameters λ_P, μ_P are initial parameters for the rupture figure. They are frequently expressed in another way, however, f.inst. as values of s for the corresponding surface points. In simple rupture figures, f.inst. with straight slip lines in the surface zones, even simpler representations may be used. Thus, the abscissa of P and its depth below the surface might represent the zone, or the parameters may not be used explicitly, but may be coupled directly to the external conditions. For example, in rupture figures with closed rupture zones such zones are frequently calculated first, and are made to conform to the external movement conditions. After this the surface

zones are determined by the condition that P shall be located on known line ruptures, the boundary slip lines being tangent and normal to these circle arcs.

Surface zones may overlap if they are generated by the same free surface, and have the same values of e_a and e_b. Overlapping surface zones are calculated as one zone, but with more end points P, each point contributing with two parameters to the rupture figure.

Statically determined rupture figures are composed solely of surface zones. They are used under the following conditions.

1. The boundary of the clay material consists of free surfaces alternating with boundaries to external rigid bodies. The domain in failure may further be limited by rigid bodies or internal boundaries inside the clay material.

2. The movements of the external rigid bodies (possibly with affixed clay bodies) relative to the surrounding rupture zones must all be in the same direction. If all (moving) rigid bodies are pressed into the clay, all surface zones will be in the passive state, and the failure problem (strictly speaking: the role of the clay material during the failure) is said to be passive. Correspondingly we have an active failure when all rigid bodies are pulled away relative to the surrounding rupture zones (or are yielding under the forces transmitted through the zones from the surface loadings or volume forces). All surface zones will then be in an active state of failure. If there are zones in contact with the boundaries to rigid bodies, they will be in the opposite state of the surface zones.

3. The part of the rupture figure which is in contact with each external rigid body (possibly through an affixed clay body) may be one-sided or two-sided. Bodies with one-sided rupture zones (walls, at the extreme ends of the rupture figure) must have their rotation points in certain domains of the plane. Bodies with two-sided rupture zones (foundations, inside the rupture figure), which are connected to the unmoving clay body through transition points, must usually be translated, and normally with the translation vector inside a certain angular sector. Thus, if there are more than one external rigid body, they must normally be supposed to be interconnected in some way. As the force resultants on all rigid bodies are statically determined, the failure problem must generally be one of controlled strain, with a sufficient number of restraints satis-

fying the above conditions. Controlled stress is only possible if all specified force components have the correct magnitudes relative to each other.

4. Even if the above conditions are satisfied the rupture figure may become geometrically impossible f. inst. because of extruding corners or loading discontinuities. Discontinuity lines may then be used, but the solution will not in this case be kinematically possible. It will also not be kinematically possible if ϵ for some reason becomes negative anywhere in the rupture zones. This will happen especially if the above mentioned movement conditions are neglected (but then the rupture figure will rapidly become too much on the safe side).
5. It needs a special investigation to ascertain that the solution is also statically possible, cf. Sec. 442.

If the rupture figure is generated from more than one free surface, surface zones from two adjacent surfaces being connected by transition points under the rigid body which separates them, care should be taken that m according to (3304) is chosen for each surface so that the zones are compatible. This is obtained if one, when passing from one free surface to the next one in the positive direction of s, changes the signs of e_a and e_b, and adds π to m_t (i.e. increases p with 1).

The surface zones in such rupture figures may have three kinds of end points, the simplest possible examples of which are shown on Fig. 42 D.

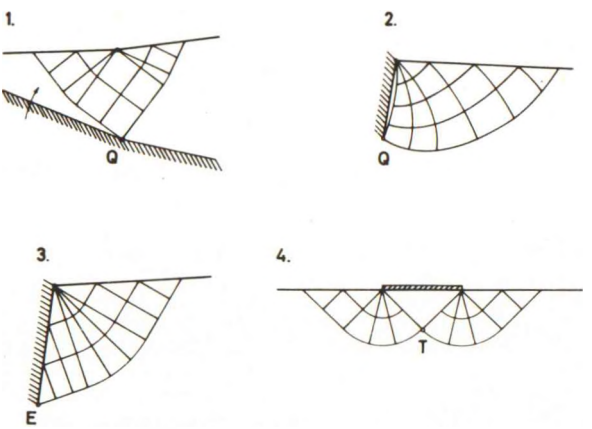

Fig. 42 D: End Points for Statically Determined Zones.

1. Points with a known position (Q), which may obtain as hinges between boundary parts to external rigid bodies, or as foot points of walls, when the boundary slip lines are concave to the walls.

2. End points (E), which may obtain as foot points of walls with normal wall zones. Only one parameter is ever used explicitly (and only as a substitute for an external, f. inst. a design, parameter). This is because the rupture zone can be calculated by strips of cells, starting at the intersection point between the wall and the surface. The parameter may f. inst. be the arc length from this point to the first point of the boundary slip line.

3. Transition points (T) between two surface zones on each side of a rigid body. The point must correspond to the same values of a and b (i. e. to m and σ) in the two zones, which determines (λ_T, μ_T) in one zone when they are chosen in the other. There are, therefore two parameters to be determined by the conditions that x and y shall also coincide.

If failure obtains by squeezing the clay material between two walls a combined surface zone with two end points E (or one E and one Q, or possibly two points Q) is developed. Similarly the last example shown in Fig. 42 D may be combined with one or two walls, unmoving so that the surface zones are constrained, or moving into the clay so that two or three end points (E, T, and E) are obtained. In fact any number of rigid bodies may be combined in this way, the intermediate ones being of the type 'foundations' (two-sided rupture zones with transition points), and the extreme ones of the type 'walls' (one-sided rupture zones with end points E or Q). Any one of the zones may be modified by the existence of a squeezing zone (cf. Fig. 42 B), or by further points of the type Q.

In this way very complicated rupture figures may obtain, so that even quite complex failure problems can be solved, provided that they satisfy the conditions listed above. Being statically determined the rupture figures can be calculated by a relatively simple routine (even for materials with much more general properties at failure than are considered in the present work). This explains the fact that until recently they have been the only type of rupture figures studied by the theory of plasticity.

Example 42 a

The conditions imposed on the failure problem by the assumption of a statically determined rupture figure may be illustrated by means of the clas-

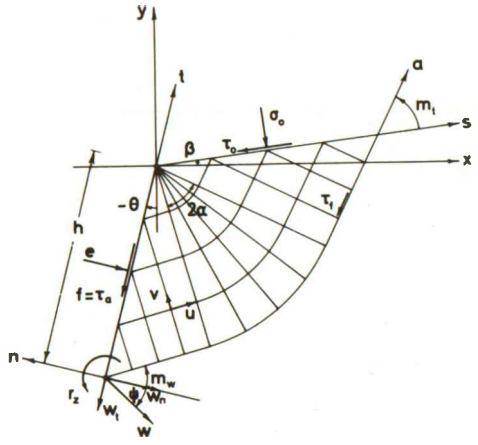

Fig. 42E: Zone Rupture (WPR) Behind a Retaining Wall.

sical Prandtl rupture figure for earth pressures, cf. Fig. 42E.

For simplicity a straight wall is assumed, with the adhesion strength c_a and the inclination θ with the vertical, retaining a clay domain with a straight surface, uniformly loaded and forming the angle β with the horizon. θ and β are positive in the positive direction of rotations. The load components are σ_o and τ_o as usual. As a first approximation the unit weight of the clay is neglected.

The above data determine completely the rupture figure, and consequently the earth pressure components e and f, when the indicators $e_f = e_a\, e_b$ and e_t are chosen. In order to be able to treat all four possible combinations of these two numbers in one operation, the failure problem is formally treated as one with $e_f = e_t = 1$, cf. Fig. 42E, but with the failure stresses

$$\tau_f = e_f\, c \tag{4201}$$

and the shear stress along the wall:

$$\tau_{nt} = \tau_a = e_t\, c_a \tag{4202}$$

Thus, in the active case ($e_f = -1$) the shear strength is taken as negative, and the boundary slip line is considered as an a-line, although it is then really a b-line. The work equation is still valid, however, because the deformation condition is now that $\epsilon \leq 0$. More generally:

$$e_f\, \epsilon \geq 0 \tag{4203}$$

This condition puts some restraints on the admissible values of the movement components w_t, w_n, r_z for the wall. These components are measured in relation to a t,n-coordinate system with origin at the foot point of the wall.

If the rotation r_z is known to be different from zero one may alternatively express the movement of the wall by the coordinates t_o, n_o to the rotation center for the wall. In a dimensionless form:

$$\rho = \frac{t_o}{h} = \frac{w_n}{r_z h}$$
$$\lambda = \frac{n_o}{h} = -\frac{w_t}{r_z h} \tag{4204}$$

Since all three movement components can be multiplied with a common factor of proportionality, without changing the failure problem, there are in fact only two independent movement parameters, as indicated by (4204). However, ρ and λ cannot be used if $r_z = 0$, at least not if w_n and w_t are both different from zero (translation in a given direction).

The geometry of the rupture figure is given by the relations:

$$m_t = \text{arc tan} \sqrt{\frac{\tau_f + \tau_o}{\tau_f - \tau_o}} \tag{4205}$$

and

$$m_w = \text{arc tan} \sqrt{\frac{\tau_f - \tau_a}{\tau_f + \tau_a}} \tag{4206}$$

The intervals $0 \leq m_t \leq \frac{\pi}{2}$ and $0 \leq m_w \leq \frac{\pi}{2}$ ($0 \leq m_w \leq \frac{\pi}{4}$ if $e_f e_t = 1$, and $\frac{\pi}{4} \leq m_w \leq \frac{\pi}{2}$ if $e_f e_t = -1$) can always be chosen. The centre angle of the radial zone is given by

$$\alpha = \frac{1}{2} (\beta - \theta + m_t - m_w) \tag{4207}$$

If $\alpha < 0$ the rupture figure is not geometrically possible. Assuming in the first place $\alpha \geq 0$ the earth pressure components are found to be:

$$e = \sigma_o + \tau_f (\sin 2 m_t + \sin 2 m_w + 4 \alpha)$$
$$= \sigma_o + e_f c \left[\sin 2 m_t + \sin 2 m_w + \sigma^z(\alpha) \right] \tag{4208}$$
$$f = \tau_a = e_t c_a$$

using Brinch Hansen's notation [1957].

Defining the velocity components u and v as usual (for $e_f = 1$, but using the same components when $e_f = -1$), we find that

$$v = 0 \tag{4209}$$

everywhere in the zone. u is constant along any a-line. It is found by the condition that it must correspond to the known normal component of the wall movement. The velocity components for a point on the wall at the distance t from the foot point are:

$$u_n = w_n - tr_z$$
$$u_t = w_t \tag{4210}$$

From this we find:

$$u = u_n \sec m_w$$
$$= (w_n - tr_z) \sec m_w$$
$$= r_z h (\rho - \frac{t}{h}) \sec m_w \tag{4211}$$

according to (4204). We have also the sliding velocity:

$$u_s = u_t + u \sin m_w$$
$$= w_t + (w_n - tr_z) \tan m_w$$
$$= r_z h \left[- \lambda + (\rho - \frac{t}{h}) \tan m_w \right] \tag{4212}$$

The condition that the unit deformation work shall be positive everywhere can in this case be separated into three specific demands:

1. In the rupture zones ϵ must have the same sign as τ_f. In the Rankine zone and the wall zone this gives:

   $$e_f \frac{\partial u}{\partial s_b} = e_f \frac{\partial u}{\partial t} \sec m_w = -e_f r_z \sec^2 m_w \geq 0$$

   or:

   $$e_f r_z \leq 0 \tag{4213}$$

   For the radial zone $e_f u \frac{\partial m}{\partial s_a} = e_f \frac{u}{(h - t) \cos m_w}$ must be added to the left hand side of the first Eq. (4213). This quantity (which is infinite when t = h) has always the same sign as e_f, compare the following condition No. 2, so (4213) represents the strongest restriction.

   Thus, r_z must be negative for passive, and positive for active earth pressures.

2. Along the boundary slip line (corresponding to t = 0) u must have the same sign as τ_f, i.e. $e_f r_z h \rho \sec m_w \geq 0$, or, using also (4213):

   $$\rho \leq 0 \tag{4214}$$

3. u_s must have the same sign as e_t along the whole height of the wall, i.e.

$$e_t\, hr_z \left[-\lambda + (\rho - \frac{t}{h}) \tan m_w \right] \geq 0$$

using also (4213) this is found to be equivalent to:

$$e_f\, e_t \left[-\lambda + (\rho - \frac{t}{h}) \tan m_w \right] \leq 0 \qquad (4215)$$

a. For $e_f\, e_t = 1$ the maximum value (for the interval $0 \leq t \leq h$) is obtained for $t = 0$. In this case, therefore:

$$\lambda \geq \rho \tan m_w \qquad (4216)$$

b. For $e_f\, e_t = -1$ the maximum value is obtained for $t = h$. In this case:

$$\lambda \leq (\rho - 1) \tan m_w \qquad (4217)$$

The conditions (4214) and (4216-7) indicate the domains in the x,y-plane in which the rotation centre for the wall must be located in order that the statically determined zone rupture shall be kinematically possible. They are shown with full lines (marked 1) on Fig. 42 F. The angle i_w on this figure is defined by the equation

$$i_w = \text{arc tan} \sqrt{\frac{c - c_a}{c + c_a}} \qquad (4218)$$

where c and c_a are always positive ($0 \leq i_w \leq \frac{\pi}{4}$).

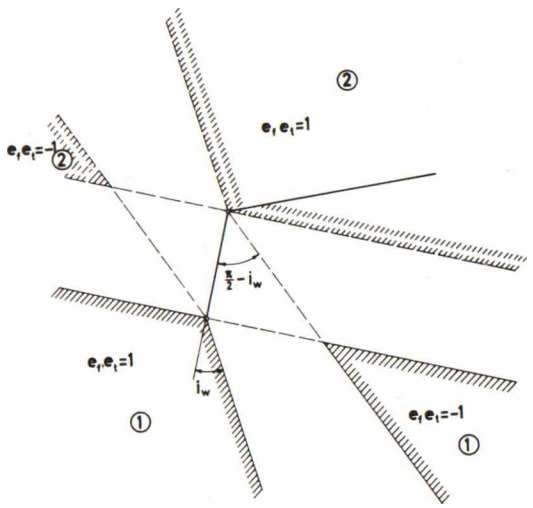

Fig. 42 F: Admissible Rotation Points for a Wall with a Zone Rupture WPR.

A pure translation ($r_z = 0$) may be defined by means of w_n and w_t alone, or by the resulting movement vector w (always positive) and the direction ψ defined by the equations:

$$w_n = w \cos \psi$$
$$w_y = w \sin \psi \tag{4219}$$

The condition (4213) is satisfied identically. The two other conditions can by means of the second Eq. (4211-2) be transformed to the following admissible intervals for ψ (the principal value in the interval $-\pi < \psi \leq \pi$ being used):

$$\begin{aligned}
-\pi < \psi &\leq -\frac{\pi}{2} && (e_f, e_t = -1, -1)\\
-\frac{\pi}{2} \leq \psi &\leq -\frac{\pi}{2} + i_w && (e_f, e_t = 1, -1)\\
-i_w \leq \psi &\leq \frac{\pi}{2} && (e_f, e_t = 1, 1)\\
\frac{\pi}{2} \leq \psi &\leq \frac{\pi}{2} + i_w && (e_f, e_t = -1, 1)\\
\pi - i_w \leq \psi &\leq \pi && (e_f, e_t = -1, -1)
\end{aligned} \tag{4220}$$

Thus, only the intervals $-\frac{\pi}{2} + i_w < \psi < -i_w$ and $\frac{\pi}{2} + i_w < \psi < \pi - i_w$ are not admissible.

If the above conditions are not, or only partially satisfied, the solution cannot be mathematically correct. It may be a relatively good, statically possible approximation, however, if the negative contributions to the deformation work integral

$$W_d = \int_V 2 \tau_f \epsilon \, dV \tag{4221}$$

are reasonably small in relation to the positive ones.

The most important contributions to this integral come from the sliding along the boundary slip line, the distortion in the radial zone near the vertex point, and (for relatively rough walls) the sliding along the wall. The weaker conditions, used to ascertain that the rupture figure will at least be a good approximation, are therefore that $e_f u$ and $e_t u_s$ shall both be positive for $0 \leq \frac{t}{h} \leq 1$.

For pure translations this gives the same conditions as before. In the general case ($r_z \neq 0$) we find again (4216-7) for $e_f r_z \leq 0$, but now this quantity may also be positive. When this is the case one must have

$$\begin{aligned}
&\rho \geq 1\\
\text{and}\quad &\lambda \leq (\rho - 1) \tan m_w \quad \text{for } e_f e_t = 1\\
&\lambda \geq \rho \tan m_w \quad\quad\ \text{for } e_f e_t = -1
\end{aligned} \tag{4222}$$

These secondary domains are shown with dotted lines on Fig. 42 F (marked 2). The approximation will be better the higher values ρ take.

As an example it can be seen that for $\beta = \theta = 0$, $\rho = 1$, $\lambda = 0$, and $c_a = c$ the zone rupture will be about 20% on the safe side. (For the rupture figure A the deformation work for $r_z = 1$ is $\frac{\pi}{2} = 1.571$, and for P it is $\frac{1}{2}(\frac{\pi}{2} + 1) = 1.285$). For a more extensive evaluation of the approximation see Ex. 53 a.

In other domains, especially when $0 < \rho < 1$, the rupture figure considered in this example may be far too much on the safe side, and will therefore be useless as an approximate solution.

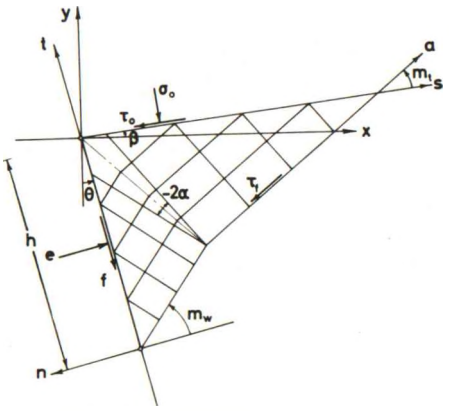

Fig. 42 G: Approximate Solution With Rupture Zones and a Discontinuity Line.

If α as given by (4207) turns out to be negative the Prandtl zone rupture will not be geometrically possible. For the simple boundary conditions assumed in this example an approximate rupture figure can, however, be constructed by means of a straight discontinuity line, as shown in Fig. 42 G.

From this rupture figure we find:

$$e = \sigma_o + e_f c \left[\sin 2 m_t + \sin 2 m_w + 2 \sin 2\alpha \right] \qquad (4223)$$

$$f = e_t c_a$$

α being taken with the correct sign.

Because of the discontinuity line the rupture figure can never be kinematically possible. It will represent the best possible approximation when the discontinuity line gives the only negative contribution to the deformation work, and it may still be useful when there are other, but small negative contributions. Consequently, the domains marked 1, and possibly also those marked 2, in Fig. 42 F should also be used in this case. For $0 < \rho < 1$ this rupture figure will also be useless as an approximation.

Example 42 b

To illustrate how the calculation procedure may be adjusted in practice consider the case of two interacting foundations shown in Fig. 42 H with the

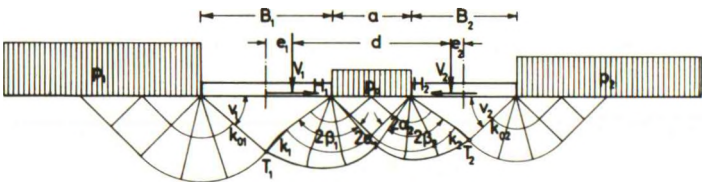

Fig. 42H: Interacting Strip Foundations on a Horizontal, Normally Loaded Clay Surface.

foundation widths B_1 and B_2, placed at the distance a on a horizontal surface with the vertical loadings p_1 and p_2 outside, and p_a between the foundations.

It is seen that the whole rupture figure (type RPTPRPTPR) may be constructed when a is known, and the angles α_1 and α_2 are assumed. Thus, by considering the conditions at the two transition points T_1 and T_2 we find:

For T_1:

condition of directions:

$$\frac{\pi}{4} + 2\,\alpha_2 - 2\,\alpha_1 - 2\,\beta_1 = -v_1 \tag{4224}$$

condition of stresses:

$$p_a + c\left[1 + 4\,(\alpha_2 + \alpha_1 + \beta_1)\right] = p_1 + c\left[1 + 2\,(\frac{3\pi}{4} - v_1)\right] \tag{4225}$$

In the same way for T_2:

$$-\frac{\pi}{4} - 2\,\alpha_1 + 2\,\alpha_2 + 2\,\beta_2 = v_2 \tag{4226}$$

and

$$p_a + c\left[1 + 4\,(\alpha_1 + \alpha_2 + \beta_2)\right] = p_2 + c\left[1 + 2\,(\frac{3\pi}{4} - v_2)\right] \tag{4227}$$

From this we find:

$$\beta_1 = \frac{\pi}{4} - \alpha_1 + \frac{p_1 - p_a}{8c}$$

$$\beta_2 = \frac{\pi}{4} - \alpha_2 + \frac{p_2 - p_a}{8c}$$

$$v_1 = \frac{\pi}{4} - 2\alpha_2 + \frac{p_1 - p_a}{4c} \qquad (4228)$$

$$v_2 = \frac{\pi}{4} - 2\alpha_1 + \frac{p_2 - p_a}{4c}$$

The rupture zone outside the simple radial zones with centre angles $2(\alpha_1 + \beta_1)$ and $2(\alpha_2 + \beta_2)$ may be constructed as usual by the method of chord lengths (second initial value problem). Along the arcs with centre angles $2\beta_1$ and $2\beta_2$ it will usually be too inaccurate to use only one cell. For reasons of continuity it is probably best to take a strip of cells, each with the maximum centre angle α_{max}, except the last one which has a fractional centre angle (if a number of cells with equal centre angles α are used, discontinuities will arise for parameter sets where the number of such cells is changed to keep α below α_{max}).

In this way the chords k_1 and k_2 are determined. They form the angles $\frac{\pi}{2} + \alpha_2$ and $\frac{\pi}{2} + \alpha_1$ with the chords k_{o1} and k_{o2}, respectively. The foundation widths B_1 and B_2 can now be calculated by simple geometry, and the resultant forces V_1, H_1 and V_2, H_2 together with the excentricities e_1 and e_2 can be found by means of the three equilibrium equations for each of the two rigid bodies of clay.

Thus, a procedure may be devised which calculates the 8 dimensionless quantities $\frac{B_1}{a}$, $\frac{B_2}{a}$, $\frac{e_1}{a}$, $\frac{e_2}{a}$, $\frac{V_1}{ca}$, $\frac{H_1}{ca}$, $\frac{V_2}{ca}$, and $\frac{H_2}{ca}$ as functions of the given quantities $\frac{p_1}{c}$, $\frac{p_2}{c}$, and $\frac{p_a}{c}$, and the two parameters α_1 and α_2.

However in practice the given quantities will usually be f. inst. $\frac{p_1}{c}$, $\frac{p_2}{c}$, $\frac{p_a}{c}$, $\frac{V_1}{cd}$, and $\frac{V_2}{cd}$ (i.e. V_1, V_2, and their distance d) and it is required to design two foundations (i.e. to find $\frac{B_1}{d}$, $\frac{B_2}{d}$, $\frac{e_1}{d}$, and $\frac{e_2}{d}$), together with the two horizontal forces $\frac{H_1}{cd}$, and $\frac{H_2}{cd}$, which should be taken by the structure, so that the statically determined rupture figure is a solution to the failure problem. This will normally ensure that the given forces are taken in the most economical way. Consequently the procedure would be applied in a program which performs an iteration, changing α_1 and α_2 until the directly calculated quantities are in accordance with the known ones.

Notice, that if the structure has no other foundations than the two shown in Fig. 42H, the difference $H_1 - H_2$ will represent an external force on the construction. It will then be required that this quantity also takes a known value, and the solution obtained above cannot be used generally. One further parameter must be introduced so that this extra condition can be satisfied (one of the PR constructions beyond T_1 or T_2 is replaced by a line rupture with an initially unknown centre angle).

422 Simple Line Ruptures and Arc Zones

The simplest possible approximate rupture figure is a single line rupture formed as a circle arc. It is normally used in kinematically admissible solutions, the parameters of the circle arc corresponding with the prescribed boundary movements (if any). This is easy to obtain because of the simple form of the rupture figure. Since an arbitrary circle arc has three free parameters, f. inst. the two coordinates to the centre and the radius, against the three equilibrium conditions for the rigid body of clay above the line rupture, the solution will in fact be quasi kinematically possible. Consequently, the equilibrium method may be used if the special stress conditions for line ruptures are applied, as pointed out by Brinch Hansen [1953].

If the surface conditions are irregular the energy method is probably the simplest to use in practice; as shown in Sec. 245 it may also be used for the purposes (f. inst. to find force resultants doing no work during the movement) to which the equilibrium method was invented. However, in sufficiently simple failure problems the latter method has the advantage that explicit calculation formulae can be derived.

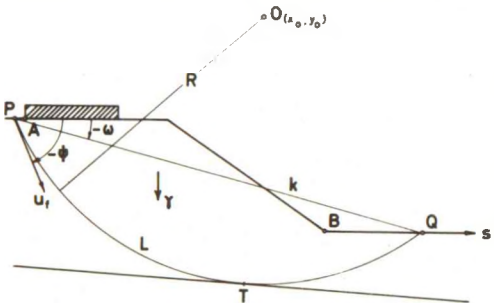

Fig. 42I: A Single Line Rupture (A) Used to Solve a Stability Problem.

Line ruptures are typically used in the so-called stability investigations (Fig. 42I). The circle arc with the length L is in principle completely free (3 parameters). In practice it is frequently restricted by the fact that one knows that in the extreme solution it must f. inst. pass through a certain discontinuity point A for the surface loading (A may also be an end point for an external rigid body), or a corner point B on the surface, or that it

must touch an internal boundary to a clay layer with a higher value of c. Further restrictions may be imposed because of the external movement conditions for rigid bodies in contact with the moving body of clay. Such restraint will decrease the number of free parameters and the number of remaining equilibrium conditions by the same amount.

The normal calculation procedure may be summarized as follows:

1. Assume a set of parameters x_o, y_o, and R (satisfying the given restraints if any).
2. Draw the circle arc, measure the length L, and calculate (semigraphically) the moment about O of all surface loadings and volume forces γ acting upon the moving rigid body of clay.
3. The energy equation is in this case simply a moment equation about O, the sliding velocity u_f entering as a simple factor of proportionality which can be disregarded.
4. The parameter set is changed in a systematical way until a minimum is found for the stability ratio (which is in fact a factor of proportionality f on all active forces on the clay body, except the shear stress along L).

Simpler calculations may possibly be obtained if the following modifications are introduced.

1. An alternative set of parameters is: the position of the first point P, or the last point Q of the circle arc, indicated f.inst. by means of the arc lengths s along the surface, the inclination ω of the chord, and the half centre angle α of the line rupture. The position of P, the tangent angle ψ, and the curvature $n = \frac{1}{R} = \frac{u_f}{r_z}$ may also be used; this set has the advantage that it is directly connected to the movement components for the rigid body.
2. The chord length k and the arc length L can easily be calculated from these data. Instead of integrating the volume forces over the clay body it is simpler to use the correction (2307), replacing in this way the volume forces by corrective surface loadings. The surface load resultants may be calculated as shown in Sec. 222.
3. Instead of using the stability ratio one may sometimes consider the problem as one of controlled strain. If the line rupture is geometrically restrained so that it cannot contract into a point an imaginary restraint may be assumed to impose a unit rotation $r_z = 1$ on the

rigid body, leaving the translation components w_x and w_y free. The corresponding restraint force is a driving moment about O necessary to produce failure. If the minimum value of this quantity is positive (after the loads and shear strengths have been provided with the required partial coefficients) the slope or construction is sufficiently stable.

4. If so desired the equilibrium method may be used, the 3 parameters being determined by the 2 remaining equilibrium equations, and the stress condition between the points P and Q. If P or Q is known we have only 2 parameters, but the stress at the known point is also unknown, so there is no stress condition. If the line rupture touches an internal boundary at a point T we have also only 2 parameters, but now a discontinuity in σ at T is possible so there is again no stress condition.

In this form the calculations are suited for a computer.

Line ruptures are also used extensively in other types of problems, f.inst. earth pressure problems (rupture figure A or X, cf. Fig. 42 J). Here they are usually known to pass through a certain point, viz. the foot point of the wall. The parameter set ω, α (or ψ, n) is frequently used, being directly connected to the known movement conditions for the wall. As a rule the equilibrium method is used instead of the energy method, at least when the boundary conditions are sufficiently regular.

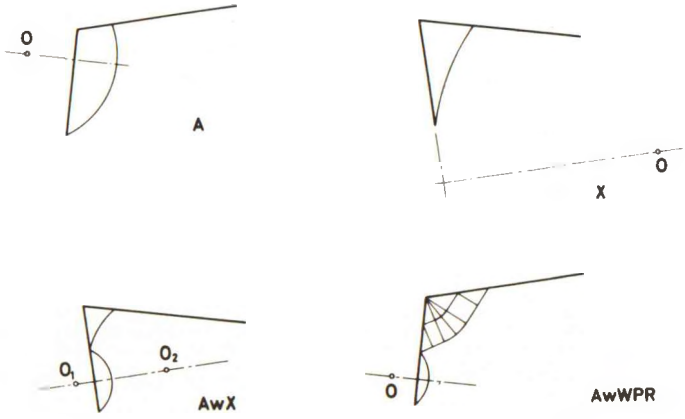

Fig. 42 J: Line Ruptures Used to Solve Simple Earth Pressure Problems.

Especially in problems of this kind two important modifications of the rupture figure consisting of a single line rupture are frequently used:

1. If the parameters for the line rupture are given completely by the movement conditions for the wall it may intersect the wall again before it reaches the clay surface. One possible solution to this problem consists in letting the line rupture be reflected from the wall (the rupture figure AwX), or in combining it with a zone rupture ending at the intersection point (AwWPR) if this is geometrically possible, cf. Fig. 42 J.

2. In the last mentioned example the rupture zone may instead be calculated so that its end point is not the intersection point with the wall (type E), but is a point on the line rupture situated so that it is a normal point. Thus, at the point the line rupture and one of the slip lines in the zone have the same tangent. The same construction (AaZ and XfZ) may also be used for combinations of line ruptures with zones of the type R and PR. In fact, it may be used with all types of statically determined rupture zones. This type of end points for the zones might be called C.

The latter modification is the most important since it is more generally applicable. It may give possible solutions provided the connection between the rupture zone and the line rupture is geometrically possible, and the rupture zone is kinematically possible ($\epsilon \geq 0$).

In the general case with arbitrary surface conditions it is not simple to construct a surface zone (i.e. to choose two surface parameters) so that the end point is a tangent point on a given line rupture. Therefore, for such rupture figures one will in practice start by assuming the two surface parameters (λ_c, μ_c). After the zone has been calculated one can then construct the line rupture from the known end point, where the tangent direction is also known, using the other point of the line rupture which is also given. By trial and error the surface parameters can then be varied until the given movement and/or equilibrium conditions are satisfied.

For simple surface conditions (surface zones with straight slip lines) it is easy to construct a rupture zone (WPR, PR, or R) with an end point of the type C in relation to a given line rupture. Therefore, in this case the calculations will start with the line rupture. Examples of this type of rupture figures are shown in Fig. 42 K.

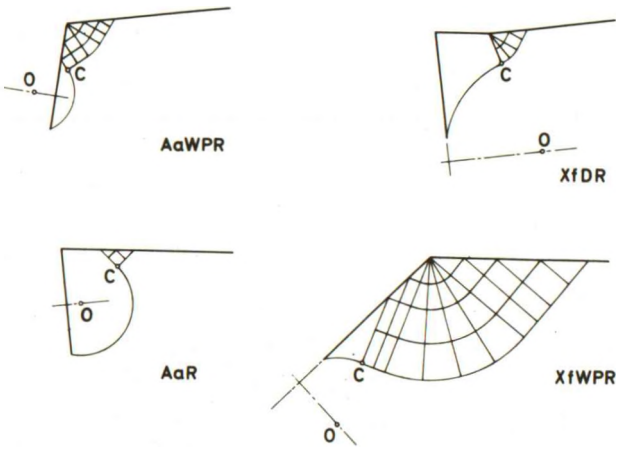

Fig. 42K: Combinations of Line Ruptures and Statically Determined Ruptures Zones.

Notice that the centre O of the circle in all cases (Fig. 42J-K) must be located on the normal to the wall in the height ρh above the foot point. If $e_t = 0$ for the rigid body of clay (no sliding between the wall and the body) the position of O is completely determined when λ is also known. For $e_t \neq 0$ the position of O must be found by the condition that $f = \tau_a = e_t c_a$ (an equilibrium condition for the components parallel to the wall of all forces acting upon the rigid body of clay).

When the surface zones are simple the possible solutions AaWPR (or AaPR) are actually quite as easy to calculate as the solutions AwX and AwWPR. They are therefore used in practice. The calculation of the rupture figures of this type depends mostly on which quantities are known initially that characterize the geometry of the rigid body of clay. Because of its importance in practice the calculation of the so-called simple rigid bodies, bounded by a wall, possibly a uniformly loaded surface, a straight, and a circular slip line, is treated separately in the following section.

Especially in bearing capacity problems line ruptures may be combined with more complicated statically determined rupture zones. Thus, the most general solution corresponding to Fig. 42H (when the resulting horizontal force $H_1 - H_2$ is also known) will for a wide range of problem parameters be of the type XfPRPTPR (or RPTPRPfX).

In the same way as a surface zone is introduced when geometrically possible to avoid that the line rupture intersects the surface under an angle which is not statically possible, a so-called arc zone, or band zone, may be introduced when the angle between a line rupture (type Xf) and a wall becomes too small (less than i_w) or even negative. In the general case such arc zones are open rupture zones with mixed boundary conditions, but when the slip lines in the surface zone perpendicular to the generating line rupture are straight the arc zone becomes a simple band containing straight and circular slip lines.

In Fig. 42 L is shown first an XfR rupture figure with a too small angle between the line rupture and the wall. Next the corresponding arc zone rupture figure, called BfR (RsX in Brinch Hansen's notation), is indicated, and finally it is shown by two rupture figures how the arc zones can be combined with line ruptures and surface zones. The last example, AaBfBfR is the most complicated single rupture figure containing simple rigid bodies. It has three rigid bodies of clay in contact with the wall, separated by two rupture zone parts. Of the three rotation centres O_1, O_2, and O_3, the middle one must be located in the rotation centre of the wall.

By comparison with Fig. 42 G it is seen that the rupture figure BfR (or XfR) can be used as a kinematically possible solution instead of a zone rupture with a discontinuity line when the rupture figure WPR is not geometrically possible because $\alpha < 0$.

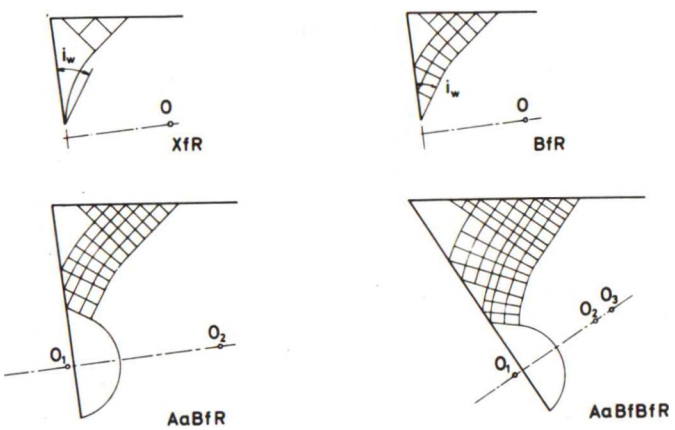

Fig. 42 L: Arc Zones Replacing Line Ruptures not Statically Possible. Other Rupture Figures With Simple Arc Zones.

When the wall (or foundation) is perfectly rough i_w will be zero, and the arc zone rupture will rarely be used except in combination with an Aa-construction. Especially for foundations one will in this case frequently use a simple Xf-construction with the line rupture tangent to the foundation, assuming this rigid body to lift away from the clay surface outside the rupture figure.

If the two first Figs. 42 L are compared it is seen that the rigid body between an arc zone and the wall is calculated in much the same way as a body bounded by a line rupture. The only difference is that the angle between the boundary slip line and the wall is now known, even if $e_t \neq 0$. On the other hand the position of the intersection point is not known initially unless $e_t = 0$.

The kinematical conditions for the simple rupture figure types considered in this section can be investigated by the same method as in Ex. 42 a. This problem is treated more fully as Ex. 51 b to Sec. 512.

Example 42 c

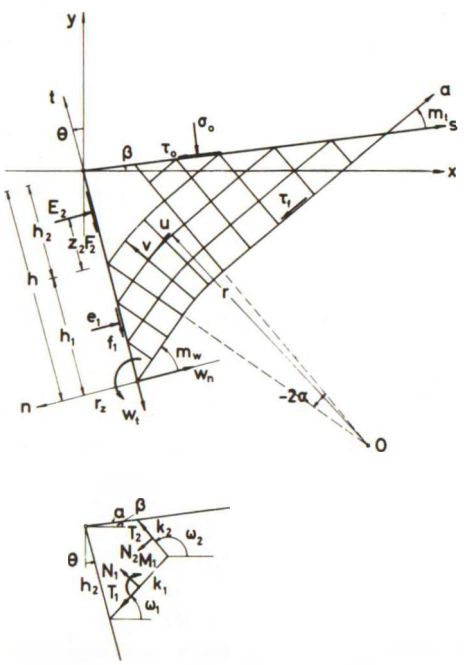

Fig. 42 M: A Simple Arc Zone Rupture (BfR) Behind a Retaining Wall.

The arc zone rupture figure BfR may be calculated as follows, cf. Fig. 42 M. The state of failure is as usual characterized by the indicator e_f, and the sliding properties of the two wall parts h_1 and h_2 are indicated by the numbers e_{t1} and e_{t2}. For kinematical reasons we must have $e_{t1} \neq 0$ and either $e_{t2} = e_{t1}$ or $e_{t2} = 0$.

m_t and m_w are calculated by means of (4205-6), using in the latter case e_{t1}. α is given by (4207). This angle is assumed to be negative. Considering the geometry and the equilibrium of the rigid body of clay we find:

$$\omega_1 = \theta + m_w + \alpha = \beta + m_t - \alpha \qquad (4229)$$

and

$$\omega_2 = \frac{\pi}{2} + \beta + m_t \qquad (4230)$$

Consequently by the geometry of the quadrangle $h_2 k_1 k_2 a$ we find:

$$k_2 = h_2 \frac{\cos(\beta - \theta)}{\cos m_t} - k_1 \frac{\sin(m_t - \alpha)}{\cos m_t}$$

and

$$a = -h_2 \frac{\sin(m_w + 2\alpha)}{\cos m_t} + k_1 \frac{\cos \alpha}{\cos m_t} \tag{4231}$$

If $e_{t2} = 0$ the centre O must be the rotation centre of the wall, having the coordinates ρh, λh in the t,n-coordinate system, cf. (4204). In this case h_2 and k_1 can be found directly, because evidently

$$\frac{h_1}{h} = \rho - \lambda \cot m_w$$

$$\frac{h_2}{h} = 1 - \frac{h_1}{h} \tag{4232}$$

$$\frac{k_1}{h} = 2\lambda \frac{\sin \alpha}{\sin m_w}$$

The rupture figure is therefore completely geometrically determined, and the resulting earth pressure components E_2 and F_2, together with the height of application z_2 can be found by the equilibrium equations.

Finding:

$$N_1 = e_f c k_1 \left[\sin 2 m_t + N^z(\alpha) \right]$$

$$T_1 = e_f c k_1 T^z(\alpha)$$

$$M_1 = e_f c k_1^2 M^z(\alpha) \tag{4233}$$

$$N_2 = e_f c k_2 \sin 2 m_t$$

$$T_2 = e_f c k_2$$

α being inserted with the correct sign, cf. Brinch Hansen [1957], we have:

$$E_2 = N_1 \sin(m_w + \alpha) + T_1 \cos(m_w + \alpha)$$
$$+ N_2 \cos(m_w + 2\alpha) + T_2 \sin(m_w + 2\alpha)$$
$$+ \sigma_o h_2 + \tau_o a \cos(\beta - \theta) \tag{4234}$$

$$F_2 = N_1 \cos(m_w + \alpha) - T_1 \sin(m_w + \alpha)$$
$$- N_2 \sin(m_w + 2\alpha) + T_2 \cos(m_w + 2\alpha)$$
$$- \tau_o a \sin(\beta - \theta) \tag{4235}$$

$$E_2 z_2 = - M_1 + \tfrac{1}{2} k_1 N_1 + \tfrac{1}{2} k_2 N_2 + k_1 (-N_2 \sin \alpha + T_2 \cos \alpha) + \tfrac{1}{2} \sigma_o h_2^2 + \tau_o a h_2 \cos (\beta - \theta) \qquad (4236)$$

If $e_{t2} \neq 0$ (4232) cannot be used directly since the position of O may not now correspond to the value of λ for the wall (but the value of ρ can still be used). Instead we must use the condition that

$$\frac{F_2}{c h_2} = e_{t2} \frac{c_a}{c} \qquad (4237)$$

When (4231) and (4233) are inserted in (4235) this gives a linear equation in $\frac{k_1}{h_2}$ from which this quantity can be found. $\frac{k_2}{h_2}$ and $\frac{a}{h_2}$ are then found from (4231). The three equations (4232) can be transformed to:

$$\frac{\lambda_o}{1 - \rho} = \frac{\frac{k_1}{h_2} \tan m_w}{\frac{2 \sin \alpha}{\cos m_w} - \frac{k_1}{h_2}} \quad (> - \tan m_w)$$

$$\frac{h_2}{h} = (1 - \rho) (1 + \frac{\lambda_o}{1-\rho} \cot m_w) = K (1 - \rho) \qquad (4238)$$

where

$$K = \frac{\frac{2 \sin \alpha}{\cos m_w}}{\frac{2 \sin \alpha}{\cos m_w} - \frac{k_1}{h_2}}$$

which defines the geometry of the rupture figure; λ_o (the coordinate $\frac{n_o}{h}$ to the centre O) can be found from the last Eq. (4232).

In both cases considered above all geometrical quantities (except α) should be positive. If not the rupture figure is not geometrically possible. It must then be replaced by another type (f. inst. XfR, X, BfPR, or BfWPR). If it is geometrically possible the earth pressure components e_1 and f_1 are found from (4208).

However, the rupture figure may also turn out to be kinematically impossible. Let ρ, λ indicate the position of the rotation centre for the wall, and $\rho_o = \rho$, λ_o the position of O. Considering the velocity components u, v (Fig. 42 M) we see that v = 0 identically. u is constant along every a-line,

so it may be regarded as a function of r, the radius vector in the radial zone. The arc zone is located in the interval $r_o \leq r \leq r_1$, where

$$\begin{aligned} r_o &= -h\,(\rho \cos m_w + \lambda_o \sin m_w) \\ r_1 &= -\lambda_o\, h \operatorname{cosec} m_w \end{aligned} \tag{4239}$$

(4210-12) is valid for the first part (h_1) of the wall. In the wall and arc zone we have

$$r = r_o + t \cos m_w$$

or

$$\begin{aligned} t &= (r - r_o) \sec m_w \\ &= r \sec m_w + \rho\, h + \lambda_o\, h \tan m_w \end{aligned} \tag{4240}$$

so that

$$\begin{aligned} u &= r_z\, h\,(\rho - \tfrac{t}{h}) \sec m_w \\ &= -r_z\, h\,(\tfrac{r}{h} \sec m_w + \lambda_o \tan m_w) \sec m_w \end{aligned} \tag{4241}$$

For $r = r_o$

$$u = r_z\, h\, \rho \sec m_w \tag{4242}$$

2ϵ is equal to

$$\frac{du}{dr} = -r_z \sec^2 m_w \tag{4243}$$

in the wall zone and the Rankine zone, and to

$$\frac{du}{dr} - \frac{u}{r} = r_z \frac{h}{r} \lambda_o \sec m_w \tan m_w \tag{4244}$$

in the arc zone.

In the rigid body, and the part of the Rankine zone adjacent to this body:

$$u = -r_z\, r \tag{4245}$$

In the former domain $2\epsilon = 0$ according to (4244); in the latter one it is equal to $-r_z$, cf. (4243).

From (4212) we find:

$$\begin{aligned} u_s &= r_z\, h \left[-\lambda + (\rho - \tfrac{t}{h}) \tan m_w \right] \\ &= -r_z\, h \left[\lambda + (\tfrac{r}{h} \sec m_w + \lambda_o \tan m_w) \tan m_w \right] \end{aligned} \tag{4246}$$

For $r = r_o$ this is equal to $-r_z\, h(\lambda - \rho \tan m_w)$, and for $r = r_1$ to $-r_z\, h(\lambda - \lambda_o)$ which is also the sliding velocity between the wall and the rigid body.

Using the same criteria as in Ex. 42a we find:

From (4243-4):

$$\begin{aligned} & e_f\, r_z \leq 0 \\ & \lambda_o \leq 0 \end{aligned} \qquad (4247)$$

the last one of which is always satisfied for geometrical reasons.

From (4242):

$$\rho \leq 0 \qquad (4248)$$

From (4246):

$$\left.\begin{aligned} & \lambda \geq \rho \tan m_w \\ \text{and} \quad & \lambda \geq \lambda_o \end{aligned}\right\} \quad \text{for } e_f e_{t1} = 1$$
$$\lambda \leq \lambda_o \quad \text{for } e_f e_{t1} = -1 \qquad (4249)$$

From this result it is seen that when $e_f e_{t1} = 1$ this rupture figure cannot exist unless the rigid body of clay slides upon the wall. For, when $e_{t2} = 0$ we have $\lambda = \lambda_o$, and from the first Eq. (4232) it is seen that $\frac{h_1}{h} \leq 0$ when $\lambda_o \geq \rho \tan m_w$.

Above the limitations (4247-9) are imposed the statical and geometrical ones, so the domain of validity for this rupture figure cannot be established without some preliminary calculations.

For example, assume the three parameters which define the rupture figure geometrically: $\beta - \theta = -20°$, $\frac{c_a}{c} = 0.5$, and $\frac{\tau_o}{c} = 0$. Without loss of generality σ_o may be put equal to zero. From (4205) and (4218) we find $m_t = 45°$ (independent of τ_f), and $i_w = 30°$.

When $e_f e_t = 1$ this gives $m_w = 30°$ and $\alpha = -2.5°$, cf. (4207). From (4231) it follows that

$$\begin{aligned} \frac{k_2}{h_2} &= 1.329 - 1.043 \frac{k_1}{h_2} \\ \frac{a}{h_2} &= -0.598 + 1.413 \frac{k_1}{h_2} \end{aligned} \qquad (4250)$$

Consequently, for geometrical reasons $\frac{k_1}{h_2}$ must be in the interval:

$$0.423 \leq \frac{k_1}{h_2} \leq 1.274 \tag{4251}$$

at the lower limit a = 0, and at the upper limit $k_2 = 0$.

From Brinch Hansen [1957] we may find:

$$N^z = -0.0873$$
$$T^z = 0.9987 \tag{4252}$$

Inserting in (4235), using also (4233) and (4250) we find:

$$e_f \frac{F_2}{c\, h_2} = 0.643 - 0.156 \frac{k_1}{h_2} \tag{4253}$$

This quantity is equal to $\frac{c_a}{c} = 0.500$ when $\frac{k_1}{h_2} = 0.916$. For statical reasons the lower limit in (4251) must therefore be replaced by this value:

$$0.916 \leq \frac{k_1}{h_2} \leq 1.274 \tag{4254}$$

According to (4238) the two limits correspond to the following positions of the centre O:

For $\frac{h_2}{h} = 1$:

$\frac{k_1}{h_2}$	K	$\frac{\lambda_o}{1-\rho}$	$1 - \rho$	λ_o
0.916	0.0991	-0.520	10.09	-5.25
1.274	0.0733	-0.535	13.65	-7.30

Using also (4248-9) it is found that the rotation centre for the wall must be located in the domain DABC on Fig. 42 N. The boundaries AD ($\rho \leq 0$) and AB ($\lambda \geq \rho \tan m_w$) are kinematically determined. EB indicates the position of O for sliding ($e_{t2} = 1$, $\frac{k_1}{h_2} = 0.916$). Since $\lambda \geq \lambda_o$ when ρ_B (= -9.09) $\leq \rho \leq 0$ we must have sliding in the whole domain. To all rotation centres on a line through the domain normal to the wall corresponds one point O, which is the intersection point between the line and FB. The lower boundary BC is given by the condition that $\frac{h_2}{h} \leq 1$ (i.e. $h_1 \geq 0$).

For rotation centres below the point B the arc zone rupture figure only exists in the limiting case where $h_1 = 0$. It is, therefore, in fact an XfR rupture figure (forming an angle to the wall normal at the foot point equal to

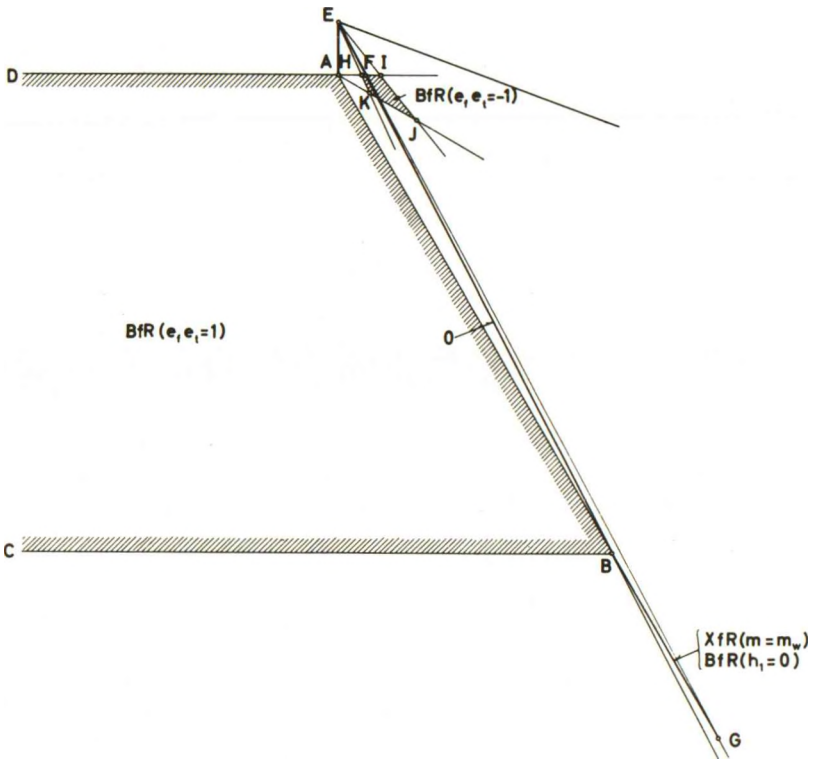

Fig. 42 N: Admissible Rotation Points for a Wall With an Arc Zone Rupture BfR.

m_w, i.e. the statically correct value). This condition obtains along the whole line ABG. $e_{t2} = 1$ for AB, and 0 for BG. The point G is the intersection point with the line corresponding to the upper limit (4254). Consequently, at this point $k_2 = 0$, i.e. the Rankine zone degenerates to a point. Thus, at the point G we have the special case of a line rupture X with statically correct angles at both end points.

For $e_f e_t = -1$ the same calculations can be performed. In this case sliding is not possible. The boundaries to the domain HIJK are determined by the following conditions:

HI: $\rho \leq 0$

HK: $a \geq 0$ $\left(e_f \frac{F}{c\,h_2} = 0.220\right)$

LJ: $k_2 \geq 0$ $\left(e_f \frac{F}{c\,h_2} = -0.367\right)$

JK: $h_1 \geq 0$

The point J also corresponds to a statically correct line rupture.

423 Rupture Figures with Simple Rigid Bodies

A simple rigid body of clay is bounded by two or three straight lines and one circle arc. The straight lines are: a wall with a constant value of c_a, a surface with a uniform surface loading (may not be present), and a slip line. The circle arc is also a slip line, the centre of which is the rotation centre (absolute or relative to another rigid body of clay) for the rigid body.

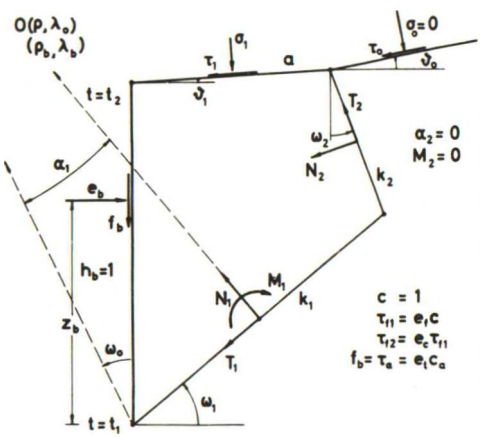

Fig. 42 O: General Case of a Simple Rigid Body.

The geometry of a simple rigid body may be defined as shown in Fig. 42 O. Its height along the wall is h_b which during the calculation of the body may be put equal to 1 (i.e. all lengths are taken relative to h_b). On the wall it is located between the absolute heights $t_1 h_w$ and $t_2 h_w$ above the foot point of the wall, h_w being its total height. The surface part a, if any, forms the angle $\vartheta_1 = \beta - \theta$ to the normal to the wall. ϑ_1 and the load components σ_1 and τ_1 (relative to c) are only prescribed when $a \neq 0$ (in which case, obviously, $t_2 = 1$). The data for the surface outside the rigid body ϑ_o, τ_o are always given. Without loss of generality σ_o may be put equal to 0.

k_2 is the straight slip line, and k_1 the chord to the circular line (with the half centre angle α_1). The rotation centre for the wall is assumed to be given, i.e. the coordinates ρ, λ, or, alternatively, the movement components w_n, w_t, r_z are known. The centre of the circle arc has the coordinates ρ, λ_o relative to the wall ($\lambda = \lambda_o$ only if $e_t = 0$). Relative to the rigid body, i.e. measured from the point $t = t_1$ relative to the height h_b, the coordinates are termed ρ_b, λ_b. They are evidently given directly from ρ, λ_o only if $t_1 = 0$.

The state of failure and the sense of sliding along the wall are characterized as usual by means of the indicators e_f and e_t. A further indicator e_c is used to show whether k_2 is of the opposite slip line family ($e_c = 1$, as in XfR) or the same family ($e_c = -1$, as in AaR) as k_1. The angles ω_o, ω_1, and ω_2 are defined so that the following identities hold:

$$\begin{aligned} \omega_1 &= \omega_o + \alpha_1 \\ \omega_2 &= \omega_1 + \alpha_1 \qquad \text{if } e_c = 1 \\ &= \omega_1 + \alpha_1 - \frac{\pi}{2} \qquad \text{if } e_c = -1 \\ \tau_{f2} &= e_c \tau_{f1} \end{aligned} \tag{4255}$$

Such rigid bodies obtain in simple rupture figures, i.e. rupture figures where all slip lines are either straight or circular. In one-sided earth pressure problems with a straight wall and a surface which is straight and uniformly loaded, except possibly for one corner point which is also a load discontinuity, simple rupture figures are obtained for a wide range of problem parameters. It should be noticed, however, that even in this case more complicated rupture figures obtain for some parameter sets. On the other hand, in other types of problems rigid bodies of clay may be obtained which have different geometries (f. inst. bounded by one or two surface parts, two straight, and three circular slip lines) but which might still be called simple rigid bodies.

The simple rupture figures considered in this section are built up of the elements which have previously been termed A, X, B, W, P, D, and R. A sketch of the elements in the λ,μ-plane is shown on Fig. 42 P, which is drawn under the assumption that $e_f = 1$ and $r_z < 0$ so that the line rupture X is an a-line, and A is a b-line.

The characteristic points (corner points for zone elements) are numbered so that in any permissible rupture figure built up of such elements each point will have a unique number. The alternative numbers shown in Fig. 42 P correspond with the fact that there may be 2 elements of the type B in the same rupture figure, and the upper right hand corner point of B may coincide with the lower left hand corner of either R, D, P, W, or B.

Apart from the numerical data of the failure problem, including the values of λ and ρ (or w_n, w_t, and r_z) for the wall and the value of e_f, it is assumed that the rupture figure is specified by means of a string of letters, indicating the constituent elements, possibly connected by the symbols a, f, or w, to indicate the connections. Besides the values of $e_f e_t$ for all wall parts (1 to 5

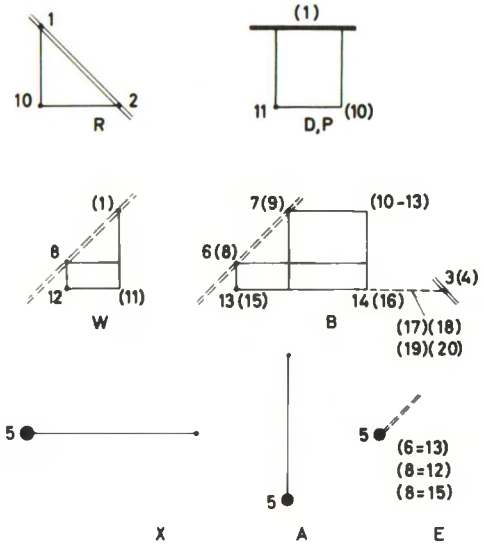

Fig. 42 P: Zone Elements for Simply Determined Rupture Figures.

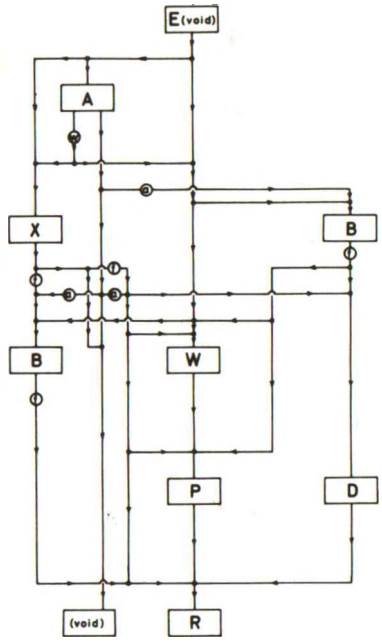

Fig. 42 Q: Admissible Schemes of Combining Simple Rupture Figure Elements.

numbers) must be given, f. inst. in the order from the foot point towards the top of the wall.

Obviously, the element symbols cannot be combined arbitrarily, but certain rules must be followed for geometrical reasons. Thus, after the symbol A there must follow either nothing or the letter a and B, W, P, R, or D, or the letter w and X, B, or W. Combinations like AwR or AaX are clearly impossible. All combinations that are geometrically possible are shown in a (rather complicated) scheme on Fig. 42 Q.

Correspondingly, the values of e_f e_t can also not be chosen arbitrarily. For kinematical reasons they should form a non-decreasing series, being different from zero for the zone parts, and of different signs for two different zone parts if such exist. For adjacent boundary parts the difference in e_f e_t must not be numerically greater than 1.

In a permissible rupture figure of the family considered in this section there will be from zero to three rigid bodies (apart from the infinite, unmoving body outside the rupture figure) of the type shown in Fig. 42 O. Three quantities will always be known in any such body, as indicated in the following table.

Table 42 A: Known Quantities in Simple Rigid Bodies.

Case No.	Body implied by the rupture figure elements	Known values of		Known quantities for			
				$r_z \neq 0$ (ρ and λ finite)		$r_z = 0$ (translation)	
		t_1	t_2	$e_f e_t = 0$	$e_f e_t \neq 0$	$e_f e_t = 0$	$e_f e_t \neq 0$
1	A, X; wX (pure line ruptures)	0; x	1	ρ_b, λ_b, k_2	ρ_b, f_b, k_2	α_1, ω_o, k_2	α_1, f_b, k_2
2	AaR, XfR	0	1	$\rho_b, \lambda_b, \omega_2$	ρ_b, f_b, ω_2	-	-
3	AaP, XfP, AaD, XfD	0	1	ρ_b, λ_b, a	ρ_b, f_b, a	α_1, ω_o, a	α_1, f_b, a
4	Aw	0	-	$\frac{\lambda_b}{\rho_b}, k_2, a$	f_b, k_2, a	-	-
5	AaW, XfW, AaB, XfB	0	-	$\frac{\lambda_b}{\rho_b}, \omega_2, a$	f_b, ω_2, a	-	-
6	BfR	-	1	$\frac{\lambda_b}{1-\rho_b}, \omega_o, \omega_2$	f_b, ω_o, ω_2	-	-
7	BfD, BfP	-	1	$\frac{\lambda_b}{1-\rho_b}, \omega_o, a$	f_b, ω_o, a	-	-
8	BfW, BfB	-	-	ω_o, ω_2, a	-	-	-

A dash in one of the columns marked t_1 or t_2 indicates that the corresponding quantity is not known. x means that it is known but is different from 0 or 1. In the four last columns a dash means that the rigid body cannot exist under the assumed circumstances. Thus, in pure translation the only possible (simple) rupture figures are WPR, X, XfR, XfPR, and XfDR, the first one of which contains no rigid bodies. A rigid body sliding upon the wall, supposed to exist between an arc zone and a wall zone (or another arc zone) would according to the rules indicated above for the variation of $e_f e_t$ separate two wall zones with the same values for e_t. It would therefore have $\alpha_1 = 0$, and would in fact simply be a part of a wall zone. For kinematical reasons, since r_z would have to be different from zero, it could not remain rigid. By a similar reasoning it is seen that XfW and XfB are only possible when $e_f e_t = 1$ for the zone, and 0 for the rigid body.

When $t_1 = 0$, although ρ_b and λ_b would not be known explicitly unless also $t_2 = 1$, their ratio $\frac{\lambda_b}{\rho_b}$ (which is equal to $\tan \omega_o$) is known when $e_t = 0$. Correspondingly the ratio $\frac{\lambda_b}{1 - \rho_b}$ is known when $t_2 = 1$ and $e_t = 0$. The ratios are evidently equal to the corresponding ratios $\frac{\lambda}{\rho}$ and $\frac{\lambda}{1 - \rho}$, respectively, inserting the coordinates to the rotation centre for the wall. Especially for combinations with Aw we must have $\rho_b = \frac{1}{2}$, and therefore $\lambda_b = \frac{\lambda}{2\rho}$ when $e_t = 0$; besides $t_2 = 2\rho$.

When $e_f e_t = 0$ the rigid body is determined by a simple geometrical construction. Thus, the centre of the circle arc is either known directly (ρ_b, λ_b) or can easily be constructed (ω_o or $\frac{\lambda_b}{\rho_b}$; and either ω_2 (or $k_2 = 0$) and a, or $\frac{\lambda_b}{1 - \rho_b}$). The circle arc can therefore be drawn until it intersects the surface ($k_2 = 0$), has a known tangent direction, or has a tangent through a known point. If $e_f e_t \neq 0$ the problem is more difficult, but one can always assume a value for the quantity replacing f_b when $e_t = 0$, and change this value by trial and error until f_b attains the given value. This is not always the most direct procedure, however, because when all angles are known (or assumed) f_b is a linear function of the chord lengths. These quantities can therefore be found by direct solution.

More specifically the following procedure may be used.

1. First ω_o is calculated from the given data, if possible:

$$\omega_o = \text{arc tan } \frac{\lambda_b}{\rho_b} \qquad \text{(Case 1-5, } e_t = 0\text{)} \qquad (4256)$$

or

$$\omega_o = \text{arc tan } \sqrt{\frac{\tau_{f1} - \tau_{a1}}{\tau_{f1} + \tau_{a1}}} \qquad \text{(Case 6-8)} \qquad (4257)$$

τ_{a1} being the value of $\tau_a = e_t c_a$ for the zone part below the rigid body of clay. ω_o should be an angle in the interval $-\frac{\pi}{2} < \omega_o \leq \frac{\pi}{2}$; when (4257) is used the lower limit will be 0 instead of $-\frac{\pi}{2}$. If ω_o is not given (Case 1-5, $e_t \neq 0$) a value is estimated.

2. α_1 and ω_2 can now be calculated. In the cases No. 2 and 6 we have

$$\omega_2 = m_t + \vartheta_o \qquad (4258)$$

where:

$$m_t = \text{arc tan } \sqrt{\frac{\tau_{f2} + \tau_o}{\tau_{f2} - \tau_o}} \qquad (4259)$$

In the cases No. 5 and 8 ω_2 is fould by (4257) inserting τ_{f2} and τ_{a2} (for the zone part above the rigid body) instead of τ_{f1} and τ_{a1}.

This gives α_1 and ω_1 directly from (4255) in these cases. By simple geometry the pertinent formulae for the other cases are found to be:

Case No. 1 (pure line rupture, $k_2 = 0$):

$$\cos(\omega_o + 2\alpha_1 - \vartheta_o) = \cos(\omega_o - \vartheta_o) - \frac{1}{\rho_b}\cos\omega_o \cos\vartheta_o \tag{4260}$$

Case No. 3: The length x, and the angles u and v are defined by the formulae:

$$\begin{aligned} x\cos u &= \lambda_b + a\cos\vartheta_1 \\ x\sin u &= (\rho_b - 1) - a\sin\vartheta_1 \\ \cos v &= \frac{\rho_b}{x\cos\omega_o} \qquad (\text{for } e_c = -1) \end{aligned} \tag{4261}$$

From this α_1 is given by

$$\begin{aligned} \alpha_1 &= \frac{\pi}{4} - \frac{\omega_o + u + v}{2} \qquad (\text{for } e_c = -1) \\ &= \frac{\pi}{4} - \frac{\omega_o + u}{2} \qquad (\text{for } e_c = 1) \end{aligned} \tag{4262}$$

Case No. 4 ($k_2 = a = 0$):

$$\alpha_1 = \frac{\pi}{2} - \omega_o \tag{4263}$$

Case No. 7: Let the angle ψ_1 be defined by the equation:

$$\tan\psi_1 = \frac{\lambda_b}{1 - \rho_b} \tag{4264}$$

ρ_b can then be found from ω_o and ψ_1 by the formula:

$$\rho_b = \frac{\cos\omega_o \sin\psi_1}{\sin(\omega_o + \psi_1)} \tag{4265}$$

3. The normal stress σ_2 along k_2 (i.e. acting at the upper point of k_1) may now be found (or without loss of generality be defined) as follows:

$$\begin{aligned} \sigma_2 &= 0 && \text{if } a = 0, \text{ or if } t_2 \neq 1 \\ &= (\tau_{f1} + \tau_o)\cot(\omega_o + 2\alpha_1 - \vartheta_o) && \text{in Case No. 1} \\ &= \tau_{f2}\sin 2m_t && \text{in Case No. 2 and 6} \\ &= \tau_{f2}\left[\sin 2m_t + 2(m_t + \vartheta_o - \omega_2)\right] && \text{else} \end{aligned} \tag{4266}$$

4. The remaining geometrical quantities, and f_b, can now be found by means of the equations:

$$\begin{aligned} k_1 \cos \omega_1 - k_2 \sin \omega_2 &= a \cos \vartheta_1 \\ k_1 \sin \omega_1 + k_2 \cos \omega_2 &= 1 + a \sin \vartheta_1 \end{aligned} \tag{4267}$$

$$\begin{aligned} &k_1 [\sigma_2 \cos \omega_1 + \tau_{f1} (N^z \cos \omega_1 - T^z \sin \omega_1)] \\ &- k_2 [\sigma_2 \sin \omega_2 - \tau_{f2} \cos \omega_2] - a [\sigma_1 \cos \vartheta_1 + \tau_1 \sin \vartheta_1] = f_b \end{aligned} \tag{4268}$$

If ρ_b is known k_1 is given by the formula:

$$k_1 = 2 \rho_b \frac{\sin \alpha_1}{\cos \omega_o} \tag{4269}$$

k_2 and a can then be found by the solution of (4267). The same method is used when a or k_2 are known (k_1 and k_2, or k_1 and a are found, respectively). f_b can then be found, and checked if $e_t \neq 0$, by means of (4268). Especially in Case No. 6, $e_t \neq 0$, where none of the above mentioned cases apply, Eq. (4267-8) can be solved as three linear equations in the three unknown quantities k_1, k_2, and a.

5. In the cases where ω_o has been estimated this quantity must be changed by trial and error until f_b attains the correct value:

$$f_b = e_t c_a \tag{4270}$$

By the other equation of projection, and by the moment equation e_b and its relative height of application z_b can finally be found. The scale of the figure, and thereby t_1 and/or t_2, can be found by simple geometry, using also (4269) if ρ_b is not known, and (4256) if λ_b is needed (Case No. 8):

$$\begin{aligned} t_1 + (t_2 - t_1) \rho_b &= \rho \\ (t_2 - t_1) \lambda_b &= \lambda \end{aligned} \tag{4271}$$

From the geometry of the rigid bodies it is easy to calculate all necessary quantities in the whole rupture figure. The velocity field can be investigated by much the same method as in the preceding Ex. 42 c.

In this way the calculations may be performed by hand. For calculations by a computer it would probably be the most useful to prepare a program which was able to decide itself what rupture figure to use (of the con-

sidered types, provided a solution can be obtained by such rupture figures). This problem is considered further in the sections 512 and 531.

The same rupture figure types may obtain for more general conditions, f. inst. with curved and non-uniformly loaded surfaces. The arc zones will now be open rupture zones with mixed boundary conditions. If an approximation is used where all zone elements are bounded by full circle arcs the rigid bodies might still be called simple, being bounded by straight lines and circle arcs with a reasonably simple variation of σ_n and τ_{nt} with the arc length along all boundaries. Another calculation method must be used in this case, however, since there is no longer a simple connection between the bounding circle arcs and the movement components of the bodies, cf. Sec. 435.

424 Straight Radial Zones and Band Zones

Radial zones with straight radial slip lines are closed rupture zone elements with mixed boundary conditions having a sufficiently simple form so that the movement conditions can easily be satisfied. They can therefore be considered as simple zone elements although they belong to a class of more complicated rupture zones.

They are used in two essentially different forms. In the first form such a zone separates two rigid bodies of clay which are both sliding upon the same (unmoving) rigid body, from which they are separated by means of line ruptures.

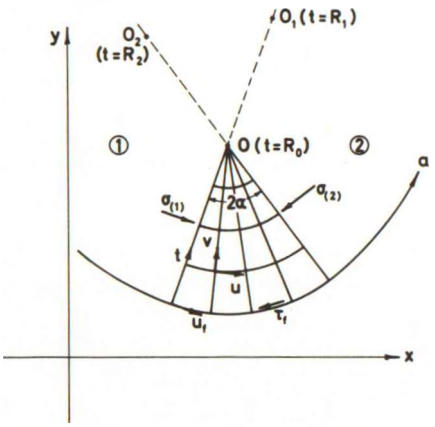

Fig. 42 R: Simple Radial Zone Separating Two Rigid Bodies (No. 1 and 2) Sliding Upon the Same Unmoving Body.

An example of this is shown in Fig. 42 R. In this figure the radial slip lines are formally considered to be b-lines, in which case $\tau_f = c$. The opposite case is obtained by taking $\tau_f = -c$.

Since $\frac{\partial m}{\partial s_b} = 0$ it is seen that $v = 0$ identically in the whole zone, so that u must be a constant along all a-lines. If t represents the distance from the boundary slip line we must have:

$$u = u_f - tr_z \qquad (4272)$$

where u_f is the sliding velocity along the boundary slip line, and r_z is the rotation of one of the rigid bodies (f. inst. No. 1).

It follows that the rotation must be the same for the other rigid body, i.e.

$$r_{z1} = r_{z2} \tag{4273}$$

The two radii to the line ruptures must therefore also be the same, $R_1 = R_2 = \frac{u_f}{r_z}$. Besides, since the deformation work must be positive everywhere in the zone:

$$\begin{aligned} 2\tau_f \epsilon &= \tau_f \left(\frac{\partial u}{\partial t} + \frac{u}{R_o - t}\right) \\ &= \tau_f r_z \frac{R_1 - R_o}{R_o - t} \\ &\rightarrow \tau_f \frac{u_f}{R_o - t} \qquad \text{for } r_z \rightarrow 0 \end{aligned} \tag{4274}$$

where R_o is the radius of the radial zone, we find that the product $r_z(R_1 - R_o)$ must have the same sign as τ_f. The same is true for u_f in order that the sliding along the boundary slip line shall have the correct sign.

Thus, R_o being always positive, for τ_{f1} positive we must have u_f positive, and R_1 and $R_1 - R_o$ must both have the same sign as r_z. This means that either $r_z > 0$, $R_1 \geq R_o$ or $r_z < 0$, $R_1 \leq 0$.

The radial zone is used as a simple zone element in kinematically admissible solutions with possible zones. The solutions will rarely be possible, or even quasi possible, so the energy method will normally have to be used. The contribution of the zone to the deformation work is:

$$\begin{aligned} W_R &= R_o \left[\sigma_{(1)} - \sigma_{(2)}\right] u_m \\ &= 4 \alpha \tau_f R_o \left(u_f - \tfrac{1}{2} R_o r_z\right) \\ &= 4 \alpha \tau_f r_z R_o \left(R_1 - \tfrac{1}{2} R_o\right) \end{aligned} \tag{4275}$$

where $\sigma_{(1)}$ and $\sigma_{(2)} = \sigma_{(1)} - 4 \tau_f \alpha$ are the normal stresses along the radial zone boundaries (2α being the centre angle) and $u_m = u_f - \frac{1}{2} R_o r_z$ is the velocity at the midpoint of these boundaries.

As an example the simple line rupture shown in Fig. 42 I may be modified by means of a radial zone with its vertex at B, cf. Fig. 42 S. In this way one further parameter (the centre angle 2α) is introduced. Three extra conditions, viz. the three equilibrium equations for the free rigid body of

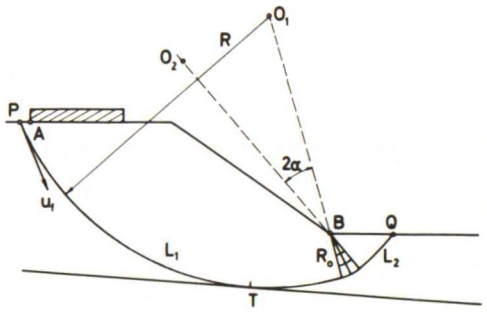

Fig. 42 S: Stability Investigation Using Circular Line Ruptures With a Simple Radial Zone.

clay between B and Q, are also introduced, so we have no longer a quasi possible solution, but only a kinematically admissible one. Nevertheless, the approximation is of course improved by the introduction of a further parameter. The improvement may be quite great, especially if the original line rupture intersects the surface at Q under a small angle (which is frequently the case in investigations of slope stability).

In the same way the approximation of an ordinary line rupture figure A (Fig. 42 J, especially for high, positive values of ρ, and rough walls) may be improved by the introduction of a radial zone. The resulting rupture figure may be called AfPfA. The calculation of such rupture figures, possibly with more than one radial zone to the same line rupture, is straightforward with the use of (4275). In the example of Fig. 42 S the total deformation work is the contribution from the radial zone plus $\tau_f u_f (L_1 + L_2)$ from the two line ruptures.

The radial zone might be used as a zone with approximate movement conditions. This means that the condition (4273) is neglected, being replaced by the weaker condition that the volume of the zone shall remain constant. It is seen to be equivalent to the condition that the mean velocity u_m on the two radial boundary slip lines shall be the same, i. e.

$$u_m = r_{z1} (R_1 - \tfrac{1}{2} R_o) = r_{z2} (R_2 - \tfrac{1}{2} R_o) \qquad (4276)$$

The deformation work is still given by (4275), on the form $4 \alpha \tau_f R_o u_m$, but the sliding velocity $u_f = u_m + \tfrac{1}{2} R_o r_z$ will now be different for the two line ruptures.

On this form the radial zone introduces yet another parameter (on dimensionless form: $\frac{(r_{z1} - r_{z2}) R_o}{u_m}$), and is still very simple to calculate. A better approximation with the same number of parameters is obtained by the use of radial zones with curved radial slip lines. The solution may in this way be made admissible with possible zones, cf. Sec. 431.

Another and a more complicated use of the simple radial zones is obtained when the two rigid bodies bounding the radial slip lines are supposed

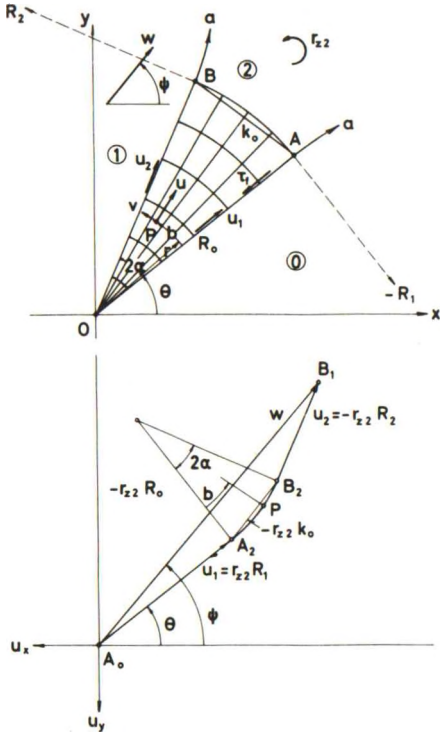

Fig. 42 T: Simple Radial Zone Separating a Translating Rigid Body (No. 1) from an Unmoving Body (No. 0). Velocity Conditions.

to be translated relative to each other whereas the third body is rotated. Without loss of generality one of the bodies which are translated can be assumed to be unmoving. Under this assumption the velocity distribution in the zone will be as shown in Fig. 42 T.

Assume that the rigid body No. 0 is unmoving, and that body No. 1 has the translation w forming the angle ψ with the horizon in relation to this body. The third rigid body, No. 2, has the rotation r_{z2} in relation to the two other bodies.

The radial zone has the centre angle 2α, its lower radial slip line forming the angle θ with the horizon. The sliding velocities along the radial boundary slip lines (assumed to be a-lines, but with shear stresses τ_f which may, formally, be negative) are u_1, between the zone and body No. 0, and u_2, between the body No. 1 and the zone. Since $\frac{\partial m}{\partial s_a} = 0$ in the zone, $\frac{\partial u}{\partial s_a}$ will also be zero, so u must be constant along all a-lines. v = 0 along the boundary slip line OA to body No. 0, so it can be concluded that v is also constant along all a-lines. Consequently u and v, and therefore also u_x and u_y, are functions of b only. For the sake of simplicity we take $m_o = \theta$ so that b is the centre angle between OA and the considered a-line.

The image zone in the hodograph plane is also shown in Fig. 42 T. Notice that the image curve A_2B_2 must be a circle arc in order that the body No. 2 shall remain rigid. The boundary slip lines OA and OB are continued beyond the points A and B as circle arcs, the radii of which, R_1 (negative) and R_2 (positive) are given when u_1, u_2, and r_{z2} are known:

$$R_1 = \frac{u_1}{r_{z2}}$$
$$R_2 = -\frac{u_2}{r_{z2}} \tag{4277}$$

If $u_1 = 0$ and/or $u_2 = 0$ the corresponding line rupture will have a vanishing radius, i.e. it will not be developed.

For any point P in the radial zone we find:

$$u_x = -u_1 \cos\theta + 2 r_{z2} R_o \sin\frac{b}{2} \cos(\theta + \frac{b}{2})$$
$$u_y = -u_1 \sin\theta + 2 r_{z2} R_o \sin\frac{b}{2} \sin(\theta + \frac{b}{2}) \tag{4278}$$

Since $m = \theta + b$ this gives:

$$u = -u_x \cos m - u_y \sin m$$
$$= u_1 \cos b - 2 r_{z2} R_o \sin\frac{b}{2} \cos\frac{b}{2}$$
$$v = u_x \sin m - u_y \cos m \tag{4279}$$
$$= -u_1 \sin b + 2 r_{z2} R_o \sin\frac{b}{2} \sin\frac{b}{2}$$

If the radius vector to P is called r we find (all derivatives relative to s_a being zero):

$$2\epsilon = \frac{\partial u}{\partial s_b} - v\frac{\partial m}{\partial s_b} = \frac{1}{r}(\frac{\partial u}{\partial b} - v) = -\frac{R_o}{r} r_{z2} \tag{4280}$$

It follows that r_{z2} must have the opposite sign of τ_f. Besides, u_1 and u_2 should have the same sign as τ_f.

From Fig. 42 T we find:

$$u_1 \cos\theta - r_{z2} k_o \cos(\theta + \alpha) + u_2 \cos(\theta + 2\alpha) = w \cos\psi$$
$$u_1 \sin\theta - r_{z2} k_o \sin(\theta + \alpha) + u_2 \sin(\theta + 2\alpha) = w \sin\psi \tag{4281}$$

This is used to find ψ (and $\frac{w}{r_{z2} R_o}$) when θ, α, $-\frac{R_1}{R_o} = -\frac{u_1}{r_{z2} R_o}$, and $\frac{R_2}{R_o} = -\frac{u_2}{r_{z2} R_o}$ are known. If instead w and ψ are given, and θ, α, and $\frac{r_{z2} R_o}{w}$ are chosen, we find:

$$\frac{u_1}{w} = \frac{\sin(\theta + 2\alpha - \psi)}{\sin 2\alpha} + \frac{r_{z2} R_o}{w} \tan\alpha$$

$$\frac{u_2}{w} = \frac{\sin(\psi - \theta)}{\sin 2\alpha} + \frac{r_{z2} R_o}{w} \tan\alpha \qquad (4282)$$

Finally, α, $\frac{u_1}{w}$, and $\frac{u_2}{w}$ may be chosen, in which case $\psi - \theta$ and $\frac{r_{z2} R_o}{w}$ may be found from:

$$\frac{\sin(\theta - \psi + \alpha)}{\sin\alpha} = \frac{u_1 - u_2}{w}$$

$$\frac{r_{z2} R_o}{w} = \frac{1}{2\sin\alpha}\left[\frac{u_1 + u_2}{w}\cos\alpha - \cos(\theta - \psi + \alpha)\right] \qquad (4283)$$

The two line ruptures beyond A and B may be connected in the usual way by normal points (type C) to surface zones, possibly continued by radial zones, wall zones, squeezing zones etc. If R = 0 (u_1 or u_2 = 0) so that the line rupture does not exist, the corresponding point may be a discontinuity point (final point of the type Q) to a surface zone, possibly continued as mentioned above.

In this way a possible rupture figure is obtained. Suppose *f. inst.* that the rigid body No. 1 is attached to an external rigid body which is bound to translate with a known velocity w in a known direction ψ. The four parameters α, $\frac{u_1}{w}$, $\frac{u_2}{w}$, and R_o will then define the radial zone, θ and r_{z2} being determined by (4283), after which R_1 and R_2 can be found from (4277). The surface zones can now be constructed, the final points being defined by the known line ruptures (and/or discontinuity points). Thus, four surface parameters can be found by purely geometrical calculations corresponding to the four initial parameters.

If the statically determined zones are very complicated the opposite construction might be performed: A set of four surface parameters are chosen, defining in this way the two final points. By a relatively simple geometrical construction the rupture zone OAB (Fig. 42 T) can now be determined, after the estimate of one parameter if both points are assumed to be of the type C (for example, the centre angles $2\alpha_1$ and $2\alpha_2$ may be chosen for the two line ruptures, subject to the condition that OA = OB). This determines θ, α, $\frac{R_1}{R_o}$, and $\frac{R_2}{R_o}$, so that ψ can be checked by means of (4281). If this value checks, $\frac{w}{r_{z2} R_o}$ can be found by the same equations.

The initial parameters may be varied until the extreme solution is obtained. If the equilibrium method is used we have the following conditions:

1. If A and B are both discontinuity points ($u_1 = u_2 = 0$) there are only two free parameters, f.inst. α and θ. They are determined, together with the stress level in the radial zone f.inst. characterized by the value of σ at the point A, by means of the three equilibrium equations for the free rigid body No. 2.
2. If one of the points A and B is a discontinuity point we have three free parameters as against the three equilibrium equations. σ_A can be found directly by the stress equation along the known line rupture.
3. If both line ruptures exist the four free parameters (one of which is, strictly speaking, an extra parameter) are determined by the three equilibrium equations plus the stress condition that σ_A shall not be in contradiction when calculated along the two possible line rupture paths.

If the surface zones are sufficiently simple, f.inst. pure Rankine zones with straight slip lines, the calculation procedure may be simplified by the following considerations.

1. The rigid body No. 2 will now form a simple rigid body, and all the necessary calculations can be performed in terms of the geometry of this body. Defining all quantities f.inst. as shown in Fig. 42 U, which implies that k_o is used as the unit length, and that all centre angles α_o, α_1, and α_2 are taken as positive, it is seen that without loss of generality σ_o may be put equal to zero.

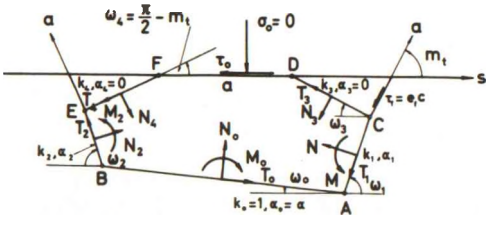

Fig. 42 U: Free Rigid Body of Clay in the Surface Zone Complex.

2. By simple geometry we have, defining:

$$m_t = \text{arc tan} \sqrt{\frac{\tau_f + \tau_o}{\tau_f - \tau_o}} \qquad (4284)$$

(τ_f being +c or -c according to whether the arc AC is in fact an a-line as supposed or not).

$$\omega_3 = \frac{\pi}{2} - m_t$$

$$\omega_1 = m_t + \alpha_1$$

$$\omega_o = \frac{\pi}{2} - m_t - 2\alpha_1 - \alpha_o \qquad (4285)$$

$$\omega_2 = \pi - m_t - 2\alpha_o - 2\alpha_1 - \alpha_2 = m_t + \alpha_2$$

$$\omega_3 = m_t + 2\alpha_1 + 2\alpha_o + 2\alpha_2 - \frac{\pi}{2} = \frac{\pi}{2} - m_t$$

so that we have the identity:

$$\alpha_o + \alpha_1 + \alpha_2 = \frac{\pi}{2} - m_t \qquad (4286)$$

when k_1 and k_2 are both different from zero.

3. The stress condition gives:

$$\sigma_C = \sigma_D = \tau_f \sin 2m_t$$

$$\sigma_A = \tau_f (\sin 2m_t - 4\alpha_1)$$

$$\sigma_B = \tau_f (\sin 2m_t - 4\alpha_1 + 4\alpha_o) = \tau_f (-\sin 2m_t + 4\alpha_2) \qquad (4287)$$

$$\sigma_E = \sigma_F = \tau_f (\sin 2m_t - 4\alpha_1 + 4\alpha_o - 4\alpha_2) = -\tau_f \sin 2m_t$$

so that we have also:

$$-\alpha_o + \alpha_1 + \alpha_2 = \frac{1}{2} \sin 2m_t \qquad (4288)$$

when k_1 and k_2 are both different from zero.

By comparison between (4286) and (4288) we find

$$2\alpha_o = \frac{\pi}{2} - m_t - \frac{1}{2} \sin 2m_t$$

$$2(\alpha_1 + \alpha_2) = \frac{\pi}{2} - m_t + \frac{1}{2} \sin 2m_t \qquad (4289)$$

If f. inst. $k_2 = 0$, ω_2 and α_2 will not be defined. The relation between σ_B and σ_E implied in (4287) will therefore not exist, so that (4286) and (4288-9) cannot be used in this case. α_1 and α_o may then be chosen independently. If also $k_1 = 0$, α_1 and ω_1 will not be defined either. The only centre angle is α_o which can be chosen freely.

4. The calculations may now proceed as follows:
   If $k_1 \neq 0$ and $k_2 \neq 0$, α_o is taken from (4289), and a value for α_1 is estimated. α_2 is then also given by (4289). All angles being now known, the five unknown lengths k_1, k_2, k_3, k_4, and a are determined by two geometrical and three equilibrium conditions, i.e. five equations, four of which are linear and the fifth quadratic in the unknown lengths. Under the above assumption k_1 or k_2 may turn out to be negative which indicates that the calculations should be performed assuming one of them to be zero.

   If $k_2 = 0$, α_1 may be estimated. The remaining five quantities k_2, k_3, k_4, a, and α_o are determined by the same equations as above. They are not linear in α_o, however, so in practice a value for this quantity is assumed, after which the four linear equations are used to find the lengths. Finally, the fifth (moment) equation is used to check the estimate of α_o. If $k_1 = k_2 = 0$, ω_o must be estimated. k_3, k_4, a, σ_A, and α_o can then be found by the same procedure as above. Finally, in all cases the scale of figure 42 U is determined together with θ and R_o by a construction of the full rupture figure (one geometrical condition, the total distance from O to the surface being known). ψ may now be checked by means of (4281). If necessary the estimated values of α_1 (or α_2) or ω_o must be changed by trial and error until ψ is correct.

5. If one of the chord lengths k_1 or k_2 have been estimated equal to zero initially, it must be checked by means of the stress condition for discontinuity points that this assumption is correct.

The rupture figure obtained in this way is a possible solution, which may be used to replace the quasi-possible one consisting of a single line rupture which intersects the surface under an angle that is not statically possible.

If the surface is straight and unloaded the improvement in accuracy from the simple line rupture to this rather more complicated rupture figure is not very great. Calculations for the case with $\tau_o = 0$ have shown that the line rupture is at most about 2% on the unsafe side. The force resultant normal to the line rupture may deviate about 0.03 c L, where L is the length of the line rupture, from the correct value. However, in problems with more complicated surface conditions, especially if the line rupture is forced to pass through or near an extruding corner or bulge, the difference might be much greater.

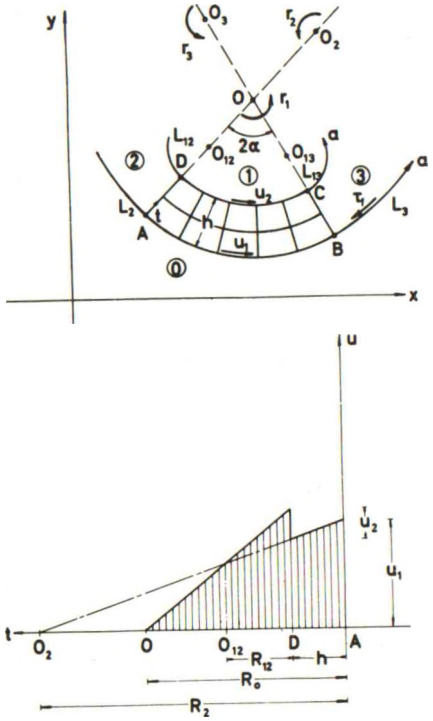

Fig. 42 V: Arc Zone With Line Ruptures Separating 4 Rigid Bodies. Velocity Distribution.

The band zone shown in Fig. 42 V may be analysed in the same way as are the two radial zones considered in this section. It is bounded by four rigid bodies, No. 0-3, the first one of which is assumed to be unmoving. The rotations for the three other bodies are called r_1, r_2, and r_3. The zone slides upon the body No. 0 (sliding velocity u_1 with the same sign as τ_f), and the body No. 1 slides upon the zone (sliding velocity u_2).

As in Fig. 42 R we have $v = 0$ everywhere in the zone and u constant along all a-lines. The distribution of u as a function of t, which is the distance from the line rupture L_2, is shown for the line AO in Fig. 42 V. Defining R_o as the distance OA, and R_1 as OD (the width of the zone $h = R_o - R_1$), the other radii having the same indices as the corresponding line ruptures:

$$R_2 = \frac{u_1}{r_2}$$

$$R_3 = \frac{u_1}{r_3}$$

$$R_{12} = \frac{u_2}{r_1 - r_2} \qquad (4290)$$

$$R_{13} = \frac{u_2}{r_1 - r_3}$$

we find that the movement conditions require that $r_2 = r_3$, and therefore $R_2 = R_3$, $R_{12} = R_{13}$. Besides u_1, u_2, and $r_1 - r_2$ should all have the same sign as τ_f. The zone contributes by the amount

$$W_d = 2 \alpha \tau_f [2 h (u_1 - \tfrac{1}{2} r_2 h) + R_1 u_2] \qquad (4291)$$

to the deformation work.

In the form shown in Fig. 42 V with 4 line ruptures the figure is determined by 4 dimensionless parameters (f. inst. α, $\frac{h}{R_o}$, $\frac{R_2}{R_o}$, and $\frac{R_{12}}{R_o}$) plus 4 quantities giving the scale, position, and orientation of the zone in the x,y-plane (f. inst. x_A, y_A, k_{AB}, and ω_{AB}). Against the 8 parameters there are 8 equilibrium and/or movement conditions for the 3 rigid bodies (plus the energy equation used to find W or f), and 3 stress conditions for the four line ruptures. The rupture figure is therefore only kinematically admissible. It is not normally used in this way unless the partitioning into 3 moving rigid bodies of clay is forced by the boundary conditions (f. inst. through the existence of two or three external rigid bodies with given (different) movement components). If the clay bodies are free a single line rupture will frequently give an almost equally good approximation.

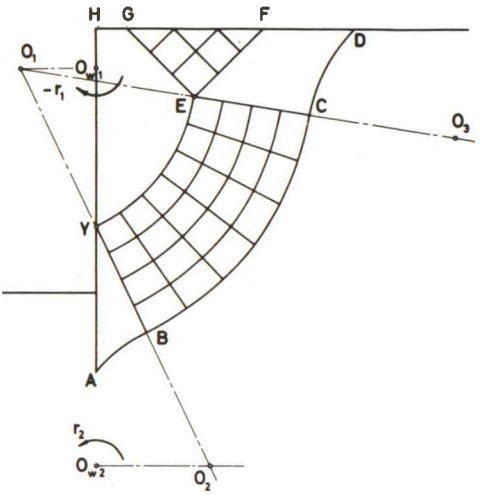

Fig. 42 W: Approximate Solution with a Simple Arc Zone for a Wall with a Yield Hinge.

In Fig. 42 W is shown an example of a failure problem where this rupture figure may be useful. Assume a sheet pile wall AH with a yield hinge Y and with known rotation points O_{w1} and O_{w2} for the two wall parts (the ratio $\frac{r_1}{r_2}$ between the two rotations will then also be known). By the construction of the arc zone BCEY (corresponding to ABCD in Fig. 42 V with $\tau_f = -c$ and $u_2 = 0$) a rupture figure is obtained which in the simplest possible way permits the given boundary movements. It has only two free parameters (f. inst. the value of λ for O_2, and the centre angle $2\alpha = \angle\, YO_1E$), the distance O_1O_3 being equal to O_1O_2. The line rupture CD may be an XfR construction if the tangent angle at D is small enough.

Against the 2 parameters there are 1 equilibrium condition for each of the two bodies ABY and YEGH (supposed to be sliding upon the wall), and 3 equilibrium conditions for the body CDFE. Since E is a discontinuity point there is no stress condition.

The same rupture figure may also be used for the problem of a partly unsupported earth front, the clay above Y being supposed to slip away from the wall (assuming that negative normal pressures cannot obtain between the wall and the clay). In this case the position of Y and the value of ρ for O_1 are also unknown parameters (O_{w2} is the rotation centre for the wall), so the rupture figure has a total number of 4 unknown parameters. There are now 7 equilibrium conditions, the body YEGH being in fact a free rigid body of clay.

By combinations of the zone elements considered in this and in the preceding sections extremely complicated rupture figures may be obtained. Thus, an arc zone construction may be used at Y in Fig. 42 W (to remove the stress singularity at this point), and the line ruptures CD and AB may be replaced by a BfR construction (or a radial zone connected to two surface zones as in Fig. 42 T) to increase the number of parameters. Finally, the rupture figure may be made possible by assuming the radial slip lines to be curved. It is seen that some of these modifications cannot be computed by the methods of simple rupture figures.

425 Systems of Line Ruptures

As an alternative to kinematically admissible rupture figures with possible zones one may in some cases use purely quasi-possible solutions consisting of line ruptures only. When the construction with line ruptures meeting in the clay is used extremely flexible rupture figures may be obtained, which are able to satisfy even rather complex boundary movement conditions caused by the existence of several external rigid bodies.

The calculation procedure is relatively simple in all cases, the most difficult problem being to represent the external movement conditions by sufficiently simple geometrical conditions for the line rupture system.

As an example consider the rupture figure shown in Fig. 42 X which can be used to calculate the bearing capacity of an excentrically loaded foundation under the clay surface, cf. Sec. 345 and Fig. 34 N, Ex. 34 a. Notice that when line ruptures are used it will not matter very much whether the surface is irregular and non-uniformly loaded. There may also be internal boundaries, and the clay may even be non-homogeneous without any serious complications in the calculations.

If such rupture figures are calculated semi-graphically, corresponding to what is usually done in stability investigations, the basic condition is giv-

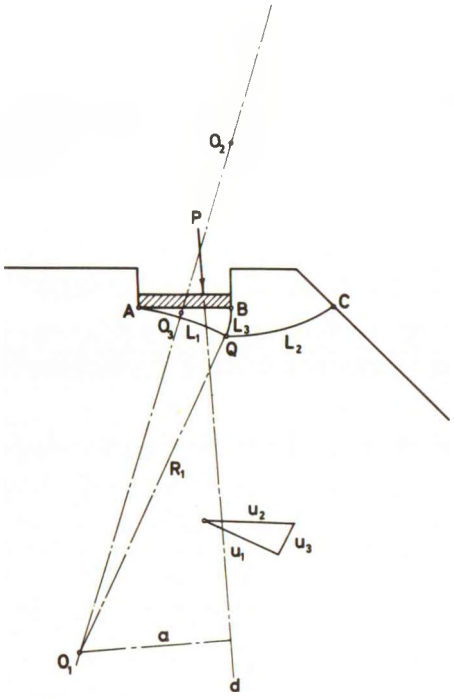

Fig. 42 X: One-Sided Bearing Capacity Problem Solved by a System of 3 Line Ruptures.

en by the fact that the centres (O_1 - O_3 on Fig. 42 X) of line ruptures meeting at a point shall be located on a straight line. Thus, a rupture figure of the type shown in Fig. 42 X may be constructed by the choice of 5 parameters, f. inst. the coordinates (x_1, y_1) and (x_3, y_3) to the centres O_1 and O_3 plus one parameter defining the position of O_2 on the line O_1O_3.

For each choice of parameters the sliding velocities u_1, u_2, u_3 can be constructed in any convenient scale. In the hodograph plane they must form a closed triangle when they are drawn parallel to the slip line directions through the intersection point Q. The lengths L_1, L_2, L_3 of the line ruptures may also be measured on the figure. If the line of attack d for the resulting foundation load P is known, P will now be given by the work equation:

$$P\, u_d = c\,(u_1 L_1 + u_2 L_2 + u_3 L_3) \tag{4292}$$

u_d, the velocity component of the foundation along d, is given by the identity:

$$-r_1 = \frac{u_d}{a} = \frac{u_1}{R_1} \tag{4293}$$

so that

$$u_d = \frac{a}{R_1}\, u_1 \tag{4294}$$

In (4293) r_1 is the rotation r_z for the rigid body above the line rupture No. 1. Inserting (4294) in (4292) we find:

$$P = \frac{c\, R_1}{a}\left(L_1 + L_2 \frac{u_2}{u_1} + L_3 \frac{u_3}{u_1}\right) \tag{4295}$$

The 5 initial parameters can now be changed until a minimum value for P is found.

The equilibrium method can also be used since the rupture figure is quasi-possible. The stress condition (3447), or $\sigma_{(1)} = \sigma_{(2)} = \sigma_{(3)}$ if L_3 is of the same slip line family as L_1 and L_2, must then be used at the point Q. However, it will probably not give a good computation economy to combine a semi-graphical method with calculations by the equilibrium method.

Alternatively, a purely numerical method may be used. This is at any rate necessary when the calculations are performed on a computer. One might characterize each line rupture by the parameter set k, ω, α, u_f (the sign of u_f defining the sign of τ_f), or by the set ψ, L, $n = \frac{1}{R}$, u_f, in both cases referring to a given starting point. The first mentioned set has the advantage that it contains directly the quantities that are used by the equilibrium method. It also corresponds to what is done in (open) rupture zones when the method of chord lengths is used.

In Fig. 42 X we have a total number of 12 parameters, subject to 3 geometrical conditions (2 from the position of Q, and 1 from the condition that C shall be located on a given curve), 2 velocity conditions at Q, cf. (3437), and 1 at A (u_d being assumed to be known), and 1 movement condition for the rigid bodies, cf. (3439). The remaining 5 free parameters are determined either by the extremum method, using that for each circle arc:

$$L = k \frac{\alpha}{\sin \alpha} \qquad (4296)$$

$$\rightarrow k \quad \text{for} \quad \alpha \rightarrow 0$$

or by the equilibrium method, using also (3420) and (3447).

The second set has the advantage that the line rupture system can be constructed in a more natural way from the given (or estimated) movements of the external rigid bodies, without the introduction of unnecessary extra parameters. Thus, in Fig. 42 X one might proceed as follows:

1. Assume a set w_x, w_y, r_z of movement components for the foundation. From this set u_d is directly given together with ψ_1, n_1, and u_{f1} for L_1 (referred to the point A).
2. A set ψ_3 and n_3 may now be chosen for L_3 (referred to the point B). The intersection point between the two circle arcs defined in this way is Q, which also defines L_1 and L_3.
3. ψ_2 (= β_2) is now chosen for L_2, referred to Q. u_{f2} and u_{f3} are now given by (3437), and n_2 by (3439). The rupture figure is now defined (apparently by means of 6 parameters, but w_x, w_y, r_z may be

multiplied by a common factor of proportionality without any change in the rupture figure or the result).

4. Instead of 2. and 3. above a set w_{xc}, w_{yc}, and r_{zc} may be chosen as the movement components for the rigid body of clay above L_2. This also determines ψ_3, n_3, and ψ_2 so the calculations proceed as before, but with a set of initial parameters even more directly connected to the general treatment of rigid body movements.

This calculation scheme contains two basic numerical operations. The first is the calculation of a set of parameters ψ, n, u_f for a line rupture through a given point P corresponding to the sliding between two rigid bodies of clay No. 1 and 2 with known movement components w_{x1}, w_{y1}, r_{z1} and w_{x2}, w_{y2}, r_{z2}. The solution is unique if the convention is adopted that the rigid body No. 2 should be in the positive direction of rotations relative to the positive direction on the line rupture, and if a direction ψ_{20} is given which is known to point into the body No. 2 (or ψ_{10} pointing into No. 1), cf. Fig. 42Y.

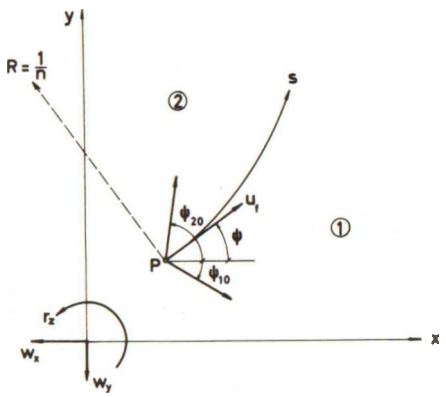

Fig. 42Y: Line Rupture Arc Separating Two Rigid Bodies with Known Movement Components.

One has evidently:

$$u_f \cos \psi = u_{x1} - u_{x2}$$

$$= w_{x1} - w_{x2} + y\,(r_{z1} - r_{z2}) \qquad (4297)$$

$$u_f \sin \psi = u_{y1} - u_{y2}$$

$$= w_{y1} - w_{y2} - x\,(r_{z1} - r_{z2})$$

The principal value of ψ ($-\pi < \psi \leq \pi$) may be found from these equations, after which an integer multiple of π is added or subtracted until $\Delta\psi = \psi_{20} - \psi$ (or $\psi - \psi_{10}$) is in the interval $0 \leq \Delta\psi < \pi$. u_f is positive or negative according to whether an even or an uneven multiple of π has been added to ψ.

Besides

$$n = \frac{1}{R} = \frac{r_{z2} - r_{z1}}{u_f} \qquad (4298)$$

This quantity can only be singular when $u_f = 0$ which implies that both right hand sides of (4297) are zero. In this case the two rigid bodies cannot slide relative to each other on a line rupture through P, since this point is their relative point of rotation.

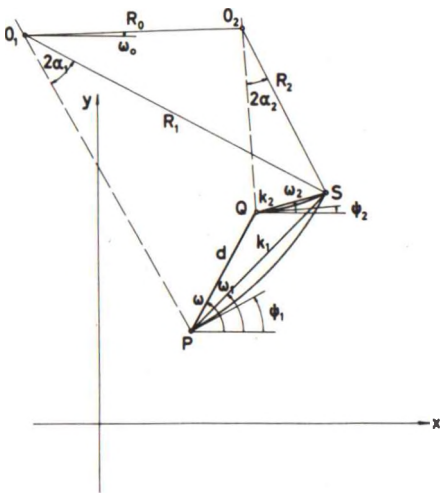

Fig. 42 Z: Intersection Between Two Line Ruptures With Known Parameters.

The second basic operation consists in the construction of the intersection point S between two curves given by the parameter sets x_1, y_1, ψ_1, n_1 (corresponding to the point P) and x_2, y_2, ψ_2, n_2 (point Q), cf. Fig. 42 Z. In some applications it may be an advantage to represent the line PQ by its length d and its inclination ω with the a-axis.

If n_1 and n_2 are both different from zero the simplest procedure is to use the radii $R_1 = \frac{1}{n_1}$ and $R_2 = \frac{1}{n_2}$. Let the line between the centres O_1 and O_2 have the length R_o and the inclination ω_o with the x-axis:

$$\begin{aligned} R_o \cos \omega_o &= x_2 - x_1 - R_2 \sin \psi_2 + R_1 \sin \psi_1 \\ &= d \cos \omega - R_2 \sin \psi_2 + R_1 \sin \psi_1 \\ R_o \sin \omega_o &= y_2 - y_1 + R_2 \cos \psi_2 - R_1 \cos \psi_1 \\ &= d \sin \omega + R_2 \cos \psi_2 - R_1 \cos \psi_1 \end{aligned} \qquad (4299)$$

From the triangle $O_1 S O_2$ we then find by simple geometry:

$$\begin{aligned} \sin (\psi_1 + 2\alpha_1 - \omega_o) &= \frac{R_o^2 + R_1^2 - R_2^2}{2 R_o R_1} \\ \sin (\omega_o - \psi_2 - 2\alpha_2) &= \frac{R_o^2 - R_1^2 + R_2^2}{2 R_o R_2} \end{aligned} \qquad (42100)$$

which defines α_1 and α_2, and by this f.inst. $L_1 = 2 R_1 \alpha_1$, $k_1 = 2 R_1 \sin \alpha_1$, and $\omega_1 = \psi_1 + \alpha_1$. Notice that α_1 and α_2 should have the same signs as R_1 and R_2 (i.e. as n_1 and n_2), respectively.

As a check the formulae

$$k_1 = d \frac{\sin(\omega - \psi_2 - \alpha_2)}{\sin(\psi_1 - \psi_2 + \alpha_1 - \alpha_2)}$$
$$k_2 = d \frac{\sin(\omega - \psi_1 - \alpha_1)}{\sin(\psi_1 - \psi_2 + \alpha_1 - \alpha_2)} \qquad (42101)$$

which are always valid, may be used.

If $n_2 = 0$ (or $n_1 = 0$) the formulae (4299-100) cannot be used, because R_2 (or R_1) will then become infinite. Correspondingly, α_2 (or α_1) will be identically zero ($k_2 = L_2$, or $k_1 = L_1$). By projection on the normal to the straight line QS (or PS) one gets instead:

$$\cos(\psi_1 - \psi_2 + 2\alpha_1) = \cos(\psi_1 - \psi_2) - n_1 d \sin(\omega - \psi_2)$$

or (42102)

$$\cos(\psi_1 - \psi_2 - 2\alpha_2) = \cos(\psi_1 - \psi_2) + n_2 d \sin(\omega - \psi_1)$$

respectively.

From these formulae α_1 or α_2 is found, and k_1, k_2 are given by (42101). Finally, if n_1 and n_2 are both zero (42101) can be used directly. The above formulae are of course also used when the intersection point between a line rupture and a surface is sought.

By an extension of the above procedure very complicated rupture figures may be built up, consisting of line rupture chains bounding in principle any number of rigid bodies of clay. If the movement components for all rigid bodies are specified (i.e. given or estimated as initial parameters) the rupture figure may be constructed successively, each line rupture (except the last one) passing through a known point (or touching a known internal boundary). In some cases free line ruptures may also be used, their defining point being also governed by a free parameter. As an example a line rupture chain may be used to keep the failure surface as long as possible in a thin soft clay layer, cf. Fig. 42 AA.

In this example the rupture figure may be constructed graphically by means of the centres $O_1, \ldots, O_7$ (14 coordinates subject to 3 geometrical conditions), or by the 12 movement components for the 4 rigid bodies of clay (1 arbitrary factor of proportionality being free). It is geometrically determined when f. inst. the points A, B and D are assumed to be known, if it is also given that the line rupture No. 5 must touch the lower internal boundary. A may also be a free point if the same condition is imposed on

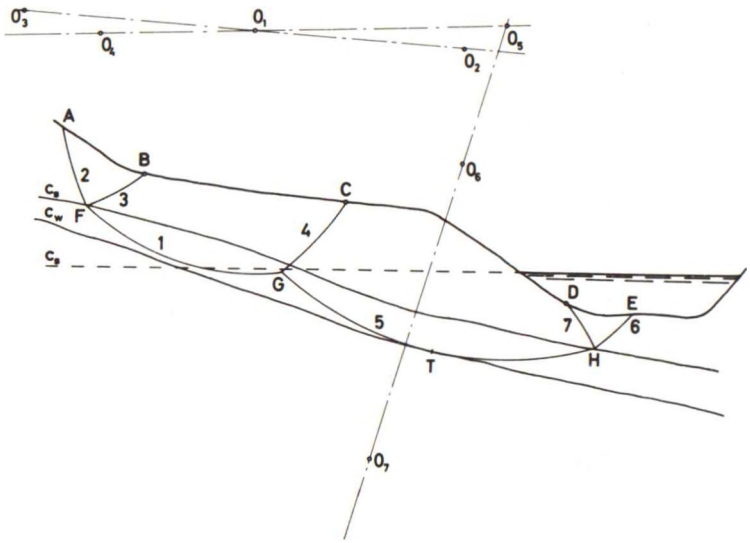

Fig. 42 AA: Stability Investigation Using a System of Line Ruptures.

the line rupture No. 1. If B and D are not reentrant corners or load discontinuities they should also be considered as free, thereby introducing two further parameters (x or s for these points). It is not an essential condition (but it simplifies the calculation work) that f. inst. the branch points F and H should be located on an internal boundary.

The same type of rupture figures is used in combined problems of earth pressure and stability (Sec. 522 and 534). If there are no internal boundaries the accuracy may some times be improved in a simple way by the replacement of some of the line ruptures by radial zones (Fig. 42 S) or by arc zones (Fig. 42 V). Notice, however, that it is only straight radial zones and circular arc zones that are as easy to calculate as a line rupture. The rupture figure may of course also be combined with surface zones as in the simple rupture figures AaR, XfR, AaWPR etc.

426 Kinematically Determined Rupture Zones

One special case exists (apart from the simple radial and arc zones hitherto considered) in which a closed rupture zone with mixed boundary conditions is completely determined by the movement conditions. It is a radial zone with curved radial slip lines, where one of the moving rigid bodies

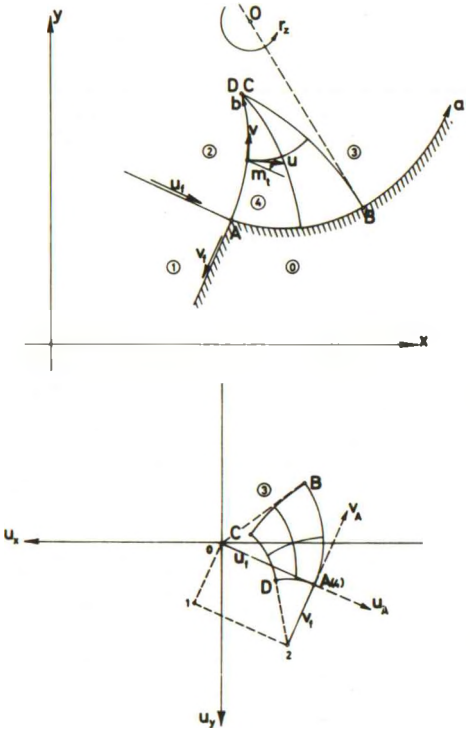

Fig. 42 AB: Kinematically Determined Rupture Zone (Rigid Body No. 2 Translated). Image in the Hodograph Plane.

of clay is translated, whereas the other one is rotated. This type of rupture zones was mentioned by Sokolovski in a colloquium (not published) at the Fifth International Conference on Soil Mechanics and Foundation Engineering, Paris 1961.

The most general case is shown (sketched) in Fig. 42 AB. In relation to the unmoving body No. 0, the body No. 2 is translated by means of the sliding velocities u_f and v_f along the two slip lines AB and AC. In practice we will usually have either $v_f = 0$, i.e. the b-line below A is not developed, or the point A will be a transition point, so the domain No. 1 will be a rupture zone, possibly of the same kind as No. 4.

Along the boundary slip line AD we have, measuring the angle m_t from the tangent direction of the a-line at the point A:

$$u = u_f \cos m_t - v_f \sin m_t = -\frac{\partial v}{\partial m_t} \tag{42103}$$

according to (3125). From this we find

$$v = -u_f \sin m_t + v_f (1 - \cos m_t) \tag{42104}$$

because $v = 0$ for $m_t = 0$.

Therefore the projections u_A and v_A on the u_f- and v_f-direction, respectively, measured from the velocity at the point A, are:

$$\begin{aligned} u_A &= u \cos m_t - v \sin m_t - u_f = -v_f \sin m_t \\ v_A &= u \sin m_t + v \cos m_t = -v_f (1 - \cos m_t) \end{aligned} \tag{42105}$$

This means that the image curve of the slip line AD in the hodograph plane is a circle arc with the radius v_f, and is touching the u_A-axis at the

point $u_A = v_A = 0$ (cf. Fig. 42 AB). For the boundary curve AB to the unmoving body No. 0 we have $u = u_f$, $v = 0$, and therefore, according to (42105):

$$u_A = -u_f (1 - \cos m_t)$$
$$v_A = u_f \sin m_t \qquad (42106)$$

Its image curve in the hodograph plane is also a circle arc. It has the radius u_f, touching the v_A-axis at the point $u_A = v_A = 0$.

Thus, the two boundary curves AB and AD are known in the hodograph plane. Therefore the image zone ABCD can be constructed when the two parameters $m_{t(B)}$ and $m_{t(D)}$ are known (or estimated). It is a zone generated from two circle arcs (second initial value problem type) in much the same way as the secondary zone used to find k_1 and k_2 on Fig. 42 H. It may be calculated f. inst. by the method of chord lengths on w_a and w_b instead of k_a and k_b.

When the zone has been calculated in the hodograph plane we may use that the configuration OBC is similar to the same figure in the x,y-plane, with the scale factor r_z (but is turned through an angle $\frac{\pi}{2}$ in the direction of r_z), cf. Sec. 337. The origin point O in the hodograph plane is therefore known to be similarly positioned in relation to the image curve BC, as the rotation point O for the clay body No. 5 in relation to the slip line BC. This determines the line rupture beyond the point B, when the zone has been constructed.

The radial zone ABCD can be calculated from the known slip line BC and the vertex point C = D. It is therefore determined, except for a scale factor and a possible rotation to bring it into the correct position in the x,y-plane, when the three parameters $\frac{v_f}{u_f}$, $2\alpha = m_{t(B)}$, and $2\beta = m_{t(D)}$ have been estimated.

In practice this rupture zone may be used in one-sided or in two-sided rupture figures. In the first case (Fig. 42 AC) the straight line rupture OA is assumed to be known (w_x, w_y, and $r_z = 0$ are known, or are estimated for the rigid body No. 1). The parameter $\frac{v_f}{u_f}$ is known to be zero, so the zone can be constructed when the parameters 2α and 2β are estimated. In the hodograph plane of Fig. 42 AB the arc AD degenerates to a point. One must therefore construct first a radial zone generated by the known arc AB (radius u_f, centre angle 2α) with the point A as vertex point and with the ver-

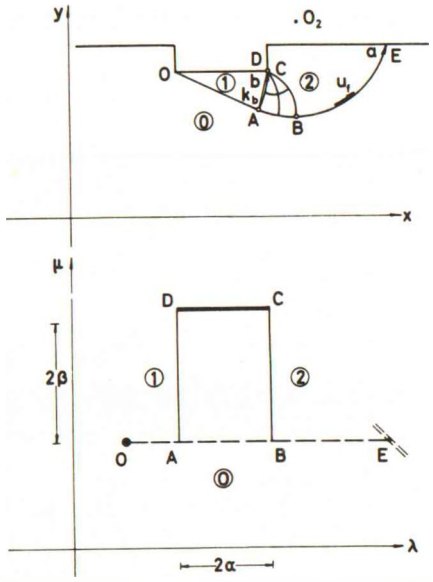

Fig.42AC: Approximate Rupture Figure with One Kinematically Determined Radial Zone (For a Translated Foundation).

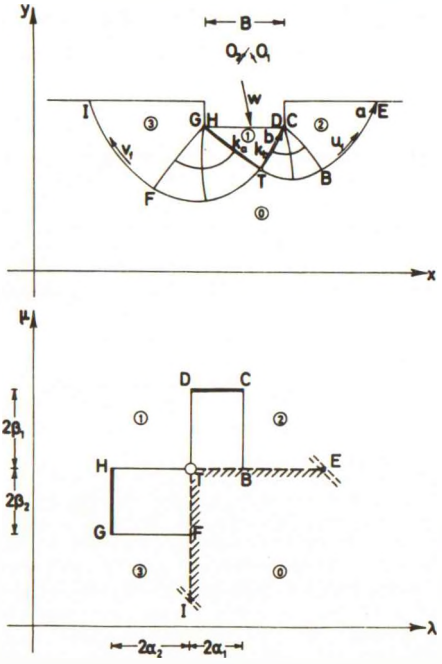

Fig. 42AD: Approximate Rupture Figure with Two Kinematically Determined Radial Zones (Two-Sided Failure of a Translated Foundation).

tex angle 2β. Upon the resulting arc BC a new radial zone is constructed with vertex point C and centre angle 2α.

Since the chord BC in the hodograph plane is equal to the chord BC in the x,y-plane times r_z, the same scale factor applies to the chord AD. Now, AD is easily constructed in the x,y-plane, the angle OAD being equal to $\frac{\pi}{2} - \beta$. The length k_b is therefore known, from which r_z and the radius $R_2 = \frac{u_f}{r_z}$ to the line rupture BC can be deduced. The scale factor being known, the zone can be constructed in the x,y-plane. Having found the point B one can easily find O_2 (or the parameters ψ, n) for the line rupture BE. The rupture figure is only admissible since we have 2 parameters but 3 equilibrium conditions for the free rigid body No. 2. The energy method must therefore be used.

The two-sided rupture figure (Fig. 42 AD) is constructed in much the same way, but now 5 parameters must be estimated ($\frac{v_f}{u_f}$, α_1, α_2, β_1, and β_2). The first parameter can be determined from the velocity diagram at the point T when the angle $-\omega_a = \angle$ THD has been chosen. The image chords TD and TH in the hodograph plane determine the values of r_{z1} and r_{z2} when compared with the chords k_b and k_a, respectively, in the x,y-plane. The latter ones are easily calculated from the given parameters.

Also in this case the rupture figure is only admissible, there being 6 equilibrium conditions for the two free rigid bodies No. 2 and 3, and one stress condition (σ_T should be the same when calculated along each of the two line ruptures, using (3420) at the points E and I).

43 RUPTURE ZONES WITH MIXED BOUNDARY CONDITIONS

431 Curved Radial and Rectangle Zones

We now leave the rupture figure types that are known by the classical theory of plasticity (Sec. 421, and partly also 426), or can be considered as relatively simple extensions of Brinch Hansen's theory (Sec. 422-3) or of the so-called $\varphi = 0$ analysis (Sec. 424-5). In order to generalize the theory so that in principle all problems can be solved it is necessary to consider rupture zones with mixed boundary conditions.

In the simplest cases such rupture zones are closed, i.e. they are only connected to surface zones by line ruptures or discontinuity points. The statical conditions for the zone boundaries will then be expressible in terms of the stress resultants only, i.e. as simple variables, not as functional dependencies. As a contrast, in open rupture zones at least one of the zone boundaries is also a boundary to a statically determined rupture zone. σ and m are therefore known functions along this boundary.

If the boundaries to a closed rupture zone contain no wall parts or internal boundaries, the external geometrical conditions for the zone will also be expressible in terms of simple variables. This case, therefore, represents the simplest possible problem with mixed boundary conditions.

Generally speaking a closed rupture zone is determined by a number of parameters representing angle differences along the zone boundaries, a number of linear parameters (ratios between sliding velocities and between rotations of the surrounding rigid bodies, and at most four geometrical parameters which do not enter directly into the calculations of the zone (a scale factor, an orientation (i.e. the value of m_0 for the zone), and the two coordinates to a characteristic point of the zone). If the zone is free all four

geometrical parameters must be found, together with the other parameters, from the equilibrium and movement conditions for the rigid bodies (together with possible stress conditions for line ruptures connecting the zone to the surface zones). Any known point, usually a vertex point, in the zone will decrease the number of free geometrical parameters by two. If there are more than two known points (which is rarely obtained) geometrical conditions are imposed on the other parameters.

This section deals with the case where the zone is represented in the λ, μ-plane by a rectangle, one side of which may be a singular (known vertex) point. If this is true the zone is surrounded by three rigid bodies of clay, one of which can be assumed to be unmoving. If not we have a free rectangle zone surrounded by four rigid bodies of clay.

The unmoving body is called No. 0. The boundary to this body is assumed to be an a-line (the shear stress τ_f may, however, be negative). The sliding velocity along this curve, which is continued by line ruptures on one or both sides of the zone, is called u_1.

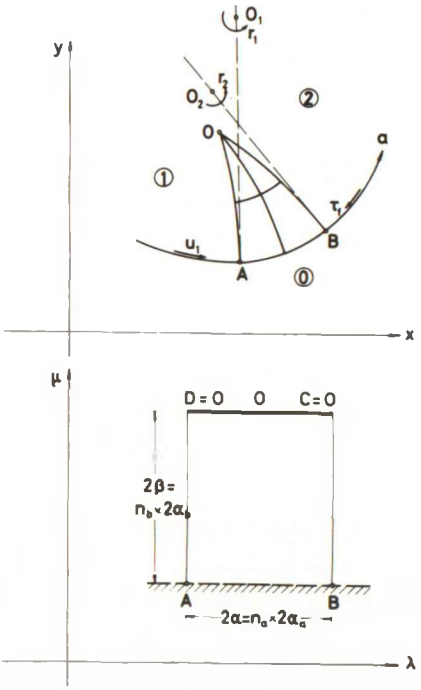

Fig. 43 A: Radial Zone with Curved Radial Slip Lines (Tangential Sliding).

The vertex point, if any, may be an a-line or a b-line vertex. In the first case the point forms the zone boundary opposite the boundary to the unmoving rigid body. The zone will then separate two bodies (No. 1 and 2), both sliding upon the body No. 0, cf. Fig. 43 A. This zone is a generalization of the simple types considered in Sec. 424 (Fig. 42 R) and Sec. 426 (Fig. 42 AB-AC).

In the second case the vertex forms one of the boundaries adjacent to the boundary to the unmoving body. The figure may without loss of generality be defined by the assumption that the a-lines are oriented so that the vertex point forms the boundary of the zone with the lowest value of λ. The two other rigid bodies are called No. 1 and 2, the first one of which slides upon the zone with the sliding velocity u_2, cf. Fig. 43 B. This zone is a generali-

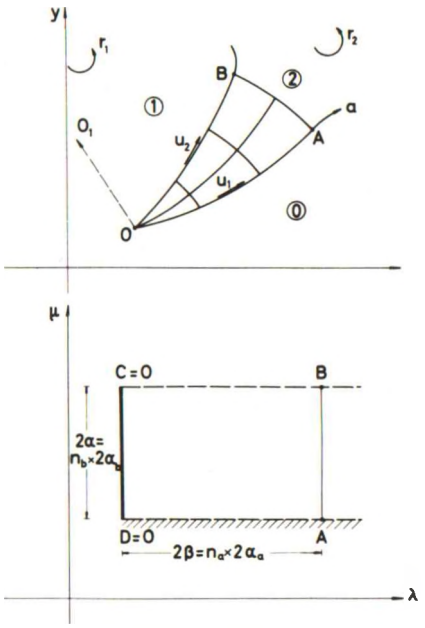

Fig. 43 B: Radial Zone with Curved Radial Slip Lines (Radial Slidings).

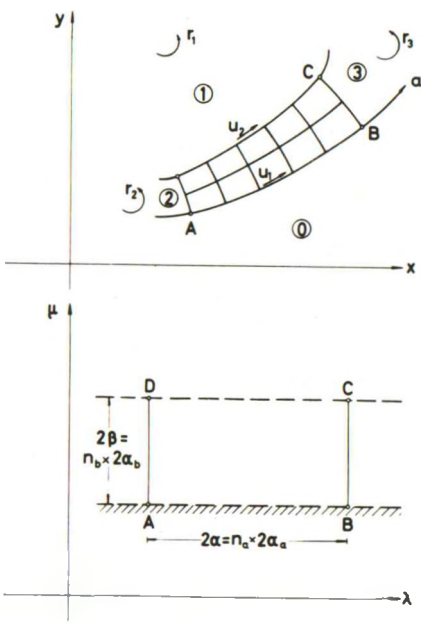

Fig. 43 C: Arc Zone with Curved Radial Slip Lines.

zation of the simple type considered in Sec. 424 (Fig. 42 T).

Finally, the general closed arc zone is obtained by replacing the vertex point in the last mentioned case by a boundary to a rigid body of clay, called No. 3, cf. Fig. 43 C (Fig. 42 V).

The problem for zones with mixed boundary conditions is to determine the form of the zone so that the boundary movements as given by the mixed conditions determine without contradiction a unique velocity field in the zone.

This may be done by means of the continuous auxiliary functions defined in Secs. 31. When the zone is closed, and is bounded by no wall or internal surface parts, the radii of curvature are the simplest to use. However, the calculations will be rather intricate in all cases.

Thus, in Fig. 43 A we have the following boundary conditions in terms of the radii of curvature.

$$\begin{aligned} &\text{Along CD:} && R = 0 \\ &\text{AD:} && G = r_1 S \\ &\text{BC:} && G = r_2 S \\ &\text{AB:} && F = u_1 \end{aligned} \qquad (4301)$$

Assume m_0 and σ_0 for the zone so that a = b = 0 at the point A and let (a, b) for the point C be $(2\alpha, 2\beta)$. If $S = S_0$ (b) along AD we must have, according to Sec. 322 (second initial value problem with the boundaries AD and DC, equation (3232)):

Along BC: $$S_{BC}(b) = S_0(b) - \int_{2\beta}^{b} S_0(t) \sqrt{\frac{2\alpha}{b-t}}\, J_1\left(2\sqrt{2\alpha(b-t)}\right) dt \qquad (4302)$$

We also have $G = r_1 S_0(b)$ along AD according to (4301), so using the boundaries AB and AD we find:

Along BC: $$G_{BC}(b) = r_1 S_0(b) - r_1 \int_0^b S_0(t) \sqrt{\frac{2\alpha}{b-t}}\, J_1\left(2\sqrt{2\alpha(b-t)}\right) dt + \int_0^{2\alpha} J_0\left(2\sqrt{(2\alpha - t)b}\right) u_1\, dt \qquad (4303)$$

The two expressions (4302-3) should be connected according to (4301). Evaluating the last integral in (4303) directly we find:

$$(r_2 - r_1) S_0(b) + r_2 \int_b^{2\beta} S_0(t) \sqrt{\frac{2\alpha}{b-t}}\, J_1\left(2\sqrt{2\alpha(b-t)}\right) dt + r_1 \int_0^b S_0(t) \sqrt{\frac{2\alpha}{b-t}}\, J_1\left(2\sqrt{2\alpha(b-t)}\right) dt = u_1 \sqrt{\frac{2\alpha}{b}}\, J_1\left(2\sqrt{2\alpha b}\right) \qquad (4304)$$

This is a functional (integral) equation that must be satisfied by S_0. It has a unique solution, apart from a factor of proportionality, when the basic (dimensionless) parameters α, β, and $\frac{r_2}{r_1}$ (or $\frac{r_1}{r_2}$ if $r_1 \to 0$) are known. The quantity $\frac{u_1}{r_1}$ (or $\frac{u_1}{r_2}$) may be taken as the scale of S_0-values so that in (4304) r_2 is replaced by $\frac{r_2}{r_1}$, and r_1 and u_1 by 1.

The solution for any given set of parameters may be obtained in a number of ways. For example:

1. An assumption for S_0 is made (f. inst. $S_0(b) = \text{const.}$). Isolating the first term on the left hand side of (4304), one can determine a better approximation for S_0 by calculating the three terms for a number of values b (the constant being determined so that the first and second approximation have the same mean value). This process may be repeated iteratively.

2. $S_0(b)$ is represented by a linear function series $A_0 + A_1 f_1(b) + A_2 f_2(b) + \ldots + A_n f_n(b)$ containing n known functions $f_1, \ldots f_n$ (f. inst. power terms, trigonometric terms, or a set of orthonormal functions) and n unknown coefficients $A_0, \ldots, A_n$. (4304) may then be solved for $S_0(b)$, giving this function as linear expressions of the coefficients A for any value of b. The coefficients may be determined either by demanding coincidence at n different values of b, or by demanding that n different integrals of $S_0(b)$ times a weighting function over the interval $0 \leq b \leq 2\beta$ should coincide.

3. The b-line AD is divided into n_b intervals, and the S_0-values at the interval points are taken as unknown quantities. By evaluating the integrals in (4304) by a numerical method (f. inst. the trapezoidal rule) for the $n_b + 1$ values of b corresponding to the interval points one obtains $n_b + 1$ linear equations in the $n_b + 1$ unknown quantities.

However, much simpler calculations are obtained when the method of chord lengths is used. Assume that AB and AD are divided into n_a and n_b intervals with half centre angles α_a and α_b, respectively, and let the intervals be numbered $i = 1, \ldots, n_b$ from A to D and $j = 1, \ldots, n_a$ from A to B.

The boundary conditions for the chords k (k_a and k_b) in the x,y-plane, and w (w_a and w_b) in the hodograph plane are:

$$\begin{aligned} &\text{Along CD:} && k_j = 0 \\ &\text{AD:} && w_i = r_1 k_i \\ &\text{BC:} && w_i = r_2 k_i \\ &\text{AB:} && w_j = 2 u_1 \sin \alpha_a \end{aligned} \tag{4305}$$

Taking the chords $k_b = x_i$ along AD as the unknown quantities, the chords k_i along BC can be expressed on the form:

$$k_i = \sum_{k=1}^{n_b} a_{ik} x_k \tag{4306}$$

It is seen that the numbers a_{ik} are functions of α_a, α_b, n_a, and k - i, being zero when i > k. They may be calculated in one operation taking $x_k = 1$ for $k = n_b$, and $x_k = 0$ for $k \neq n_b$ (e_a, $e_b = 1, -1$). $[a_{ik}]$ is a triangular matrix with zeroes below the diagonal, and with $a_{i+p,\,k+p} = a_{ik}$ for any number p.

The velocity difference chords w_b along AD are equal to $r_1 x_i$. The corresponding quantities along BC can be expressed on the form:

$$w_i = r_1 \sum_{k=1}^{n_b} b_{ik} x_k + u_1 c_i \qquad (4307)$$

The coefficients b_{ik} are functions of α_a, α_b, n_a, and i - k, being zero when $i < k$. They may also be calculated in one operation taking $x_1 = 1$ and $x_k = 0$ for $k > 1$ (together with $x_j = 0$ along AB; e_a, $e_b = 1,1$). It is seen that $[b_{ik}]$ is a triangular matrix with zeroes above the diagonal, and with $b_{i+p,k+p} = b_{ik}$ for any number p.

The coefficients c_i are calculated taking all $x_i = 0$ along AD, and all $x_j = 2 \sin \alpha_a$ along AB (e_a, $e_b = 1,1$). The geometrical constructions corresponding to the calculation of the coefficients a_{ik}, b_{ik}, and c_i are shown in Fig. 43 D (assuming $\alpha_a = \alpha_b$ both positive, and $n_a = n_b = 5$). The constructions are quite simple due to the simple geometry of the basic quadrangles (cf. Fig. 32 H), but they are far too inaccurate for practical purposes. The coefficients may be calculated numerically to any desired accuracy, however. Finite expressions may be derived by repeated use of (3260).

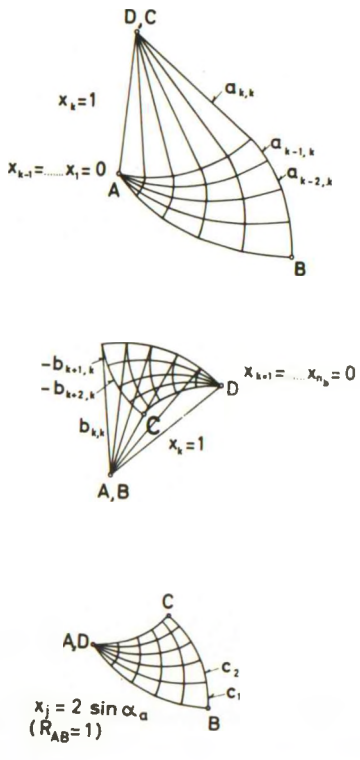

Fig. 43 D: Unit Constructions for Solutions by the Method of Chord Lengths.

Thus, $a_{kk} = \frac{1}{b_{kk}} = \left[\frac{\cos(\alpha_a - \alpha_b)}{\cos(\alpha_a + \alpha_b)}\right]^{n_a}$.

For n_a and n_b greater than 1 or 2 rather complex polynomia of degree n_a are obtained, so in practice it is simpler to find the coefficients by means of the slip line net calculations corresponding to the constructions sketched in Fig. 43 D.

Inserting the expressions (4306-7) in the boundary condition (4305) for BC we find

$$\sum_{k=1}^{n_b} x_k (r_2 a_{ik} - r_1 b_{ik}) = u_1 c_i \qquad (4308)$$

i.e. n_b linear equations in the n_b unknown quantities x_k.

In practice these equations may be used in different ways. For example:

1. α, β, and $\frac{r_2}{r_1}$ (or $\frac{r_1}{r_2}$ if $r_1 \to 0$) may be used as standard parameters, the greatest permissible half centre angle α_{max} determining the actual values of n_a, n_b, α_a, and α_b. (4308) will then determine a unique set of initial chord lengths $\frac{x_i r_1}{u_1}$ (i.e. measured with the radius O_1A on Fig. 43 A as the scale of lengths), which permits the satisfaction of all boundary conditions for the zone. By a normal calculation of the zone its geometry can now be completely determined. Thus, the ratio $\frac{k_o r_1}{u_1} = \frac{OA}{O_1A}$ and the angle $\alpha_o = \angle\, OAO_1$ can also be found:

$$\sum_{i=1}^{n_b} x_i \cos(2i - 1)\, \alpha_b = k_o \cos \alpha_o$$
$$\sum_{i=1}^{n_b} x_i \sin(2i - 1)\, \alpha_b = k_o \sin \alpha_o \qquad (4309)$$

together with the corresponding quantities for the boundaries OB and AB, and the stress resultants N, T, and M (scale $\tau_f O_1A$ and $\tau_f O_1A^2$) for all three boundaries, and possibly also the deformation work W_d (scale $\tau_f u_1 O_1A$) for the whole zone. These quantities tabulated as functions of the original parameters (or obtained as output from a standard procedure in a computer program) will describe the zone geometrically and statically so that it can be used directly as an element in a rupture figure.

2. Since either one of the two quantities r_1 and r_2 may be zero a more generally useful representation may be obtained by using k_o as the scale of lengths (scale of forces: $\tau_f k_o$, of moments: $\tau_f k_o^2$, and of work: $\tau_f u_1 k_o$). By considering (4309) together with (4308) the initial parameters may be taken as α, β, and α_o, the $n_b + 2$

unknown quantities being $\frac{x_i}{k_o}$, $\frac{r_1 k_o}{u_1}$, and $\frac{r_2 k_o}{u_1}$.

3. In practice, when the rupture zone is applied in a rupture figure like the one shown in Fig. 42 AC a slightly different representation is necessary: Assume a line rupture OA, which must be a straight line or a circle arc. The end point A (1 parameter, if ψ, n, and u_1 for the line rupture are given by the movement of the rigid body) determines k_o and α_o, and the parameter $\frac{r_1 k_o}{u_1}$ is also known. α and β must now be chosen so that (4308-9) determine the $n_b + 1$ quantities $\frac{x_i}{k_o}$ and $\frac{r_2 k_o}{u_1}$ without contradiction (2 parameters subject to 1 supplementary condition). The energy equation must be used to find the extreme solution since we have only 2 free parameters against 3 equilibrium equations for the free rigid body No. 2.

4. If the line rupture OA is not determined by the movements of the rigid body (1 or 2 remaining equilibrium equations for the rigid body No. 1), α, β, and α_o (or α, β, and $\frac{r_1}{r_2}$) may be taken as free parameters. The zone and the two line ruptures may then be constructed, treating its scale (f. inst. the ratio $\frac{k_o}{OD}$) and its orientation (f. inst. ω_{AD}) as further parameters subject to the condition that the line rupture OA must pass through the known point O, and possibly also to one condition for the movement of the external rigid body. Thus, in this case we have 3 or 4 free parameters against 4 or 5 equilibrium conditions for the two rigid bodies of clay.

The last mentioned method can also be used when there are 2 movement conditions for the rigid body No. 2. One of the three initial parameters must then be varied by trial and error until all conditions for the line rupture OA are satisfied. The method mentioned under 3. above would then seem to give a more direct flow of calculations, however.

The radial zone of Fig. 43 B is calculated in much the same way. We can also here use the continuous auxiliary functions, but much simpler calculations are obtained by means of the method of chord lengths. With the geometry of the rupture zone as assumed in Fig. 43 B the boundary conditions are:

Along AD: $w_j = 2 u_1 \sin \alpha_a$

DC: $k_i = 0$

$$\text{BC:} \quad w_j = r_1 k_j - 2 u_2 \sin \alpha_a \tag{4310}$$
$$\text{AB:} \quad w_i = r_2 k_i$$

The n_a chord lengths x_j along DA (numbered from D in the direction of A) may be taken as unknown quantities. The chords along CB and along AB can then be expressed on the form

$$\text{Along CB:} \quad k_j = \sum_{k=1}^{n_a} a_{jk} x_k$$
$$\text{AB:} \quad k_i = \sum_{k=1}^{n_a} b_{ik} x_k \tag{4311}$$

using also the boundary condition along DC (e_a, e_b = 1,1)

$[a_{jk}]$ is a square matrix (n_a by n_a) with zeroes above the diagonal ($j < k$). Its elements are functions of α_a, α_b, n_a, and $j - k$, $a_{j+p,k+p}$ being equal to a_{jk} for any number p. $[b_{ik}]$ is a rectangular matrix (n_b by n_a). Its elements are functions of α_a, α_b, i, and $n_a - k$.

Using the boundary condition along AB we find

$$\text{Along AB:} \quad w_i = r_2 \sum_{k=1}^{n_a} b_{ik} x_k \tag{4312}$$

If this is used together with the boundary condition along AD we may find (e_a, e_b = -1,1):

$$\text{Along CB:} \quad w_j = r_2 \sum_{i=1}^{n_b} c_{ji} \sum_{k=1}^{n_a} b_{ik} x_k + u_1 d_j \tag{4313}$$

$[c_{ji}]$ is a rectangular matrix (n_a by n_b) whose elements are functions of α_a, α_b, $n_b - i$, and $n_a - j$. Performing the matrix multiplication (4313) may be written:

$$w_j = r_2 \sum_{k=1}^{n_a} e_{jk} x_k + u_1 d_j \tag{4314}$$

which taken together with (4311) and the boundary condition along CB gives:

$$\sum_{k=1}^{n_a} x_k (r_1 a_{jk} - r_2 e_{jk}) = u_1 d_j + u_2 2 \sin \alpha_a \qquad (4315)$$

From these equations the n_a unknown quantities may be determined on the form $\frac{x_i r_1}{u_1}$ when the four parameters α, β, $\frac{r_2}{r_1}$, and $\frac{u_2}{u_1}$ are known or have been estimated. As in the previous example one of the total lengths, f. inst. OA or OB, may be taken as the scale of lengths, using also a set of equations equivalent to (4309). If the quantities w_i along DC are calculated (scale u_1) the resultant velocity at O for the rigid body No. 1 may be determined together with its direction by means of the equations (cf. Fig. 42 T):

$$\begin{aligned} u_1 + u_2 \cos 2\alpha + \sum_{i=1}^{n_b} w_i \cos (2i - 1) \alpha_b &= w \cos (\psi - \theta) \\ u_2 \sin 2\alpha + \sum_{i=1}^{n_b} w_i \sin (2i - 1) \alpha_b &= w \sin (\psi - \theta) \end{aligned} \qquad (4316)$$

θ being the value of m at O for the a-line OA.

Thus, relative to the rigid body No. 1 the radial zone shown in Fig. 43 B acts as a line rupture with the parameters ψ, $u_f = w$, and $n_1 = \frac{1}{OO_1} = \frac{r_1}{w}$. The zone may also be determined by $\psi - \theta$ and n_1 together with α and β (or $\frac{u_1}{w}$ and $\frac{u_2}{w}$), i.e. by 4 parameters (6 when the scale and orientation are introduced by means of k_o and θ) against 2 remaining movement and/or equilibrium conditions for the rigid body No. 1, 3 equilibrium conditions for the body No. 2, and 1 stress condition between the line ruptures extending beyond A and B. For these two line ruptures ψ, u_f, n_1 are respectively $\theta + 2\beta$, u_1, $\frac{r_2}{u_1}$ and $\theta + 2\beta + 2\alpha$, u_2, $\frac{r_1 - r_2}{u_2}$. They are replaced by discontinuity points when the respective sliding velocities are zero.

By means of this rupture zone a possible solution can therefore be obtained to replace the quasi-possible one consisting of a simple line rupture. The rigid body No. 2 will no longer be simple, the arc AB being not generally a circle arc. In most practical cases n_b will be put equal to 1, however, and under this approximation AB is a circle arc.

In the third example (Fig. 43 C) it is necessary to use $n_a + n_b$ unknown quantities, f. inst. the chord lengths x_i along AB, and y_j along AD. Along DC

and BC we then find expressions on the form

$$\text{Along DC:} \quad k_i = \sum_{k=1}^{n_a} a_{ik} x_k + \sum_{l=1}^{n_b} b_{il} y_l$$

$$\text{BC:} \quad k_j = \sum_{k=1}^{n_a} c_{jk} x_k + \sum_{l=1}^{n_b} d_{jl} y_l \tag{4317}$$

Along AD we also have, according to the boundary condition:

$$w_l = r_2 y_l \tag{4318}$$

so that we may also find along DC and BC:

$$\text{Along DC:} \quad w_i = u_1 e_i + r_2 \sum_{l=1}^{n_b} b_{il} y_l$$

$$\text{BC:} \quad w_j = u_1 f_j + r_2 \sum_{l=1}^{n_b} d_{jl} y_l \tag{4319}$$

Notice that $e_i = 2 \sin \alpha_a \sum_{k=1}^{n_a} a_{ik}$, and $f_j = 2 \sin \alpha_a \sum_{k=1}^{n_a} c_{jk}$.

Using the boundary conditions along DC and BC we find, finally:

$$r_1 \sum_{k=1}^{n_a} a_{ik} x_k + (r_1 - r_2) \sum_{l=1}^{n_b} b_{il} y_l = u_1 e_i + u_2 \, 2 \sin \alpha_a$$

$$r_3 \sum_{k=1}^{n_a} c_{jk} x_k + (r_3 - r_2) \sum_{l=1}^{n_b} d_{jl} y_l = u_1 f_j \tag{4320}$$

which are $n_a + n_b$ equations in the $n_a + n_b$ unknown quantities (scale $\frac{u_1}{r_1}$ when the parameters $\frac{r_2}{r_1}$, $\frac{r_3}{r_1}$, and $\frac{u_2}{u_1}$, together with α and β, are assumed to be known). As before a total chord length AB or DC may be introduced as scale of lengths, and the parameters $\psi - \theta$, $\frac{1}{n_1} = O_1 D$ for the rigid body movement No. 1 at the point D may also be introduced.

This rupture zone used alone cannot give possible solutions since we have only 9 parameters (the 5 mentioned above plus 4 giving the position, scale and orientation of the zone) against 8 remaining movement and/or equilibrium conditions for the 3 rigid bodies, and 3 stress conditions between the 4 line ruptures. To remove the deficiency of parameters two of the line ruptures must be replaced by arc zones (connected to surface zones). This, however, transforms the rupture figure into an open multiple arc zone rupture.

A modified form of the zone may be used as in Fig. 42 W, introducing one further parameter in the simple rupture figure shown in this figure.

Example 43 a

The calculation procedures sketched in this section can in practice only be performed on a computer. This is also not too difficult, however, the basic operations being quite simple. For calculations by hand, when it is at all justified to use these more complex rupture zone types, a great simplification can be obtained if one takes $n_a = n_b = 1$ (the whole rupture zone being one unit cell). At least for the rupture zones considered in this section the rupture figures may under this assumption still be considered as simple.

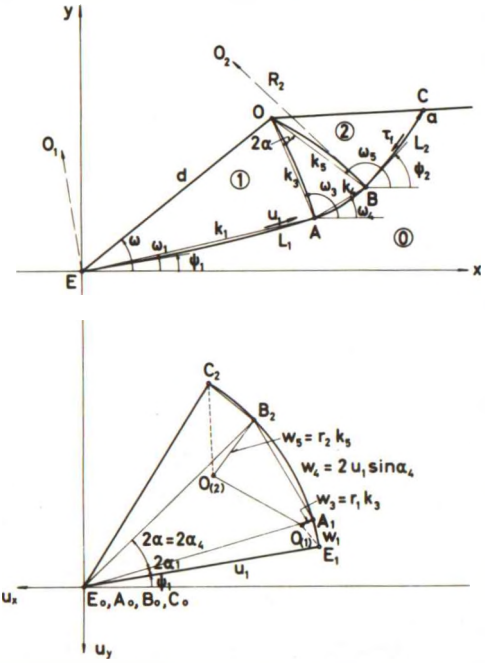

Fig. 43 E: Two Line Ruptures Connected by a Radial Zone with Curved Radial Slip Lines (AfCfA). Image in the Hodograph Plane.

Thus, in the general AfCfA rupture figure (Fig. 43 E) we may assume the movement components w_x, w_y, r_z for the rigid body No. 1 to be given, or to be the basic external parameters of the failure problem. From this the parameters ψ_1, $n_1 = \frac{1}{R_1}$, and u_1 for the line rupture L_1 are given.

The boundary OAE to the rigid body No. 1 is determined in the simplest way be means of the angles ω_1 and ω_3 (or α_1 and α_3)

$$\omega_1 = \psi_1 + \alpha_1$$

$$\omega_3 = \omega_1 + \alpha_1 + \frac{\pi}{2} + \alpha_3 \qquad (4321)$$

$$= \frac{\pi}{2} + \psi_1 + 2\alpha_1 + \alpha_3$$

so that

$$\alpha_1 = \omega_1 - \psi_1$$
$$\alpha_3 = \omega_3 - \psi_1 - 2\alpha_1 - \frac{\pi}{2} \tag{4322}$$

Besides

$$k_1 = d\,\frac{\sin(\omega_3 - \omega)}{\cos(\alpha_1 + \alpha_3)}$$
$$k_3 = d\,\frac{\sin(\omega - \omega_1)}{\cos(\alpha_1 + \alpha_3)} \tag{4323}$$

and

$$n_1 = \frac{2\sin\alpha_1}{k_1} = \frac{2}{d}\,\frac{\sin\alpha_1\cos(\alpha_1 + \alpha_3)}{\sin(\omega_3 - \omega)}$$

If ψ_1 and n_1 are given, α_1 may therefore be chosen freely, after which α_3 is determined by trial and error until the last equation (4323) is satisfied.

$\alpha = \alpha_4$ may now be chosen after which the geometry of the rupture zone is given:

$$\alpha_5 = \alpha_3$$
$$\omega_4 = \omega_1 + \alpha_1 + \alpha_4 \tag{4324}$$
$$\omega_5 = \omega_3 + 2\alpha_4$$

and

$$k_4 = k_3\,\frac{\sin 2\alpha_4}{\cos(\alpha_3 + \alpha_4)}$$
$$k_5 = k_3\,\frac{\cos(\alpha_3 - \alpha_4)}{\cos(\alpha_3 + \alpha_4)} \tag{4325}$$

From the corresponding figure in the hodograph plane, which is also shown in Fig. 43 E, we find, the angle between $O_{(1)}\,O_{(2)}$ and $A_1\,B_2$ being $2\alpha_3$:

$$w_5 = w_3\,\frac{\cos(\alpha_3 + \alpha_4)}{\cos(\alpha_3 - \alpha_4)} + w_4\,\frac{\sin 2\alpha_3}{\cos(\alpha_3 - \alpha_4)} \tag{4326}$$

or, inserting the boundary conditions:

$$r_2 k_5 = r_1 k_3\,\frac{\cos(\alpha_3 + \alpha_4)}{\cos(\alpha_3 - \alpha_4)} + 2u_1\,\frac{\sin\alpha_4 \sin 2\alpha_3}{\cos(\alpha_3 - \alpha_4)} \tag{4327}$$

This determines r_2, and the parameters for the line rupture L_2. In the coordinate system of Fig. 43 E we have:

$$
\begin{aligned}
x_A &= k_1 \cos \omega_1 \\
y_A &= k_1 \sin \omega_1 \\
x_B &= x_A + k_4 \cos \omega_4 \\
y_B &= y_A + k_4 \sin \omega_4 \\
\psi_2 &= \omega_4 + \alpha_4 \\
n_2 &= \frac{r_2}{u_1} = n_1 \frac{\cos^2 (\alpha_3 + \alpha_4)}{\cos^2 (\alpha_3 - \alpha_4)} + \frac{2}{k_5} \frac{\sin \alpha_4 \sin 2\alpha_3}{\cos (\alpha_3 - \alpha_4)}
\end{aligned}
\tag{4328}
$$

From this the point C can be determined when the surface form to the right of O is known. Finally L_1 ($= k_1 \frac{\alpha_1}{\sin \alpha_1}$) and L_2 are found, and the work equation is applied to the rupture figure. The contribution from the line ruptures is simply $\tau_f u_1 (L_1 + L_2)$. For the rupture zone the deformation work is found in the simplest way by using the normal, tangential, and rotational movement components referred to the mid point of each of the chords k_3 and k_5.

Thus,

$$
\begin{aligned}
u_{n3} &= u_1 \cos \alpha_3 - \tfrac{1}{2} r_1 k_3 \quad \text{(directed into the zone)} \\
u_{t3} &= u_1 \sin \alpha_3 \quad \text{(directed from O to A)} \\
r_{z3} &= r_1
\end{aligned}
\tag{4329}
$$

and

$$
\begin{aligned}
u_{n5} &= u_1 \cos \alpha_3 - \tfrac{1}{2} r_2 k_5 \quad \text{(directed away from the zone)} \\
u_{t5} &= u_1 \sin \alpha_3 \quad \text{(directed from O to B)} \\
r_{z5} &= r_2
\end{aligned}
$$

The corresponding stress resultants are:

$$
\begin{aligned}
N_3 &= k_3 \left[\sigma_B + \tau_f \left(N^Z (\alpha_3) + \sigma^Z (\alpha_4) \right) \right] \\
T_3 &= \tau_f k_3 T^Z (\alpha_3) \\
M_3 &= \tau_f k_3^2 M^Z (\alpha_3) \\
N_5 &= k_5 \left[\sigma_B + \tau_f N^Z (\alpha_3) \right] \\
T_5 &= \tau_f k_5 T^Z (\alpha_3) \\
M_5 &= \tau_f k_5^2 M^Z (\alpha_3)
\end{aligned}
\tag{4330}
$$

From this we find:

$$W_d = N_3\, u_{n3} + T_3\, u_{t3} - M_3\, r_{z3} - N_5\, u_{n5} - T_5\, u_{t5} + M_5\, r_{z5} \qquad (4331)$$

By insertion of (4329), (4327), and (4325) it can be verified that the total contribution from σ_B is zero. This quantity (and the term $\tau_f\, N^z\, (\alpha_3)$) can therefore be neglected in (4330). N_3 can therefore be taken simply as $\tau_f\, k_3\, \sigma^z\, (\alpha_4) = 4\, \tau_f\, k_3\, \alpha_4$, and N_5 as zero. The final result is:

$$W_d = \tau_f\, k_3\, u_1 \left[4\, \alpha_4\, (\cos \alpha_3 - \tfrac{1}{2} n_1\, k_3) + \sin \alpha_3\, T^z\, (\alpha_3)\, (1 - \frac{k_5}{k_3}) + 2\, M^z\, (\alpha_3)\, \frac{\sin \alpha_4\, \sin 2\, \alpha_3}{\cos (\alpha_3 + \alpha_4)} \right] \qquad (4332)$$

The two last terms are of the second order in α_3.

432 Multiple Radial Zones

If a solution is obtained by means of the rupture figure shown in Fig. 43 B, all equilibrium and movement conditions may be satisfied for a set of initial parameters for which the line ruptures beyond A and B do not permit the construction of surface zones, and yet intersect the surface under an angle which is not statically correct. The solution is then only quasi-possible, and it can only be made possible if the line ruptures themselves are replaced by radial zones, ending in a surface zone complex.

In this way multiple radial zones may obtain, cf. Fig. 43 F. Strictly speaking it is not correct to draw the rupture figure on one sheet in the λ,μ-plane. This is because α_2 and α_3 need not have the same sign, so the coordinates λ may not have a unique meaning to the right of AD. In cases where it is important that a is a unique function of λ (f. inst. in a table of computations) the rectangle CDHG must be considered to be drawn on a separate sheet.

Assuming the initial parameters α_1, α_2, α_3, β_1, β_2, β_3, u_2/u_1, u_3/u_1, and u_4/u_1 to be known we may take the $m = m_1 + m_2 + m_3$ chords k_{oa} along A_oA, AE, and CG as the unknown quantities. The k_b-values along EF, BC, and GH may now be found as linear expressions of these chords. They are used, together with the boundary conditions along the initial boundaries,

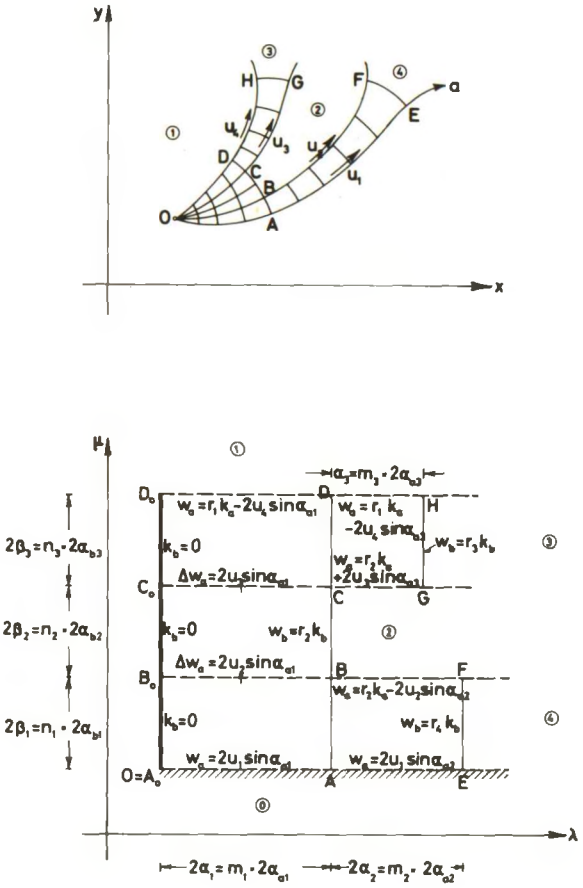

Fig. 43 F: Multiple Radial Zone.

to find w_a along D_oD, DH, and BF, where also k_a are found directly from k_{oa} (all quantities as linear sums, each containing m terms).

During these calculations the ratios r_2/r_1, r_3/r_1, and r_4/r_1 may be assumed beforehand. We will then end up with m equations in the m unknown quantities k_{oa} (expressed as ratios to the unit length u_1/r_1). Afterwards the positions of the four rotation centres may be found, and the whole rupture figure may be rotated and multiplied to another scale in order to obtain the best possible satisfaction of the given conditions. In this way we have 14 free parameters to satisfy the 9 equilibrium conditions for the 3 clay bodies No. 2, 3, and 4; 3 stress conditions for the 4 line ruptures contacting the surface zones, and f. inst. two conditions for the position of the rotation centre for clay body No. 1.

During the readjustments of the rupture figure to satisfy all these conditions the parameters must be varied. However, it is only when the six basic angle differences, α_1, ..., β_3, are changed that the whole rupture zone must be calculated anew. The m x m matrix of coefficients for the chord lengths $k_{oa}\ r_1/u_1$ may be split up into sub-matrices, forming the constant term and the factors in a linear expression of the three rotation parameters r_2/r_1, r_3/r_1, r_4/r_1. Correspondingly, the m-dimensional vector of constant terms may be written as a linear expression of the three velocity parameters u_2/u_1, u_3/u_1, u_4/u_1. In this way the recalculations for 8 of the 14 free parameters become relatively simple. Furthermore, if the angle differences are, at least in the initial steps, altered only by multiples of the respective α_a or α_b, the calculations of new matrices and vectors may be simplified.

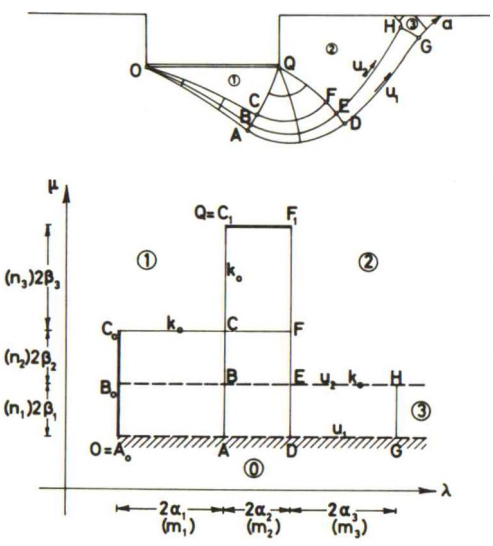

Fig. 43 G: Possible Solution to One-Sided Bearing Capacity Problem.

Much the same procedure is used when the closed rupture zone has more than one vertex point, cf. Fig. 43 G in which is sketched a possible, presumably the mathematically correct rupture figure corresponding to the admissible solution shown in Fig. 43 E (cf. Fig. 42 AC). We have 9 initial parameters: α_1, α_2, α_3, β_1, β_2, β_3, r_2/r_1, r_3/r_1, and u_2/u_1, corresponding to 9 conditions: 3 equilibrium conditions for the clay body No. 2, 3 for the body No. 3, 1 stress condition for the surface zone complex beyond GH, and 2 conditions for the movements and/or total forces of body No. 1. The possible rotation and multiplication to scale of the rupture zone give no extra parameters, because this process is determined by the condition that the vertex points O and Q shall have the correct position relative to each other, i.e. the chord OQ, when calculated from the chord lengths along C_oC and CC_1, shall have a known length and orientation.

The $m_1 + m_3 + n_3$ chords along the slip line portions marked k_o are taken as the unknown quantities. This determines all other chords in the rup-

ture figure. After using the boundary conditions along A_oADG, GH, and EFF_1, the quantities w can now be determined, and the values of k_o are then determined by considering the boundary conditions along C_oC, CC_1, and EH.

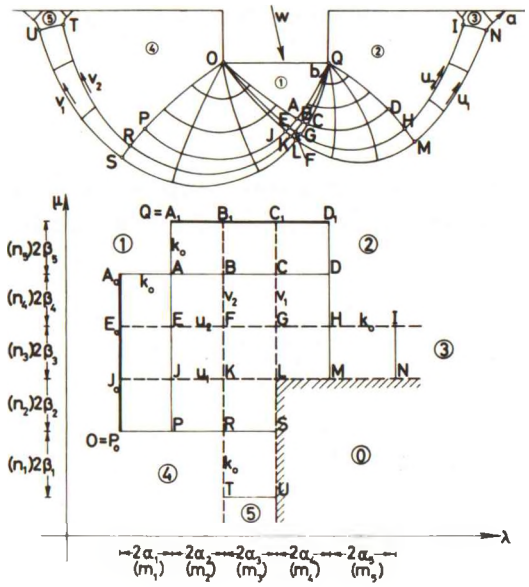

Fig. 43 H: Possible Solution to Two-Sided Bearing Capacity Problem.

Similarly the rupture figure shown sketched on Fig. 43 H is a possible, presumably the mathematically correct solution corresponding to the approximate rupture figure in Fig. 42 AD. It has 16 initial parameters: $\alpha_1, \ldots, \alpha_5$, $\beta_1, \ldots, \beta_5$, r_3/r_2, r_4/r_2, r_5/r_2, u_1/u_2, v_1/u_2, and v_2/u_2. The four free rigid bodies of clay give altogether 12 equilibrium conditions, and there are 3 stress conditions for the surface zone complexes beyond IN and TU, and for the connection between these two complexes. The orientation and scale of the closed rupture zone are determined by the known length and orientation of the chord OQ. Finally there is one condition for the known direction of translations w.

The zone is calculated in the usual way, using the $m_1 + m_5 + n_1 + n_5$ chords on the slip line portions marked k_o as unknown quantities, and satisfying the boundary conditions on the same boundary portions.

In the symmetrical case (w vertical) the number of parameters reduces to 7, corresponding to 6 equilibrium conditions and one stress condition. The complexity of this rupture figure explains, perhaps, why the mathematically correct solution to the bearing capacity problem for a foundation below the clay surface has never been published. Even in the simplest possible case (all numbers m and n equal to unity) the calculations for the rupture figure in Fig. 43 H (and also in Fig. 43 G) are rather laborious. However, a compromise replacing the construction EDGH in Fig. 43 G and the constructions HMNI and RSUT in Fig. 43 H by line ruptures would save respectively 4 and 8 parameters. The remaining (quasi-possible) solutions would therefore have 5 and 8 initial parameters, respectively. This could be managed, at least on a computer, and it would give calculations which were accurate enough for all theoretical and practical purposes. These rupture figures have the advantage that the equilibrium method can be used. On the other hand, the calculations may show in some cases that β_2 (on Fig. 43 G) or α_2 and/or β_4 (on Fig. 43 H) becomes negative, or that the corresponding radial zones OBC or OAE and OAB are not kinematically possible. This would indicate that the correct rupture figures are much more complicated. In practice the AfCfA rupture figure on Fig. 43 E (or the corresponding one for the two-sided failure) should then be used.

433 Combinations with Wall Zones and Simple Arc Zones

The radial zone of Fig. 43 B may become statically impossible if the angle between the tangent to the zone boundary OB and a wall through the point O becomes too small (less than i_w). A better approximation (less on the safe side) may then be obtained by continuing the radial zone through a wall zone. This development is similar to the transition from an XfR rupture figure into a BfR failure zone. Rupture figures of the same kind can also obtain in lieu of BfR rupture figures if the Rankine zone is not geometrically possible ($k_2 < 0$ in Fig. 42 M).

Several types exist, one of which is shown in Fig. 43 I. This rupture figure has 5 parameters: α_1, α_2, β_1 (which determines the value of m at the point O for the slip line OA, the wall inclination and the angle COB being known when e_{t1} for the zone part OC is known), r_2 (r_1 being known if the movement components for the wall are known), and u_1 (ρ for the wall being assumed to be known).

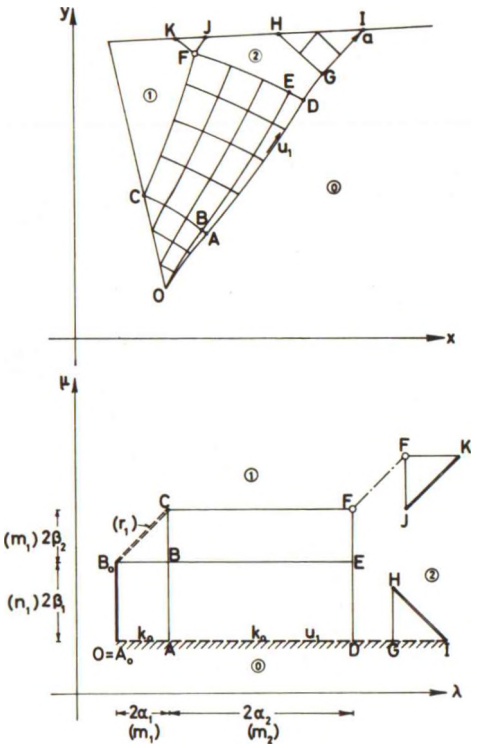

Fig. 43 I: Rupture Figure with a Radial Zone Augmented by a Wall Zone.

The $m_1 + m_2$ chord lengths marked k_o may be taken as unknown quantities. If the wall is straight all chords along CF and FD can be expressed as linear functions of the quantities k_o. The boundary conditions for movements can now be used along A_oD and DE, which determines the quantities w, and also u_s along B_oC as linear functions of k_o. The boundary conditions along CF and FE will then represent $m_1 + m_2$ linear equations in the unknown quantities. If $e_{t2} = 0$ (the rigid body No. 1 is not sliding upon the wall) a further equation is obtained by the condition that $u_s = 0$ at C, so that u_1 can also be determined, all equations being also linear in u_1. The four (or five for $e_{t2} \neq 0$) remaining parameters are checked by the three equilibrium conditions for the rigid body No. 2 (after the line rupture DG and the surface zone GHI have been constructed), the value of ρ for the body No. 1, and possibly the projection parallel to the wall of the forces acting upon the body No. 1.

Some possible modifications are shown (sketched) in Fig. 43 J, assuming the surface conditions to be simple (straight slip lines in the Rankine zones) so that arc zone ruptures connected to surface zones have straight radial slip lines, and circular tangential slip lines.

1. In the first sketch on Fig. 43 J the boundary slip line on Fig. 43 I is replaced by a radial zone with a surface zone complex beyond G and H. This figure has four parameters above those indicated in Fig. 43 I, viz. the centre angle AOB, the difference in a between D and G, the sliding velocity along OBEH, and the rotation of the rigid body No. 3. Against this there are also four supplementary conditions: the three equilibrium equations for the rigid body No. 3, and a stress condition between the line ruptures beyond G and H. A

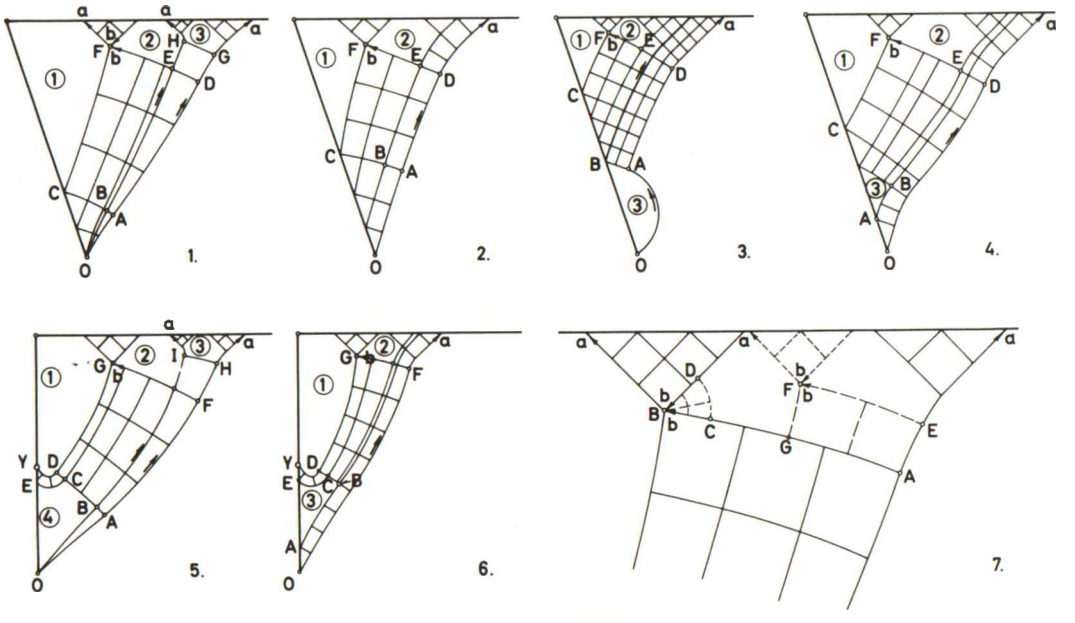

Fig. 43 J: Variants of Rupture Figures with Closed Wall Zones, Including Yield Hinges Y and Secondary Failures in Rigid Bodies of Clay.

further variant exists in which H is a discontinuity point. The sliding velocity u_2 (along OBEH) will then be identically zero, but there will also be no stress condition between G and H.

2. In the second sketch the radial zone and the line rupture on Fig. 43 I are replaced by an arc zone construction (BfR instead of PfXfR). We have the same number of parameters as in Fig. 43 I, the angle β_1 being replaced by the width DE (= AB since the radial slip lines are straight) of the arc zone. Notice that the a-lines between the b-lines through O and D need not be circular.

3. If the rotation point for the wall is above the foot point, the rupture figure may be modified by an Aa-construction (for kinematical reasons this presupposes a BfR construction of the surface as in Fig. 43 J 2). Notice that all b-lines between the a-lines through D and E are straight, so the Aa-construction is calculated exactly as indicated in Sec. 423. The remaining part of the rupture figure, above the point B, is identical to the one shown in the preceding sketch.

4. In the lower part of the rupture figure a construction Bf (or Xf, or AaBf) may also obtain. The secondary rigid bodies of clay obtained in this way along the wall are calculated much like the simple rigid bodies considered in Sec. 423. The b-line through the point B will not be straight over its whole length, however, so above this point the rupture figure must be calculated as a general band zone with a wall part boundary. The restrictions on the variation of the indicator e_t along the wall are also valid in this case.

5. If there is a yield hinge in the wall (or the earth front is partly unsupported) more complicated rupture figures may obtain. For some combinations of the rotations of the two wall parts a yield hinge may also obtain in an ordinary WPR or BfR rupture figure, however, or in fact in any rupture figure with a wall zone part, provided only that the yield hinge is located in the wall part covered by the zone, and that the different movements of the wall parts do not produce negative values of ϵ in the zones. The variant shown in Fig. 43 J 5 (cf. Fig. 42 W) has 11 parameters: the differences in a along OA, AF, FH, and CE, the differences in b along AB, BC, and CD, the sliding velocities along OH and OI, and the rotations of the rigid bodies No. 2 and 3. There are also 11 conditions: 3 equilibrium conditions for each of the bodies No. 2 and 3, 1 equilibrium and 1 movement condition for No. 1, and 1 equilibrium condition for No. 4, 1 stress condition between the line ruptures beyond H and I, and 1 geometrical condition representing the fact that the directions EY and OY must coincide. If there is no yield hinge at Y, but the earth front above Y is unsupported, the body No. 1 will be free. There are now two further parameters (the rotation of the body No. 1, and a scale factor representing the unknown distance OY) against two further conditions (two equilibrium equations for the body No. 1; the movement condition mentioned above, corresponding to a known value of ρ for the wall, is still valid, but is now applied to the body No. 4).

6. In this case too the radial zone construction OHI may be replaced by an arc zone construction. Below the point B the rupture figure may start with the elements Xf, Bf, XfBf, AaBf, BfBf, or AaBfBf. The rupture figures shown in Fig. 43 J 1-4 may also apply (with the yield hinge situated somewhere in the wall zone parts).

7. Finally, two possible modifications of the rigid body (No. 2) below the surface are shown. If the discontinuity point supposed to exist at the left hand corner does not satisfy the stress condition ($|\sigma_C - \sigma_D| \leq 2\,|\tau_f|\,(m_D - m_C)$), it will be replaced by an arc zone. This zone may degenerate into a radial zone since the sliding velocity along the a-line through the point is zero. This gives one further parameter (the width BC of the zone) against one further stress condition.

   At the right hand side a secondary rupture figure may develop (compare Fig. 43 I with Fig. 43 J 1). If the point F is a discontinuity point this introduces 3 further parameters (the differences in m along AE and AG, and the rotation of the secondary rigid body) against the 3 equilibrium conditions for this body. If there is an arc zone, a radial zone, or a line-rupture at F one further parameter is introduced (the width of the zone, or a sliding velocity) against a stress condition between E and F. Notice that the surface zones above B and F are of the same kind (both active when $\tau_f = c$), so they may overlap if necessary. The original right hand boundary to the body No. 2 may of course be an arc zone instead of a line rupture.

Generally speaking, it is seen that there are in principle no difficulties in the calculation of even very complicated rupture figures with closed rupture zones (or quasi-closed, if they are connected to surface zones by means of simple arc zones). The worst problem is that of the great number of parameters, between 6 and 11 being used in the figures shown in Fig. 43 I-J. This gives a great work of calculation, even if all zone element boundaries consist of one circle arc only.

However, reasonably simple approximate solutions are obtained if all b-lines are considered as straight, all radial zones, as in Fig. 43 J 1 and 5, are replaced by simple line ruptures (an XfR or BfR construction being used if possible), and the arc zone construction CDYE in Fig. 43 J 5-6 is replaced by a single point (with a stress singularity). In this way Fig. 43 J 5 is replaced by Fig. 42 W, and correspondingly simple solutions are also obtained in the other cases. The solutions will then only be kinematically admissible, but they will at least represent the major points in the failure problem.

434 Open Rupture Zones

The general case of open rupture zones have the property in common with the curved radial and rectangle zones that the movement conditions are not connected in a simple way to the geometry of the zone. As a further complication they are partly determined by the parameters to a, usually not simple, surface zone. This imposes a geometrical restraint on the angle parameters, that for the closed zones could be considered independent, and the length parameters (the unknown chord lengths) are connected in a non-linear way to the angle parameters.

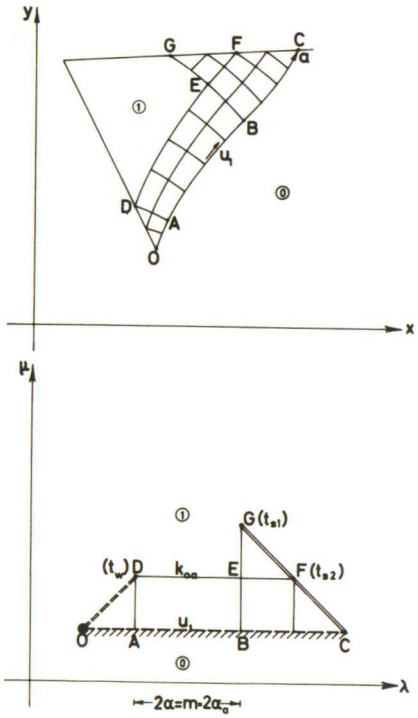

Fig. 43 K: A General Arc Zone Rupture Figure.

The method of finding the unknown chord lengths by the solution of a set of linear equations after the angle parameters have been estimated cannot therefore be used in this case. In principle the unknown chord lengths must be estimated in exactly the same way as the unknown angle parameters. Consider for example the general arc zone shown in Fig. 43 K (the slip line BEG being curved). It should be calculated by the following procedure.

1. First the geometrical parameters are estimated, and are corrected if necessary, until a geometrically possible solution is obtained:
   a. First the surface zone EFG is determined, f. inst. by the two parameters t_{s1} and t_{s2} (arc lengths, values of x etc.) which define the positions of the points G and F on the surface. The zone EFG is then statically determined.
   b. If the wall is straight and has a constant value of c_a this determines the angle parameter 2α (= m_E - m_D, both of these quantities being known). If the wall is curved, the position of D must also be estimated (one parameter, t_w, f. inst. the height OD).

c. The number m of circle arcs along DE is chosen, and all of the m unknown chord lengths marked k_{oa} are estimated, subject to one geometrical condition if the wall is straight (the end point D of the chain of chords must be located on the wall). If the wall is curved there are two conditions (D must be located in the point corresponding to the value of t_w). If necessary (m = 1 in the second case) one of the initial parameters must be changed until these conditions are satisfied.

d. The remaining part of the rupture figure is constructed as in an ordinary statically determined rupture zone, the end point O being of the type E (Sec. 421; in practice the surface parameter for the point C is changed by trial and error until the end point coincides exactly with the point O).

2. Next the kinematical conditions are satisfied in the zone. This will usually imply a change of some, or all, of the remaining initial parameters (1 + m in this example), so during this operation the rupture figure must be recalculated by trial and error.

   a. Using the known (or estimated) movement parameters for the wall the boundary conditions along OD, OABC, and EG can in this case be used to determine the sliding velocity u_1 along the boundary slip line, u_s along the wall part OD, and the rotation chords w in the whole rupture zone. In more complicated rupture figures it may be necessary to introduce some further parameters (other sliding velocities, rotations of rigid bodies of clay) in order to define the velocity field completely.

   b. The boundary condition along DE gives m conditions for the estimated parameters. If the rigid body No.1 is not supposed to slide along the wall we have the further condition that $u_s = 0$ at the point D. In this case, therefore, the kinematical conditions define the rupture figure completely.

   c. In all cases we have now a kinematically admissible solution with possible zones, so the energy equation can be applied. The remaining parameters (1 in Fig. 43 K, if the body is sliding along the wall) may now be varied, entailing recalculations as under 1 a - d and 2 a - b above, until a minimum is found.

3. Alternatively the equilibrium method may be used, changing the remaining parameters (with corresponding recalculations of the rup-

ture figure) until all equilibrium conditions, and also possible stress conditions, are satisfied. In the example of Fig. 43 K there is only the equation of projection of all forces acting on the body No. 1, to a line parallel to the wall (known value of τ_a), but in more complicated cases there will also be equilibrium conditions for free rigid bodies of clay, and possibly also stress conditions between line ruptures and/or arc zones.

The method may easily be extended to all rupture figures considered in Sec. 422-3, the Rankine zones being no longer assumed to have straight slip lines. Thus, if only the elements shown in Fig. 43 L are considered the procedure may be summarized as follows.

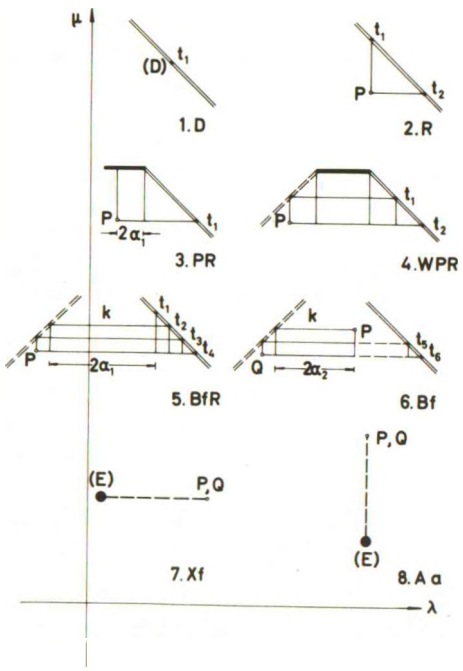

Fig. 43 L: Elements for the Calculation of Generalized Simple Rupture Figures.

1. If D then estimate the surface parameter t_1 and the inclination of the line rupture through the point D. Proceed with Xf or Aa below (alternatively: calculate the line rupture as in Sec. 425).
2. Else if R then estimate t_1 and t_2. Calculate the surface zone until the end point P.
3. Else if PR then estimate t_1 and the centre angle α_1. Calculate the continued surface zone.
4. Else if WPR then estimate t_1 and calculate the WPR-zone above this point. Estimate t_2 and continue the zone until the end point P (if E then $t_2 = t_1$, this parameter being found directly from the end point condition).
5. Else if BfR then estimate t_1 and t_2, and calculate the small Rankine zone. This determines the value of α_1, and also k if there is only one circle arc between the Rankine zone and the wall. Else estimate the values of k subject to one geometrical condition (end point of chord chain on the wall). Estimate t_3 and t_4 and continue the zone

until the end point P (if E then $t_3 = t_4$, directly determined by the end condition).

6. If Bf then α_2 is given directly, the point P being known. k is also given if there is only one circle arc. Else estimate the values of k subject to one geometrical condition (end point of chord chain on the wall). Estimate t_5 and t_6 and continue the zone until the end point Q (if E then $t_5 = t_6$, directly determined by the end condition).

7. If Xf or Aa then construct the line rupture from the known point and inclination (D, P, or Q) and the known foot point of the wall. The case E has been treated separately above.

8. The rupture figure is now geometrically determined with a number of estimated parameters equal to 2 + the number of chord lengths (marked k) - 1, for each rigid body of clay. The velocity field can now be constructed starting at the foot point of the wall. Since r_z is known for all rigid bodies (being equal to the value for the wall) a number of conditions equal to the number of chord lengths must be satisfied ($w = r_z k$). During this calculation the values of u_s along the wall, and the values of u_f along possible slip lines with sliding are determined.

9. The remaining parameters, 1 for each rigid body of clay, are determined by the condition either that $u_s = 0$ for the rigid body ($e_t = 0$), or that the resultant force parallel to the wall shall have a known value ($e_t \neq 0$, $f = e_t c_a$).

It is easily seen to make no difference in principles when the surface zones are allowed to be modified by radial zones (type D in Sec. 422-3), or even to be continued in all the possible ways shown in Sec. 421.

It should be noticed that when the slip lines in the surface zone are curved the rules indicated in Sec. 423 for the variation of e_t along the wall must be modified. We may now for geometrical or kinematical reasons have to introduce a rigid body in contact with the wall which has a value of e_t equal to the values for the two neighbouring wall zones. Thus, constructions of the type XfBfBfR or BfBfBfR may now be possible.

The method indicated above is perfectly general. It can be used for the calculation of all rupture figures containing open rupture zones. However, in its most general formulation it may also be regarded simply as the general calculation method for all types of rupture figures, the methods indicated in the preceding sections being specializations obtained when the problem para-

meters, or the type of rupture figures, permit one to telescope the different operations into each other, using some of the later mentioned conditions simultaneously with the earlier ones to determine final values for the parameters in one step.

Thus, the exposition in the preceding sections may be reviewed in the reverse order to see more clearly the different possible specializations of the general calculation method:

1. In the closed rupture zones with curved slip lines (Sec. 431-433) the geometrical and kinematical conditions are considered simultaneously, all boundary conditions being linear in the chord lengths. Since they are only connected to the surface zones by line ruptures, discontinuity points, or simple arc zones, the surface parameters t_s do not influence the choice of angle parameters for the zone proper. They can be represented indirectly by the parameters determining the scale and orientation of the zone (which may be the last parameters that are chosen). If the surface zones are simple Rankine zones the stress conditions between the line ruptures may be used to determine one or more angle parameters explicitly.

2. Simple radial and rectangle zones, kinematically determined rupture zones, and systems of line ruptures (Sec. 424-426) are further specializations characterized by the fact that a number of parameters have been put equal to zero so that the kinematical conditions can be interpreted directly in terms of the geometry of the rupture figure.

3. Rupture figures with simple rigid bodies permit the further simplification that the equilibrium conditions can also be expressed in a simple way in terms of the chord lengths (and a few angle parameters). All kinds of conditions (geometrical, kinematical, and statical ones) are therefore treated simultaneously, so that the final solution is obtained in one operation, although some calculations by trial and error may be necessary.

4. Finally, the statically determined rupture figures (Sec. 421) are characterized by the fact that no kinematical or statical condition (in the sense of movement or equilibrium for rigid bodies) enter the solution at all. There are only the geometrical conditions implied in f. inst. transition points.

The full procedure in which each parameter can in principle only be determined by a more or less complete recalculation of the whole rupture

figure may not be used very much in practice for economical reasons. It is always useful to keep it in mind, however, when the calculation procedure for any given rupture figure is planned, because it gives the natural sequence of operations. If some of these can be performed simultaneously in any special case, this should of course be utilized as far as possible.

However, in some rupture figures no short cuts are possible. In this connection it should be noticed that irregular surface zones may be generated by relatively simple features in the failure problem, cf. f. inst. the radial zones which obtain on both sides of discontinuous surface loadings. Fig. 43 M shows (sketched) a possible rupture figure corresponding to an active zone rupture on a retaining wall when a narrow strip surface loading is present. This rupture figure may obtain in several variants, depending on the actual values of the loading parameters d_1/h, d_2/h, and q/c (the surface is supposed to be horizontal, and the wall vertical with a known point of rotation below the foot point; since the state of stress is active τ_f is negative).

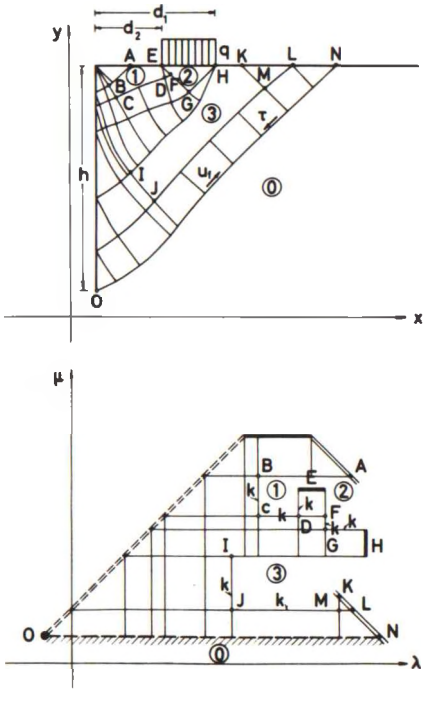

Fig. 43 M: Possible Solution to an Earth Pressure Problem with a Strip Load Behind a Retaining Wall.

For example:

1. The rupture zones above the rigid body No. 1, and between No. 0 and 3 may not actually develop. If both zones disappear we have a case resembling the one shown in Fig. 43 K.
2. The rigid body No. 2 is shown bounded by two radial zones (with curved radial slip lines). A surface zone may for some parameter sets develop along each of the boundary slip lines; the whole rigid body may develop into a triangle zone, or be partitioned into two rigid bodies separated by a local arc zone construction; or the rupture zones separating the three rigid bodies may fail to develop (for sufficiently small values of q/c). For sufficiently high values of q/c the radial zone on either side may be continued in a region near the vertex point into a surface zone outside the loading (as in Prandtl's bearing capacity rupture figure).

3. The arc zone construction between the bodies No. 0 and 3 may develop into one of the constructions considered in Sec. 433 (Fig. 43 I - J).

For the variant shown in Fig. 43 M the calculations by the general method are straightforward, but they will of course entail a great work of calculations. The procedure is summarized in the following Table 43 A. Notice that if more than one circle arc is used along each boundary to a zone element the number of parameters and conditions will increase, each of the symbols k representing now a number of variables. The problem is somewhat simplified if the arc zone construction between the bodies No. 0 and 3 is simple.

435 Rigid Bodies in Zones

In the rupture figures considered so far several different types of rigid bodies of clay have been encountered. On closer inspection it is seen that they fall roughly into two classes, the point of distinction being whether they are topologically equivalent to a domain in an ordinary slip line net or not:

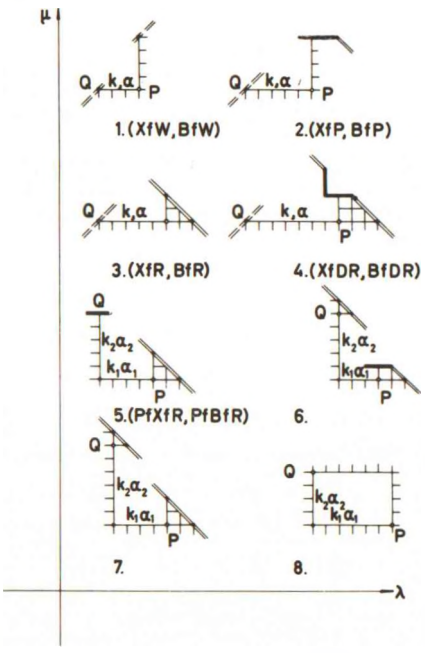

Fig. 43 N: Rigid Bodies of Clay in Rupture Zones.

The first class, which has this property, is characterized by the fact that its members, except for some special cases, are bounded by an even number of slip lines (the same number of a- and b-lines), possibly together with a surface and/or a wall. They may obtain instead of parts of statically determined rupture zones, and also in other types of open or closed rupture zones, which are not geometrically or kinematically possible.

Some examples are shown in Fig. 43 N. The first four types have been considered before, obtaining in simple rupture figures (Sec. 423). They can be considered as modifications to the classical Prandtl rupture figure (WPR), obtained for kinematical or geometrical

Table 43 A: Calculation Procedure for a Rupture Figure with Open Zones (Fig. 43 M).

Operation	Step No.	Assume	Calculate	Conditions	Numbers param.	Numbers cond.	Sum param.	Sum cond.
Geometrical construction	1	Surface param. t_A	WPR-zone between A and wall	none	1	0		
	2	λ_B, α_{BC}, k_{BC}	Zone between BC and wall	none	3	0		
	3	α_{CD}, k_{CD}, α_{DE}, k_{DE}	Chord chain CDE	End point at E	4	2		
	4	$\alpha_E = \alpha_{DF}$	Radial zone DEF	none	1	0		
	5	α_{FG}, k_{FG}, α_{GH}, k_{GH}	Chord chain FGH, zone FG-wall	End point at H	4	2		
	6	α_H	Radial zone from H to wall	none	1	0		
	7	λ_I, t_L, k_{IJ}	Zone between IJ and wall	none	3	0		
	8	t_k, k_{JM}	Surface zone KLM, chain JM	End point at M	2	2		
	9		Zone until NO	none	0	0	19	6
Velocity field	10		u_f and $u_{s(0)}$	none (given by known ρ for wall)	0	0		
	11	r_3	Zone until a-line through I	k_{JM} and k_{JI} compared with w	1	2		
	12	r_2	Zone until a-line through F	k_{GH} and k_{GF}	1	2		
	13	r_1	Zone FED, and until B	k_{DE}, k_{CD}, and k_{CB}	1	3	3	7
Equilibrium	14		Equilibrium for body No. 3	3 equations	0	3		
	15		Equilibrium for body No. 2	3 equations	0	3		
	16		Equilibrium for body No. 1	3 equations	0	3	0	9
				Total sums of parameters and conditions:			22	22

reasons between two wall zone parts with different values of e_t (No. 1; in zones with curved slip lines the two values of e_t may, however, also be equal), because the centre angle of a normal radial zone would be negative (No. 2 and 3), or because of a surface discontinuity (corner point or end point of a surface loading, No. 4).

Assuming the rupture zone to be calculated from the right hand side (e_a, e_b = -1, -1) all four types are determined geometrically by two parameters (λ, μ for the point P), which determine also the total centre angle α. The chord lengths along PQ must also be estimated, subject to one geometrical condition. When the velocity field is calculated (e_a, e_b = 1, 1) r_z is known since the rigid body is in contact with the wall. This will give a number of conditions equal to the number of chord lengths. The remaining condition is either that $u_s = 0$ ($e_t = 0$) or that the projection parallel to the wall shall correspond to the known value of f ($e_t \neq 0$).

The four next types of rigid bodies are free. They are determined by four geometrical parameters, viz. λ, μ for the point P and either the total centre angles α_1 and α_2 (No. 5) or λ, μ for the point Q. The chord chain between P and Q is subject to two geometrical conditions. When the velocity field is calculated r_z must be assumed, and we have a number of conditions equal to the number of chord lengths between P and Q. The remaining three parameters correspond to the three equilibrium conditions for the rigid body.

The type No. 6 has been encountered in Fig. 43 M (rigid bodies No. 1 and 3). No. 5 is a special case with an uneven number of boundary slip lines. It seems that this construction is possible when there is no stress or angle condition between the points P and Q, so that α_1 and α_2 are not known even if the positions of P and Q are known (another example is the rigid body No. 2 on Fig. 43 M, but here the number of boundary slip lines is again even because both end points are of the type Q on Fig. 43 N 5). The types No. 7 and 8 show that the rigid bodies need not be connected to singular points, but may also obtain in continuous zones. No. 7 might f. inst. be produced by a continuous bulge on the surface, see Fig. 43 O (rigid body No. 1).

Since there may be any number of surface irregularities in a given failure problem - there may f. inst. be any number of strip loads in Fig. 43 M, or the surface may have a sinusoidal form with a small wave length - an originally quite regular rupture figure may have to be modified by the inclusion of any number of rigid bodies of clay, all of them being of the even-numbered type. It is seen that in this way rather complex rupture fig-

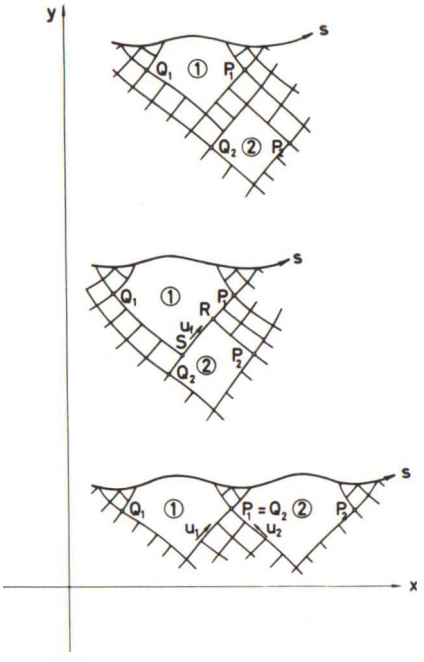

Fig. 43 O: Rigid Bodies Generated by Surface Irregularities.

ures may be obtained. Two neighbouring rigid bodies may be separated by an arc zone construction, a line rupture, or a transition point, cf. Fig. 43 O.

The first mentioned case is normal, the general procedure described above being directly applicable. In the second case one parameter vanishes, λ_{P_1} being equal to λ_{Q_2}. On the other hand, the sliding velocity u_f along the line rupture RS (i.e. along the slip line connecting P_1 and Q_2) must be a free parameter. Similarly, the third case is only possible when both sliding velocities, u_1 and u_2, through the transition point are free parameters. One or more of the boundary slip lines may be broken, or be replaced, by a discontinuity point, cf. the body No. 2 on Fig. 43 J, 1 and 5, and DCGF on Fig. 43 J 7.

The second class of rigid bodies of clay contain the irregular bodies which cannot be considered as parts of rupture zones, so to speak, which have become rigid. They have mostly an uneven number of boundary slip lines, some of which may be replaced by discontinuity points, but bodies of this type with an even number of boundary slip lines also exist. They may be roughly subdivided into the following types.

1. Bodies with one boundary slip line, bounding an Aa-construction (No. 3 on Fig. 43 J 3), possibly together with a boundary to a radial zone (No. 1 on Fig. 43 B) or an arc zone construction (No. 1 on Fig. 43 C, 43 I, and 43 J 1-5).

2. Two boundary slip lines may obtain (corresponding to the type No. 5 on Fig. 43 N) when a rigid body of the first mentioned kind is subdivided by a radial zone, cf. No. 2 on Fig. 43 G, and No. 2 and 4 on Fig. 43 H (in both cases No. 1 is a regular, even-numbered rigid body). Between two radial zones a body bounded by three slip lines may be cut out.

3. Bodies with three boundary slip lines may also separate wall zones in different states of failure (different values of e_f), cf. No. 4 on Fig. 43 J 5 and No. 3 on 43 J 6. Such bodies might conceivably be partitioned by radial zones into one body bounded by two slip lines (regular), a number of bodies bounded by three slip lines, and one body bounded by four slip lines.

4. Finally, bodies with five boundary slip lines may separate surface zones in different states of failure, cf. No. 2 on Fig. 43 B, No. 2, 3 and 4 on Fig. 43 F, No. 3 on 43 G, No. 3 and 5 on 43 H, No. 2 on 43 I (one slip line being replaced by a discontinuity point), No. 2 on 43 J, 2-4 and 6, and No. 3 on Fig. 43 J, 1 and 5.

Such bodies mostly obtain in rupture figures with closed rupture zones. However, as shown in Fig. 43 J arc zone constructions are also possible, and they may not be simple (they may f. inst. contain any number of regular rigid bodies, as may also the closed zones themselves, cf. No. 3 on Fig. 43 J 4). In this case the calculation procedure is much like the one used for the corresponding regular bodies, except that one further parameter may have to be estimated, subject to one stress condition between two surface zones in different states of failure.

Bodies bounded by line ruptures with singular end points (in admissible solutions) form a transitional class between the two classes considered above. They will usually obtain in relatively simple, at most quasi correct solutions.

436 Problems with Internal Boundaries

If there are different clay layers in the failure problem the mathematically correct rupture figures may be very complicated. Relatively simple approximations obtain when the rupture figure in the upper clay layer is statically determined. Then the velocity conditions (3351) may frequently be satisfied directly, without altering the rupture figure. Three examples are shown in Fig. 43 P. The two first examples are concerned with the modification of a zone rupture behind a perfectly smooth wall by an inclined internal boundary. For rotation points of the wall below the foot point the velocity difference across the boundary slip line will produce slidings along the lines shown dotted in the figure. It is seen that in the stronger clay material (supposed to be the lower clay layer) a radial zone or an arc zone may be developed. In the last mentioned case the rupture figure may for low positions of the rotation point be modified into an XfWPR-type.

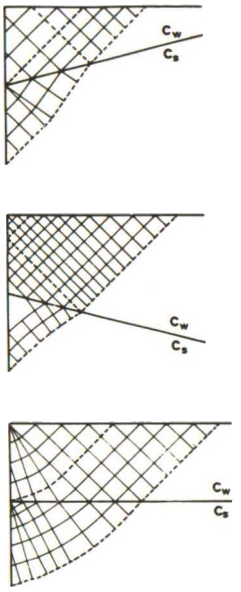

Fig. 43 P: Rupture Figures for Earth Pressure Problems with a Stratified Clay Profile (Statically Determined Zone Ruptures).

The third example shows the modification of a zone rupture corresponding to a partly rough wall. In the lower clay layer the types XfWPR, BfWPR, XfPR, or BfPR may become actual. In all three cases the internal boundary acts as a clay surface with known surface loadings, determined by the statically determined rupture zones in the upper clay layer.

The velocity field in the upper clay layer may clearly become kinematically impossible in some cases, opposite signs for u_f and τ_f obtaining along some of the slip lines (f. inst. the b-line in the first example). In such cases the approximation is comparable to that of a zone rupture with one or more discontinuity lines. The correct solution will have a complicated construction with an arc zone crossing the internal boundary.

For zones with mixed boundary conditions the statical and kinematical conditions for an internal boundary will influence the zones on both sides of the boundary. This makes the calculations rather difficult. In principle the boundary stresses may first be assumed after which the rupture figure in the lower clay layer can be constructed. For the upper clay layer the internal boundary will then have known boundary deformations which determine the rupture figure in this domain of the clay (the solution to this problem may not be easy to find or simple to calculate, however). Finally it is ascertained whether the boundary stresses found by the latter rupture figure are identical with the assumed ones. If not the above process must be repeated until a sufficiently good agreement is obtained.

As an example Fig. 43 Q shows (by a rough sketch) one of the possible rupture figures corresponding to Fig. 43 B when an internal boundary exists in the clay. Dependent on the position of the boundary, and on the ratio c_w/c_s, different constructions may be obtained (cf. the limits $c_w/c_s = 0$ and 1). Corresponding constructions obtain when band zones or line ruptures intersect the boundary.

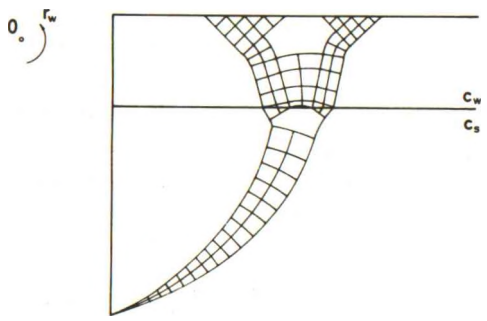

Fig. 43 Q: Radial Zone Modified by the Transgression of an Internal Boundary.

The mathematically correct rupture figures may also be rather complex for bearing capacity problems on stratified soil profiles. As an example Fig. 43 R shows on the right hand side the rupture figure corresponding to squeezing of a weak clay layer between a foundation and a rigid layer (type RPsWTWsPR, cf. Fig. 42 B in section 421). On the left hand side is shown a possible modification (not proved to exist) when the shear strength of the lower clay layer is decreased so that an additional rupture figure (type RfAfR) is on the verge of failure. It may not be kinematically possible; if not it must be replaced by a more complex figure containing a band zone with two surface zone complexes.

For decreasing values of c_s (or increasing values of the foundation width) integrated rupture figures are obtained. For even smaller values of c_s a radial zone will develop in the lower clay layer, starting from the boundary slip line shown in Fig. 43 R. An outer rupture figure much like the one shown in Fig. 43 H is developed (with a special construction like the one shown in Fig. 43 Q where the arc zone intersects the internal boundary). Eventually the rupture zones near the symmetry line will disappear so that for $c_s = c_w$ the normal Prandtl figure is obtained.

Evidently such rupture figures are not suited for practical calculations. In practice problems of this kind will therefore be solved by approximate

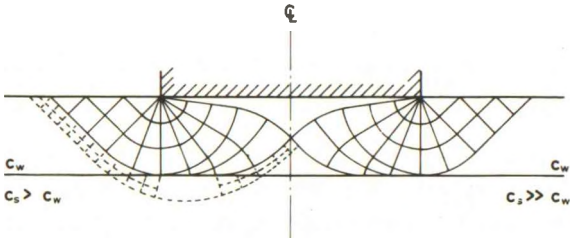

Fig. 43 R: Squeezing of a Weak Clay Layer Between a Foundation and a Stronger Clay Layer. Limiting Case with a Rupture Figure on the Verge of Failure in the Stronger Clay.

rupture figures, using systems of line ruptures (Sec. 425) when possible. If rupture figures with other types of rupture zones (f. inst. band zones or radial zones in AfPfA rupture figures) intersecting the boundary cannot be avoided one may use the velocity fields for the solutions in homogeneous clay in kinematically admissible solutions. The zones will then not be statically possible, however.

Especially for earth pressures an even simpler approximation has been proposed by Brinch Hansen who uses his approximate earth pressure distribution for rigid bodies of clay in contact with the wall. The earth pressure coefficients characterizing this distribution are in a homogeneous clay independent of the value of c. In a stratified clay the same coefficients are used, inserting in each clay layer the actual value of c to find the earth pressure.

The method is exact for a zone rupture behind a vertical, perfectly smooth wall if the surface and all internal boundaries are horizontal (vertical and constant surface loading). For other rupture figures it may in unfavourable cases be quite far off. For example, it is not able to distinguish between different inclinations of the internal boundary. The method could be elaborated to cover also such cases, however, using f. inst. the earth pressure coefficients corresponding to inclined surfaces.

44 SPECIAL PROBLEMS

441 Stresses in Rigid Bodies

It is frequently necessary to be able to calculate internal forces and moments in external rigid bodies in the state of failure. This is of course easy when the rigid body is not in contact with the soil, and also when the boundary to the clay is completely covered by a wall zone. In these cases the pressure distribution on the external rigid body is known in details, and the normal theory of structures may be used. The problem is also simple even if there are rigid bodies of clay in contact with the external rigid body, when f. inst. only the maximum moment in a wall is required, and the point of maximum moment is located in a wall zone part. Then the known values of the force resultants between the rigid body of the clay and the wall may

be used in exactly the same way as if the complete earth pressure distribution was known.

However, if the point of maximum moment is located in a wall part in contact with a rigid body of clay the point and the moment cannot be determined directly since the stress distribution is in principle unknown inside a rigid body, the state of failure being assumed to be plastic-rigid.

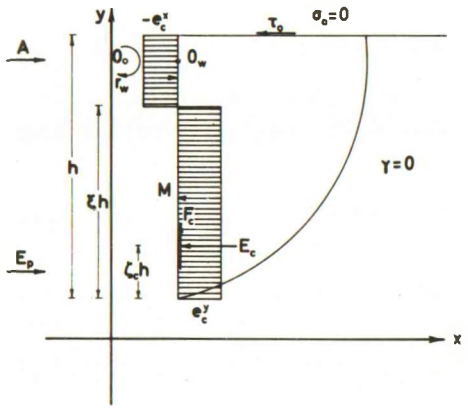

Fig. 44 A: An Anchored Sheet Wall. Earth Pressure Distribution by Brinch Hansen's Approximation.

Brinch Hansen has proposed an approximate solution to this problem, cf. Fig. 44 A in which a simple line rupture is assumed to be used in an active earth pressure problem. The rotation point for the wall is O_w; for the clay body it is O, the wall being partly rough ($0 < c_a < c$). If the clay surface is horizontal and uniformly loaded the earth pressure corresponding to the normal load σ_o, and to the unit weight γ of the clay will be independent of the rupture figure. Its distribution can therefore be assumed to be the same as in zone ruptures ($e_p = \sigma_o$, $e_\gamma = \gamma z$, $f_p = f_\gamma = 0$, where z is the depth below the clay surface). For the remaining earth pressure, corresponding to $\sigma_o = 0$ and to $\gamma = 0$, only the resultants E_c and F_c are known, together with the height of E_c above the foot point of the wall. F_c may be distributed uniformly along the wall, also if the body is not sliding upon the wall, so that $|f| < c_a$. E_c may be represented by an earth pressure distribution dividing the wall into two uniformly loaded parts. If one of the pressure amplitudes, f. inst. e_c^x is fixed (arbitrarily) at the value obtained in a WPR zone rupture (the maximum value that can be taken by the clay near the top of the wall), the known values of E_c and ζ_c will determine the remaining quantities e_c^y and ξ. When the restraint forces A and possible earth pressures E_p acting on the other side of the wall are also determined the point of maximum moment M, and the moment itself, can be determined in the usual way, the maximum moment obtaining in the point where the transversal force in the wall is zero.

This method has the advantage that it is one of the simplest possible rational approximations. Its treatment of e_p and e_γ is correct, these earth

pressure components being in fact corrective boundary loadings of the type K (with negative sign) considered in (2305-7). They must be added on all clay boundaries (or as external loadings on external rigid bodies in contact with such clay boundaries) in order to bring the substitute failure problem with $\sigma_o = 0$ and $\gamma = 0$ back to the original one.

An alternative method is suggested by the following observations. The wall will normally also be calculated by the theory of plasticity. Redistributions of stresses until the final state of failure is obtained are therefore permitted in the structure of external rigid bodies, and also between such bodies and the clay, as they are in the clay material itself (where the final, plastic-rigid state of failure is expressly assumed). Hence, for design purposes it is not necessary to assume that the yield moment in the wall should obtain simultaneously with an elastic-plastic state of failure in an adjacent rigid body of clay; this body may instead be assumed to be on the verge of failure. In this way a continuous variation of the design moment is also obtained between walls in which a yield hinge is assumed to develop, and walls assumed to be unyielding: the last mentioned case is calculated as if there were a yield hinge, but the relative rotation between the wall parts is assumed to be zero relative to the overall plastic movements in the rupture figure.

In this connection the rupture zones and line ruptures bounding the rigid body of clay may be considered as if they were free surfaces with known (or at least calculable) surface loadings: the plastic deformations in the body cannot change the rupture figure since they are assumed to be zero. The proposed method may therefore more specifically be formulated in the following points.

1. The rupture figure is first calculated in the normal way, assuming the wall to remain rigid.
2. The rigid body is then considered as a clay domain at rest, acted upon by the known surface loadings and stresses along boundary slip lines, and by the forces transmitted through the external rigid body. If the rupture figure gives a possible or a quasi-possible solution the collection of external forces upon the rigid body of clay will be in equilibrium.
3. In this case the required moment may be found as the (negative) restraint force (P_r, cf. Sec. 223) in a secondary failure problem in controlled strain, the prescribed movement (d_r) being a relative rotation between the two wall parts. Evidently one of the wall parts

may be assumed to remain unmoving, the other part rotating about the assumed point of maximum moment. The secondary rupture figure is treated exactly as in an ordinary failure problem. If the equilibrium method is used the choice of moment point may be checked by the condition that the transversal force shall be zero. If the energy method is used the condition is that the moment shall be a maximum (minimum of P_r) for variations in the position of the moment point.

4. If the primary rupture figure is itself approximate (admissible with possible zones) the rigid body may not be in equilibrium. The solution will then not be unique, but an estimate of the moment can still be obtained by arbitrarily considering one of the wall parts to be fixed (taking in this way the corrective forces that are necessary to obtain equilibrium). One should of course choose the wall part which gives the greatest maximum moment found as under 3. above.

5. In the last mentioned case the transition to a state of failure with a finite relative movement may not be continuous, since the original rupture figure will not have a sufficient number of parameters. However, the rupture figure corresponding to a finite movement in the yield hinge need not be possible or quasi-possible to ensure that the transition is continuous. It is only required that the work done by the movement in the yield hinge can be separated from the other terms in the energy equation ($P_r = \frac{\partial W}{\partial d_r}$). The rupture figure for the case with an unyielding wall should therefore be the limiting case ($d_r \rightarrow 0$) of a more general rupture figure which satisfies this condition, see f. inst. Ex. 24 c.

The same principle may be used to find other internal force resultants in the rigid bodies insofar as they depend on unknown stresses in rigid bodies of clay. Notice, however, that the forces found in this way are not independent. Thus, it is evident that one cannot find f. inst. first a moment in a wall by assuming one rupture figure on the verge of failure in an adjacent rigid body of clay, and then a shear force by assuming a quite different state of failure in the same rigid body. In fact, problems of this kind must be considered as design problems, in which a mode of failure in the rigid body is assumed, although the movements corresponding to this secondary failure are small in relation to the primary failure movements. This means that the ratios between the different values of d_r must be decided upon, if

there are more than one restraint, possibly by a consideration of an economical optimum, and a consistent secondary rupture figure (on the verge of failure) must be constructed.

Undetermined values of σ in the neighbouring rupture zones may be chosen arbitrarily, subject to the condition that the rupture figure shall be statically possible. If σ has any influence on the required internal forces this condition will frequently be the effective condition of design. In this way the secondary rupture figure may be made to extend on both sides of a rupture zone with an undetermined value of σ.

A (rather special) case obtains when some of the values of d_r are small in relation to some other values. It may then be necessary to construct tertiary rupture figures inside the rigid bodies of the secondary ones. In principle such a hierarchy of rupture figures may extend to an arbitrarily high order, but in practice cases of this kind will probably be exceedingly rare.

Since the secondary (and possibly higher order) rupture figures are calculated under the same assumptions and by the same methods as the primary rupture figures hitherto considered in this work the same conclusions apply as to the uniqueness of solutions and to the properties of approximate solutions (except that the clay domain may not be in equilibrium). Thus, statically admissible approximations are on the safe side, and kinematically admissible ones on the unsafe side, if they are not correct. Notice, however, that in these statements it is tacitly assumed that the primary rupture figure is correct. If this is not the case the rigid body of clay may be acted upon by corrective forces which do no work during the movements in the primary rupture figure. Therefore, this body may well be in equilibrium in this rupture figure (the corrective forces being taken as reactions by the wall), but the moments determined by the secondary rupture figure are influenced by these forces to an unknown extent and in an unknown direction. However, if the primary rupture figure represents a good approximation to the correct one it seems safe to conclude that the moments etc. determined by the secondary rupture figures will also give good estimates of the required quantities, even if it cannot be proved.

Example 44a

The method outlined above may be illustrated by the problem of finding the maximum bending moment in a slab foundation acted upon by a known system of loads in equilibrium with the earth reaction Q at failure (in practical design problems it will usually be a nominal state of failure).

For a centrally and vertically loaded foundation on the surface of the clay the classical Prandtl rupture figure applies. Assuming the foundation to be perfectly rough in relation to the clay (c_a = c) there will be a triangular rigid body of clay directly beneath the foundation. This clay body may fail in three different ways, shown on Fig. 44 B.

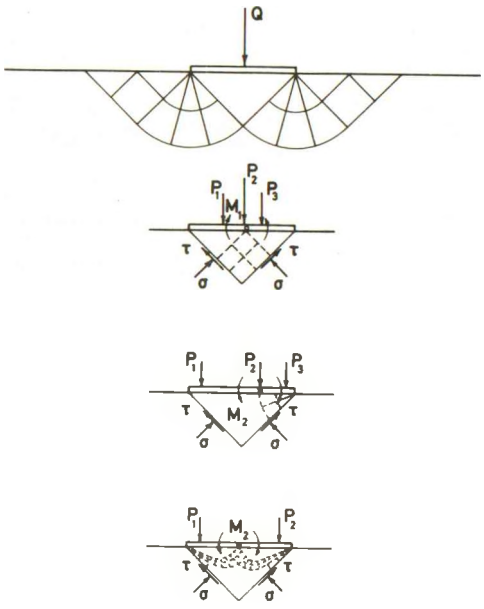

Fig. 44 B: Rupture Figures on the Verge of Failure in the Rigid Body Below a Strip Foundation.

In the first case the active loads (P_1, P_2, P_3, acting as line loads or as continuous loadings), which are in equilibrium with Q, are concentrated about the centre line of the foundation so that the maximum bending moment M_1 will be positive. The secondary rupture figure, shown with dotted lines in Fig. 44 B, is obtained simply as a statically determined rupture zone, constructed by means of the boundaries with known boundary stresses σ and τ (second initial value problem type, since the boundaries are slip lines). The end point of the zone must be located at the point of maximum moment.

For the Prandtl rupture figure this construction is seen to be equivalent to the assumption of a uniformly distributed subgrade reaction, so no special rupture zone construction is necessary in this case. However, the same construction may be used in more general cases (rupture figure XfPR, XfWPR etc.) where the corresponding reaction may not be uniformly distributed. The point of maximum moment may then have to be found by trial and error, or the stress distribution found by covering the rigid body by a rupture zone constructed from the boundary slip lines may formally be used.

If, on the other hand, the forces P are concentrated near the edges of the foundation so that the maximum moment M_2 is negative, the secondary rupture figure will correspond to an ordinary passive earth pressure problem. In this special case where the foundation is rough, and the boundary

curve is a slip line, the rupture figure (normally of the type WPR) will reduce to a simple radial zone. This assumption evidently gives smaller values for M_2 than does the uniformly distributed subgrade reaction. Only if the foundation is assumed to be perfectly smooth will the two results be identical. Evidently, in some cases it may be necessary to investigate by trial whether the design moment is in fact positive or negative.

For some distributions of P the simple radial zone may only be possible if it is assumed that the foundation can lift away from the clay surface, when the negative maximum moment obtains near the centre line. If this cannot be assumed the secondary rupture figure may be as sketched in the lower Fig. 44 B. It is a sort of arc zone rupture figure with special properties arising from the facts that $\tau = c$ along the boundary curve (corresponding to a free surface in an earth pressure problem) and that the moment point is not a foot point of a wall, but is a hinge between two rough walls.

The last rupture figure is by no means simple, but the constituent rupture zone elements are ordinary open rupture zones with mixed boundary conditions. The lower tip of the triangular rigid body may be assumed to remain fixed.

Example 44 b

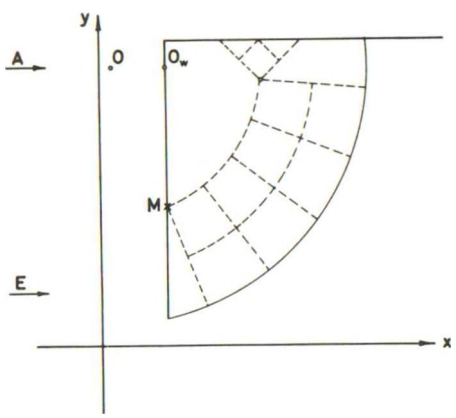

Fig. 44 C: Rupture Figure on the Verge of Failure in the Rigid Body above an a-Line Rupture (Bending of the Wall at the Point M).

The earth pressure problem considered in Fig. 44 A may be solved approximately by the finding of the maximum moment from a secondary rupture figure as shown in Fig. 44 C (cf. Fig. 42 W). It has only one free parameter, apart from the one used to find the position of the maximum moment, so it will probably only give a relatively rough estimate (on the unsafe side). On the other hand, it is reasonably easy to calculate, and is therefore well suited for design work in practice. If closer approximations are needed, rupture figures of the types shown in Fig. 43 J must be used. The primary rupture figure should then also be replaced by the correct solution.

442 Statical Possibility

The most difficult problem in the calculation of a rupture figure which is intended to give the correct solution is the proof that the solution arrived at is statically possible. In principle this investigation has a meaning only if the solution is possible, i.e. if the equilibrium and failure conditions are satisfied at all points of the rupture zones. Thus, it is a provision that under the calculation of the rupture figure it has been shown that for example:

1. no line rupture meets the surface or any other line rupture under a statically incorrect angle.
2. no angle through a rigid body between a slip line and a wall is smaller than the statically possible value.
3. no two boundary slip lines for zones meet each other at statically incorrect angles ($\neq \frac{\pi}{2}$ for ordinary corner points and transition points, $\leq \frac{\Delta \sigma}{2c}$ for discontinuity points).

The maximum shear stress is then known not to exceed the shear strength at any point of the boundaries to the rigid bodies of clay. To this may be added the further condition that it shall be possible to construct rupture zones of an infinitesimal width from the boundary slip lines into all rigid bodies of clay without exceeding the failure condition. If we consider the zones which are generated by the two boundary slip lines meeting in the normal corner points of a rigid body (Fig. 44 D) this condition is equivalent to the demand that two such zones obtained from two corner points on the same boundary slip line shall not overlap when they are both continued until they meet at a point on the slip line. Let O and A be two such corner points on the same a-line, taken in the order of increasing values of λ, and let O and B be two corner points on the same b-line, in the order of increasing values of μ. Radii of curvature, R_O, S_O, S_A, and R_B are measured at the corresponding points on the parts of the slip lines bounding the rigid body.

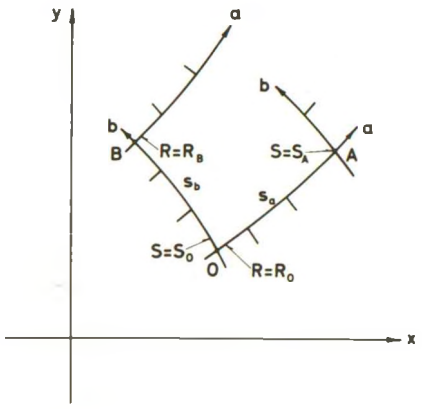

Fig. 44 D: Radii of Curvature at the Corners of a Rigid Body Bounded by Rupture Zones.

By the use of (3113) it is seen that the condition of non-overlapping zones can be formulated as follows.

For a-lines: either $S_O \geq 0$, and $S_A \leq 0$ or $S_O + s_a \leq S_A$;
or $S_O \leq -s_a$ and $S_O + s_a \leq S_A \leq 0$ (4401)

For b-lines: either $R_B \geq 0$, and $R_O \leq 0$ or $R_B + s_b \leq R_O$;
or $R_B \leq -s_b$ and $R_B + s_b \leq R_O \leq 0$ (4402)

If one of the points is a singularity point (vertex point for a radial zone or end point for a line rupture) the corresponding value for R or S is put equal to zero. For an end point at a wall (3309) must be used ($S \cos m_t = R \sin m_t$) if the angle between the slip line and the wall is statically correct (R or S = 0 if the angle is greater.)

However, the shear stresses in the interior of the clay bodies may exceed the shear strength even if the above conditions are all satisfied. On the other hand, in quasi-possible solutions where some of the conditions are known not to be satisfied one may wish to ascertain that the interior of the clay bodies are not stressed to failure, even if the boundary parts are. The solution will then be quasi statically possible, and it may be used as a basis upon which the correct solution can be constructed.

This investigation has much in common with the one considered in the preceding section, and it is performed in much the same way. The only difference is that an extra parameter must be introduced, the value of which should indicate whether the body is in a state of failure or not. Except in the rare cases where the body is exactly on the verge of failure, and can be covered completely by a rupture zone constructed from the boundary slip lines (or a statically admissible stress distribution can be shown to exist in the body), the simplest way is to consider the problem as one of controlled strain, using the following procedure.

1. The body is considered as a clay domain with known boundary loadings along all free surfaces and boundary slip lines. Since the solution is at least quasi-possible all external loadings on this domain will be in equilibrium.

2. Any rupture figure in the interior of the body will divide it into at least two rigid bodies of clay separated by a system of line ruptures and/or rupture zones. If their movements are not determined by external conditions, one of these bodies can be considered as unmoving, the movements in the rupture figure being governed by one imaginary restraint movement d_r which is compatible with the rupture figure and with the external movement conditions (d_r will fre-

quently be the value of the rotation r_z of another one of the secondary rigid bodies).

3. The rupture figure is calculated in the normal way, giving the restraint force P_r corresponding to the restraint movement d_r. If the work $P_r d_r$ can be shown to be negative for any secondary rupture figure (possible or admissible) which is known to be on the unsafe side, the original rigid body will certainly not be stable. On the other hand, if $P_r d_r$ is positive then either the body is stable or the secondary rupture figure itself is on the unsafe side (i.e. not statically possible).

4. This process is seen to be recursive. In principle a possible secondary rupture figure should be shown to be statically possible by the construction of tertiary rupture figures in its rigid bodies of clay. However, in practice one will soon arrive at a stage in which all remaining rigid bodies are easily seen to be stable.

5. If $P_r d_r$ is exactly zero in a statically possible secondary rupture figure it is seen that this figure does in fact exist on the verge of failure. This indicates that a boundary point for the regime of the primary rupture figure has been reached, considering the external parameters as variables. Thus, the type of rupture figure can be changed by an infinitesimal change of the external parameters.

The last mentioned state may, however, also be said to obtain in other connections. Thus, the rupture figure may be on the point of becoming geometrically impossible (a chord length or a centre angle being exactly zero), or kinematically impossible (ϵ is exactly zero at a point, along a curve, or in a whole region of the rupture figure. The last mentioned case is seen to be identical to the one considered under the point No. 5 above. It is obtained when the considered rupture figure has included both the primary and the secondary one).

It is seen that the investigation of the statical possibility of a rupture figure may be rather complicated, involving the calculation of a number of secondary and possibly higher order rupture figures in the bodies assumed to remain rigid. However, for the bodies in the interior of the rupture figure, i.e. bodies that are completely surrounded by rupture zones, only a relatively small number of secondary rupture figures are at all possible. Some characteristic examples of this are given in the following.

1. The rigid body along a wall indicated by the rupture figure elements XfW, XfB, XfP, BfW, BfB, or BfP can be covered completely by a

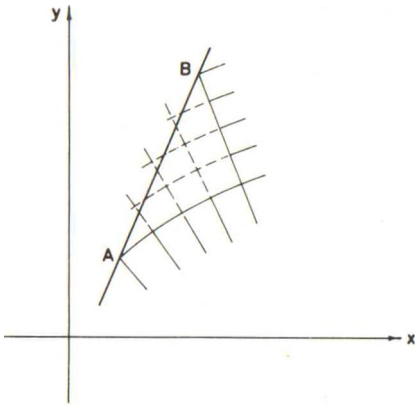

Fig. 44 E: Secondary Rupture Zone Covering a Rigid Body Near a Wall.

statically admissible rupture zone, determined by the boundary slip lines (Fig. 44 E). Because of the convex slip line all angles between the interior slip lines and the wall (i.e. all values of τ_{nt}) will be statically admissible, if they are at the end points A and B. Such bodies are therefore always statically possible.

2. A rigid body in an AaW, AaB, AaP, or AaR rupture figure may sometimes fail by a secondary AaB rupture figure (Fig. 44 F). The rotation points O_2 (for the secondary A-rupture line) and O_3 (for the arc zone) must be located on the same normal to the wall, but not necessarily on the normal through O_1 (the centre of the primary line rupture). The secondary rupture figure has 3 parameters: $\rho_2 = \rho_3$, λ_2, and λ_3, to be found together with P_r (f. inst. the shearing force along the wall part AC) by the 3 equilibrium conditions for the rigid body between the two line ruptures and the projection parallel to the wall of the forces acting upon the secondary body AC. It is seen that the primary rigid body ACB will not as a rule slide upon the wall, and that it fails by the sliding away of the secondary body AC.

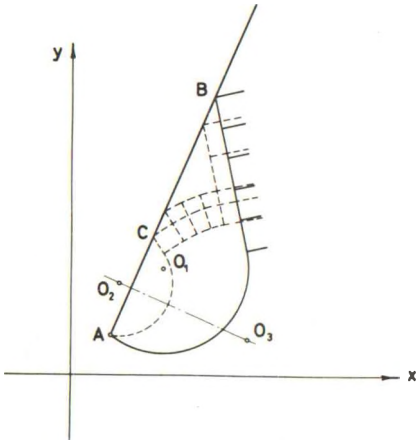

Fig. 44 F: Secondary Rupture Figure (AaBfW) in a Rigid Body to an AaW-Construction.

3. Correspondingly, a secondary A-line rupture may be critical in the unmoving rigid body bounding a rupture figure of the type f. inst. AaBfR, AaBfPR, or AaBfWPR (replace the dotted lines by full lines and vice versa in Fig. 44 F).

4. The more or less triangular rigid body bounded by a wall, a free surface, and a rupture figure of the type XfR, X, A (or the corresponding possible solutions with a curved radial zone as in Fig. 43 B, cf. Fig. 31 H and 33 K), BfR etc. may fail by a secondary rupture figure constructed as shown in Fig. 43 I (to the left of OADG) and Fig. 43 J 1-4 (to the left of the a-lines through the points E). In principle this process is recursive, since the rigid bodies No. 1 in the above mentioned rupture figures might evidently fail by a similar construction. The same type of failure may also obtain f. inst. in the bodies No. 2 in Fig. 43 G, and No. 2 and 4 in Fig. 43 H. The construction AEFG in Fig. 43 J 7 is quite similar. In all cases we have 2 parameters and the value of P_r (an unbalanced moment) against the 3 equilibrium conditions for the new rigid body. The secondary rupture figure is seen to correspond to a failure of the primary rigid body by bending.

5. The rigid body bounded by an A-line rupture (or the corresponding possible solution) may also fail by a sort of combined shear and bending, if it is narrowed too much by a reentrant corner or a load discontinuity. The simplest secondary rupture figure is in this case a line rupture (L_2 on Fig. 44 G) starting at the discontinuity or corner point. In this way the investigation of the statical possibility will be a simple calculation of stability, the stresses along the primary line rupture L_1 being known. However, the secondary rupture figure is only quasi-possible so it will only give an estimate (on the unsafe side, although it will probably be rather close) of the branch point between a simple line rupture and a combined rupture figure. Besides, it has no continuous transition, for a further variation of the external parameters, to rupture figures of the type AfPfA. Fig. 44 G is logically continued by rupture figures consisting of three ruptures meeting in the clay.

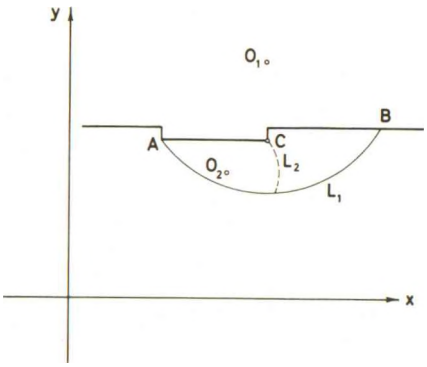

Fig. 44 G: Secondary Line Rupture Between a Corner Point and a Line Rupture.

If it is required that a continuous transition to a figure AfCfA should exist, the condition must be imposed on the line rupture L_2 that it shall intersect L_1 under a right angle. It may then open up into a radial zone when the external parameters are changed. In this case it has only one free parameter, so it will as a rule be more on the unsafe side than if this condition was not imposed. If a radial zone with straight radial slip lines (P instead of C) is required, L_2 should be straight. It is then uniquely determined (no free parameters).

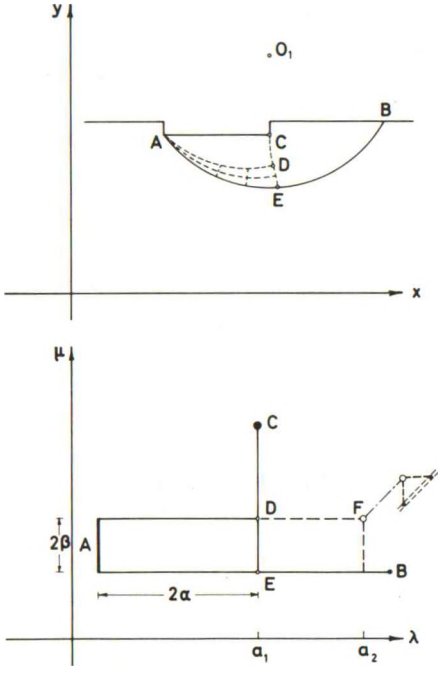

Fig. 44 H: Secondary (Possible) Rupture Figure Including Also a Radial Zone (or, Alternatively, an Arc Zone with a Surface Zone Complex).

6. A possible secondary rupture figure will in this case be composed of a radial zone ADE (Fig. 44 H), which is statically determined, and a line rupture CD. For this rupture figure we have two parameters (f. inst. α and β) as in the ordinary line rupture Fig. 44 G. Notice that the zone may also be placed to the other side, along the part BE of the line rupture (shown with dotted lines on the lower Fig. 44 H). This version obtains if β turns out to be negative. It has 5 parameters (a_1, a_2, β, r_z for the rigid body between B and the discontinuity point F, and f. inst. the chord length DE), corresponding to the fact that there are now 3 secondary rigid bodies instead of the 2 shown in the upper Fig. 44 H. The two versions may also be combined, corresponding to a tertiary rupture figure of the type No. 4 above in the body CDEB of the upper Fig. 44 H. For a further change of parameters the line rupture CD will open up into a radial zone, cf. Fig. 43 G.

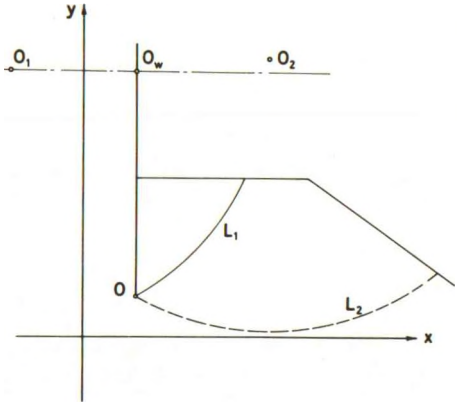

Fig. 44 I: An Alternative Line Rupture L_2 as a Secondary Rupture Figure to the Primary Line Rupture L_1.

The investigation of the statical possibility should be extended to the unmoving rigid body outside the rupture figure (cf. the point No. 3 above). In principle the same procedure as above should be used. This is important because one will frequently find that the secondary rupture figure is more or less completely separated from the primary one. For example, in an earth pressure problem with a slope at some distance from the wall the primary rupture figure may correspond to a local earth pressure which does not include the influence from the slope, whereas the secondary rupture figure extends to the slope, cf. Fig. 44 I.

In this example (passive earth pressure) the rotation point for the wall is O_w. The primary rupture figure is supposed to be a line rupture L_1 whose rotation point O_1 is at the wall normal through O_w. There are no restrictions on the position of the rotation point O_2 of the secondary line rupture L_2, however, since its movements are zero in relation to the movements of L_1. Note carefully that it is not sufficient to calculate separately each of the two line ruptures L_1 and L_2, afterwards selecting the most critical one to represent the true rupture figure. This is because during these calculations O_1 and O_2 must both be on the wall normal through O_w, whereas, when the statical possibility is investigated after assuming one of the line ruptures as the primary rupture figure, the rotation point for the secondary one is unrestricted. The method of selection may therefore be on the unsafe side.

This will show by the fact that the secondary rupture figure is unstable for both choices of primary rupture figures. The correct rupture figure will then not be any single one of the two alternatives, but will be a combination of the two rupture figures, acting simultaneously. Neither O_1 nor O_2 need then be on the wall normal through O_w (but they should be located on each side of it), cf. also Ex. 24a (Fig. 24C).

443 Rupture Figure Complexes

In Fig. 44 I we had an example of two rupture figures corresponding to two different movements of the same external rigid body acting simultaneously. Another example is shown in Fig. 44 F. Such rupture figure complexes may be characterized in the following way:

1. Each rupture figure is in itself a solution to the given failure problem for one set of values of the external parameters.
2. In a domain of parameter sets the combined rupture figure is more critical than any one of the two constituent figures.
3. By a linear combination of the movements corresponding to each of the two rupture figures a one-dimensional subset of the external parameters is obtained in which the geometry of the rupture figure and the force resultants acting upon the external rigid body are constant, while the movements of the body change.
4. At the two end points of this subset one or the other of the constituent rupture figures is just on the verge of failure (zero movements).

However, the distinction between composite rupture figures of this type and complicated ordinary rupture figures is not sharp. For example, the correct solution to the problem shown in Fig. 44 I may well have a multiple radial zone as shown in Fig. 43 F. The statement No. 3 above will then no longer be true. The rupture figure with connected rupture zones will change for any variation of the external parameters. On the other hand, it is still true that for some parameter sets parts of the rupture figure (all zones above OBF or below OCG on Fig. 43 F) are just on the verge of failure.

This example shows that in such cases a great saving in calculation work may be obtained if the possible rupture figure is replaced by a quasi-possible one in which the two constituent rupture figures are not connected.

A similar, but more complicated problem obtains when the primary and secondary rupture figures do not cover the same parts of the external rigid bodies. Thus, in the examples shown in Fig. 43 G and H it is assumed that the foundation OQ is thin. If one has instead a block foundation extending to the original clay surface secondary rupture figures must develop in the rigid bodies No. 2 and 4 along the vertical faces to permit the relative movements between these bodies and the block foundation. The calculation of the combined rupture figure obtained in this way (assuming the primary and secondary rupture figures to be separated) must take into regard that

the equilibrium conditions for the remaining parts of the bodies No. 2 and 4 are influenced by the forces from the secondary rupture figures. These forces, on the other hand, depend on the movements of the rigid bodies, unless the secondary rupture figures are statically determined. The parameters of the primary and secondary rupture figures are therefore interdependent.

In this connection the corner points O and Q act as a sort of discontinuity points (as does the point O in Fig. 44 I). If the stress condition between the slip lines meeting at the point is not satisfied, the primary and secondary rupture figures will in the correct solution be connected. We have then again one rupture figure with connected zones instead of a complex of simpler rupture figures.

As an example consider the rupture figure for a quadratic bar being pulled transversally in the interior of a clay domain. The problem is assumed to be one of controlled strain, the transversal movement w_o, horizontal and parallel to a pair of opposite sides of the quadrangle being known. The pulling force Q per unit length of the bar is required.

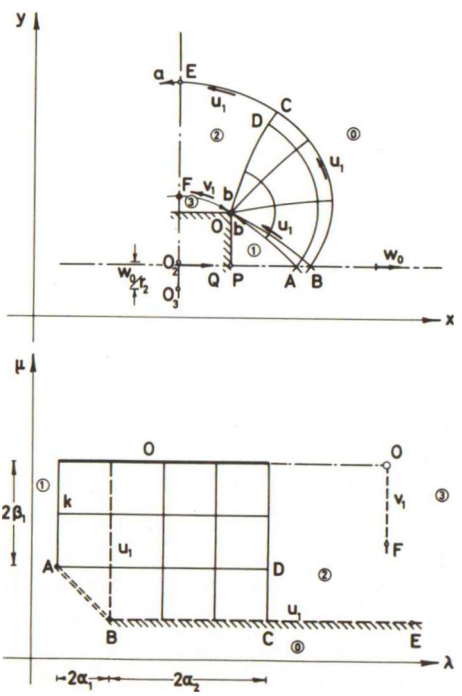

Fig. 44 J: Rupture Figure Around a Quadratic Bar Translated Inside a Clay Mass.

A possible solution to this problem is shown in Fig. 44 J. The rigid bodies No. 1 and 3 adhere to the bar, which is assumed to be rough. The body No. 2 is rotating about a point O_2. Because of the symmetry only one quarter of the rupture figure need to be considered, and O_2 must be located on the vertical axis of symmetry of the bar. The line rupture CE is connected by a normal point C to the zone OABC. The line rupture OF represents a secondary rupture figure which is caused by the movement of the body No. 2 relative to the bar. O is a discontinuity point between the two rupture figures OABCE and OF.

This rupture figure is calculated in the normal way. Thus, after an estimate of the parameters α_1, α_2, and β_1 has been made, the chord lengths along OA may be estimated, subject

to one geometrical condition (A must be located on the horizontal axis of symmetry for the bar). The rupture zone OABC can now be constructed. Because of the symmetry the portion AB of the horizontal axis may be considered as a perfectly smooth wall. The position of the corner point C, and the value of m at this point, determine the position of O_2, the line O_2C (length R_2) which is the radius to CE being a tangent to the slip line OC at C.

The sliding velocity u_1 may now be assumed. This also determines the value of r_2, the rotation of the rigid body No. 2, since $u_1 = r_2 R_2$. The boundary conditions along BC and OC will now determine the values of w in the zone. u_1 is determined by the fact that u_s, the sliding velocity along the imaginary wall AB, should be equal to w_o at the point A, and the boundary conditions along OA ($w = 0$) determine the unknown chord lengths (if any) together with one of the initial parameters α_1, α_2, or β_1.

When the above mentioned conditions have been satisfied the line rupture OF may be constructed, using that O_3 must be located on the same axis as O_2, and for kinematical reasons the distance O_2O_3 must be equal to $\frac{w_o}{r_2}$. From the value of $R_3 = O_3O$ the sliding velocity v_1 may be found. It is equal to r_2R_3.

The admissible solution with possible zones obtained in this way may be used to find an estimate for Q. The extreme solution may be found by varying the remaining two parameters. Alternatively the three equilibrium conditions for the rigid body No. 2 may be used to find the stress difference $\sigma_F - \sigma_E$, and the two parameters.

If the parameter α_1 turns out to be negative, the rupture figure shown in Fig. 44J is geometrically impossible. The radial zone OAB will then not obtain, but the line rupture CE may instead be replaced by an arc zone. Because of the symmetry it must have straight radial slip lines. In this case the width of the arc zone replaces α_1 as an initial parameter.

If the bar is only partially rough, so that the rigid body No. 3 may slide upon the bar, the distance between O_2 and O_3 may be smaller than $\frac{w_o}{r_2}$. It must then be determined by the equation of horizontal projection for the body No. 3. Finally, if the stress condition for discontinuity points is not satisfied at O between the slip lines OC and OF, a radial zone must exist between these two slip lines. This introduces an extra parameter, representing the length of the radial slip lines, but we have now the condition that σ

shall revert to its original value after a full circulation of the boundaries to the body No. 2.

Notice that in rupture figures of this kind, that are not connected to free surfaces, the absolute values of σ are unknown. σ_E may be put equal to zero, which determines σ at all points in the rupture zones, but an arbitrary constant may be added to all values of σ found in this way. This constant will have no influence on the value of Q, but if any upper (or lower) limit is required f. inst. to design the walls of a hollow bar, it must be determined by a secondary rupture figure, connecting the outer boundary of the rupture figure to another rupture figure or to a free surface. A corresponding secondary rupture figure may have to be constructed in the rigid bodies No. 1 and/or 3.

444 Approximate Movement Conditions

The rupture figures considered in this work have assumed the solutions to be kinematically admissible with possible zones. However, as explained in Sec. 424 it is sometimes possible to use rupture figures of the same types to even simpler approximations. Thus, in simple radial zones one may neglect the movement conditions, demanding only that the volume of the zone shall remain constant.

This method may be generalized to cover in principle all the rupture figure types considered in the previous sections. In the general case it may be defined as follows.

1. The mixed boundary conditions are not used for the rupture zones. The statical and geometrical conditions are all satisfied, however. When they are not sufficient to determine the zone some arbitrary geometrical condition is imposed. Thus, for radial zones and arc zones (Fig. 43 A-C and Fig. 43 G-K) one or more of the unknown boundary slip lines may be assumed to be circle arcs (which will not be very far off).
2. The zones are constructed geometrically in the usual way and the movement components for the rigid bodies are determined, disregarding the movement conditions in the zones, but satisfying the conditions along line ruptures, and keeping also the total volumes of the zones constant. If these conditions are not sufficient the remaining movement components are regarded as free parameters.

3. The work equation (2426) may now be used, all terms being known. The extreme solution may be sought, or, if there is a sufficient number of free parameters, the equilibrium method may be used (the movement components for the rigid bodies are then only needed to show that the volumes of the rupture zones can in fact be kept constant). If all equilibrium conditions are satisfied the solution will at least be quasi statically admissible.

Some approximate calculations in practice are very close to this method. Alternatively, all movement conditions may be completely disregarded, and the number of equilibrium conditions to be satisfied (chosen arbitrarily) is exactly equal to the number of free parameters. This version might be called the method of disregarded movement conditions.

Strictly speaking these methods are outside the scope of the present work because they do not satisfy the conditions indicated in Sec. 243 for approximate solutions. Thus, since the true movement conditions are not used, but are replaced by arbitrary geometrical conditions it is impossible to ascertain whether the solution to a given problem is correct or not, and the relation of any solution by this method to the correct solution cannot be indicated (except that the calculation result will presumably be more reliable the more it resembles the correct rupture figure).

The methods permit the calculation of rupture figures resembling quasi-possible or even possible figures but with very much simpler calculations. The value of this should not be overestimated, however. It seems more rational, if approximate solutions are required, to use an admissible solution with possible (perhaps simple) rupture zones. It has been shown that such solutions may be calculated in an equally simple way, and they have a well defined relation to the correct solution.

However, the methods defined in this section may have one rather important function in practical calculations: They may be used to assess by a rough estimate the result of replacing a given approximate solution by another one defined by a more complex rupture figure. Thus, if an admissible solution with possible zones is known it is usually reasonably easy to indicate at least roughly how a possible or quasi-possible solution to the same problem should be constructed. One can also sketch a likely rupture figure and give more or less close estimates for its parameters. It may be reasonable to calculate roughly a rupture figure sketched in this way so that the rupture zones are at least geometrically and statically possible. By the use of the pertinent equilibrium equations it can then be ascertained whether

the required force terms (f. inst. an earth pressure resultant or a bearing capacity) has changed sufficiently from the values found by the previous rupture figure to justify the calculation work involved in finding the true solution to the more complicated rupture figure.

Considering the general calculation method as defined in Sec. 434 this amounts to the following: After the first stage of the calculations for the new rupture figure has been completed, i. e. after the rupture figure has been constructed geometrically, but before the movement conditions are used (or after a slight readjustment so that a movement is possible with at least approximately constant volumes in the rupture zones), the statical conditions are considered, or an approximate work equation is used, and the result is compared with that of the old rupture figure. From this comparison it is determined whether the calculations of the new rupture figure should be continued, or the result of the old calculation should be accepted.

Care should be taken, however, in the interpretation of the results of this comparison. If all equilibrium conditions are not satisfied (so that the solution is quasi statically admissible) the determination of a restraint force by any one of them may be quite far off. On the other hand, in a complicated rupture figure it may necessitate rather lengthy calculations to satisfy all equilibrium conditions. It seems to be simpler, and also safer, to use the work equation. But to do this one must have at least an estimate of the movement components for all rigid bodies.

5 CONSTRUCTION OF SOLUTIONS

In this chapter the problem of constructing solutions to given failure problems is considered. It is assumed that the method of admissible solutions with possible zones is used, and that the general calculation method derived in Chap. 4 is applied. It is therefore a question of choosing the rupture figures that are best suited for the calculations in practice, depending on the type of failure problem and also on what use shall be made of the solution.

The choice of rupture figure involves a general evaluation of what types of rupture figures may be expected to solve the given failure problem. It also includes an evaluation of the economy of the calculations. One must decide how complex solutions are justified, and how great the accuracy should be. On this choice depend the type of rupture figure to be calculated, and also some details in the calculation procedure.

These problems are discussed in the first subsection of the chapter. In the following sections some examples from typical failure problems in soil mechanics are considered. Since a full account of the problems would require an extensive work of calculations which can better be treated in separate reports, most weight has been placed upon the general planning of the numerical calculations and the representation of the results for practical use. Numerical results are only given in some relatively simple cases.

51 CHOICE OF RUPTURE FIGURE

511 General Problems

When it is required to find a solution to a given failure problem one must as explained in Chap. 4 choose a rupture figure from which the calculation procedure can be derived. The rupture figure must evidently be chosen so that it is reasonable to expect that a solution can be found in terms of the parameters implied by the figure. Thus, it should be relevant and determinable, and it should at least be plausible that it will not fail to give a solution by becoming geometrically or kinematically impossible.

There will usually be a number of rupture figures which satisfy these conditions. Depending on the type of failure problem, very simple approximations and also very complicated types may be included in the alternatives. If some of the external parameters are variables, or it is required to find the solutions for a range of parameters, it may also be necessary to consider different types of rupture figures, valid in different domains of parameter sets.

In this way a sort of two-dimensional (discrete) space of rupture figure types is defined, the "dimensions" being the level of complexity, and the parameter variations. The main problem is to indicate a criterion for what rupture figures shall be investigated in connection with the given problem, and to find rupture figures that are permissible under the criterion.

The first question depends on the purpose of the calculations, and is therefore outside the scope of this work. However, some general remarks are called for:

1. In design problems in practice it must, strictly speaking, be decided on the basis of the overall economy for the calculations and the project: More accurate calculations will justify a smaller margin of safety, but will also give a greater work of calculations. Therefore, if appreciable savings can be obtained by increasing the accuracy of calculations, rather complicated solutions may be justified. If this is not the case, f.inst. because the margin of safety must be kept high for other reasons (uncertainties in the geometry, the loadings, or the shear strengths), relatively simple approximations may have to be used.

2. For research purposes one may wish to solve a type of problems once and for all with a view of obtaining a series of results for future uses in design work. The accuracy should then as a rule be at least as high as in any single design job. However, since the number of parameters will usually be too great to permit a direct tabulation of the results as functions of the parameters, one must usually give them in the form of more or less simplified design formulae, using the principles of linearization and superposition as far as possible. The accuracy of the calculations should of course be balanced to the subsequent simplification of the results.

3. In more special cases one might wish expressly to compare approximate and mathematically correct solutions to the same problems, or to test the theory by comparing observed forces and rupture figures with the ones predicted by approximate methods as used in practice, design formulae developed by more accurate calculations, and/or the mathematically correct solutions.

In this connection it should also be remembered that in some types of failure problems, f. inst. simple earth pressures, the mathematically correct solution may be so easy to find that it should be used in all but the most rough estimates. In other problems it may be extremely complicated, so that it is hardly ever justified to embark on the corresponding work of calculations. The number of different approximate solutions will of course be much greater in the latter case than in the former one.

As explained in Sec. 412 the reasoning used to decide upon the types of rupture figures to investigate will also indicate the level of numerical accuracy that should be attained in the calculations. As a general rule, in relatively rough approximations the rupture zones, if any, should obviously not be calculated with a large number of cells in the zone elements, and if the energy equation is used the accepted solution should only satisfy the extreme condition with a reasonable accuracy. On the other hand, when the total number of circle arcs (in the method of chord lengths) has been decided, all geometrical, kinematical, and used statical conditions (in this order of preference) should if possible be satisfied within the obtainable numerical accuracy, i.e. with the full number of figures that can be obtained by the method that is used (f. inst. slide rule, desk calculation machine, or electronic computer). This is necessary in order to obtain a unique numerical solution, which can also be checked numerically.

To find the actual rupture figures to calculate one will usually start with an approximate or presumably correct figure known by experience. One may then proceed in one of two different directions, assessing the changes in the rupture figure induced by changes in the external parameters of the failure problem, or by improvements in the approximation (or the opposite, if simpler rupture figures are required). The two methods might be called the method of rupture figure loci, and the method of developing rupture figures, respectively. They are treated by means of some few examples in the following two sections.

Each of the two methods may be used to plan a series of calculations of rupture figures, the results of each step indicating the rupture figure to calculate next. The series will end with the rupture figure that corresponds to the given parameters of the failure problem, and has the required level of complexity. However, in practice the methods are frequently used qualitatively, without actually performing the implied calculations. One will then end with a number of likely alternatives, and the scheme of calculations must include a decision on the order in which they are to be tried, the tests that should be performed on the solutions, and the criterion upon which the final solution should be accepted. This presents no problem when the mathematically correct solution is required, because this solution is uniquely determined, but if an approximate solution is acceptable it is necessary to specify something about the required standard of approximation. In practice one will usually start the calculations with what one considers the most likely alternative, and will only reject the solution if it is plainly (f. inst. geometrically) impossible.

Naturally, if the problem includes a range of (or variable) external parameters the method of rupture figure loci must be incorporated in the scheme of calculations. On the other hand, if the purpose of the calculations is to compare different approximate solutions to the same problem, they must be derived from each other by the method of developing rupture figures. A summary of the general solution method for failure problems is given in Sec. 514.

Example 51 a

The construction of rupture figures by means of the two principles of variation mentioned in this section can be illustrated by the family of rupture figures shown in Fig. 51 A. However, both methods have been used implicitly several times in the preceding sections, so many other examples can be found among the previous figures.

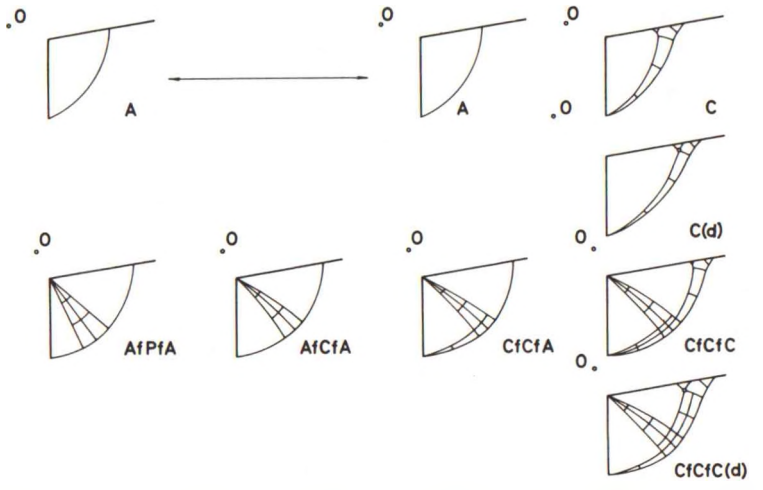

Fig. 51 A: Alternative Rupture Figures to the Same Failure Problem.

The problem considered in this example is an earth pressure problem with a vertical wall with a known rotation centre, O, and an inclined, unloaded surface. The rotation centre is in a domain of the x,y-plane (near the top point of the wall) which makes the simple line rupture A a reasonable approximation.

This rupture figure is a very simple kinematically admissible approximation, but because of the simplicity of the rupture figure it is in fact also quasi-possible. If a possible solution is required the rupture figure Cf(XfRs AaR), or briefly C, must be used. However, since this rupture figure shows more details than does the simple line rupture, different variants may exist for different positions of O, all of which correspond to the simple line rupture A. Thus, one of the small line ruptures may have to be replaced by a discontinuity point. If no calculation is performed to find the exact position of the transition points between the two variants, both alternatives must be tried for any given position of O (or, rather, one variant is tried and is tested by considering the sign of the chord lengths, or the stress condition for the discontinuity point, respectively).

The original line rupture A may for some positions of O give a solution that is not statically possible. According to how accurate solutions are required one may in this situation use one of a number of increasingly complex rupture figures: AfPfA, AfCfA (with a curved radial zone), or CfCfA (with a double radial zone), only the last one of which is quasi-possible. As

suggested in the figure all three alternatives may be considered as equivalent to the line rupture A, but different transition points to the line rupture must be expected.

Conceivably, the last mentioned alternative may become geometrically impossible, the centre angle for the radial zone starting at the foot point of the wall being negative. In this case the rupture figure cannot be used as a quasi-possible solution, but one must take either the figure AfCfA or one of the possible variants CfCfC (presumably the last rupture figure shown on Fig. 51 A with a discontinuity point under the surface). If a possible solution is required, i. e. one wishes to find the mathematically correct solution, there will presumably be more alternatives than the two shown in the figure. Thus, also in the first alternative a small line rupture may have to be replaced by a discontinuity point.

The example shows, which is also immediately clear, that the more complex rupture figures are used, the more variants have to be considered. Thus, the possible solutions shown in the last column in Fig. 51 A will be sensitive to even small changes in the surface form, or to small variations in the surface loadings, three parameters being used to describe the geometry of a small rigid body directly below the surface. However, such changes, which may alter the form of the small rigid body considerably, may have no great influence on the magnitude or position of the total earth pressure on the wall which in most cases will be the primary object of the calculations. For that reason one will in most practical cases confine oneself to the consideration of the rupture figures shown in the two (or three) first columns of Fig. 51 A. It is seen that one obtains in this way a considerable reduction in the work of calculations, not only because the number of parameters decreases but also because the number of variants of the rupture figure is smaller. It will therefore be more probable that the final rupture figure to calculate can be chosen at the first try, so that time-consuming recalculations can be avoided.

512 Rupture Figure Loci

In the method of rupture figure loci in its most general form some or all of the external parameters describing a family of failure problems are transformed into a space of characteristic variables, and the interest is concentrated on the boundaries in this space between the regimes of the different rupture figure types.

In the space of characteristic variables a curve may be defined by the expression of the variables as functions of one parameter t. A boundary point on such a curve for a given rupture figure type corresponds to a set of external parameters consistent with one unique value of t for which the rupture figure is on the point of becoming geometrically, kinematically, or statically impossible.

This concept may be used f. inst. in one of the following ways.

1. In the space of characteristic variables a curve is defined joining a point with a known rupture figure to the point corresponding to the given parameter set. Starting with the known rupture figure the first boundary point on the curve is found by finding the set of external parameters for which the rupture figure has a geometrical quantity (a chord length or a centre angle) or a value of ϵ (in a point or in a connected set of rupture zones) equal to zero, or for which a secondary rupture figure in one of the rigid bodies of clay is just on the verge of failure. Such cases, especially the first mentioned one, may even be simpler to calculate than the general case for the rupture figure in question, because the quantity known to be zero may be an initial parameter for the figure. The next boundary point is then calculated by means of the new rupture figure, and so forth until the end point of the curve is reached.

2. The method is most useful when the problem is to find some quantity, f. inst. f or W, a restraint force, or a design quantity, as a function of the external parameters over a region in the space of characteristic variables. Obviously, the boundaries between the regimes in this space of the different rupture figure types will be characteristic points of such functions, which should therefore be calculated primarily in boundary points, especially in intersection points between two or more boundaries if such exist in the given region. Points in the interior of the regimes are in this connection only supporting points, to be calculated when necessary to make possible an interpolation between the boundary points. Thus, the method may be used to determine what failure problems to calculate in a given range of external parameters. This is important f. inst. when it is required to derive a design formula for a class of failure problems (which will have to include some coefficients that are functions of the external parameters).

3. In design problems, especially when more than one design quantity are to be determined, the most economical solution will frequently obtain at boundary points between the regimes of the rupture figure types in the space of characteristic variables (considering the design quantities as variable external parameters). This is because all functions of the external variables (forces etc., and also a cost function) will often be continuous everywhere in the space and differentiable in the interiors of the regimes, but will have discontinuous derivatives across the boundaries of the regimes. Generally speaking, in all problems in which the external parameters can be varied the boundary points of the regimes will usually be the most important points (together with the boundaries for the region of permissible variations), and also the points that are most easily calculated.

In practice it is usually easy to see what changes will obtain in a rupture figure for a given change of external parameters. If the figure changes because of the geometrical conditions the boundary points can frequently be constructed directly in the case of simple rupture figures. In more complicated cases, the exact position of the boundary points, and frequently also the order in which the different changes obtain, can only be found by actual calculations of the rupture figure. The intermediate stages of the rupture figure types are of course only calculated if they are expressly needed, so if the method is only used to predict what kind of rupture figure to expect for the given set of external parameters, one will usually follow the different stages through sketches of the figure. The method will then not be perfectly unique, but one will end up with a (usually small) number of alternative rupture figures.

Example 51 b

In Ex. 42 a (Fig. 42 F) and Ex. 42 c (Fig. 42 N) the regimes of two different rupture figures were investigated in the space defined by the characteristic variables ρ and λ that indicate the position of the rotation centre for a wall.

Naturally, in some problems it might be more helpful to use other variables, f. inst. the relative height $\frac{z}{h}$ and the inclination δ = arc tan $(\frac{F}{E})$, or the mean tangential stress $\frac{F}{ch}$, of the total earth pressure. However, in this example we use ρ and λ together with the same parameters, viz. $\beta - \theta$, $\frac{c_a}{c}$, and $\frac{\tau_o}{c}$, as in the two other examples (cf. Fig. 42 E). It is seen that the

rupture figure is completely given by these parameters when also the indicator e_f (or the direction of rotation around the point ρ, λ) is specified.

If $\tau_o = 0$ one gets geometrically the same rupture figure for the two directions of rotation corresponding to the same rotation point, so in this case the 4 remaining parameters will specify the rupture figure.

Assuming now $\frac{\tau_o}{c} = 0$, $\frac{c_a}{c} = 0.5$, and $\beta - \theta$ so great that α according to (4207) is positive also for $e_f e_t = -1$ ($\beta - \theta$ is also assumed great enough so that a further condition to be mentioned later is also satisfied) we find the regimes of the different possible rupture figures in the ρ, λ-plane indicated on Fig. 51 B. Each rupture figure is characterized by a string of letters according to the notation of Fig. 42 P-Q and Fig. 51 A, and also by the values of $e_f e_t$ for the different wall parts in the figure. The numbers are given in the order from the foot point upwards, and $e_f = 1$ corresponds to a rotation of the wall in the negative direction.

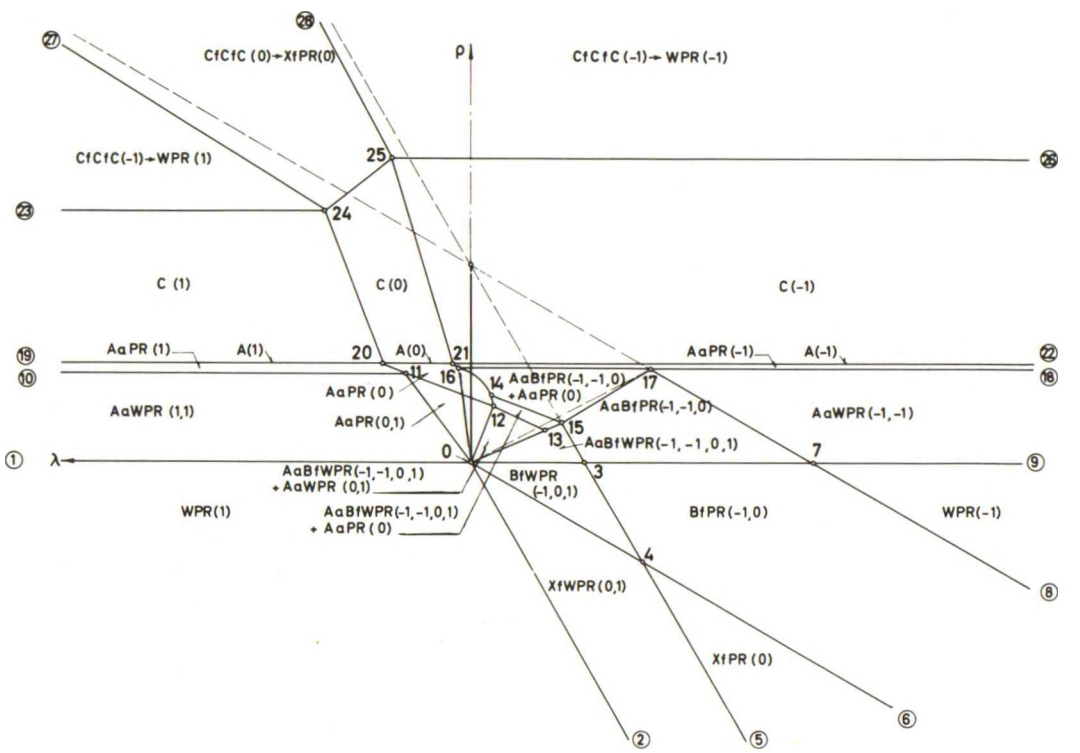

Fig. 51 B: Rupture Figure Loci (Domains of Rotation Points) for a Simple Earth Pressure Problem.

The domains for the rupture figures WPR, bounded by the lines 0-1, 0-2 and 7-8, 7-9 are identical to the ones shown in Fig. 42 F. Starting with the first mentioned domain we find that on the line 0-2 (which forms the angle i_w with the wall) the value of ϵ becomes zero in the wall zone at the foot point of the wall. To the right of the line we will therefore have a rigid body along the lower part of the wall (rupture figure XfWPR).

When the line 0-4 (which forms the angle $\frac{\pi}{2} - i_w$ with the wall) is reached the line rupture will form the angle i_w with the wall. To the right of 0-4 it will not be statically possible, and it must be replaced by an arc zone (rupture figure BfWPR).

On the line 3-4-5, which is parallel to 0-2 but passes through the top point of the wall, the rigid body will extend to the wall top. To the right of this line a wall zone will therefore not be geometrically possible, and the rupture figures BfWPR and XfWPR must be replaced by BfPR and XfPR, respectively. The boundary line between the two last mentioned rupture figures is 4-6, which is the extension of 0-4.

The line 7-8, parallel to 0-4-6 through the top point, is the locus of the points where the rigid body vanishes. To the right of this line we therefore have a pure zone rupture WPR again, but now with $e_f e_t = -1$ for the wall zone.

On the line 1-0-3-7-9, normal to the wall through the foot point, the value of ϵ (and the sliding velocity u_f) will be zero along the lower boundary slip line for the rupture figure. Above this line all rupture figures must therefore be modified by the introduction of an Aa-construction. To the extreme left hand side (rupture figure AaWPR) the rigid body will slide upon the wall, the centre for the line rupture being on the line 0-11. The upper boundary 10-11 is determined by the condition that the body extends upwards to the top point. Above this line the rupture figure will therefore be of the type AaPR (centre of the line rupture on the curve 11-20).

To the right of the boundary 0-11-20 the rigid body will not slide on the wall, so the centres of the line ruptures in the rupture figures AaWPR, AaPR, and A will coincide with the rotation points for the wall. This applies until the line 0-12, extended by the curve 12-14-16. Along this boundary the rigid body will contain a secondary rupture figure on the verge of failure (cf. Fig. 44 F). The secondary figure will be of the type AaBfWPR along 0-12-14, and of the type AaBfPR along 14-16. On the boundary 16-21 the rigid body will again slide in relation to the wall, but now with $e_f e_t = -1$.

To the extreme right in the domain 9-7-17-18 we have a rupture figure AaWPR in which the rigid body slides upon the wall (centre of the line rupture on the line 0-16). Correspondingly, in the domain 18-17-16-21-22 the figure AaPR obtains, also with a sliding rigid body (centre on the curve 16-21). Notice that this is only geometrically possible if $\beta - \theta$ is greater than a certain value (which is assumed as mentioned previously).

On the line 17-7 ϵ becomes zero in the upper point of the wall zone, so in the domain 3-7-17-15 a rigid body develops near the top point of the wall (figure AaBfPR). On the line 15-3 the lower radial slip line forms the angle i_w with the wall, so in the domain 0-3-15-13 a wall zone is again developed (with $e_f e_t = 1$, rupture figure AaBfWPR). In all cases the centre of the A-line rupture is on the line 0-16.

The two last mentioned rupture figures become geometrically impossible along the line 0-17, because the two rigid bodies along the wall (the lower one sliding, the upper one fixed to the wall) will then touch. However, before this line is reached the rigid body outside the rupture will become statically impossible, a secondary rupture figure AaWPR (along 0-13) or AaPR (along 13-15-17) forming in this body. For the secondary rupture figure the centre of the line rupture is located on the curve 0-12-14-16.

In each of the domains 0-12-13, 12-14-15-13, and 14-16-17-15 we will have two simultaneous rupture figures of the types AaBfWPR + AaWPR, AaBfWPR + AaPR, and AaBfPR + AaPR, respectively.

On the line 19-20-21-22, normal to the mid point of the wall we have a pure line rupture A. The rigid body slides upon the wall for the parts 19-20 ($e_f e_t = 1$, centre of line rupture at 20) and 21-22 ($e_f e_t = -1$, centre of line rupture at 21). In this special case, obtained from the corresponding rupture figure AaPR, assuming the surface zone to degenerate into a point, the earth pressure is not uniquely determined since the value of σ at the upper point of the line rupture may be decreased, without changing the rupture figure or the deformation work, from the limiting value obtained in this way to the value for which the rigid body outside the line rupture becomes unstable. A rupture figure of the type C (Fig. 51 A, but with a degenerated surface zone at the top point of the wall) will then be on the point of being developed.

This rupture figure will also obtain in three versions, according to whether $e_f e_t$ for the rigid body along the wall is 1, 0, or -1. At some curve higher above the mid point of the wall (23-24-25-26 in Fig. 51 B) the rigid body will become unstable as shown in Fig. 51 A. The rupture figure CfCfC

will then obtain, also in three versions. When the distance to the rotation point becomes infinite, i.e. when the movement of the wall becomes a pure translation, the outer radial zone in the CfCfC rupture figure degenerates into a single slip line which intersects the surface under the statically correct angle. At the same time the radial slip lines become straight, the rigid body under the surface is on the point of failure (it is covered by an ordinary surface zone), and if the rigid body below the radial zone slides upon the wall, it will also be on the point of failure (being covered by a wall zone).

This example shows that in some regions of the space of characteristic variables it may be possible to select the correct rupture figure on the basis of very simple geometrical reasonings (f.inst. $\rho \leq 0$). In other parts ($0 < \rho \leq 0.5$) reasonably precise estimates may be made, but the exact position of the boundaries can only be found after some, more or less complicated, preliminary calculations. Finally, in some regions ($0.5 < \rho$) it is only possible to obtain rather rough estimates. In a critical domain, f.inst. in the neighbourhood of the point $\rho,\lambda = (1.5, 0.5)$, it is virtually impossible to determine beforehand whether a radial zone will be developed or not, and also whether the value of $e_f e_t$ will be 1, 0, or -1.

513 Development of Rupture Figures

If the mathematically correct solution to a given failure problem has a simple rupture figure one will presumably always use this solution, except possibly for rough preliminary estimates. Thus, an approximate solution may never be needed, and will possibly also be difficult to find. On the other hand, if the correct solution is very complex a wide range of approximate solutions may exist, and will also be much needed in practice.

The problem considered in this section is, from a known admissible solution with possible zones corresponding to a given failure problem to find another solution to the same problem, the calculation of which gives the answer with the required accuracy in the most economical way.

In principle this problem can be solved by a stepwise modification of the rupture figure: After having ascertained that it is in fact geometrically and kinematically admissible it is easy to determine the number of free parameters so that it can be determined whether it is possible, quasi-possible, or only admissible. One can also find out, by calculations of secondary rupture figures or by estimates, whether the rigid bodies in the rupture figure are stable or not.

In any case, by an increase of the number of zone elements (possibly a decrease, if the solution is not kinematically possible), or of the number of free parameters used to describe the existing zone elements, one may obtain another rupture figure which can form the basis for a solution which is closer to the mathematically correct one. The process can be repeated on the new rupture figure, and so on, until the required accuracy is reached.

Since the economy of the calculation work is usually important, it makes a difference how one chooses to change the rupture figure. As a rule good approximations can only be obtained if all major zone elements in the correct solution are also present in the accepted one. On the other hand, local stress singularities (or small domains with $\epsilon < 0$) may have no great influence on the overall accuracy of the solution. Therefore, the conditions for the solution should be satisfied in the following order of preference.

1. When only admissible solutions with possible zones are considered it is indispensable that the rupture figure is able to transmit the given boundary movements. If the movements of the external rigid bodies are rather completely specified this may in itself introduce a number of rupture figure elements (f. inst. the arc zone behind a sheet wall with a yield hinge). If such movements are not specified (problems in controlled stress, or with only a few restraints on each body) much simpler rupture figures may be permissible under the method, but in order to obtain a good approximation it may be necessary to introduce a sufficient number of elements so that a rather general type of movements for the bodies is possible. Thus, if a wall has a hinge the rupture figure should permit movements in the hinge even if they are not specified (if not the final rupture figure may turn out to be statically impossible).

2. The preliminary rupture figures should contain as few rigid bodies of clay as possible. However, it is important that the rigid bodies are not patently statically impossible, being unstable along secondary line ruptures or radial zones. Correspondingly, if the solution is only quasi kinematically admissible it is important that the negative contributions to the total deformation work are relatively small in relation to the positive ones. Thus, in portions with large or even infinite values of ϵ (velocity jumps by slidings along slip lines, or neighbourhoods of top points of radial zones) τ and ϵ should always have the same sign.

3. Depending on the failure problem a solution satisfying the above

conditions may be correct (a simple solution), possible, quasi-possible, or admissible. In the latter cases some alternative variants may exist (f. inst. systems of line ruptures as alternatives to combinations of line ruptures with curved or straight radial zones), but in all cases the solution will usually represent a quite good approximation. It may be improved by the increase of the number of parameters without increasing the number of rigid bodies of clay, until the solution is at least quasi-possible. This is in most cases obtained by replacing some line rupture by radial zones or arc zones, and straight zone boundaries by curved ones.

A solution satisfying these conditions will normally represent a good approximation. It should be noticed, however, that the availability of simple approximate solutions will also depend on how completely the movements of the external rigid bodies are specified. If the number of restraints, n_r, is high, a number of simple rupture figures, f. inst. AfPfA, may be kinematically impossible, although they may give reasonably good approximations in terms of the magnitude of the total force between the clay and the rigid body when the failure problem is reformulated so that f. inst. the position and direction of this force is specified by means of one restraining rod.

The rupture figure shown in Fig. 34 N is an example of this. The three line ruptures of this figure determine the bearing capacity of the foundation reasonably well, although the movement of the foundation (a rotation about O_3) is not close to the correct movement (a translation forming the angle $\frac{\pi}{4}$ with the horizon).

This special difficulty might be solved in an approximate way by means of a procedure explained in Sec. 532. It replaces some of the given restraints by a maximum condition on the resulting forces. In this way simple approximate solutions may be obtained to almost any given failure problem, provided the number of interfaces between the clay and external rigid bodies is not too great.

A solution, refined and possibly modified as indicated above, may still contain some singularities of less importance. It may f. inst. have stress singularities at the end points of line ruptures or at corner points of rigid bodies of clay. Some regions of the rupture zones may also have negative values of ϵ, and there may be less evident secondary rupture zones in some rigid bodies of clay that are unstable.

Some of these points may be removable without any great increase of the number of parameters. Thus, discontinuity points may be replaced by

line ruptures or (simple) arc zones, and line ruptures intersecting a wall under a statically impossible angle may be replaced by a simple arc zone with no or only a slight increase in the calculation work. The elimination of other singularities, f. inst. intersection points between line ruptures and free surfaces, a possible difference between the true and the approximate external movement conditions, or the introduction of free rigid bodies in rupture zones or secondary, possibly simultaneous rupture figures in rigid bodies may mean a drastic increase in the work of calculations. This should only be done if it is strictly necessary, f. inst. because the mathematically correct solution is expressly required. As explained in Sec. 444 one may at an early stage in the calculation of the improved rupture figure obtain at least a rough estimate on the corrected forces to see whether the full calculations will be worth the trouble.

As explained previously an increase of the number of rupture figure elements will also mean that the rupture figure exists in a greater number of variants. Since it is evidently illogical to introduce a number of elements and not also find the correct combination of these elements (or the most correct, if the rupture figure is still not mathematically correct), a large part of the calculation work will be used on the exact fitting of the rupture figure to relatively unimportant details in the failure problem. This if of course necessary if the mathematically correct solution is required for some reason, but for practical engineering purposes it may clearly be very uneconomical.

Example 51 c

The method of developing rupture figures has also been used implicitly several times in the preceding sections. Thus, Fig. 24 H (Ex. 24 f) shows a number of rupture figures that can be used to give a solution to the bearing capacity problem for a shallow strip foundations. Fig. 34 N and Fig. 42 AC show two alternative solutions (comparable to d or e in Fig. 24 H). An alternative to f in Fig. 24 H is suggested by the last rupture figure shown in Fig. 51 A.

Another example is given by a comparison of Fig. 42 W with the variants shown in Fig. 43 J. In this example a number of intermediate stages can evidently be conceived. It also shows the great number of variants that may have to be considered if the mathematically correct solution is required.

The most striking examples of this are obtained when there are corner points or loading irregularities on a free surface. Thus, in Fig. 51 C is con-

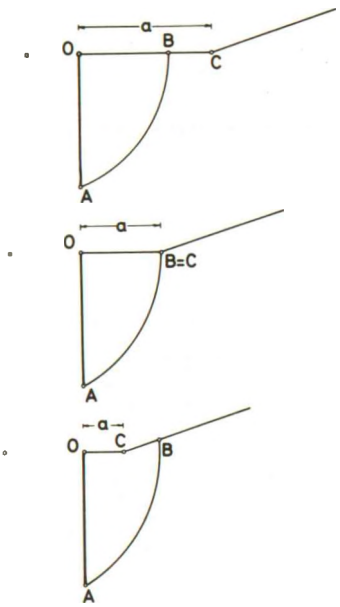

Fig. 51 C: A Line Rupture in Different Positions Relative to a Corner Point.

sidered an earth pressure problem in which a smooth wall is rotated about its top point O. The surface has a (reentrant) corner point C, and the problem is assumed to be that of finding the earth pressure E as a function of the distance a between the top point O and the corner point C.

A simple solution is found easily by means of a line rupture. It exists in three variants, dependent on the position of C in relation to the end point of the line rupture:

1. If B is between O and C we have the simplest case in which a has no influence on the rupture figure or the earth pressure.
2. For decreasing values of a a point is reached in which B and C coincide. In a certain interval of a after this point the line rupture is bound to pass through C.
3. When a becomes too small the rupture figure will intersect the surface beyond C. If the slope beyond C is too steep the rigid body above the line rupture may not be stable. A secondary radial zone with straight or curved radial slip lines, or a secondary line rupture, may then be introduced between C and the line rupture. The two first mentioned solutions are not quasi-possible, so the magnitude of E can only be found approximately by an equilibrium equation, or by the solution of an additional failure problem with a slightly changed position of the rotation point (the resulting earth pressure E should have a position so that the known position of the rotation point is the most critical one, cf. Ex. 24 d).

The mathematically correct solution must be based on the rupture figure C shown in Fig. 51 A, possibly modified to CfCfC when the corner point is located in the surface of the moving rigid body (this modification is not assumed in the following). It is seen, however, that due to the two surface zones rather complex intermediate stages may exist, in which one of the

two Rankine zones must be replaced either by a construction with one or two radial zones (RD or RDR, cf. Fig. 42 A) or with an ordinary end point for a line rupture. If the corner angle is small enough it may not be possible to satisfy the stress condition between the two line ruptures, when C is located between the two surface zones. The second rupture figure in Fig. 51 C will then be mathematically correct for some values of a.

If only a working estimate of the value of E is required, f. inst. within an accuracy of 5 %, it seems uneconomical to use too much time and work of calculations to study these variants. However, for research purposes it may sometimes be necessary to carry through the development of the actual rupture figures until the mathematically correct solution has been obtained.

514 General Solution Method

The methods considered in the first sections of this chapter complete the theory that is necessary to solve the general type of failure problems defined in Sec. 22.

The general method may be summarized as follows; for details in the calculation of rupture figures see Chap. 4, and in the numerical method see Chap. 3.

1. The parameters of the failure problem are assessed.
2. A rupture figure type is chosen together with a mode of failure (in design problems).
3. Its parameters are estimated and are subsequently adjusted simultaneous with a determination of values for the design parameters, the external parameters that are variable, and the parameters that determine a range of failure problems so that:
   a. The rupture figure is geometrically determined.
   b. Its movement conditions are satisfied.
   c. It is an extreme solution for the set of internal and variable external parameters.
   d. It is located within the range of parameters, possibly at a characteristic point of its regime.
4. The kinematical and statical possibility is investigated (secondary rupture figures are calculated as under 2-3 above), and in design

problems a cost function may be evaluated. It is now decided:

a. Whether the rupture figure is accurate enough. If not, how it should be modified.

b. For design problems: whether the solution is economical. If not, how the mode of failure should be changed.

c. Whether the intended range is covered sufficiently. If not, how the rupture figure (or the point in its regime) should be changed.

5. Depending on the result the calculations are finished or are repeated as under 2-3 above.

Notice that design problems, or problems with variable external parameters may sometimes be treated as problems with a range of parameters, i.e. fundamentally as a problem with rupture figure loci or, for each rupture figure, as problems with variable internal parameters. In this way a set of solutions is obtained from which the extreme solution, or the most economical solution, can be derived afterwards by a numerical interpolation.

For that reason no special distinction is made in the following between design problems and other failure problems. In research one will usually be interested in the solution of fairly general problems, i.e. problems in which the most important of the external parameters are considered as variables. If the characteristic quantities of the solution are represented as functions of these variables the resulting curves or tables can be used in an evident way to solve design problems within the considered range of variables.

If the number of variables is too great a direct tabulation of the results will be impossible. One must then either express the results by a more or less approximate formula (even if the results come from mathematically correct solutions), or prepare a standard program or procedure that will give the solution to any given set of variables. In the latter case the program should be able to utilize the method of rupture figure loci when a range of variable sets is specified.

In practice a general solution to a given class of failure problems would preferably contain all of the above mentioned elements. Thus, for research purposes one would proceed as follows:

1. After the class of problems has been defined a general program of solutions on the required level of accuracy is prepared. This program is later used on all problems, or sets of problems not covered by the special solutions.

2. For a convenient subspace of the variables (or a number of subspaces assumed to be the most important in practice) a sufficient number of solutions is calculated so that a general approximate formula can be derived, using the principles of linearization and superposition as far as possible. The necessary coefficients or functions of the variables are also expressed by empirical formulae or are tabulated or given by curves.
3. Finally, for some special (degenerate) cases with only two or three non-vanishing parameters the correct solutions can be tabulated directly, or can be given as curves.

In the following sections some examples of the choice of rupture figures, the planning and performance of the calculation work, and the representation of the final results are given for some typical failure problems in soil mechanics. Most weight has been placed on the principal questions of definition of problems, feasibility of solutions and calculations, and schemes of computation, so final results of calculation are only given in a few simple cases.

52 STABILITY INVESTIGATIONS

521 Stability of Slopes

The so-called stability investigations are concerned with failure problems in which the considered structure moves as a whole. The distinction to bearing capacity problems and to problems with combined earth pressure and bearing capacity calculations is not sharp. However, it is a typical feature in stability problems that most of the soil that is moving consists of one or a few rigid bodies. Possible external rigid bodies, that may not be present at all, do not as a rule impart any movement restraints on the rigid bodies of clay, except in the form of geometrical restraints (f. inst. sheet walls that must not be sheared by line ruptures). Occasionally some weak coupling may exist, amounting to about one rod connection per external rigid body (cf. Sec. 223), or less, but in many cases it is then a matter of defi-

nition whether the problem is one of stability or of (possibly connected) earth pressures or bearing capacities.

Stability problems as defined above are primarily problems in controlled stress, although they may also be formulated in controlled strain, using a real or imaginary rod or moment restraint. Which formulation to prefer depends on whether a dominant single force is acting (f. inst. a construction load or a water pressure) and also on the definition of the safety. A procedure that is much used is to consider all active forces, including unit weights, as loading rates in controlled stress. The common factor of proportionality, f, is then effectively a safety factor on the shear strength.

Stability problems may roughly be divided into stability of slopes and stability of structures. In the first mentioned type the forces acting upon external rigid bodies, if any, are relatively small in relation to the weights of the moving clay bodies. The failure problem is therefore mostly due to the geometry of the soil profile, although it may be modified f. inst. by the presence of sheet walls or by loadings on the top of the slope. In the second kind the rupture figures are to a large extent determined geometrically by an external rigid body, or a collection of such bodies moving as a rigid whole. In this case there may be special problems of interacting failures of earth pressures or bearing capacities and stability.

Problems in stability of slopes constitute the classical field of application for the energy method, cf. the well known $\varphi = 0$ analysis (Sec. 422). This is because the geometry of the failure problem may be extremely complicated with irregular external and internal boundaries, so that mathematically correct or even possible solutions can hardly ever be used. For the same reason the problems encountered in practice depend on so many parameters that a general, even an empirical solution in closed form is out of the question, except for a few special cases (f. inst. a straight slope between two horizontal levels in heavy clay with no surface loading, resting on a horizontal rigid base, cf. Fellenius [1927] and Taylor [1937]).

In this situation the best procedure consists in the general use of a simple class of rupture figures. Systems of line ruptures (Sec. 425) are the most generally applicable when the external rigid bodies are only weakly restrained, but if the rupture figure is located in one clay layer only, combinations of line ruptures with radial zones and possibly arc zones can also be used. For simplicity the following discussion will assume the use of line ruptures only.

As explained in Sec. 425 the calculation of each rupture figure is relatively simple, but it may be rather tedious due to the great number of parameters that must be varied in some cases to find the minimum solution. The calculations are well suited to performance on a computer, however, the basic operations being:

1. The parameters characterizing the failure problem are read and stored, using f.inst. the form of Fig. 22 E, Ex. 22 a.
2. The parameters of a preliminary rupture figure are read and stored. A special convention may be used to show which parameters (positions of points, values of α etc.) are assumed to remain fixed and which ones can be varied.
3. The preliminary rupture figure is calculated, correcting if necessary contradictions between the given parameters (satisfaction of possible geometrical and kinematical conditions that are violated through an overdetermination of the rupture figure).
4. By a systematic variation of the parameters the minimum solution is obtained by a continuous transformation of the preliminary rupture figure. During this process it should be possible to take into account possible variations of the number of rupture figure elements (rigid bodies of clay degenerating into points, or line ruptures vanishing because the movement components of the surrounding rigid bodies of clay become equal).
5. After the minimum solution has been found it should be possible to continue the calculations by adding new elements to the rupture figure, or by replacing it with an alternative one (chosen and indicated under No. 2 above, or read into the computer at this stage on the basis of the output from the primary calculations), e.g.:
   a. to subdivide the rigid bodies of clay by secondary rupture figures.
   b. to transform the rupture figure into another one with another minimum solution.

Notice that since two separated rupture figures in this type of failure problems cannot be coupled by external movement conditions, only the one corresponding to the smallest value of f (or W) will develop. They may be connected by a branch point, however, and the combined rupture figure may by more critical than any one of them.

Schematically the surface of a slope may be divided into parts that tend to generate failures (so-called active parts, f. inst. high surface loadings, extruding bulges) alternating with parts that tend to collect line ruptures (so-called passive parts, f. inst. low surface loadings, reentrant curves). A typical rupture figure that is influenced by a number of such parts will contain the elements sketched in Fig. 52 A. The following points should be noticed.

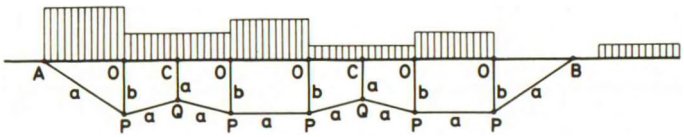

Fig. 52 A: General Type of Systems of Line Ruptures Used on Stability of Slopes.

1. The rupture figure (supposed to be an a-line corresponding to a slide in the direction from left to right) starts at a point A which is in or at a left boundary of an active surface part. It ends at a point B in or at the right boundary of a passive part. For each internal boundary point O between an active and a passive part a secondary (b-line) rupture may extend to a branch point P. Under each internal passive part an (a-line) rupture may branch off from a point Q to a surface point C.

2. The geometry of the whole rupture figure may be determined by the assumption that either A or B has known positions (corner points or load discontinuities). If no such limitation exists (surface loads increasing indefinitely to the left or decreasing to the right) it may be confined by a lower internal boundary to a clay with a higher shear strength. In inhomogeneous materials the confinement may obtain by a continuously increasing shear strength with depth.

3. If the boundary points between active and passive surface parts are not sharp (or the load discontinuities are too small) the corresponding b-line ruptures may not develop. Correspondingly, a part of the rupture figure at the end and/or at the start (from a point Q to B and/or from A to a point Q) may not develop. In the first case the remaining construction PQC becomes a single line rupture PB; in

the second case a rigid body COPQ may degenerate into a point A (or into a body AOP if A is not located in a fixed point).

4. If a passive surface part is too weakly developed the three line ruptures OP, QC, and OP may fail to develop. On the other hand, if it contracts into a single reentrant corner the construction may be replaced by a single (b-line) rupture OP.

5. The alternatives mentioned under No.3 and 4 above may obtain as locally extreme solutions to the failure problem. This means that from any one of them it may not be possible by a continuous transformation of the rupture figure through monotonously decreasing values of f or W to obtain the absolutely extreme (and therefore quasi-correct) solution. However, an extreme that is only local will always be statically impossible. It can therefore be detected by the investigation of secondary rupture figures in the moving rigid bodies or outside the rupture figure (built up in the same way). Alternative rupture figures can also be investigated, and the one with the lowest value of f or W be chosen, unless it intersects, or runs close to, another rupture figure with only a slightly higher value of f or W. In the latter case a combined rupture figure may be more critical. In any case care should be taken that the system of rupture figures that are investigated is compatible with the assumption of a unique stress distribution in the clay.

In a number of cases in practice a single line rupture will be a good enough approximation. It may be rather far off, however, if the soil profile is stratified, or if it passes too close to a reentrant corner (especially if it passes through or near below the foot point of a sheet pile wall). In natural slopes the former case will frequently obtain, and here the terraces, f. inst. in a river bed, will also represent a number of alternating active and passive surface parts. In such cases the so-called method of slices is sometimes used in soil mechanics as an alternative to the ordinary $\varphi = 0$ analysis.

This method has, strictly speaking, an infinite number of parameters since it admits of an arbitrarily shaped rupture line. In its best versions it satisfies all equilibrium conditions for the clay mass that is assumed to move, and also approximately the stress conditions along the slip line. No kinematical conditions are imposed on the rupture figure, and the failure condition may also be exceeded in the clay domain (but the value of τ_{max} is limited due to the special partitioning of the moving clay mass into slices).

In the terms of Sec. 243 (cf. Ex. 24 e) the method is therefore (approximately) quasi statically admissible, so that the minimum solution may be assumed to be somewhat on the safe side. However, the absolute minimum is never found since the variable quantities do not form a finite set of parameters, but an arbitrary function.

As an alternative the rupture figure type sketched in Fig. 52 A may be used, cf. Fig. 42 AA. Since this represents a kinematically admissible solution it will tend to be more on the unsafe side than the method of slices used on the same boundary to the moving mass of clay, provided that the safety is interpreted in the same way (in terms of a force necessary to produce failure, or a shear strength necessary to prevent failure). With the system of line ruptures greater care should therefore be taken to find the minimum solution. This is also possible since the number of parameters, although it may be high, is at least finite.

In artificial slopes or cuts the problems are usually simpler since it is only necessary to investigate a small number of rupture figures. They will, moreover, frequently be quite simple, containing at most one branch point. Special calculation problems, resembling those of natural slopes, may arise, however, if a deep cut is terraced or if strip loads are placed near the top of the slope, especially if an economic optimum design is sought.

Example 52 a

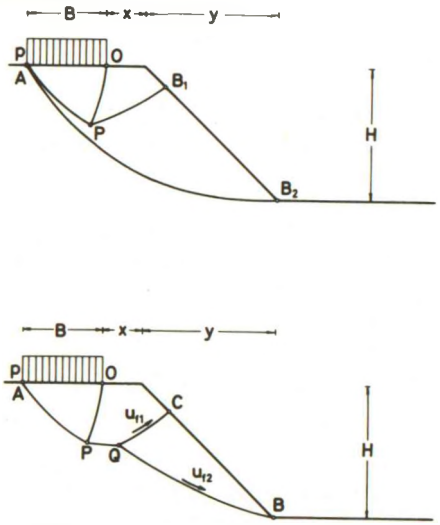

Fig. 52 B: A Combined Problem of Slope Failure. Separated and Integrated Rupture Figures.

Assume the intensity p and the width B of a strip load to be given together with the height H of a nearby slope (Fig. 52 B). If the minimum permissible values of the horizontal distances x and y are required, the foot point of the slope being given for a cut, or the position of the strip load being given for a fill, they could be determined by the condition that the two separate rupture figures $APOB_1$ (local bearing capacity) and AB_2 (slope failure) have the same, i.e. the required, value of f. The calculations could therefore be planned as follows (upper Fig. 52 B):

1. The value of y is estimated.
2. For an assumed value of x the rupture figure $APOB_1$ is calculated. x is varied, and the calculation is repeated, until f for this rupture figure has the required value.
3. For the values of x and y found in this way the rupture figure AB_2 is calculated (possibly continued below the foot point of the slope with a POB-construction, cf. Fig. 52 A). If the value of f is different from the required value the calculations from No. 1 above are repeated starting with another value of y.

However, this method may not be correct since no regard has been taken to the possible interaction between the two rupture figures. If in the upper Fig. 52 B a toe failure starting at some point along the slip line APB_1 is more critical than the line rupture AB_2 (the stresses along APB_1 being found by means of the stress conditions of Sec. 34), then a combined rupture figure like the one shown in the lower Fig. 52 B will be more critical.

In this case x and y cannot be found separately. For any value of y in a certain range one value of x can be found for which the combined rupture figure has the required value of f. The rupture figures for different values of y are distinguished by different values of the ratio between the sliding velocities u_f along the two line ruptures QC and QB (the parameter $\frac{u_{f1}}{\sqrt{u_{f1}^2 + u_{f2}^2}}$ will increase from 0 to 1 when y is increased within the actual range; during the same process x will decrease). The optimal combination must be chosen by means of some economic criterion, f. inst. minimum of x + y, minimum of cut volume, or of fill volume.

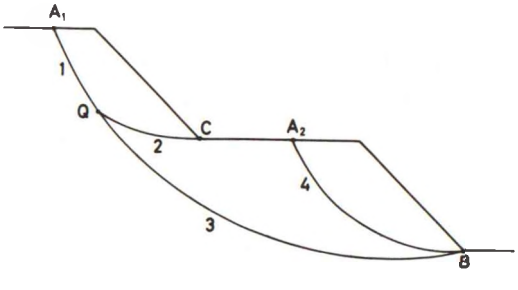

Fig. 52 C: Stability of a Terraced Slope.

Similar problems obtain when cuts or fillings with terraces are investigated (Fig. 52C). Here again the optimal design may have to be determined by means of a composite rupture figure (line ruptures No. 1 through 4) that is more critical than the collection of separate rupture figures, each of them calculated without any regard to the stresses produced by the other figures.

522 Stability of Structures

Stability problems in which structures, i.e. external rigid bodies, are more directly involved are not essentially different from the problems considered in the preceding section. By the definition of stability problems (in the sense used in soil mechanics) the existence of structures may impose certain geometrical constraints on the rupture figures, but the kinematical restraints will only be weak. A simple example of this is shown in the rupture figure, indicated by Brinch Hansen [1953], corresponding to an overturning of a cofferdam, cf. Ex. 24a (Fig. 24C). Other examples obtain in the stability of quay constructions.

The rupture figures are usually not difficult to find; they are built up in much the same way as in the problems of the preceding section. The only difference is that the existence of external rigid bodies will tend to increase the number of sharp reentrant corners in the clay domain. In a great number of cases the rupture figure will pass through, or be connected by secondary line ruptures to, such corners.

The main problem is that such rupture figures cannot normally, as it is often done in practice, be calculated separate from the earth pressure or bearing capacity figures that are bounded by the same corners. Therefore, in many cases that are treated as special, or secondary stability investigations to a problem that is primarily one of earth pressures or bearing capacities, one has in reality a combined rupture figure. This is due to the fact that for any given set of parameters to a failure problem a unique stress distribution should be assumed to exist in the clay.

Thus, for a sheet wall construction as shown in Fig. 52D the calculation procedure corresponding to the sketched rupture figures is usually applied:

1. First the driving depth D is determined by an ordinary earth pressure investigation, using the line ruptures No. 1 and 2 corresponding to an unmoving anchor construction. In the same process the wall is designed.
2. The depth D_a' of the anchor wall and the points of application for the tie rods (depth z_a) are then determined by the rupture figure 3 which is chosen to correspond to a translation of the anchor wall (zero relative to the movements of the sheet wall).
3. Finally the length a of the tie rods are determined by means of the line rupture No. 4. The rupture figure No. 3 for the active earth

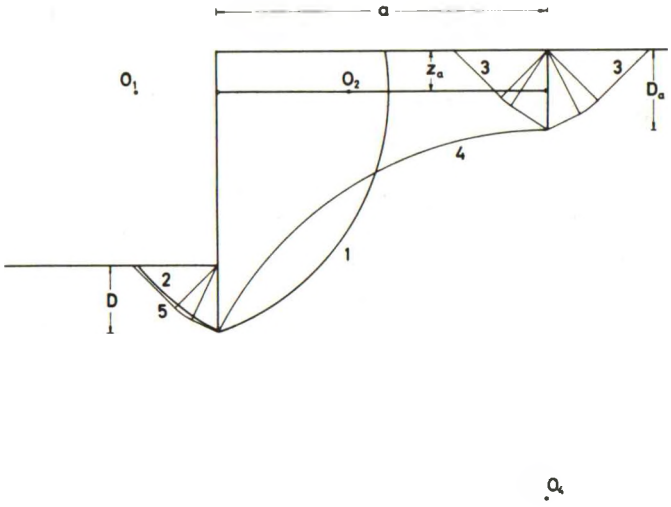

Fig. 52 D: Rupture Figures for the Investigation of an Anchored Sheet Wall. Usual Approximation with Separate Rupture Figures for Earth Pressures and Stability.

pressure on the anchor wall is not changed, but for the passive earth pressure on the sheet wall a new rupture figure (No. 5 corresponding to a zone rupture) must now be assumed.

This scheme is simple and straightforward, and it is not changed very much if the anchor construction is assumed to move instead of remaining fixed. The only difference is that the normal through the rotation points O_1 and O_2 need then no longer be located in the anchor level.

However, the line ruptures 1 and 4, and the rupture figures 2 and 5 cannot be assumed to exist simultaneously. If we maintain the assumptions that the movements in the rupture figures No. 3 are zero relative to those in No. 4 and 5, and that these again are zero relative to those in No. 1 and 2 the least changes in calculation method are necessary. In fact, the sheet wall and the anchor construction can be calculated as usual (rupture figures 1, 2, and 3). For the determination of a the line rupture 4 should be assumed to go from the foot point of the anchor wall to the line rupture 1 which in this connection is considered as a surface with known surface loadings ($\sigma_o = \sigma$ and $\tau_o = c$ along the line rupture). The rupture figure 5 is not used.

This mode of failure should be assumed for one definite set of variable external parameters (f. inst. surface loadings if such exist), and this set

should be the most critical one. In order to prove this one may have to calculate the sheet wall construction for another set of external parameters that tends to increase the value of f for the line rupture No. 4 and to decrease it for the slip lines No. 1 and 2.

For the failure problem obtained in this way the correct rupture figure (with a unique value of f) may not correspond to the assumed mode of failure. The two ratios of movements mentioned above ($\frac{u_3}{u_4}$ and $\frac{u_4}{u_1}$) may be finite numbers rather than zero. The same case obtains if savings are required on a and/or D_a at the cost of an increased value of D (and of the wall modulus). The rupture figure shown in Fig. 52 E may then obtain, assuming that the anchor wall is still translated during failure.

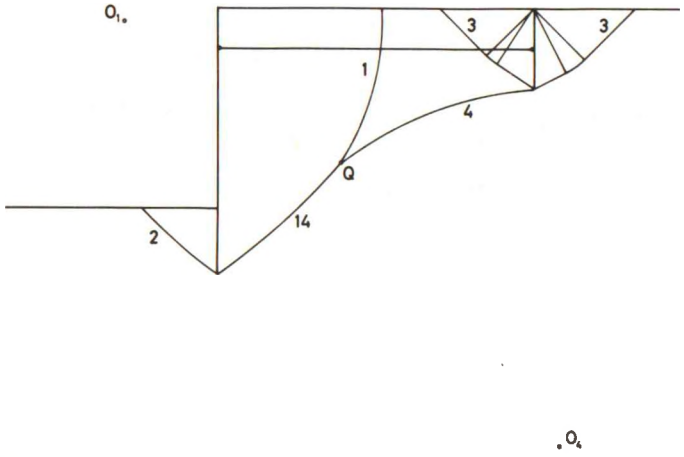

Fig. 52 E: Integrated Rupture Figure Corresponding (Approximately) to a Unique Stress Distribution in the Clay.

If $\frac{u_3}{u_4} > 0$, O_1 need not be located in the tie rod level. The line ruptures 1 and 4 intersect in a branch point Q and are continued in a single line rupture 14 (whose centre is located somewhere on the line through O_1 and O_4, but outside this interval) ending at the foot point of the sheet wall.

The passive earth pressure is determined by a rupture figure, assumed to be a single line rupture 2, whose centre is located on the same wall normal as O_{14}. The same addition of movements along No. 1 and 4 to obtain the resulting movement of the wall, which determines the rupture figure for the passive earth pressure, should also be made even if the two line ruptures can both be extended to the foot point of the wall without intersecting.

The same principle applies when the stability failure behind the wall is caused by a slope or heavy loadings located behind the anchor construction: If the movements in such failures can be assumed zero in relation to the movements of the wall the corresponding rupture figures should be calculated using the known stresses along the boundaries of the known rupture figures (it is in fact an investigation of the statical possibility of the rupture figure, considering secondary rupture figures in the unmoving earth mass). On the other hand, if the ratio between the movements turns out to be finite, f being smaller in the secondary rupture figure than in the primary one, a combined rupture figure must be considered, and the resulting movement of the wall must be found by a combination of the movements in the two rupture figures. The same type of problems obtains for retaining walls and for foundations.

If the rupture figure for a problem of total stability of a quay construction passes entirely below the construction, embedding the sheet wall and the anchor construction completely in the moving rigid body, this investigation has no influence whatever on the earth pressure problem. However, since a full circular line rupture may frequently become too much on the unsafe side (1-1' in Fig. 52 F) one may have to modify this rupture figure by means of a secondary line rupture through the foot point of the wall (the construction 2-3 in Fig. 52 F). This has no influence on the earth pressures if the movements in the rupture figure for the stability can be assumed zero. If this is not the case the different movements of the clay on the active and the passive side of the sheet wall will give modified earth pressures.

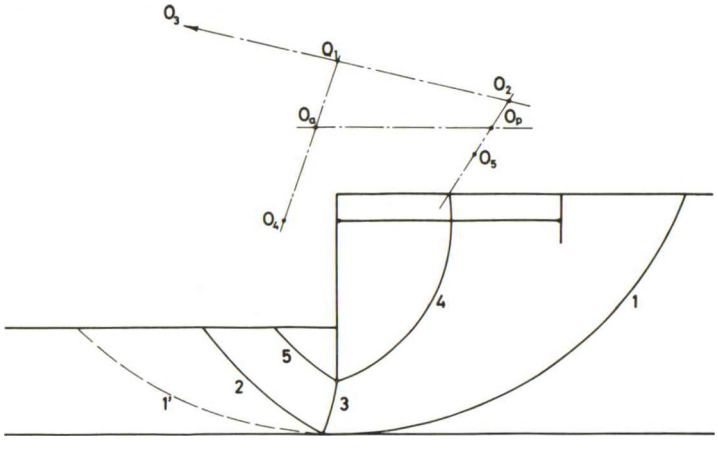

Fig. 52 F: An Earth Pressure Problem Modified by a Total Stability Failure under the Sheet Wall.

The active earth pressure in Fig. 52 F is calculated by means of a line rupture 4 whose centre is located in the tie rod level (assuming an unmoving anchor construction). From the ratio between the slidings along 1 and 4 the centre O_a for the resulting movement of the rigid body of clay on the active side can be constructed. The corresponding centre O_p for the body on the passive side should be located on the same wall normal. When its position has been assumed the centre O_5 can be constructed from the known rotations and movements.

It is seen that a rather complex rupture figure is obtained (8 free parameters). It presents no special difficulty, however, and it could easily be calculated on a computer. The only way to avoid such complications is to ensure that the safety against the total failure is somewhat greater than the safety against local failure of the sheet wall. This is also desirable in some cases, since the economic consequences of a total failure are usually much greater than for a local one, but it is not always possible to obtain because the measures that can be taken against total failure are also more expensive.

For combined problems of bearing capacity and stability rupture figures much like the ones shown in Fig. 52 B are used. If so desired other rupture figures can also be used for the bearing capacity problem, f. inst. AfPfA or an ordinary Prandtl rupture figure if the boundary conditions permit, at least when the movements in the stability figure are zero relative to those in the bearing capacity figure. If not this figure may have to be modified, using an AfPfA-construction on each side of the branch point. The combination of branch points and rupture zones seems rather illogical, however.

In problems with combined bearing capacity or earth pressure and stability the specification of the required safety may present a difficulty. For economical reasons it is customary to demand a higher factor of safety in bearing capacity problems than in stability investigations. On the other hand, in a combined rupture figure, or in a complex of simultaneous rupture figures as in Fig. 52 F, one must evidently calculate with one definite set of partial coefficients (or require one definite value of f). It is clearly illogical to specify zero movements in the stability failure and yet calculate this failure for a lower safety than the primary one. Questions of policy in specifying safeties are considered to be outside the scope of this work, however.

53 EARTH PRESSURE PROBLEMS

531 Simple Earth Pressures

By simple earth pressure problems we understand problems with one-sided failures between a straight wall and a straight, uniformly loaded surface, cf. Fig. 53 A. If the unit weight γ of the clay is taken into account the problem is, strictly speaking, only simple if the surface is horizontal ($\beta = 0$). In most cases in practice the parameter $\frac{\gamma h \sin\beta}{c}$ will be small, however, so the variation of the normal load along the surface can usually be disregarded. If not, the problem is of a more general type in which the normal load can be linearly distributed (the tangential load, if any, being a constant). Such problems are only a little more simple than the general type in which the surface load can be arbitrarily, but continuously, varying.

In the simplest case an earth pressure problem of the considered type is characterized by the 4 parameters $\beta - \theta$, $\frac{c_a}{c}$, $\frac{\tau_o}{c}$, $\frac{\sigma_o}{c}$, together with the movement and/or equilibrium conditions for the wall. If the movement of the wall is completely specified the rupture figure will be determined by $\beta - \theta$, $\frac{c_a}{c}$, and $\frac{\tau_o}{c}$ together with ρ, λ, and the indicator e_f (or with u_n, u_t, r_z with an arbitrary factor of proportionality).

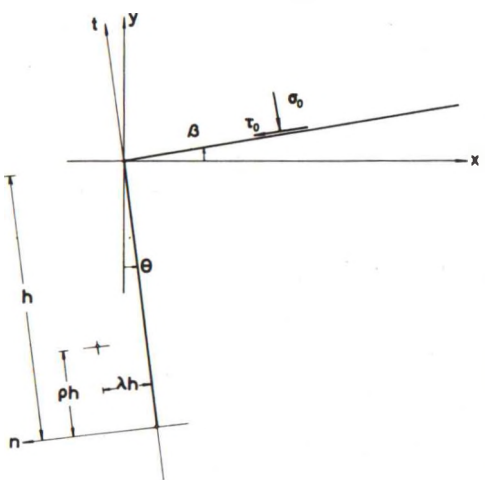

Fig. 53 A: Parameters for a Simple Earth Pressure Problem.

In a way such problems are exactly opposite to those considered in the preceding sections, because now the failure problem can be characterized by a few numerical values. But in a general solution a large number of different rupture figures will have to be used, cf. Fig. 51 B, Ex. 51 b. It follows from this example that although the rupture figure in many cases will be simple, or quasi-statically determined (Sec. 423) more complicated forms with closed rupture zones can

also obtain. Variants with wall zones and simple arc zones (Fig. 43 I-J) are also possible, especially if it is assumed that the normal stresses between the wall and the clay cannot be negative. Rupture figures with partly unsupported earth fronts may then become actual, and the values of the parameters $\frac{\sigma_o}{c}$ and $\frac{\gamma h}{c}$ have a direct influence on the form of the rupture figure.

However, if the last mentioned complication is disregarded for the moment (cf. Sec. 533), it is found to be relatively easy to indicate the proper rupture figure to investigate for any given set of movement components for the wall.

Thus, if $\rho \leq 0$ and $\lambda \geq \rho \tan i_w$ one can always start either with a full zone rupture WPR or with an arc zone rupture BfR (1,1). If in the latter case h_1 becomes negative (Ex. 42 c, Fig. 42 M-N) XfR must be used or, if the Rankine zone is geometrically impossible: X. When $\lambda < \rho \tan i_w$ one of the rupture figures XfWPR, XfPR, XfR or X may be used as a first approximation.

For $0 < \rho \leq \frac{1}{2}$ combinations of Aa or Aw with one of the above mentioned figures may be used if AaPR or AaR is not geometrically possible. Alternatively, when a partly unsupported earth front is assumed (especially for rough foundations) one may when $\lambda < 0$ use a construction Xf tangent to the wall.

Finally, for $\frac{1}{2} < \rho$ rupture figures of the types AaR, A, or AfPfA (or AfCfA, CfCfA, or three line ruptures meeting in the soil) are used.

In this way kinematically admissible solutions with possible zones are obtained. If the solution is not correct, and better approximations are required, the method of developing rupture figures should be applied. For example, a rupture figure XfR may be replaced by BfR if the angle between the line rupture and the wall is too small. However, if the same condition obtains in a line rupture X, or if the chord length k_2 (Fig. 42 M) in the arc zone rupture becomes negative, a closed wall zone connected to surface zones may have to be used. Constructions with Aw may be replaced by Aa with the same possibility of complications.

The above procedure is used for the first (or only) set of movement components in a given range of parameter sets, or for the first estimate of the movement components if the problem is stated in another way (f. inst. with given values of F and the point of application for E). By changes of the components, to cover a given range or to obtain a closer estimate, the rupture figure should be changed according to the method of rupture figure loci.

One might contemplate the calculation of simple earth pressures by means of a general program that were able to perform the operations indicated above. In order to be useful such a program should also be able to output the geometry of the rupture figure and the required force resultants (earth pressure distributions in the wall zone parts), so that f. inst. limiting states of failure in the rigid bodies of soil could afterwards be considered in connection with plastic bending of the wall (Sec. 441).

In practice one will not encounter all possible sets of the external parameters with equal frequency. The most important practical problems are:

1. Retaining walls or other types of combined earth pressure and bearing capacity problems. Here β and θ may vary over a wide range, as may also c_a, σ_o, and τ_o, but one will usually have $\rho < 0$ and frequently also $\lambda > \rho \tan i_w$.
2. Sheet walls in which frequently $\beta = \theta = 0$ and $\lambda = 0$ (normal rotation of the wall). τ_o is usually equal to zero. ρ may take any value, but values either in the vicinity of 0 or 1, or high positive or negative are the most frequent. For free sheet walls ρ may be in the middle part of the wall and λ may be slightly positive or negative.
3. The earth pressure on block foundation (usually with $\beta = \theta = 0$) is frequently either as for retaining walls (a large foundation load) or as for free sheet walls ($\lambda > 0$ and somewhat greater, cf. Sec. 542).
4. One-sided simple bearing capacity problems (with a slope through the foundation edge, cf. Sec. 541) have $\theta = -\frac{\pi}{2}$ but any value of β. c_a is usually equal to c. λ will normally be rather large and negative. $\rho < 1$.

However, occasionally other types of problems may arise, so no geometrically possible set of external parameters can be considered improbable a priori. Consequently, althrough a program of the type indicated above might be constructed and tested so that workable solutions to the most important problems are available first, it should eventually be extended to cover all possible sets of parameters.

It is seen that the range of such a program does not correspond very logically with the ranges of its sub-routines. It is evident that some of the rupture figures (f. inst. A, X, and AfPfA) can easily be used on much more complicated problems, whereas for other figures (f. inst. BfR) it is a provision that the earth pressure problem is simple. If this assumption is a-

bandoned, f. inst. by the introduction of a linearly varying surface load, the calculation procedure must be changed, although the computations will not become much more complicated than for some of the rupture figures that can be used in the simple case (f. inst. C). Besides the earth pressure problem as stated above gives only a partial solution since the resulting earth pressure must subsequently be used together with other earth pressures or bearing capacities acting upon the same construction.

The conclusion seems to be that the simple earth pressure problems defined as above do not in themselves form a sufficiently meaningful field of research. Instead, the different failure problems, f. inst. retaining walls, free sheet walls, anchored sheet walls with possible yield hinges, block foundations, and one-sided bearing capacity problems, should be studied by means of integrated programs that calculate the structures in question completely, using in each case as subroutines only the rupture figures that can actually be expected to develop.

An exception to this obtains in problems where the earth pressures can be described by a number of parameters sufficiently small to permit the recording of the solution on a closed form once and for all. Examples of this are: earth pressures on retaining walls (supposed to be full zone ruptures, WPR, expressible by a closed formula, cf. (4205-8)), rigid sheet walls with normal rotation ($\beta - \theta = \tau_o = 0$, so that the parameters are only ρ and $\frac{c_a}{c}$), and simple one-sided bearing capacity problems (rupture figure XfWPR, the solution of which can also be given by a diagram and a closed formula). In such cases the separate solution to the earth pressure problem may be used as an independent element in the total solution to the failure problem, at least in calculations by hand. In calculations by a computer it is not easy to introduce partial solutions expressed by graphs (represented by complicated formulae of numerical interpolation), so for this use it may actually be simpler to calculate the original rupture figures directly.

Example 53 a

The simple case with $\beta = \theta = \lambda = 0$ (normal rotation) has been solved by Brinch Hansen [1953] who considers perfectly rough ($c_a = c$) and perfectly smooth ($c_a = 0$) walls. The results for the two cases are so close that as far as the total earth pressure components are concerned, and also the parameters describing Brinch Hansen's approximate earth pressure distribution, it is sufficiently accurate to interpolate linearly when intermediate values of c_a obtain.

The rupture figures that are used in this investigation (with $\varphi = 0$) are all kinematically admissible with possible zones, and with one exception they are all solved by the equilibrium method. Of the rupture figures WPR, AaPR, and AaR (R, P, AaP, and AaR in Brinch Hansen's notation) are possible whereas A is quasi-possible and PfA is admissible.

The last mentioned rupture figure (Fig. 53 B) is obtained instead of AfPfA with straight radial slip lines when $\lambda = 0$ and the wall is perfectly rough. If the value of ρ is fixed it has only one free parameter, f. inst. $2\alpha_2$. It should therefore be solved by the extremum method, determing α_2 by the condition that the deformation work for a unit rotation about O shall be minimum.

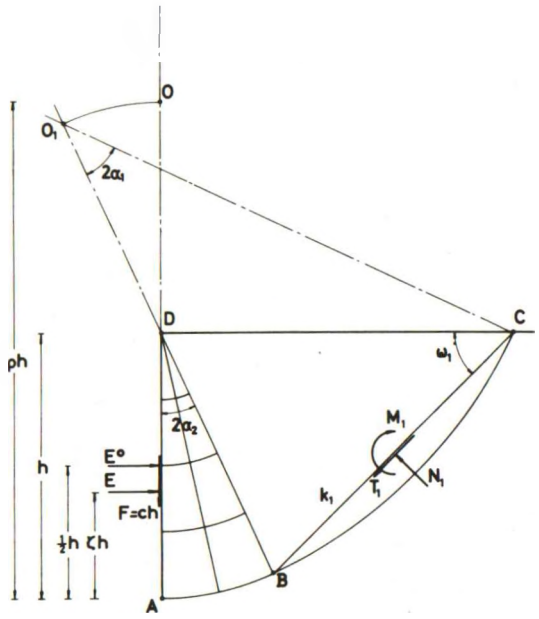

Fig. 53 B: A Rupture Figure PfA.

Since an infinitesimal change in α_2 will move the position of O_1 perpendicular to the line O_1B without changing the rotation r of the rigid body BCD, the extreme condition is seen from (2436-7) to be equivalent to the condition that the sum of the projections parallel to O_1B of the forces acting upon the body BCD shall be zero (including the shear stress along DB).

According to (3285) and (3420) we have:

$$N_1 = ck_1 \left[\cot(\omega_1 + \alpha_1) + 2\alpha_1\right]$$
$$T_1 = ck_1 \left[2\alpha_1 \cot\alpha_1 - 1\right] \tag{5301}$$

Besides:

$$\frac{k_1}{h} = 2\rho \sin\alpha_1 = \frac{\cos(\omega_1 - \alpha_1)}{\sin\omega_1} \tag{5302}$$

so that the above condition is equivalent to:

$$\left[\cot(\omega_1 + \alpha_1) + 2\alpha_1\right] \cos\alpha_1 - \left[2\alpha_1 \cot\alpha_1 - 1\right] \sin\alpha_1 = \frac{\sin\omega_1}{\cos(\omega_1 - \alpha_1)} \tag{5303}$$

By contraction we find:

$$\frac{\cos\omega_1}{\sin(\omega_1 + \alpha_1)} = \frac{\sin\omega_1}{\cos(\omega_1 - \alpha_1)}$$

or

$$\cos\alpha_1 \cos 2\omega_1 = 0 \tag{5304}$$

This means, evidently, that $\omega_1 = \frac{\pi}{4}$. Inserting this result in (5302) we find:

$$\rho = \frac{1}{2}(1 + \cot\omega_1 \cot\alpha_1) = \frac{1}{2}(1 + \cot\alpha_1) \tag{5305}$$

Using α_1 as a parameter ($0 \leq \alpha_1 \leq \frac{\pi}{4}$) solutions can be obtained for the interval $\infty \geq \rho \geq 1$. One has evidently:

$$2\alpha_1 + 2\alpha_2 = \frac{\pi}{4} + \alpha_1$$

i.e.

$$2\alpha_2 = \frac{\pi}{4} - \alpha_1 \tag{5306}$$

The value of σ at the point A, and therefore along the whole height of the wall, can also be found:

$$\frac{\sigma_A}{c} = \cot\left(\frac{\pi}{4} + \alpha_1\right) + \frac{\pi}{2} + 2\alpha_1 \tag{5307}$$

However, this is not a good approximation for the earth pressure along the wall. According to the general theory of admissible solutions with possible zones the energy method should be used, and by (2426) it is seen that the work done by σ_A should be corrected, using also the work done by the forces acting upon the rigid body BCD.

If the movements during failure are normalized so that the displacement of the mid point of the wall is unity, the horizontal earth pressure component E^o, supposed to be acting at this point is found from (2426):

$$\frac{E^o}{ch} = K_c^o = \frac{\sigma_A - \sigma_B}{c} + \frac{\rho^2}{\rho - 0.5} \; 2\alpha_1$$
$$= \frac{\pi}{2} + \frac{2\alpha_1}{\sin 2\alpha_1} \tag{5308}$$

inserting also (5305).

A better approximation is obtained if the horizontal earth pressure E is assumed to act at a height ζh above the foot point. The corresponding value of K_c is found from ζ and K_c^o by the formula

$$K_c = K_c^o \frac{\rho - 0.5}{\rho - \zeta} \tag{5309}$$

the deformation work $K_c(\rho - \zeta) = K_c^o(\rho - 0.5)$ being known when the rotation centre O is fixed.

The best value for ζ can be found as follows. Assume that ζ were known, and that the problem were to find E by varying ρ and α_2 until the extreme value obtained. The condition $\frac{\partial E}{\partial \alpha_2} = 0$ (with a fixed value of ρ) would evidently give the same solution $\omega_1 = \frac{\pi}{4}$ as above. However, ρ should afterwards be determined by the condition that $\frac{\partial E}{\partial \rho} = 0$. Since $\frac{\partial E}{\partial \alpha_2} = 0$ it does not matter whether α_2 is kept constant or it is also varied, keeping ω_1 equal to $\frac{\pi}{4}$.

Therefore, the connection between ρ, ζ, and K_c should be found from (5308-9) by the condition that $\frac{\partial K_c}{\partial \rho} = 0$ when ζ is assumed to be a constant. This will evidently make the solution consistent with the solution to the problem where the rotation centre is not fixed. Thus, if an external force E acts upon the wall at the height ζh the restraint force at O has a vanishing horizontal component.

By the use of (2436-7) this can be shown to be equivalent to the condition that the total work done by a rotation of the wall about its mid point is zero. Equating the works done by the earth pressure resultant E, and by the forces acting upon the rigid body BCD (rotating about the mid point of BD) we find:

$$K_c(0.5 - \zeta) = \frac{0.5}{ch}(N_1 \sin\alpha_1 + T_1 \cos\alpha_1) + \frac{M_1}{ch^2} - \frac{1}{2}\frac{k_1 N_1}{ch^2} \tag{5310}$$

Inserting (5301-2) and also:

$$M_1 = \frac{1}{2} c k_1^2 \, (\alpha_1 - \alpha_1 \cot^2 \alpha_1 + \cot \alpha_1) \tag{5311}$$

cf. (3284-5), we find after some calculations:

$$K_c \, (0.5 - \zeta) = \rho - 0.5 + 2 \, \alpha_1 \, \rho \, (1 - \rho)$$

$$= \frac{1}{2} [\cot \alpha_1 + \alpha_1 \, (1 - \cot^2 \alpha_1)] = M^z \, (\alpha_1) \tag{5312}$$

The same formula can be obtained by direct differentiation of (5309):

$$\frac{\partial K_c}{\partial \rho} = \frac{\partial K_c^o}{\partial \rho} \, \frac{\rho - 0.5}{\rho - \zeta} + K_c^o \, \frac{0.5 - \zeta}{(\rho - \zeta)^2} = 0 \tag{5313}$$

which can be written:

$$K_c \, (0.5 - \zeta) = - \frac{\partial K_c^o}{\partial \rho} (\rho - 0.5)^2 \tag{5314}$$

If we use that $\frac{\partial K_c^o}{\partial \rho} = \frac{\partial K_c^o / \partial \alpha_1}{\partial \rho / \partial \alpha_1}$, calculated by means of (5305) and (5308), we find again (5312).

From (5309) and (5312) we may find:

$$\zeta = \frac{\frac{1}{2} K_c^o \, (\rho - 0.5) - M^z \, (\alpha_1)}{K_c^o \, (\rho - 0.5) - M^z \, (\alpha_1)} \tag{5315}$$

after which K_c is found from (5309).

The results of these calculations are shown in Table 53 A. K_c and ζ as functions of $\frac{1}{\rho}$ (= $1 - \tan (\frac{\pi}{4} - \alpha_1)$) are given in Fig. 53 C (curves with full lines).

For the sake of simplicity Brinch Hansen has calculated the rupture figure, after introducing the kinematical condition $O_1B = O_1C = OA$, as if it were a zone rupture. Thus, for each value of α_1 (in the interval $0 \leq \alpha_1 \leq 33.4^o$) ω_1 and therefore also α_2 are determined by the condition that the vertical equilibrium for all forces upon the clay domain ABCD shall be satisfied. After this K_c and ζ are determined by the horizontal equilibrium and the moment equation about the foot point of the wall.

The corresponding results are shown in Fig. 53 C (dotted lines). It is seen that K_c and ζ are both smaller than the values found in Table 53 A. The unit deformation work $K_c \, (\rho - \zeta)$ is also a little smaller, so Brinch Hansen's method is in this case on the safe side. The deviation is only at

Table 53 A: Earth Pressure Coefficients Calculated from Rupture Figure PfA.

α_1 deg.	ρ	K_c^o	ζ	K_c	$\frac{1}{\rho}$
0	∞	2.571	.500	2.571	.000
5	6.215	2.576	.477	2.566	.161
10	3.336	2.591	.454	2.550	.300
15	2.366	2.618	.431	2.525	.423
20	1.874	2.657	.407	2.489	.534
25	1.572	2.710	.382	2.442	.636
30	1.366	2.780	.356	2.385	.732
35	1.214	2.871	.329	2.316	.824
40	1.096	2.989	.299	2.235	.913
45	1.000	3.142	.267	2.142	1.000

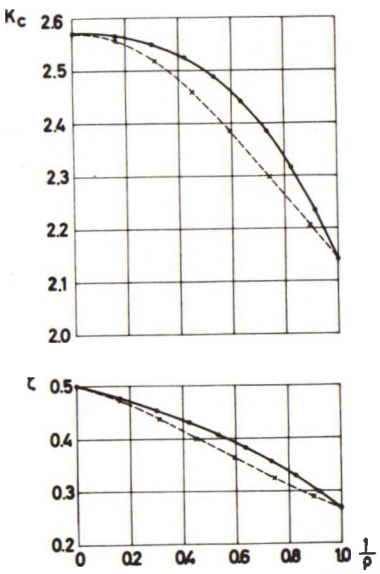

Fig. 53 C: K_c and ζ as Functions of $\frac{1}{\rho}$ Calculated for a Rupture Figure PfA ($\beta = \theta = 0$, $\tau_o = \sigma_o = 0$).

most 1 %, however. It contains a contribution (to the unsafe side) from the fact that the most critical combination of α_1 and α_2 has not been used, and another (to the safe side) from the use of an equilibrium equation instead of the work equation.

It might be noticed that Table 53 A can be used to evaluate the approximation involved in the use of the zone rupture WPR for values of ρ in the interval $1 \leq \rho < \infty$ (cf. Ex. 42 a). This is obtained simply by comparing the value of K_c^o for $\rho = \infty$ (the normalized deformation work for the zone rupture) with the values of the same quantity for the actual values of ρ. The comparison shows that the zone rupture, which is about 20 % on the safe side for $\rho = 1$, will be less than 10 % wrong for $\rho > 1.25$, less than 5 % wrong for $\rho > 1.6$, and less than 1 %

wrong for $\rho > 3$. In this comparison it is used that the rupture figure PfA is only a few per cent wrong (on the unsafe side) for $\rho = 1$ (the line rupture A compared with C, cf. Fig. 51 A), and is correct for $\rho = \infty$.

532 Special Surface Conditions

If more general surface conditions than those considered in the preceding section are permitted the number of parameters will as a rule become so great that even for the individual failure problems considered above, e.g. free sheet pile walls, a general solution cannot be obtained.

In practice one must therefore prepare a calculation program for each case that does not fall into one of the following classes.

1. It can be calculated by hand using a simple, admissible or even quasi correct, rupture figure, f.inst. a line rupture (A) that is not affected much by irregular surface conditions.
2. It is preferred to approximate it with a corresponding simple problem. For example, a variable surface loading is smoothed out so that a uniform mean loading is used instead, and/or a broken surface curve is replaced by a straight mean line.
3. A corresponding interpolation can be made directly on the required quantities. For example, the earth pressure for a broken surface may be obtained by an interpolation between the values for the two surface directions through the corner point.
4. A general program (f.inst. for stability problems) that solves a class of arbitrary failure problems by means of a special type of rupture figures (f.inst. systems of line ruptures, general statically determined surface zones continued by line ruptures, or AfCfA-figures) can be used, possibly after some approximation of the failure parameters.

In such programs existing procedures for the calculation of special rupture figure elements should be utilized as far as possible. Moreover, the rupture figures should if possible be chosen so that they contain the simple (correct or quasi-correct) solutions as special cases that are obtained for the parameter sets corresponding to simple failure problems (zero corner angle, uniform load etc.). This is not always possible, cf. Ex. 34a, but the deviation from known solutions in the simple cases should always be checked.

Earth pressure problems with a straight wall having a constant value of c_a, but with arbitrary surface conditions, fall roughly into the following classes. Notice, however, that it is only problems with rupture figures that have surface zones that are seriously influenced by irregular surface conditions.

1. If the surface is straight and the surface loading variable but continuous and not too rapidly changing, much the same basic approximate rupture figures can be used as in the preceding section. The surface zones will be of a more general class, and possible arc zone ruptures will no longer be simple, but the calculation work need not be much more complicated, if all zone elements can be bounded by single circle arcs, cf. Sec. 434.

2. The same state of affairs obtains if the surface is curved (upwards concave or with a relatively large radius of curvature). Reentrant corners introduce radial zones and will therefore increase the number of zone elements. The same applies to jumps in the normal loading, but in all these cases it is still basically the same rupture figure types that are used, provided the loading jumps are not too great or too close to the wall, and that for active surface zones the higher load, and for passive zones the lower one is on the side of the jump towards the wall (cf. Ex. 33 e-f, Fig. 33 S).

3. In other cases, f. inst. extruding corners, convex surface curves with a small radius, and more general types of load discontinuities, rather more difficult rupture figures may obtain. Normal surface zones may have to be replaced by complicated constructions of open zones separated by rigid bodies of clay (Fig. 43 M and Sec. 435), and other simple rupture figures by rupture figure complexes (Fig. 44 I).

The general types of rupture figures to use in each case can to some extent be deduced from the preceding chapters. In some cases relatively simple approximate solutions can be given, whereas in other cases, especially if open rupture zones are present in the correct rupture figure, all solutions that distinguish the main features of the failure problem are complicated, unless a special expedient to be mentioned later in this section is used. It permits the use of the same rupture figures, f. inst. systems of line ruptures, as in stability investigations, but the boundary movement conditions are neglected.

The most important problems in practice with irregular surface conditions are the ones mentioned in the preceding sections made more complicated by the existence of a uniform surface loading acting only over a part of the surface (discontinued surface loadings or strip loads). Occasionally the surface loading may be linearly increasing or decreasing over some surface parts, f. inst. due to the correction for volume forces on a slope, and the surface itself may consist of a horizontal and one or two sloping parts separated by corner points.

The basic construction at a load discontinuity (with increased loading in active and with decreased loading in passive surface zones) is BfDR, cf. the first Fig. 53 D. Correspondingly, for extruding corners (in passive surface zones) it is BfR. Naturally, they may for different movements of the wall be modified into XfDR, AaBfDR etc., and the rigid body may also be separated from the wall, being f. inst. a local body in the surface zone corresponding to an AaR-rupture figure.

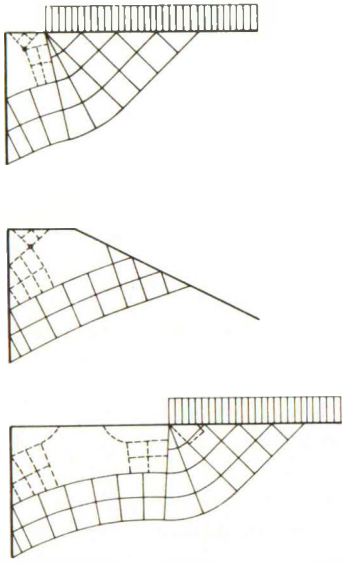

Fig. 53 D: Arc Zone Ruptures for Earth Pressure Problems with Discontinued Surface Loadings or Extruding Corners. Secondary Rupture Figures in the Rigid Body, and Formation of a Rigid Body in the Surface Zone.

This construction may be modified by the existence of secondary rupture figures in the rigid body, starting at the surface zone or at the wall, cf. Fig. 53 D (sketched with dotted lines). The secondary rupture figures may be connected by discontinuity points to surface zones as shown in the two first Figs. 53 D. They may also be continued by line ruptures, cf. the last figure, that are approximations to arc zone constructions ending in a surface zone complex. Local constructions of the types XfR, AaR etc. are also possible.

If the breaking up of the primary rigid body into secondary bodies produces negative values of ϵ in the surface zone, rigid bodies may also be formed in this zone as suggested by a dotted line in the third Fig. 53 D.

For extruding corners in active surface zones rupture figures of the same kinds will be developed. The only dif-

ference is that the tendency for the rupture figure to intersect the surface part between the wall and the corner will be stronger.

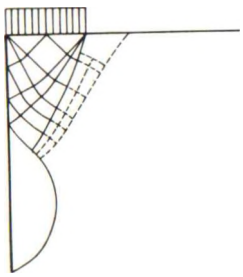

Fig. 53 E: Rupture Figure AaWPR for a Discontinued Surface Loading Behind a Wall.

For load discontinuities in the opposite directions of those considered above (i.e. positive for passive and negative for active surface zones) the basic construction is the continuation of the surface zone near the wall through a radial zone (Fig. 53 E, cf. Fig. 33 S). Thus, at the first hand it is simply a modification of an otherwise normal surface zone, when it obtains in a rupture figure WPR, AaR, BfR etc. In Fig. 53 E this feature is shown for an AaWPR rupture figure (r_z positive for the wall).

If the load discontinuity comes too close to the wall a secondary rupture figure may develop in the unmoving rigid body outside the rupture figure as suggested by dotted lines in Fig. 53 E. By combinations of the above mentioned modifications complicated rupture figures like the one shown in Fig. 43 M are obtained. For strip loads that are narrow in relation to the extent of the surface zone the rupture figure may be considered as a modification obtained by the introduction of free rigid bodies into the zone (Sec. 435). An example of this is shown in Fig. 53 F ($\rho < 0$) for active and passive earth pressure (upper and lower figure, respectively).

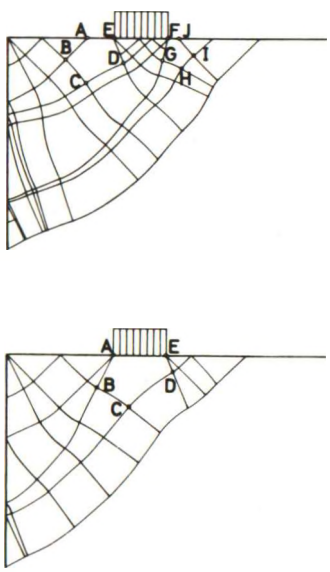

Fig. 53 F: Zone Ruptures Modified by Strip Loads in the Active and the Passive Case.

The rigid bodies ABCDE and FGHIJ are calculated as indicated in Sec. 435. For each body the geometry is determined by 5 parameters subject to one stress condition. The velocity field

determines the rotation of the body and imposes one further condition on the parameters so that the remaining 3 parameters can be determined by the equilibrium conditions.

These calculations will give solutions for sufficiently small values of the unit load. From Fig. 53 F it is seen that the curvature of the arcs BC and GH may for higher unit loads make the rupture figure geometrically or kinematically impossible (producing negative chord lengths or negative values of ϵ further down in the rupture zone). For other modifications see Fig. 43 M with comments.

Quasi-possible solutions with line ruptures ending at the surface are not made much more difficult by the existence of irregular surface conditions. It should be noticed, however, that the number of secondary rupture figures to investigate will usually be increased. Thus, a-line ruptures ending under high load concentrations (and b-line ruptures under low ones) will tend to split up into a combined rupture figure as will also line ruptures of both denominations in the vicinity of extruding corners. If more correct (possible) rupture figures are required, one will either get distorted surface zone complexes, with the active zones under high and the passive zones under low unit loads, or the ordinary C-rupture figure will split up into more complicated figures with simultaneous or combined multiple radial zones.

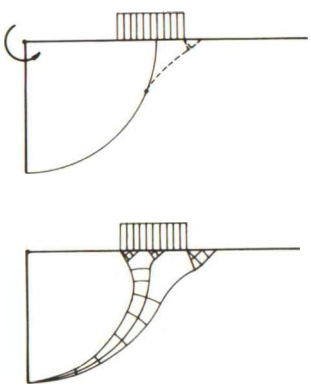

Fig. 53 G: Modification of a Line Rupture, and the Corresponding C-Rupture Figure, Near a Strip Load.

For example, the line rupture shown in Fig. 53 G, supposed to be obtained by rotating a perfectly rough wall about its upper point, may be statically impossible because of a secondary rupture figure, shown with dotted lines, being unstable. A combined rupture figure containing a line rupture branching off in another line rupture and an XfDR construction may in this case give a quasi-correct solution. The mathematically correct solution may have a rupture figure as shown in the lower Fig. 53 G. This rupture figure evidently exists in a great number of variations, so the calculation work may be very large. However, it should be noticed that the combined quasi correct solutions may have a significantly

smaller deformation work than has the simple line rupture. Some modifications may therefore be necessary even if the correct solution is not required.

If one wishes to avoid the open rupture zones of Fig. 53 D-F, that can in practice only be calculated by means of rather far advanced computer programs which are able to develop and modify rupture figures, one may replace the zone ruptures by systems of line ruptures as in Fig. 53 G (cf. also Ex. 34 a, Fig. 34 M), or other simple rupture figures (AfPfA, AfCfA etc.). This method, which is analogous to Coulomb's classical earth pressure solution, does not always permit the use of the correct value of ρ. This parameter should therefore be considered as unknown. Instead a point of application for the total earth pressure must be assumed. An approximate optimal position of this point may be found by the condition that the work done by the total earth pressure, if the movement of the wall is supposed to be a rotation about the true rotation point, shall be a maximum.

This rule is based on the following reasoning. If the point of application were given (f. inst. by the relative height ζ) we might investigate the failure problem by a series of ruptures figures like the ones shown in Fig. 53 D-F, i.e. corresponding to at least approximately correct values of ρ. As explained in Ex. 53 a the best solution would be characterized by the condition that $\frac{\partial E}{\partial \rho} = 0$ (a minimum). If another value of ζ is chosen, another set of values for E and ρ is found. Considering any given value of ρ, ρ_o, the corresponding values E_o and ζ_o may be found as the set for which $\rho = \rho_o$. However, it is also equal to the set for which $W = E\,(\rho_o - \zeta)$ is a maximum.

This can be verified directly in Table 53 A. It can also be seen from the fact that this deformation work can be obtained by using the velocity field of the solution E_o, ζ_o (rotation point at ρ_o) together with the stress distribution of the solution E, ζ. If the first mentioned solution (σ_o, u_o) is compared with a consecutive one (σ, u), the difference $\rho - \rho_o$ being infinitesimal, it is seen that the difference

$$\Delta W = \int_V (\sigma_{ij} - \sigma^o_{ij})\, \epsilon^o_{ij}\, dV$$

$$= \int_V 2\,[\tau \cos 2\,(\theta - \theta_o) - c]\, \epsilon_o\, dV \qquad (5316)$$

is less than zero (regardless of the sign of $\rho - \rho_o$), provided the solutions are kinematically admissible with possible zones, cf. Sec. 245.

Therefore the maximum condition is true for rupture figures that give the true movements of the external rigid bodies. But, since the failure problem with a fixed value of ζ has a unique solution any other approximate solution, even if it does not have this property, will give an approximation to the correct value of E. Consequently, the maximum condition can also be used approximately for such solutions, and if they are reasonably close the final result may also be expected to be a good approximation.

In this way a solution method is defined which more generally can be stated as follows. A movement restraint on the system of external rigid bodies can as an approximation be neglected provided that one of the other movement conditions (the position of a rod, or a ratio between two rod deformations) is considered as a variable parameter, the value of which is chosen (after the minimum solution has been found in the normal way for each considered value) so that the work done by the prescribed movements, assuming the neglected restraint to be now operating, is a maximum.

The goodness of the approximation in this minimax procedure will of course depend on the choice of the alternative variable parameter. For example, the system of three line ruptures does not give a very good approximation for $\rho_o \leq 0$ (it will be somewhat on the unsafe side). However, if the full number of parameters, viz. 5, is used, solutions with $\rho = \rho_o$ will be both statically and kinematically quasi-possible, and they will of course be found whether the ordinary extremum method (with $\rho = \rho_o$) or the minimax procedure is used. To obtain a better approximation, i.e. one that is more on the safe side, the minimax procedure should be used with a lower number of parameters, or ζ should be assumed to be known. With this modification the solution method does not, strictly speaking, follow the standards of Sec. 243, and the position of the solution relative to the mathematically correct one is not known.

However, the approximation may not be too far off (cf. Ex. 34a), and applied to the problems considered in this section the method has the advantage that all earth pressure problems with rigid walls can be considered as if they were stability problems. Thus, rupture figures with systems of line ruptures or other simple rupture figures can be used instead of complicated open rupture zones. This may give important savings in the calculation work, especially when the surface conditions are irregular, although the ordinary extreme method is replaced by a minimax procedure.

Example 53 b

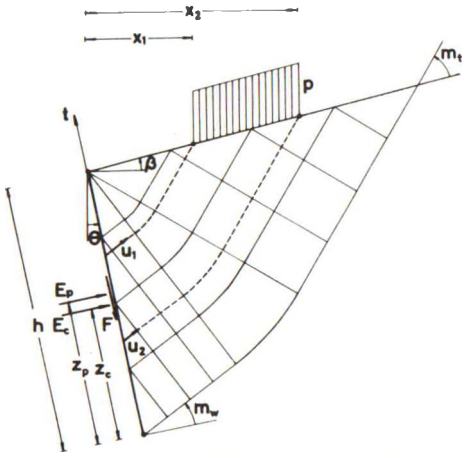

Fig. 53 H: A Kinematically Admissible Solution to the Problem of a Strip Load Behind a Retaining Wall (Velocity Field from the Ordinary WPR-Zone Rupture).

Consider as an example the problem of a vertical, uniform strip load behind a retaining wall (Fig. 53 H). The number of parameters is not very great: β, θ, $\frac{c_a}{c}$, $\frac{p}{c}$, $\frac{x_1}{h}$, $\frac{x_2}{h}$, and also ρ and λ. The influence of the position of the rotation point will probably be weak if a full zone rupture (WPR, active case) is supposed to be developed in the unloaded case ($p = 0$).

As a first and rather rough approximation the velocity field corresponding to the full zone rupture may be used for $p \neq 0$. Since the rupture figure is unaltered from the case $p = 0$ the deformation work in the clay will be the same. The work necessary to move the wall will therefore simply be decreased by the work done by the strip load during the deformation.

This means that an additional earth pressure E_p is obtained above the earth pressure E_c that corresponds to the case $p = 0$, cf. (4208). $e_f = e_t = -1$ and $\sigma_o = \tau_o = 0$ ($m_t = \frac{\pi}{4}$). From the notations in Fig. 53 H we find:

$$r_z E_p (z_p - \rho h) = -\frac{1}{2} p (x_2 - x_1) (u_1 + u_2) \sin (m_t + \beta) \qquad (5317)$$

Inserting (4211), using also that for both of the subscripts 1 and 2:

$$t = h - x \frac{\sin m_t}{\cos \beta \cos m_w} \qquad (5318)$$

(5317) can be written:

$$E_p \left(\frac{z_p}{h} - \rho\right) = p (x_2 - x_1) \left[1 - \frac{x_1 + x_2}{2h} \frac{\sin m_t}{\cos \beta \cos m_w} - \rho\right] \frac{\sin (m_t + \beta)}{\cos m_w} \qquad (5319)$$

As explained in Ex. 53 a z_p can be found from the condition that $\frac{\partial E_p}{\partial \rho} = 0$, assuming z_p to be a constant. This gives directly:

$$E_p = p\,(x_2 - x_1)\,\frac{\sin\,(m_t + \beta)}{\cos\,m_w}$$

and (5320)

$$\frac{z_p}{h} = 1 - \frac{x_1 + x_2}{2h}\,\frac{\sin\,m_t}{\cos\,\beta\,\cos\,m_w} = \frac{t_1 + t_2}{2h}$$

Thus, E_p acts at the mid point between the intersection points with the wall of the slip lines through the load boundaries. Assuming it to be uniformly distributed between these two points its intensity is found to be:

$$\frac{e_p}{p} = \frac{\sin\,(m_t + \beta)\,\cos\,\beta}{\sin\,m_t} \tag{5321}$$

with $m_t = \frac{\pi}{4}$. Since the wall zone is fully developed the shear force F will in all cases be equal to $-c_a\,h$.

This is a reasonably simple rule, that is on the unsafe side, however. It is seen that for $\beta = 0$ we have $e_p = p$. For $\beta \neq 0$ this method has the disadvantage that in the limit, i.e. for $t_1 = h$, $t_2 = 0$, the intensity (5321) will not have its correct value which is obtained from (4205-8), inserting $\tau_o = p \sin \beta$, $\sigma_o = p \cos \beta$ (for $e_c + e_p$) and subtracting the corresponding expression (for e_c) with $\sigma_o = \tau_o = 0$:

$$e_p = p \cos \beta + c\,(\tfrac{\pi}{2} + 1 - 2\,m_{tp} - \sin 2\,m_{tp}) \tag{5322}$$

where

$$m_{tp} = \arctan \sqrt{\frac{c - p \sin \beta}{c + p \sin \beta}}$$

$$\cos 2\,m_{tp} = \frac{p}{c} \sin \beta \tag{5323}$$

$$\sin 2\,m_{tp} = \sqrt{1 - (\tfrac{p}{c})^2 \sin^2 \beta}$$

If a smooth transition between the two expressions is required one should (for $\beta \neq 0$) determine the total work done by the prescribed boundary movements:

$$W = r_z[\,E_c\,(z_c - \rho h) + E_p\,(z_p - \rho h)] \tag{5324}$$

considering m_t as a variable and demanding that $\frac{\partial W}{\partial m_t} = 0$. Assuming $z_c = \frac{h}{2}$ and z_p as given by (5319) the total earth pressures E_c and E_p can be found from the further condition that the derivative of the resultant earth pressure force with respect to ρ shall be zero. Alternatively E_c and z_c are considered as known, and E_p and z_p are determined by this condition. The principle of superposition can then still be used, but as it can be seen from (5321-2) $\frac{e_p}{p}$ will now depend on $\frac{p}{c}$, and probably also on $\frac{x_1}{h}$ and $\frac{x_2}{h}$.

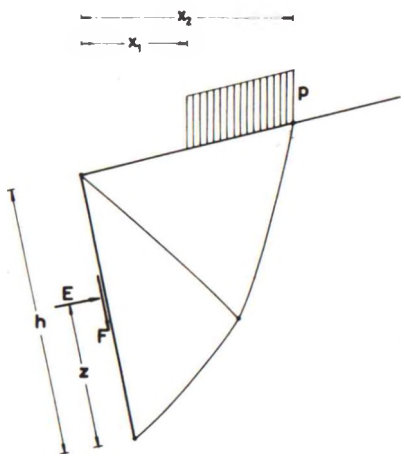

Fig. 53 I: Approximate Solution with 3 Line Ruptures.

A better approximation is probably obtained if the shear force $F = -c_a h$ (acting on the clay) is put on as a known force, after which the total normal earth pressure E is found for some different values of z f.inst. by means of a rupture figure with three line ruptures meeting in the soil (Fig. 53 I). During this investigation the wall is assumed to be free, but afterwards the set E, z is chosen for which the work done by E, i.e. $-E(z - \rho h)$ - negative because the values of u are negative - is a maximum. In practice the position of this maximum will presumably often be assumed to be known by experience, using f.inst. (5320), or the number of parameters is decreased f.inst. by the use of a fixed curvature for the lower slip line (or a fixed, high positive value of ρ is used).

If still better approximations, or possibly the correct solutions are required the rupture figure of Fig. 53 F with variants must be used. Possible solutions of this type may have 8 parameters or more, but even if admissible solutions with the same number of parameters as in Fig. 53 I (viz. 3-5) are used, it is easy to see that the calculation work will be much greater because of the more complicated rupture figure (a considerably greater number of zone elements).

533 Yield Hinges and Partly Unsupported Earth Fronts

In the problems considered in this section the surface conditions may be irregular, f. inst. because of the existence of strip loads, but they will frequently be perfectly regular. The problems considered now arise from a crack opening between the wall and the soil, the interface being unable to sustain negative normal stresses, or from the development of a (yield) hinge in the wall. As explained in Sec. 433 the two cases may in the important practical case of anchored sheet walls give much the same rupture figures.

This special case has been treated rather extensively, cf. Fig. 43 I-J. In practice the simple approximation shown in Fig. 42 W (cf. Fig. 44 C) will probably be very useful. With a few modifications the same rupture figures may be used f. inst. for earth pressures acting upon retaining walls, if a crack is supposed to open along the upper part of the wall. This approximation is presumably better than the usual one in which the earth pressure distribution is calculated by means of the ordinary zone rupture WPR, after which negative normal earth pressures (and the corresponding adhesion stresses) are simply disregarded.

If ρ takes a small positive value one may, depending on the values of λ and e_f, obtain rupture figures f. inst. of the type Aw, wAa, wW, wBf, or wXf (for $c_a = c$), cf. Fig. 53 J. Such rupture figures may become actual around free sheet walls, f. inst. of the types Aw on one side and wWPR, wAaPR, or wBfWPR on the other side. If λ becomes too large and negative, rupture figures of the types wBfPR, wBfR etc. may also develop, ending

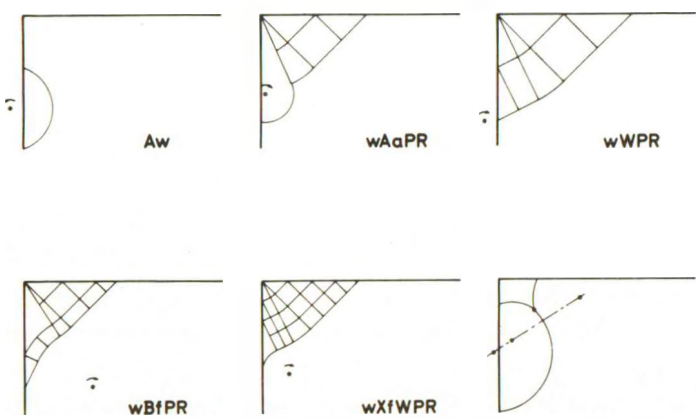

Fig. 53 J: Simple Rupture Figures for Partly Unsupported Earth Fronts.

with wX or w plus an arc zone with a surface zone complex (Fig. 43 I-J, cf. Sec. 531 with $\rho = 0$).

All these rupture figures are simple, and are in fact as easy to calculate as the ordinary simple earth pressure figures. Notice that in the upper point of the line rupture Aw, and in the lower point of wA, the value of σ is not directly determined by (3420) since σ_o, and also τ_o if the wall is not sliding upon the clay, are unknown at these points on the side of the moving rigid body. However, (3435) may be used if all terms containing the index 1 are neglected (cf. Fig. 34G; this is equivalent to the use of only the second and fourth term in (3417)). For simplicity one may change the signs so that $\tau_f = +c$ when the line rupture is an a-line, and it may also be used that:

$$\frac{r_w n_r}{u_n} - \cot(\beta - \beta_w) = -\frac{u_s}{u_f} \operatorname{cosec}(\beta - \beta_w) \qquad (5325)$$

u_s being the sliding velocity between the wall and the clay, and u_f the sliding velocity along the line rupture. We find:

$$\sigma = \tau_f \cot(\beta - \beta_w) + c_a \frac{u_s}{u_f} \operatorname{cosec}(\beta - \beta_w) \qquad (5326)$$

cf. (3420).

In rupture figures of the type wA this imposes a stress condition on the lower point of the line rupture, the stress at this point being also calculated from the surface through the rupture figure.

As shown in the last Fig. 53 J the rigid body above a line rupture Aw may become unstable if the line rupture comes too close to the surface. A combined rupture figure may then obtain in which the top point of the clay front against the wall acts as an extruding corner.

In heavy clay the corrective normal loading (2307) should be supposed to act upon all free clay surfaces including the faces to the cracks between the wall and the clay. It should also be added as an external load on the wall parts facing such cracks. For wall parts along which no crack is supposed to open it is an internal force, however.

If this correction is of any significance one may for relatively high values of ρ obtain a rupture figure of the general type LsZ in Brinch Hansen's notation. The same type, an example of which is sketched in Fig. 53 K, may also obtain for walls with yield hinges as an alternative to the rupture figures shown in Fig. 42 W and Fig. 43 I-J (ZsL in Brinch Hansen's notation).

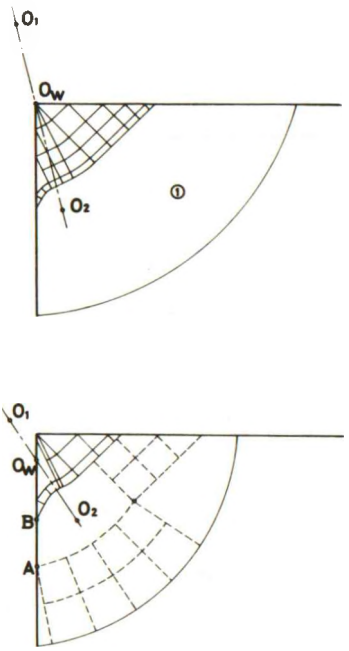

Fig. 53 K: Rupture Figures AsBfWPR (LsZ). Secondary Rupture Figure in the Rigid Body.

In the general case the upper rupture figure will be one of the types shown in Fig. 53 J (except Aw).

In Fig. 53 K O_w is the rotation point for the wall (or the upper wall part); O_1 is the rotation point for the moving rigid body (No. 1) of clay (possibly also for the lower wall part if a yield hinge develops), and O_2 is the rotation point for the relative movement between the body No. 1 and the wall (the upper wall part). If there is a yield hinge, its position (i.e. ρ_2) and ρ_1 should be assumed to be known. This determines the rupture figure if no sliding is assumed to take place between the body No. 1 and the wall. Else λ_1 must be assumed from which λ_2 is given. This parameter must be determined by the equation of vertical equilibrium for the body No. 1 (or the entire clay domain above the line rupture).

On the other hand, if the lower wall part is out of contact with the clay ρ_1, ρ_2 and λ_1 must be assumed beforehand, to be determined by all three equilibrium equations for the body No. 1. It is seen that rupture figures of this type are simpler to calculate than the figures of the type ZsL. The rigid body No. 1 may become unstable by a sort of shear failure (sketched in the lower Fig. 53 K). Correspondingly, the rigid body in a ZsL failure may become unstable by the development of a secondary rupture figure (interchange the full and dotted lines in the lower Fig. 53 K). Evidently, if the wall has a yield hinge (and no cracks develop) the points A and B should both coincide with the hinge. There might be a hinge somewhere between A and B and a crack from A to B, however.

An intermediate stage between a ZsL and an LsZ failure may therefore obtain, having a combined rupture figure with movements in both the upper and the lower rupture zones. One of the pure cases is again reached when ϵ becomes zero throughout the upper or the lower part of the figure. It is not difficult to investigate these stages by means of the method of rup-

ture figure loci, using f.inst. the approximation of Fig. 42 W together with the simple rupture figures of Fig. 53 J.

Example 53 c

The maximum height of a vertical unsupported slope in homogeneous clay with a horizontal surface can be found by means of a simple line rupture A (Fig. 53 L). Assuming first that $p = 0$, the condition is clearly that $F = 0$, $\zeta = \frac{1}{3}$, and $E = ch K_c = -\frac{1}{2}\gamma h^2$. The solution has been found by Brinch Hansen [1953]. From the table of results for line ruptures (par. 531 in the cited work) it follows that for a smooth wall ($c_a = 0$) with $\rho = 2.207$ ($\alpha = 15°$, $\omega = 47.6°$, i.e. $\lambda = \rho \tan(\omega - \alpha) = 1.411$) we have $\zeta = 0.333$ and $\kappa = K_c = -1.916$. Therefore:

$$\frac{\gamma h}{c} = -2\kappa = 3.832 \tag{5327}$$

If the surface load is p we must have correspondingly:

$$-K_c = \frac{1}{2}\frac{\gamma h}{c} + \frac{p}{c}$$

and (5328)

$$-\zeta K_c = \frac{1}{6}\frac{\gamma h}{c} + \frac{1}{2}\frac{p}{c}$$

so that:

$$\frac{\gamma h}{c} = -12\left(\frac{1}{2} - \zeta\right) K_c$$

$$\frac{p}{c} = -6\left(\zeta - \frac{1}{3}\right) K_c \tag{5329}$$

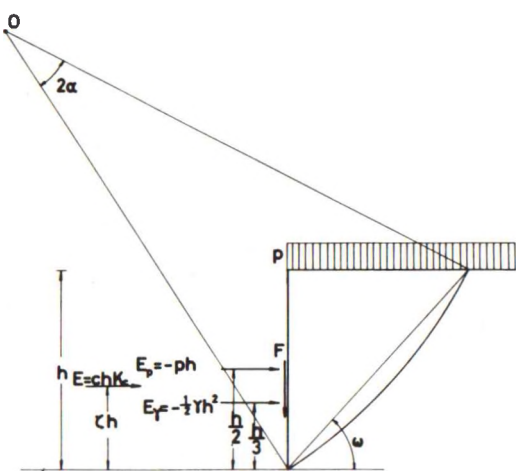

Fig. 53 L: A Vertical Slope Investigated By a Single Line Rupture.

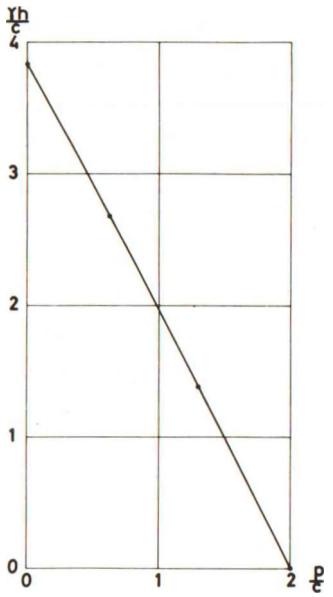

Fig. 53 M: Failure Combinations for the Parameters $\frac{p}{c}$ and $\frac{\gamma h}{c}$ of a Vertical Slope.

The curve corresponding to these parameter sets for different values of ζ ($2.2 \leq \rho \leq \infty$) is shown on Fig. 53 M. If the point corresponding to the parameters $\frac{\gamma h}{c}$ and $\frac{p}{c}$ for any given slope is located below this curve the slope is stable, and a possible support will receive no active earth pressure (but possibly a water pressure if cracks are formed, and are filled by rain water). On the other hand, if the point is above the curve on Fig. 53 M the slope must be supported, f. inst. by a retaining wall.

If the rotation point for a retaining wall in such a case is assumed to be known (or estimated, to be determined later by the investigation of the bearing capacity problem) we have the classical earth pressure problem with a partly unsupported earth front. It can be solved in several different ways, assuming in all cases that cracks will only form along the wall, not in the interior of the clay domain (since the theory of plasticity for cracked materials, i.e. materials with an additional failure condition: $\sigma_3 \geq \sigma_t$, is outside the scope of the present work).

1. The simplest thing to do is to calculate an earth pressure distribution by means of an ordinary simple rupture figure. Negative earth pressures, and corresponding adhesion stresses are then neglected.

2. Brinch Hansen's method may be used for a supposed wall with a yield hinge. The upper wall part is assumed perfectly smooth, and for this part ρ is determined, together with the position of the hinge, by the conditions that K_c and $K_c \zeta$ shall both be identically zero (in the final solution; when corrected surface loadings are used the two quantities shall correspond to an earth pressure distribution with $e = -\gamma z$, $f = 0$, where z is the depth under the level at which $K = 0$, cf. (2305)). The lower wall part moves as the real retaining wall, and the earth pressures on this part are the required actions

on the wall. The method has the disadvantage that it is in principle only developed for so-called normal rotations ($\lambda = 0$). This condition is not as a rule satisfied for retaining walls.

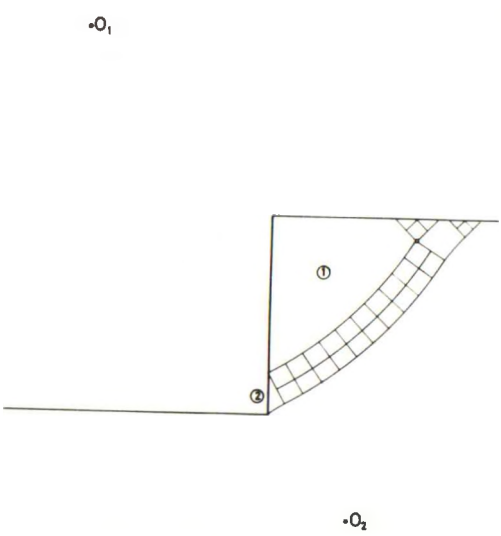

Fig. 53 N: Approximate Solution for a Partly Supported Vertical Slope.

3. Finally, one may use a ZsL rupture figure (Fig. 53 N), based on the previously discussed principles. Although simple the rupture figure has at least 4 parameters (f. inst. ρ and λ for O_1, and the width and centre angle for the arc zone). If the lower rigid body is sliding along the wall we have one further parameter (λ for O_2). The rupture figure can therefore in practice only be calculated on a computer. By the method of developing rupture figures a possible solution may be obtained with at least 7 free parameters (Fig. 43 I-J).

There is no special problem in the preparation of a computer program for the cases shown in Fig. 53 N and K, the latter one of which will also cover the cases with high values of ρ for the wall. This is a typical example of a problem where it might be useful to express the result of a computer calculation in the form of a simplified rule, f. inst. a corrected version of the method No. 1 indicated above, for future practical use.

534 Interacting Walls

Problems with interacting walls may obtain in several different types. They can be divided roughly into weak interactions, where only the movement parameters for the walls are interconnected, and strong interactions, when the individual rupture figures fuse into combined rupture figures.

For example, consider the cofferdam shown in Fig. 53 O. If a state with a low water table on both sides of the cofferdam is considered we have a case of simultaneous active earth pressures on both walls.

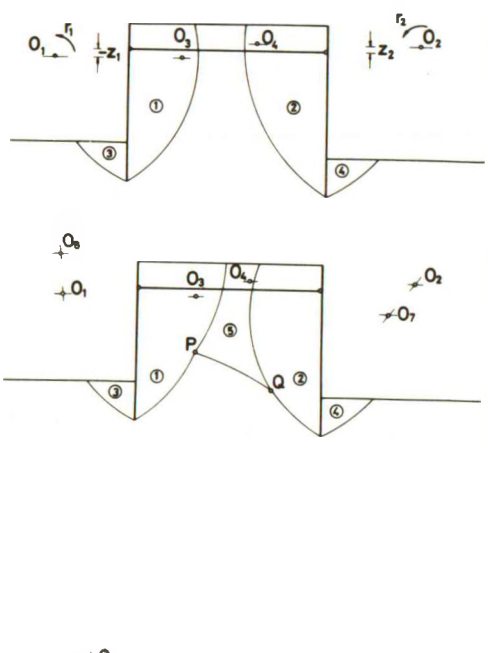

Fig. 53 O: Interacting Rupture Figures for the Earth Pressures on the Walls of a Cofferdam (Drawdown Case). Mutual Anchoring and Integrated Rupture Figure with Line Ruptures.

If the walls are sufficiently far apart the interaction between the walls only operate by the fact that the tie rod may translate instead of remaining fixed. Thus, in the rupture figures shown in the first Fig. 53 O the rotation points for the line ruptures need not be located in the tie rod level. The differences in height, z_1 and z_2, should be connected with the rotations, r_1 and r_2 (having different signs), so that the translation of the tie rod is a unique quantity. Thus,

$$r_1 z_1 = r_2 z_2 \qquad (5330)$$

so that z_1 and z_2 should also have different signs.

It is seen that for the rupture figure we have 6 parameters (f. inst. ρ, λ for O_1 and O_2 and λ for O_3 and O_4; by virtue of (5330) this also determines the ratio r_1/r_2). Since we have a quasi-possible solution they may be determined by the 4 equations of vertical equilibrium for the bodies No. 1-4, and by the 2 equations of moment and horizontal equilibrium for the collection of moving rigid bodies (i. e. 2 equations to the effect that the anchor force shall be the same for the two walls, and shall be located at the same level; the condition (5330) ascertains that this will be the tie rod level).

If the width of the cofferdam is decreased the rigid body between No. 1 and 2 will become unstable. As a first approximation a combined rupture figure like the one shown in the second Fig. 53 O may then be used. It has 10 parameters (f. inst. ρ, λ for O_1, O_2, and O_5; λ for O_3 and O_4; and ρ for O_6 and O_7). They determine all ratios between the rotations so they are subject to the condition (5330). The remaining 9 parameters are determined by the 6 conditions mentioned above plus the 3 equilibrium conditions for the rigid body No. 5.

In the symmetrical case the velocity fields of two symmetric rupture figures may be superimposed, and corresponding approximations may be used in nearly symmetrical cases. However, a better approximation is obtained, especially if the walls are brought still closer together, when a part of the system of line ruptures in Fig. 53 O is replaced by a closed rupture zone. This is because in the extreme case with a narrow cofferdam a sort of squeezing zone is developed between the walls, and squeezing zones are not easily represented by systems of line ruptures.

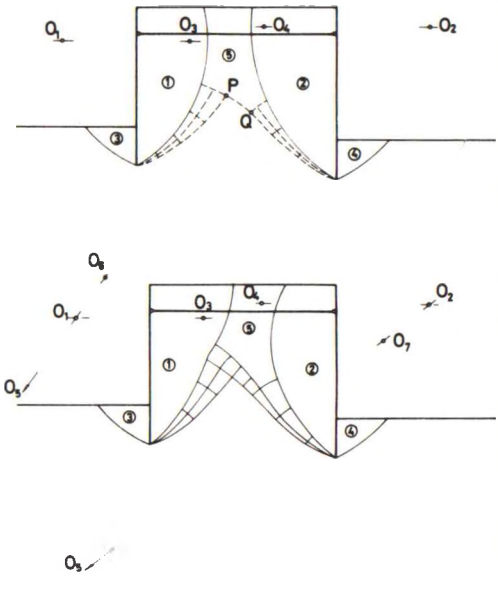

Fig. 53 P: Alternative Solutions with Closed Rupture Zones.

The secondary rupture figure corresponding to a state of failure in the unmoving rigid body is shown in the first Fig. 53 P. The line rupture PQ corresponds to the same construction in Fig. 53 O, but it is seen that the radial zones leave a greater scope for the development of the rupture figure. In this state the rupture figure is determined by 2 parameters, f. inst. a, b (or λ, μ) for the point Q, the radial zone to the right of Q being determined geometrically by the line rupture and the singular point at the foot point of the wall. The curvature of the line rupture PQ is another parameter that defines the tangent point P to the other radial zone. It is determined by the stress condition between the two parts of the rupture figure. The two parameters and the critical width of the cofferdam are determined by the 3 equilibrium equations for the rigid body No. 5.

When the width of the cofferdam is still further decreased the movements in the secondary rupture figure increase from zero, and the rupture figure develops into forms like the one shown in the second Fig. 53 P. Its similarity to Fig. 53 O is evident. The closed double radial zone construction has 9 initial parameters (3 differences in a, and 3 in b, together with 2 ratios between rotations and 1 ratio between sliding velocities). The position, scale, and orientation of the zone corresponding to each parameter set are

determined by the known positions of the two vertex points, after which the rotation points O_1, O_2, O_5, and, after construction of the line ruptures, O_6 and O_7 are also known. 2 further parameters (λ for O_3 and O_4) finishes the construction of the rupture figure. It is quasi-possible since we have also 11 conditions (4 equations of vertical equilibrium, 1 of horizontal, and 1 of moments, plus the condition (5330) for the bodies No. 1-4; 3 equilibrium equations for No. 5; and 1 stress condition between the two line ruptures).

If the width of the cofferdam is further decreased, which case will hardly become actual in practice, one or both of the rigid bodies No. 1 and 2 may be sheared by an arc zone extending from the radial zones to the wall, and being continued until the clay surface by a reflected arc zone ending in a surface zone complex. This construction, that can be approximated by two line ruptures, may for very narrow cofferdams develop into extremely complicated patterns of rupture zones, the arc zones being reflected several times back and forth between the walls.

However, rupture figures of this type have no great practical use. The examples shown in Fig. 53 O-P will probably be all that is needed in practice. Interactions between other types of active, or passive, earth pressures will follow the same principles. Thus, the general type of failure with a double radial zone may also be used if the simple line ruptures are replaced by other types of rupture figures, f. inst. the ones shown in Fig. 53 K or N corresponding to partly unsupported earth fronts.

Since the interaction between the rupture figures starts with a failure in the unmoving rigid body, and later takes the character of a squeezing phenomenon, the overall safety as a function of the distance between the walls will first decrease and will then increase again, for decreasing distances. Therefore, one may define a critical distance between the walls for which the overall safety of the construction is a minimum. For most constructions of this kind the design shall also take one-sided loading into account (f. inst. a water pressure for a cofferdam). Therefore, the small widths cannot be used, and the width that gives an economic optimum design may actually be in the neighbourhood of the point for which the safety against the two-sided failure is a minimum.

The one-sided failure corresponds to an interaction between a passive earth pressure on one side and an active earth pressure on the other side, but in practice the purely passive pressure will rarely develop, so it will usually be a combination between a stability and an active earth pressure problem. The stability problem for an anchor wall to a sheet pile wall

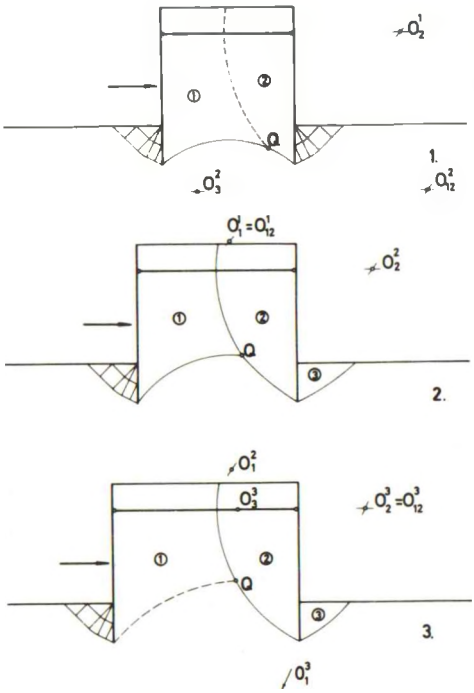

Fig. 53 Q: Simultaneous Stability and Earth Pressure Problem. Relative Movement in Earth Pressure Figure Zero, Finite, or Infinite (Case No. Indicated as Superscripts for Rotation Points).

(Fig. 52 E) belongs to this type. The application to the cofferdam problem is shown in Fig. 53 Q in three versions, dependent on whether the ratio between the movements in the earth pressure and the stability failure is assumed zero (No. 1), finite (No. 2), or infinite (No. 3). In such cases the overall safety will of course decrease monotonically for decreasing width of the cofferdam. The case No. 1 will probably always represent the economical optimum in practice.

If the passive rupture figure is also developed the connecting stability failure will have a branch point Q at both end points (cf. Fig. 52 E). The corresponding possible solutions in this and in the preceding case will have multiple radial zones (Sec. 432), possibly connected by line ruptures, and possibly continued by arc zones if the walls are designed with yield hinges. It is seen that we may have rather complicated rupture figures as we also had in the corresponding stability problems. However, this cannot be avoided unless one either designs the construction so that some of the rupture figure parts are only on the verge of failure, or makes the usual approximation (on the unsafe side) implying that a number of mutually inconsistent states of stress exist simultaneously in the soil.

54 BEARING CAPACITY PROBLEMS

541 Simple Foundations

Simple foundation problems, i.e. problems that can be solved by simple rupture figures, may be considered as a special class of simple earth pressure problems (with θ about $-\frac{\pi}{2}$). In practice they will usually fall into one of three possible classes:

1. Problems that can be solved by statically determined rupture zones connected by transition points. An example of this, containing interacting foundations, has been given in Ex. 42 b (Fig. 42 H). The classical Prandtl rupture figure (Fig. 31 G) shows the simplest possible case. A more complicated example is given by the squeezing problem (right hand side of Fig. 43 R).
2. Problems that can be solved by the combination of such zones with line ruptures. Since the foundation will usually be perfectly rough, the composite rupture figures will frequently be very simple XfPR-constructions, especially if it is assumed that the foundation can lift away from the clay surface. In certain cases other types may also obtain, however. Thus, Aw or wA are frequent under block foundations that are overturned (combined with AaWPR for the earth pressures on the vertical faces).
3. Other simple rupture figures, f. inst. the simple AfPfA (or AfCfA) rupture figure, systems of line ruptures, and kinematically determined rupture zones (Fig. 24 H, 34 M-N, 42 X, and 42 AC-AD).

As an example of a problem with a simple rupture figure, and a number of parameters sufficiently small so that a final representation of the solution can be given, consider the strip foundation shown in Fig. 54 A. It is placed on a horizontal clay surface with one edge on the top of a rectilinear slope. The surface loading on the slope (if any) is assumed to be constant, and the unit weight of the clay is taken to be negligible.

The foundation may be loaded to failure in several different ways. For simplicity it is first assumed that the line of attack is known for the resulting force P on the foundation, i.e. that a and i are known. The problem is therefore to determine P as a function of the parameters c, B, a (or a_k), i,

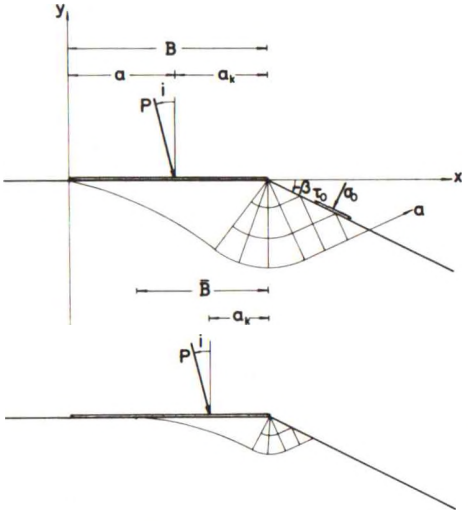

Fig. 54 A: Simple One-Sided Bearing Capacity Problem Solved by the Rupture Figure XfPR or wXfPR.

β, σ_o, and τ_o. It is assumed that a $\geq \frac{B}{2}$, and i $\geq$ 0, and that the foundation is perfectly rough (c_a = c).

Under these assumptions the rupture figure will be the simple type XfPR shown on Fig. 54 A, with straight b-lines and straight or circular a-lines. Two possible cases are shown on the figure, the first one being the ordinary XfPR rupture figure. Here the movement component u_n is positive along the whole foundation width. This case obtains for small excentricities of the load. For a certain value of a, u_n becomes zero at the edge furthest from the load. If a is increased above this value we may, instead of using rupture figures covering the whole foundation, assume that for negative values of u_n a crack will appear between the foundation and the clay. In this way the second case is obtained. Under this assumption the rupture figure is still of the type XfPR, but only a part of the foundation, of the width $\bar{B}$, is in contact with the clay. For kinematical reasons the underside of the foundation must then be a tangent to the line rupture.

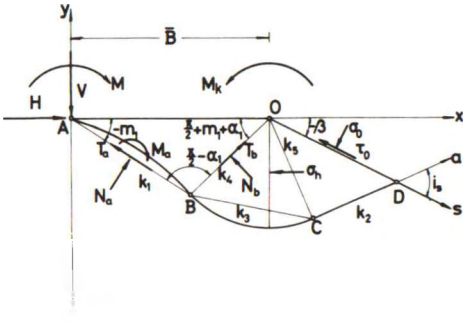

Fig. 54 B: Notations.

In both cases the symbols indicated on Fig. 54 B can be used. Notice that the effective width $\bar{B}$ of the foundation is always taken as the unit length. The unknown quantities which define the rupture figure may then be either m_1 and α_1 ($\bar{B}$ = B) or m_1 = α_1 and $\bar{B}$/B ($\bar{B}$ < B).

By simple geometry we find:

$$\frac{k_1}{\bar{B}} = \frac{\cos(m_1 + \alpha_1)}{\cos \alpha_1} \qquad (5401)$$

$$\frac{k_4}{\bar{B}} = -\frac{\sin m_1}{\cos \alpha_1}$$

From (3284-5) we obtain, cf. Fig. 32Q:

$$\frac{N_a}{c\bar{B}} = \frac{k_1}{\bar{B}}\left[N^z(\alpha_1) + \frac{\sigma_h}{c} - 2(m_1 + \alpha_1)\right]$$

$$\frac{T_a}{c\bar{B}} = \frac{k_1}{\bar{B}} T^z(\alpha_1) \qquad (5402)$$

$$\frac{M_a}{c\bar{B}^2} = \left(\frac{k_1}{\bar{B}}\right)^2 M^z(\alpha_1)$$

and

$$\frac{N_b}{c\bar{B}} = \frac{k_4}{\bar{B}}\left[\frac{\sigma_h}{c} - 2(m_1 + \alpha_1)\right] \qquad (5403)$$

$$\frac{T_b}{c\bar{B}} = \frac{k_4}{\bar{B}}$$

α_4 being equal to zero.

In (5402-3) σ_h is the normal stress acting on the vertical slip line through O. It is independent of m_1 and α_1; from (3303-6) we find, using:

$$i_s = \arctan\sqrt{\frac{c + \tau_o}{c - \tau_o}} \qquad (5404)$$

that

$$\frac{\sigma_h}{c} = \frac{\sigma_o}{c} + 2 i_s + \sin 2 i_s + 2\beta \qquad (5405)$$

Isolating the terms which depend on m_1 and α_1 we define:

$$\frac{V_o}{c\bar{B}} = \frac{k_1}{\bar{B}}\left[N^z(\alpha_1)\cos m_1 - T^z(\alpha_1)\sin m_1\right] + \frac{k_4}{\bar{B}}\cos(m_1 + \alpha_1) - 2(m_1 + \alpha_1)$$

$$\frac{H_o}{c\bar{B}} = \frac{k_1}{\bar{B}}\left[N^z(\alpha_1)\sin m_1 + T^z(\alpha_1)\cos m_1\right] + \frac{k_4}{\bar{B}}\sin(m_1 + \alpha_1) \qquad (5406)$$

$$\frac{M_o}{c\bar{B}^2} = \frac{k_1}{\bar{B}}\left[\frac{k_1}{\bar{B}}\left(-M^z(\alpha_1) + \frac{1}{2}N^z(\alpha_1)\right) - \sin m_1\right] - (m_1 + \alpha_1)$$

and

$$\frac{M_{ko}}{c\bar{B}^2} = \frac{V_o}{c\bar{B}} - \frac{M_o}{c\bar{B}^2} \tag{5407}$$

The final quantities are then found from:

$$\frac{V}{c\bar{B}} = \frac{V_o}{c\bar{B}} + \frac{\sigma_h}{c}$$

$$\frac{H}{c\bar{B}} = \frac{H_o}{c\bar{B}} \tag{5408}$$

$$\frac{M}{c\bar{B}^2} = \frac{M_o}{c\bar{B}^2} + \frac{1}{2}\frac{\sigma_h}{c}$$

and

$$\frac{M_k}{c\bar{B}^2} = \frac{M_{ko}}{c\bar{B}^2} + \frac{1}{2}\frac{\sigma_h}{c}$$

The two unknown quantities are determined by the conditions that

$$\frac{V}{c\bar{B}} \sin i - \frac{H}{c\bar{B}} \cos i = 0$$

and (5409)

$$\frac{V}{c\bar{B}} \frac{a_k}{B} - \frac{M_k}{c\bar{B}^2} \frac{\bar{B}}{B} = 0$$

The fact that the parameters can be separated as shown in (5408) makes it possible to represent the solution to the problems in a closed form. This can be done by representing the quantities $\frac{H_o}{c\bar{B}}$ and $\frac{M_{ko}}{c\bar{B}^2}$ as functions of $\frac{V_o}{c\bar{B}}$ with α_1 and m_1 as parameters as shown in Fig. 54C. Notice that $m_1 \leq \alpha_1 \leq 0$, and $m_{10} \leq m_1 \leq 0$, where m_{10} is the value (dependent on α_1) for which $H_o = 0$. For $m_1 < \alpha_1$ we always have $\bar{B} = B$.

For the two special cases $\alpha_1 = 0$ and $\alpha_1 = m_1$ the formulae (5402) become simple expressions so that (5409) can be satisfied by a simple interpolation. Thus, for $\alpha_1 = 0$ (a straight line rupture) we have $N^z = M^z = 0$, $T^z = 1$. Inserting also (5401) we find:

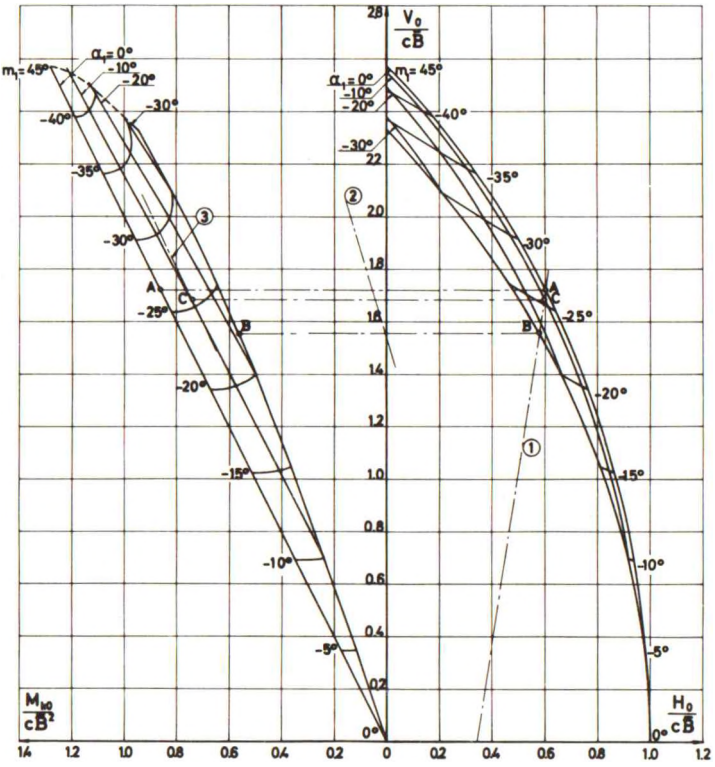

Fig. 54C: Graphical Solution to the Simple One-Sided Bearing Capacity Problem.

$$\frac{V_o}{cB} = -2\,m_1 - \sin 2\,m_1$$

$$\frac{H_o}{cB} = \cos 2\,m_1 \qquad (5410)$$

$$\frac{M_o}{cB^2} = \frac{M_{ko}}{cB^2} = -m_1 - \frac{1}{2}\sin 2\,m_1$$

For $\alpha_1 = m_1$ we find by inserting the expressions (3285) and contracting:

$$\frac{V_o}{cB} = -N^z\,(2\,\alpha_1)$$

$$\frac{H_o}{c\,\bar{B}} = T^z\,(2\,\alpha_1)$$

$$\frac{M_o}{c\,\bar{B}^2} = -2\,M^z\,(2\,\alpha_1) \qquad (5411)$$

so that

$$\frac{M_{ko}}{c\,\bar{B}^2} = 2\,M^z\,(2\,\alpha_1) - N^z\,(2\,\alpha_1)$$

For other cases the formulae (5401-3) and (5406) must be used directly.

The diagram Fig. 54C is used as follows to solve a problem represented by the conditions (5409).

1. First the basic stress σ_h is found from (5404-5).
2. From the point $(0, -\frac{\sigma_h}{c})$ in the coordinate system $\frac{H_o}{c\,\bar{B}}$, $\frac{V_o}{c\,\bar{B}}$ a line is drawn with the inclination i to the $\frac{V_o}{c\bar{B}}$ - axis (measured in the negative direction of rotations in this coordinate system, cf. the line No. 1 in the diagram). This line represents the first condition (5409).
3. From the point $(\frac{\sigma_h}{2c}, -\frac{\sigma_h}{c})$ another line (No. 2 or 3) is drawn with the inclination arc tan $\frac{a_k}{B}$ to the $\frac{V_o}{c\,\bar{B}}$ - axis (measured in the positive direction of rotations). This line represents the second condition (5409).
4. If $\frac{a_k}{\bar{B}} = \frac{1}{2}$ we can see directly from the left part of the diagram that $\alpha_1 = 0$. In the right part the intersection point between the line No. 1 and the outer boundary curve ($\alpha_1 = 0$) will therefore represent the solution (using also (5408)).
5. If the line does not intersect the curves in the left part (No. 2, $\frac{a_k}{\bar{B}}$ being too small) we have the second case of Fig. 54A, i.e. $\alpha_1 = m_1$ and $\bar{B} < B$. In the right part the intersection point with the inner boundary curve ($\alpha_1 = m_1$) will therefore give the solution. The corresponding point on the left part (same value of $\frac{V_o}{c\,\bar{B}}$) determines $\frac{a_k}{\bar{B}}$ as the ratio $(\frac{M_{ko}}{c\,\bar{B}^2} + \frac{\sigma_h}{2c})/(\frac{V_o}{c\,\bar{B}} + \frac{\sigma_h}{c})$, so that $\frac{\bar{B}}{B}$ can be found as $\frac{a_k}{B} / \frac{a_k}{\bar{B}}$. In this way $\frac{V}{c\,B}$ and $\frac{H}{c\,B}$ are found.

6. If, finally, the line (No. 3) passes through the curves in the left diagram we have the case No. 1 of Fig. 54 A ($\overline{B} = B$). The solution must then be found by trial and error, seeking the value of $\frac{V_o}{c\,\overline{B}}$ ($= \frac{V_o}{c\,\overline{B}}$) which corresponds to the same value of α_1 on the two lines No. 1 and 3.

Alternatively the formulae (5410), (5411), or (5401-3) and (5406) may be used for direct numerical calculations. In the first two cases a single interpolation in m_1 or α_1 is necessary, but in the last case both m_1 and α_1 must be varied until both conditions (5409) are satisfied.

This is certainly feasible, but for all practical purposes the semi-graphical method indicated above will probably be accurate enough. For a rapid orientation the same approximation may be used as in the simple bearing capacity formula, cf. Brinch Hansen [1961]. A fictive foundation is here used, symmetrically situated in relation to the point of application for the force, i.e. $\frac{a_k}{\overline{B}}$ is always taken to be 0.5, so that α_1 is always zero.

Thus, taking $\overline{B} = 2\,a_k$ we may use (5408) and (5410) directly:

$$\frac{V}{c\,\overline{B}} = \frac{\sigma_h}{c} - 2\,m_1 - \sin 2\,m_1$$

$$\frac{H}{c\overline{B}} = \cos 2\,m_1 \qquad (5412)$$

This approximation is always on the safe side.

In the bearing capacity formula as indicated by Brinch Hansen [1961] (5412) is further simplified by expressing $\frac{V}{c\,\overline{B}}$ as an approximate function of $\frac{H}{c\overline{B}}$:

$$\frac{V}{c\,\overline{B}} = \frac{\sigma_h}{c} + (\frac{\pi}{2} + 1)\sqrt{1 - \frac{H}{c\,\overline{B}}} \qquad (5413)$$

This approximation to (5412) is remarkably good, and is a little further on the safe side. It is a question, however, whether it is in fact easier to use (5412) when the ratio H/V is given (and not just H). In the work cited above the formula (5413) is only used for $\beta = \tau_o = 0$ (and σ_o is termed q). It can then be written, $\frac{\sigma_h}{c}$ being in this case $\frac{\pi}{2} + 1 + \frac{q}{c}$:

$$\frac{V}{c\,\overline{B}} = N_c\,i_c + \frac{q}{c}$$

where

$$N_c = \pi + 2 \tag{5414}$$

and

$$i_c = \frac{1}{2} + \frac{1}{2}\sqrt{1 - \frac{H}{c\,\overline{B}}}$$

By (5405) it is indicated how this formula must be corrected for more general surface conditions. It follows that a combined slope and inclination factor t_c (say) may be defined. We find:

$$\frac{V}{c\,\overline{B}} = N_c\, t_c + \frac{\sigma_o}{c}$$

with

$$N_c = \pi + 2 \tag{5415}$$

and

$$t_c = \frac{2\, i_s + \sin 2\, i_s + 2\beta}{\pi + 2} + \frac{1}{2}\sqrt{1 - \frac{H}{c\,\overline{B}}}$$

The lines No. 1-3 in Fig. 54C are drawn corresponding to a problem with $\beta = -15^o$ and a vertical surface loading $q = 0.364\,c$; to this corresponds a value of 2.301 for $\frac{\sigma_h}{c}$.

Assuming the two other parameters to be $\frac{H}{V} = 0.15$ (line No. 1) and $\frac{a}{\overline{B}} = 0.5$ (points A), 0.7 (points B), or 0.525 (points C) we find:

1. $\frac{a}{\overline{B}} = 0.5$, points A:

From the curve, or directly from (5410), we find ($B = \overline{B}$):

$$m_1 = -26.5^o, \quad \frac{V_o}{c\,\overline{B}} = 1.721, \quad \frac{H_o}{c\,\overline{B}} = 0.603$$

i.e. according to (5408):

$$\frac{V}{c\,\overline{B}} = 4.022 \tag{5416}$$

$$\frac{H}{c\,\overline{B}} = 0.603$$

The formula (5413) gives:

$$\frac{V}{c\,\overline{B}} = 3.944 \tag{5417}$$

$$\frac{H}{c\,\overline{B}} = 0.592$$

which is about 2% on the safe side.

2. $\frac{a}{\overline{B}} = 0.7$, points B:

We have $\frac{a_k}{\overline{B}} = 0.3$ (line No. 2). It is seen that $\overline{B} < B$ so that $\alpha_1 = m_1$. From the curve, or directly from (5411) we find:

$$m_1 = \alpha_1 = -22.3^\circ, \quad \frac{V_o}{c\overline{B}} = 1.557, \quad \frac{H_o}{c\overline{B}} = 0.579, \quad \frac{M_{ko}}{c\overline{B}^2} = 0.565$$

so that:

$$\frac{V}{c\overline{B}} = 3.858, \quad \frac{H}{c\overline{B}} = 0.579, \quad \frac{M_k}{c\overline{B}^2} = 1.716, \text{ and } \frac{a_k}{\overline{B}} = 0.445$$

This gives:

$$\frac{\overline{B}}{B} = 0.675$$

$$\frac{V}{c\overline{B}} = 2.602 \qquad (5418)$$

$$\frac{H}{c\overline{B}} = 0.390$$

If the approximation (5412) is used we must take the results (5416) together with the value $\frac{\overline{B}}{B} = 0.600$. This gives:

$$\frac{V}{c\overline{B}} = 2.413$$

$$(5419)$$

$$\frac{H}{c\overline{B}} = 0.362$$

which is about 7% below the values of (5418).

The approximation (5413) gives, using (5417) together with $\frac{\overline{B}}{B} = 0.600$:

$$\frac{V}{c\overline{B}} = 2.367$$

$$(5420)$$

$$\frac{H}{c\overline{B}} = 0.355$$

which is about 9% below the values of (5418).

From this example it is seen that for the assumed conditions the case No. 2 on Fig. 54 A applies for all values of $\frac{a}{B}$ above 0.555, i.e. even for very small excentricities of the foundation load.

3. $\frac{a}{\overline{B}} = 0.525$, points C:

By interpolation between the curves we find $a \sim -11^\circ$, $m_1 \sim -25.4^\circ$ (line No. 3, $\overline{B} = B$), and:

$$\frac{V_o}{c\overline{B}} = 1.684, \quad \frac{H_o}{c\overline{B}} = 0.598$$

This gives directly:

$$\frac{V}{c\overline{B}} = 3.985$$

$$\frac{H}{c\overline{B}} = 0.598 \qquad (5421)$$

The approximations (5412) and (5413) give, respectively, with $\frac{\overline{B}}{B} = 0.950$:

$$\frac{V}{c\overline{B}} = 3.821$$

$$\frac{H}{c\overline{B}} = 0.573 \qquad (5422)$$

which is about 4% below the values (5421), and:

$$\frac{V}{c\overline{B}} = 3.747$$

$$\frac{H}{c\overline{B}} = 0.562 \qquad (5423)$$

which is about 6% below the values (5421).

Evidently Fig. 54C, or the approximate formulae (5412-3) can also be used for more general forces in controlled stress. In controlled strain, if there is more than one rod connection to the foundation the corresponding movement conditions can be interpreted as conditions on the values of α_1 and m_1. Thus, if w_x, w_y, and r_z are given or estimated (in the coordinate system of Fig. 54A; assuming $w_x < 0$, $r_z \leq 0$) we find:

1. If $r_z = 0$, then $\alpha_1 = 0$, $m_1 = \text{arc tan } (\frac{w_y}{w_x})$; else $\rho = \frac{w_y}{r_z}$, $\lambda = -\frac{w_x}{r_z}$.

2. If $\rho \geq 0$ then $\overline{B} = B - \rho$; $\alpha_1 = m_1 = \frac{1}{2} \text{arc tan } (\frac{\overline{B}}{\lambda})$.

3. (General case): putting $v_1 = \text{arc tan } (\frac{-\rho}{\lambda})$ and $v_2 = \text{arc tan } (\frac{B-\rho}{\lambda})$:
$\alpha_1 = \frac{v_2 - v_1}{2}$ and $m_1 = \frac{v_2 + v_1}{2}$.

In a computer program, instead of calculating the terms in (5402-3) and (5406-8) in order to satisfy (5409) or the corresponding conditions for a more general system of forces and/or restraints, it may be simpler to use the energy method, the numerical operations being then simpler. Assuming a constant reference velocity w_o to be given we may find the sliding velocity u_f along the line rupture from the formulae:

$$\frac{u_f}{w_o} = -\frac{w_x}{w_o}\cos(m_1 - \alpha_1) - \frac{w_y}{w_o}\sin(m_1 - \alpha_1) \quad (\text{if } \alpha_1 \neq m_1)$$
$$= -\frac{w_x}{w_o} \quad (\text{if } \alpha_1 = m_1) \tag{5424}$$

In the latter case we also find:

$$\frac{\bar{B}}{B} = 1 - \frac{w_y}{Br_z} \tag{5425}$$

We then have, using also (5401) and (5405):

$$\frac{W_r}{cw_oB} = \frac{P_r}{cB}\frac{d_r}{w_o}$$
$$= \frac{\bar{B}}{B}\left\{\frac{u_f}{w_o}\frac{k_1}{\bar{B}}\frac{\alpha_1}{\sin\alpha_1} + \left(\frac{u_f}{w_o} - \frac{1}{2}\frac{k_4}{\bar{B}}\frac{Br_z}{w_o}\frac{\bar{B}}{B}\right)\frac{k_4}{\bar{B}}\left[\frac{\sigma_h}{c} - 2(m_1 + \alpha_1)\right]\right\}$$
$$-\sum\frac{Q_i}{cB}\frac{w_i}{w_o} \tag{5426}$$

The limit value of $\frac{\alpha_1}{\sin\alpha_1}$ being 1 for $\alpha_1 \to 0$.

In some cases with shallow foundation and possibly irregular surface conditions the simple AfCfA rupture figure, Fig. 43 E, Ex. 43 a, can be used (or its two-sided variant where the line rupture under the foundation is replaced by another CfA-construction). If there are no movement restraints on the foundation we have now 4 free parameters (8 in the two-sided case, subject to 1 stress condition) against the 2 considered in this section. Because of the simple calculation the problem may still be considered as simple, however. The same is true for systems of 3 or 5 line ruptures (Ex. 34 a), or kinematically determined rupture zones (Sec. 426, to be used under the effective foundation width $\bar{B}$, cf. the lower Fig. 54 A).

542 Complex Foundation Problems

Bearing capacity problems of the types considered within the scope of the present work may exactly as earth pressure problems be complicated

because their rupture figure interact with other bearing capacity, earth pressure, or stability failures, because they are part of rupture figure complexes (Sec. 443), or because of special irregularities in the failure problem (f. inst. a stratified soil profile as in Fig. 43 R).

The problems obtained in this way are not radically different from those considered in the preceding sections, however. Since they are typically obtained in individual projects in practice, and the number of parameters does not permit of a general solution to be calculated beforehand, one should as a rule seek to obtain the solution by means of rupture figure types that can be used for arbitrary problem parameters. Thus, systems of line ruptures will frequently be as useful here as they are in general stability problems and in earth pressure problems with irregular surface conditions.

However, there are certain exceptions such as the block foundation shown in Fig. 54 D. The failure problem itself has only 3 parameters (the ratio width/depth of the foundation plus two quantities indicating the line of attack for the resulting loading), so in this case a general solution might be obtained and tabulated. There are in principle three different rupture figure types, two of which are shown in Fig. 54 D.

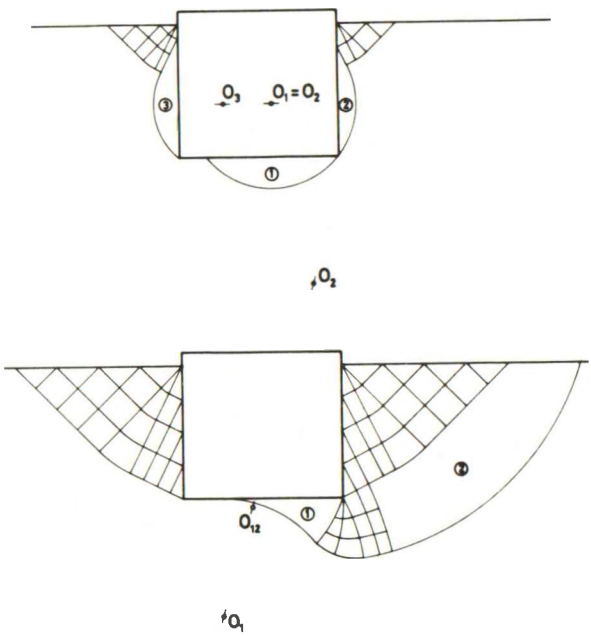

Fig. 54 D: Combined Earth Pressure and Bearing Capacity Failures for a Block Foundation.

In the first type the rotation point O_1 for the foundation is located somewhere in the foundation block itself. The two earth pressures are found by means of simple AaWPR-rupture figures, and a simple line rupture extends under the foundation. If the vertical faces are supposed to be partly unsupported, figures of the types shown in Fig. 53 J may have to be used instead (possibly with the introduction of a fourth parameter of the type $\frac{\gamma B}{c}$).

If the rotation point is below the foundation we have a combined earth pressure and bearing capacity rupture figure on the passive side of the foundation as shown in the lower Fig. 54 D, O_{12} being the point of relative rotation between the block and the rigid body No. 2. On the active side we may have an ordinary WPR-zone, but Fig. 53 N may also apply if the earth is partly unsupported. If $\frac{\gamma B}{c}$ is small enough the whole active face may crack away from the clay.

The third case (not shown) has two-sided bearing capacity failures with only a small (possibly vanishing) interaction between the vertical faces and the rigid bodies of clay. If the clay is assumed to be firmly adhering to the vertical faces a quasi-possible solution may be obtained by a rupture figure much like the one shown in Fig. 44 J (the clay surface replacing the symmetry line EF of this figure). Some cases of minor importance exist where the block is pulled out of the soil and where no bearing capacity failure is at all developed. The whole problem, two limiting cases of which are a simple surface foundation on one hand and a free sheet wall on the other, could clearly form the subject of a useful and sufficiently well defined investigation; f. inst. limited to the cases that are most frequently met with in practice:

1. An overturning (first Fig. 54 D) of the foundation due to a force resulting from its weight and an active force (horizontal or inclined, f. inst. a wind pressure or a pull of a cable) on a structure placed upon the foundation.

2. A bearing capacity failure (second Fig. 54 D or the corresponding two-sided rupture figure) when the active force is relatively large, vertical or somewhat inclined, and with an excentricity less than or of the same order of magnitude as the width of the foundation.

3. An upward pull of the foundation, acting as an anchor block. In this case the problem will frequently be to design the block so that its movement is a pure translation.

In the most general case, in which no restrictions are put on the possible lines of attack for the resulting force, one would have to consider all types of bearing capacity and (simple) earth pressure rupture figures together with a number of possible modes of combination. Large parts of the resulting very comprehensive program would rarely be used in practice, however.

If foundations are placed on or in clay surfaces behind earth pressure resisting structures we have a special case of interacting bearing capacity and earth pressure problems (usually in active state). They are very similar to earth pressure problems with discontinuous surface loadings (Fig. 53 D-F). The main difference is that now the load is transmitted to the clay through an external rigid body, whose width is determined by economic considerations. Therefore the bearing capacity failure will be fully or partly developed, depending on the chosen ratio between movements in the bearing capacity and the earth pressure failure.

If this ratio is chosen near infinity, which will frequently be required by the nature of the problem (small dimensions of the foundation and small settlements in the actual state due to the movement of the wall) a rupture figure like the one shown in Fig. 54 E may obtain. It has a rotation point for the wall somewhere below the foot point. However, the rupture figure for the bearing capacity can equally well be combined with other types of movements for the wall. For example, a line rupture of the type A should be tangent to an a-line, possibly in the continued rupture zone below the two radial zones.

The rupture figure on Fig. 54 E is an open arc zone rupture and it will as such have a rather great number of zone elements. If the approximate minimax procedure of Sec. 532 is used it may be replaced by a system of line ruptures. This may not decrease the number of initial parameters very much, but it gives a simpler calculation of each rupture figure.

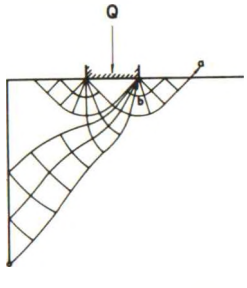

Fig. 54 E: Strip Foundation Behind a Retaining Wall.

In such combined problems as also in problems of bearing capacities combined with stabilities (the rupture figure shown in Fig. 52 B may be an example of this) it may be difficult to decide upon a satisfactory system of safeties (partial coefficients) that gives a continuous transition to the cases of

pure bearing capacity or pure earth pressure or stability. As a matter of fact it may be necessary to let the partial coefficient on the shear strength of the clay be a function of the chosen mode of failure. Such problems of policy are, however, considered to be outside the scope of the present work.

6 CONCLUSIONS

As a result of the investigation in the preceding chapters we may conclude that by the solution method of admissible solutions with possible rupture zones it is possible to construct rupture figures that are able to solve in principle all failure problems in practice that fall within the scope of the present work. Because of the flexibility of the method the solutions that are permissible under the method range from sometimes very simple and rough approximations to the mathematically correct solutions. It is therefore possible in each case to choose a solution that is neither too inaccurate nor too difficult to calculate, considering the actual need for accuracy against the cost of calculations.

The simplest calculations are in most cases obtained when the method of chord lengths is applied. This calculation method uses a modified integration by finite differences, utilizing the special geometrical properties of slip line nets in homogeneous clays. By a decrease of the step widths the method can give as accurate numerical results as required. In practice, however, all rupture zone elements should as a rule be bounded by single arcs.

However, despite the flexibility of the solution method and the simplicity of the calculation method some problems in soil mechanics are in themselves so complicated that the calculation work needed to obtain a solution cannot with certainty be kept within even rather wide limits. Such problems can therefore only be solved by means of a computer. In order to avoid duplicate programming work the most useful computer programs would be of the following types (in this order of preference): General types of rupture figures that can be used on arbitrary or at least very flexible problems, programs that develop and choose between rupture figures solving special classes of failure problems, and special programs that tabulate solutions to particular failure problems or parts of problems.

In this chapter the methods introduced in the present work are reviewed in some details, after which the general applicability of the methods to other types of failure problems and other materials is briefly discussed.

61 REVIEW OF METHODS

611 Solution Method

The solution method is based on the following facts.

1. The general assumptions indicated in Sec. 211 and more specifically in Sec. 213 (and Sec. 241-2) are sufficient, i.e. the mathematically correct solution to a failure problem, defined as in Sec. 212 and more specifically in Sec. 221-3, will be unique in the sense defined in Sec. 242. Thus, apart from certain possibilities of variations that are not important in practice they determine one definite rupture figure from which all necessary failure loads and restraint forces can be calculated.

2. For the so-called kinematically admissible solutions, defined as in Sec. 243 by a velocity field satisfying the condition of constant volume and agreeing with the given boundary movements, the work equation can be used. They are always on the unsafe side, and the mathematically correct solution is contained as a member, so the solution with a minimum work (for the chosen variable parameters) done by the prescribed movements shall always be used.

3. Any velocity field indicates a partitioning of the clay mass into rigid bodies that move without deformations, and rupture zones in which every soil element is deformed. If the local conditions are satisfied for all points in the rupture zones they will be possible, and the work equation can be expressed in terms of the works done by the forces acting upon the rigid bodies (Sec. 244). The condition of minimum work for a given rupture figure type can be expressed as a number, equal to the number of free parameters in the rupture figure, of combined equilibrium conditions for the collection of rigid bodies (Sec. 245), provided a special set of stress conditions are introduced at possible singular end points for line ruptures (Sec. 341-5). When the calculations are based on rupture figure types it is also a provision that the resulting extreme solution has a geometrically possible rupture figure. Solutions that are only quasi kinematically admissible ($\epsilon < 0$ somewhere in the zones) are permissible under the method, however.

4. If the number of free parameters in the rupture figure is great enough the equilibrium conditions for the rigid bodies can be used directly. The solution will then be quasi-possible (Sec. 246). It is possible if there are no singular points on the line ruptures. Whether it is correct depends on the stability of the assumed rigid bodies of clay, and on the kinematical possibility of the deformations in the zones.

5. Forces doing no work during the movement, also internal forces in adjacent structures, can in some cases be found directly by means of the stress distribution in the rupture figure. Sometimes this is not possible (Sec. 441), and at any rate they may be inaccurate if the solution is only admissible. By a special use of the work equation (Sec. 245) such forces may be obtained as derivatives of the deformation work corresponding to appropriate changes in the parameters of the problem. Such changes may have to violate the movement conditions of the failure problem, and if the solution is not at least quasi-possible the rupture figure should again be calculated by means of the extremum method for each change in the external parameters. This amounts to the calculation of a more general failure problem, choosing afterwards the original problem as a separate case (Ex. 53 a). In some cases the calculation work may be simplified by using this method in an approximate way (Sec. 532), replacing an external movement condition by an extremum condition for a force.

6. The stress distribution in rigid bodies of clay may be found as a limiting case by the construction of a secondary rupture figure inside the rigid bodies (Sec. 441). The same technique is used for the investigation of the statical possibility of the rupture figure (Sec. 442).

It should be noticed that the solution method presupposes one definite velocity field with an accompanying stress distribution to exist in the clay for any specific set of variable external parameters and design quantities, if such exist. Therefore, it may not be permissible to investigate alternative modes of failure separately for the same set of parameters, because they may correspond to stress distributions that cannot obtain simultaneously. If only line ruptures intersect, an admissible solution might obtain by the superposition of the corresponding velocity fields, but an intersection of rupture zones with line ruptures or with other zones is inconsistent with the

assumption of possible zones. Therefore, integrated rupture figures should, if necessary, be applied in such cases (but the design quantities may frequently be fixed so that parts of the rupture figures are only on the verge of failure, i.e. with zero relative movements).

For any given failure problem a rupture figure type must be chosen that represents the major features of the problem in a reasonable way and yet is simplified as much as is consistent with the required accuracy of the solution. If necessary one must start with an approximation, and after having investigated its kinematical and statical possibility one may repeat the calculations with an improved rupture figure (possibly after some preliminary calculations to see whether the improvement is worth the trouble, cf. Sec. 444). Alternatively the final rupture figure may be obtained by considering the changes in a known rupture figure imposed by a systematic change of the corresponding external parameters into the given ones (Sec. 511-4).

612 Calculation Methods

The numerical calculations of rupture figures permissible under the general solution method can be performed in a number of different ways. Thus, if the rupture zones, utilizing the special geometrical properties of the slip line net under the present assumptions (Sec. 311), are described by means of continuous functions (Sec. 311-4) one has the choice between a system of equivalent coordinates and velocity components ($\bar{x}$, $\bar{y}$, u, v, cf. Sec. 313-4) and a system of radii of curvature and rotation functions (R, S, F, G, cf. Sec. 312 and 314). The first mentioned set of functions is the best suited to the calculation of statically determined rupture zones. The second set is the best for closed zones with mixed boundary conditions. Either one of the function sets may be calculated by the method of Riemann integration (Sec. 322) or by an integration in finite steps (Sec. 323), after the boundary conditions for the zones have been assessed (Sec. 331-8).

However, the simplest calculations are obtained if the so-called method of chord lengths (Sec. 325) is applied. It presupposes a division of the slip line net into finite cells, the chords and centre angles of the strings being the objects of calculation. If the maximum centre angle is decreased until zero, the number of cells in a given zone will increase to infinity, and the net of cells will converge to the mathematically correct slip line net. Actually, for equal centre angles the method of chord lengths will be more accurate than the method of finite differences, so when a given accuracy is prescribed it will give the least work of calculation (Sec. 324).

The number of cells to use in any given rupture figure should of course be fixed with a view to the accuracy that can at all be obtained by the rupture figure (Sec. 412). If it defines only an approximate solution it would clearly be uneconomical to spend too much work in obtaining an illusory high accuracy in the calculation of the rupture zones. Therefore, in most cases in practice the cells in the slip line net would cover entire zone elements (domains with continuous radii of curvature).

On the other hand, in order to obtain a unique calculation result that can subsequently be checked, all numerical calculations performed on a given system of cells should in principle be accurate. Thus, round-off and truncation errors should be kept as small as possible, all geometrical, stress, and equilibrium conditions should be satisfied within the obtainable numerical accuracy, and if the minimum condition is not satisfied exactly it should at least be possible to demonstrate that the location and magnitude of the minimum is approximately known. Especially if forces doing no work during the movement are required it may be necessary to find partial derivatives to the deformation work in the point of (relative) minimum.

The method of chord lengths may be stated formally in a rigid system of notations (Sec. 325 and Sec. 331-8) that facilitates the administration of general types of rupture figures on a computer. For more closed calculation purposes in which all zone elements can be designated individually it is simpler to deduce the necessary formulae by direct geometrical reasoning in the physical plane and the hodograph plane.

In the general scheme of calculations (Sec. 434) a number of parameters for the rupture figure must be assumed initially in order to define the figure geometrically. The parameters must then be changed, possibly by trial and error, until the movement conditions are satisfied so that the figure defines an admissible velocity field. The work equation can now be used and any remaining parameters can be varied, subject to the condition that the rupture figure shall still be geometrically possible and kinematically admissible, until either the minimum solution has been found or all relevant stress and equilibrium conditions have been satisfied.

For certain types of rupture figures this process can be simplified f.inst. because of the fact that the figure is statically determined (Sec. 421), or the movement and equilibrium conditions can be interpreted in a simple geometrical way (Sec. 422-6), or the rupture zones are closed so that the movement conditions can be satisfied by a relatively simple method of solving linear equations (Sec. 431-3). In the general case (open rupture zones,

Sec. 434-5) it may lead to rather laborious calculations even if all zone elements are single cells. Therefore, a number of rupture figures can in practice only be calculated on a computer, and even if calculations by hand are possible it will frequently be more economical to use a computer.

Failure problems of the types considered in this work cannot therefore be expected to be solved in the course of normal engineering practice unless the solutions can be obtained by hand or by very simple programs. Most of the solutions would have to be developed in research work or, possibly, on very large jobs. For ordinary engineering purposes one would prefer to do one of the following things (in this order of preference).

1. Find the solution to the problem in question (possibly after some simplifications of the original problem) either directly tabulated, given in a graphical form, or expressed by more or less approximate formulae. The solution might be built up from partial solutions of this kind (treating f. inst. earth pressures and bearing capacities acting on the same structure separately). It is clearly a duty of research institutions to prepare and publish such basic solutions.

2. If the number of parameters in the problem is too great, or the conditions are too irregular to be safely approximated by the known standard solutions, one may instead borrow a standard program (sufficiently general, finished, and thoroughly tested) that is able either to apply a general class of rupture figures on a wide range of failure problems or to solve a special class of failure problems choosing itself in each case the appropriate rupture figure, possibly to a required standard of accuracy. Such programs would be prepared by research institutions and also (when inspired by actual jobs) by engineering firms or computing centres.

It should be noticed, however, that some of the procedures, especially of the second class, would only be really useful if they are prepared for more general circumstances than those considered in the present work. Thus, rupture figures consisting of line ruptures should be generalized to cover also the case of inhomogeneous clays.

62 MORE GENERAL APPLICATIONS

621 General Problems in Clay

Since the general solution method of kinematically admissible solutions with possible zones is based on considerations of the deformation work (Sec. 241) that are also valid for much more general properties of the material and the failure problems, this method can be given a much wider use than the one indicated in the present work.

Thus, the development in Sec. 241, except for the four last equations, is clearly valid for all failure problems whatever the material. It can also be extended to cover three-dimensional problems with the following modifications.

1. The volume forces have now three components: X, Y, Z or in tensor notation: X_i. If they are gradients to a potential function: $X_i = \frac{\partial K}{\partial x_i}$ (or, if the comma notation is used for brevity to indicate derivatives: $X_i = K_{,i}$) their action can be replaced by the action of a normal loading $\sigma_n = K$ on the clay boundaries, provided that an additional hydrostatic stress distribution does not influence the failure condition.

2. The velocity field has also three components: u_x, u_y, u_z or in tensor notation: u_i. Correspondingly, the total forces and movements of rigid bodies have six components (3 forces or translations and 3 moments or rotations): Q_x, Q_y, Q_z, M_x, M_y, M_z and w_x, w_y, w_z, r_x, r_y, r_z or in tensor notation: Q_i and w_i ($i = 1 \ldots 6$). Rod connections between rigid bodies are also described by six numbers a_{ri} (the projections and moments of a unit vector in the rod).

3. Surface loadings and movements must be described by three components: σ_n^o, τ_t^o, τ_s^o, (σ_i^o) and u_n, u_t, u_s (u_i^o) relative to a local surface coordinate system n, t, s of which t and s are tangents to the surface, whereas n is the surface normal. Alternatively, the surface loading may be described by three components p_x, p_y, p_z (p_i) taken per unit area of the coordinate planes (dy dz, dx dz, and dx dy, the sign being dependent on the direction cosines n_i of the normal vector).

4. The stress tensor has also six components, σ_x, σ_y, σ_z, τ_{xy}, τ_{yz}, τ_{xz} (σ_{ij}). The same is true for the strain tensor (ϵ_{ij}). Since the latter one shall correspond without contradiction to a unique velocity field that has only three components, there will now be three compatibility equations instead of one.

The basic equations in the three-dimensional case are, expressed in tensor notation so that they are also valid in the two-dimensional case hitherto considered:

The equilibrium equations inside the clay:

$$\sigma_{ij,j} + X_i = 0 \tag{6201}$$

and along the clay surface:

$$\frac{dQ_i}{dS} = \sigma_{ij}\, n_j = p_i\, n_i \text{ (no sum)} = a^o_{ik}\, \sigma^o_k \tag{6202}$$

In this equation ($i = 1, 2, 3$) dQ_i are the contributions to the three first components of the total force, and $dS = dt\, ds$ is the surface element. n_j are the direction cosines of the surface normal, and a^o_{ik} is the direction cosine No. i to the surface coordinate axis No. k ($a^o_{i1} = n_i$).

The strain components depend on the movement components by the equation:

$$\epsilon_{ij} = \frac{1}{2}\,(u_{i,j} + u_{j,i}) \tag{6203}$$

The connection between the surface movements u^o_i and the ordinary movement components u_i is given by:

$$u_i = a^o_{ik}\, u^o_k \tag{6204}$$

Correspondingly, if n, t, s is a right handed coordinate system:

$$u^o_i = a^o_{ki}\, u_k \tag{6205}$$

The sliding velocity u_s between an external rigid body and the clay may be described by the components u^s_i. Since it is orthogonal to the normal vector its components must satisfy the condition

$$u^s_i\, n_i = 0 \tag{6206}$$

Besides

$$u^s_i\, u^s_i = (u_s)^2 \tag{6207}$$

If sliding takes place the resulting shear stress on the clay surface should have the same direction as u_s, and should be equal to c_a. Hence, the rigid body acts upon the clay with a surface loading σ_i^s that satisfies the condition that for i = 2 and 3:

$$u_s \, \sigma_i^s = c_a \, u_i^s \tag{6208}$$

Since u_i^s is orthogonal to σ_1^s we have evidently $u_i^s \, \sigma_i^s = c_a \, u_s$.

The equations of Sec. 223 that are given in tensor notation are also valid for the three dimensional case.

The development in Sec. 241 can now be written:

$$W_d = \int_V \sigma_{ij} \, \epsilon_{ij} \, dV = \int_V \sigma_{ij} \, u_{i,j} \, dV$$

$$= \int_V (\sigma_{ij} \, u_i)_{,j} \, dV - \int_V \sigma_{ij,j} \, u_i \, dV$$

$$= \int_S \sigma_{ij} \, u_i \, n_j \, dS + \int_V X_i \, u_i \, dV \tag{6209}$$

The first transformation of the deformation work integral follows from (6203), utilizing the symmetries in the stress and strain tensors; the second transformation is a simple integration by parts; the first integral in the final expression follows from Gauss' integral theorem, and the second one from (6201). According to (6202) the surface integral can be written:

$$W_s = \int_S a_{ik}^o \, \sigma_k^o \, u_i \, dS = \int_S p_i \, u_i \, dS^i \tag{6210}$$

cf. (2404-5), where $dS^i = n_i \, dS$. Thus, for the term $p_z \, u_z$ in the sum one should use the area element $dS^i = dx \, dy$, with the same sign as $n_3 = n_z$.

The contribution from a surface to a rigid body of clay is equal to:

$$W_{cs} = Q_i^c \, w_i^c \tag{6211}$$

cf. (2406), and from the system of external rigid bodies it is equal to:

$$W_{rs} = P_r \, d_r + Q_{pi}^e \, w_{pi}^e - \int_S c_a \, u_s \, dS \tag{6212}$$

cf. (2409). According to (6207-8) u_s is always positive.

The uniqueness of solutions (Sec. 242) and the definition of the method of kinematically admissible solutions (Sec. 243) with variants (Sec. 244-6) are based on the comparison between (2411) and (2412) and also on (2414). The extremum property in this way depends on the type of failure condition. It may clearly be true for other materials than the homogeneous, isotropic clay in plane strain that is considered in the present work.

A more general failure criterion than (2308) can be obtained on the following form, cf. Hill [1950]:

$$c_{ijkl}\ \sigma_{ij}\ \sigma_{kl} = K \tag{6213}$$

where K may be a function of x and y (and z in the three dimensional case), but not of σ_{ij} or ϵ_{ij}. c_{ijkl} is a tensor of the fourth order. Because of the symmetries in the stress tensor it should satisfy the symmetry condition:

$$c_{ijkl} = c_{jikl} = c_{ijlk} = c_{klij} \tag{6214}$$

Since the failure condition shall not depend on the mean normal stress $\sigma = \frac{1}{n}\ \sigma_{ii}$ the c-tensor should also satisfy the condition:

$$c_{iikl} = 0 \tag{6215}$$

If now the deformation condition (2333) is replaced by:

$$\epsilon_{ij} = \lambda\ c_{ijkl}\ \sigma_{kl} \tag{6216}$$

where λ is an arbitrary factor, we find that provided the quadratic form (6213) is non-negative, i.e. the equation $f(\sigma_{ij}) = c_{ijkl}\ \sigma_{ij}\ \sigma_{kl} = \text{const.}$, of the n^2 stress components, represents an $(n^2 - 1)$-dimensional hypersurface in the n^2-dimensional space of the stress components that is convex about the origin point $\sigma_{ij} = 0$ (but with rectilinear generators parallel to the direction $\sigma_{ij} = \delta_{ij}$), the following extremum condition will hold:

Assume that to any given failure problem a velocity field is specified that agrees with the known boundary movements and satisfies the condition of constant volume:

$$u_{i,i} = \epsilon_{ii} = 0 \tag{6217}$$

cf. (6215-6), and also that all such stress distributions are considered as agree with the known boundary stresses and total forces, and satisfy the equilibrium condition (6201), and nowhere exceed the failure condition (i.e. $c_{ijkl}\ \sigma_{ij}\ \sigma_{kl} \leq K$). The unit deformation work

$$dW_d = \sigma_{ij}\ \epsilon_{ij}\, dV \tag{6218}$$

will then be a maximum for the stress distribution that further satisfies the condition (6216).

For any given velocity field this stress distribution is found at each point, except for an unknown factor of proportionality k and an unknown mean normal stress σ, by the solution of the equations (6216):

$$\sigma_{ij} = k\, e_{ijkl}\, \epsilon_{kl} + \sigma \tag{6219}$$

where e_{ijkl} is the inverse transformation tensor to the c-tensor:

$$c_{mnij}\, e_{ijkl} = \delta_{km}\, \delta_{ln} \tag{6220}$$

The factor of proportionality k can be found by insertion into (6213), but σ cannot be found in this way. In most cases it will be given by the equilibrium and boundary conditions, however.

A still more general formulation of the failure and deformation conditions exist for which the same maximum principle holds:

$$f(\sigma_{ij}) = K$$

and (6221)

$$\epsilon_{ij} = \lambda \frac{\partial f}{\partial \sigma_{ij}}$$

cf. Drucker, Prager, and Greenberg [1951]. $f(\sigma_{ij}) = \text{const.}$ shall again be a convex hypersurface about the origin point. The formulation (6213-6) is general enough for most practical purposes, however. It may be used for the following special cases.

1. If c_{ijkl} is defined as in Table 62A below we have an ordinary clay in plane strain. If K is a constant ($= 4c^2$) the clay is homogeneous as it has been assumed in the preceding chapters. On the other hand, if K is taken to be an arbitrary function of x and y the clay is inhomogeneous. This will not change the definition of the stress or strain characteristics, or their position relative to the principal stress directions, but (2318) must now be changed. One finds (provided the volume forces have been corrected as in (2305-7)):

$$\frac{\delta \sigma}{\delta s_a} + 2c \frac{\delta m}{\delta s_a} = -\frac{\partial c}{\partial x} \sin m + \frac{\partial c}{\partial y} \cos m = \frac{\delta c}{\delta s_b}$$

$$\frac{\delta \sigma}{\delta s_b} - 2c \frac{\delta m}{\delta s_b} = \frac{\partial c}{\partial x} \cos m + \frac{\partial c}{\partial y} \sin m = \frac{\delta c}{\delta s_a} \tag{6222}$$

Therefore, the Hencky conditions (3104) will no longer be valid. This

makes it somewhat more difficult to calculate possible zones, because m and σ must be calculated as functions of λ and μ simultaneous with f. inst. $\overline{x}$ and $\overline{y}$. If the gradients $\frac{\partial c}{\partial x}$ and $\frac{\partial c}{\partial y}$ can be considered as piecewise constants, which will be admissible in most practical cases, the calculations are somewhat simplified. A workable method can be obtained by the use of a modified method of chord lengths (a second order approximation), but in principle all zones will now have to be calculated as open zones, so in practice it is presumably simpler, except for statically determined zones or systems of line ruptures, to use the method of kinematically admissible solutions in all cases (possibly with velocity fields taken from solutions in homogeneous clay). Alternatively solutions with kinematically possible zones (Ex. 24 e) may be used.

Table 62 A: Elements c_{ijkl} for isotropic clay in plane strain.

k,l \ i,j	1,1	1,2	2,1	2,2
1,1	1	0	0	-1
1,2	0	1	1	0
2,1	0	1	1	0
2,2	-1	0	0	1

2. If c_{ijkl} is changed to the pattern shown in Table 62 B we have an anisotropic clay with axes of anisotropy parallel to the coordinate axes, cf. Hill [1950]. This corresponds to a replacement of the failure condition (2308) by:

$$\tau^2 \ (a \cos^2 2\theta + b \sin^2 2\theta) = c^2 \qquad (6223)$$

when K is again put equal to $4c^2$. If anisotropy axes forming an angle θ_o with the coordinate system are required the c-tensor shown in Table 62 B may be transformed by the equation:

$$c'_{ijkl} = a_{pi} \, a_{qj} \, a_{rk} \, a_{sl} \, c_{pqrs} \qquad (6224)$$

before it is inserted in (6213). a_{ij} is the matrix of direction cosines to the anisotropy axes relative to the coordinate system.

In this case, and especially if the clay is also assumed to be inhomogeneous, the calculation of possible zones becomes rather difficult. The principal stress and strain directions will no longer coin-

cide (unless θ is an integer multiple of $\frac{\pi}{2}$), but the stress and strain characteristics will, m being equal to $\psi + \frac{\pi}{4}$ where $\tan 2\psi = \frac{b}{a} \tan 2\theta$. Therefore, in this case also a workable method for the calculation of possible zones may be devised, based on the method of chord lengths (or finite differences). The calculations will be rather extensive, however, so if statically determined zones or systems of line ruptures are not used, it is much simpler to use only kinematically admissible solutions, or solutions with kinematically possible zones.

Table 62 B: Elements c_{ijkl} for anisotropic clay in plane strain.

k,l \ i,j =	1,1	1,2	2,1	2,2
1,1	a	0	0	-a
1,2	0	b	b	0
2,1	0	b	b	0
2,2	-a	0	0	a

3. For isotropic clay in the three-dimensional case the c-matrix will be as shown in Table 62C below (to be used with $K = 6c^2$ where c is the shear strength in plane strain). Problems of this kind have been studied very little, mainly because possible zones are in general extremely difficult. Since we have only 3 equilibrium equations and one failure condition against the 6 unknown stress components statically determined zones can no longer obtain, but the stress distribution and the velocity field must be calculated simultaneously. Therefore, all rupture zones, even if bounded by free surfaces with known surface loadings, have mixed boundary conditions, and the basic differential equations are rather complicated. However, it is relatively easy to specify kinematically admissible solutions in the usual way by means of velocity fields (using now 3 components instead of 2), so the extremum method can always be used. As in problems in plane strain forces doing no work during the movement may be found by considering derivatives of the deformation work. The parameter K in (6213) may be considered as a function in x, y, and z, and the elements in Table 62C may be transformed as under No. 2 above, to obtain more general problems in inhomogeneous and anisotropic materials.

Table 62C: Elements c_{ijkl} for isotropic clay in the three-dimensional case.

k,l = \ i,j =	1,1	1,2	1,3	2,1	2,2	2,3	3,1	3,2	3,3
1,1	2	0	0	0	-1	0	0	0	-1
1,2	0	$\frac{3}{2}$	0	$\frac{3}{2}$	0	0	0	0	0
1,3	0	0	$\frac{3}{2}$	0	0	0	$\frac{3}{2}$	0	0
2,1	0	$\frac{3}{2}$	0	$\frac{3}{2}$	0	0	0	0	0
2,2	-1	0	0	0	2	0	0	0	-1
2,3	0	0	0	0	0	$\frac{3}{2}$	0	$\frac{3}{2}$	0
3,1	0	0	$\frac{3}{2}$	0	0	0	$\frac{3}{2}$	0	0
3,2	0	0	0	0	0	$\frac{3}{2}$	0	$\frac{3}{2}$	0
3,3	-1	0	0	0	-1	0	0	0	2

622 Frictional Materials

In principle the general formula (6213) may also represent a material with internal friction, giving f. inst. a failure criterion on the form:

$$\sigma^2 \sin^2 \varphi - \tau^2 = 0 \qquad (6225)$$

in plane strain. The deformation condition (6216), however, will in this case specify an angle of dilatation ν defined by the formula

$$\sin \nu = -\frac{\epsilon_v}{\epsilon} \qquad (6226)$$

where $\epsilon_v = \frac{1}{2}(\epsilon_x + \epsilon_y)$, equal to the angle φ of internal friction. This would mean that the deformation work was zero, the work due to the volume increase against the normal stresses being equal to the energy of distorsion. Thus, no work would be used on non-conservative friction forces between the grains of the material.

This is not a realistic assumption and, in fact, angles of dilatation are always measured smaller than φ (even negative in loose sands). Therefore, although (6225) may be a reasonable assumption for sand it cannot be fitted into the general scheme of the preceding section. Another deformation condition than (6216), or the second Eq. (6221) in more general cases, must be

used, f.inst. $\epsilon_v = 0$ as in the previous chapters of this work.

This gives a number of difficulties, however, because under these assumptions the general extremum principle will no longer be generally true; at least it cannot be proved simply by considering the deformation work integrals. Thus, one cannot in a simple way prove that solutions are unique, or that kinematically admissible solutions are always on the unsafe and statically admissible solutions on the safe side. It seems, in fact, that the work done by the prescribed movements will within certain limits depend on forces doing no work during the movement, resulting f.inst. partially from prestressings in the material before the loading until failure.

Other problems arise from the fact that the stress and the strain characteristics do not coincide if $\nu \neq \varphi$. This makes the construction of solutions with rupture zones with mixed boundary conditions rather difficult. Presumably the assumption of coinciding principal stress and strain directions cannot be retained, cf. de Josselin de Jong [1959], but then another deformation condition must be found in order to have a sufficient number of conditions. The nature of this condition has not yet been determined; it should probably not specify a local connection between the stress and strain components at each point but should rather be an extremum condition for the entire sand mass.

However, statically determined rupture zones can be calculated also in materials with internal friction, and in fact in any plastic material in plane strain. As proposed by Brinch Hansen [1953] line ruptures may be calculated under the assumption that they are stress characteristics, at least in homogeneous materials, so some types of rupture figures (relatively simple, quasi-possible solutions) can be calculated, apparently with a good accuracy although their position relative to the mathematically correct solution, if such exist under the given assumptions, is not known. In relation to the present work the best methods in sand may be compared with the method of approximate movement conditions (Sec. 444). They might therefore be extended to cover more complex rupture figures (including closed radial zones, and arc zones), but it is a question whether the accuracy would be much increased.

As a conclusion it seems that the most fruitful research work in the present field, and the one that is most needed, could be divided into the following types.

1. Implementation of the present theory: Preparation of computation programs for general calculation purposes, special types of failure problems, and particular solutions of special interest.

2. First order extension: Reformation of the programs to cover also problems in inhomogeneous and anisotropic clays as needed (for example: general types of rupture figures applied to inhomogeneous clay and particular solutions also for anisotropic clay).

3. Second order extension: A corresponding investigation (with reasonably simple types of velocity fields) for three-dimensional cases. Possibly more advanced methods including (at least kinematically) possible zones for problems with axial symmetry.

4. The most important studies at present are concerned with frictional materials, however. Although some solutions can be obtained with a surprisingly high accuracy the correct basic approach is still wanted. Apart from the calculation of particular solutions with approximate movement conditions when needed, the fundamental problem of defining a sufficient set of assumptions and formulating a general method that will give a unique calculation result, or at least upper and lower limits when regard is taken to the possible states of prestressings, should be given a high priority.

NOTATIONS

In this section only the most important, generally used symbols are indicated together with their sign rules. Notice that the positive direction of rotations (xy) is defined by the Cartesian coordinate system x,y.

a,b — Slip line directions, positive so that the direction of rotations (ab) is positive, and so that the minor principal stress direction σ_3 lies in the first and third quadrant of the local a,b coordinate system.

Also angular coordinates, i.e. the difference in m measured along a- and b-lines respectively.

c — The shear strength of the clay. If necessary distinguished by indices, especially c_s for the stronger, and c_w for the weaker clay on the two sides of an internal boundary.

c_a — The adhesion strength between an external rigid body and the clay.

d — Prescribed movement. Especially: d_r = deformation of a constraint rod in controlled strain; positive as extension.

e — Indicator, equal to $\pm$ 1 (or 0). Shows the direction of calculations (e_a, e_b, e_s, e_w), of slidings (e_t), or failure (e_f).

e,f — Normal and shear stress, respectively, between an external rigid body and the clay (considered as unit earth pressures). Identical with σ_n and τ_{nt}.

f — Factor of safety, i.e. proportionality factor on loading rate in controlled stress.

i — An angle in connection with the surface. With sign: the inclination of the resulting surface load in relation to the normal (positive in the negative direction (tn)). Absolute quantity (also distinguished by an index s,w etc.): basic angle between a slip line and the boundary.

k — A chord length (always positive).

m	The angle between the positive direction of x and the positive a-direction. m_a, m_b direction angles for chords.
p	Surface loading. Especially p_x, p_y loading components per unit length of the perpendicular coordinate axis (taken with sign for increasing values of s). Positive when acting in the negative direction of the corresponding coordinate axis.
r	Rotation of a direction. Especially r_a, r_b: rotation of the a- and b-direction, respectively. r_z: movement component (rotation) of a rigid body. Positive in the direction from x to y.
s	Arc length. For free surfaces: positive when encircling the clay material in the negative direction of rotations. For the slip lines: s_a, s_b positive in the positive a- and b-direction, respectively.
t, n	A local surface coordinate system, in the tangential and (outward) normal direction, respectively.
u	A velocity at a point. Especially u_x, u_y: components of the velocity field, positive in the negative directions of the respective coordinate axes. Also u_n, u_t.
u_f, u_d, u_s	Sliding velocity along slip lines or between an external rigid body and the clay.
u, v	Velocity component in the a- and b-direction, respectively. Positive in the positive slip line directions.
w	Movement component or velocity difference. w_x, w_y: movement components for a rigid body. Positive in the negative coordinate directions. w_a, w_b: arc lengths along the slip lines in the hodograph plane. Also chord lengths in the hodograph plane. With the same sign as r_a and r_b, respectively. Also (in tensor notation): a general movement component.
x, y	The Cartesian coordinate system of reference.
$\bar{x}, \bar{y}$	Equivalent coordinates. Measured in a special coordinate system with the same origo as the system x, y but turned the angle m for each point to which the coordinates are measured.
F, G	Rotation functions, i.e. radii of curvature to the slip lines in the hodograph plane.

K	A constant. Also used to indicate a scalar function the gradient vector of which is the resulting volume force.
M	Moment. Especially: M_z: resultant moment acting upon a rigid body. Without any index: the moment about the mid point of the chord of the stress resultant for a circle arc.
M^z	A dimensionless function depending on α only, used to calculate M.
N	The component perpendicular to the chord of the stress resultant for a circle arc.
N^z	A dimensionless function depending on α only, used to calculate N.
Q	Force component for a rigid body. Q_x, Q_y: components positive in the negative coordinate directions. Also (in tensor notation) a general force component.
R, S	Radii of curvature for the slip lines. Positive when m is increasing in the positive direction of a and b, respectively.
T	The component in the line of the chord of the stress resultant for a circle arc.
T^z	Dimensionless function, depending on α only. Used to calculate T.
W	Work, usually the work $P_r d_r$ done by the prescribed boundary movements. W_d: deformation work in the clay.
X, Y	Volume forces. Positive in the negative coordinate directions.
α	An angle. Usually half the centre angle for a circle arc. α_a, α_b: half centre angles for slip line arcs, positive for increasing values of m in the positive slip line directions. α_1, α_2, .., without index, or α_c (for surface arcs): frequently always positive (geometrical angles).
β	Angle between positive x-direction and positive tangent direction for curve.
γ	Unit weight of the clay.

ϵ Unit deformation. ϵ_x, ϵ_y, ϵ_{xy}: components of the strain tensor in the coordinate directions. Positive as shortenings, and when the angle between the positive x- and y-directions is increased. ϵ_1, ϵ_3: principal strains. ϵ: radius in Mohr's circle of deformations (with sign = $(\epsilon_1 - \epsilon_3)/2$). Also (in tensor notation) general strain components.

θ, ψ Angles. Especially θ or θ_s: angle between the positive x-direction and the first principal stress direction. θ_d (if necessary) the same for the first principal strain direction.

λ, μ Dummy coordinates in the curvilinear coordinate system of slip lines. Increasing in the positive a- and b-direction, respectively.

ρ, λ Dimensionless coordinates used to characterize the rotation point for a rectilinear wall. Origo fixed at the foot point; coordinate directions coincident with the t- and n-direction, respectively, for this point.

σ Normal stress, positive as compression. σ_x, σ_y or σ_n, σ_t: components relative to the respective coordinate directions. σ_o: normal loading component on a surface. σ_1, σ_3: principal stresses. Without index: mean normal stress (= abscissa to the centre in Mohr's circle). Also (in tensor notation) general stress components.

τ Shear stress, positive in the same direction as ϵ_{xy}. τ_{xy} or τ_{nt}: components relative to the respective coordinate directions. τ_o: shear loading on a surface. Without index: radius in Mohr's circle for stresses.

ϖ Direction angle for chords. Measured from the positive x-direction to the chord direction.

REFERENCES

Caquot, A. et Kerisel, J.
Traité de mécanique des sols.
Gauthier-Villars, Paris 1956.

Carathéodory, C. und Schmidt, E.
Über die Hencky-Prandtlschen Kurvenscharen.
Zeits. ang. Math. Mech. 3, 1923, 468.

Coulomb, C.A.
Essai sur une application des règles de maximis et minimis à quelques problèmes de statique relatifs à i'architecture.
Mém. Acad. R. prés. p. div. sav. T. VII, 1773, Paris 1776.

Cox, A.D., Eason, G., and Hopkins, H.G.
Axially Symmetric Plastic Deformations in Soils.
Phil. Trans. Roy. Soc. A 254, 1961, 1036.

Damgaard, J.J.
Om Sands Bæreevne.
Master Thesis. The Technical University of Denmark 1951 (unpublished).

Drucker, D.C., Prager, W., and Greenberg, H.J.
Extended Limit Design Theorems for Continuous Media.
Quart. Appl. Math. 9, 1951, 381.

Drucker, D.C. and Prager, W.
Soil Mechanics and Plastic Analysis or Limit Design.
Quart. Appl. Math. 10, 1952, 157.

Fellenius, W.
Erdstatische Berechnungen mit Reibung und Kohäsion und unter Annahme kreiszylindrischer Gleitflächen.
Ernst, Berlin 1927.

Frazer, R.A., Duncan, W.S., and Collar, A.R.
Elementary Matrices.
Cambridge University Press, London 1938.

Geiringer, H.
Beitrag zum vollständigen ebenen Plastizitätsproblem.
Proc. 3rd Int. Cong. Appl. Mech. Stockholm, 2, 1930, 185.

Geiringer, H. und Prager, W.
Mechanik isotroper Körper im plastischen Zustand.
Ergebn. Exakt. Naturwiss. 13,310. J. Springer, Berlin 1934.

Geiringer, H.
Some Recent Results in the Theory of an Ideal Plastic Body.
Adv. Appl. Mech. 3, 1953.

Haar, A. und Kármán, Th. v.
Zur Theorie der Spannungszustände in plastischen und sandartigen Medien.
Nachr. Ges. Wiss. Göttingen, Math.-phys. Klasse 1909, 204.

Hansen, J. Brinch.
A General Plasticity Theory for Clay.
Géotechnique, 3, no. 4, 1952.

Hansen, J. Brinch.
Earth Pressure Calculation.
Teknisk Forlag, Copenhagen 1953.

Hansen, J. Brinch.
The Internal Forces in a Circle of Rupture.
Dan. Geot. Inst. Bull. 2, Copenhagen 1957.

Hansen, J. Brinch and Hessner, J.
Geotekniske Beregninger.
Teknisk Forlag, Copenhagen 1959.

Hansen, J. Brinch und Lundgren, H.
Hauptprobleme der Bodenmechanik.
Springer, Berlin 1960.

Hansen, J. Brinch.
A General Formula for Bearing Capacity.
Dan. Geot. Inst. Bull. 11, Copenhagen 1961.

Hartman, L.
Distribution des déformations dans les métaux soumis à des efforts.
Berger-Levrault, Paris 1896.

Haythornthwaite, R. M.
Stress and Strain in Soils, Plasticity.
Pergamon Press, London etc., 1960.

Hencky, H.
Über einige statisch bestimmte Fälle des Gleichgewichts in plastischen Körpern.
Zeits. ang. Math. Mech. 3, 1923, 241.

Hill, R.
The Mathematical Theory of Plasticity.
Clarendon Press, Oxford, 1950.

Hodge, P. G., Jr.
The Method of Characteristics Applied to Problems of Steady Motion in Plane Plastic Stress.
Quart. Appl. Math. 8, 1951, 381.

Hodge, P. G., Jr.
The Theory of Piecewise Linear Isotropic Plasticity.
I. U. T. A. M. Colloquium, Madrid 1955; Springer, Berlin 1956.

Huber, M. I.
Strain Energy of Distorsion as Measure of Strength of Material.
Chasopismo Technichne, Lemberg, 22, 1904, 81.

Hvorslev, J.
Über die Festigkeitseigenschaften gestörter bindiger Böden.
Ingeniørvidenskabelige Skrifter A Nr. 45, Copenhagen 1937.

Jáky, J.
Sur la stabilité des masses de terre complètement plastiques.
I. II. III. Müegyetemi Kösletnények, Budapest 1947-48.

Jelinek, R.
Gleitlinienfelder und Spannungsverteilung der Grenzzustände im Coulombschen Halbraum.
Diss. T.H. Wien 1943.

Josselin de Jong, G. de.
Statics and Kinematics in the Failable Zone of a Granular Material.
Waltman, Delft 1959.

Kézdi, A.
Erddrucktheorien.
Springer, Berlin 1962.

Korn, G.A., and Korn, T.M.
Mathematical Handbook for Scientists and Engineers.
McGraw-Hill, New York etc. 1961.

Kötter, F.
Über das Problem der Erddruckbestimmung.
Verhandl. Phys. Ges. Berlin, 7, 1888.

Kötter, F.
Die Entwiklung der Lehre vom Erddruck.
Jahresber. deutsch. math. Ver., 2, 1892, 75.

Kötter, F.
Die Bestimmung des Druckes an gekrümmten Gleitflächen.
Sitzungsber. Kgl. Preuss. Akad. der Wiss. Berlin 1903.

Krey, H. und Ehrenberg, J.
Erddruck, Erdwiderstand und Tragfähigkeit des Baugrundes.
4. Aufl. W. Ernst & Sohn, Berlin 1932.

Lévy, M.
Sur une théorie rationelle de l'équilibre des terres fraîchement remuées et ses applications au calcul de la stabilité des murs de soutènement.
J. Mathém. de Liouville, 1873.

Lundgren, H. and Hansen, J. Brinch.
Geoteknik.
Teknisk Forlag, Copenhagen 1958.

Lundgren, H. and Mortensen, K.
Determination by the Theory of Plasticity of the Bearing Capacity of Continuous Footings on Sand.
Proc. 3rd Int. Conf. Soil Mech. and Found. Eng. Zürich 1953.

Mandel, J.
Equilibres par tranches planes des solides à la limite d'écoulement.
Imprimerie Louis-Jean, Gap, 1942.

Meyerhof, G.G.
The Ultimate Bearing Capacity of Foundations.
Géotechnique, 2, no.4, 1951.

Mises, R.v.
Mechanik der festen Körper im plastisch-deformablen Zustand.
Nachr. Ges. d. Wiss. zu Göttingen 1913, 582.

Mises, R.v.
Mechanik der plastischen Formänderung von Kristallen.
Zeits. ang. Math. Mech. 5, 1925, 147; 8, 1928, 161.

Mohr, O.
Abhandlungen aus dem Gebiete der technischen Mechanik.
2nd Ed., W. Ernst & Sohn, Berlin 1914.

Müller-Breslau, H.
Erddruck auf Stützmauern.
Kröner, Stuttgart 1906 and 1947.

Nadai, A.
Plastizität und Erddruck.
Handbuch der Physik, Vol. 6, ch. 6, J. Springer, Berlin 1928.

Nadai, A.
Theory of Flow and Fracture of Solids.
McGraw-Hill, New York 1950.

Ohde, J.
Zur Theorie des Erddruckes unter besondere Berücksichtigung der Erddruckverteilung.
Die Bautechnik, Heft 10, 11, 13, 19, 25, 37, 42, 53, 54, 1938.

Olszak, W., Perzyna, P., and Szymanski, C.
Two-dimensional Plastic Problems of Nonhomogeneous Anisotropic Media.
Bull. Acad. Polon. Sci. Sér. Sci. Techn. 7, no.7, 1959.

Prager, W. and Hodge, Ph.
Theory of Perfectly Plastic Solids.
John Wiley & Sons, New York 1951.

Prager, W.
A Geometrical Discussion of the Slip Line Field in Plane Plastic Flow.
Kungl. Tekn. Högsk. Handlingar, No.65, Stockholm 1953.

Prager, W.
Probleme der Plastizitätstheorie.
Birkhäuser, Basel-Stuttgart 1955.

Prandtl, L.
Über die Härte plastischer Körper.
Nachr. d. Ges. d. Wiss., math.-phys. Kl., Göttingen 1920, 74.

Prandtl, L.
Anwendungsbeispiele zu einem Henckyschen Satz über das plastische Gleichgewicht.
Zeits. ang. Math. Mech. 3, 1923, 401.

Prandtl, L.
Spannungsverteilung in plastischen Körpern.
Proc. Int. Congr. Appl. Mech. Delft 1924.

Prandtl, L.
Über die Eindringungsfestigkeit plastischer Baustoffe und die Festigkeit der Schneiden.
Zeits. ang. Math. Mech. 1927.

Rankine, W.
On the Stability of Loose Earth.
Trans. Royal Soc. London, 147, 1857.

Rendulic, L.
Gleitflächen, Prüfflächen und Erddruck.
Die Bautechnik H. 13/14, 1940.

Résal, J.
La poussée des terres.
Béranger, Paris 1903.

Saint Venant, B. de.
Comptes Rendus Acad. Sci. Paris 70, 1870, 473; 13, 1871, 1181; 74, 1872, 1009.

Schultze, E.
Strenge Lösungen von Erddruckaufgaben und ihre Bedeutung für die Praxis.
Bauplanung u. Bautechnik, 1950.

Skempton, A.W.
The φ=0 Analysis and Its Theoretical Basis.
Proc. 2nd Int. Conf. Soil Mech. Found. Eng., Rotterdam 1948.

Skempton, A.W. and Bishop, A.W.
Building Materials: Their Elasticity and Inelasticity.
(ed. M. Reiner). Ch. X, Soils. North-Holland Publ. Co., Amsterdam 1954.

Sobotka, Z.
Limiting States of Equilibrium of Soils and Other Continuous Media.
(In Czech), Prague 1956.

Sobotka, Z.
The Limiting Equilibrium of Nonhomogeneous Soils.
Nonhomogeneity in Elasticity and Plasticity.
Proc. of I.U.T.A.M. Symposium, Warsaw 1958;
Pergamon Press, London etc.

Sobotka, Z.
On a New Approach to the Analysis of Limit States in Soils and in Other Continuous Media.
Bull. Acad. Polon. Sci. Sér. Sci. Techn., 9, no.2, 1961.

Sokolovski, V.V.
Statics of Soil Media.
Butterworths, London 1960.

Steen, Ole.
Brudfigurer i ler ved stive, glatte vægge.
Master Thesis. The Technical University of Denmark 1961 (unpublished).

Szymanski, C.
Some Plane Problems of the Theory of Limiting Equilibrium of Loose and Cohesive Nonhomogeneous Isotropic Media in the Case of a Non-linear Limit Curve.
Nonhomogeneity in Elasticity and Plasticity.
Pergamon Press, London etc., 1958.

Taylor, D.W.
Stability of Earth Slopes.
Boston Soc. Civil Engrs., 24, 1937, 197.

Taylor, D.W.
Fundamentals of Soil Mechanics.
J. Wiley & Sons, New York 1948.

Terzaghi, K.
Erdbaumechanik auf bodenphysikalischer Grundlage.
F. Deuticke, Leipzig u. Wien, 1925.

Terzaghi, K.
A Fundamental Fallacy in Earth Pressure Computations.
Journ. Bost. Soc. Civ. Engrs., Apr. 1936.

Terzaghi, K.
Theoretical Soil Mechanics.
J. Wiley & Sons, New York 1943.

Terzaghi, K. and Peck, R.B.
Soil Mechanics in Engineering Practice.
J. Wiley & Sons, New York 1948.

Terzaghi, K. und Jelinek, R.
Theoretische Bodenmechanik.
Springer, Berlin 1954.

Tresca, H.
Comptes rendus Acad. Sci. Paris 59, 1864, 754; 64, 1867, 809.
Mém. Sav. Acad. Sci. Paris 18, 1868, 733; 20, 1872, 75.

U.S. Department of Commerce.
National Bureau of Standards.
Tables of Bessel-Clifford Functions of Orders Zero and One.
Applied Mathematics Series 28, 1953.

Whittaker, E.T. and Watson, G.N.
A Course of Modern Analysis.
Univ. Press Cambridge, 1952.

SUMMARY

The aim of the present work has been to complete the existing theory of plasticity so that in principle all problems in practice concerning the final state of failure in ideal frictionless materials in plane strain can be solved in an economical way.

In order to obtain this a general solution method, called the method of kinematically admissible solutions with possible zones, has been developed from general considerations of the deformation work. Solutions of this kind, which have not been studied before to the author's knowledge, are special cases of the so-called kinematically admissible solutions that can be considered as generalizations of the well-known $\varphi = 0$ analysis.

It is shown how the general energy method is connected with the equilibrium method. The results of this investigation give a generalization of Brinch Hansen's method, including a more general formulation of the approximate stress conditions for line ruptures. By means of the equilibrium method the so-called quasi-possible and possible solutions are defined, in which the equilibrium conditions may be used instead of the extremum condition.

In the general solution methods, rupture zones with mixed boundary conditions are used. They have not been studied before to the author's knowledge. It is shown how they can be calculated either by an extension of the known methods of Riemann integration or integration by finite differences, using the so-called rotation functions F and G together with the radii of curvature R and S in the slip line net, or more economically by a new method, the so-called method of chord lengths. The different rupture figure types have been classified in an increasing order of complexity, and a general calculation method has been developed to cover all cases encountered in practice.

The above methods are also used to investigate limiting states of stress in rigid bodies of clay, finding in this way distributions of earth pressures and other soil reactions that are not given by the primary rupture figure, and also to investigate whether the assumed rupture figures are the most critical ones.

The use of the methods are shown by some examples from soil mechanics. During this part of the work some problems connected with the construction of solutions, including modes of failure, interacting and alternative rupture figures, and choice of approximations are discussed. Some special uses of the extremum method, including an approximate minimax principle, are also shown.

DANSK RESUME

Det er forsøgt at udvide den eksisterende plasticitetsteori, således at i princippet alle i praksis forekommende problemer vedrørende den endelige brudtilstand i idealt friktionsløst materiale i plan spændingstilstand kan løses på en økonomisk måde.

Dette er søgt opnået ved indførelsen af en generel løsningsmetode, den såkaldte metode med kinematisk tilladelige løsninger med mulige brudzoner, som kan udledes ved betragtning af forskellige udtryk for deformationsarbejdet i lermassen. Denne løsningsmetode, der såvidt vides ikke tidligere har været angivet, er et specialtilfælde af metoden med kinematisk tilladelige løsninger, der kan opfattes som en generalisation af den velkendte $\varphi = 0$ analyse.

Forbindelsen mellem den generelle arbejdsligning og ligevægtsligningerne er nøjere klarlagt. Som resultat af denne undersøgelse er opnået en generalisering af Brinch Hansens ligevægtsmetode, herunder en mere generel formulering af de tilnærmede betingelser for normalspændingerne på liniebrud. Ved hjælp af ligevægtsmetoden er de såkaldte quasi-mulige og mulige løsninger defineret. I disse løsninger kan ekstremumbetingelsen erstattes af ligevægtsligningerne.

I den generelle løsningsmetode er anvendt brudzoner med blandede grænsebetingelser, som såvidt vides ikke tidligere har været undersøgt. Det er vist, hvorledes sådanne brudzoner kan beregnes, enten ved en udvidelse af de kendte beregningsmetoder (Riemann integration eller trinvis integration), idet de såkaldte rotationsfunktioner F og G kan anvendes sammen med krumningsradierne R og S i brudlinienettet, eller lettere ved hjælp af en ny beregningsmetode, den såkaldte kordelængdemetode. De forskellige typer brudfigurer er klassificeret efter stigende sværhedsgrad, og en beregningsmetode er udviklet, som dækker alle i praksis forekommende tilfælde.

De nævnte metoder bruges også til at undersøge grænsetilfælde for spændingstilstanden i stive lerlegemer, hvorved man kan bestemme jordtryks- og andre reaktionsfordelinger, som ikke direkte fremgår af brudfiguren. De benyttes også til at undersøge, om de anvendte brudfigurer er de mest kritiske.

Anvendelsen af metoderne er illustreret ved hjælp af nogle eksempler inden for geoteknikken. Herunder er også diskuteret forskellige problemer i forbindelse med konstruktion af løsninger, kombinerede og alternative brudfigurer samt valg af tilnærmede løsninger. Der er desuden vist specielle anvendelser af ekstremmetoden, herunder et tilnærmet minimax-princip.

INDEX

Numbers refer to pages. Brackets indicate that the subject has been referred to, but has not been mentioned explicitly, at the page in question.

a, b-coordinates, 58, 110-2, 131, 145, 157.

Adhesion strength (c_a), 23, 29, 35f, 70, 71, 72, 75, 170, 203.

Anchor force, 98.

Anchor walls, 26f, 386, 418f.

Anisotropic materials, 12, 446f.

Arc zones, 31, 244f, 268-70, 273, 293-5, 307, 324-6, 327, 337f, 339.

Auxiliary (continuous) function set, 17, 128, 131, 246f, 307-9.

Bar, transversally loaded, 356-8.

Bearing capacity formula, 426f.

Bearing capacity problems, 16, 48.

- on stratified soil, 340.
- one-sided, 48, 95f, 104-7, 199f, 253, 303f, 321, 393f, 420f.
- simple, 246, 420f.
- two-sided, 48, 253, 304, 322f, 432.
- with interacting foundations, 246, 261-4.
- with squeezing, 246, 340.
- combined with stability, 386, 390.

Bessel functions, 135f, 137f, 140, (143f).

Boundary conditions, 13, 19.

- Brinch Hansen's (line ruptures), 18f, 33, 89, 96, 106, 225.
- movements, 29, 31, 36, 38, 43-6, 48, 68, 75, 81, 329, 442.
- stresses, 29, 31, 37, 55, 68, 442.

(see also Free surfaces, Rigid bodies of clay etc.).

Boundary load, normal corrective, 54, 196, 228, 343.

Boundary parts, 34f, 39-43, 48.

- circle arcs, 39-43, 123, 158, 164f, 203f, 205f, 208.

Calculations, numerical, 20, 128, 132, 168f, 243, 246-8, 333.

- accuracy, 30, 99, 104, 107, 120, 150f, 160-2, 167f, 247f, 359f, 362f.
- by hand, 33, 147, 170, 210, 243.
- economy, 13, 93, 107, 168, 243, 247f, 359f, 362f, 373, 375.
- on computer, 33, 87, 174, 210, 243, 245f, 266, 381, 393f, 415, 430, 440.

Caquot, A., 16.

Carathéodory, C., 17, 131f.

Centre angles, 39, 40, 146, 157f, 161f, 163, 167f, 210.

Chord lengths, method of, 123, 162-9, 172, 178f, 182f, 184, 189, 207-9, 210f, 216f, 246f, 250f, 309.

Chords, 40, 156-9, 162f, 167f, 210.

Clay layer on rock, 55f.

Cofferdams (double sheet walls), 77-9, 86, 415-8.

Compatibility conditions, 13, 64f, 442.

Conjugate functions (solutions to Telegraphist's equation), 132, 133-5.
Conjugate (complementary) solutions, 24, 179, 248f.
Controlled stress or strain, 23-5, 26f, 29, 48, 51, 72-5, 82, 86, 92.
Coordinate systems, 34f, 52, 55, 110f, 175, 203.
Coordinates, to points in rupture figure, 117, 121, 159, 164.
Corner points, 179f, 183, 191-3, 226f, 228, 254, 264, 337, 401-3.
Coulomb, C.A., 15, 59.
Coulomb's method, 15, 16, 18, 405.
Cracks, 36, 218, 410f, 421, 432.
Cuts, 385.
Cycloids, 61, 156, 159.

Damgaard, J.J., 6.
Danish Geotechnical Institute, 6.
Deformation conditions, 13, 17, 29, 63-5, (68), (72), 444f, 448.
Deformation work, 29f, 68f, 71, 72-4, 83, 219, 260, 373, 443, 448f.
Design problems, 24, 27, 51, 75, 362f, 377f.
Design quantities, see Parameters, external.
Developing rupture figures, method of, 364, 372-5.
Dilatation, angle of, 448.
Discontinuity lines, 91, 187-93, 250, 254.
Discontinuity points, 91, 193-6, 289f, 305, 327, 356.
Driving depth, 18, 26f, 386.
Drucker, D.C., 17, 18, 81, 445.

Earth front, (partly) unsupported, 76f, 295, 410-5.
Earth pressure:
  components, 170, 214, 229, 232.
  total (resulting), 98, 171, 214, 271f, 366, 397-9.
  (see also Line of attack).
Earth pressure distribution, 18, 19, 20, 341, 342f, 410, 414.
Earth pressure problems, 48.
  in stratified soil, 338f.
  simple, 246, 256, 277f, 365f, 368-72, 391-3.
  with interacting walls, 246, 415-9.
  with irregular surface conditions, 210f, 333f, 375f, 400-5.
  with partly unsupported earth fronts, 295, 326, 410-5.
  with yield hinges, 294, 326, 410-2.
  combined with bearing capacity, 433f.
  combined with stability, 28, 246, 301, 354, 386, 419.
Economy of construction, 25, 28, 362, 378.
Elastic deformations, 12, 205, 218.
Envelope of slip lines, 120f, 198, 206f, 250.
Equilibrium conditions (equations), 12, 15, 18, 23, 29f, 46f, 53f, 56f, 60, 68, 76, 80, 91f, 94, 96, 106, 167f, 220, 248, 266, 330, 442.
Equilibrium method, 18, 87-93, (96), (98), 220, 248, 266, 329f.
Equivalent coordinates, 17, 121-4, 125, 127, 137, 178, 181f, 183f, 202-5, (215), 247, 251.
External rigid bodies, 23-5, 27, 34, 43-8.
  boundaries to, 23, 34, 68-70, 84, 91, 113, 121, 170f, 187, 196, 200-10, 220, 229-32, 249f, 253f, 264, 442-4.
  equilibrium conditions, 27, 29, 46f, 68.
  force resultants on, 23-4, 36f, 43, 46f, 50, 68, 87f, 171, 218, 443.
  internal forces in, 341-5.
  movement conditions (restraints),

12, 23-5, 27, 36, 43-6, 70, 85f, 265.

movements of, 23-5, 27f, 43-6, 68, 86, 205f, 297, 373.

Extremum (maximum or minimum), extreme:

condition (minimum of W), 18, 30, 83, 86, 88f, 92, 94, 449.

method (energy method, use of work equation), 16, 31, 87, 93f, 96f, 219, 220, 396, 447.

principles (position of approximate solution), 18, 80, (81), (82), (345), 444f, 449.

solution, 15, 18, 30f, 81, 85, 93, 329, 377.

Failure, final state of, 13-5, 26.

Failure condition, 12f, 14, 29, 54f, 444, 448.

Failure problems, 12, 23-5, 33f, 243f, 245f.

Fellenius, W., 16, 380.

Finite differences, method of, 17, 128, 132, 142f, 145-51, 162, 172, 189, 202-7, 247.

Force components (total), 36, 43f, 441.

Foundation load, 238, 241, 346, 374.

excentric and inclined, 95f, 104-7, 295f, 420-9.

line of attack, 95, 420.

Foundation width, effective, 106, 421.

Foundations, 16, 246.

block, 355f, 393, 431-3.

moments in, 96, 345-7.

near a slope (interface), 199, 420-30.

on clay surface, 115, 128f, 238.

rough, 115, 128, 269, 346.

shallow, 16, 95f, 104-7, 295f, 303f.

smooth, 115, 199, 347.

Friction forces, 218.

Function set (continuous), see see Auxiliary functions.

Gauss' integral theorem, 69, 138, 443.

Geiringer, H., 17, 66, 125.

Geometrical conditions, 85, (131), 158, 243, 328f, 358.

Geometrical methods:

analytical, 20, 155, 157-62.

graphical, 20, 154-8.

Haar, A., 17.

Hansen, J. Brinch, 5, 6, 12, 18-20, 25, 75, 77, 83, 88, 104, 116, 168, 172, 173f, 221, 225, 243, 257, 264, 275, 341, 342, 349, 398, 414, 426, 449.

Hencky, H., 16, 58, 109, 117.

Hencky's conditions, 17, 131, 157, 158, 445.

Hill, R., 16, 17, 109, 115, 121, 141, 146, 444, 446.

Hinges:

between rigid bodies, 43, 46, 56.

in walls (see Yield hinges).

on rods, 43, 95.

Hodograph plane, 124-30, 156f, 158, 165f, 168, 287, 302f.

Homogeneous materials, 22, 77.

Huber, M. T., 16.

Indicators (e), 113, 146, 163f, 172, 178, 201f, 215, 249, 278.

Inhomogeneous materials, 12, 68, 77, 103, 123, 445-7.

Initial value problems, 133f, 136, 141f, 148f, 164, 179, 201.

Internal boundaries, 23, 35, 37, 84, 91, 196-9, 205, 214, 227f, 249, 265, 338-40.

Internal friction, materials with, 15-7, 22, 103, 218f, 448f.

Isotropic materials, 13, 22.

Josselin de Jong, G. de, 17, 449.

Kézdi, A., 17.

Kinematic conditions, 15, 18, (30), 64-7, (68), (72), 83f, 91, (99), (167), 329.

Kronecker's delta, 47.

Kötter, F., equation of, 16, 58, (449).

Line of attack, position, 77f, 263, 397-9, 405-6.

Line ruptures, 16, 18, 31, 84, 87-9, 92, 113, 195f, 220-41, 264-8, 284-8, 314, 319, 325, 352f.

force resultants, 87f, 93, 97, 172-4.

meeting in soil, 232-7, 295-300.

meeting at wall, 229-32, 267.

stress conditions, 18, 19, 89, 92, 220-37.

(see also Rupture figure, A, X etc., and Slip Lines).

Linearization, principle of, 363, 379.

Lundgren, H., 6.

Maximum shear strain, 29, 167.

Maximum shear stress, 14, 16, 29, 53f.

Mean normal stress, 13, 53, 72, 76, 79f, 81f, 175f.

Meyerhof, G.G., 16.

Mikhlin, 17, 121.

Minimax procedure, 405f, 409, 433.

Mises, R. v., 16.

Mohr circle for strains, 63.

Mohr circle for stresses, 52, 59, 155f, 177, 187, 197, 229.

Movement components (rigid body), 36, 38, 43f, 441.

Multiple radial zones, (107), 245, 319-23, 355.

Parameters, external (defining failure problems), 23-6, 33-51, 98, 243, 362, 364, 367f.

design, 24f, 94, 367f.

variable, 26f, 94, 362, 364.

Parameters, internal (defining solutions), 18, 30, 33, 81, 83, 85-7, 89f, 92-4, 100-2, 243, 305, 328f, 344.

movement, 25, 27f, 46, 48, 86.

Plane strain, state of, 14, 16, 22.

Plastic deformations, 13, 15, 55, 205, 218.

Plastic-rigid state (or material), 14, 16, 22, 54, 75, 343.

Pole trail method, 17, 155-7, 159.

Prager, W., 17, 155.

Prandtl, L., 17.

Principal directions (stress and strain), 22, 29, 53, 63, 71f, 81, 181, 446f, 449.

Radial zones, 15, 19, 31, 95, 113, 116, 122f, 134, 183-6, 198, 244f, 249-51, 284-9, 306f, 323-5, 336-8.

Radii of curvature, 17, 117-20, 122f, 126f, 137, 178, 181f, 183, 186, 205-7, (216), 223, 247, 348f.

Rankine, W., 15.

Rankine zones, 15, 143, 179, 198, 249, 251, 273, 330.

Rectangle zones, 134f, 142, 184, 249f, 306-16.

Rendulic, L., 16.

Restraint forces, 23, 25, 28, 45-7, 72, 75, 94, 106, 443.

Retaining walls, 16, 210f, 256, 333f, 393f, 407-9.

Riemann integration, 17, 138-45, 202, 247, (308f).

Rigid bodies of clay, 16, 28, 84, 99, 129, 198, 334-8, 373.

boundaries to, 19, 84, 113, 129f, 171f, 214-6.

equilibrium conditions, 18, 29, 68, 80, 82, 99f.

force resultants on, 36f, 42f, 87f, 171, 196.

limiting state of stress (secondary rupture figure) in, 20, 93f, 96, 99, 115, 327, 343-54, 358, 367, 375.

movement restraints, 84, 87, 92f, 104, 336.

movements of, 28, 233f, 265f, 298, 301f, 329.

possible stress distribution in, 30, (72), (81), (82), 99, 348-54, 373.

simple, 268, 277-84, 332.

Rod connections, 43-6, 48, 51.

Rotation (component), 36, 45f, (51), 67, 78f, 85, 125f, 128-30, 195.

Rotation functions, 126f, 206f, (216).

Rotation point, 77f, 116, 230-2, 234, 256f, 268, 275f, 278f, 296, 354, 369-72.

Rupture figure :

A, 32, 85, (97f), 266, 279-80, 365.

AaBfBfR, 268f.

AaBfR, 269.

AaPR, 32, 85, 395.

AaR, 267f, 395.

AaWPR, 267f.

AfCfA, (107), (316-9), 365f.

AfPfA, 19, 33, 85, (95), 98f, 106, 286, 341, 365, 395.

Aw, 410f.

AwWPR, (232), 267.

AwX, 229-32, 267.

BfR, 32, 85, 268-76.

BfR, general (curved slip lines), 32, 328-30.

C or Cf (XfRsAaR), 33, 98, 116, 195, 339f, 365f.

CfCfA, (321), 365f.

L (simple line rupture), 16, 77f, 85, 93, 97, 104f, 238, 244, 246, 264-6, 354.

PfA, 395-9.

R (Rankine), 76.

R, general (curved slip lines), 61-3, 114, 120f, 123f, 137f, 143f, 150f, 159-61.

RPTPR (Prandtl), 17, 115, 128-30, 195, 199, 346.

SfPfS, 95f, 106.

System of line ruptures, 198, 239-41, 244, 246, 295-301, 341, 380-3, 446, 447.

wA, 410f.

WPR (Prandtl), 32, 99, 212, 255-61, 335f, 342, 347, 395, 399.

WPR, modified (discontinuous surface loading), 212, 216f.

X, 266, 276, 279-80.

XfPR (or XfDR), 267f, 346, 421-5.

XfR, 268f, 275.

XfWPR, 267f, 338f, 346.

Rupture figure elements, (A, X, B, W, P, D, R), 267, 278f, 326, 330f, 350-2.

Rupture figure loci, method of, 364, 366-8, 392.

Rupture figures, 20, 29-32, 32f, 80, 84f, 100, 104, 116, 243-6, 362-4.

composite, 18, 244.

geometrically impossible, 183, 188, 254, 268, 272, 350, 362, 364.

integrated (composite), 355, 356, 385, 387-90, 417-9.

simply determined, 19, 31, 32f, 244f, 278-80, 332, 449.

simultaneous, 245, 354-6, 384f.

statically determined, 16, 31f, 188, 244f, 253-5, 332, 338f, 446, 447.

Rupture zones, 16, 28-30, 68, 81, 83-91, 99f.

closed, 32, 85, 215, 245, 247, 305f, 327, 332, 338.

kinematically determined, 17, 31, 244, 301-5.

open, 32, 245, 247, 328f.

statically determined, 14, 15, 17, 19, 31, 83, 86, 244, 249-55.

with mixed boundary conditions, 19, 31, 216, 244f, 247, 305.

kinematically possible, 101, 103, 239, 241, 254, 258f, 267, 446f.

possible, 83f, 86, 89, 100.

quasi-admissible, 102.

with approximate movement conditions, 101, 106, 286, 358-60.

with disregarded movement conditions, 102, 359.

Safe side, solutions on the, 18, 80f, 99-102.

Safety factor (f), 15, 24, 29, 75, 82, 86, 265, 390, 433f.

Saint Venant, B. de, 17.

Shear box test, 79.

Shear strength, 14, 16, 22, 23, 35, 54f, 72, 83.

Sheet walls, 116, 246, 393f.

anchored, 18, 25-8, 97f, 294, 342, 347, 386-90, 418f.

connected, 416-9.

free, 393, 410f.

Slices, method of, 383f.

Sliding velocity, 29f, 70, 84f, 204-7, 215f, 221, 230f, 233f, 297f, 442f.

Slip line net, 16f, 61, 109-16, 154-9, 168.

Slip lines, 15, 59f, 77, 85, 214.

arc lengths, 112, 117f, 119, 122, 127f, 183.

circular, 157f, 162, 172f, 252, 277.

sliding along, (29), (67), 127, 135, 147, 167, 194, 215f.

straight, 112, 119f, 122, 127, 135, 147, 277.

stress resultants, 87f, 170-4.

Slopes, 39, 77-9, (256), 380, 382-4, 391, 393, 413f, 420, 427.

Sokolovski, V.V., 17, 109, 302.

Solution method, 80, 99, 103f, 377f.

Solutions, 28-33, 100-4, 362.

mathematically correct, 18-20, 29-32, 72, 75, 80f, 98, 100, 363f, 375.

quasi-correct, 19, 99f.

approximate, 16, 18, 20, 30-2, 80-3, 362-4.

possible, 30-3, 98-100.

kinematically possible, 100, 254, 272.

statically possible, 100, 254, 260f, 348-54.

quasi-possible, 30, 32, 98-101, 374.

admissible with possible zones, 83-7, 98, 101, 104, 246, 329.

kinematically admissible, 18, 30f, 33, 81-3, 101f, 198, 239, 341, 444-7.

statically admissible, 18, 30f, 80f, 101-3.

with approximate movement conditions, 31, 101, 358-60, 449.

Squeezing zones, 244, 340, 418.

Stability problems, 16, 33, 39, 77-9, 264-6, 285f, 300f, 379-90.

State of failure, active or passive, 176-9, 194, 197, 201, 253. (see also Conjugate solutions).

Steen, O., 6, 116.

Strain characteristics, 65f, 103, 447.

Strain components, 14, 63, 442.

Stratified clay, 22, 26f, 196, 300f, 338-40, 380, 383.

Stress characteristics, 56-60, 91, 109, (120f), 447.

Stress components, 14, 37f, 52f, 442.

Stress conditions, 85, 110f, 131, (194), 243, (255), 262, 291.

Stress distributions, 15, 16, 17, 29f, 55, 68, 80f, 109, 115.

statically admissible, 18, 80, 89f, 103.

Stress resultants, 170-4.

Superposition, principle of, 363, 379.

Surface loading, 12, 23, 29, 36, 39f, 50, 69, 82, 86, 175f, 218.

components, 36, 441.

discontinuous, 16, 183, 210, 226f, 254, 264, 295, 333f, 336, 401-4, 407-9.

resultant, 36f, 40-3.

uniform, 76, 278.

variable, 26f, 62f, 401.

Surface zone complex, 107, 116, 289-92, (314), 321f.

Surface zones, 31, 184, 237, 244f, 249-53, 267.

Surfaces, free, 23, 31, 34f, 37, 68, 84, 113, 175-9, 225-7, 249, 253f, 343.

boundary conditions for zones, 29, 68, 87, 91, 175-9.

bounding rigid bodies, 69, 174.

irregular, 16, 149, 295, 336.

Taylor, D.W., 380.

Telegraphist's equation, 132.

Tensor notation, 43f, 441-3.

Terzaghi, K., 16, 18.

Three-dimensional problems, 12, 14, 16, 68, 83, 103, 441-3, 447f.

Tie rods, 26f, 386f, 416.

Transition points, 31, 115, 193f, 195, 254f, 262, 337.

Translation, 36, 45f, 95f, 106, 116, 128, 194.

Tresca, H., 16.

Triangle zones, 134, 142, 179, 199, 249f.

Undrained failure (clay), 13-7, 22.

Uniqueness of solutions, 17, 72-8, 219, 345, 444.

Unit weight, 22, 26, 35.

Unsafe side, solutions on the, 18, 80, 82, 99-102.

Velocity components, 15, 17, 36, 38, 64, 66, 124-6.

Velocity fields, 17, 23, 28f, 64-7, 68, 75-9, 80-3, 86, 115, 124, 165f, 190, 204f, 209f, 215-8, 441.

kinematically admissible, 18, 81-4, 446.

Vertex points, 84, 91, (113), 183-7, 251, 306.

Virtual displacements, principle of, 71, 96.

Volume change, 13, 22, 29, 63, 68, 81, 101, 286, 358, 360, 448f.

Volume forces, 14, 22, 23, 35, 53f, 62, 68, 70, 82f, 86, 123, 441.

Wall zones, 31, 135, 149, 165, 198, 201f, 244, 249-51, 273, 323f, 336, 338.

Work (W), done by specified movements, 24, 25, 75, 82, 87.

Work (energy) equation, 17f, (69), 86f, 88f, 96, 219, 329.

Work hardening, 13, 22.

Yield hinges, 26f, 343f, 410-2.

Zone elements, 84, 211, 248, 249f, 252, 316, 373.

λ, μ-plane, 112-6, 177f, 185f, 195, 199, 201, 215, 243.

$\varphi = 0$ analysis, 18, (264f), (285f), 380.